

# **Activation of Carboxylic Acids *via* Self-Assembly Organocatalysis**

**Inaugural-Dissertation**

zur

Erlangung des Doktorgrades

der Mathematisch-Naturwissenschaftlichen Fakultät

der Universität zu Köln

vorgelegt von

Mattia Riccardo Monaco

aus Naples (Italien)

Köln 2015

Berichterstatter:

Prof. Dr. Benjamin List  
Prof. Dr. Albrecht Berkessel  
Prof. Dr. Axel Klein

Tag der letzten mündlichen Prüfung:

27.10.2015

**Table of Contents**

<b>Abstract</b> .....	<b>IV</b>
<b>List of Abbreviations</b> .....	<b>V</b>
<b>Acknowledgements</b> .....	<b>VIII</b>
<b>1. Introduction</b> .....	<b>1</b>
<b>1.1. Chirality</b> .....	<b>1</b>
<b>1.2. Asymmetric catalysis</b> .....	<b>3</b>
<b>2. Background</b> .....	<b>6</b>
<b>2.1. Asymmetric organocatalysis</b> .....	<b>6</b>
2.1.2. Activation modes and establishment of modern organocatalysis .....	8
<b>2.2. Asymmetric Brønsted acid catalysis</b> .....	<b>11</b>
2.2.1. General Brønsted acid catalysis: hydrogen bonding catalysts.....	12
2.2.2. Specific Brønsted acid catalysis: acid catalysts .....	13
<b>2.3. Carboxylic acids</b> .....	<b>20</b>
<b>2.4. Epoxides and aziridines in organocatalysis</b> .....	<b>27</b>
<b>2.5. Asymmetric hydrolysis</b> .....	<b>31</b>
2.5.1. Asymmetric sulfhydrolysis .....	33
<b>3. Objectives</b> .....	<b>36</b>
<b>3.1. Premise</b> .....	<b>36</b>
<b>3.2. Studies towards heterodimeric self-assembly</b> .....	<b>39</b>
<b>3.3. Activation of carboxylic acids in asymmetric organocatalysis</b> .....	<b>40</b>
<b>3.4. Asymmetric synthesis of <math>\beta</math>-hydroxythiols</b> .....	<b>41</b>
<b>3.5. Mechanistic investigation and codification of a novel activation mode</b> .....	<b>42</b>
<b>4. Results and Discussions</b> .....	<b>44</b>
<b>4.1. Studies on heterodimeric self-assembly</b> .....	<b>44</b>
4.1.1. Identification of the supramolecular association .....	44
4.1.2. Evaluation of binding constants and structure elucidation .....	47
<b>4.2. Asymmetric carboxylysis of aziridines</b> .....	<b>51</b>
4.2.1. Reaction design and optimization.....	51
4.2.2. Reaction scope .....	59

---

4.2.3. Discussion .....	64
<b>4.3. Asymmetric hydrolysis of epoxides in organocatalysis .....</b>	<b>69</b>
4.3.1. Reaction design and initial optimization.....	69
4.3.2. Catalyst design and synthesis.....	75
4.3.3. Evaluation of novel catalysts and reaction optimization.....	83
4.3.4. Reaction scope .....	89
4.3.5. Biomimetic, asymmetric <i>anti</i> -dihydroxylation strategy .....	94
<b>4.4. Asymmetric synthesis of <math>\beta</math>-hydroxythiols.....</b>	<b>98</b>
4.4.1. Reaction design and heterodimer studies .....	98
4.4.2. Preliminary studies and optimization of reaction conditions.....	101
4.4.3. Reaction scope .....	104
<b>4.5. Mechanistic investigations.....</b>	<b>109</b>
4.5.1. Studies on heterodimeric activation .....	109
4.5.2. Studies on the catalytic cycle .....	112
4.5.3. Investigations on the transition states.....	118
<b>5. Summary .....</b>	<b>121</b>
<b>5.1. Activation of carboxylic acids in asymmetric organocatalysis .....</b>	<b>121</b>
<b>5.2. Highly enantioselective carboxylolysis of aziridines.....</b>	<b>123</b>
<b>5.3. Asymmetric, biomimetic hydrolysis of epoxides.....</b>	<b>124</b>
<b>5.4. Enantioselective organocascade approach to <math>\beta</math>-hydroxythiols.....</b>	<b>125</b>
<b>5.5. Exploration of novel classes of confined phosphoric acid catalysts .....</b>	<b>126</b>
<b>6. Outlook .....</b>	<b>129</b>
<b>6.1. Enantioselective recognition of chiral carboxylic acids by heterodimerization. ....</b>	<b>129</b>
<b>6.2. Stereodivergent resolution of racemic carboxylic acids. ....</b>	<b>131</b>
<b>6.3. Regiodivergent, enantioconvergent dihydroxylation of unsymmetrical olefins. ....</b>	<b>132</b>
<b>6.4. Towards other heterodimeric self-assemblies. ....</b>	<b>133</b>
<b>7. Experimental Section .....</b>	<b>136</b>
<b>7.1. General experimental conditions .....</b>	<b>136</b>
<b>7.2. Studies on heterodimeric self-assembly.....</b>	<b>139</b>
7.2.1. 1D-NMR studies .....	139
7.2.3. Binding isotherm studies.....	143
7.2.4. Crystal structure determination of TRIP·AcOH .....	147



---

<b>7.3. Asymmetric carboxylation of aziridines</b> .....	<b>155</b>
7.3.1. Preparation of starting materials.....	155
7.3.2. General procedure for the desymmetrization of <i>meso</i> -aziridines.....	161
7.3.3. General procedure for the kinetic resolution of terminal aziridines.....	168
7.3.4. Determination of the absolute configuration of products.....	172
7.3.5. Kinetic studies.....	174
7.3.6. Non-linear effect studies.....	176
<b>7.4. Asymmetric hydrolysis of epoxides in organocatalysis</b> .....	<b>177</b>
7.4.1. Preparation of catalysts.....	177
7.4.1.1. Crystallographic data of compound 139.....	194
7.4.2. Preparation of starting materials.....	207
7.4.3. General procedure for the desymmetrization of <i>meso</i> -epoxides.....	212
7.4.4. General procedure for the kinetic resolution of racemic epoxides.....	222
7.4.5. General procedure for the <i>anti</i> -dihydroxylation strategy.....	228
<b>7.5. Asymmetric synthesis of <math>\beta</math>-hydroxythiols</b> .....	<b>231</b>
7.5.1. Heterodimer studies.....	231
7.5.2. General procedure for the thiocarboxylation of <i>meso</i> -epoxides.....	237
7.5.3. General procedure for the organocascade synthesis of thiols 148.....	251
7.5.4. One-pot synthesis of 1,2-thioalcohols 150.....	256
7.6.1. Molecular orbital energies of acetic acid.....	258
7.6.2. Brønsted acidity of TRIP·AcOH heterodimer.....	259
7.6.3. Studies on the catalytic cycle.....	271
<b>8. Bibliography</b> .....	<b>297</b>
<b>9. Appendix</b> .....	<b>312</b>
<b>9.1. Erklärung/Declaration</b> .....	<b>312</b>
<b>9.2. Lebenslauf/CV</b> .....	<b>313</b>

## Abstract

This work describes the development of a novel enantioselective activation mode for carboxylic acids *via* self-assembly organocatalysis. In the first part, the heterodimerization between sterically congested chiral phosphoric acid catalysts and carboxylic acids is presented. Upon association, an exceptionally synergistic effect is observed: the acidity of the catalyst is enhanced and the nucleophilicity of the carboxylic acid is increased. Explorations on this catalytic system allowed to unlock the first enantioselective ring openings of aziridines and epoxides to 1,2-diols, 1,2-aminoalcohols and 1,2-thioalcohols in Brønsted acid catalysis. An unusual reaction mechanism was harnessed, in which the phosphoric acid primarily establishes an interaction with the nucleophile rather than with the electrophile. This apparent change of polarity of the catalytic cycle allowed to effectively override the instability of the acid organocatalyst towards an alkylative deactivation in the presence of highly reactive electrophiles. Thorough mechanistic investigations, including theoretical analysis on the heterodimeric species and kinetic studies on the catalytic cycle were conducted in order to allow the detailed codification of this new reaction mode.

## Kurzzusammenfassung

Diese Arbeit beschreibt die Entwicklung eines neuen enantioselektiven Aktivierungsmodus von Carbonsäuren durch selbstorganisierte Organokatalyse. Im ersten Teil wird die Heterodimerisierung von sterisch anspruchsvollen chiralen Phosphorsäure-Katalysatoren und Carbonsäuren erläutert. Bei deren Wechselwirkung wurde ein synergistischer Effekt beobachtet: Sowohl die Azidität des Katalysators, als auch die Nukleophilie der Carbonsäure wurden erhöht. Untersuchungen des katalytischen Systems ermöglichten die erste Brønstedsäure-katalysierte enantioselektive Ringöffnung von Aziridinen und Epoxiden zu den entsprechenden 1,2-Diolen, 1,2-Aminoalkoholen und 1,2-Thioalkoholen. Hierfür wurde ein ungewöhnlicher Reaktionsmechanismus angewandt, bei dem die Phosphorsäure zunächst eine Wechselwirkung mit dem Nukleophil, anstelle des Elektrophils eingeht. Dieser offensichtliche Wechsel der Polarität im katalytischen Zyklus verhinderte eine Deaktivierung des Katalysators über eine mögliche Alkylierung durch hochreaktive Elektrophile. Mechanistische Studien, unter anderem theoretische Untersuchungen der Heterodimer-Spezies sowie kinetische Studien zur Aufklärung des katalytischen Zyklus wurden durchgeführt um detaillierte Einblicke in diesen neuartigen Reaktionsmodus zu erhalten.

**List of Abbreviations**

*	designating chiral element
A	acid
Ac	acyl
ACDC	asymmetric counteranion-directed catalysis
Alk	alkyl
Ar	aryl
Asp	aspartate
aq.	aqueous
B	base
BINOL	1,1'-bi-2-naphthol
Bn	benzyl
Boc	<i>tert</i> -butyloxycarbonyl
br	broad
brsm	based on recovered starting material
Bu	butyl
calcd	calculated
cat.	catalyst or catalytic
chloranil	tetrachloro- <i>p</i> -benzoquinone
conc.	concentrated
conv.	Conversion
cy	cyclohexyl
d	doublet or day(s)
DCE	dichloroethane
DCM	dichloromethane
DFT	density functional theory
DMAP	4-dimethylaminopyridine
DOSY	diffusion ordered spectroscopy
DMF	dimethylformamide
DMSO	dimethylsulfoxide
DPP	diphenyl phosphoric acid
dppf	1,1'-Bis(diphenylphosphino)ferrocene
d.r.	diastereomeric ratio
E	electrophile
E <sub>a</sub>	activation energy
ee	enantiomeric excess
EI	electron impact ionization
e.r.	enantiomeric ratio
equiv.	equivalents
Et	ethyl
<i>et al.</i>	<i>et alii/et aliae</i> – and others
ESI	electrospray ionization
GC	gas chromatography (gas chromatography coupled with mass detection)
h	hour(s)
H <sub>8</sub> -BINOL	5,5'.6,6',7,7',8,8'-octahydro-1,1'-2-naphtol
HOMO	highest occupied molecular orbital

## List of Abbreviations

---

HPLC	high performance liquid chromatography
HRMS	high resolution mass spectrometry
HX*	designating chiral Brønsted acids, e.g. chiral phosphoric acid diesters
<i>i</i>	iso
L	ligand
LUMO	lowest unoccupied molecular orbital
<i>m</i>	meta
m	multiplet
M	molar or metal
<i>m</i> CPBA	<i>meta</i> -chloroperbenzoic acid
Me	methyl
MS	mass spectrometry or molecular sieves
MTBE	methyl <i>tert</i> -butyl ether
MW	molecular weight
<i>n</i>	normal
NCS	N-chlorosuccinimide
NBS	N-bromosuccinimide
NMR	nuclear magnetic resonance (spectroscopy)
NOE	nuclear Overhauser effect
NuH/Nu	nucleophile
<i>o</i>	ortho
obs	observed
P	product
<i>p</i>	para
PAA	<i>p</i> -anisaldehyde
PG	protecting group
Py	pyridine
Ph	phenyl
PMA	phosphomolybdic acid
<i>Pr</i>	propyl
quant.	quantitative
quint	quintet
rac	racemic
r.t.	room temperature
S	substrate or selectivity factor
sat.	saturated
sol.	Solution
SOMO	singly occupied molecular orbital
SPINOL	1,1'-spirobiindane-7,7'-diol
STRIP	spiro-TRIP
<i>t</i>	<i>tert</i> , tertiary
t	triplet
T	temperature
TADDOL	$\alpha,\alpha',\alpha'$ -tetraaryl-1,3-dioxolan-4,5-dimethanol
TBCO	2,4,4,6-Tetrabromo-2,5-cyclohexadienone
Tf	trifluoromethylsulfonyl
THF	tetrahydrofuran
TLC	thin layer chromatography

## List of Abbreviations

---

TMP	2,2,6,6-tetramethyl piperidine
TMS	trimethylsilyl
TON	turnover number
TRIP	3,3'-bis(2,4,6-triisopropylphenyl)-1,1'-binaphthyl-2,2'-diyl-hydrogen phosphate
TsOH	<i>para</i> -toluene sulfonic acid
Tyr	tyrosine
VAPOL	2,2'-diphenyl-(4-biphenanthrol)

## Acknowledgements

*“Ah Mattia... remember to be curious!”*

Ben, November 2011 (after our very first meeting)

I am grateful to Prof. Dr. Benjamin List for giving me the opportunity to work and grow up as a chemist in the perfect research environment of the Max-Planck-Institut für Kohlenforschung. Being part of his group has been both an incredible experience and a great honor for me. I had the chance to experience some of the most exciting, challenging and forefront chemistry while surrounded by talented and brilliant chemists. I am indebted to Ben for being always supportive and motivating and for the trust and freedom given to me. I believe that the most important lesson I have learnt from him goes well beyond chemistry: to tackle difficult challenges both bravery and happiness are needed.

I would also like to extend my sincerest thanks to Prof. Dr. Albrecht Berkessel for accepting to review this thesis, to Prof. Dr. Axel Klein and Dr. Martin Klußmann for serving on my defence committee. I also thank Dr. Thomas James, Gabriele Pupo, Lisa Kötzner, Dr. Aurelian Tap and Dr. Sunggi Lee for kindly proofreading this work and for their valuable suggestions.

I am extremely thankful to those who have directly worked with me, being passionate and motivated towards our results, sharing both the successes and the difficult moments that we met during the investigations: Dr. Belen Poladura and Dr. Miriam Diaz for our productive collaboration on the aziridines ring opening and Dr. Sebastien Prévost for his contribution in the epoxides carboxylysis and thio-carboxylysis projects. For the analytical characterization of heterodimeric species, the assistance by Markus Leutzsch and Dr. Richard Goddard is gratefully acknowledged. It was truly a pleasure to collaborate with Dr. Daniele Fazzi from the Thiel group for the theoretical investigations.

I also owe my sincere gratitude to Prof. Dr. Nuno Maulide and to Dr. Martin Klußmann for leading various highly educative Ph.D. seminars and for being always available for additional discussions.

The technical support from our technician team has been very valuable during my studies. I would like to thank in particular Marianne Hannappel, Natascha Wippich, Hendrik

## Acknowledgements

---

van Thienen, Arno Döring, and Simone Marcus for providing me with valuable catalysts and for their routine assistance in the lab. I thank our GC, HPLC and mass departments for their assistance and prompt work. Adrienne Hermes, Alexandra Kaltsidis and Monika Lindner are also gratefully acknowledged for their administrative support.

I am indebted to my labmates Jiwoong Lee, Sebastien Prévost and Thomas James for their incredible support, for sharing their creativity and knowledge and for being always willing to discuss chemistry with me. I wish I could be a source of inspiration and help for someone as they have been for me during these four years.

I also would like to address special thanks to Jihye, Fabio, Tom, Seb, Gabri, Jiwoong, Fred, Marco, Desi, Dani, Anto, Aurélien, Alberto, Ilija, Nathalie, Tim, Manu, Vivi, Tere, Boommina, Olgi, Nohemy and Saul. They are my Mülheim family and the time spent inside and outside the lab with them has been simply unforgettable.

Finally, I would like to thank the closest people in my life for their constant encouragement and support: my parents Mario and Patrizia, my brother Maurizio and my “apple” Camilla. *Perché il vostro sostegno é la mia lanterna.*

### 1. Introduction

#### 1.1. Chirality

*“I call any geometrical figure, or group of points, chiral, and say that it has chirality if its image in a plane mirror, ideally realized, cannot be brought to coincide with itself”*

W. T. Kelvin, Robert Boyle Lecture, 1893

Chirality, as defined by Lord *Kelvin* in 1893,<sup>1</sup> is the geometrical property of any object which is not super-imposable upon its mirror-image. Molecules, if chiral, can occur in two chemically equivalent structures, termed enantiomers, which are specular to each other.<sup>2</sup> Early investigations in the 19<sup>th</sup> century by *Biot*<sup>3</sup> and *Pasteur*<sup>4</sup> pioneered the discovery of this concept, whereas the first rationalization about molecular chirality can be traced back to the theorizations on the tetravalency of carbon atoms by *van't Hoff*<sup>5</sup> and *LeBel*<sup>6</sup>. This three-dimensional property represents a prominent feature of life and its consequences are of unique importance in both material and natural sciences.

At the edge between biology and chemistry the “handedness” of enantiomers has enormous relevance. Besides rare exceptions, aminoacids, nucleotides, lipids and sugars are incorporated as single enantiomers in nature. Although the origins of this phenomenon are still debated,<sup>7</sup> it is widely accepted that the defined chirality of life’s building blocks effectively translates in the formation of enantiomerically pure natural macromolecules (i.e. enzymes and nucleic acids). As a consequence, biological systems are mostly homochiral and they dissimilarly interact with enantiomers of chiral compounds, thus resulting in different physiological responses. Flavours, odours and drug responses are strongly affected by such biomolecular recognition, which found its primordial postulation in *Fischer’s* “lock and key principle” (Figure 1.1).<sup>8,9</sup>

Arguably, one of the most important consequences of the handedness is found in the use of chiral compounds as medicinal agents, since the desired activity is usually displayed only by one of the enantiomers of chiral antibiotics and pharmaceutical drugs.<sup>10</sup> In the past years, the vast majority of synthetic drugs has been marketed as racemic mixture and the potential side effects of the undesired mirror-image compound have been considerably overlooked until late 1950’s, when the “thalidomide tragedy” landmarked a change of attitude.<sup>11</sup>



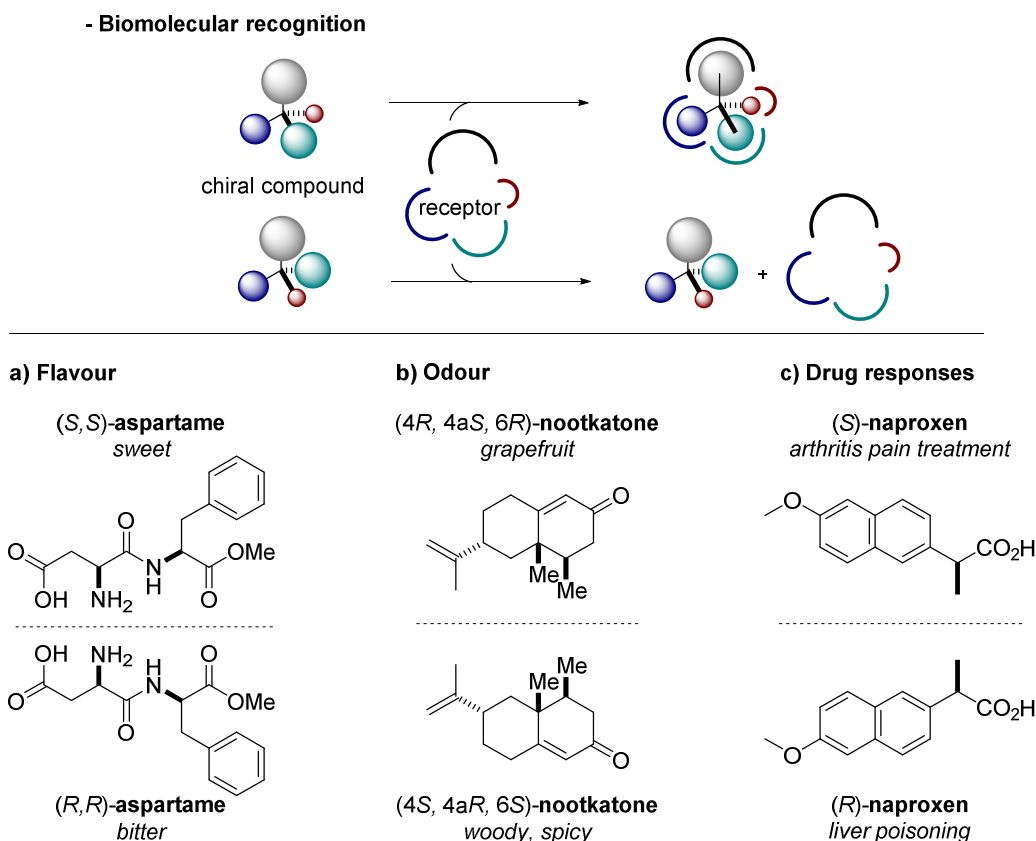


**Figure 1.1.** Biomolecular recognition and examples of bioactive chiral molecules.

Such sorrowful experience induced a significant switch of paradigm for drug regulation and more structured rules were introduced aiming towards the prevention of undesired effects by the “wrong” mirror-image compound.<sup>12</sup> Since then, most of the newly commercialized chiral medicinal compounds are single enantiomers and, very often, the previously marketed racemic drugs are reinvestigated in their enantiopure form.<sup>13</sup>

Nowadays, the demand for chiral compounds as single enantiomers is a primary issue for chemical industries and chemical synthesis is no longer limited to producing racemic mixtures that contain undesired stereoisomers. Traditional strategies rely either on the exploitation of enantiopure reagents, often derived from nature’s chiral pool, or on resolution techniques for racemic mixtures. However, the requirement for stoichiometric amounts of the chiral precursor for the former approach and the usual waste of the undesired second enantiomer for the latter, are generally identified as major drawbacks for these processes.<sup>14</sup> On the other hand, during the last decades, asymmetric catalysis has emerged as a complementary strategy with considerable advantages over the older techniques.<sup>15</sup> The possibility to use a chiral catalyst, ideally in sub-stoichiometric amounts,

for the synthesis of large quantities of a desired product is arguably the most elegant approach to chiral enantiopure compounds. The catalyst is regenerated during the course of the reaction and therefore can theoretically promote the transformation with high efficiency and minimal amount of waste.

## 1.2. Asymmetric catalysis

Either thermodynamically favored or disfavored, chemical transformations generally require activation energy to occur. A highly energetic transition state is formed along the reaction coordinate and eventually evolves in the formation of the products. Catalysis is the chemical phenomenon of the acceleration of the rate of a given transformation by means of an additional substance, which is not consumed and can be recycled. Interacting with the reagents, the catalyst allows the same reaction to occur *via* a different less-energetic pathway. In other words, the potential barrier of the overall process is reduced and the reaction rate is increased (Figure 1.2).<sup>16</sup>

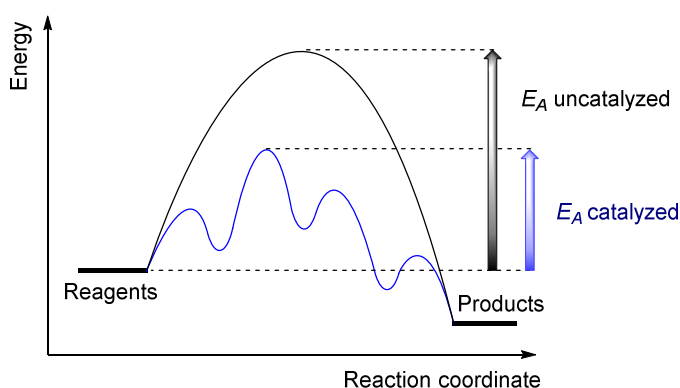
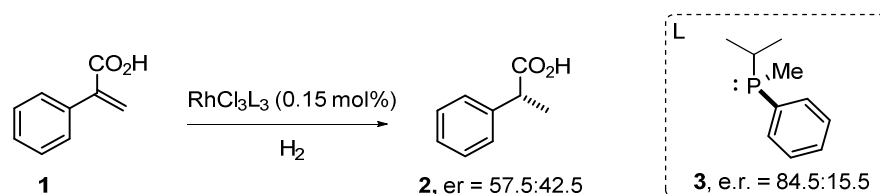


**Figure 1.2.** Generic energy diagram of a catalyzed- and a related non-catalyzed process.

If the catalyst is chiral (and enantiopure), stereogenic elements may be assembled in a selective fashion. Despite having the same absolute energy, the two mirror-image products are obtained through energetically non-equivalent reaction pathways: different activation energy is required due to the formation of diastereomeric transition states. This phenomenon accounts for a possible asymmetric induction and it is for this reason that the vast majority of bio-catalyzed transformations occur in an enantioselective fashion.

In analogy with the concept of biomolecular recognition, enantioselective enzyme catalysis has been long established; interestingly however, the potential of artificial enantiomerically pure catalysts was discovered more recently. Arguably, one of the most important breakthrough was represented by the investigations by *Knowles* at Monsanto Company in 1968. A modest, but significant selectivity was reported for the reduction of  $\alpha$ -phenylacrylic acid with hydrogen gas catalyzed by a rhodium complex with a scalemic phosphine ligand (Scheme 1.1).<sup>17a</sup>



**Scheme 1.1.** *Knowles'* pioneering achievement in asymmetric catalysis

*"...The inherent generality of this method offers almost unlimited opportunities for matching substrates with catalysts in a rational manner and we are hopeful that our current effort will result in real progress towards complete stereospecificity"*

W. S. Knowles, M. J. Sabacky, 1968

The efficacy of this approach was immediately recognized by the scientific community and very soon the first industrial application of a similar catalytic system was developed by Monsanto for the highly enantioselective synthesis of L-DOPA.<sup>17b</sup> In recognition of his milestone achievements, *Knowles* shared the Nobel prize in 2001 with *Noyori*, also for asymmetric hydrogenation reactions, and *Sharpless* for his studies on asymmetric oxidation reactions.<sup>18</sup>

Over the years, metal-based processes have dominated asymmetric catalysis with remarkable advances; however, shortly before the Nobel prize award, a new area emerged in this research field. In 2000, independent investigations by *List*<sup>19</sup> and *MacMillan*<sup>20</sup> introduced asymmetric organocatalysis as the "catalysis with small organic molecules, where an inorganic element is not part of the active principle".<sup>21</sup> The easy access to chiral organic catalysts, together with the remarkable stability and low toxicity exhibited with respect to chiral metal complexes, rendered this concept highly attractive to the scientific community. From its disclosure, organocatalysis has been increasingly investigated, finding wide

applications in synthetic chemistry on both academic and industrial scale. Complementing metal-catalysis and biocatalysis, organocatalysis is nowadays accepted as the third cornerstone for asymmetric synthesis.<sup>22</sup> Today, this research area seems to be unlimited and continuous explorations are focused on the development of different activation modes, the disclosure of novel transformations and the design and preparation of highly active and selective catalysts.

In the following chapters an overview of organocatalysis is presented, with special focus on Brønsted acid catalysis, followed by the discussion of the investigations conducted during these doctoral studies. In particular, this work has been aimed at the development and the codification of a novel activation mode for carboxylic acid substrates in asymmetric organocatalysis.

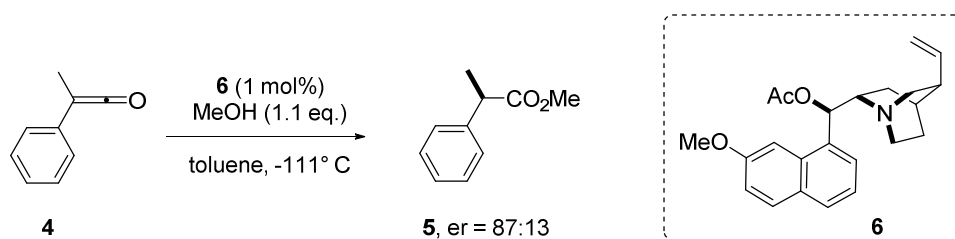
## 2. Background

### 2.1. Asymmetric organocatalysis

#### 2.1.1. Introduction and historical background

Nature has always been a source of inspiration for the mankind and the development of asymmetric catalysis is not an exception.<sup>23</sup> In biological systems, enzymes catalyze reactions with extraordinary activity and selectivity, thus allowing life-sustaining chemical processes. Such biocatalysts rely either on the activity of aminoacidic residues or on the role of cofactors and coenzymes, which are present in their active pockets.<sup>24</sup> Surprisingly, although non-metallic proteins are about half of the known biocatalysts, chemists have rarely investigated the possibility to mimic their catalytic principles until recently. As a consequence the development of asymmetric organocatalysis has lagged significantly behind that of enantioselective metal-based catalysis and, before the year 2000, consisted only in a small collection of poorly understood transformations.<sup>25</sup>

The possibility to promote chemical reactions by means of simple organic molecules may be traced back to more than hundred years ago to the pioneering findings by *von Liebig*<sup>26</sup> and *Bredig*<sup>27</sup>. However, the first significant example of chirality transfer was only observed in 1960 by *Precejus* in an asymmetric addition of methanol to ketenes catalyzed by a quinine-derived catalyst (Scheme 2.1).<sup>28</sup>

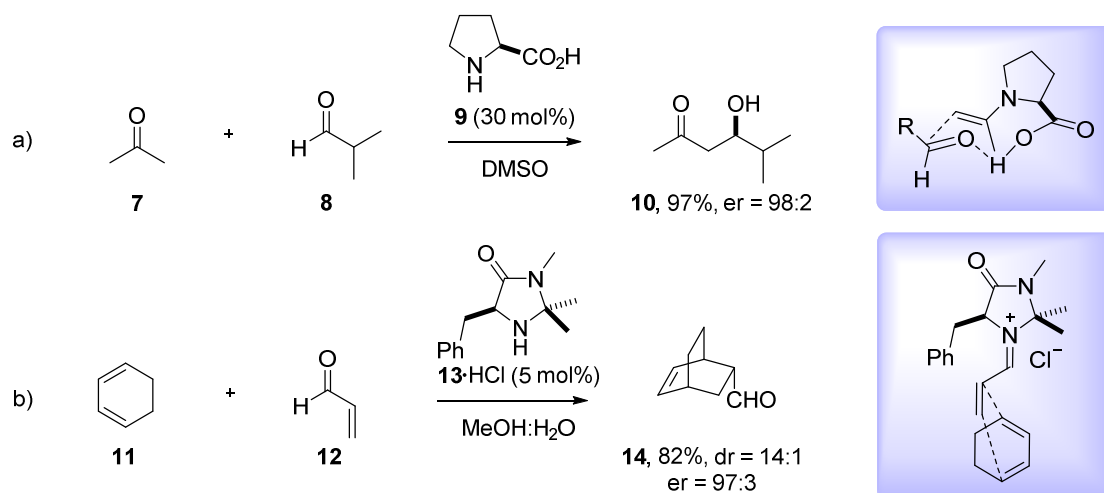


**Scheme 2.1.** *Precejus'* pioneering achievement in asymmetric organocatalysis

Other isolated examples appeared later, such as the *Julia-Colonna* epoxidation and the enantioselective approach to the *Wieland-Mischer* ketone independently described by *Hajos* and *Parrish* and by *Eder*, *Sauer* and *Wiechert*.<sup>29</sup> Nevertheless, the lack of a mechanistic rationalization hampered a general recognition of this type of asymmetric catalysis.

## 2. Background

It was with the ground breaking works by *List* and *MacMillan* that the generality and the potential of the concept were realized and the field of asymmetric organocatalysis entered its modern era. Two complementary activation modes for carbonyl compounds by means of secondary amine catalysts were disclosed. *List* reported the enantioselective aldol reaction of acetone with aldehydes catalyzed by the aminoacid proline (Scheme 2.2.a).<sup>19</sup> Slightly later the same year, *MacMillan* reported that chiral imidazolidinone catalysts can promote the asymmetric *Diels-Alder* reaction between enals and dienes (Scheme 2.2.b).<sup>20</sup> Importantly, a detailed mechanistic rationalization supported the understanding of the catalytic principles of both transformations. It is evident that the activation of the substrates occurs in a chiral environment and the highly organized transition states allow the transfer of the stereochemical information held in the structure of the chiral catalyst.



**Scheme 2.2.** *List's* (equation a) and *MacMillan's* (equation b) seminal works

These two reports triggered the development of the new research field, which has rapidly grown during the subsequent years. Impressively, the number of reported organocatalytic reactions has increased exponentially and, to date, over ten thousands scientific contributions have appeared demonstrating an exceptional interest both from the academic and the industrial chemical community.<sup>30</sup> Currently, organocatalysis is among the most intensively investigated areas of organic chemistry and it is widely accepted as one of the main branches of enantioselective synthesis.<sup>31</sup>

### 2.1.2. Activation modes and establishment of modern organocatalysis

The success of organocatalysis relies on the introduction and the detailed codification of various activation modes. Organic catalysts significantly affect the reactivity profile of basic functional groups through the formation of covalent adducts or the establishment of non-covalent interactions (hydrogen bonding or ion pairing). The frontier molecular orbitals of the reacting species are influenced by these associations and, when the activation occurs in a chiral microenvironment, enantioselective catalysis may take place.<sup>32</sup> Simple moieties (aldehydes, ketones, imines, etc...) assemble with chiral catalysts in a highly defined manner thus facilitating a predictive understanding of the reactions.<sup>33</sup> Today, a platform of different asymmetric catalytic modes is available and constitutes a useful and powerful tool for organic synthetic chemists.

A key example can be found in the activation of carbonyl compounds and related substrates. A variety of asymmetric strategies have been reported and, therefore, the organocatalytic exploitation of these functional groups is well-established (Figure 2.1).

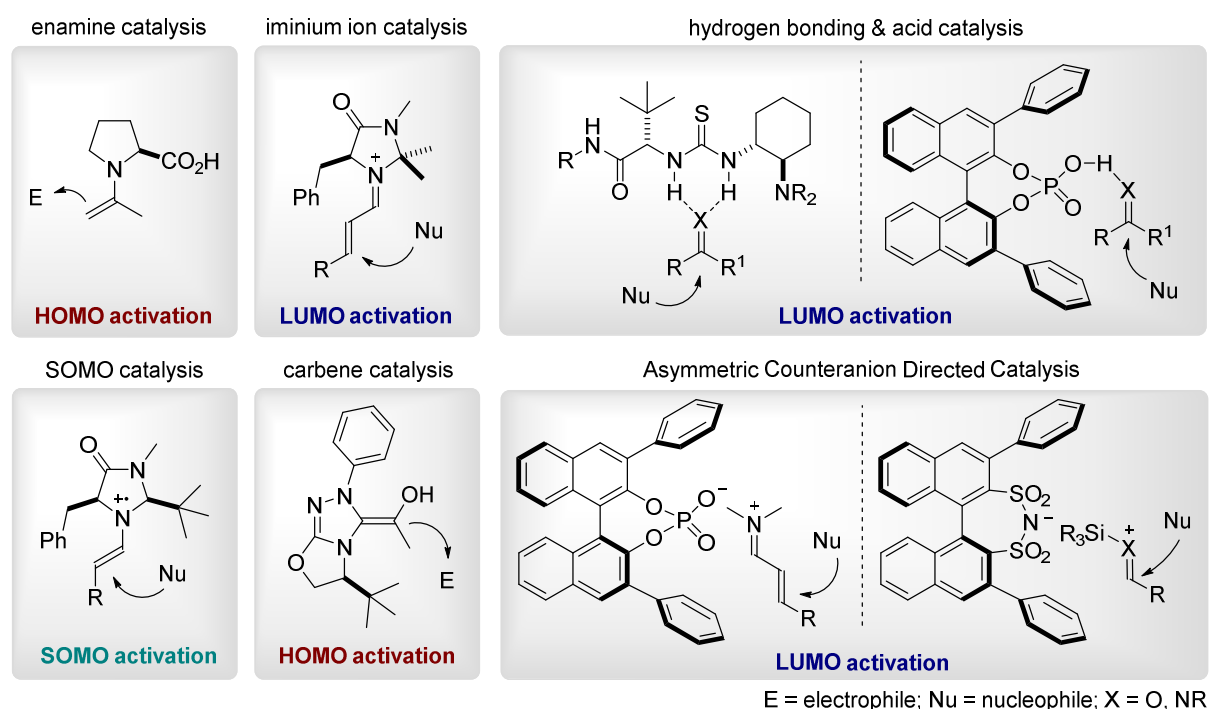


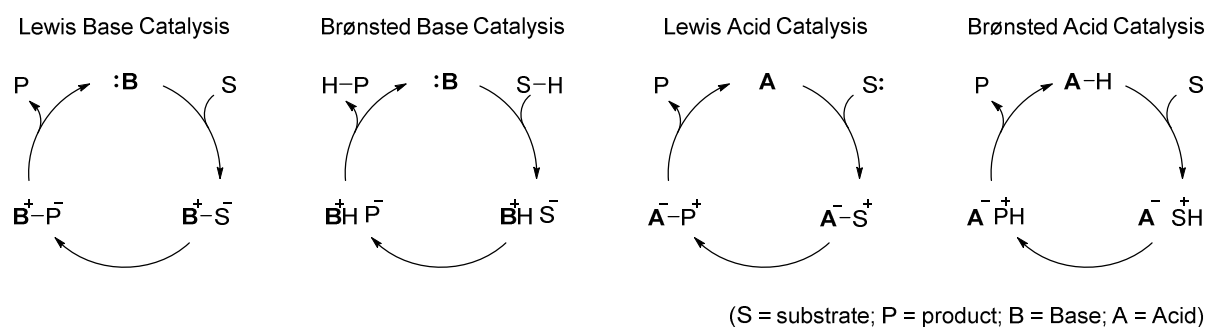
**Figure 2.1.** Selected organocatalytic modes for carbonyl compounds and related substrates.

As introduced in the previous paragraph, aminocatalysis can be useful both for nucleophilic and electrophilic activation. The  $\alpha$ -functionalization can be obtained through enamine catalysis: these species have a higher-lying HOMO (highest occupied molecular orbital) than

the corresponding enols, resulting in being more reactive towards electrophilic reaction partners.<sup>19,34</sup> On the other hand, iminium ion intermediates exhibit a low-lying LUMO (lowest unoccupied molecular orbital), thus being more available for incoming nucleophiles compared to the parent carbonyl substrate.<sup>20,35</sup> In addition, the SOMO (singly occupied molecular orbital) activation can be unlocked by oxidation of enamine intermediates to radical cations, complementing enamine catalysis for the  $\alpha$ -functionalization of aldehydes and ketones.<sup>36</sup> Catalysis by carbenes can be exploited for nucleophilic reactions of aldehydes, due to the formation of chiral Breslow intermediates,<sup>37</sup> while LUMO lowering activations are also successfully realized through hydrogen bonding or acid catalysis.<sup>38,39</sup> Finally, a recent asymmetric approach to electrophilic activation is represented by Asymmetric Counteranion Directed Catalysis (ACDC). This mode of catalysis exploits the formation of achiral cationic reactive intermediates (*i.e.* iminium ions, oxonium ions) in a coulombic ion pairing interaction with the chiral anion derived from the catalyst.<sup>40</sup>

However, despite the broad success of the already investigated catalytic modes, many functional groups are not yet amenable to asymmetric organocatalysis. The introduction of novel activation strategies provides valuable alternatives in synthetic chemistry, especially for the enantioselective transformations of such elusive substrates.

Aiming to an organization of the various activation modes and considering the huge number of reported organocatalytic transformations, *Seayad* and *List* have suggested a classification based on the role of the organic catalyst.<sup>41</sup> Although any reaction exhibits peculiar mechanistic features, four distinct classes can be identified: Lewis base catalysis, Brønsted base catalysis, Lewis acid catalysis and Brønsted acid catalysis (Scheme 2.3).



**Scheme 2.3.** Classification of organocatalytic transformations based on the role of the organic catalyst.



## 2. Background

Lewis base catalysis, in which the catalyst promotes the reaction donating one (or more) electrons to the substrate, encompasses the majority of the reported transformations and both enamine and iminium ion catalysis, together with SOMO catalysis and carbene catalysis, operate through this type of mechanism.

However, although this classification may appear rigid, it is worth to mention that several reactions simultaneously exploit multiple activation modes, possibly lying at the edges between two different mechanisms. Many organocatalysts have been proposed to play a bifunctional role, when the primary activation is assisted by a secondary interaction that tunes the reactivity of the reaction partner. Perhaps, one of the clearest examples of this phenomenon is represented by the above-mentioned proline-catalyzed aldol reaction. The enamine activation of acetone is assisted by the Brønsted acid activation of the aldehyde thus facilitating the transformation (Figure 2.1).<sup>42</sup>

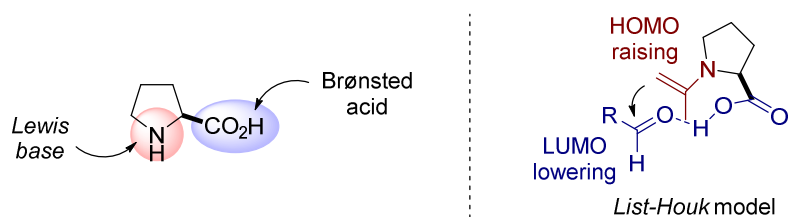


**Figure 2.1.** Proline as bifunctional catalyst: the List-Houk model for the asymmetric aldol reaction.

## 2.2. Asymmetric Brønsted acid catalysis

The Brønsted-Lowry acid-base theory was independently introduced in 1923 by the two physical chemists aiming at the correction of the previously accepted paradigm, which had been postulated by *Arrhenius*.<sup>43</sup> Their concept is based on the understanding that acidity and basicity are not absolute properties, but are better described as the relative features of two species when in interaction with each other. Accordingly, acids are defined as species capable of proton donation to bases, which are proton acceptors. The field of Brønsted acid catalysis is essentially based on this definition, since the activation of the substrates is realized *via* a preliminary acid-base equilibrium: the acidic catalyst donates a proton to the substrate which acts as a base.

A strict affinity can be imagined with enantioselective Lewis acid catalysis, which combines metals or metalloid central atoms with chiral ligands. From this point of view, hydrogen can be imagined as the smallest centered element and the backbone of an organic catalyst may be the effective source of stereoselectivity (Figure 2.2).<sup>39a</sup>

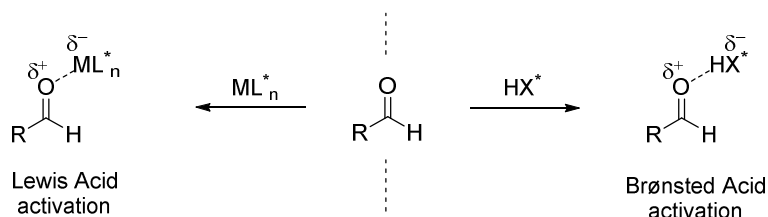
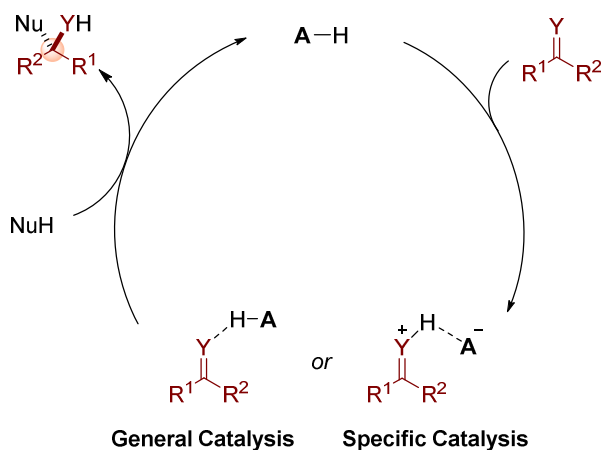


**Figure 2.2.** Lewis acid activation and Brønsted acid activation.

Asymmetric catalysis by Brønsted acids may be mechanistically divided into two different classes: general catalysis and specific catalysis.<sup>44</sup> The former type of catalysis is promoted by catalysts which are not truly capable of donating protons and activates substrates *via* hydrogen bonding coordination. The latter activation relies instead on the real protonation of substrates and a more pronounced ion pair character is exhibited (Scheme 2.4). Obviously, in both cases the Lewis acidity of the substrate is increased and the LUMO is lowered, thus being activated towards nucleophiles. The distinction between these two mechanisms is subtle and it is based on the inherent acidity difference between the catalyst and the conjugated acid of the substrate. Nevertheless, in the majority of cases it is not possible to draw the line, a classification into hydrogen bonding catalysts and acid catalysts, which are relatively prone to protonation, is commonly accepted.

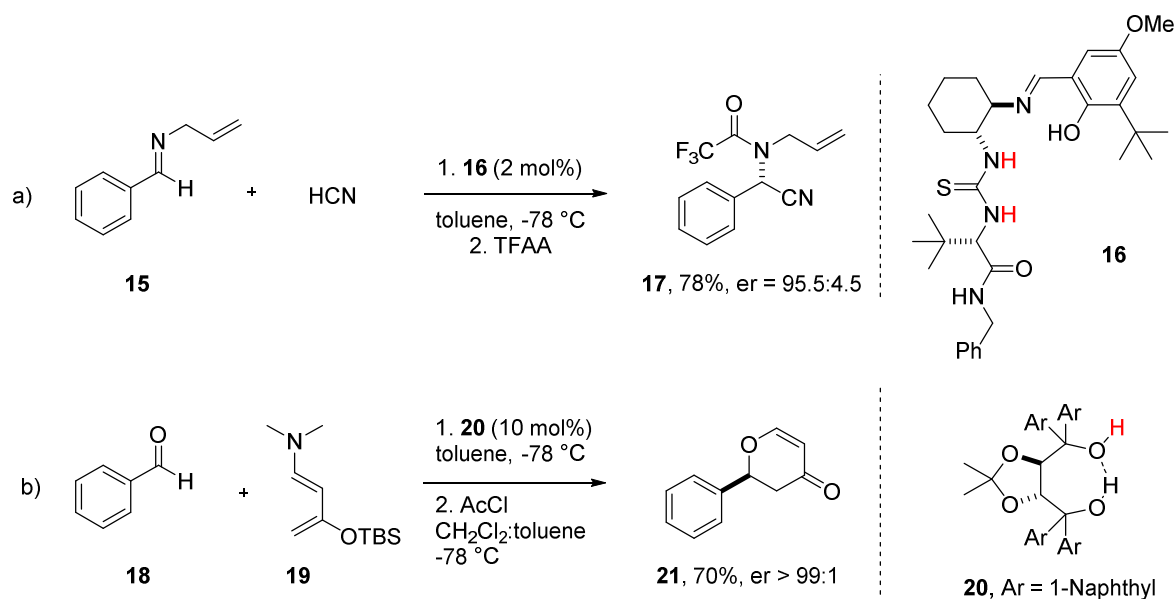


**Scheme 2.4.** General Brønsted acid catalysis and specific Brønsted acid catalysis

### 2.2.1. General Brønsted acid catalysis: hydrogen bonding catalysts

It is widely accepted that many enzymes exploit hydrogen bonding networks to facilitate their catalyzed transformations. Perhaps, one of the most noteworthy examples is represented by the importance of the “oxyanion hole” in the mechanism of the *serine proteases*. In the catalytic pocket, the amide substrate is coordinated to two N-H hydrogen bond donors, thus being more reactive for the incoming nucleophilic attack.<sup>45</sup> After the advent of modern organocatalysis, chemists have successfully mimicked this natural activation strategy and intensively explored artificial chiral hydrogen bonding catalysts.

The first catalytic system for enantioselective transformations was serendipitously discovered by the *Jacobsen* group. Catalyzed by chiral thiourea **16**, which had been initially designed as ligand for metal catalysis, a highly enantioselective *Strecker* reaction between allyl-imines and hydrogen cyanide was reported (Scheme 2.5.a).<sup>46</sup> Few years later, chiral diols were also identified as effective catalysts by the *Rawal* group. An enantioselective hetero *Diels-Alder* reaction between aldehydes and activated dienes was reported to be promoted by TADDOL **20** (Scheme 2.5.b).<sup>47</sup>



**Scheme 2.5.** (a) *Strecker* reaction catalyzed by a chiral thiourea and (b) hetero *Diels-Alder* reaction catalyzed by a chiral TADDOL.

Interestingly, these catalysts operate *via* different binding systems. Thiourea catalysts promote transformations through a dual hydrogen bonding interaction, which may either activates electrophiles or act as binding site for anion nucleophiles. Conversely, it is accepted that the more flexible TADDOL acts as a single hydrogen donor. The intramolecular hydrogen bonding network increases the acidity of the alcohol moiety in a phenomenon which has been termed by *Yamamoto* “Brønsted acid assisted Brønsted acid catalysis”.<sup>48</sup>

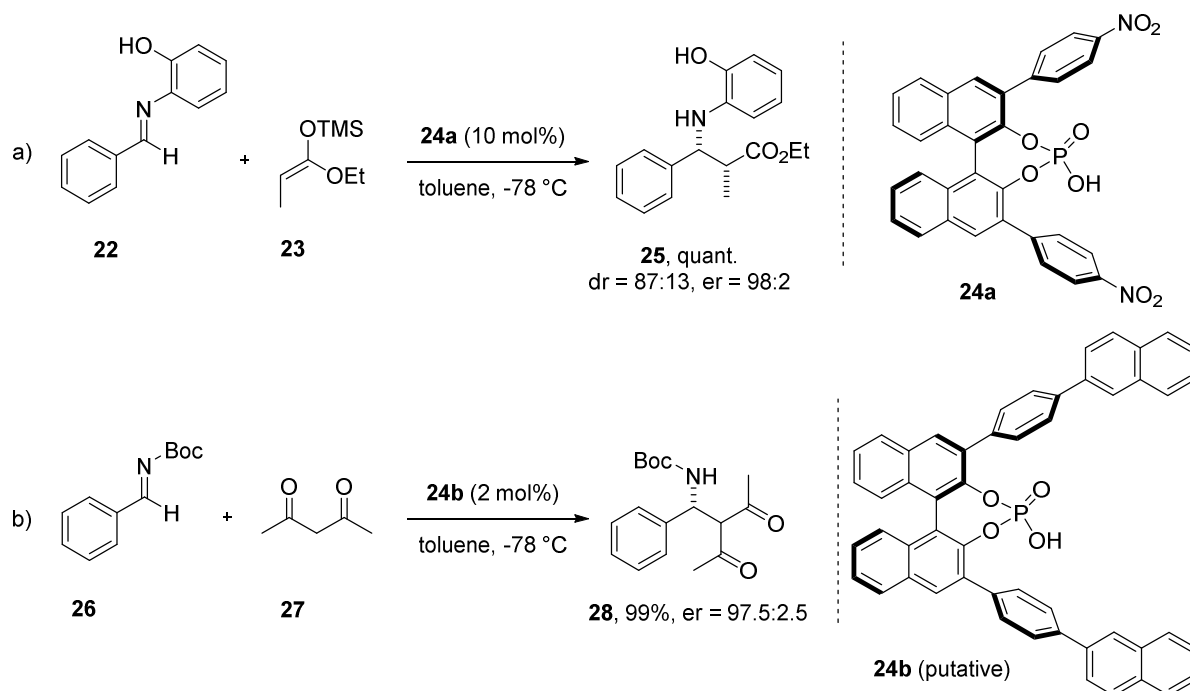
Today TADDOLs and thioureas, together with chiral ureas, squaramides, BINOLs and many other scaffolds, are intensively investigated and hydrogen bonding catalysis is among the most explored fields in organocatalysis.<sup>38</sup>

### 2.2.2. Specific Brønsted acid catalysis: acid catalysts

Catalysis by strong Brønsted acids has long been used in synthetic chemistry. The effect of mineral acids on the rate of certain organic reactions has been known to chemists since many centuries. In contrast, the exploration of this type of catalysis for asymmetric reactions only started in 2004. Seminal works by *Akiyama* and *Terada* proposed the use of chiral organic acids for the electrophilic activation of imines. The two research groups simultaneously introduced axially chiral BINOL-derived phosphoric acid diesters to promote

## 2. Background

highly stereoselective *Mannich* reactions. *Akiyama* and coworkers reported the addition of silyl ketene acetals to aromatic imines catalyzed by phosphoric acid **24a** (Scheme 2.6.a),<sup>49</sup> while a similar acid catalyst **24b**, bearing a different substitution pattern at the 3-3' position of the binaphthyl backbone, was introduced by the *Terada* group for the addition of  $\beta$ -diketones to Boc-protected imines (Scheme 2.6.b).<sup>50a</sup>



**Scheme 2.6.** (a) *Akiyama's* enantioselective *Mannich* reaction catalyzed by phosphoric acid **24a** and (b) *Terada's* enantioselective *Mannich* reaction catalyzed by putative phosphoric acid **24b**.

In 2010, reinvestigating the reaction by the *Terada* group, *Ishihara* and coworkers suggested that the actual catalyst was not the phosphoric acid, but the corresponding calcium salt formed as an impurity during the purification by silica gel chromatography.<sup>50b</sup> Despite this finding, these two Japanese groups share the prestige of the discovery of the potential of acid catalysis. After the disclosure of this concept the scientific community was extremely inspired and the design and tuning of novel catalysts has evolved with remarkable progress.<sup>39</sup>

### Acid catalysts for asymmetric catalysis

Due to the possible structure modulation, chiral phosphoric acid derivatives are the most exploited acid catalysts to date. A fine tuning of the electronic and steric properties can be achieved, thus facilitating the optimization of the catalytic performances for a large number of reactions (Figure 2.3).

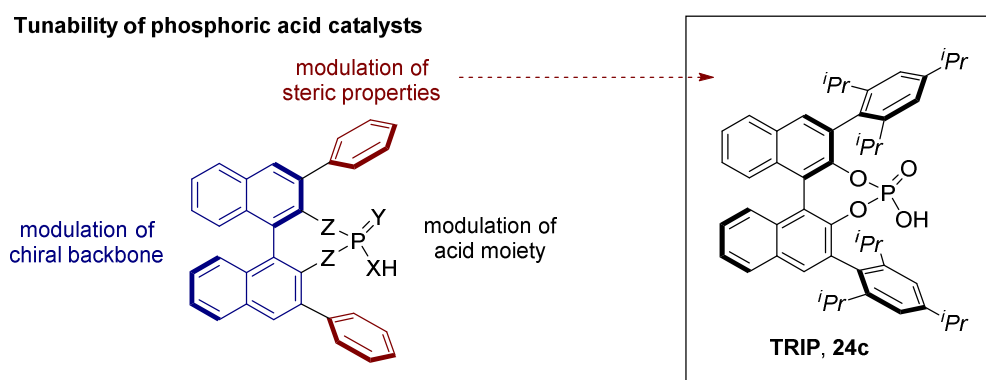


**Figure 2.3.** Modulation of phosphoric acid diesters and **TRIP (24c)**, one of the most used organocatalysts.

Introduced in 2004, BINOL-derived axially chiral phosphoric acid catalysts have been intensively investigated.<sup>51</sup> Their success relies on two main aspects: the availability of chiral enantioenriched binaphthol and the possibility to easily access a library of relatively different catalysts. Chiral binaphthyl derivatives have been introduced in asymmetric catalysis by *Noyori* and several diverse functionalizations have appeared over the years.<sup>52</sup> For example, a late stage cross coupling reaction at the 3-3' position allows the synthesis of phosphoric acids with variously substituted binaphthyl moieties. Such modulation may significantly affect the structure of the catalytic pocket, hence influencing the catalytic properties. Limiting the number of possible less-selective isomeric transition states and increasing the steric hindrance of the catalyst active site often translates into higher selectivity. Despite not being a general phenomenon, this empirical rule is generally helpful for the design of novel catalysts. Introduced by the *List* group in 2006, **TRIP 24c** represents one of the most popular organic catalyst and, bearing a bulky 2,4,6-triisopropyl phenyl substituent, it is a noteworthy example of this concept (Figure 2.3).<sup>53</sup>

The modification of the chiral backbone may also be particularly useful and has been thoroughly investigated. Next to the axially chiral binaphthyl-moiety, other stereogenic units

have been explored with the introduction of several other classes of catalysts.<sup>54</sup> Phosphoric acid **29**, bearing a hydrogenated H<sub>8</sub>-BINOL motif, was reported by the *Gong* group,<sup>54a</sup> while the first application of a VAPOL-derived phosphoric acid (**30**) in asymmetric catalysis was presented by *Antilla* and coworkers.<sup>54b</sup>

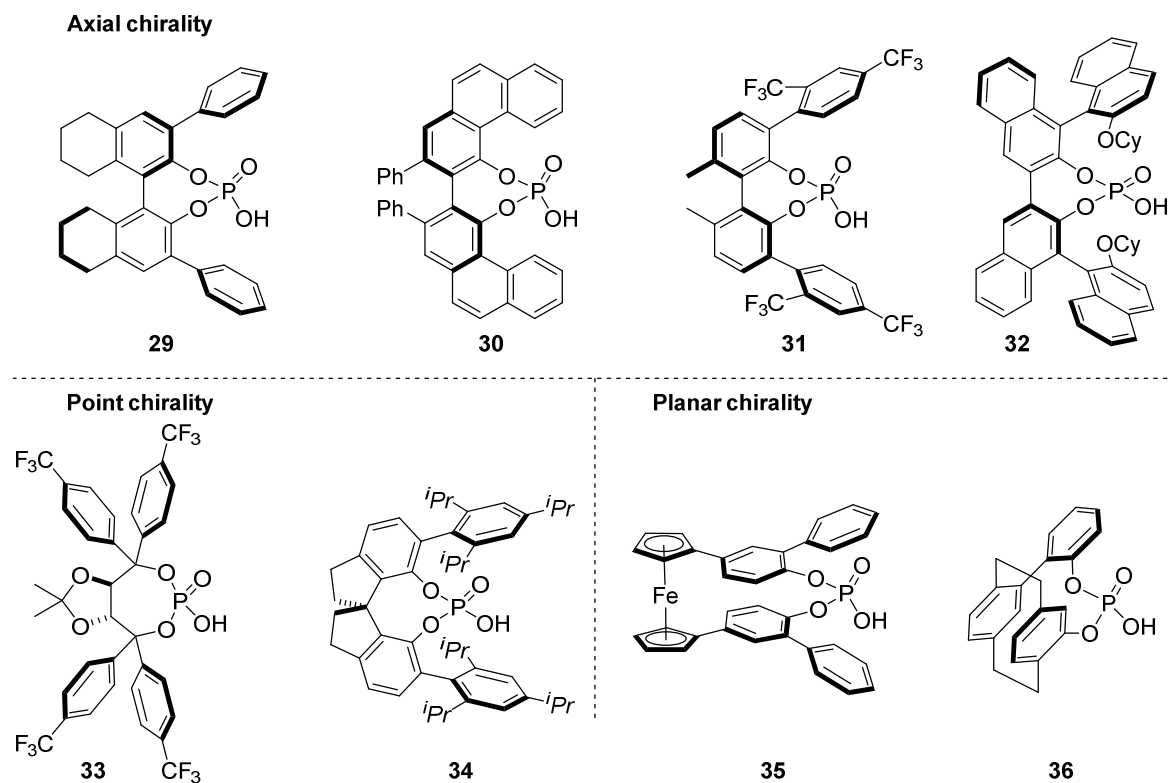


**Figure 2.4.** Alternative backbones for phosphoric acid catalysts.

A chiral biphenol backbone has also been developed by the *Akiyama* group (**31**), while the double axially chiral phosphoric acid **32** was identified by *Du* as the optimal catalyst for an asymmetric reduction of quinolines.<sup>54c,d</sup> Point and planar chiral scaffolds have also been explored and the corresponding catalysts were reported to exhibit significantly different performance profiles. In 2005 *Akiyama* developed the TADDOL-derived catalyst **33** for certain *Mukaiyama-Mannich* reactions,<sup>54e</sup> while in 2010 a novel class of chiral phosphoric acids bearing a SPINOL backbone was introduced independently by the *List* group and by *Liu, Wang* and coworkers. **STRIP 34** was used for an efficient kinetic resolution of alcohols *via* transacetalization, while a related 1-naphthyl substituted catalyst was developed for a *Friedel-Crafts* reaction.<sup>54f,g</sup> Catalysts **35** and **36**, with planar chiral backbones have recently been introduced by the groups of *Enders* and *Marinetti*, however only preliminary explorations have been reported to date.<sup>54h,j</sup>

Since the acidity of catalysts often translates into their catalytic performances, the tuning of the acid moiety is largely investigated and it is of primary interest for synthetic purposes. The possibility to reduce the catalyst loading is always an ambitious target and, in addition, the desired reactivity is often unlocked only by adjusting the features of the active site.

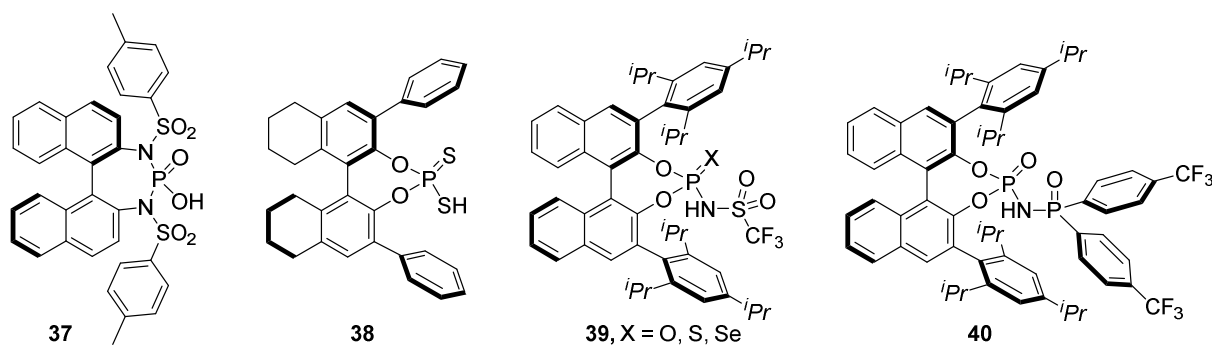


**Figure 2.5.** Overview of modifications to the phosphoric acid moiety.

A phosphoric acid diamide catalyst **37** was reported by *Terada*, however, despite the introduction of a novel tunable site, limited success has been reported so far.<sup>55a</sup> Dithiophosphoric acids **38** were first introduced by the *Blanchet* group and later employed by *Toste* and coworkers for a highly enantioselective hydroamination of allenes.<sup>55b,c</sup> An important development was represented by the introduction of N-triflyl phosphoramidates **39** by *Yamamoto* in 2006. This class of catalyst have found several applications in organocatalysis, presumably due to their remarkable acidity, and also thio- and seleno-derivatives have been developed.<sup>53d,e</sup> N-phosphinyl phosphoramidate catalysts **40** have been recently reported by *List* and coworkers for an enantioselective N,O-acetalization reaction.<sup>55f</sup>

Beyond phosphoric acid derivatives, different moieties have appeared, complementing the field of acid catalysis.<sup>56</sup> In 2007, BINOL-derived dicarboxylic acids **41** have been reported by the *Maruoka* group,<sup>56a</sup> while highly acidic axially chiral disulfonic acids **42** were initially introduced in 2008 by the *List* group and later utilized by *Ishihara* and coworkers, who investigated their pyridinium salts in enantioselective catalysis.<sup>56b,c</sup> Recently, *List* and coworkers reported the synthesis of chiral disulfonimide catalysts **43** for their applications as precatalysts in Lewis acid organocatalysis. Interestingly, this class of catalyst also found applications as strong Brønsted acid catalysts, as witnessed by an elegant and



## 2. Background

straightforward approach to the enantioselective synthesis of estrone using an asymmetric *Torgov* cyclization as the key step.<sup>56d,e</sup> Very recently, the challenging stereocontrol of the reactions of small and structurally unbiased substrates prompted the *List* group to develop confined catalysts. For this reason, dimeric imidodiphosphoric acids **44** were designed and successfully utilized in acid catalyzed asymmetric acetalization and spiro-acetalization reactions, as well as in an elegant, highly selective sulfoxidation of thioethers.<sup>56f-h</sup>

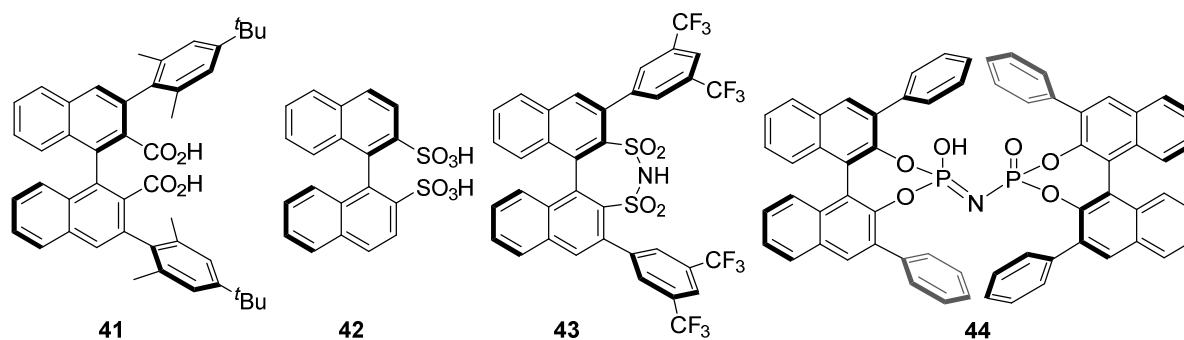


**Figure 2.6.** Overview of non-phosphoric acid chiral catalysts.

In parallel to the use of chiral acid organocatalysts, a different approach to acid catalysis is represented by the combination of a strong achiral acid and a chiral base.<sup>57</sup> Depending on the pK<sub>a</sub> of the conjugated acid of the basic compound, this approach delivers moderately to strong acidic species. In other words, the chiral base operates as a proton shuttle, attenuating the overall reactivity thus allowing enantioselective catalysis. Two remarkable examples are the catalytic systems developed by *Johnston* and *Jacobsen* (Figure 2.7).

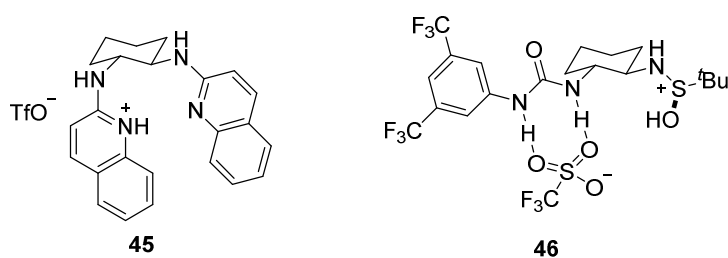


**Figure 2.7.** Combination of strong achiral acids with chiral bases.

The *Johnston* group developed chiral bisamidinium sulfonate catalyst **45** in 2004 and explored its activity over the years with multiple applications.<sup>57a</sup> The *Jacobsen* group designed a combination of a chiral urea-sulfoxide catalyst and sulfonic acids (**46**) and applied

this system to an asymmetric *Povarov* reaction between N-aryl imines and electron-rich alkenes.<sup>57b</sup>

Clearly, the overview presented in this paragraph is not aimed at a comprehensive review of the field of Brønsted acid catalysis, but to broadly outline this intensively explored subject. The interest of the scientific community towards asymmetric acid catalysis is always growing and presumably any present description of this field is destined to be soon outdated. The concepts sketched here are continuously applied to new transformations and, additionally, a considerable interest is given to the broadening of the activation principles to previously unexplored compounds. One class of substrates, which has been elusive to asymmetric organocatalysis is represented by carboxylic acids.

### 2.3. Carboxylic acids

The carboxylic acid moiety is among the most common functionalities in organic molecules, and it is abundantly incorporated in natural compounds.<sup>58</sup> All aminoacids, lactic acid, mandelic acid and pyruvic acid, to name just a few, bear witness to the ubiquity of these substances among the molecules of life. Furthermore, carboxylic acid intermediates are considered linchpin raw materials for synthetic purposes as they are significantly stable compounds, easy to store and to handle and preparatively accessible by a variety of established routes.<sup>59</sup> Presumably due to all these aspects, they are commercially available in a wide structural variety.

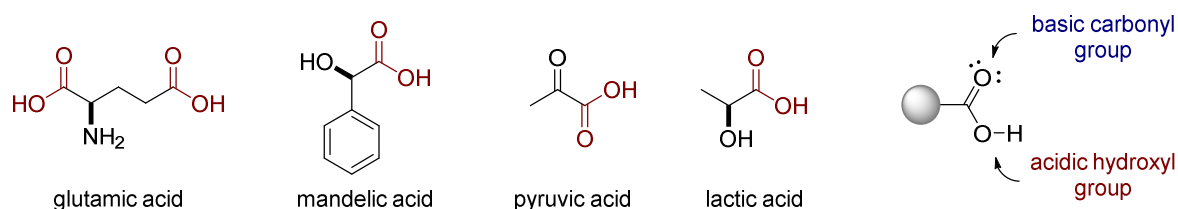


**Figure 2.8.** Naturally occurring carboxylic acids and dichotomous polarity of the moiety.

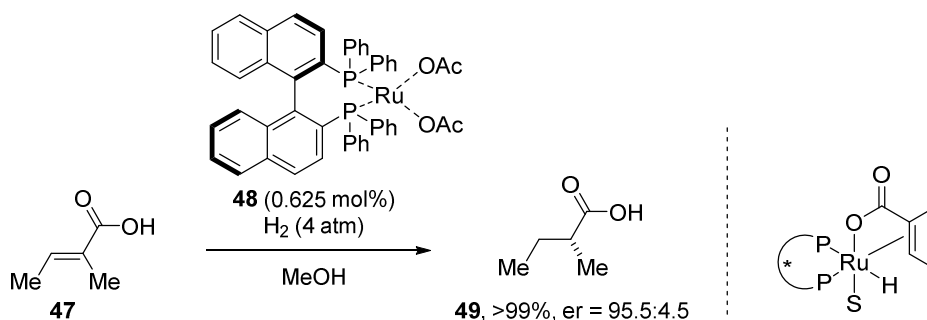
The normal reactivity of this functional group is based on its peculiar dichotomous structure. In fact, two geminal oxygen atoms characterize the carboxylic moiety: the basic carbonyl moiety and the acidic hydroxyl group (Figure 2.8). Under basic conditions a deprotonation reaction delivers a reactive carboxylate anion which can be exploited for nucleophilic reactions. On the other hand, under acidic conditions the electrophilicity of the carbonyl group is enhanced and addition-elimination reactions may occur resulting in the substitution of the hydroxyl moiety with various nucleophiles. In addition, powerful routes towards  $\alpha$ -functionalization reactions and decarboxylative transformations have been established.<sup>60</sup>

Despite the importance of these compounds as versatile synthetic intermediates, the development of catalytic transformations is still rather limited. As a matter of fact, the conversion into carboxylic acid derivatives is usually required for their exploitation under catalytic conditions, while the possibility to avoid the additional derivatization step is often a desired, yet challenging, target.<sup>61</sup> In recent years, various investigations in non-symmetric metal-catalysis have actually made possible the direct use of carboxylic acid substrates,

however this exploitation has been generally elusive in enantioselective transformations (*vide infra*).

### Metal-based asymmetric catalysis with carboxylic acid substrates

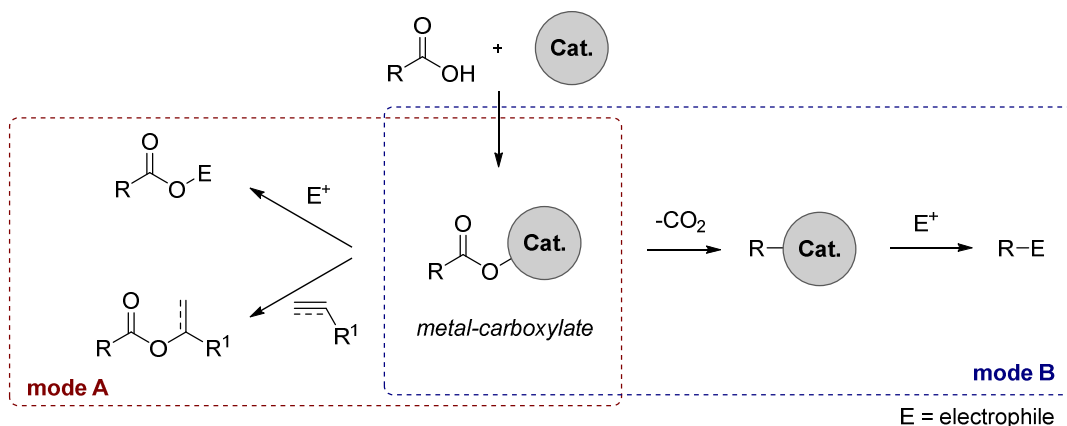
Interestingly, carboxylic acids were investigated at the very onset of metal-based asymmetric catalysis. The first asymmetric hydrogenation reaction disclosed by *Knowles* at Monsanto<sup>17a</sup> was later followed by several reports in which the catalytic system was modified, thus allowing high enantioselectivity. For example, *Noyori* reported the asymmetric reduction of  $\alpha,\beta$ - and  $\beta,\gamma$ -unsaturated carboxylic acids catalyzed by a ruthenium complex with a chiral BINAP ligand (Scheme 2.7).<sup>62</sup> This transformation proceeds *via* the formation of a metal-carboxylate intermediate, which facilitates the coordination of the olefin moiety and allows the following asymmetric hydrogenation reaction. A formal activation of the carboxylic acid moiety is not realized in this type of transformation, but the functional group effectively serves as directing group.



**Scheme 2.7.** Carboxylic acid as directing group in *Noyori's* hydrogenation reaction

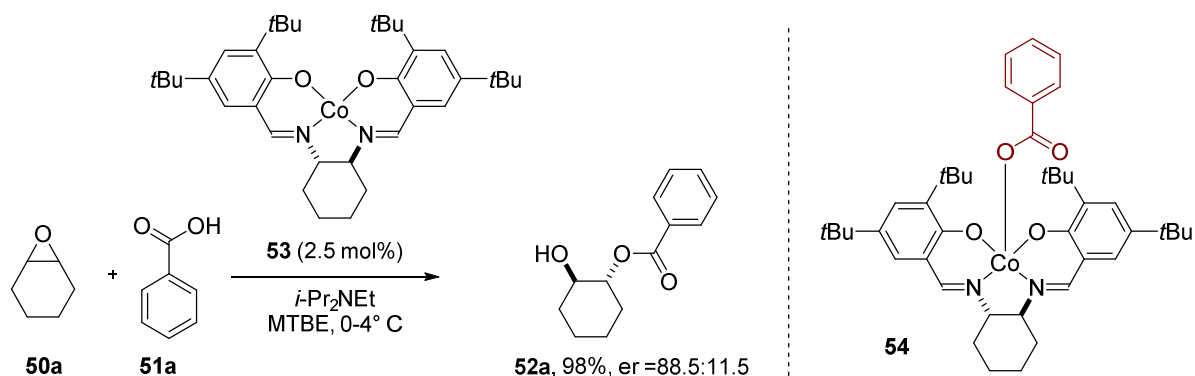
On the other hand, the formation of metal-carboxylates can also result in a direct activation and two main approaches have been proposed: the exploitation of the nucleophilicity of the organometallic intermediate towards activated electrophiles (mode A, Scheme 2.8) or a decarboxylative strategy for addition reactions (mode B, Scheme 2.8).<sup>61a</sup> Importantly, the first type of transformation involves a C-O bond formation giving ester products, while the second approach, after the extrusion of carbon dioxide, provides a C-C bond formation.

## 2. Background



**Scheme 2.8.** Direct activation of carboxylic acids *via* metal-carboxylate.

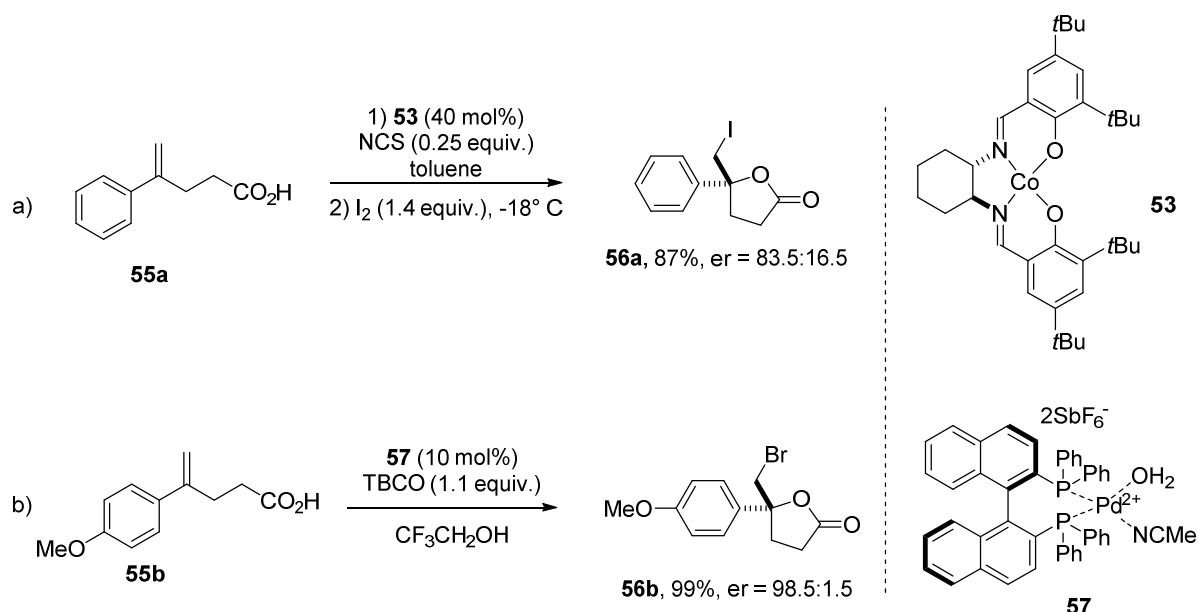
In 1997, the *Jacobsen* group reported an elegant approach to the desymmetrization of *meso*-epoxides with benzoic acid catalyzed by cobalt-SALEN complex **53** (Scheme 2.9).<sup>63</sup> Similarly to the later developed hydrolytic kinetic resolution of racemic epoxides (*vide infra*), the transformation exploits a double activation strategy. Catalyzed by an *in-situ* formed Co(III) species, the reaction involves the activation of benzoic acid as metal carboxylate (intermediate **54**) and the concurrent Lewis acid activation of the epoxide substrate by a second catalyst molecule.<sup>64</sup>



**Scheme 2.9.** Metal-mediated desymmetrization of *meso*-epoxides with benzoic acid.

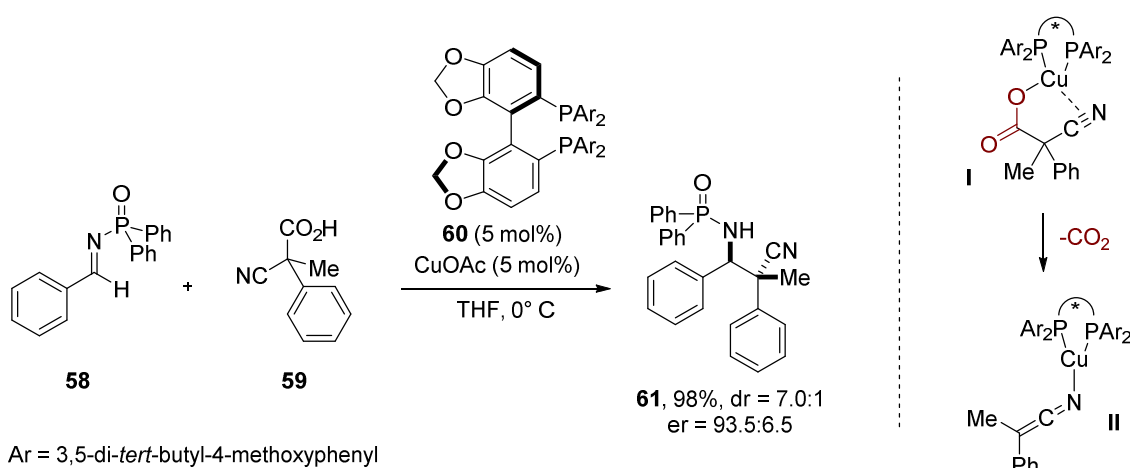
A similar strategy for the asymmetric halolactonization of alkenoic acids has also been explored. The *Gao* group reported an intramolecular iodocyclization reaction catalyzed by the same Co-catalyst **53** (Scheme 2.10.a),<sup>65</sup> while palladium-BINAP complex **57** was developed by the *Kim* group for a related bromolactonization strategy (Scheme 2.10.b).<sup>66</sup>

## 2. Background



**Scheme 2.10.** Metal-catalyzed enantioselective intramolecular iodolactonization.

Despite being less investigated, decarboxylative reactions of carboxylic acids are also amenable to asymmetric catalysis. A remarkable example is represented by the asymmetric *Mannich*-type reaction with racemic cyanocarboxylic acids recently disclosed by *Shibasaki* and coworkers (Scheme 2.11).<sup>67</sup> The reaction involves the decarboxylation of the copper-carboxylate species **I** to deliver a metal-ketenimine intermediate **II** in which the stereocenter of the substrate is lost. The following nucleophilic addition to imines is controlled by chiral DTBM-SEGPHOS ligand **60**.

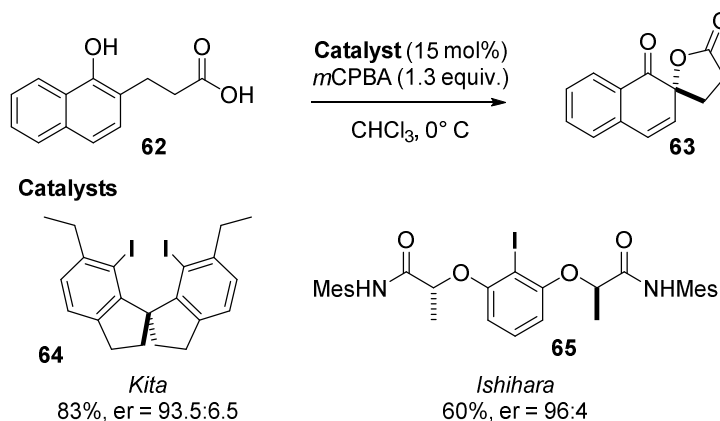


**Scheme 2.11.** Decarboxylative metal-catalyzed asymmetric *Mannich* reaction.

### Asymmetric organocatalysis with carboxylic acid substrates

The considerable acidity and the significant stability render the development of enantioselective transformations of carboxylic acids in organocatalysis quite challenging. Brønsted basic catalysts may generate a stable ion pairing associations, thus rendering difficult an efficient catalytic turnover; whereas the acidity of the substrates may interfere with acid catalysis. Actually, carboxylic acids can themselves be employed as catalysts and they have been applied to several asymmetric methodologies.<sup>56a</sup> For these reasons, prior to the investigations by our group, the use of carboxylic acids as substrates was seldom investigated and limited to certain specific intramolecular lactonization reactions.

Using chiral hypervalent iodine species, *Kita* and coworkers reported a stereoselective dearomatizing spirocyclization reaction.<sup>68</sup> Initially promoted by a stoichiometric amount of chiral reagent, this methodology was more recently reinvestigated in a catalytic fashion using *m*CPBA as terminal oxidant. The *Kita* group proposed the use of spirobiindane **64** as catalyst,<sup>68b</sup> while *Ishihara et al.* discovered that the reaction could be effectively catalyzed by iodoarene **65** (Scheme 2.12).<sup>68c</sup>

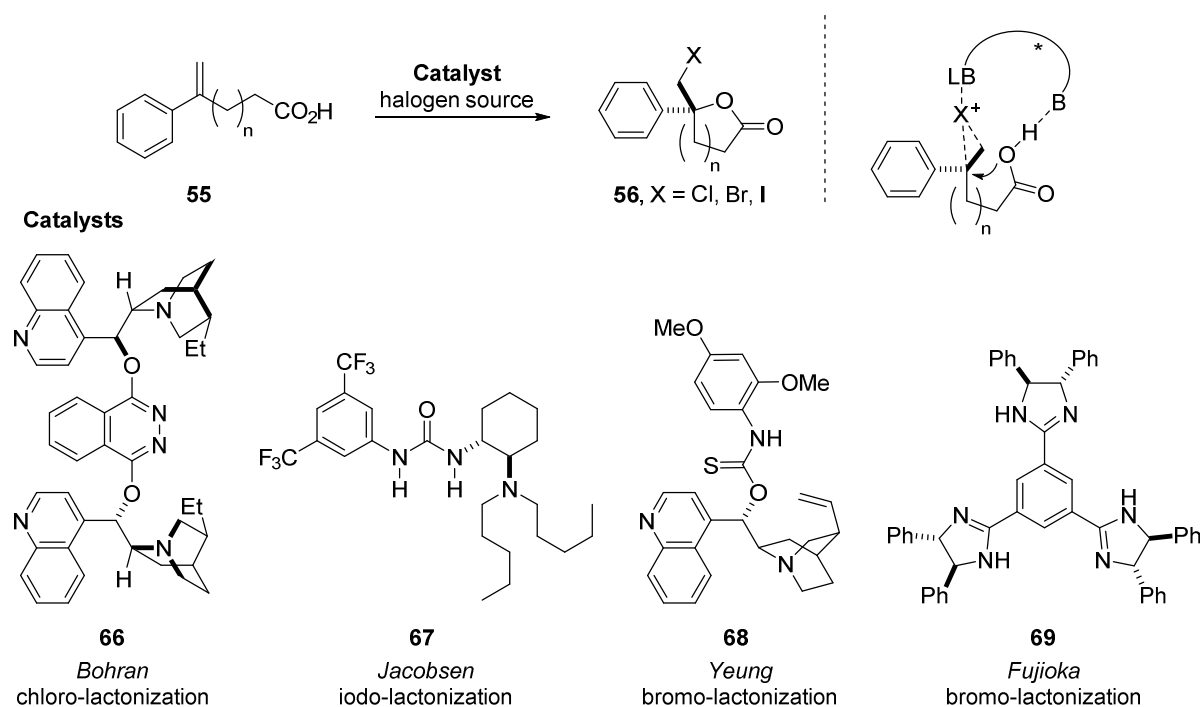


**Scheme 2.12.** *Kita*' and *Ishihara*'s asymmetric spirocyclization.

Intensive explorations have been focused on the development of intramolecular halolactonization reactions.<sup>69</sup> Early attempts to induce this transformation were reported in phase-transfer catalysis, although only poor results were obtained.<sup>69a</sup> A significant interest of the scientific community was revealed in 2010, when four different enantioselective methodologies were disclosed (Scheme 2.13). All these reactions exhibit a common feature: they presumably occur *via* organized transition states in which the stabilization of the highly

## 2. Background

reactive halonium species by a Lewis basic site is combined with the partial deprotonation of the carboxylic acid.



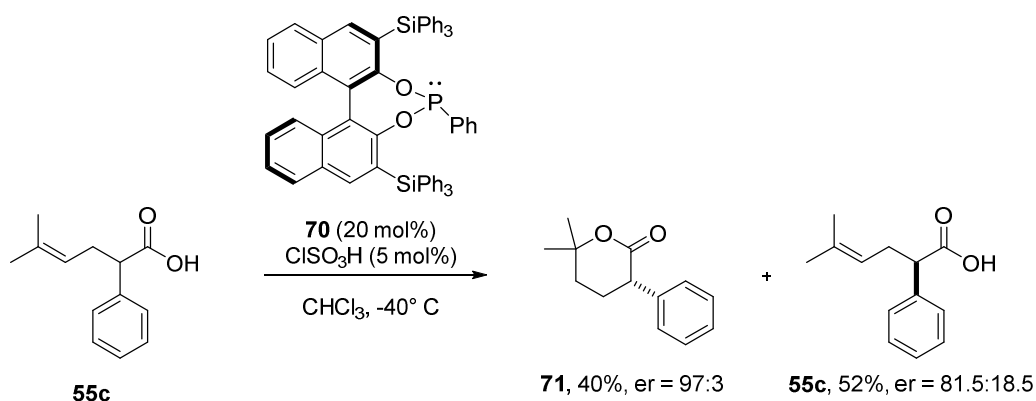
**Scheme 2.13.** Asymmetric organocatalytic halolactonizations of alkenoic acids.

*Bohran* reported a chloro-lactonization catalyzed by (DHQD)<sub>2</sub>PHAL **66**,<sup>69b</sup> while chiral urea-tertiary amine catalyst was developed by the *Jacobsen* group for a iodo-cyclization reaction.<sup>70c</sup> Bromo-lactonization strategies were instead reported by the groups of *Yeung* and *Fujioka*: the former employed quinidine-derived thiocarbamate **68**,<sup>69d</sup> while the latter used as catalyst chiral C<sub>3</sub>-symmetric tris-imidazoline **69**.<sup>69e</sup> Importantly, the tuning of the reactivity of the halogen species was also facilitated by the judicious choice of the halogen source, which was identified as key parameter for all these reactions. These reports triggered the developments of other bifunctional catalysts for this type of cyclization but, despite such advances, the reported catalytic systems have found no further application towards different transformations.<sup>70</sup>

In 2013, the group of *Ishihara* developed a kinetic resolution of racemic alkenoic carboxylic acids *via* a protolactonization reaction.<sup>71</sup> The employed catalytic system consists of an elegant combination of chiral BINOL-derived Lewis base **70** and an achiral strong Brønsted acid (Scheme 2.14). The functionalization of unactivated olefins using this



phosphonium salt catalyst is remarkable; however the applicability of this system remains to be fully explored.



**Scheme 2.14.** *Ishihara's* protolactonization of alkenoic acids.

An interesting strategy for the utilization of carboxylic acids in asymmetric Lewis base catalysis was disclosed by the *Romo* group.<sup>72</sup> However, in order to circumvent the difficult activation of the acidic moiety, a preliminary *in-situ* conversion into ester derivatives is required, thus affecting the atom economy of the methodology.

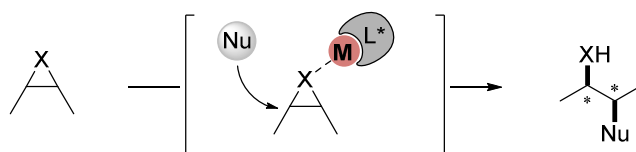
Arguably, asymmetric organocatalysis still lacks a well-defined activation strategy for carboxylic acids. Given the abundance of the carboxylate functional group in natural products and the undoubted synthetic utility of carboxylic acids, the development of general reaction modes for enantioselective transformations is desirable.

## 2.4. Epoxides and aziridines in organocatalysis

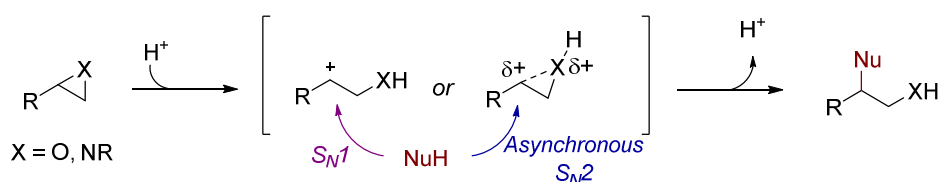
Epoxides and aziridines, three membered heterocyclic compounds, exhibit an uncommon balance between stability and reactivity and are therefore considered linchpin intermediates for organic synthesis.<sup>73</sup> Perhaps, the main feature of these structures is represented by the inherent ring strain, which makes them susceptible to nucleophilic ring opening with a variety of nucleophiles (oxirane strain energy = 26.3 kcal·mol<sup>-1</sup>; aziridine strain energy = 26.7 kcal·mol<sup>-1</sup>).<sup>74a</sup> These heterocycles are easily accessed from carbonyls or imines,<sup>75</sup> but also directly obtained from the corresponding alkenes, providing intriguing possibilities for the functionalization of simple hydrocarbon fragments.<sup>76</sup> In recognition of the high synthetic usefulness of such “spring-loaded intermediates”,<sup>74b</sup> their ring opening reactions have been even identified by *Sharpless* as important transformations for the development of the click chemistry approach.

The development of novel synthetic routes and transformations assumes a prominent role in enantioselective catalysis due to the possibility to introduce two adjacent chiral centers. In particular, the Lewis acid activation towards stereoselective ring opening reactions has been intensively investigated in the field of metal-based catalysis,<sup>77,78</sup> yet there is a surprising dearth of related approaches in asymmetric organocatalysis. Interestingly however, an activation of these heterocycles in Brønsted acid catalysis is textbook knowledge (Scheme 2.15).<sup>60</sup>

### Generic Lewis acid activation mode



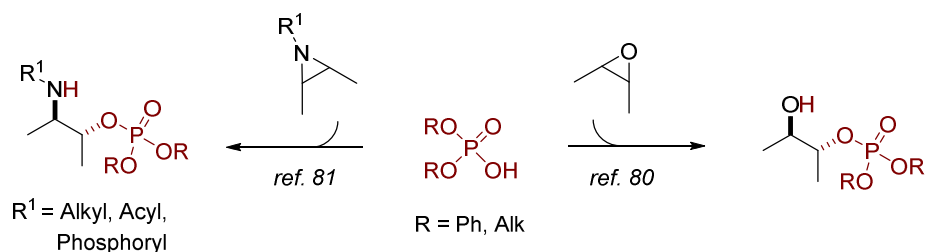
### Textbook Brønsted acid catalysis



**Scheme 2.15.** Metal-based Lewis acid catalysis and Brønsted acid catalysis for the ring opening of epoxides and aziridines.

## 2. Background

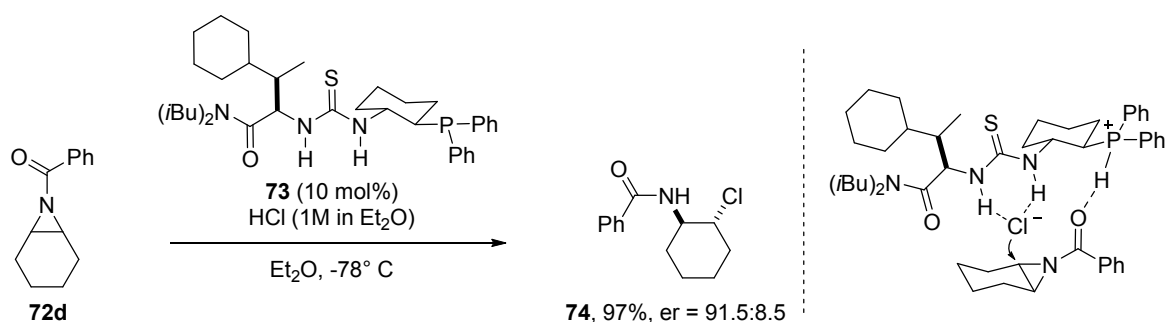
A protonation of the heteroatoms may facilitate the bond-breaking event, thus inducing the attack of the incoming nucleophile. Under these conditions, the transformation can occur either *via* a carbocation intermediate or through an asynchronous  $S_N2$  pathway. In both cases, even when a concerted mechanism is involved, the nucleophilic attack preferentially occurs at the most substituted carbon center due to the presence of a localized (partial) cationic charge.<sup>79</sup> Remarkably, this activation mode has been significantly overlooked for asymmetric methodologies. Perhaps, the lack of developments may be ascribable to the instability of chiral phosphoric acid catalysts and their derivatives towards these compounds. Phosphoric acid diesters can effectively react with these electrophiles: a protonation of the substrates delivers an oxiranium or aziridinium intermediate which is prone to be opened by the phosphate counteranion (Scheme 2.16).<sup>80, 81</sup>



**Scheme 2.16.** Alkylation of phosphoric acid diesters with epoxides and aziridines.

Alkylation of catalysts, leading to the formation of catalytically inactive species, represents one of the main limitations for the exploitation of organic catalysts in combination with highly reactive substrates. It is a fact that the activation of epoxides and aziridines in the various branches of asymmetric organocatalysis has been significantly elusive.

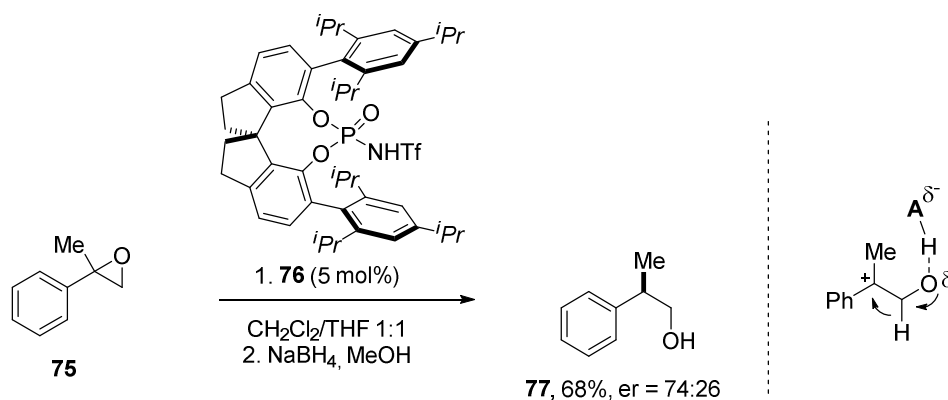
The *Jacobsen* group investigated the enantioselective hydrochlorination of aziridines, a valuable transformation due to the possible exploitation of  $\beta$ -chloro amine products.<sup>82</sup>



**Scheme 2.17.** Desymmetrization of *meso*-aziridines *via* activation of hydrochloric acid.

An elegant combination of chiral basic phosphine-thiourea catalyst **73** with a stoichiometric amount of hydrogen chloride (cf. paragraph 2.2.2) delivers an acidic species which activates the electrophilic substrate while directing nucleophilic attack of the chloride ion (Scheme 2.17).

An interesting rearrangement of racemic tertiary epoxides to aldehydes was instead reported during our investigations.<sup>83</sup> Catalyzed by SPINOL-derived N-triflyl phosphoramidate catalyst **76**, this reaction is proposed to involve a 1,2-hydride shift on the tertiary carbocation intermediate (Scheme 2.18). Nevertheless, despite representing an interesting approach to chiral aldehydes, the moderate selectivities achieved and the rather limited reaction scope limit the synthetic usefulness of this methodology.



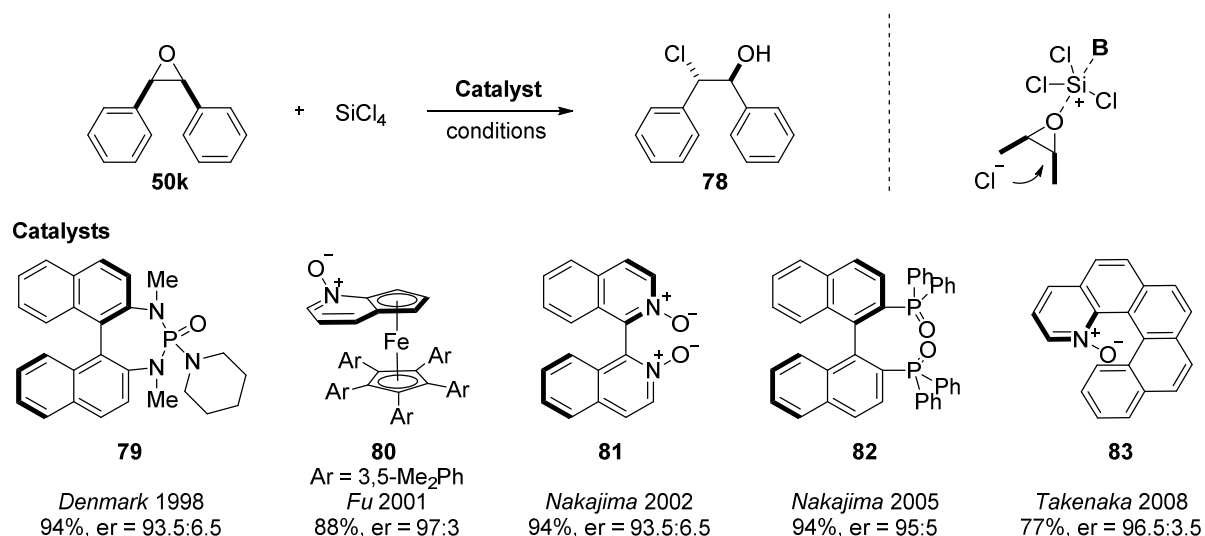
**Scheme 2.18.** Brønsted acid-catalyzed rearrangement of epoxides.

Catalyzed by a phosphoric acid catalyst, a desymmetrization of *meso*-aziridines with silylated nucleophiles was proposed by the groups of *Antilla* and *Della Sala*.<sup>84</sup> However, the putative organic Lewis acid mechanism was later disproved and the reaction was described to be promoted by alkaline metals salt impurities of the organocatalyst.<sup>85</sup>

Given the difficult activation of epoxides and aziridines in acid catalysis, the activation of nucleophilic compounds towards ring opening reactions has been attempted in Lewis base catalysis.<sup>86</sup> An enantioselective desymmetrization of *meso*-epoxides towards chiral chlorohydrins was initially reported by the *Denmark* group in 1998.<sup>87</sup> The association between catalyst **79** and silicon tetrachloride delivers a nucleophilic chloride species and a stabilized silicon cation which is presumably providing an additional Lewis acid activation of the epoxide. Notably, over the years different Lewis basic catalysts were reported to

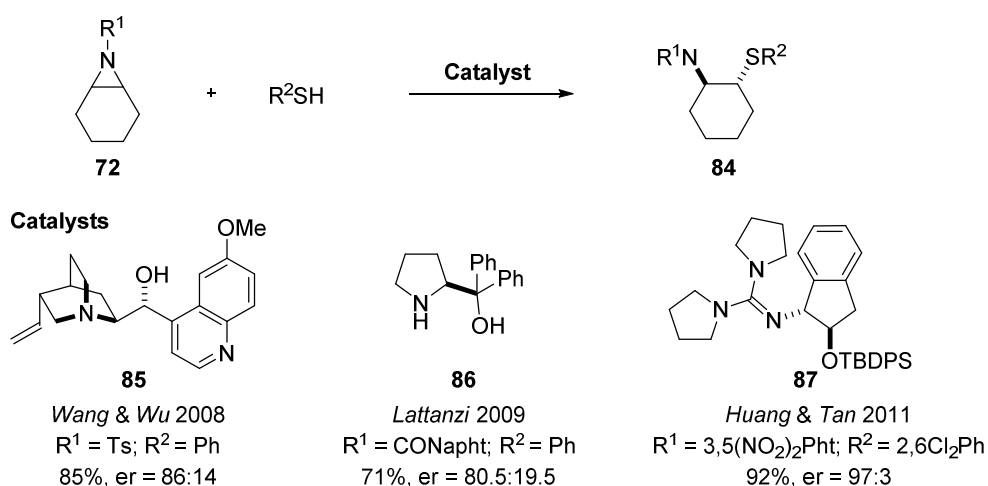
## 2. Background

promote this transformation with improved enantioselectivity and significantly broader reaction scope (Scheme 2.19).<sup>87</sup>



**Scheme 2.19.** Desymmetrization of *meso*-epoxides to chlorohydrins.

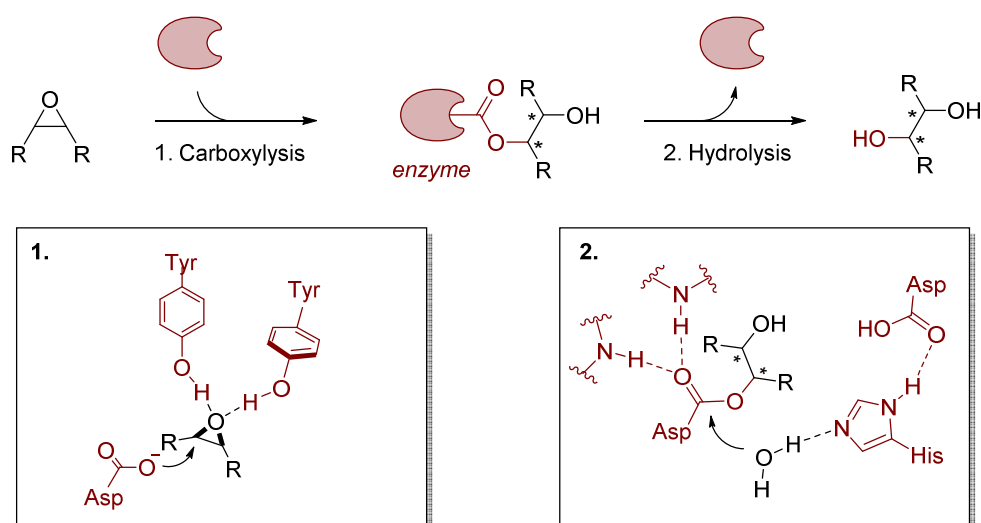
The ring opening of aziridines to 1,2-thioamines was also reported to some extent (Scheme 2.20). Owing to the large-sized valence orbitals, thiol substrates are highly nucleophilic species and their activation by base catalysis is well-established. Different catalytic systems have been studied to date, however, only chiral guanidine **87**, developed by *Huang, Tan* and coworkers, exhibits a synthetically valuable stereocontrol combined with a wide scope of the reaction.<sup>88</sup>



**Scheme 2.20.** Brønsted base-catalyzed thiolysis of aziridines

## 2.5. Asymmetric hydrolysis

The asymmetric hydrolytic ring opening of epoxides is an important transformation in synthetic chemistry since chiral vicinal diols are valuable building blocks and represent a common motif in bioactive compounds and medicinal drugs.<sup>89</sup> In nature this transformation occurs in the xenobiotic metabolism for the detoxification of exogenous substances in living organisms.<sup>90</sup> Lipophilic compounds are generally converted into more hydrophilic ones, thus facilitating their excretion; hence chiral diols are also ubiquitous as secondary metabolites and very often incorporated into the scaffolds of natural products. In biological systems epoxides are formed from the cytochrome P-450 oxidation of alkenes and their conversion to diols is catalyzed by the *epoxide hydrolase*.<sup>91</sup> Intriguingly, the hydrolysis reaction proceeds through a metal-free catalytic pathway and the active site is entirely characterized by aminoacidic residues. The mechanism occurs *via* two sequential transformations: the epoxide is activated by hydrogen-bonding and the nucleophilic attack of an aspartate residue delivers an enzyme bound intermediate, which is eventually subjected to ester hydrolysis giving the diol product (Scheme 2.21).<sup>92</sup>



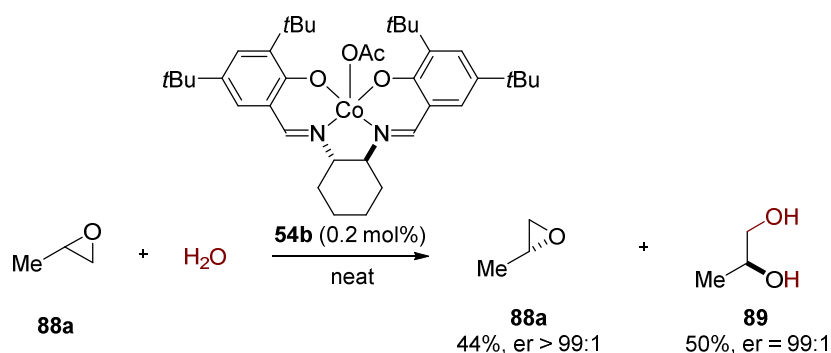
**Scheme 2.21.** Enzymatic mechanism of the *epoxide hydrolase*.

Importantly, the *epoxide hydrolase* is also active in the conversion of aziridines to 1,2-aminoalcohols, which presumably proceeds according to a similar mechanism.<sup>93</sup>

In non-enzymatic asymmetric catalysis the activation of the epoxide moiety and the concomitant enhancement of the typically moderate reactivity of oxygen nucleophiles render this reaction still challenging. The few successful catalytic systems have been

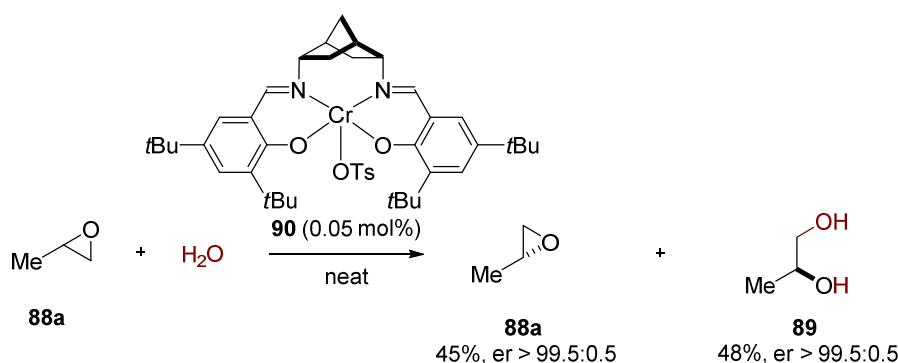
## 2. Background

reported in the field of metal-promoted transformations. The *Jacobsen* group has importantly contributed with the development of a hydrolysis reaction catalyzed by cobalt-SALEN complexes, which had been initially designed for the ring opening with carboxylic acids (cf. paragraph 2.3).<sup>94</sup> An elegant kinetic resolution of terminal epoxides was reported to proceed with remarkably high selectivity (Scheme 2.22) and the same methodology could also later be applied to the desymmetrization of *meso*-epoxides. It is noteworthy that, over the years, this reaction has also found application on an industrial scale.



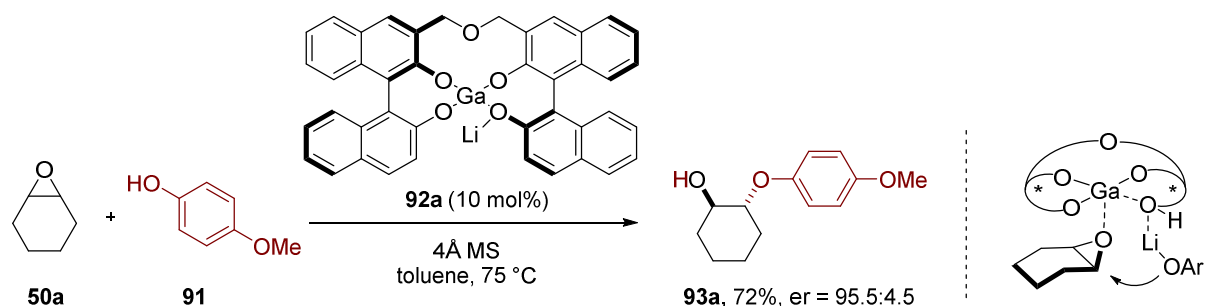
**Scheme 2.22.** The hydrolytic kinetic resolution (HKR) of epoxides developed by *Jacobsen*.

This kinetic resolution strategy has been also reinvestigated by the *Berkessel* group with a different catalytic system.<sup>95</sup> Remarkably, in many cases, the designed chromium-DIANANE-SALEN complex **90** was shown to outperform the benchmarked cobalt-SALEN system (Scheme 2.23).



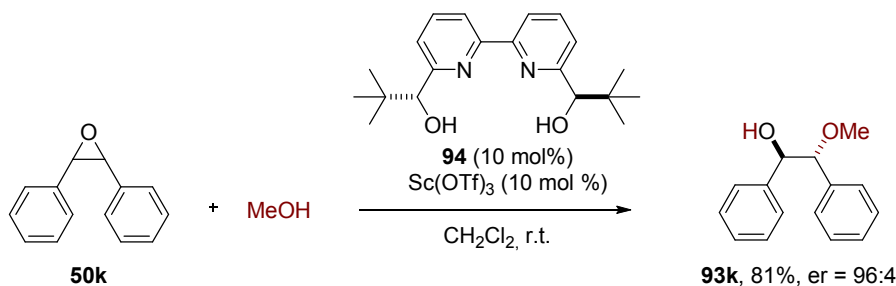
**Scheme 2.23.** The hydrolytic kinetic resolution of epoxides reported by *Berkessel*.

A desymmetrizing asymmetric alcoholysis of *meso*-epoxides was reported by *Shibasaki* and coworkers.<sup>96</sup> Catalyzed by the bimetallic gallium-lithium binaphthoxide complex **92a**, they reported an effective ring opening reaction with *p*-methoxy phenol **91**, which was effective for alkyl substituted oxiranes (Scheme 2.24).



**Scheme 2.24.** Bimetallic Ga-Li complex for the desymmetrization of *meso*-epoxides.

A complementary approach for the enantioselective alcoholysis of stilbene-derived epoxides was investigated by the *Schneider* group (Scheme 2.25).<sup>97</sup> For this purpose scandium triflate was employed as catalyst together with chiral bipyridine ligand **94** affording aromatic  $\beta$ -hydroxyethers in high enantiopurity. This catalytic system was also studied for the reactions of alkyl substrates, albeit only moderate selectivity was observed.



**Scheme 2.25.** Alcoholysis of stilbene-derived epoxides by a Sc-bipyridine complex.

Although the activation of aziridines under metal-based Lewis acidic conditions has been explored with various nucleophiles, an asymmetric hydrolysis of this heterocycle has never been reported. Due to the robust and straightforward routes to access aziridines from the corresponding olefins, such methodology would provide a powerful route to introduce chiral  $\beta$ -aminoalcohol moieties in a large variety of molecular scaffolds.

### 2.5.1. Asymmetric sulfhydrolysis

Sulfur is a frequent constituent of bioactive molecules and medicinal compounds, therefore its selective incorporation into complex molecular frameworks is highly relevant in pharmaceutical chemistry.<sup>98</sup> Despite the value of enantiopure thiols as building blocks for the synthesis of sulfurous compounds,<sup>99</sup> the development of direct asymmetric approaches



to their preparations have been particularly challenging.<sup>100</sup> Chiral  $\beta$ -hydroxythiol molecules are often associated with privileged bioactivity as illustrated with dihydrobenzoxathiins, cysteinyl leukotrienes, or the marketed drugs diltiazem, emtricitabine and cevimeline (Figure 2.9).<sup>101</sup> Therefore the development of enantioselective routes to these chiral compounds is of particular synthetic interest.

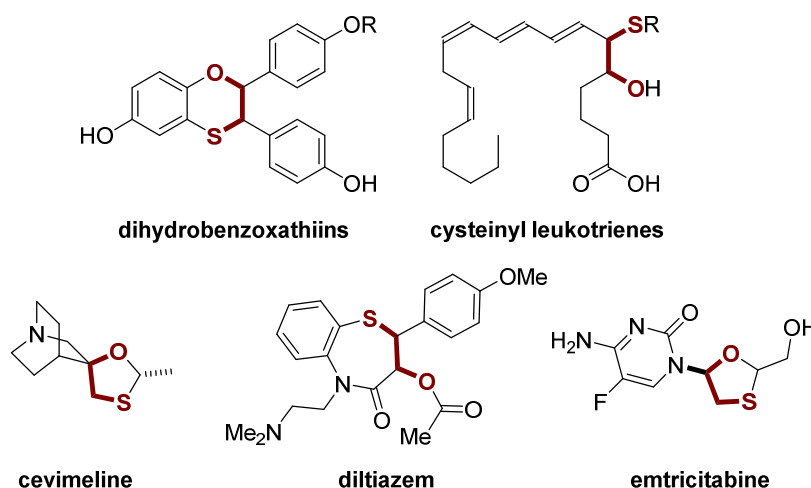
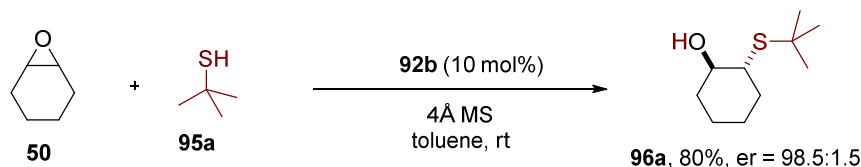


**Figure 2.9.** Bioactive molecules that incorporate a  $\beta$ -hydroxythiol framework.

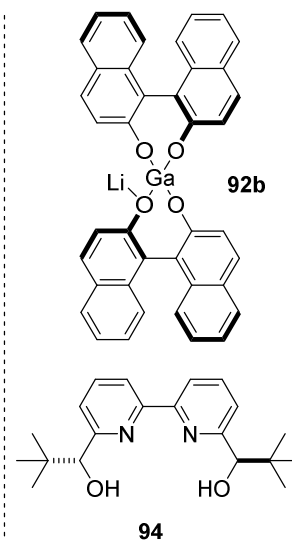
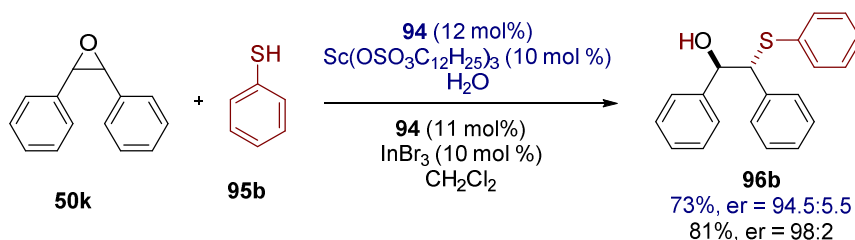
An enantioselective ring opening of epoxides with hydrogen sulfide would arguably represent the most elegant and straightforward approach to this scaffold. Nevertheless, because of the difficult exploitation of  $\text{H}_2\text{S}$ , an asymmetric sulfhydrolysis reaction remains elusive. Most investigated routes rely on the thiolysis of epoxides and have been developed using metal-based Lewis acid catalysis.<sup>102</sup> The first attempts to this transformation can be traced back to the studies by *Mukaiyama* on zinc-tartrate complexes in the 1980's.<sup>102a</sup> Despite several catalytic systems having been reported, these methodologies generally suffer from the difficulty of satisfying both substrate generality and high stereoselectivity. The best performing catalysts in the thiolysis of *meso*-epoxides were those developed by *Shibasaki* and by the groups of *Schneider* and *Kobayashi* (Scheme 2.26).<sup>102b-d</sup> The gallium-lithium binaphthoxide complex **92b** was found to promote the thiolysis of alkyl *meso*-epoxides with high selectivity. Unfortunately, the use of hindered *tert*butyl thiol is required in order to avoid a possible ligand exchange pathway, which results in non-asymmetric catalysis, thus significantly limiting the applicability of this process. Based on scandium or indium bipyridinyl complexes, the asymmetric thiolysis reported by *Schneider* and *Kobayashi*

is instead applicable to different thiols, although the reaction is specific for stilbene-derived epoxides thus limiting the utility of this methodology.

a) *Shibasaki 1997*

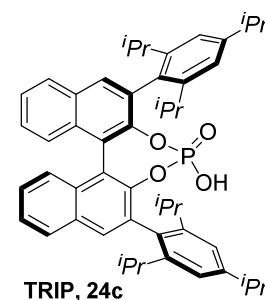
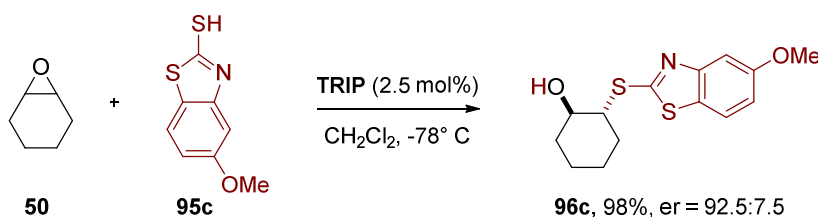


b) *Kobayashi, Schneider 2007*



**Scheme 2.26.** Metal-catalyzed asymmetric thiolysis of *meso*-epoxides.

Very recently, during our studies, an organocatalytic approach to this transformation was reported by *Sun* and coworkers.<sup>103</sup> Broadening the scope of the ring opening of oxetanes with 2-mercaptobenzothiazoles **95c**, they reported a desymmetrization of *meso*-epoxides which proceeds with moderate selectivity (Scheme 2.27).



**Scheme 2.27.** TRIP-catalyzed thiolysis of epoxides with 2-mercaptobenzothiazoles.

In addition to the substrates and nucleophiles limitations, thioether products are delivered in all these transformations and the conversion into the desired free thiols generally requires additional steps and typically harsh conditions. A general and straightforward access to  $\beta$ -hydroxy thiols is unprecedented; thus an enantioselective approach to the sulfhydrolysis reaction, which could directly give enantiopure thiol products, represents a challenging target.

### 3. Objectives

The main objectives of the doctoral studies presented herein were:

1. The identification and development of a novel activation mode for the exploitation of carboxylic acid compounds as substrates in asymmetric organocatalysis.
2. The development of an organocatalytic, biomimetic, asymmetric hydrolysis of epoxides and aziridines utilising Brønsted acid catalysis, which would provide an enantioselective approach to 1,2-diols and 1,2-aminoalcohols.
3. The investigation towards an effective variant of the asymmetric sulfhydrolysis reaction for the synthesis of  $\beta$ -hydroxythiols.
4. The design and the synthesis of novel, confined, chiral phosphoric acids. Catalysts bearing a congested active pocket may potentially provide a complementary tool for asymmetric Brønsted acid catalysis.

#### 3.1. Premise

Carboxylic acids are characterized by the combination of a hydrogen-bond donor and a hydrogen-bond acceptor in a geminal relationship. The opposite polarity and the proximity of these moieties confer peculiar features to this class of compounds. Due to geometrical constraints, an intramolecular stabilization of the two groups is not possible and thus an intermolecular dimerization is commonly observed in apolar solvents and is accepted as a general phenomenon. A double hydrogen bonding interaction is established and a stable eight-membered non-covalent network is formed. Initially described by *Sidgwick* in 1933,<sup>104</sup> the tendency to self-associate has been intensively investigated and it is today known that both physical and chemical properties of carboxylic acids (*i.e.* boiling point, solubility, etc...) are influenced. Importantly, the capability to self-assembly in organic media also leads to an enhancement of the acidity of the carboxylic acid by itself, due to the so-called homoconjugation phenomenon.<sup>105</sup> Upon deprotonation, the hydrogen bonding interaction accounts for a higher stabilization of the conjugate base of the dimer with respect to the monomeric carboxylate anion (Figure 3.1).<sup>106</sup>

### 3. Objectives

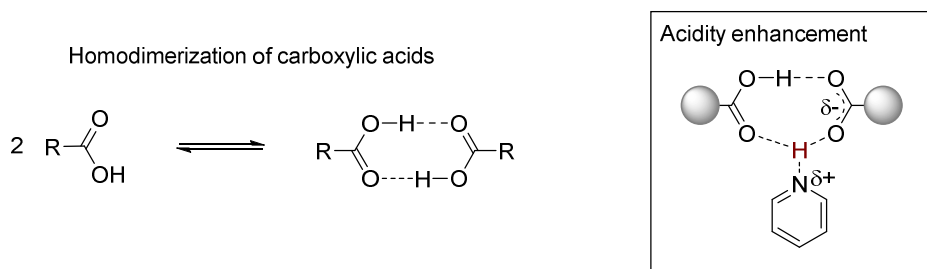


**Figure 3.1.** Homodimerization equilibrium of carboxylic acids and its effect on the acidity.

In the middle of the last century a similar tendency towards homodimeric self-assembly was also observed for phosphoric acid diesters by *Peppard et al.*<sup>107</sup> In fact, in strict analogy with carboxylic acids, these compounds have two groups with opposite polarity connected to the same phosphorous atom. For these species the association was found to be even stronger on account of the higher acidity and the concurrent large dipolar nature of the P=O bond. In 1996, studying the effect of these features on the binding constants, *Anslyn* suggested that the ylide-mesomeric structure ( $P^+-O^-$ ) could even be more representative for the species.<sup>108</sup> Notably, also in this case the effect of the homodimerization on the acid base equilibria could be observed (Figure 3.2).

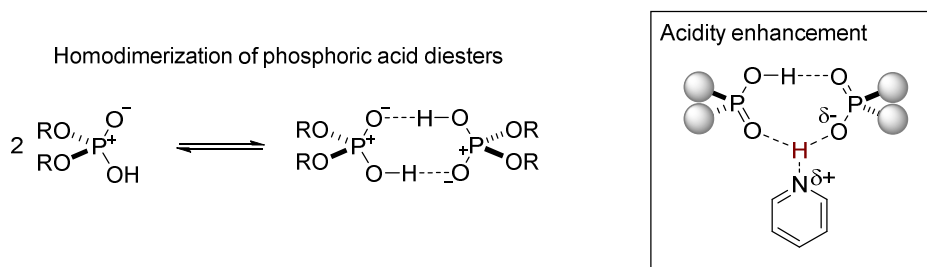


**Figure 3.2.** Homodimerization equilibrium of phosphoric acids and its effect on the acidity.

It is noteworthy that, although chiral phosphoric acids dominate the field of asymmetric Brønsted acid catalysis, this type of association has neither been explored nor proposed. Presumably, the homo-association is sterically prevented for 3-3' substituted BINOL-derived phosphoric acids, which, in contrast to their small congeners, are generally monomers in solution. However, in the solid state, the dimerization tendency of phosphoric acid catalysts is apparent. For example, in the crystal structure of **TRIP** phosphoric acid a molecule of water is incorporated in a hydrogen-bonding network to bridge within the heterodimer (Figure 3.3).<sup>53</sup> Notably, a similar behavior is also displayed in the crystal lattice of other chiral hindered phosphoric acid catalysts.<sup>109</sup>

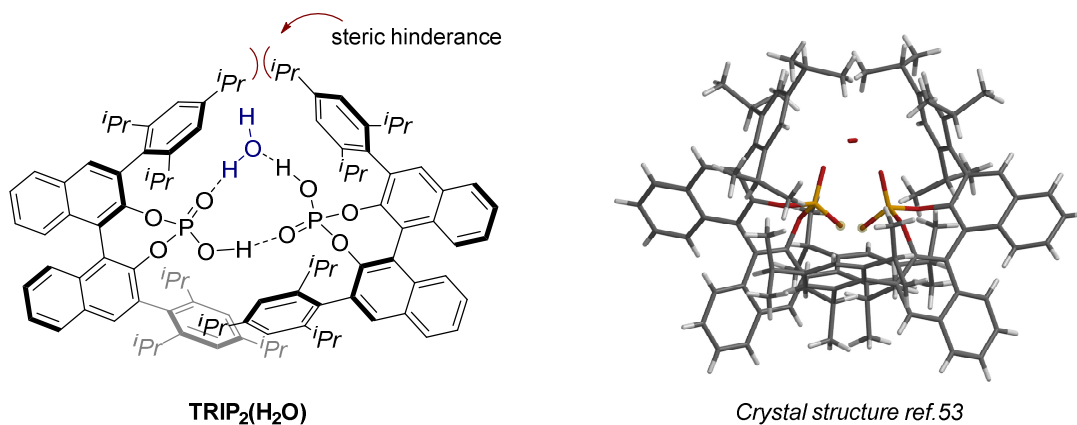
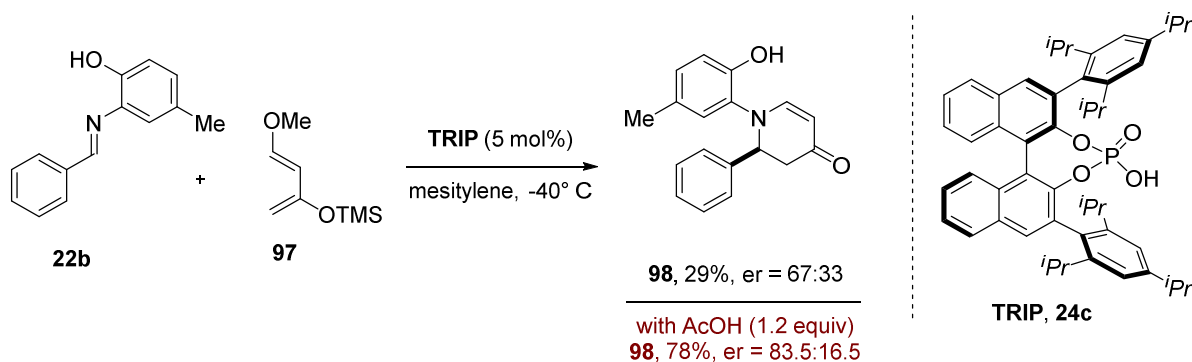


**Figure 3.3.** Crystal structure of (*R*)-TRIP phosphoric acid catalyst.

On these bases, we hypothesized that a small-sized carboxylic acid molecule may, in solution, enter the pocket of the phosphoric acid catalyst, thus providing stabilization in the absence of large repulsive forces. Indeed, a beneficial effect from the use of achiral carboxylic acids as additive in phosphoric acid catalysis can be traced back in a report by *Akiyama*.<sup>110a</sup> The addition of a carboxylic acid significantly improved both the reactivity and the enantioselectivity of a **TRIP**-catalyzed *aza-Diels-Alder* reaction between imines and *Danishefsky's* diene **97** (Scheme 3.1). A similar effect was also later observed by the groups of *Rueping* and *Antilla*.<sup>110b-d</sup>



**Scheme 3.1.** Acetic acid as additive in phosphoric acid catalysis: *Akiyama's* report.

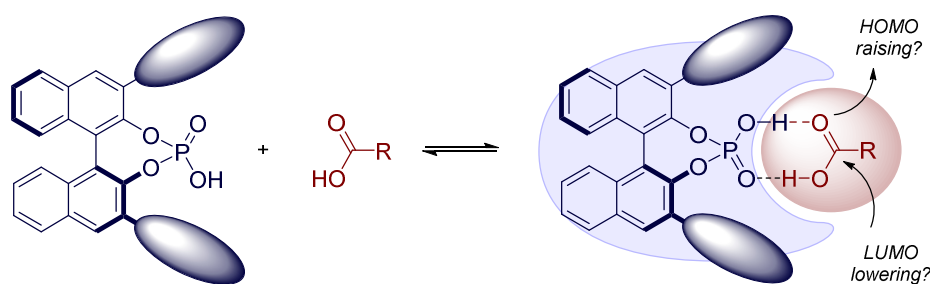
“...At the present stage the role of the protic additive is not clear.”

T. Akiyama *et al.*, 2006.

### 3.2. Studies towards heterodimeric self-assembly

Despite homo-dimerization processes of carboxylic acids and phosphoric acids having been largely investigated and established, significantly less effort has been devoted to the study of mixed carboxylic-phosphoric acid dimers. However, it is reasonable that an association may occur as the homodimerization tendency of phosphoric acid diesters was observed to be significantly reduced in acetic acid.<sup>111</sup> Nevertheless, a direct study on specific hetero-association equilibria or an investigation on the reactivity of heterodimeric species has never been reported.

As mentioned earlier, bulky phosphoric acid catalysts cannot reach stabilization *via* homo-association in solution and, given to the unreleased stabilization energy, they could be formally considered “frustrated Brønsted pairs”. Therefore, an equilibrium towards a heterodimeric species with carboxylic might be energetically favored (Scheme 3.2).



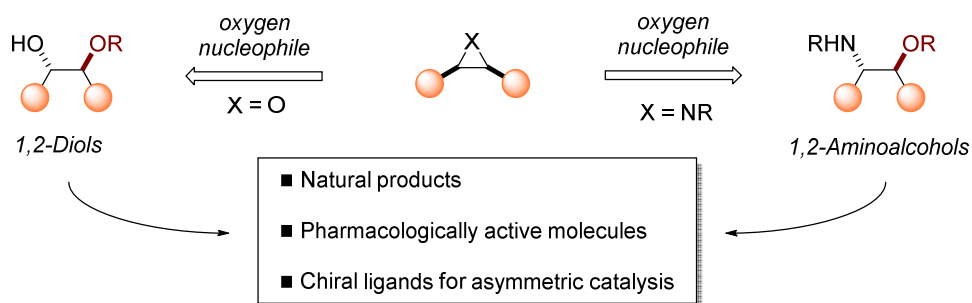
**Scheme 3.2.** Developing an activation mode for carboxylic acids in Brønsted acid catalysis.

We were intrigued by this combination since no solid prediction on the reactivity of these designed species was possible at first sight. Nevertheless, based on the established heteroconjugation effect and on the previously reported findings, an increase of the overall acidity could be proposed. Our curiosity was especially aimed towards the effect of such self-assembly on the frontier molecular orbital of the carboxylic acid molecule. The heterodimeric species would not be symmetrical and the two hydrogen bonding interaction could account for opposite effects. The acid moiety of the phosphoric acid may potentially increase the electrophilicity of the carbonyl group; whereas the highly basic P=O double bond, participating in a partial deprotonation, may raise the nucleophilicity of the carboxylate moiety.

A full physico-chemical investigation would establish the possibility to achieve a supramolecular heterodimeric self-assembly and provide further insights on this ambiguous “pull-push” effect. Due to the recognized importance of carboxylic acids in synthetic chemistry, we aimed at the exploration of this self-assembly as a novel activation mode. Given the difficult exploitation of these substrates in asymmetric catalysis, such development could significantly broaden the perspectives of organocatalysis both from the academic and the industrial point of view.

### 3.3. Activation of carboxylic acids in asymmetric organocatalysis

The synthesis of chiral 1,2-aminoalcohols and 1,2-diols from the corresponding alkenes is an ambitious target in synthetic chemistry. Indeed, such moieties are widely occurring in the scaffolds of natural products, pharmacologically active molecules and in chiral ligands for asymmetric catalysis.<sup>89, 112</sup> Therefore, an asymmetric ring opening reaction of epoxides and aziridines with oxygen nucleophile in Brønsted acid catalysis would represent a valuable alternative to existing methodology.

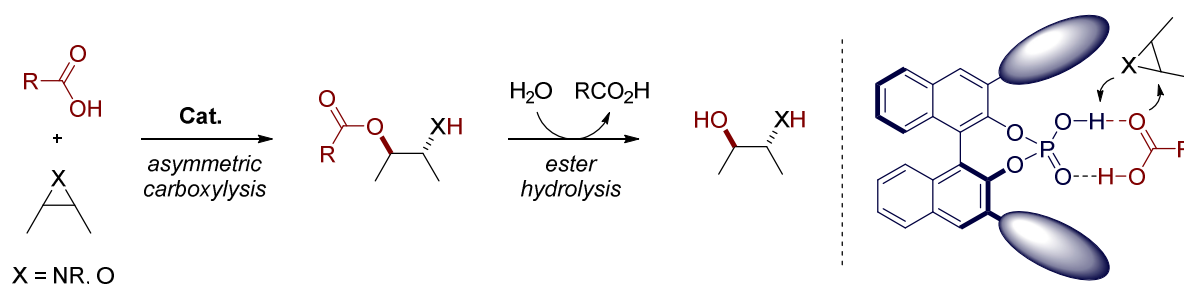


**Scheme 3.3.** Asymmetric ring opening of epoxides and aziridines to aminoalcohols and diols.

However, the moderate reactivity of oxygen nucleophiles and the need to avoid the alkylative deactivation of the catalyst render this target significantly challenging in Brønsted acid asymmetric organocatalysis. The disclosure of an effective variant to the asymmetric hydrolysis reaction represents an objective of the present investigation. Intrigued by the previously discussed enzymatic mechanism of the *epoxide hydrolase*, we focused on the development of an enantioselective carboxylolysis of epoxides and aziridines. If followed by a mild basic hydrolysis of the ester product, this methodology would represent an elegant biomimetic transformation.

### 3. Objectives

The envisaged heterodimerization with confined phosphoric acid catalysts may potentially activate carboxylic acids towards nucleophilic reactions in Brønsted acid organocatalysis, thus providing a new catalytic mode for the targeted methodologies (Scheme 3.4). By favoring such hypothetical self-assembly over the direct interaction with the highly reactive electrophile, we aimed to prevent the alkylative deactivation of the acid catalyst.

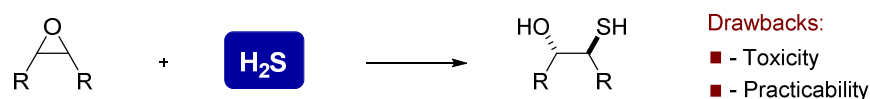


**Scheme 3.4.** A biomimetic, asymmetric hydrolysis *via* hetero-dimeric self-assembly.

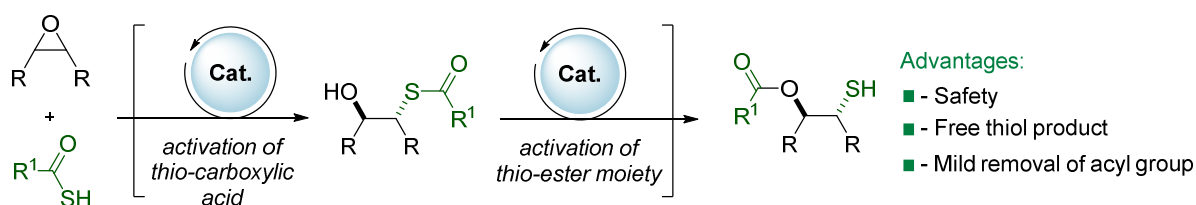
#### 3.4. Asymmetric synthesis of $\beta$ -hydroxythiols

Although the thiolysis of epoxides has been investigated, the developed methodologies do not provide a facile approach to free  $\beta$ -hydroxythiols. In more general terms, the direct introduction of a thiol moiety in a hydrocarbon framework is still a challenging target. The investigations towards an organocatalytic variant of the sulfhydrolysis of epoxides are reported herein.

##### Sulfhydrolysis of epoxides



##### Designed organocatalytic variant



**Scheme 3.5.** Design of an organocatalytic route to chiral *O*-protected  $\beta$ -hydroxythiols.

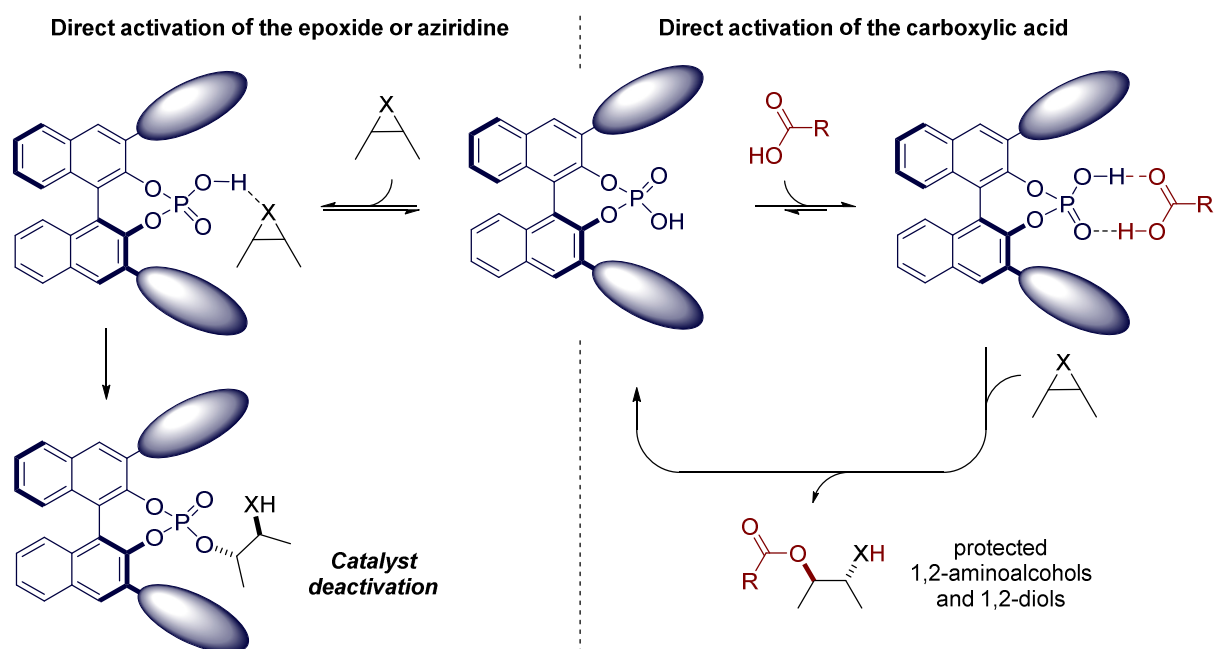
Broadening the activation of carboxylic acid to its sulfur variant, the asymmetric ring opening of oxiranes with thio-carboxylic acids was targeted and an organocascade



transformation was envisioned. The asymmetric thiocarboxyls of epoxides would yield a  $\beta$ -hydroxythioester moiety that, under Brønsted acid catalysis, could undergo a thermodynamically favored acyl-transfer process. The designed transformation would directly deliver *O*-protected thiol products (Scheme 3.5); however, the possibility to interrupt the cascade sequence prior to the intramolecular transesterification is also desirable. Such orthogonal control would give the chance to access the same molecular scaffold protected either on sulfur or on oxygen, thus giving interesting perspectives in synthetic applications. Moreover, chiral 1,2-thioalcohols may be directly obtained upon *in-situ* removal of the protecting group and, due to the safe and non-toxic conditions of the overall process, the methodology would be an ideal alternative to the sought after asymmetric sulfhydrolysis.

### 3.5. Mechanistic investigation and codification of a novel activation mode

Over the course of this doctoral work, all the developed transformations have been designed and explored using the hetero-dimeric self-assembly as central feature. The thermodynamically favored association between the phosphoric acid catalyst and carboxylic acids was found to override the unproductive catalyst deactivation. We proposed an unprecedented catalytic cycle, which relies on the direct activation of carboxylic acids as nucleophiles, thus reversing the usual polarity in Brønsted acid catalysis (Scheme 3.6).



**Scheme 3.6.** Asymmetric approach to carboxylation of epoxides and aziridines.

### 3. Objectives

---

Given the wide applicability of this system, we ultimately aimed towards the detailed investigation of this reaction mode in organocatalysis. Therefore theoretical investigations on heterodimeric species, as well as kinetic studies on the reaction pathways and an analysis on the catalyst structure-selectivity relationship were targeted. We expected that this exploration should facilitate a predictive understanding, thus underpinning the development of further enantioselective transformations of carboxylic acids.

*“In the middle of difficulties lies opportunity.”*

A. Einstein

## 4. Results and Discussions

### 4.1. Studies on heterodimeric self-assembly<sup>113</sup>

The first part of this section describes the characterization of the interaction between carboxylic acids and chiral, hindered, phosphoric acids. Spectroscopic analyses were undertaken to gain evidence for a supramolecular non-covalent association, while X-ray crystallography elucidated the heterodimeric structure of the self-assembly. Based on these experiments, the structural properties were disclosed and some of the reactivity features could be predicted, thus igniting the synthetic investigations described in the following paragraphs.

*The spectroscopic investigations described in this section were performed in collaboration with M. Leutzsch, while the crystal structure determination of **99b** by X-ray diffraction was performed by Dr. R. Goddard.*

#### 4.1.1. Identification of the supramolecular association

The hindered homodimerization of chiral phosphoric acids encouraged us to investigate whether a heterodimeric association with carboxylic acids could be thermodynamically favored in organic non-polar solvents. Spectroscopic measurements usually represent the most accessible techniques for the elucidation of supramolecular equilibria in solution and are based on the influence of the binding event on a defined observable.<sup>114</sup> We hypothesized that the targeted association may provide a significant change of the electronic distribution from the phosphoric acid monomer, thus enabling an analysis by nuclear magnetic resonance. Therefore, at the onset of our studies we investigated the NMR spectra of mixtures of **TRIP** and acetic acid in deuterated dichloromethane (Figure 4.1). Indeed, comparing the proton and the phosphorous NMR spectra of the simple phosphoric acid (blue spectra) with a sample in which the two acids were simultaneously contained (ratio 1:6, red spectra), a sharp difference was observed. The presence of the carboxylic acid influenced both the shape and the chemical shift of the signals of the phosphoric acid molecule. The phosphorous peak in the <sup>31</sup>P-NMR experienced a significant shift downfield (from 2.32 ppm to 4.64 ppm) and a similar shift towards lower field was also observed for all the proton signals of the phosphoric acid molecule in the <sup>1</sup>H-

NMR, hinting at the establishment of a different chemical environment. In addition, the coalescence of non-equivalent proton signals of the 3-3' substituents resulted cleared (signals at 2.5-3.0 ppm and 6.9-7.1 ppm). These observations reinforced us in the belief that an equilibrium favoring the heterodimeric species with carboxylic acid was occurring.

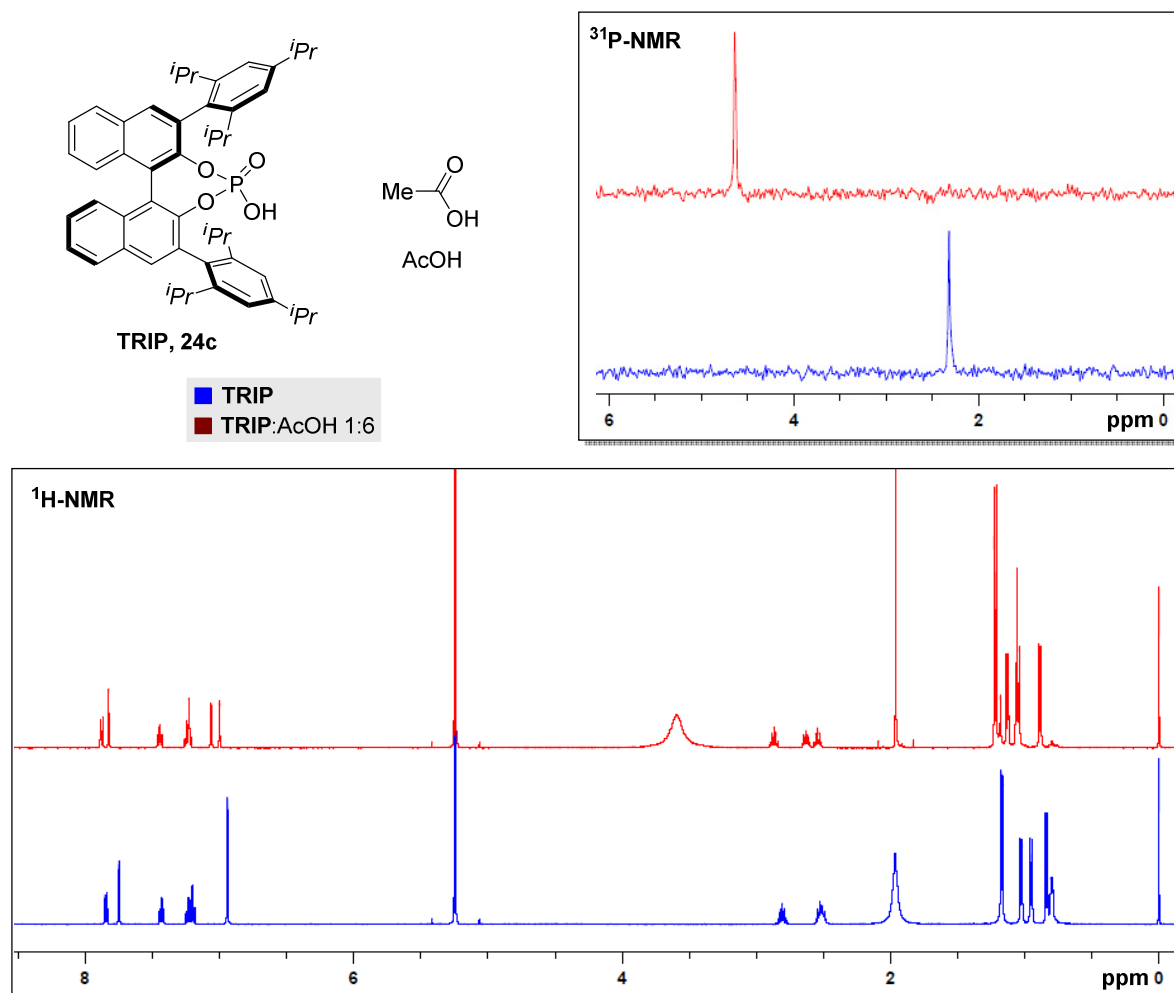
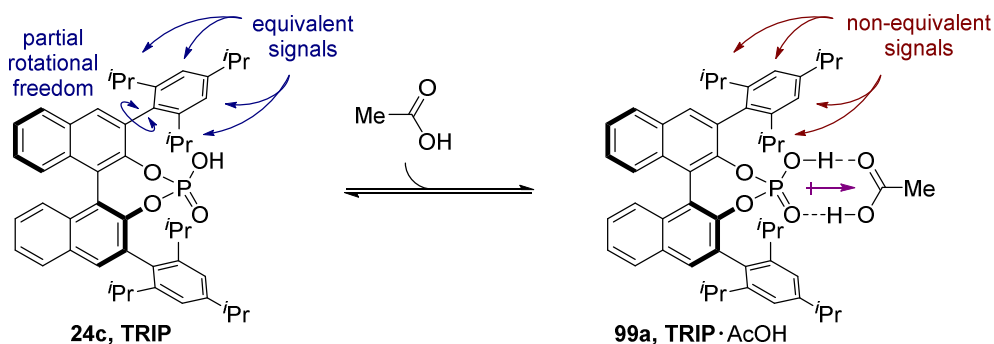


**Figure 4.1.** Association studies *via* 1D-NMR.  $^1\text{H}$ -NMR and  $^{31}\text{P}$ -NMR of **TRIP** (blue spectra) and a mixture 1:6 **TRIP**:AcOH (red spectra) in  $\text{CD}_2\text{Cl}_2$  are shown.

On the one hand, the observed splitting of the proton signals suggested a lower rotational freedom of the 3-3' aryl substituent, thus indicating the presence of the guest molecule in the catalyst pocket. On the other hand, the general downfield shift of the signals of **TRIP** in the proton NMR was intriguing and suggested an overall decrease of the electronic density on the phosphoric acid. The saturation of a solution of acetic acid with **TRIP** resulted in an upfield shift of the methyl signal revealing a higher electron density on the carboxylic acid molecule, thus confirming this hypothesis (see experimental section, cf. paragraph

7.2.1). This phenomenon is postulated to be caused by the double hydrogen bonding interaction which characterizes the **TRIP**·AcOH complex.



**Scheme 4.1.** Spectroscopic analysis of **TRIP**·AcOH heterodimerization.

Prompted by these initial findings, a series of DOSY experiments (Diffusion-Ordered Spectroscopy) was performed in order to gain further evidence on the proposed heterodimerization.<sup>115</sup> Based on the *Stokes-Einstein* equation, this analysis offers the possibility to investigate the molecular size of solute species in solution and could effectively be applied to our association studies. In supramolecular chemistry, the hydrodynamic volume of the solvated aggregates is larger than the corresponding monomeric species and therefore their diffusion rate is decreased. Applying the related pulse sequence to <sup>1</sup>H-NMR, we independently measured the diffusion coefficients of **TRIP** ( $D_{TRIP} = 8.3 \times 10^{-10} \text{ m}^2 \text{ s}^{-1}$ ) and benzoic acid ( $D_{BzOH} = 16.4 \times 10^{-10} \text{ m}^2 \text{ s}^{-1}$ ) in deuterated dichloromethane and then we evaluated the same parameters in mixtures of the two components (Figures 4.2).

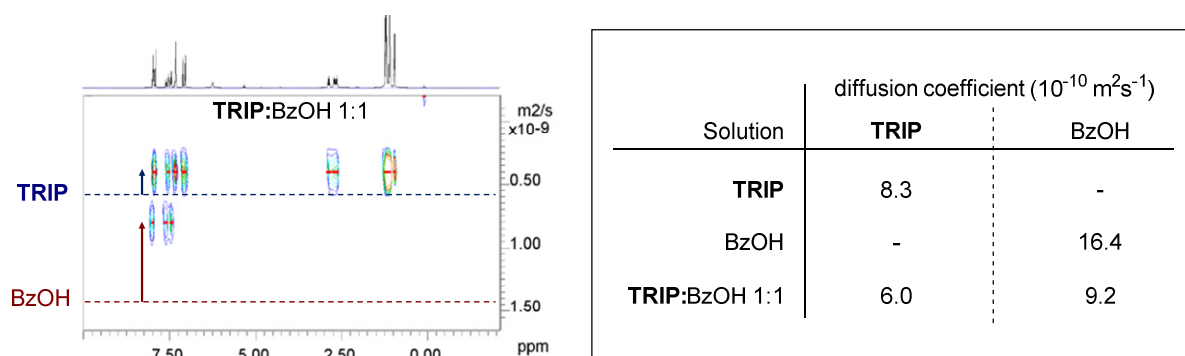


**Figure 4.2.** Evaluation of diffusion coefficients by <sup>1</sup>H-DOSY.

This experiment provided full confirmation of the binding between the two acids: in an equimolar mixture, the diffusion coefficients of the two species were found to be significantly lowered with respect to their independent values. Upon self-assembly, the

relatively small benzoic acid experienced the highest variation of hydrodynamic volume ( $D_{BzOH} = 9.2 \times 10^{-10} \text{ m}^2 \text{ s}^{-1}$ ) but a significant influence was also observed on the phosphoric acid ( $D_{TRIP} = 6.0 \times 10^{-10} \text{ m}^2 \text{ s}^{-1}$ ).

#### 4.1.2. Evaluation of binding constants and structure elucidation

Having obtained qualitative insights on the heterodimerization between **TRIP** catalyst and carboxylic acids in organic non-polar solvents, we targeted the evaluation of the binding strength and a more detailed elucidation of the supramolecular structure. Taking advantage of our previous investigations, we initially focused on the determination of the association constant by NMR spectroscopic analysis.<sup>116</sup> In particular, the shift of the phosphorous signal was identified as a suitable physical observable for the quantitative study of the dimerization equilibrium. In fact, the observed chemical shift should be mathematically dependent on the mole fraction of the heterodimer in solution (equation 4.1).

$$\delta_{\text{OBS}} = \frac{[\text{TRIP} \cdot \text{RCO}_2\text{H}]}{[\text{TRIP}_0]} (\delta_{\text{TRIP} \cdot \text{RCO}_2\text{H}} - \delta_{\text{TRIP}}) + \delta_{\text{TRIP}} \quad (4.1)$$

Hence we preliminary confirmed the stoichiometry of the binding event using the method of continuous variations (Job's method).<sup>117</sup> Keeping constant the total concentration but varying the proportion between **TRIP** and acetic acid, several samples were measured. The curved plot obtained ( $\Delta\delta^* \chi_{\text{TRIP}}$  VS  $\chi_{\text{TRIP}}$ ) showed a maximum for  $\chi_{\text{TRIP}} = 0.5$ , thus revealing a 1:1 stoichiometry of the self-assembly (figure 4.3).

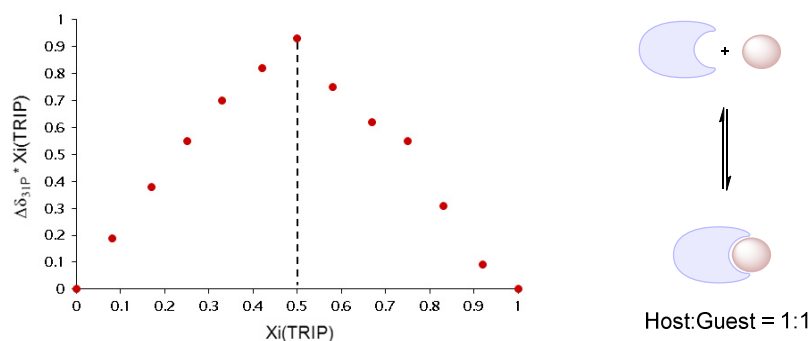


**Figure 4.3.** Job plot for **TRIP**-AcOH.

## 4. Results and Discussion

With the the stoichiometry of our host-guest system determined, we investigated the binding isotherms for **TRIP**·AcOH and **TRIP**·BzOH heterodimers in order to obtain the equilibrium constants (Figure 4.4).

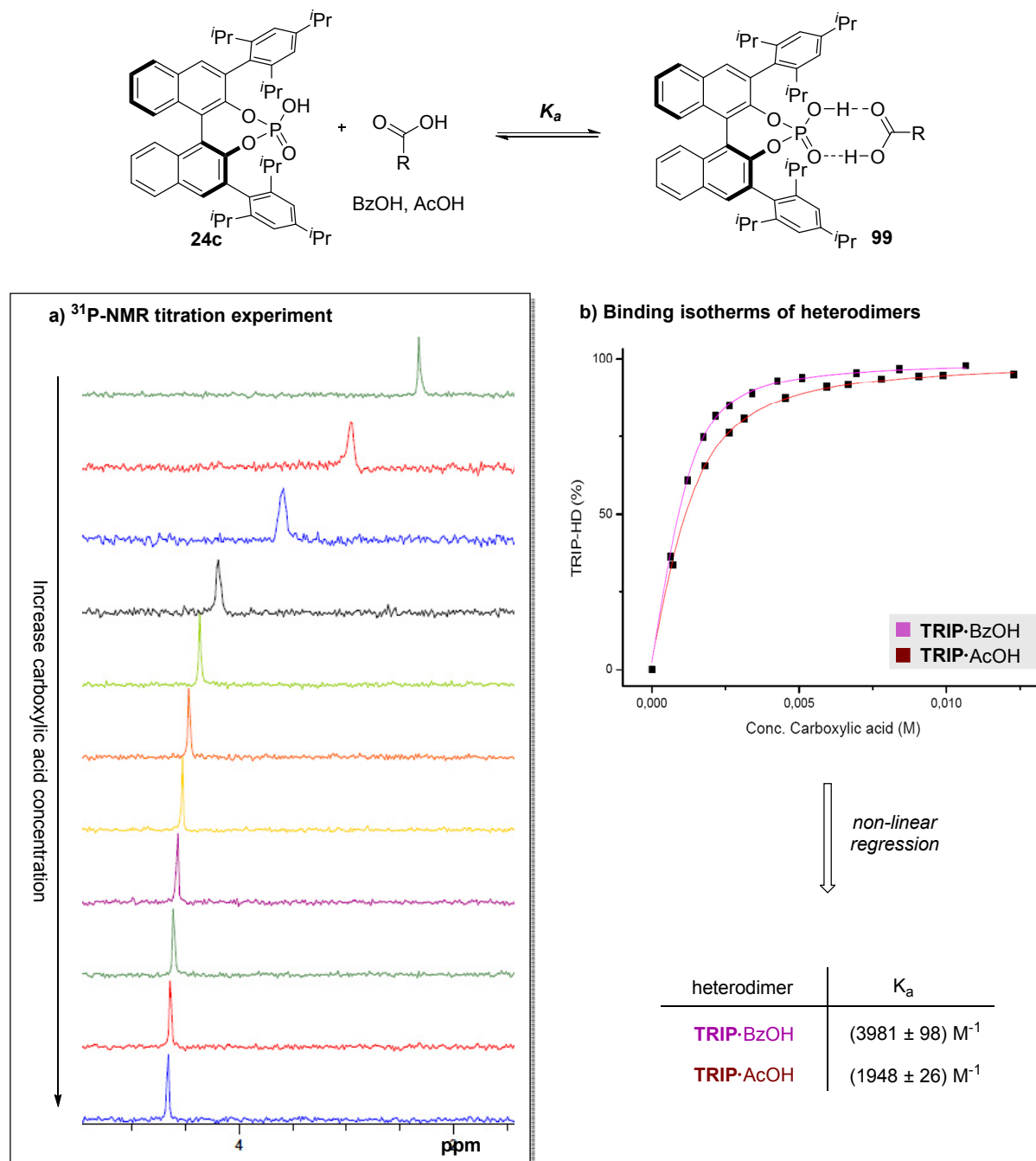


**Figure 4.4.** Evaluation of association constants. a) Example of  $^{31}\text{P}$ -NMR titration experiment for **TRIP**·AcOH. b) Binding isotherms of **TRIP**·BzOH (magenta) and **TRIP**·AcOH (blue) and association constants for the heterodimers.

Upon addition of carboxylic acid to a solution of the phosphoric acid in dichloromethane, the asymptotic approach to complete heterodimer formation was monitored following the shift of the phosphorous signal. Once the binding isotherms were obtained, a non-linear regression method was followed and, implementing the known equation for 1:1 complexes (equation 4.2;  $H$ =host,  $G$ =guest,  $HG$ =complex) together with equation 4.1, the association constants were successfully derived.<sup>116</sup>

$$[HG] = \frac{1}{2} \left( [G_0] + [H_0] + \frac{1}{K_a} \right) - \sqrt{\frac{1}{4} \left( [G_0] + [H_0] + \frac{1}{K_a} \right)^2 - [H_0][G_0]} \quad (4.2)$$

Two different sets of experiments have been performed for both heterodimeric systems, and the values were given as the mathematical average (**TRIP**·BzOH  $K_a = (3981 \pm 98) \text{ M}^{-1}$ ; **TRIP**·AcOH  $K_a = (1948 \pm 26) \text{ M}^{-1}$ ).

These numerical values are remarkably high for supramolecular association and this highlights the thermodynamic favor of the process, which is considerable despite the steric hindrance of **TRIP** active pocket. The stronger association which is observed with benzoic acid rather than with acetic acid may be explained on the basis of the two-fold contribution of the aromatic ring, which concurrently increases the availability of the lone pairs on the carbonyl moiety and the acidity of the hydroxyl group. In other words, benzoic acid is preferred as binding partner due to being simultaneously a stronger hydrogen-bonding donor and hydrogen-bonding acceptor compared to acetic acid. In fact, the same considerations are applied to the homodimerization equilibria of benzoic acid and acetic acid.

It is noteworthy that the obtained values significantly matched with our expectations, lying in between those of carboxylic acids ( $10$ - $100 \text{ M}^{-1}$ ) and phosphoric acid diester homodimers ( $>10^5 \text{ M}^{-1}$ ) (Figure 4.5).<sup>118,108</sup>



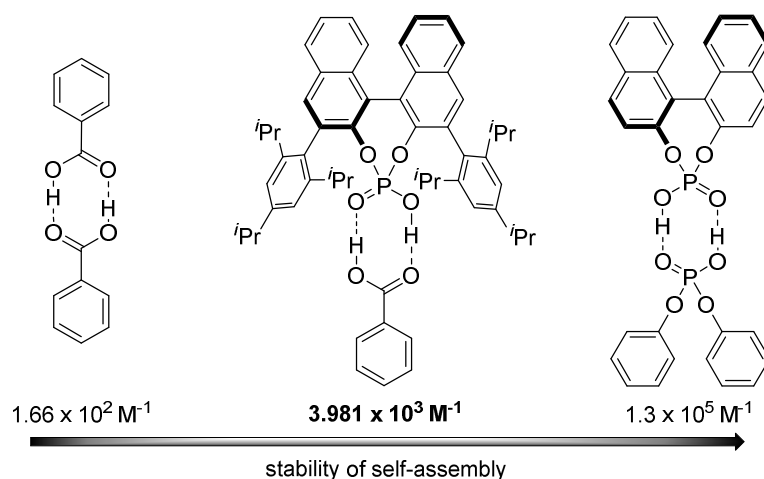


**Figure 4.5.** Stability scale for dimeric self-assembly

A final unambiguous confirmation of the structure of the heterodimeric association was given by X-ray crystallography. A single crystal suitable for diffraction analysis was obtained by co-crystallizing acetic acid and **TRIP** *via* slow evaporation of dichloromethane solvent. The isolation of **TRIP**·AcOH heterodimer suggests that this interaction is not only favored in solution, but also in the solid state (Figure 4.6). In agreement with our spectroscopic observations, the species appears pseudo  $C_2$ -symmetric and the molecule sits on a crystallographic 2-fold axis which passes through the phosphorous atom and the two carbon atoms of the acetic acid molecule. The hydrogen bonding network could be clearly identified and the relative short distance between the oxygen atoms accounts for such a strong interaction (2.565 Å).

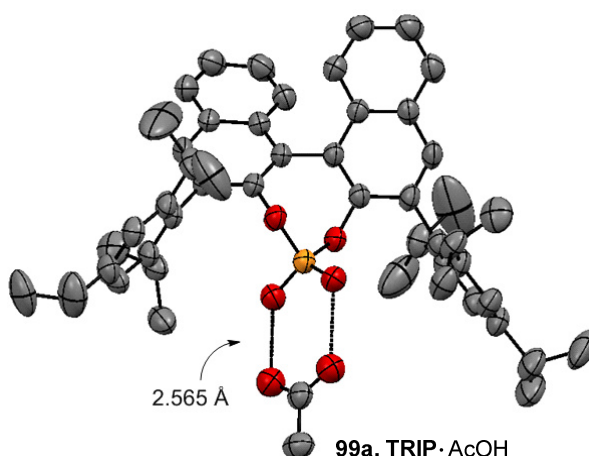


**Figure 4.6.** Crystal structure of **TRIP**·AcOH.

This crystal structure represents the first reported example of a defined dimeric interaction between these two acidic moieties.

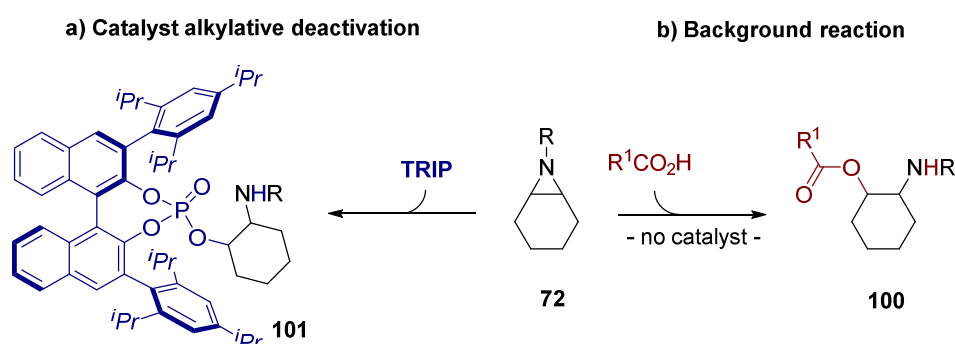
## 4.2. Asymmetric carboxylation of aziridines<sup>113</sup>

As discussed in the introduction, prior to the studies presented in this thesis, an asymmetric catalytic conversion of aziridines into chiral 1,2-aminoalcohols was unprecedented. At the onset of our investigations we were particularly motivated in exploring the reactivity of the observed phosphoric-carboxylic acids mixed dimers. Due to the synthetic value of the transformation, we selected the carboxylation of aziridines as testing ground for our investigations in organocatalysis.

*The work described in this section was performed in collaboration with B. Poladura and M. Diaz de los Bernardos.*

### 4.2.1. Reaction design and optimization

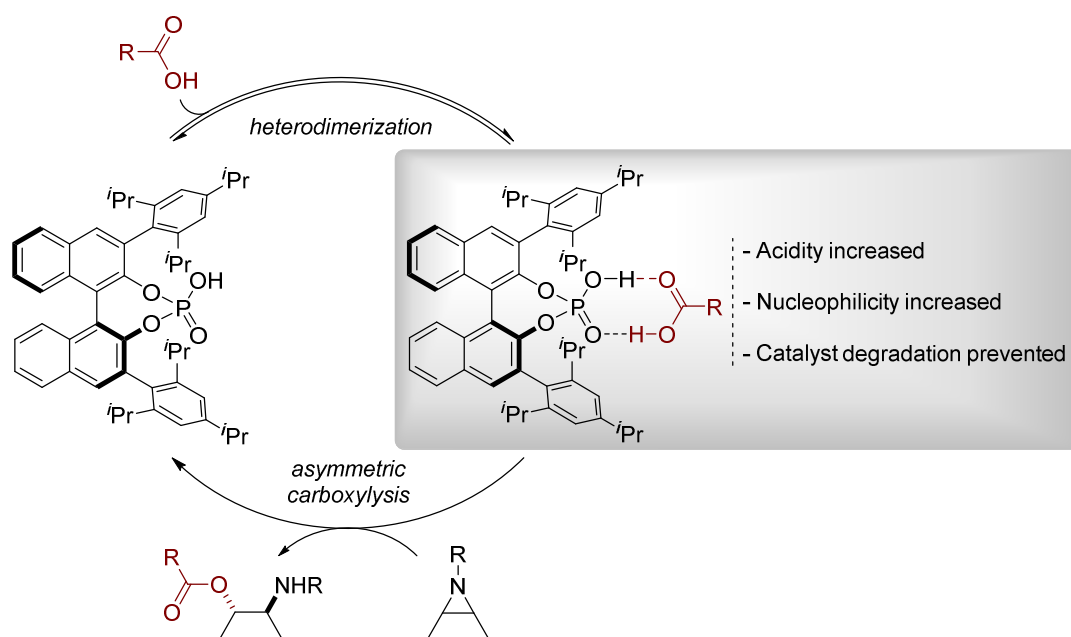
Due to the high reactivity of aziridines, the development of a carboxylation reaction is particularly challenging in asymmetric Brønsted acid catalysis. This transformation faces two major difficulties in phosphoric acid catalysis: an alkylative deactivation of the organic catalyst and the possible background reaction (Scheme 4.2). On the one hand, aziridinium phosphate intermediates are short-lived species and they commonly decompose leading to the phosphate ester before being intercepted by external nucleophiles (i.e. water, alcohols...).<sup>81,119</sup> On the other hand, the acidity of carboxylic acids may lead to the activation of the aziridine substrate in a non-asymmetric environment, giving the desired product through a racemic pathway.<sup>120</sup>



**Scheme 4.2.** Major issues for an asymmetric carboxylation reaction in phosphoric acid catalysis.

However, having established the thermodynamic favor of the association between phosphoric acid catalysts and carboxylic acids, we hypothesized that this system may provide an effective solution to these limitations. In particular, we investigated a novel approach based on self-assembly organocatalysis, which involves the heterodimeric species as the crucial intermediate. Based on our heterodimerization studies, we envisioned a two-fold beneficial effect due to association: both acidity of the catalyst and nucleophilicity of the carboxylic acid may be enhanced. Indeed, the spectroscopic analysis had suggested the significant role of the Lewis basic site of the catalyst in a partial deprotonation, thus revealing a possible activation of the carboxylic acid as nucleophile. We also expected an increased acidity of this species with respect to the free catalyst because of the established *heteroconjugation* (cf. paragraph 3.1), which may facilitate the activation of the aziridine. Furthermore, the direct formation of an aziridinium phosphate species could be prevented, thus avoiding the undesired catalyst alkylation pathway.

Therefore, we began our exploration focusing on the development of a novel catalytic cycle in Brønsted acid catalysis, which intriguingly resembles, at first glance, a base catalyzed pathway (Scheme 4.3).<sup>41</sup> The phosphoric acid catalyst primarily establishes a hydrogen-bonding interaction with the nucleophile and this heterodimeric intermediate eventually engages the reaction with the electrophilic species.



**Scheme 4.3.** Carboxylation of aziridines *via* heterodimer intermediate

### Desymmetrization of *meso*-aziridines

At the onset of our studies we focused our attention on a desymmetrization strategy for *meso*-aziridines. In the presence of **TRIP** phosphoric acid, the ring opening of differently protected cyclohexene derived aziridines **72** with benzoic acid was explored (Table 4.1).<sup>121</sup>

**Table 4.1.** Preliminary screening of *N*-protecting group in the carboxylis of aziridines.

**72** + **BzOH** (1.6 equiv.)  $\xrightarrow[\text{CH}_2\text{Cl}_2 (0.125 \text{ M}), \text{rt, 2h}]{(S)\text{-TRIP (4 mol\%)}}$  **100**

Aziridines			entry	aziridine	conv <sup>a</sup>	notes
			1	<b>72a</b>	22%	background
			2	<b>72b</b>	12%	background
			3	<b>72c</b>	-	no reaction
			4	<b>72d</b>	<5%	degradation of <b>TRIP</b>
			5	<b>72e</b>	96%	background
			6	<b>72f</b>	<5%	degradation of <b>TRIP</b>
			7	<b>72g</b>	2%	degradation of <b>TRIP</b>
			8	<b>72h</b>	10%	degradation of <b>TRIP</b>
			9	<b>72i</b>	23% <sup>b</sup>	degradation of <b>TRIP</b>

<sup>a</sup> Determined by <sup>1</sup>H-NMR; <sup>b</sup> er = 78.5:21.5

Initial attempts confirmed the difficulties of the methodology under investigation. Presumably due to their significant basicity, unprotected or phenyl-protected substrates (**72a** and **72b**) exhibited significant background reactivity: control experiments without the phosphoric acid catalyst showed similar conversion into the desired product (entries 1-2, Table 4.1). Under these conditions **TRIP** was also found to be prone to deactivation and its alkylated species was observed by NMR investigation of the reaction mixtures. Reducing the basicity of the aziridines by tuning the nitrogen protecting group, we made an interesting observation. While sulfonyl-protected substrate **72c** was unreactive, the benzoyl-protected compound **72d** gave a rapid alkylation of the catalyst, albeit significantly lowering the background reactivity. This last experiment suggested that the simple activation by the carboxylic acid is difficult with this protecting group and therefore we promptly explored substituted benzoyl-protecting group with electronically different properties. In particular,

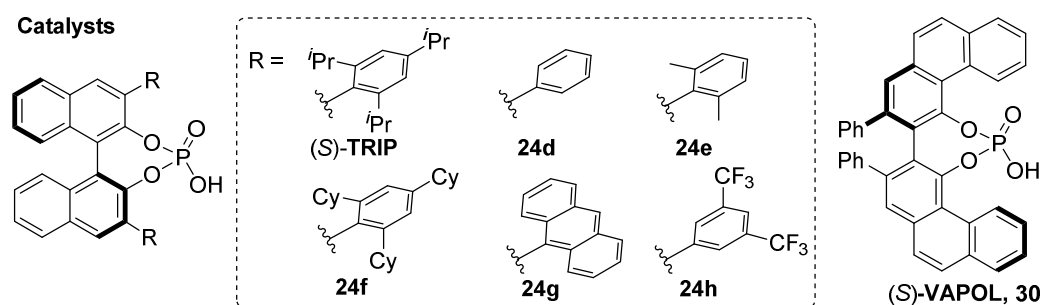
we aimed at the identification of a protecting group in which the interaction with the simple phosphoric acid could also be suppressed, favoring the activation by the more acidic heterodimeric species. The presence of an electron-donating substituent resulted again in the fast deactivation of the catalyst (entry 6, Table 4.1), while the basic nicotinic moiety was unsuitable as protecting group due to significant background reaction. Gratifyingly, electron-poor benzamide moieties gave promising results (entry 7-9, Table 4.1). Next to the common degradation of the catalyst, these reactions showed the formation of a significant amount of product. In particular, aziridine **72i**, bearing an *o*-nitro benzoyl protecting group, gave the desired protected 1,2 aminoalcohol product **100i** in 23% yield and 78.5:21.5 enantiomeric ratio (entry 9, Table 4.1).

Encouraged by this result, aziridine **72i** was selected as model substrate and, aiming at the improvement of both reactivity and selectivity, an evaluation of different chiral phosphoric acid catalyst was performed (Table 4.2). The structure of the catalyst was found to be crucial for the reaction outcome, however **TRIP** was still found to give the best results.

**Table 4.2.** Evaluation of chiral phosphoric acid catalysts in the carboxylation of **72i**.

entry	catalyst	conv <sup>[a]</sup>	er <sup>[b]</sup>	entry	catalyst	conv <sup>[a]</sup>	er <sup>[b]</sup>
1	(PhO) <sub>2</sub> POOH	-	-	6	<b>24g</b>	10%	74:26
2	( <i>S</i> )- <b>TRIP</b>	23%	78.5:21.5	7	<b>24h</b>	<5%	-
3	<b>24d</b>	<5%	nd	8	( <i>S</i> )- <b>VAPOL</b>	<5%	-
4	<b>24e</b>	<5%	54:46	g <sup>[c]</sup> ( <i>S</i> )- <b>TRIP</b> 41% 88.5:11.5			
5	<b>24f</b>	20%	77:23				

<sup>a</sup> Determined by <sup>1</sup>H-NMR; <sup>b</sup> Determined by HPLC on chiral stationary phase; <sup>c</sup> 8 mol% catalyst loading



Sterically less hindered phosphoric acids gave disappointing results, since these compounds underwent the deactivation reaction at a superior rate (entries 3,4 and 7, Table 4.2). It is worth to mention that achiral diphenyl phosphoric acid was also ineffective for the transformation (entry 1, Table 4.2) and even the preparation of the racemic product for analytical purposes had to be performed using a 1:1 mixture of **TRIP** enantiomers.<sup>81c</sup> Catalyst **24f**, bearing a significantly hindered pocket, exhibited similar performances with respect to **TRIP** (entry 5, Table 4.2),<sup>122</sup> while anthracenyl substituted catalyst **24g** gave the desired product in lower yield and selectivity (entry 6, Table 4.2). Increasing the catalyst loading of **TRIP** from 4 to 8 mol% resulted both in a higher yield and higher enantioenrichment of the desired product (entry 9, Table 4.2). In this last experiment, the turnover number of the catalyst is presumably unchanged, while the higher selectivity observed may be due to the lower detrimental effect of the residual background reactivity.

Aiming to decrease the formation of the aziridinium phosphate, thus limiting the catalyst loss, we investigated the effect of the loading of the carboxylic acid substrate on the reaction outcome. A large excess of benzoic acid may further promote the heterodimeric association and facilitate the desired reactivity through the inhibition of the decomposition pathway. As shown in Table 4.3, this parameter was found to be critical for the transformation. The rate of the catalyst deactivation was significantly lowered and a beneficial effect was observed on the yield of the desired product. When performing the reaction with 7 or 8 equivalents of benzoic acid with respect to the aziridine the desired product could be obtained in excellent yield and enantioselectivity (entries 7-8, Table 4.3). Under these conditions, an optimal balance between catalyst alkylation and background reactivity was achieved and therefore the excess of such inexpensive nucleophile was maintained during the optimization of the other reaction parameters.

The effect of the reaction medium and temperature was then carefully evaluated. Performing the reaction at 0° C in dichloromethane, the selectivity was improved to 97.5:2.5 enantiomeric ratio (entry 2, Table 4.4). However, further lowering the temperature was instead found to be detrimental (entries 3-4, Table 4.4). A little deviation in the selectivity was observed with organic non-polar solvents (entries 1, 5 and 7, Table 4.4), while in tetrahydrofuran the reactivity was completely suppressed (entry 6, Table 4.4). Presumably the presence of competing hydrogen-bond acceptors effectively impedes the self-assembly

## 4. Results and Discussion

with the catalyst. Finally, performing the reaction in chloroform at ambient temperature the desired product was obtained in quantitative yield and 98.5:1.5 enantiomeric ratio.

**Table 4.3.** Screen of the carboxylic acid loading in the carboxylation of **72i**.

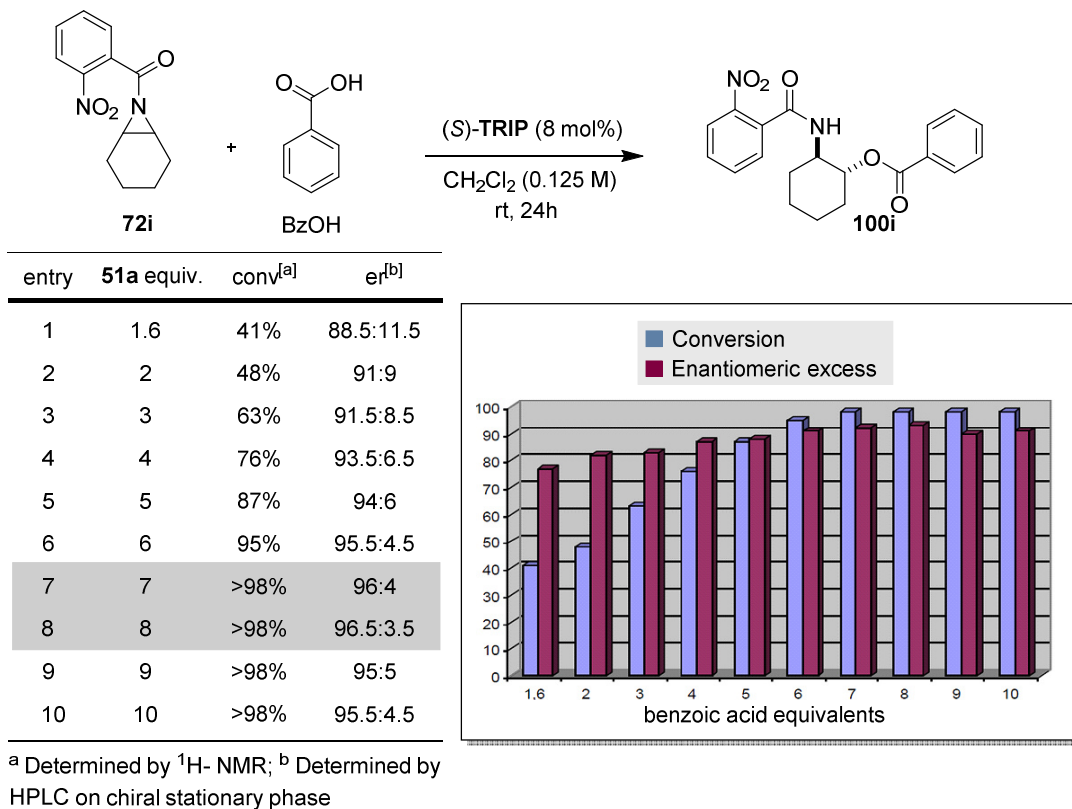
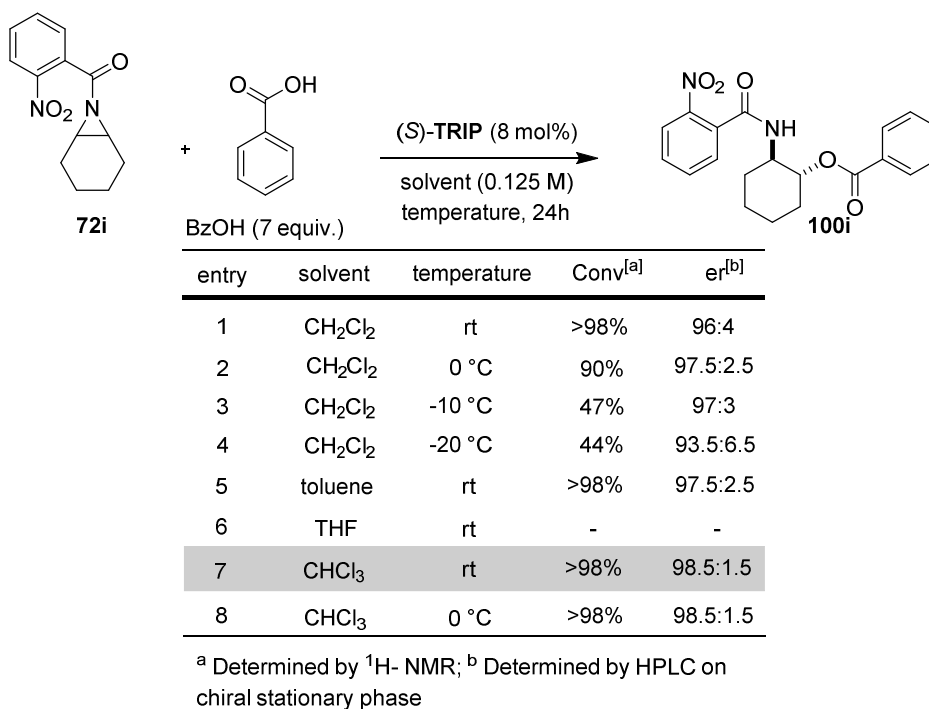
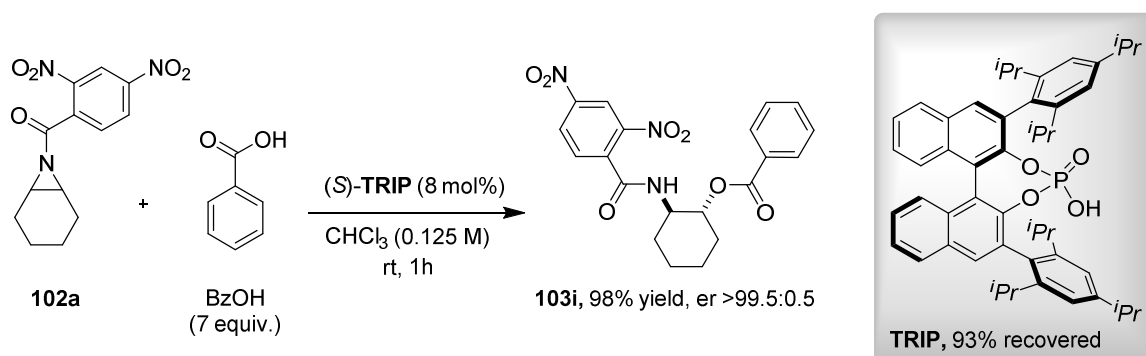


**Table 4.4.** Screen of the solvents and temperature for the carboxylation of **72i**.



Having established a suitable catalytic system for the enantioselective conversion of aziridine **72i** into the corresponding protected aminoalcohol, we were curious to evaluate the effect of an even more electron-poor benzamide moiety as protecting group. To our delight, under optimized conditions cyclohexene-derived aziridine **102a**, with nitro groups in the *ortho* and in the *para* position of the benzoyl moiety underwent the reaction in less than one hour with outstanding enantioselectivity (er = >99.5:0.5; Scheme 4.4). Moreover, the catalyst deactivation pathway was found to be completely prevented and the phosphoric acid could be almost quantitatively recovered by column chromatography.



**Scheme 4.4.** Asymmetric carboxylation of aziridine **102a** under optimized conditions.

#### Kinetic resolution of terminal aziridines

Chiral aziridines are considered linchpins for the synthesis of various building blocks such as 1,2-amino alcohols, 1,2-diamines and 1,2-thioamines.<sup>123</sup> The remarkable results obtained in the desymmetrization of *meso*-aziridines encouraged us to further apply our catalytic system to a kinetic resolution strategy for racemic terminal aziridines. It is noteworthy that in this transformation both the product and the unreacted starting material would be potentially useful. Since in a kinetic resolution the catalytic system should discriminate between two enantiomeric starting materials rather than performing an asymmetric ring opening of an achiral substrate, we expected factors governing selectivity to be slightly different from our previous optimization.

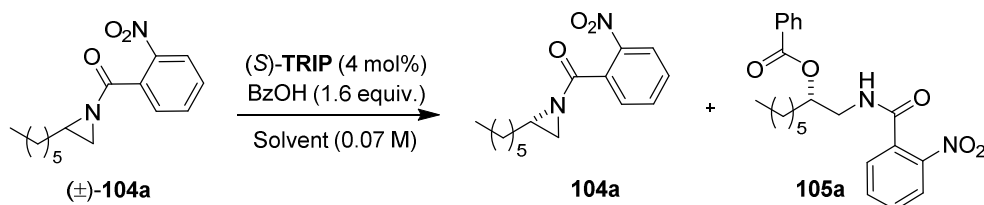
The aziridine derived from 1-octene with an *ortho* nitro-benzoyl protecting group was chosen as model system for a preliminary screening of chlorinated non-polar organic solvents (Table 4.5). Dichloromethane was found to be the most suitable solvent and the reaction proceeded with good selectivity (entry 1). Both starting material and product were



## 4. Results and Discussion

isolated in an enantioenriched form and by using the *Kagan* equation,<sup>124</sup> the selectivity factor ( $k_S/k_R$ ) was calculated to be 13.4 (entry 1, Table 4.5).

**Table 4.5.** Preliminary solvent screening for the kinetic resolution of terminal aziridine **104a**.

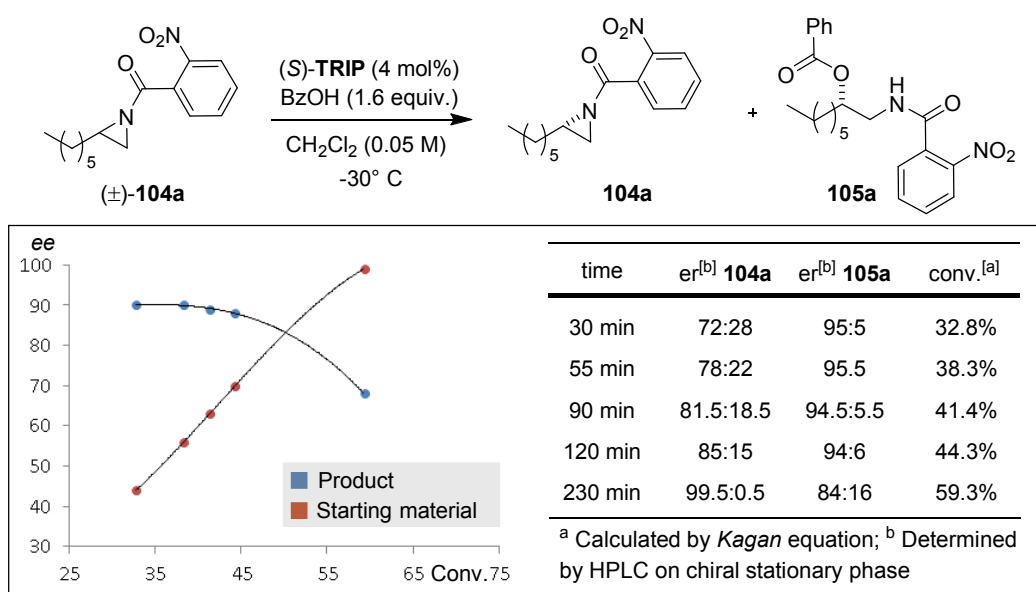


entry	solvent	time	er <sup>[b]</sup> <b>104a</b>	er <sup>[b]</sup> <b>105a</b>	Conv. <sup>[a]</sup>	s <sup>[a]</sup>
1	CH <sub>2</sub> Cl <sub>2</sub>	2h	94.8:5.2	82.1:17.9	58.2%	13.4
2	ClCH <sub>2</sub> CH <sub>2</sub> Cl	2h	72.2:27.5	85.5:14.5	38.5%	9.1
3	CCl <sub>4</sub>	2h	76:24	76:24	50%	5.2
4	CHCl <sub>3</sub>	2h	72.5:27.5	81.5:18.5	41.7%	6.8

<sup>a</sup> Calculated by the *Kagan* equation; <sup>b</sup> Determined by HPLC on chiral stationary phase

Remarkably, the ring opening occurred at the internal carbon center with perfect regiocontrol. This observation suggests that a partial positive charge on the aziridine substrate is developed in the transition state, thus directing the reaction at the most substituted center. Two possible scenarios are in line with this experimental observation: *S<sub>N</sub>1*-type process or a concerted but asynchronous substitution (cf. paragraph 2.4). However, investigating the dependence of the product enantioenrichment on the reaction progress, the involvement of a carbocationic intermediate could be excluded.

**Table 4.6.** Dependence of the enantioenrichment on the reaction progress.



In an  $S_N1$ -process, the reaction of both enantiomers of aziridine **104a** would occur *via* the same carbocation intermediate, thus giving the desired product with same enantioselectivity. However, over the course of the reaction we observed an erosion of the enantiopurity of the protected aminoalcohol **105a**, thus suggesting a borderline  $S_N2$  transformation.<sup>79</sup>

A final optimization of the reaction parameters revealed the beneficial effect of the loading of the carboxylic acid and excellent selectivity was observed by performing the reaction under cryogenic conditions (entry 3, Table 4.7). Given the positive influence observed upon introduction of a more electron-withdrawing protecting group in the desymmetrization reaction, we also attempted the kinetic resolution with aziridine **106a**, with an *ortho-para* dinitro benzamide moiety. However, in this transformation a lower selectivity was observed (entry 4, Table 4.7).

**Table 4.7.** Optimization of the kinetic resolution of terminal aziridines.

**104a**, Ar = 2-(NO<sub>2</sub>)C<sub>6</sub>H<sub>4</sub>  
**106a**, Ar = 2,4-(NO<sub>2</sub>)<sub>2</sub>C<sub>6</sub>H<sub>3</sub>

entry	aziridine	acid equiv.	time	er <sup>[b]</sup> <b>SM</b>	er <sup>[b]</sup> <b>P</b>	Conv. <sup>[a]</sup>	s <sup>[a]</sup>
1	<b>104a</b>	1.6	2h	85:15	94:6	44.5%	32.8
2	<b>104a</b>	3	2h	80:20	96:4	39.5%	44.2
3 <sup>c</sup>	<b>104a</b>	7	2.5h	98:2	92.5:7.5	53%	48
4 <sup>c</sup>	<b>106a</b>	7	16h	98:2	91:9	52%	40.0

<sup>a</sup> Calculated by *Kagan* equation; <sup>b</sup> Determined by HPLC on chiral stationary phase;

<sup>c</sup> Concentration of the reaction 0.016 M

#### 4.2.2. Reaction scope

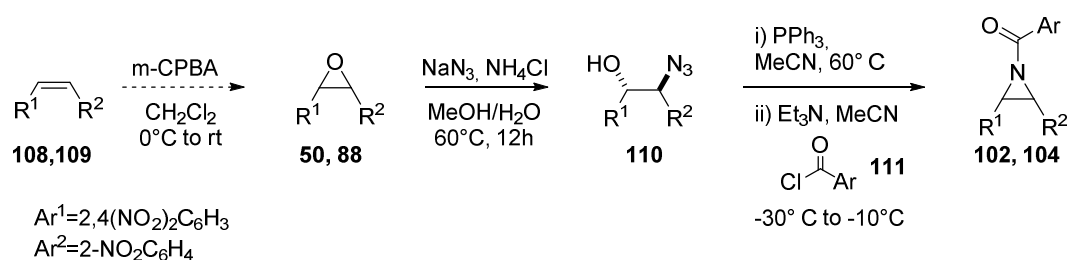
##### Preparation of starting materials

With the optimized conditions in hand, both for desymmetrization of *meso*-aziridines and kinetic resolution of terminal aziridines, we set out to explore the substrate scope of the novel asymmetric carboxylolysis reaction. The starting materials **102** and **104** were prepared

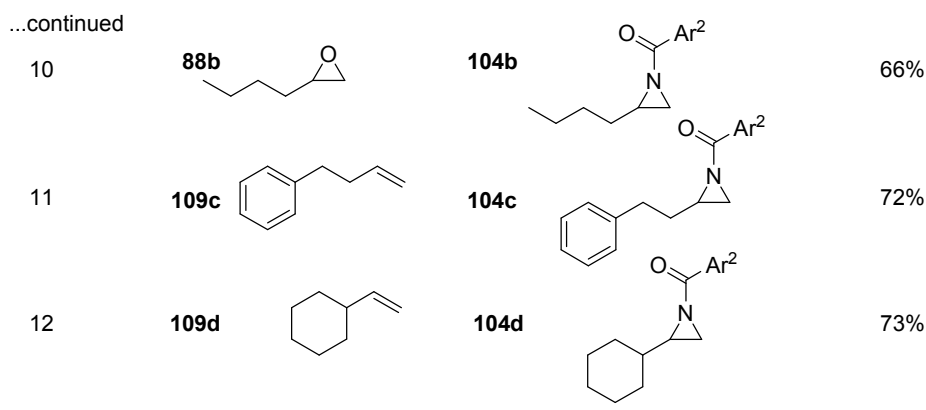
## 4. Results and Discussion

from the corresponding epoxides **50** and **88** following a three-step protocol.<sup>84a</sup> The epoxides were first subjected to an azidolysis reaction, followed by a *Staudinger* reaction and acylation in a one-pot sequence (*Blum* aziridine synthesis).<sup>125</sup> When not commercially available, epoxides **50** were prepared by *Prilezhaev* epoxidation of the corresponding olefin with *m*-CPBA (cf. paragraph 4.3.4).<sup>126</sup> Notably, the reaction sequence could be performed in a straightforward fashion with a single purification step by silica gel chromatography.

**Table 4.8.** Preparation of starting materials for the asymmetric carboxylisis.



entry	starting material	product	Yield
1	<b>50a</b>	<b>102a</b>	50%
2	<b>108b</b>	<b>102b</b>	24%
3	<b>108c</b>	<b>102c</b>	59%
4	<b>50d</b>	<b>100d</b>	42%
5	<b>50e</b>	<b>102e</b>	48%
6	<b>108i</b>	<b>102i</b>	27%
7	<b>108j</b>	<b>102j</b>	33%
8	<b>108k</b>	<b>102k</b>	30%
9	<b>88a</b>	<b>104a</b>	56%

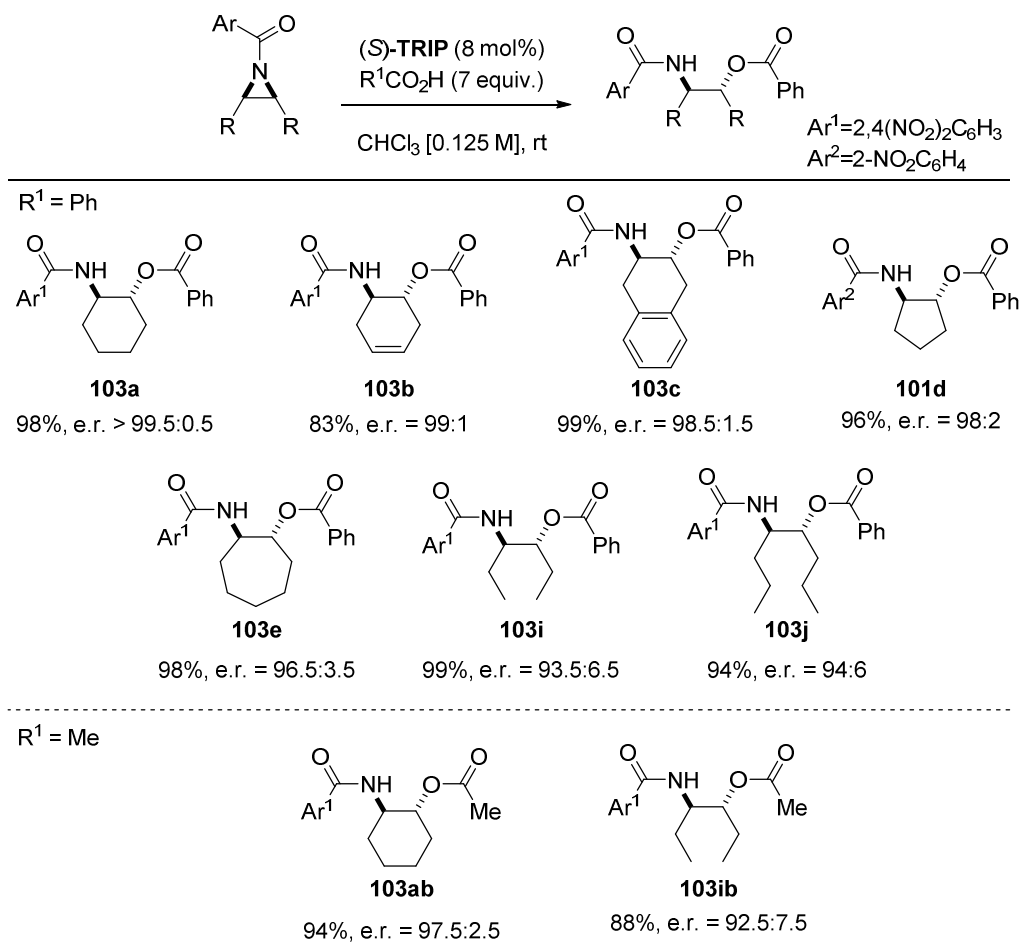


### Scope of the desymmetrization of *meso*-aziridines

With a selection of aziridines in hand, the enantioselective carboxylolysis reaction, utilizing the previously optimized conditions, was studied (Scheme 4.5). To our delight, the corresponding products were generally obtained with excellent yields and enantioselectivities and the methodology seemed to be only minorly influenced by the steric features of the starting materials. Cyclic protected aminoalcohols were obtained with outstanding results regardless the ring size and the presence of  $sp^2$  centers (products **103a-c** and **103e**). Compound **101d**, bearing a five-membered ring scaffold and only one nitro group on the benzamide moiety, was also readily reacted although lower temperature ( $-10^\circ\text{C}$ ) and more dilute conditions were required (96% yield, er = 98:2). Aziridines derived from acyclic substrates were also well tolerated although with a slight loss in stereocontrol. Protected amino alcohols **103i** and **103j** could be obtained in excellent yield and good enantiocontrol when the reaction was performed under more diluted conditions.

Other carboxylic acids are also effective in this transformation. For example, we tested substrates **102a** and **102i** in the corresponding reaction with acetic acid and similar results were obtained (products **103ab** and **103ib**, Scheme 4.5). However, the acetolysis reaction required longer reaction time and therefore a higher loading of the carboxylic acid (10 equiv.) was required to further prevent catalyst alkylation.

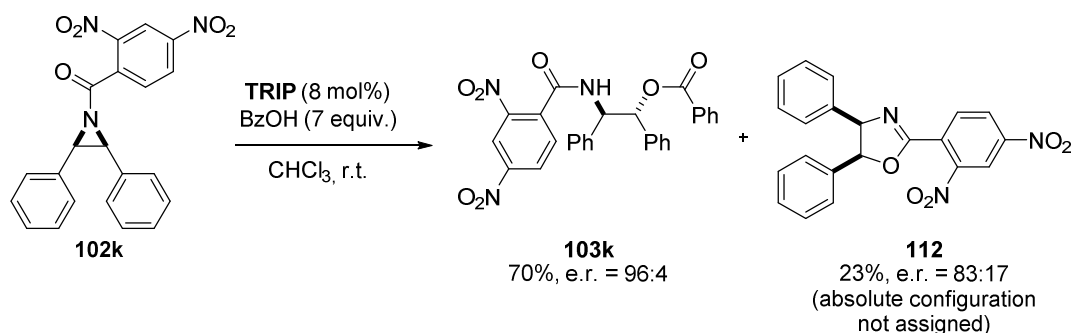
## 4. Results and Discussion



Reactions were performed on a 0.2 mmol scale. Substrate **102a** was reacted on a 1 mmol scale. Substrate **100d** was reacted at  $-10\text{ }^\circ\text{C}$  in a 0.07 M solution. The loading of AcOH in the reaction to products **103ab-ib** was increased to 10 equivalents. Enantiomeric ratios were determined by HPLC on chiral stationary phase.

### Scheme 4.5. Scope of the desymmetrization of *meso*-aziridines

An interesting observation was made while performing the catalytic carboxylation on the challenging stilbene derived aziridine **102k** (Scheme 4.6).<sup>127</sup> Under the standard reaction conditions, the desired protected 1,2-aminoalcohol product **103k** was effectively delivered (70% yield, er = 96:4) together with a significant amount of a rearranged *cis*-oxazoline **112** (23% yield, er = 83:17). Such result is presumably due to the electronic features of the substrate, since the phenyl moiety may provide an additional stabilization to a localized cationic charge at the benzylic position. Product **103k** was not observed to be converted into this byproduct; therefore, a double substitution process seems unlikely while a rearrangement occurring *via* carbocationic intermediate may be speculated.<sup>127b</sup> However, this compound was isolated with moderate enantioselectivity suggesting an important role of the chiral phosphoric acid catalyst in the process.



**Scheme 4.6.** Carboxylation of stilbene derived aziridines **102k**.

The absolute configuration of compound **103i** was determined by comparison of the optical rotation of the *N*-Boc aminoalcohol readily obtained by Boc-protection and basic hydrolysis, with a literature value (*R,R*). The configurations of other 1,2-aminoalcohol products were assigned by analogy.<sup>128</sup>

#### Scope of the kinetic resolution of terminal aziridines

The investigation on the scope of the kinetic resolution of terminal aziridines further confirmed the potential of the developed asymmetric methodology. As shown in Table 4.9, not only linear chain aziridines **104a,c** were suitable for the resolution, but even the branched compound **104d** was found to be smoothly converted to product under optimized conditions. Rewardingly, all the substrates tested in the transformation were generally converted with excellent selectivity factors (from 37 to 51), affording both the ring opened products and the unreacted starting materials in high enantiopurity.

Compound **105a** was subjected to a straightforward Boc protection/hydrolysis sequence providing the corresponding *N*-Boc aminoalcohol. The comparison of the optical rotation with a literature value allowed the assignment of the absolute configuration (*S*) and the configurations of the other products were assigned by analogy.<sup>129</sup> It is intriguing that the desymmetrization reaction gives enantioselectively the (*R,R*)-aminoalcohol while the kinetic resolution preferentially converts the (*R*)-aziridine (cf. paragraph 4.2.3).

**Table 4.9.** Kinetic resolution of terminal aziridines.

entry	recovered aziridine	Yield	er <sup>[b]</sup>	product	Yield	er <sup>[b]</sup>	S <sup>[c]</sup>
1		42%	98:2		48%	92.5:7.5	48
2		46%	95.5:4.5		49%	94:6	50
3		44%	98.5:1.5		51%	92.5:7.5	51
4		58%	71.5:28.5		28%	96:4	37

[a] Reactions performed on 0.1 mmol scale in a 0.016 M solution. [b] Determined by HPLC on chiral stationary phase. [c] Measured by the *Kagan* equation.

#### 4.2.3. Discussion

The established asymmetric carboxylolysis gives access to highly enantioenriched protected aminoalcohols and represents the first enantioselective ring opening of aziridines with an oxygen nucleophile. The key to the success of the methodology was the prevention of the phosphoric acid catalyst deactivation pathway *via* heterodimeric self-assembly. Fascinated by the mechanistic features of the methodology, we further investigated the reaction profile by NMR analysis in order to gain further insights on the new catalytic mode.

Our optimization studies revealed that the desired pathway could be unlocked by matching the electronic properties of protecting group of the nitrogen atom with a proper loading of the carboxylic acid nucleophile. In this way optimal conditions have been identified and the catalyst could be also recovered from the reaction mixture. We therefore

## 4. Results and Discussion

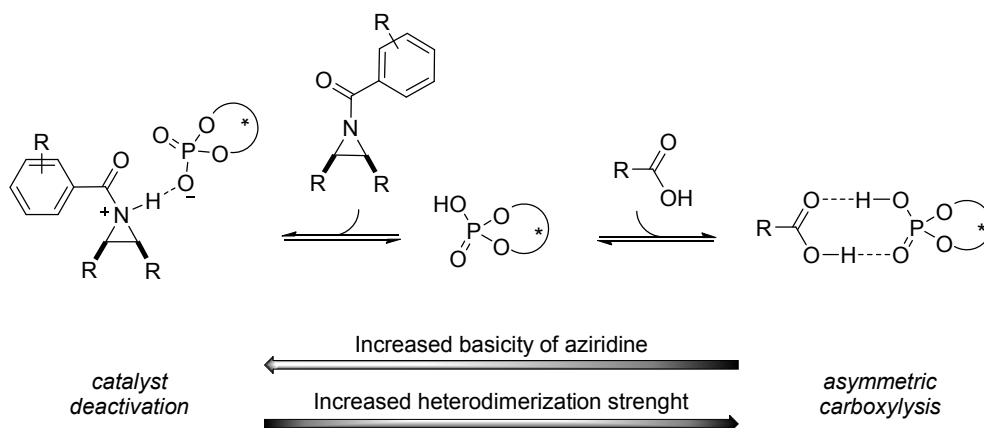
decided to examine more carefully this fine tuning and we decided to monitor the alkylation of catalyst by  $^{31}\text{P}$ -NMR in the reaction with differently protected aziridines. In particular, we set out the investigation of the carboxylation of **72d**, **72i** and **102a** with benzoic acid and acetic acid (Table 4.10).

**Table 4.10.** Comparative evaluation of the effect of the protecting group and carboxylic acid.

	Ar = <b>72d</b>	<b>72i</b>	<b>102a</b>
 10 equiv.	20 min Desired product Yield < 5% Degradation of the catalyst = full	10 min Desired product Yield = 15% Degradation of the catalyst > 95%	10 min Desired product Yield = 35% Degradation of the catalyst = 15%  18 h Desired product Yield > 95% Degradation of the catalyst = 55%
 7 equiv.	40 min Desired product Yield < 5% Degradation of the catalyst = full	5 min Desired product Yield = 48% Degradation of the catalyst = 20%  60 min Desired product Yield = 88% Degradation of the catalyst = 63%	10 min Desired product Yield = 88% Degradation of the catalyst = 0%  30 min Desired product Yield = quant Degradation of the catalyst = 0%

As expected, these experiments showed a defined trend. A fast catalyst deactivation is obtained when employing more electron-rich aziridines in combination with acetic acid (up-left corner, Table 4.10), while the desired product is preferentially formed by utilizing benzoic acid and an electron-poor protecting group (right-down corner, Table 4.10). Taking into consideration the simple acid-base equilibrium for the formation of the aziridinium phosphate, lowering the affinity of the aziridine for the acidic catalyst by decreasing its basicity was found to exhibit a beneficial effect. We also realized that our evaluation of the binding constants of heterodimers had revealed a higher tendency for the association of **TRIP** with benzoic acid rather than with acetic acid. Therefore, confirming our initial hypothesis, our exploration suggested that favoring the formation of an aziridinium phosphate intermediate accelerates the alkylation of the catalyst, while a more stable self-assembly with carboxylic acids favors the desired carboxylation (Scheme 4.7).





**Scheme 4.7.** Generalised results of the effect of the basicity of the aziridine substrates and the heterodimerization strength on the reaction outcome.

Moreover, the heteroconjugation effect should increase the acidity of the dimeric species with respect to the simple phosphoric acid, thus allowing a selective activation for the heterocycle with lower Lewis basicity. From this point of view, **TRIP**·BzOH heterodimer is more stable than **TRIP**·AcOH but also presumably more acidic, due to the higher acidity of the carboxylic acid molecule. On this basis, the reactivity scale observed can also find a reasonable mechanistic support in the *Bell-Evans-Polanyi* principle.<sup>130</sup>

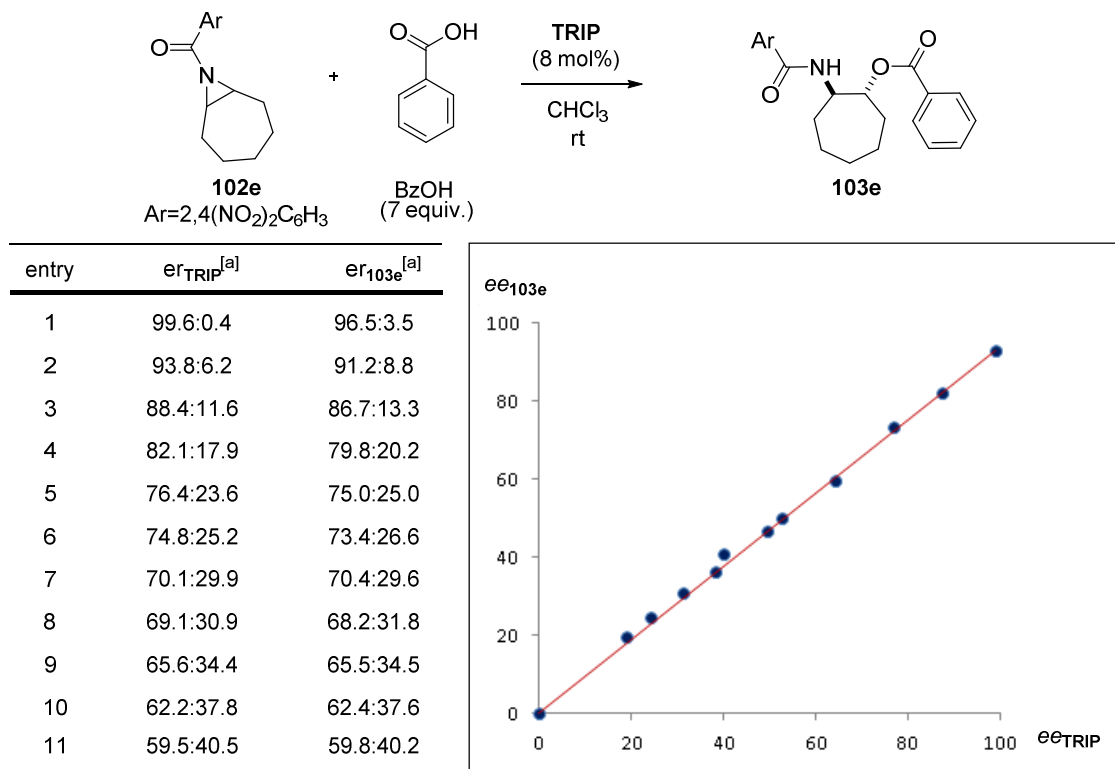
### Transition state model

Based on the experimental results we speculate that the reaction might occur *via* an asynchronous  $S_N2$  pathway and that the heterodimeric complexation is a crucial intermediate along the reaction coordinate to avoid the direct degradation of the catalyst. The involvement of a carbocationic intermediate is unlikely because of the exclusivity of the *anti*-product in the desymmetrization, while the complete regioselectivity of the kinetic resolution suggests the presence of a localized  $\delta^+$ -charge at the reacting carbon center.

The presence of two molecules of the catalyst in the transition state of the stereodiscriminating event would provide a very crowded arrangement and therefore is unlikely. However, in order to exclude this possibility we performed a study of non-linear effects by employing scalemic mixtures of **TRIP** as the catalyst in the ring opening of **102e** (Table 4.11).<sup>131</sup> The experiment shows a linear correlation between the enantioenrichment of the isolated product and the enantiopurity of the catalyst used, thus suggesting that in

the transition state one molecule of the catalyst simultaneously interacts with both coupling partners.

**Table 4.11.** Study of non-linear effects in the carboxylation of **102e**.



<sup>a</sup> Determined by HPLC on chiral stationary phase

Although a proper stereochemical rationalization is currently not available, the identification of the main parameters which contribute to enantioselective catalysis is of certain interest. Our speculations can be based on two assumptions: (1) the activation of the heterocycle may occur *via* the direct protonation of the nitrogen atom, due to the high *s* character of the corresponding lone pair and (2) both the *trans*- and *cis*-invertomers of the aziridine can engage the heterodimer.

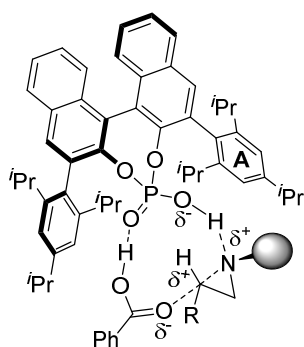


**Figure 4.7.** Transition state model for the carboxylation of aziridines.

The benzamido moiety is the widest stereo-discriminating element of the substrate and thus it preferentially avoids the catalyst bulky substituent **A** (Figure 4.7). The reaction of the *cis*-invertomer (less thermodynamically favored) may further reduce the non-stabilizing interaction of the R-group with the catalyst, while the *trans*-invertomer would reduce the steric clash within the substrate.

Possibly, the energetic difference between these competitive pathways results in the remarkable selectivity towards (*R,R*)-aminoalcohols in the desymmetrization protocol and in the selective transformation of the *R*-aziridine in the kinetic resolution.

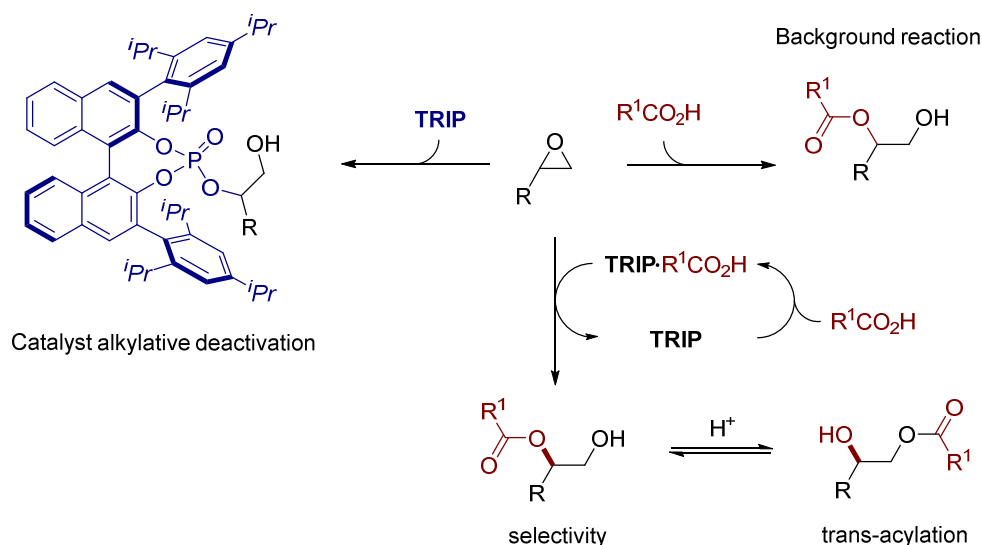
### 4.3. Asymmetric hydrolysis of epoxides in organocatalysis<sup>132</sup>

The excellent reactivity shown by our catalytic system in the asymmetric ring opening of aziridines prompted us to investigate this novel concept in reactions with different electrophiles. Given the high synthetic interest of epoxide hydrolysis reactions, we aimed at the development of the first asymmetric metal-free approach by coupling a stereoselective carboxylation with the mild hydrolysis of the formed ester product. This methodology would be particularly useful if applicable both to the desymmetrization of *meso*-epoxides and to the kinetic resolution of chiral racemic substrates.

*The work described in this section was performed in collaboration with Dr. S. Prévost.*

#### 4.3.1. Reaction design and initial optimization

With respect to the carboxylation of aziridines, the development of a related transformation on the epoxide ring system may encounter more difficulties (Scheme 4.8).



**Scheme 4.8.** Envisioned issues for the asymmetric carboxylation of epoxides.

In fact, the undesired tendency towards catalyst alkylation was expected and the absence of a tunable protecting group for the oxygen heteroatom, in analogy with the aziridine protection, significantly increased the chance of catalyst deactivation.<sup>80</sup> Moreover, next to a possible competing background reaction by means of carboxylic acid catalysis, the facile acid-catalyzed trans-acylation reaction on the obtained products would yield an

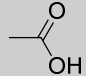
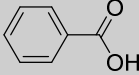
additional regioisomer, thus rendering the reaction profile more complex. Considering the possible asymmetric induction, we also hypothesized that the lack of the stereo-discriminating protecting group of the aziridine in the transition state would presumably render enantioselective catalysis significantly challenging.

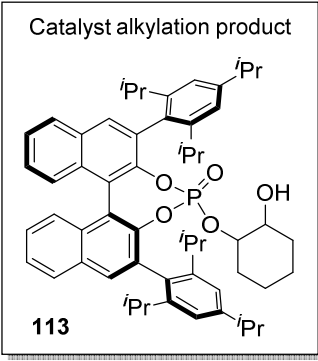
### Desymmetrization of *meso*-epoxides

Since the possible trans-acylation reaction is degenerative for monoesters derived from  $C_2$ -symmetric diols,<sup>63</sup> we initially focused our attention on the development of a desymmetrization strategy and we selected cyclohexene oxide **50a** as the model substrate.

Confirming the instability of phosphoric acids with oxiranes previously described by *Chan and Di Raddo*,<sup>80</sup> at the beginning of our exploration we verified a remarkable reactivity of **TRIP** catalyst towards the alkylative deactivation (entry 1, Table 4.12). As expected, this fast decomposition effectively hampers a possible catalyzed reaction with alcohol nucleophiles (entries 2-3, Table 4.12) whereas, to our delight, the approach *via* heterodimeric self-assembly was successful. Indeed, both the reactions with acetic acid and benzoic acid yielded the desired product in good yield and moderate selectivity (entries 4-5, Table 4.12).

**Table 4.12.** Initial studies towards the ring-opening of **50a** catalyzed by **TRIP**.

entry	ROH	conv <sup>[a]</sup>	er <sup>[b]</sup>	notes
1 <sup>[c]</sup>	-	>98%	dr = 2:1 <sup>[a]</sup>	TRIP alkylation
2	MeOH	-	-	TRIP alkylation
3	PhOH	-	-	TRIP alkylation
4		85%	79:21	TRIP alkylation
5		>98% (96%) <sup>[d]</sup>	78.5:21.5	TRIP alkylation detected



Catalyst alkylation product  
**113**

<sup>a</sup> Determined by <sup>1</sup>H- NMR; <sup>b</sup> Determined by HPLC on chiral stationary phase;

<sup>c</sup> Loading of **TRIP** 1 equiv.; <sup>d</sup> Isolated yield

## 4. Results and Discussion

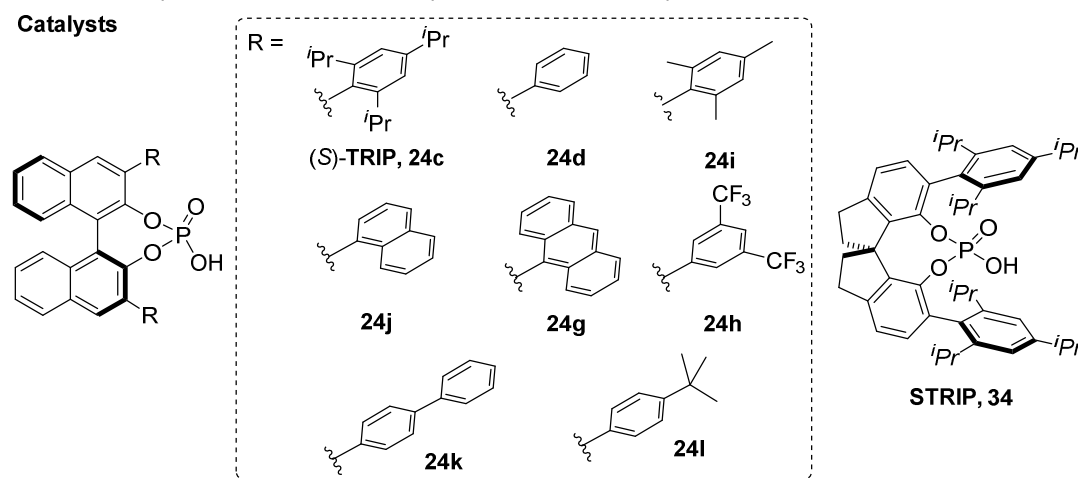
Despite the success of both carboxylic acid nucleophiles in this transformation, it is worth to mention that the reaction with acetic acid was found to be slower and the competing alkylation of **TRIP** occurred more significantly, thus confirming our previous expectations.

The moderate selectivity observed in these initial studies encouraged us to evaluate different phosphoric acid catalysts (Table 4.13). Disappointingly however, all the common phosphoric acid catalysts, bearing less hindered catalyst pockets were found to exhibit a higher alkylation rate and the desired glycol monoester product was obtained always in residual amount and in very low enantiopurity. The catalyst **34** (**STRIP**), derived from a SPINOL backbone, was also found to be similarly selective to **TRIP**,<sup>54</sup> however the product was obtained in lower yield (entry 10, Table 4.13).

**Table 4.13.** Preliminary screen of phosphoric acid catalysts for the acetolysis of **50a**.

entry	catalyst	Conv <sup>[a]</sup>	er <sup>[b]</sup>	entry	catalyst	Conv <sup>[a]</sup>	er <sup>[b]</sup>
1	(PhO) <sub>2</sub> POOH	<5%	-	6	<b>24g</b>	nd	53.5:46.5
2	( <i>S</i> )- <b>TRIP</b>	85%	79:21	7	<b>24h</b>	<5%	56:44
3	<b>24d</b>	<5%	51.5:48.5	8	<b>24k</b>	<5%	50:50
4	<b>24i</b>	<5%	54:46	9	<b>24l</b>	<5%	46.5:53.5
5	<b>24j</b>	<5%	47.5:52.5	10	<b>STRIP, 34</b>	nd	20:80

<sup>a</sup> Determined by <sup>1</sup>H- NMR; <sup>b</sup> Determined by GC on chiral stationary phase

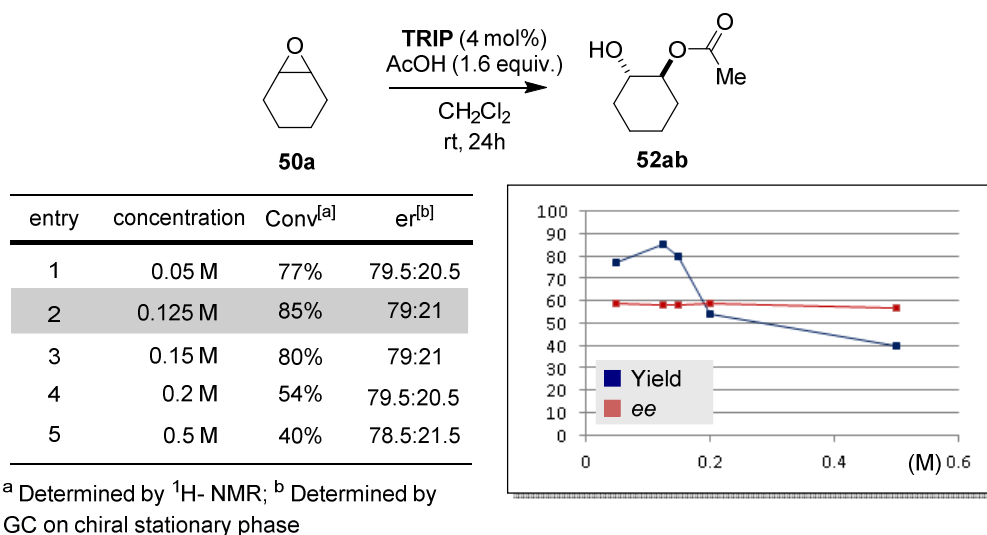


Therefore **TRIP** was selected as the most promising catalyst and a careful evaluation of the other reaction parameters was undertaken. As shown in Table 4.14, the yield of the

## 4. Results and Discussion

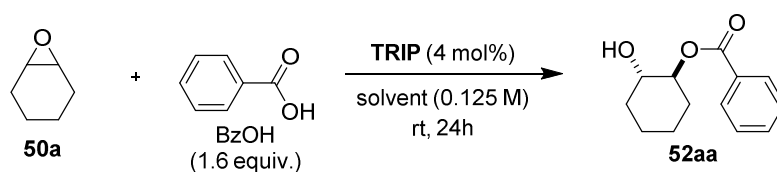
reaction was significantly influenced by the concentration of the mixture, while the enantioselectivity was found to be essentially insensitive. Upon diluting the reaction mixture the rate of the transformation was decreased. Conversely, a concentration led to a significant degradation in yield due to the more effective catalyst deactivation.

**Table 4.14.** Concentration screening for the acetolysis of **50a**.



With a clear optimization of the reaction concentration in hand, the nature of the solvent was investigated (Table 4.15). Notably, this study revealed that the level of enantioselectivity was maintained in all non-polar media tried. Using benzoic acid as nucleophile, the yield was always excellent, with the only exception of cyclohexane due to solubility issues (entry 5, Table 4.15). Polar aprotic solvents instead were not suitable for the reaction (i.e. tetrahydrofuran; entry 8, Table 4.15), presumably due to the interference with the establishment of hydrogen bonding assemblies. Lowering the temperature was found to have a beneficial influence on the selectivity of the transformation and, under cryogenic conditions the enantiomeric ratio was improved to 86:14, albeit with a detrimental effect on the reactivity (entry 11, Table 4.15).

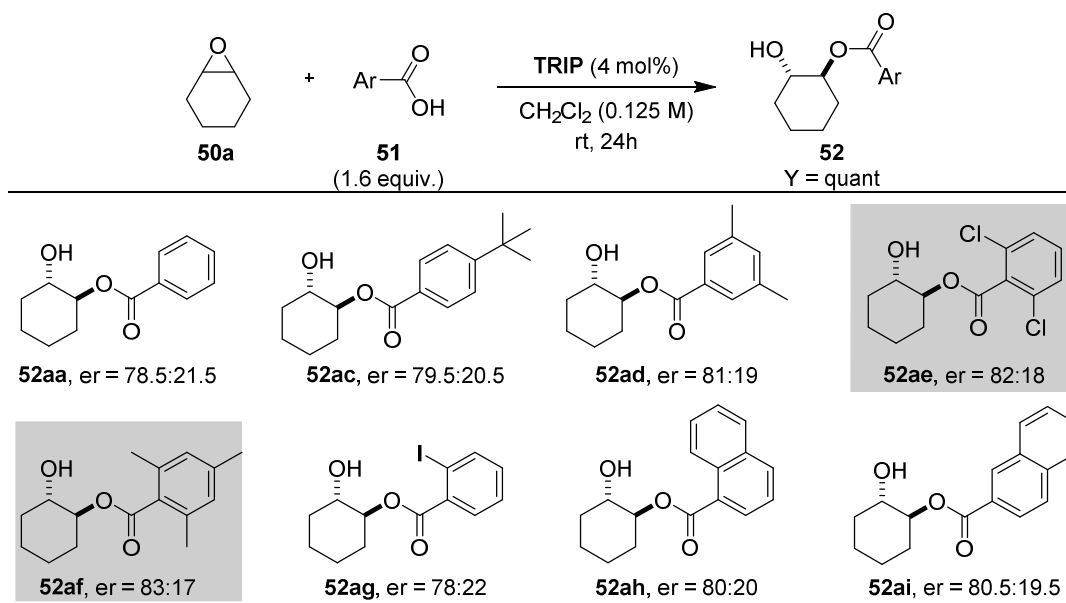
Hoping to further differentiate the energy of the diastereotopic transition states leading to the opposite enantiomers, we explored the effect of different carboxylic acid nucleophiles (Scheme 4.9). Various substituted benzoic acids were reacted and the corresponding products were always obtained with excellent yields.

**Table 4.15.** Solvent and temperature evaluation in the carboxylisis of **50a**.

entry	solvent	temperature	Conv <sup>[a]</sup>	er <sup>[b]</sup>
1	CH <sub>2</sub> Cl <sub>2</sub>	rt	>98%	78.5:21.5
2	CH <sub>3</sub> Cl	rt	>98%	75.5:24.5
3	CCl <sub>4</sub>	rt	92%	79:21
4	(CH <sub>2</sub> Cl) <sub>2</sub>	rt	>98%	76.5:23.5
5	cyclohexane	rt	22%	75.5:24.5
6	benzene	rt	>98%	77:23
7	toluene	rt	94%	78.5:21.5
8	THF	rt	<5%	-
9	CH <sub>2</sub> Cl <sub>2</sub>	-10° C	>98%	83:17
10	CH <sub>2</sub> Cl <sub>2</sub>	-20° C	96%	84:16
11	CH <sub>2</sub> Cl <sub>2</sub>	-30° C	72%	86:14

<sup>a</sup> Determined by <sup>1</sup>H- NMR; <sup>b</sup> Determined by HPLC on chiral stationary phase

A low but non-negligible effect on the enantioselectivity was observed and curiously, the highest results were obtained when reacting *ortho,ortho*-disubstituted benzoic acids **51e** and **51f**, which have a significant torsional angle between the phenyl ring and the carboxylate moiety.



Yield determined by <sup>1</sup>H- NMR; Er determined by HPLC on chiral stationary phase

**Scheme 4.9.** Evaluation of different carboxylic acids in the ring opening of **50a**.



## 4. Results and Discussion

An additional temperature screening was also attempted for 2,4,6-trimethyl benzoic acid and 2,6-dichloro benzoic acid (Table 4.16). Upon lowering the temperature to -35° C the product **52af** was obtained with 90.5:9.5 enantiomeric ratio but with reduced conversion (entry 3, Table 4.16). Instead, the transformation with dihalogenated benzoic acid showed a significantly improved reactivity and could be performed at -55° C obtaining excellent yield and 93:7 enantiomeric ratio (entry 9, Table 4.16). Presumably the high acidity of this carboxylic acid ( $pK_{a_{H_2O}} = 1.82$ )<sup>133</sup> further strengthen the heteroconjugation effect, thus explaining such remarkable reactivity.

**Table 4.16.** Temperature screening with different carboxylic acids.

Reaction scheme: Epoxide **50a** + Carboxylic acid **51** (1.6 equiv.)  $\xrightarrow[\text{CH}_2\text{Cl}_2 (0.125 \text{ M}), \text{rt}, 24 \text{ h}]{\text{TRIP (4 mol\%)}}$  Product **52af** (Ar = Mes) or **52ae** (Ar = 2,6-Cl<sub>2</sub>Ph)

entry	carboxylic acid	temperature	conv <sup>[a]</sup>	er <sup>[b]</sup>
1	 <b>51f</b>	rt	>98%	83:17
2		-20° C	76%	89:11
3		-35° C	55%	90.5:9.5
-----				
4	 <b>51e</b>	rt	>98%	82:18
5		-20° C	>98%	88.5:11.5
6		-35° C	84%	89:11
7		-40° C	96% <sup>[c]</sup>	90:10
8		-50° C	89% <sup>[c]</sup>	91.5:8.5
9	-55° C	91% <sup>[d]</sup>	93:7	

<sup>a</sup> Determined by <sup>1</sup>H-NMR; <sup>b</sup> Determined by HPLC on chiral stationary phase; <sup>c</sup> reaction time 42h; <sup>d</sup> reaction time 96h

Despite not yet being satisfactory, the good enantioselectivity obtained in this last transformation encouraged us in again evaluating the role of the phosphoric acid catalyst. The above-mentioned lack of stereo-controlling elements in the epoxide substrate rendered the optimization of the reaction quite challenging; however, upon modifying the steric properties of the nucleophile a noteworthy effect was identified. The beneficial effect given by *ortho*-substituents suggested that the selectivity might be improved by further crowding the transition state. Therefore, we decided to re-evaluate the organic catalyst, this time exploring a fine modulation of the highly hindered active site. In particular, BINOL-derived phosphoric acids with 2,6-diisopropyl aryl substituents were tested (Table 4.17).<sup>134</sup>

**Table 4.17.** Re-evaluation of the phosphoric acid: screen of highly hindered catalysts.

entry	catalyst	acid	conv <sup>[a]</sup>	er <sup>[b]</sup>
1	(S)-TRIP	51a	>98%	78.5:21.5
2	24m	51a	>98%	81.5:18.5
3	24n	51a	>98%	76.5:23.5
4	24o	51a	82%	82:18
5	24f	51a	>98%	78.5:21.5
6 <sup>[c]</sup>	24m	51f	39%	91:9
7 <sup>[d]</sup>	24o	51f	38%	86.5:13.5
8 <sup>[c]</sup>	24o	51e	>98%	90.5:9.5
9 <sup>[d]</sup>	24f	51e	78%	77.5:22.5

**Catalysts**

R =

(S)-TRIP, 24c

24m

24n

24o

24f

**Carboxylic acids**

51a

51e

51f

<sup>a</sup> Determined by <sup>1</sup>H- NMR; <sup>b</sup> Determined by HPLC on chiral stationary phase; <sup>c</sup> Performed at -40 °C; <sup>d</sup> Performed at -20° C

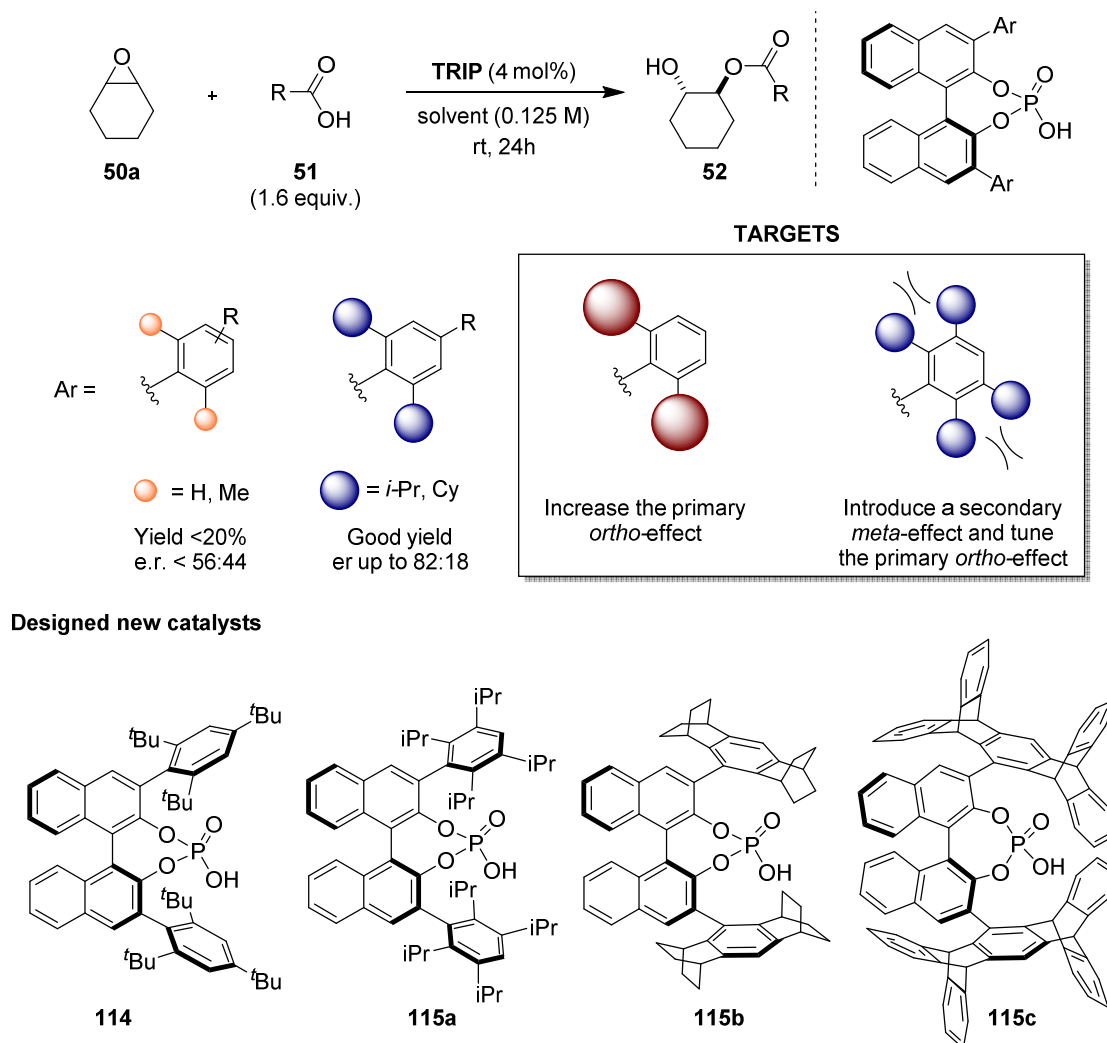
Interestingly, catalyst **24m** with unsubstituted *para*-position performed slightly better than **TRIP** (entry 2, Table 4.17),<sup>134a</sup> while **24n** bearing a bulky adamantyl moiety in that position was found to be less selective (entry 3, Table 4.17).<sup>134b</sup> The highest selectivity was obtained with catalyst **24o**,<sup>134c</sup> however the product was formed with a lower conversion (entry 4, Table 4.17).

Hoping to match the combination of the catalyst and the substituted carboxylic acids, we tried the reaction using **50e** and **50f** as nucleophiles under cryogenic conditions (entries 6-9, Table 4.17). However, our expectations were not fulfilled and no improvement was obtained on the selectivity with respect to the corresponding **TRIP**-catalyzed transformations.

### 4.3.2. Catalyst design and synthesis

As the optimization process clearly revealed the requirement of even more sterically demanding phosphoric acids, we attempted the design and the synthesis of an optimal

catalyst. In fact, although hindered active sites are commonly useful in asymmetric catalysis (cf. paragraph 2.2.2), we surprisingly realized that this particular class of phosphoric acid catalysts, by contrast, was significantly underrepresented. Therefore, the development of novel types of bulky catalysts would not only be a possible solution for the carboxylation reaction but at the same time the new catalysts may find applications in various methodologies. Our investigations were targeted towards two different goals (Scheme 4.10).



**Scheme 4.10.** Design of confined chiral phosphoric acid catalysts.

On the one hand, the introduction of even more sterically-demanding fragments in the *ortho*-position of the 3-3' aryl substituent should result in an enlargement of the steric features. Such modification could potentially develop a higher *van der Waals* strain, thus affecting the torsional angle of the C-C bond between the phenyl ring and the binaphthyl backbone. On the other hand a combined *ortho-meta* substitution pattern had never been

explored. We wondered whether the additional presence of an alkyl fragments in the *meta*-position could contribute to enantioselective transformations by introducing a secondary effect and by simultaneously providing a fine tuning of the primary effect of the *ortho*-substituent.<sup>135</sup>

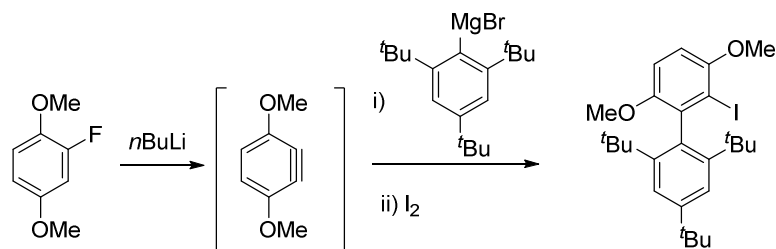
Aiming towards the evaluation of our hypotheses, we designed and developed synthetic routes towards catalysts **114** and **115a-c**.

### Synthesis of **114**

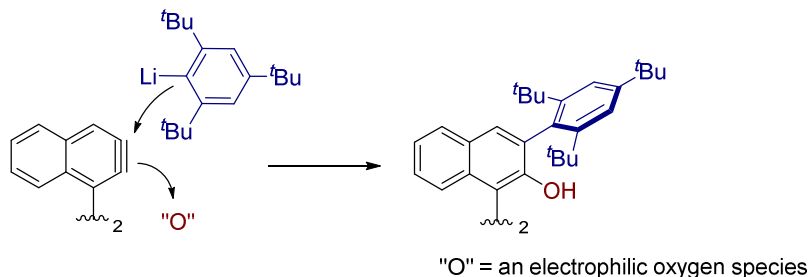
Despite appearing as a simple member of the family of 3,3'-Bis(2,4,6-trisubstituted phenyl)-BINOL phosphoric acids, catalyst **114** has never previously been reported, presumably due to the significant difficulties encountered during the synthesis. In fact, a metal-catalyzed cross coupling reaction is usually exploited to assemble biaryl compounds; however, this type of transformation is challenging when the two coupling partners are relevantly hindered. As an example, the synthesis of **TRIP** has to be accomplished through a Ni-catalyzed *Kumada* reaction,<sup>53</sup> while the robust *Suzuki-Miyaura* coupling is instead generally used for the preparation of less bulky catalysts.<sup>49,50</sup> Nevertheless, similar protocols were found to be unsuccessful for the preparation of catalyst **114**. More in general, the *Schimdt* group have so far reported the only example of cross coupling reaction with an *ortho,ortho*-ditertbutyl aryl fragment and this lack of methodologies further highlights the synthetic challenge of our goal.<sup>136</sup>

Over the years, many attempts toward **114** have been tried in our laboratories, unfortunately without any significant breakthrough. Performing the *Kumada*-type coupling under various conditions resulted in no desired biaryl coupling. Furthermore, *Suzuki-Miyaura* conditions lead to disappointing results, as independently reported by the *Buchwald* group.<sup>137</sup>

Fascinated by such synthetic challenge, we focused our attention on the methodology described by *Buchwald* for the synthesis of bulky biaryl phosphine ligands.<sup>138</sup> A completely novel route towards chiral binaphthyl phosphoric acids was designed aiming at the exploitation of the reactivity of aryne intermediates (Scheme 4.11).

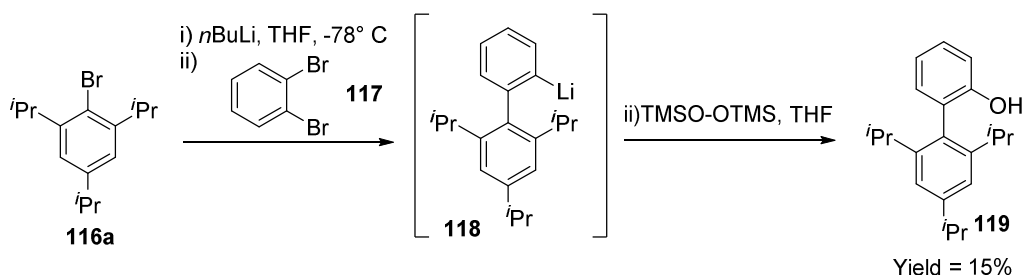
Buchwald *et al.* - Coupling *via* aryne intermediate for hindered phosphine ligands

## Designed approach to BINOL-derivatives



**Scheme 4.11.** Access to hindered biaryl fragments: synthesis of phosphine ligands *via* aryne intermediates and designed approach to BINOL derivatives.

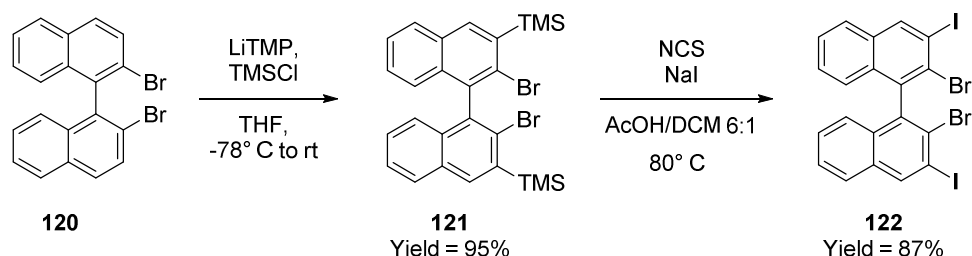
We hypothesized that a 1,2-dihalogenated aryl substrate may undergo a controlled lithium halogen exchange in the presence of an excess of a hindered aryl lithium species, thus generating *in situ* the corresponding aryne compound *via* elimination of lithium halide.<sup>139</sup> This reactive intermediate may promptly react with the excess of the organolithium species, thus yielding a biaryl lithium species, which could be eventually trapped by an electrophilic oxygen reagent (i.e. TMS-peroxide).<sup>140</sup> Indeed, this elegant one-pot protocol was attempted using 1,2-dibromobenzene and 2,4,6-triisopropyl bromobenzene as model system and the isolation of the corresponding compound confirmed the feasibility of such synthetic plan (Scheme 4.12).



**Scheme 4.12.** Model study for the synthesis of hindered biaryl compounds.

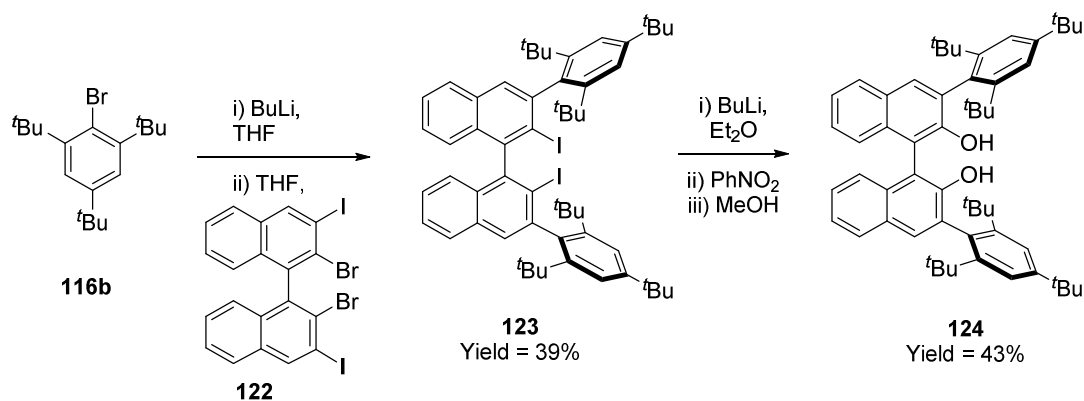
Encouraged by this preliminary result, we set out the synthesis of the targeted catalyst. Tetrahalogenated binaphthyl compound **122** was straightforwardly prepared by a

simple *ortho*-silylation followed by an *ipso*-desilylation/halogenation reaction (Scheme 4.13).<sup>141, 142</sup> The synthetic procedure was developed using racemic starting material due to the envisioned low racemization barrier for the chiral aryne intermediate, which may have in any case resulted in the deterioration of the enantioenrichment.



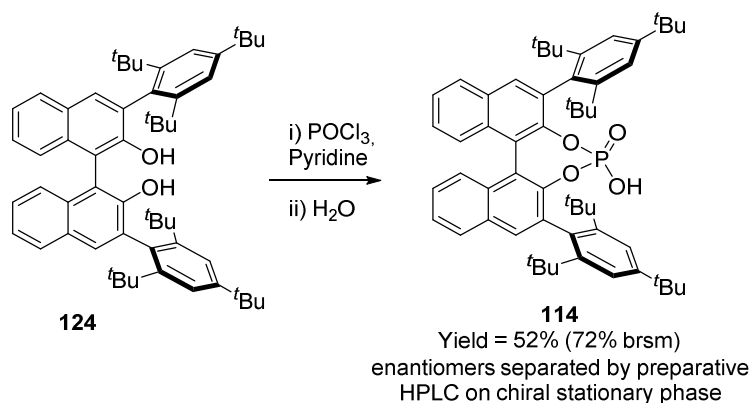
**Scheme 4.13.** Preparation of compound **122**.

We then attempted the simple one-pot protocol, which gave promising results in the model studies. Despite the poor solubility of **122** under the reaction conditions, the aryne intermediate was generated quantitatively due to the mass action law and the biaryl coupling occurred as expected. However, to our surprise, the addition of TMS-peroxide was unfruitful and we isolated the iodinated species **123** instead of binaphthol compound **124**. This outcome may be due to an unexpected lithium-halogen exchange from the organolithium intermediate; such reactive intermediate could effectively propagate a chain-type mechanism.<sup>139b</sup> Indeed, simply avoiding the final addition of the electrophilic oxygen reagent, product **123** was obtained in moderate yield (39%, Scheme 4.14). The conversion of compound **123** into the desired BINOL-derivative **124** was eventually achieved using the oxygenation procedure previously developed by *Power* and coworkers for the preparation of highly hindered phenols (Scheme 4.14).<sup>143</sup>



**Scheme 4.14.** Preparation of binaphthol **124**.

Unexpectedly, the final formation of the phosphoric acid suffered from a remarkably slow formation of the phosphoryl chloride intermediate; nevertheless, the desired compound could be obtained and the racemic mixture was resolved by preparative HPLC on chiral stationary phase (Scheme 4.15).



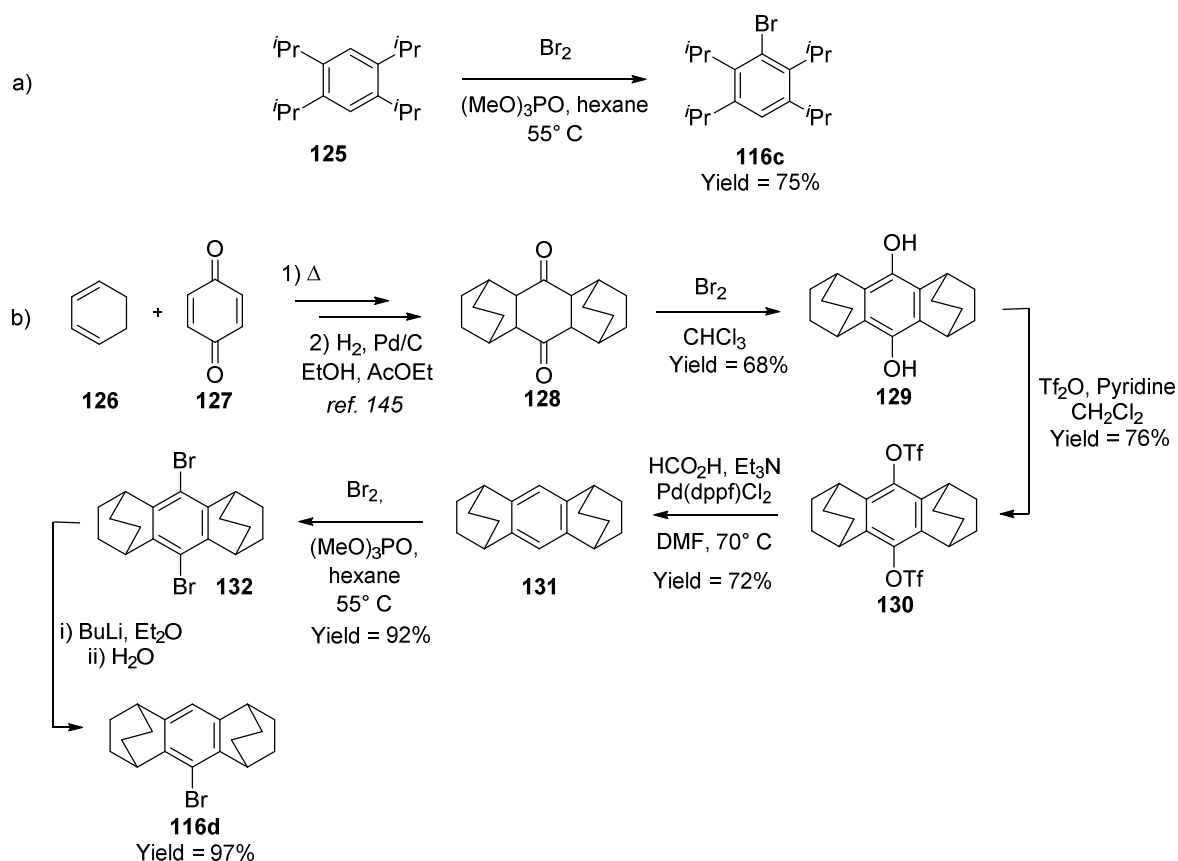
**Scheme 4.15.** Synthesis of catalyst **114**: end-game.

This completely novel route to chiral phosphoric acids may provide a secure access to even more hindered catalysts and, given the importance of binaphthol ligands in asymmetric catalysis, could also find application for the preparation of chiral metal-based catalysts.<sup>52</sup>

### Synthesis of **115a-c**

The synthesis of the binaphthol scaffolds of catalysts **115a-c** (Scheme 4.10) was instead possible *via* cross-coupling reaction using the Ni-catalyzed *Kumada* reaction usually applied to the synthesis of **TRIP**.<sup>53</sup> However, in this case, the preparation of the required aryl bromides was challenging from the synthetic point of view. While *tetra*-isopropyl bromobenzene **116c** was prepared by simple electrophilic aromatic bromination of the corresponding hydrocarbon compound (Scheme 4.16.a),<sup>135</sup> the synthesis of complex architectures for polycyclic aryl-bromides **116d-e** required more challenging routes.

However, despite the need for a stepwise approach, compound **116d** was prepared on multi-grams scale, thus highlighting the robustness of the developed procedure (Scheme 4.16.b).<sup>144</sup>



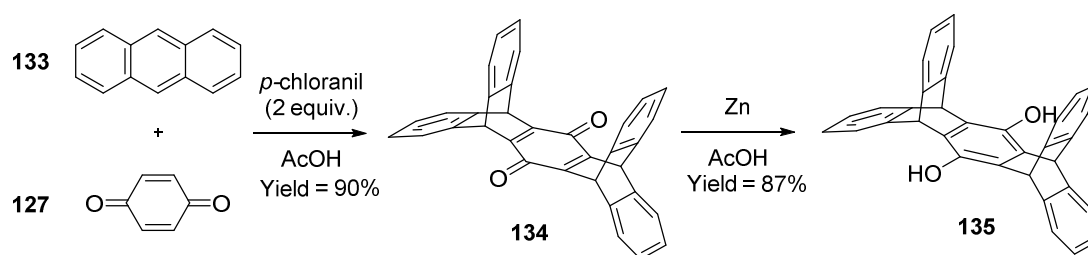
**Scheme 4.16** Preparation of aryl bromides **116c** and **116d**.

An initial *Diels-Alder* reaction followed by olefin reduction gave diketone **128** starting from benzoquinone and cyclohexadiene.<sup>145</sup> This product was then converted into the corresponding hydroquinone through  $\alpha$ -bromination/elimination sequence and subjected to triflation conditions in order to be eventually reduced in a Pd-catalyzed hydrogenolysis.<sup>146</sup> Due to solubility issues, the following electrophilic aromatic bromination could not be interrupted at the desired monobrominated product; nevertheless a clean dibromination reaction was carried out and product **116d** was finally obtained after mono-lithiation and protonation.

A similar synthetic approach was not attempted for the preparation of pentyptcene bromide **116e**, since the presence of five aromatic moieties discouraged us from planning a final electrophilic bromination. Synthetic routes towards pentyptcenes are significantly challenging and a long linear synthesis of dibromide **136** has been disclosed and previously reported in literature.<sup>147</sup> However, we designed a much shorter route, which could be useful on a preparative scale. In the presence of *p*-chloranil as an oxidant, anthracene and benzoquinone were coupled in a double *Diels-Alder* reaction giving quinone compound **134**



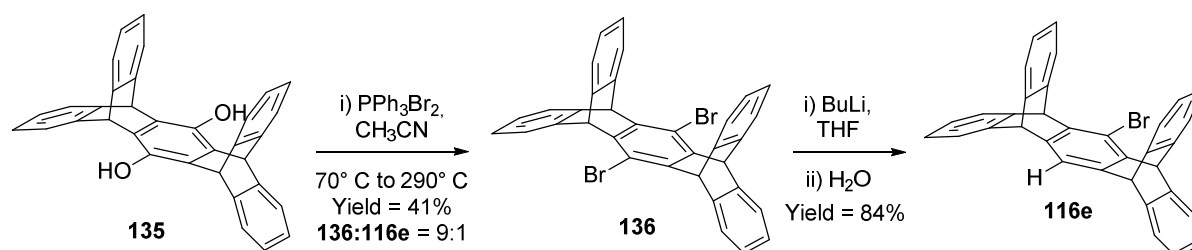
and afterwards a simple reduction with zinc powder gave the corresponding hydroquinone **135** (Scheme 4.17).<sup>148, 149</sup>



**Scheme 4.17.** Preparation of hydroquinone **135**.

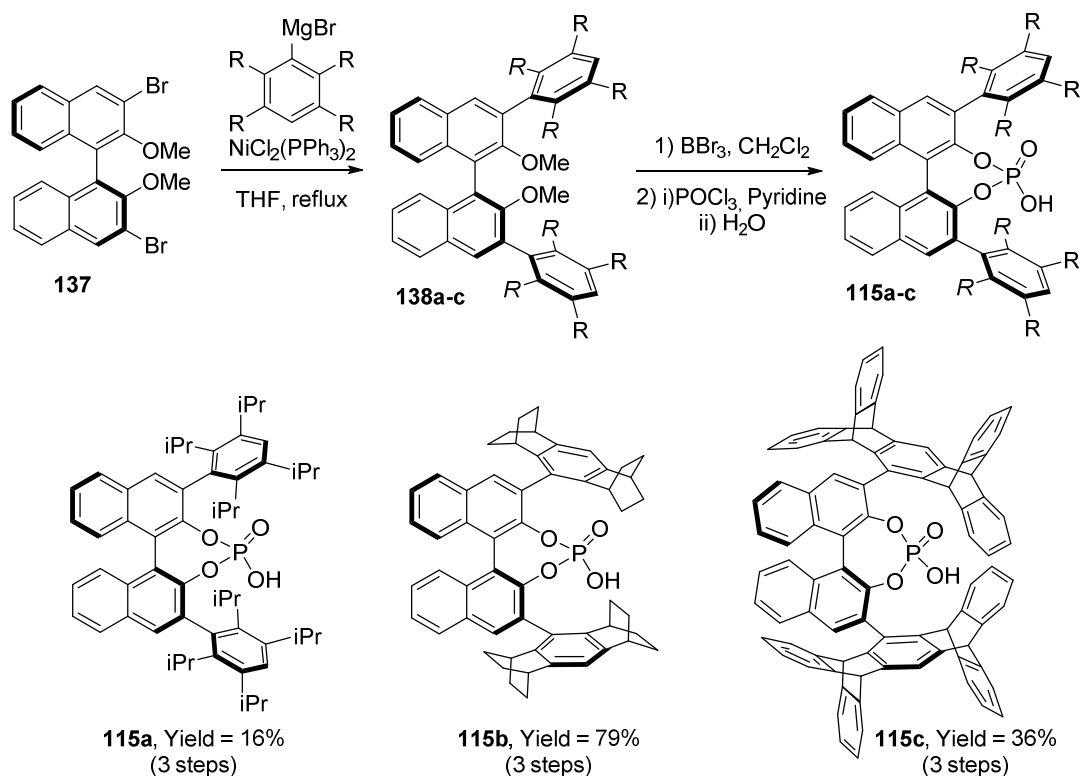
We then developed a novel *Appel*-type transformation at elevated temperature (290° C), which provided a remarkably clean reaction profile and the dibrominated species **136** was obtained in a single step and moderate yield. Intriguingly, the analysis of the reaction mixture allowed the identification of the bromo-pentiptycene compound **116e** as a minor byproduct of the transformation. A final mono-lithiation/protonation sequence provided the desired product **116e** in an overall four-step approach (Scheme 4.18).

Notably, iptycene scaffolds are unique three-dimensional rigid structures and find promising applications in molecular machines, supramolecular chemistry, material science and coordination chemistry.<sup>150</sup> Therefore, this novel and straightforward protocol could also provide an interesting novel entry to these highly investigated molecules.



**Scheme 4.18.** Preparation of bromo pentiptycene **116e**.

Having established reliable, multigram approaches, for the preparation of aryl bromides **116c-e**, the synthesis of the corresponding phosphoric acid catalysts was performed. As mentioned above, the *Kumada* biaryl coupling allowed the synthesis of the complex binaphthyl scaffolds. Then a simple ether cleavage using boron tribromide gave the desired BINOL- derivatives, which were next converted under standard conditions into the corresponding phosphoric acids (Scheme 4.19).<sup>53</sup>



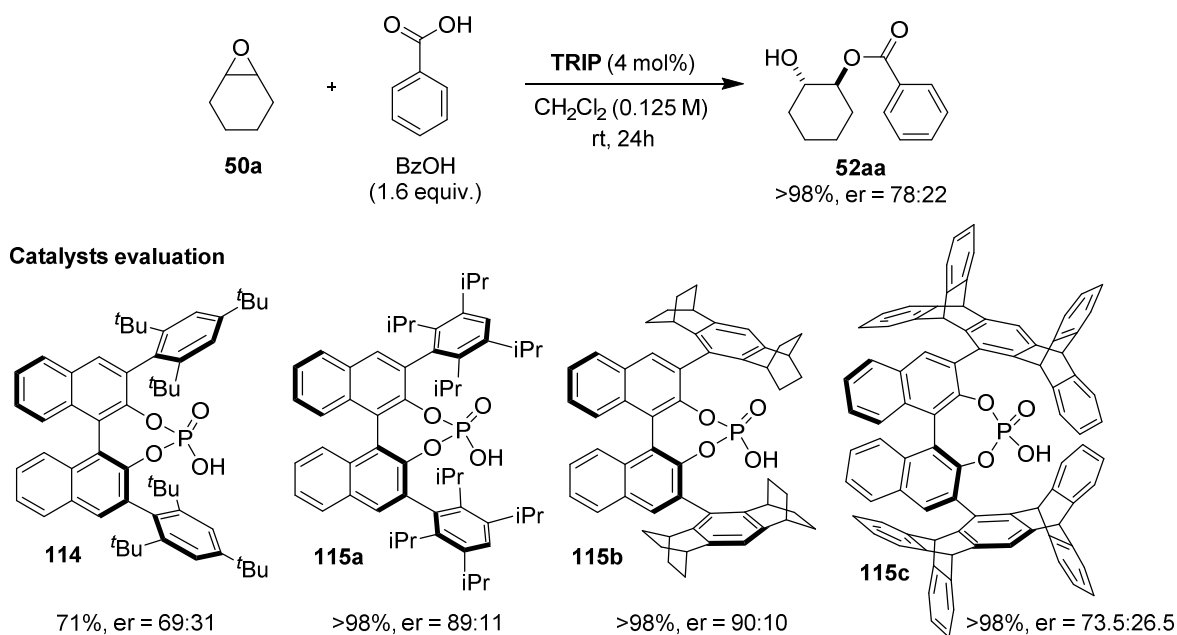
**Scheme 4.19.** Synthesis of catalysts **115a-c**: end-game.

#### 4.3.3. Evaluation of novel catalysts and reaction optimization

Having synthesized the newly designed chiral phosphoric acids, we explored their catalytic performances in the carboxylation of cyclohexane oxide with benzoic acid (Scheme 4.20). Unexpectedly, increasing the size the *ortho*-substituents did not result in the desired effect: as a matter of fact, catalyst **114** showed lower selectivity than **TRIP** in the ring opening reaction (er = 69:31). Gratifyingly however, catalysts with *ortho,meta*-substituted aryl moieties outperformed the previously known catalysts, providing a two-fold beneficial effect. On one hand, confinement of the phosphate pocket reduced its nucleophilicity, thus further limiting the deactivation pathway. On the other hand, the steric demand enhanced the stereochemical communication within the interacting intermediates. In particular, catalyst **115a** considerably improved the selectivity of the reaction (er = 89:11) and the conformationally constrained polycyclic catalyst **115b** proved to be even more effective (er = 90:10). Finally we investigated the iptycene-substituted organocatalyst **115c** and we observed a detrimental effect on the reaction outcome (er = 73.5:26.5). Possibly, such active site is barely accessible due to the considerable steric features and relevant non-stabilizing

## 4. Results and Discussion

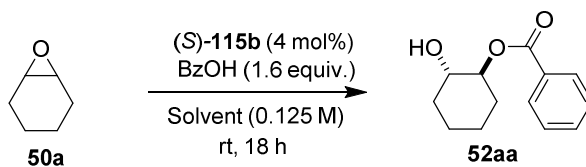
interactions also characterize the transition state leading to the favored product enantiomer.



**Scheme 4.20.** Evaluation of novel catalysts in the carboxylation of **50a**.

Having finally identified **115b** as the optimal catalyst for our transformation, we started evaluating the other reaction parameters. The transformation was observed to be essentially insensitive to the polarity of the reaction medium and similar results were obtained in a large variety of non-polar solvents (Table 4.18).

**Table 4.18.** Screen of solvents for the carboxylation of **50a** catalyzed by **115b**.



entry	solvent	Conv <sup>[a]</sup>	er <sup>[b]</sup>
1	CH <sub>2</sub> Cl <sub>2</sub>	>95%	90:10
2	benzene	>95%	90:10
3	toluene	>95%	90.5:9.5
4	mesitylene	>95%	90.5:9.5
5	<i>p</i> -xylene	>95%	90.3:9.7
6	<i>o</i> -xylene	>95%	90.2:9.8

<sup>a</sup> Determined by <sup>1</sup>H-NMR; <sup>b</sup> Determined by HPLC on chiral stationary phase

Presumably, due to the hindrance of the phosphoric acid moiety and the rigidity of its structure, solvent molecules cannot be intercalated inside the catalytic pocket in the transition state and the external solvation sphere does not significantly influence its well-defined conformation. Toluene was chosen as the optimal solvent ( $er = 90.5:9.5$ ; entry 3, Table 4.17), due to a small beneficial effect and low-toxicity with respect to dichloromethane ( $er = 90:10$ ; entry 1, Table 4.18).

The exploration of various carboxylic acids suggested a wide applicability of the methodology and only a minor contribution to the selectivity could be attributed to the nucleophile backbone. Both aliphatic and aromatic carboxylic acids were investigated and benzoic acid was found to slightly outperform the others (entry 1, Table 4.19). Intriguingly, the benefits provided by the 2,6-substitution pattern in the **TRIP**-catalyzed reaction were not observed in the transformation with catalyst **115b** and the selectivity was reduced when using carboxylic acid **51e** (entry 7, Table 4.19).

**Table 4.19.** Screen of carboxylic acids for the ring opening of **50a** catalyzed by **115b**.

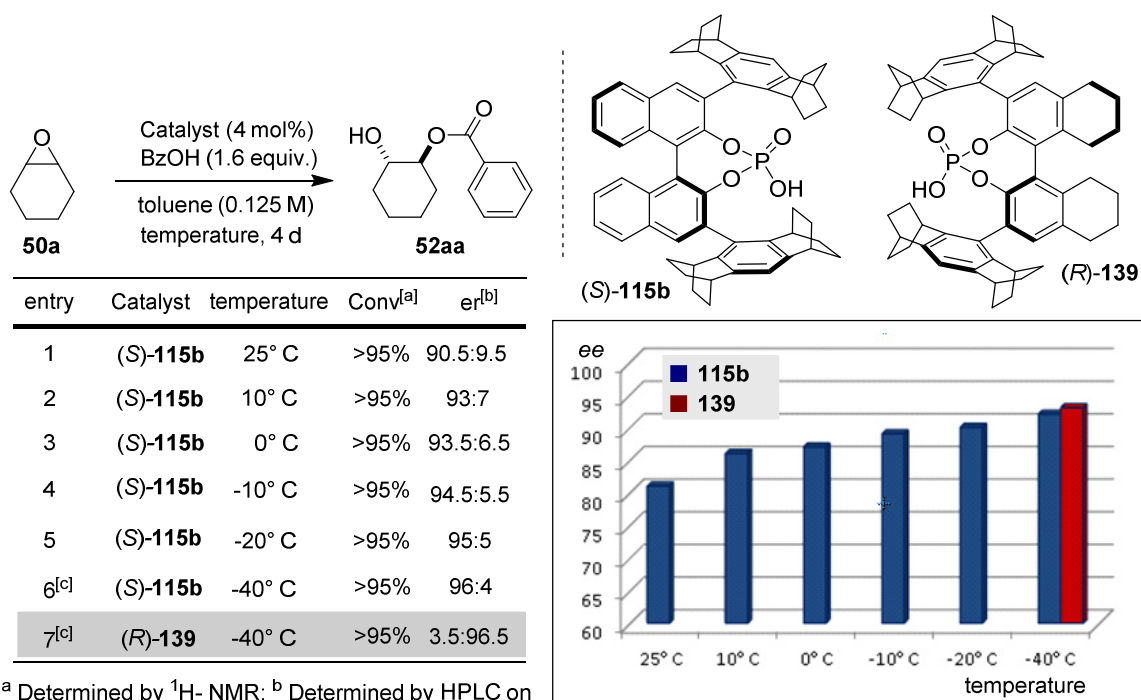
entry	RCO <sub>2</sub> H	er <sup>[a]</sup>	entry	RCO <sub>2</sub> H	er <sup>[a]</sup>
1		90.5:9.5	5		89.5:10.5
2	AcOH	89.5:10.5	6		89:11
3		89:11	7		72.5:27.5
4		89.5:10.5			

<sup>a</sup> Determined by HPLC on chiral stationary phase

Remarkably, under cryogenic conditions, an excellent level of enantioselectivity was achieved. Lowering the temperature to  $-40^{\circ}\text{C}$ , the chiral monoprotected 1,2-diol **52aa** was quantitatively obtained in 96:4 enantiomeric ratio (entry 6, Table 4.19).

A final effort for the ultimate optimization of the catalyst led us to explore catalyst **139**, the tetra-hydrogenated variant of catalyst **115b**.<sup>151</sup> This catalyst, which was designed and prepared according to the same strategy showed in the previous paragraph, gave superior results under the optimized conditions and allowed the isolation of the product with 96.5:3.5 enantiomeric ratio (entry 7, Table 4.20).

**Table 4.20.** Final optimization for the asymmetric carboxylation of **50a**.



<sup>a</sup> Determined by <sup>1</sup>H-NMR; <sup>b</sup> Determined by HPLC on chiral stationary phase; <sup>c</sup> Reaction performed with 10 mol% catalyst loading and 3 equivalents of PhCO<sub>2</sub>H

### Structural rationalization of the catalyst design

A comparison between catalysts **139** or **115b** and **TRIP** helps to sketch out the achievements of our confinement-oriented catalyst synthesis. The experimental analysis of the catalytic performances highlighted a superior selectivity of the novel catalysts but a lower turnover frequency. Both these effects can be attributed to a less accessible catalytic site. Indeed, the analysis of the X-ray crystal structure of catalyst (R)-**139** provides further insights and significant differences can be appreciated with respect to (S)-**TRIP** in the solid state (Figure 4.8).

Considering the closest carbon atoms to the phosphate group, a comparative analysis of the space diagonals reveals that catalyst **139** exhibits a tighter available space between the two hydrophobic substituents (**TRIP**: 10.40 Å and 9.00 Å; **139**: 9.79 Å and 8.78 Å). The confined nature of the novel catalytic pocket appears even more evident when considering the *Van der Waals* surface through a space-filling model. While the active site of the previously known catalyst is relatively open, the less flexible substituents of the novel catalyst effectively translates into a more compact cavity, thus providing a more hindered moiety (front view, Figure 4.8). This analysis also suggests the importance of the *meta*-substituents of the phenyl groups: the polycyclic framework provides an extended rigid structure which further reduces the exposition of the phosphoric acid (side view, Figure 4.8).

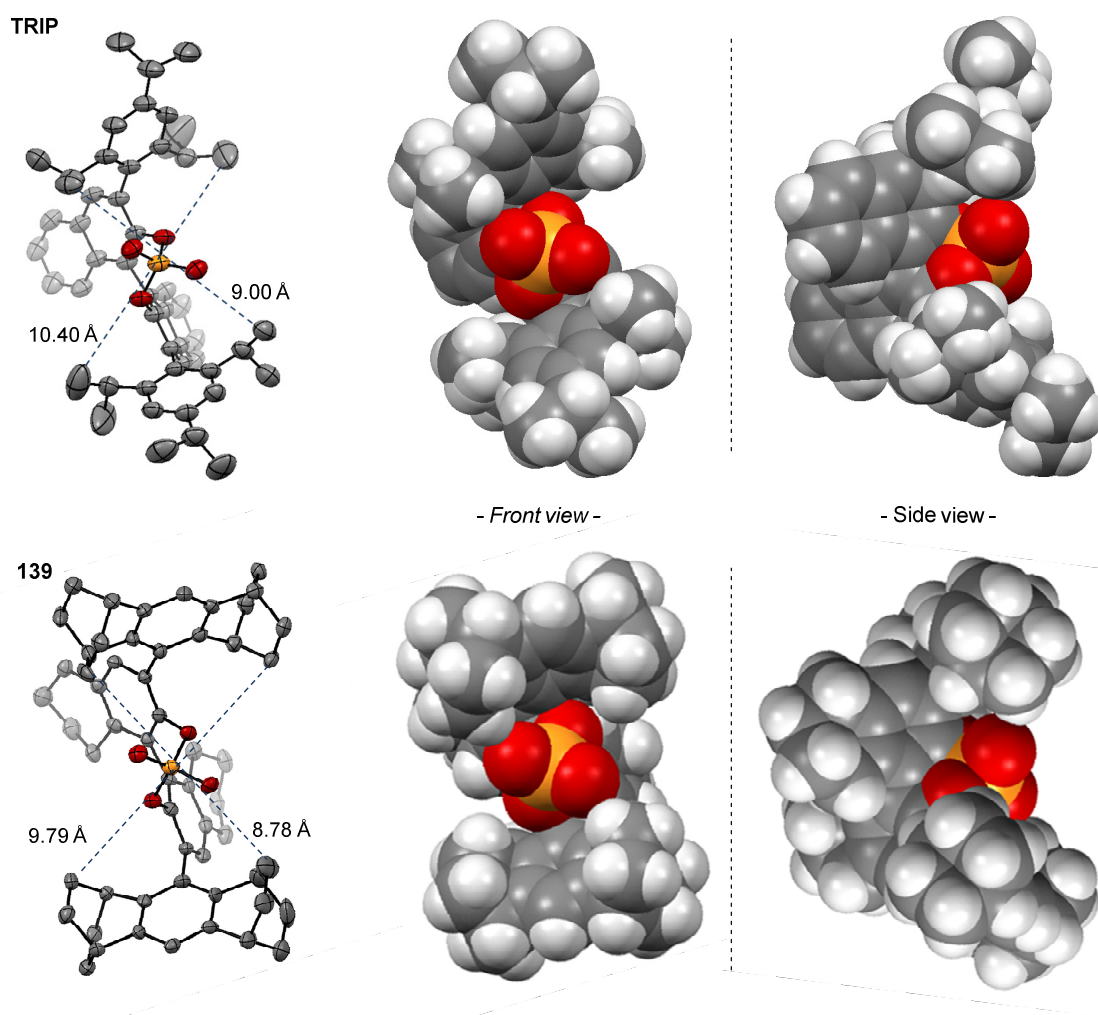


**Figure 4.8.** Comparison between **TRIP** and catalyst **139**. The crystal structure of (*R*)-**139** has been flipped for clarity.

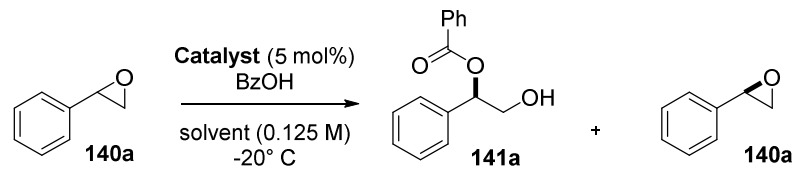
A theoretical exploration of the transition states of the transformation is presented in section 4.5.3, aiming at a rationalization of how these structural features translate into an effective stereochemical communication between the catalysts and the reaction partners.

### Kinetic resolution of racemic epoxides

Having identified optimal conditions for the asymmetric carboxylation of *meso*-epoxides, we wondered whether the scope of our methodology could also include a resolution strategy. Although chiral epoxides are recognized as important building blocks in stereoselective synthesis, the development of highly enantioselective epoxidation reactions of unactivated olefins is still in need.<sup>152</sup> Racemic epoxides are inexpensively derived from the corresponding alkenes and thus the development of efficient resolution strategies is practically useful. Fascinated to contribute to this field, we turned our attention to the ring opening of non-symmetrical racemic epoxides.

Employing styrene oxide **140a** as model substrate and **TRIP** as the catalyst, we could verify that a highly selective kinetic resolution to *O*-benzoylated phenyl ethyleneglycol **141a** was occurring (*S* = 19.8; entry 1, Table 4.21). As expected from our previous studies on aziridine substrates, the ring opening reaction selectively occurs on the internal carbon center and no regioisomer could be detected in the reaction mixture.

**Table 4.21.** Kinetic resolution of styrene oxide **140a**.

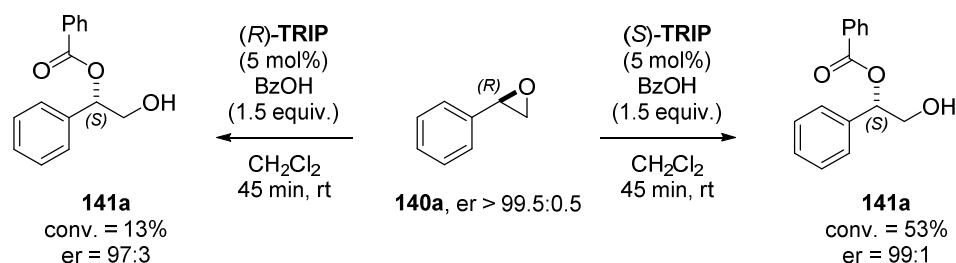


entry	catalyst	BzOH equiv.	solvent	time	er <sup>[b]</sup> <b>140a</b>	er <sup>[b]</sup> <b>141a</b>	Conv. <sup>[a]</sup>	<i>S</i> <sup>[a]</sup>
1	( <i>S</i> )- <b>TRIP</b>	0.5	DCM	24 h	33.5:66.5	6.5:93.5	27.5%	19.8
2	( <i>R</i> )- <b>139</b>	0.5	toluene	3 days	60.5:39.6	97:3	18.5%	39.7
3	( <i>R</i> )- <b>139</b>	0.6	toluene	36 h	63.3:36.7	97.2:2.8	22%	45
4	( <i>R</i> )- <b>139</b>	3	toluene	36 h	64.8:35.2	96.8:3.2	24%	40.4
5	( <i>R</i> )- <b>139</b>	0.6	toluene	3.5 days	71.7:28.3	96.7:3.3	32%	44.9
6	( <i>R</i> )- <b>139</b>	3	toluene	3.5 days	74.4:25.6	96.2:3.8	34.5%	41.1

[a] Calculated by the *Kagan* equation. [b] Determined by HPLC on chiral stationary phase.

An optimization of the reaction conditions confirmed the superior selectivity of catalyst **139** ( $S = 45$ ; entry 3, Table 4.21) and revealed that a substoichiometric amount of carboxylic acid could be used in this case to facilitate the control of the reaction progress.

We also investigated the nature of the nucleophilic substitution in order to exclude the possibility of a  $S_N1$  reaction pathway with a carbocationic intermediate. As presented in Scheme 4.21, enantiopure ( $R$ )-styrene oxide was subjected to the ring opening reaction with the two enantiomers of **TRIP** catalyst and the same enantiomer of the product was obtained in both reactions, albeit at different rates. This outcome is consistent with an  $S_N2$  pathway, which proceeds with inversion of configuration at the chiral center.



**Scheme 4.21.** Stereoselectivity study for the carboxylic kinetic resolution of **140a**.

#### 4.3.4. Reaction scope

##### Preparation of starting materials

Having identified conditions for both desymmetrization and kinetic resolution strategies, we set out to explore the substrate scope. When not commercially available, epoxides **50** and **140** were generally prepared according to a standard epoxidation protocol of the corresponding olefin by *Prilezhaev* reaction with *m*-CPBA (Table 4.22).<sup>126</sup>

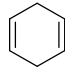
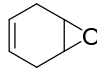
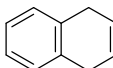
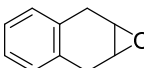
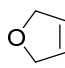
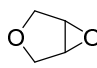
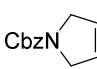
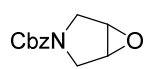
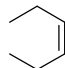
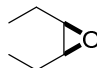
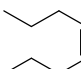
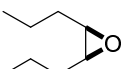
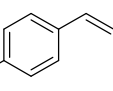
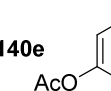
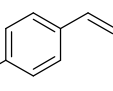
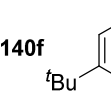
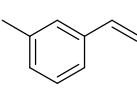
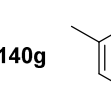
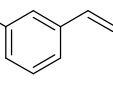
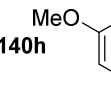
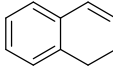
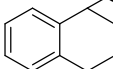
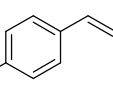
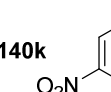
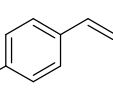
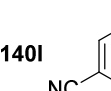
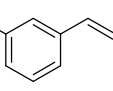
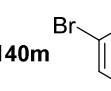


## 4. Results and Discussion

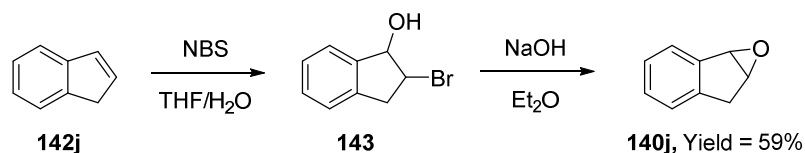
**Table 4.22.** Preparation of epoxides starting materials.

$$\text{R}^1\text{-CH=CH-R}^2 \xrightarrow[\text{CH}_2\text{Cl}_2, 0^\circ\text{C to rt}]{\text{m-CPBA}} \text{R}^1\text{-CH(O)-CH(O)-R}^2$$

**107, 142**  **50, 140**

entry	starting	product	Yield
1	<b>107b</b> 	<b>50b</b> 	61%
2	<b>107c</b> 	<b>50c</b> 	75%
3	<b>107f</b> 	<b>50f</b> 	58%
4	<b>107g</b> 	<b>50g</b> 	79%
5	<b>107i</b> 	<b>50i</b> 	37%
6	<b>107j</b> 	<b>50j</b> 	63%
7	<b>142e</b> 	<b>140e</b> 	75%
8	<b>142f</b> 	<b>140f</b> 	28%
9	<b>142g</b> 	<b>140g</b> 	55%
10	<b>142h</b> 	<b>140h</b> 	84%
11	<b>142i</b> 	<b>140i</b> 	77%
12	<b>142k</b> 	<b>140k</b> 	35%
13	<b>142l</b> 	<b>140l</b> 	50%
13	<b>142m</b> 	<b>140m</b> 	48%

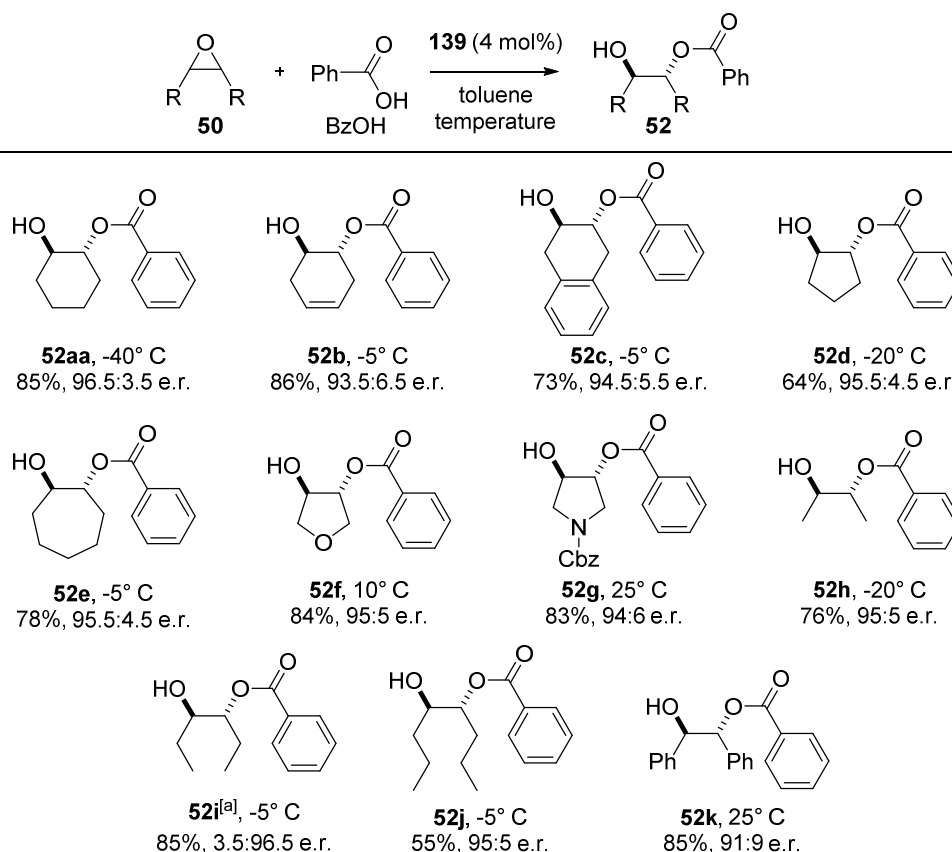
Due to the instability of epoxide **140j** under the acidic conditions of the epoxidation with peracids, this compound was prepared *via* a stepwise process. Bromohydrin **143** was obtained from indene **142j** and the desired epoxide was then delivered through a base-promoted intramolecular substitution reaction (Scheme 4.22).<sup>153</sup>



**Scheme 4.22.** Synthesis of indene oxide **140j** via bromohydrin intermediate **143**.

### Desymmetrization of *meso*-epoxides

Several *meso*-epoxides, cyclic and acyclic, were successfully transformed into the corresponding glycol monoesters with high levels of stereocontrol (Scheme 4.23).



Reactions were performed on a 0.1 mmol scale. Enantiomeric ratios were determined by HPLC on chiral stationary phase. <sup>a</sup> Reaction catalyzed by (S)-**115b**.

**Scheme 4.23.** Reaction scope for the desymmetrization of *meso*-epoxides to monoprotected 1,2-diols.

Six-membered-ring substrates **50b** and **50c** reacted smoothly giving the desired products in good yields and very good enantioselectivity (respectively **52b**: 86% yield, er = 93.5:6.5 and **52c**: 73% yield, er = 94.5:5.5). Monoprotected *trans*-diols bearing a five- or seven-membered-ring scaffold were obtained with excellent stereocontrol (**52d** and **52e**; er = 95.5:4.5). Presumably, the presence of additional competing hydrogen-bonding acceptors was the reason for a lower reactivity observed when reacting epoxides with heteroatoms in the cyclic scaffold; however, the reactions proceeded smoothly at slight elevated temperature and the corresponding products **52f** and **52g** were also obtained with very good selectivity. The remarkable generality of the system was furthermore demonstrated when acyclic substrates **50h-j** were investigated. It is noteworthy that even the small epoxide **50h** was converted into the corresponding product **52h** in excellent enantiomeric ratio (76% yield, er=95:5), highlighting the potential of our new sterically confined catalyst to handle small substrates. In case of epoxide **50i**, both catalyst **139** and its fully aromatic version **115b** gave the desired product enantioselectively, with the latter catalyst being slightly superior (er<sub>139</sub>=96:4, er<sub>115b</sub>=3.5:96.5; see the experimental section, cf. paragraph 7.4.3.1). The challenging *cis*-stilbene derived epoxide **50k** was compatible with the reaction conditions and the desired product was isolated in high yield and good enantioselectivity (85% yield, er = 91:9).

#### Kinetic resolution of racemic epoxides

Under optimized conditions a variety of unsymmetric epoxides were investigated in the carboxylic kinetic resolution and the results are collected in Table 4.23.

The reaction generally proceeds with excellent selectivity (*S* from 29 to 93) and different substitution patterns on the phenyl ring of the starting epoxides are well tolerated. It is worth to notice that the reactivity of the different substrates was found to be related to the electronic properties and the position of the substituents. Rate acceleration due to the presence of electron-donating groups was observed and a qualitative correlation with the *Hammett* sigma constants was possible.<sup>154</sup> For example, styrene oxide **140a** reacted at -20° C ( $\sigma = 0.00$ ; *S* = 44; entry 1, Table 4.23), its *para*-tertbutyl substituted congener **140f** was found to be reactive even at -40° C ( $\sigma = -0.20$ ; *S* = 73; entry 6, Table 4.23), while for the reaction of *meta*-methoxy styrene oxide **140h** the temperature had to be raised at +4° C ( $\sigma = +0.12$ ; *S* =

## 4. Results and Discussion

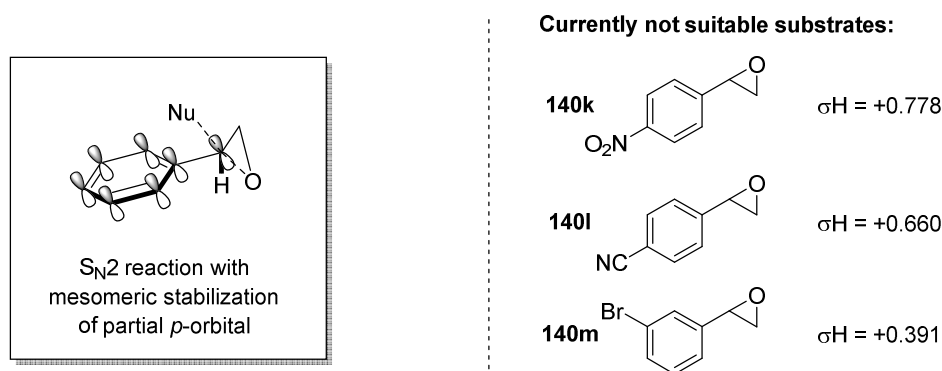
29; entry 8, Table 4.23). Halogenated epoxides **140b-d** underwent the resolution with excellent selectivity factors ( $S = 48-50$ ; entries 2-4, Table 4.23) and also the presence of an acetyl-group in the starting material was effectively tolerated (**140e**,  $S = 46$ , entry 5, Table 4.23). An influence on the reactivity due to the steric features of the epoxide was also observed. Presumably, due to the geometrically constrained structure, epoxides **140i** and **140j** exhibited the highest reactivity and were resolved with outstanding selectivities ( $S = 93$  and  $S = 87$ ) at  $-50^\circ\text{C}$  with reduced catalyst loading (2 mol%, entries 9-10, Table 4.23).

**Table 4.23.** Reaction scope for the carboxylic kinetic resolution of racemic epoxides.

entry	Products	Yield <sup>[a]</sup>	er <sup>[b]</sup>	S <sup>[c]</sup>	entry	Products	Yield <sup>[a]</sup>	er <sup>[b]</sup>	S <sup>[c]</sup>
1	<b>141a</b> 	40%	95.7:4.3	44	6	<b>141f</b> 	50%	95.3:4.7	73
	<b>140a</b> 	55%	82.6:14.4			<b>140f</b> 	47%	97.2:2.8	
2	<b>141b</b> 	50%	93.3:6.7	48	7	<b>141g</b> 	47%	94.3:5.7	61
	<b>140b</b> 	46%	96.7:3.3			<b>140g</b> 	44%	97.5:2.5	
3	<b>141c</b> 	30%	96.9:3.1	50	8	<b>141h</b> 	48%	91.2:8.8	29
	<b>140c</b> 	61%	73.5:23.5			<b>140h</b> 	45%	93.2:6.8	
4	<b>141d</b> 	28%	97:3	49	9	<b>141i</b> 	45%	98:2	93
	<b>140d</b> 	51%	71:29			<b>140i</b> 	55%	81.2:18.8	
5	<b>141e</b> 	46%	93.4:6.6	46	10	<b>141j</b> 	53%	94.1:5.9	46
	<b>140e</b> 	45%	95.8:4.2			<b>140j</b> 	44%	99.6:0.4	

[a] Reactions performed on 0.1 mmol scale in a 0.016 M solution. [b] Determined by HPLC on chiral stationary phase. [c] Measured by Kagan's equation.

The rate accelerating effect of electron-donating substrates suggests the presence of a mesomeric stabilization of a localized cationic charge at the carbon center which undergoes the ring opening reaction. However, the presence of a carbocationic intermediate had been disproved and a concerted  $S_N2$  transformation was proposed. Therefore, an asynchronous reacting event can be hypothesized with the transient formation of cationic charge localized in an orbital with a partial  $p$ -character, thus benefitting from the resonance stabilization of the phenyl moiety (Scheme 4.24).



**Scheme 4.24.** Mesomeric effect in the asynchronous  $S_N2$  ring opening of epoxides and current limitations of the kinetic resolution.

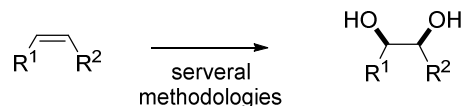
This phenomenon is common in nucleophilic ring opening reactions occurring at a benzylic position.<sup>155</sup> As a consequence, strong electron-withdrawing groups significantly decreases the reaction rate and substrates **140k-m** ( $\sigma > +0.391$ ) were found to be limitations of this methodology.

#### 4.3.5. Biomimetic, asymmetric *anti*-dihydroxylation strategy

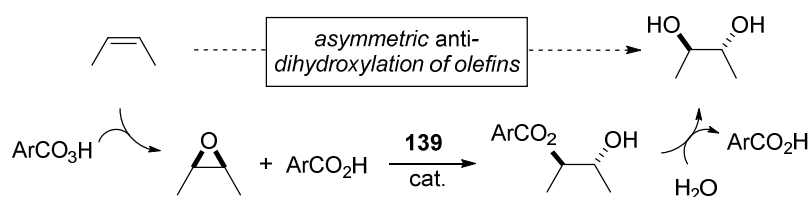
With the optimal conditions for the asymmetric carboxylation in hand, we reasoned that our reaction may be exploited for the development of an enantioselective *anti*-dihydroxylation of unactivated alkenes. Although enantioselective *syn*-dihydroxylations of olefins are well developed,<sup>156-157</sup> analogous non-enzymatic asymmetric *anti*-dihydroxylations are unknown. Therefore developing a catalytic dihydroxylation reaction which proceeds with such topicity is particularly interesting. We realized that the oxidation of alkenes with simple peracids (*Prilezhaev* reaction), delivers both an epoxide and a carboxylic acid, which is the exact combination of substrates for the asymmetric reaction under investigation.

Accordingly, adding catalyst **139** to this reaction mixture should directly furnish the corresponding monoprotected dihydroxylation product in an enantioenriched fashion (Scheme 4.25).

**Syn-dihydroxylation:**

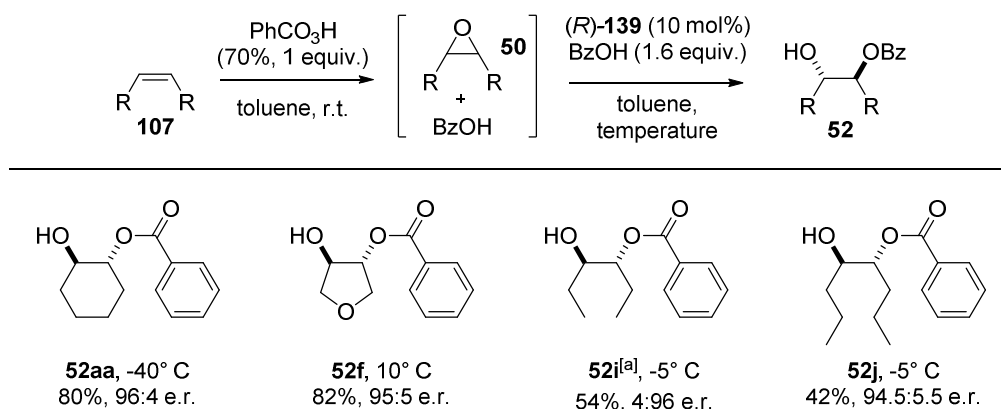


**Anti-dihydroxylation:**



**Scheme 4.25.** Developing an *anti*-dihydroxylation of simple olefins.

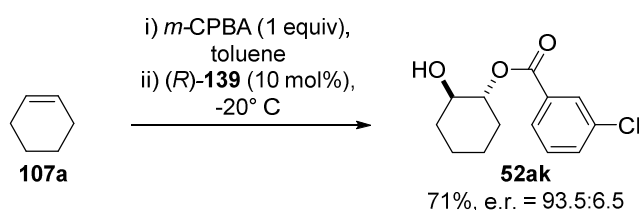
To test this idea, we treated a variety of olefins **107** with perbenzoic acid in toluene and subjected the resulting reaction mixture to our desymmetrization conditions (Scheme 4.26). The expected glycol monoester products were obtained in good yields and with enantioselectivities similar to those previously obtained for the simple ring opening reaction (Scheme 4.23). In these reactions, the catalyst was always added in solution together with additional benzoic acid to reach the previously optimized conditions (**139** 10 mol% and benzoic acid 3 equivalents).



Reactions were performed on a 0.1 mmol scale. Enantiomeric ratios were determined by HPLC on chiral stationary phase. <sup>a</sup> Reaction catalyzed by (*S*)-**115b**.

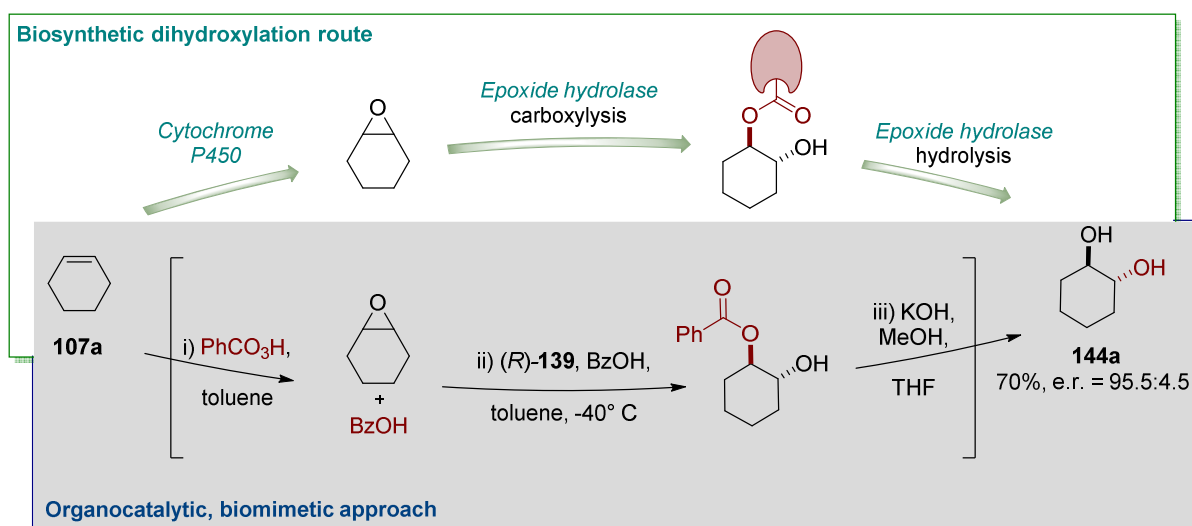
**Scheme 4.26.** Organocatalytic asymmetric dihydroxylation strategy.

We also performed the reaction sequence with the commonly used *meta*-chloroperbenzoic acid as oxidant. Remarkably, in this reaction the catalyst was added without additional carboxylic acid and the desired product was obtained in 71% yield and 93.5:6.5 enantiomeric ratio (Scheme 4.27). It is noteworthy that the overall sequence of *Prilezhaev* epoxidation followed by carboxylolysis exhibits perfect atom economy and the product obtained can be converted into the corresponding diols in under mild basic conditions.



**Scheme 4.27.** Asymmetric dihydroxylation strategy using *m*-CPBA.

Fascinatingly, our designed overall *anti*-dihydroxylation of olefins, perfectly mimics the enzymatic biosynthetic pathway (Scheme 4.28). In the living organisms, epoxides are commonly delivered by the *cytochrome P-450*-mediated oxidation of olefins. Subsequently, an aspartate residue of an *epoxide hydrolase* performs a nucleophilic attack on the activated oxirane generating an enzyme-bound intermediate, which is sequentially hydrolyzed.<sup>23, 91</sup>



**Scheme 4.28.** Organocatalytic, biomimetic dihydroxylation of cyclohexene **107a**.

In an analogous way, using our methodology, we explored the first biomimetic asymmetric synthesis of 1,2-cyclohexandiol **144a** starting from cyclohexene **107a**. In fact, a

three-step, one-pot protocol was devised including a final hydrolysis step, which terminates the epoxidation/desymmetrization sequence. According to such protocol, the desired diol product was straightforwardly obtained in good yield and excellent enantioselectivity (70% yield, er = 95.5:4.5; Scheme 4.28).

*“...a jumbo jet is not just a scaled-up pigeon. In biomimetic chemistry, we also take inspiration, but not blueprints, from natural chemistry”*

R. Breslow (*J. Biol. Chem.* 2009)



#### 4.4. Asymmetric synthesis of $\beta$ -hydroxythiols<sup>158</sup>

Having successfully developed a catalytic system for the asymmetric ring opening of aziridines and epoxides towards 1,2-aminoalcohols and 1,2-diols, we investigated whether this approach could be applied to other nucleophiles. Due to the importance of chiral  $\beta$ -hydroxythiol scaffolds,<sup>101</sup> broadening the perspectives of our novel activation mode to a sulfur-variant could be of synthetic value. Intrigued by the possible heterodimer formation, we focused on thiocarboxylic acids. In particular, we aimed at the development of an organocascade strategy which directly delivers chiral thiols, thus representing a valuable alternative to the long sought-after asymmetric sulfhydrolysis reaction.<sup>159</sup>

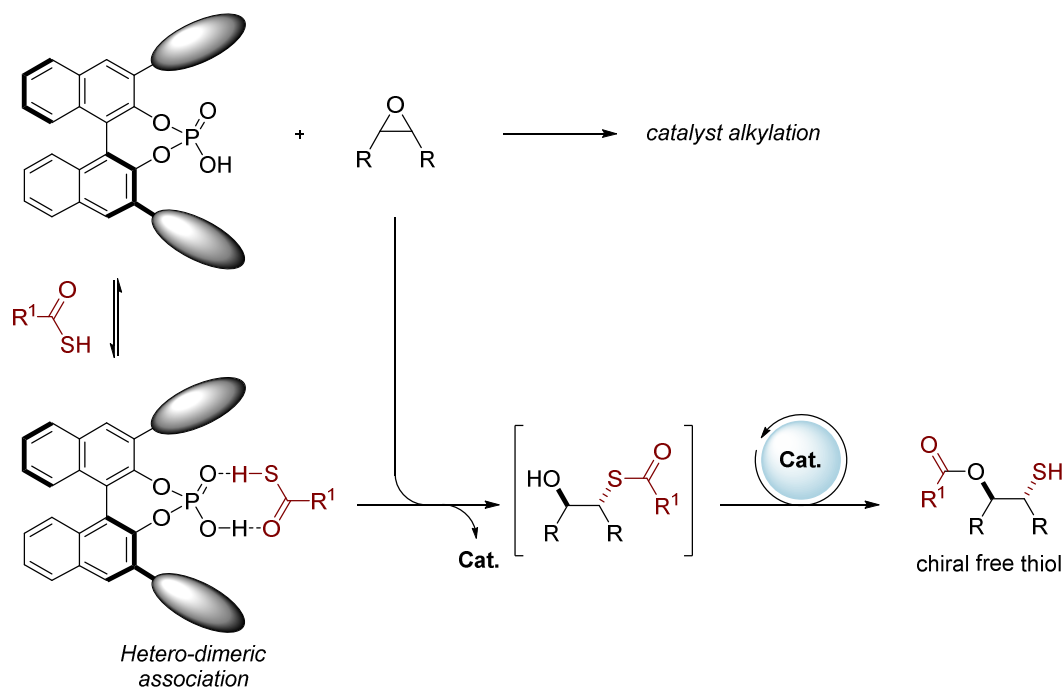
*The work described in this section was performed in collaboration with Dr. S. Prévost. The density functional theory calculation presented in Figure 4.10 was performed in collaboration with Dr. D. Fazzi (AK Prof. Thiel, MPI Mülheim). The crystal structure determination of **147ab** by X-ray diffraction was performed by Dr. R. Goddard.*

##### 4.4.1. Reaction design and heterodimer studies

The exploration presented in the previous chapters revealed that the heterodimerization with carboxylic acids inhibits the alkylation of phosphoric acid catalysts in the presence of epoxides and aziridines, thus allowing an highly enantioselective carboxyls of these substrates. Similarly to carboxylic acids, thiocarboxylic acids are capable of self-assembling through hydrogen-bonding interactions. However, mainly due to the moderate electronegativity of sulfur, this association is less pronounced.<sup>160</sup> Thiol moieties are weaker hydrogen-bonding donors than hydroxyl groups and this translates in the formation of less stable homodimeric species. On this basis, we wondered whether a hypothetical heterodimeric self-assembly between hindered phosphoric acids and thiocarboxylic acids could be sufficiently stable to prevent the decomposition pathway in favor of the catalytic transformation.

We designed a thiocarboxyls ring opening reaction which may benefit from the high nucleophilicity associated with the large valence orbital of the sulfur atom. This reactivity should be extendable into an organocascade process: the initially generated  $\beta$ -hydroxythioester may undergo an *in situ* Brønsted acid catalyzed intramolecular *trans-*

esterification reaction to the thermodynamically more stable ester, thus giving direct access to the free thiol moiety. Given the significant challenge associated to the asymmetric synthesis of thiols,<sup>100</sup> our transformation should provide a valuable and attractive alternative (Scheme 4.29).



**Scheme 4.29.** Design of an asymmetric variant of the sulfhydrolysis of epoxides *via* heterodimeric association.

At the onset of our investigation, we studied the proposed self-assembly between **TRIP** phosphoric acid and thiobenzoic acid. NMR spectroscopic analysis indeed supported our speculations, confirming that in mixtures of the two acids in organic non-polar media, an equilibrium towards an associative interaction exists. As shown in Figure 4.9, in accordance with our experiments with carboxylic acids (cf. paragraph 4.1), the interaction caused evident changes in both the <sup>31</sup>P-NMR and in the <sup>1</sup>H-NMR of the phosphoric acid upon addition of a large excess of thiocarboxylic acid. The phosphorous signal experienced a remarkable downfield shift (**TRIP** BzSH: 4.16 ppm; **TRIP**: 2.36 ppm) while in the proton spectrum the presence of the guest molecule in the catalyst pocket could be hypothesized due to resolution of the coalescence of the signals at 2.5-3.0 ppm and 6.9-7.1 ppm.

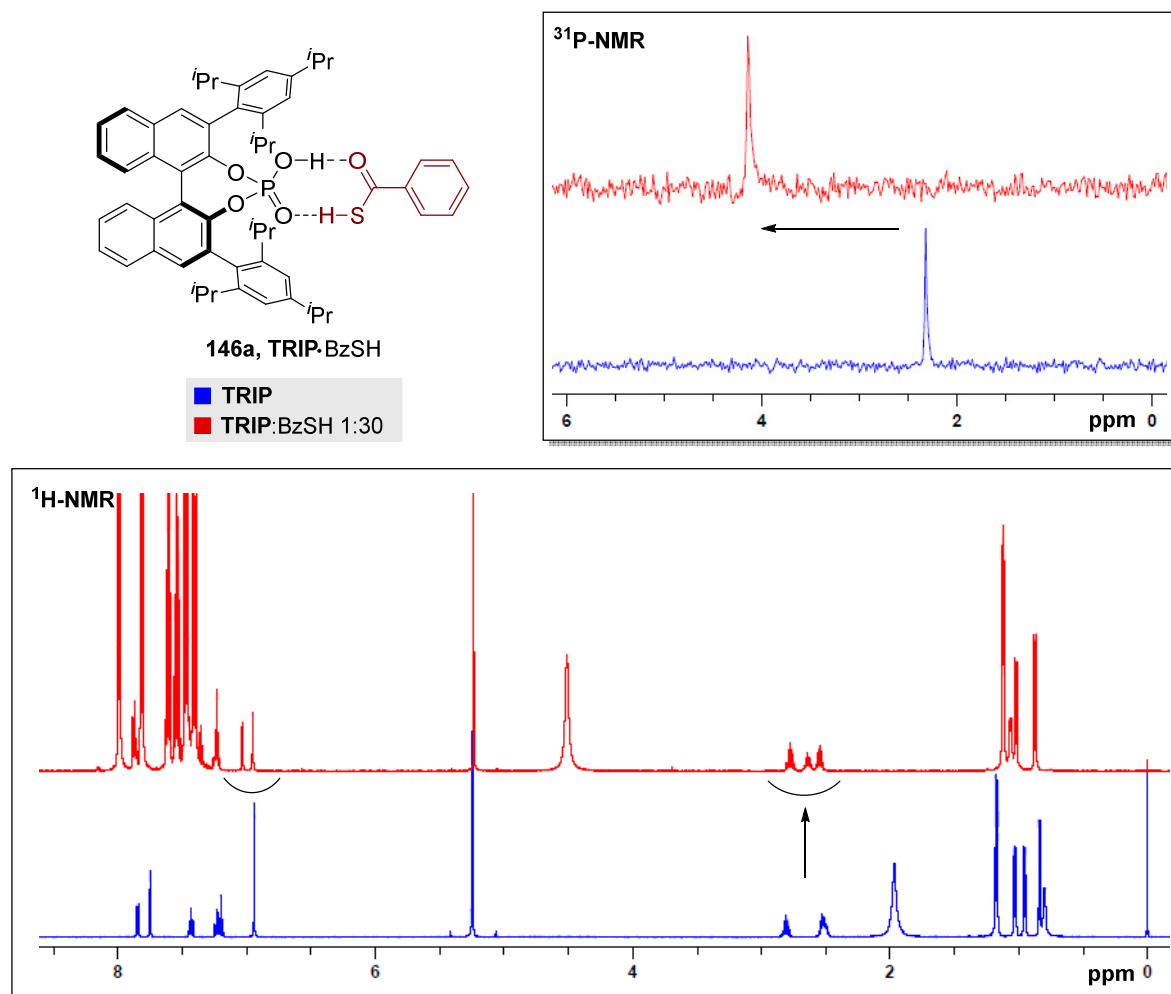


**Figure 4.9.** Qualitative investigation of self-assembly heterodimerization between TRIP and thiobenzoic acid (TRIP blue spectra; TRIP·BzSH red spectra).

Although the spectroscopic analysis confirmed the interaction, the definition of the structure was not trivial. The formation of two tautomeric species may be envisioned and therefore we also investigated the self-assembly by density functional theory calculations (Figure 4.10). In fact, both the thiol and the thione isomers of the thiocarboxylic acid may be suitable partners for the self-assembly with the phosphoric acid catalyst.<sup>161</sup> The computational analysis predicted a higher stability of the thione tautomer **146b<sub>2</sub>** with respect to the thiol form **146b<sub>1</sub>** ( $\Delta G = 0.9 \text{ kcal mol}^{-1}$ ) and therefore we suggest that the former isomeric state is more populated than the latter.

Nevertheless, this equilibrium should be relatively fast in solution since proton transfer in dimeric structures is usually characterized by low energy barriers and often affected by quantum tunneling.<sup>162</sup>

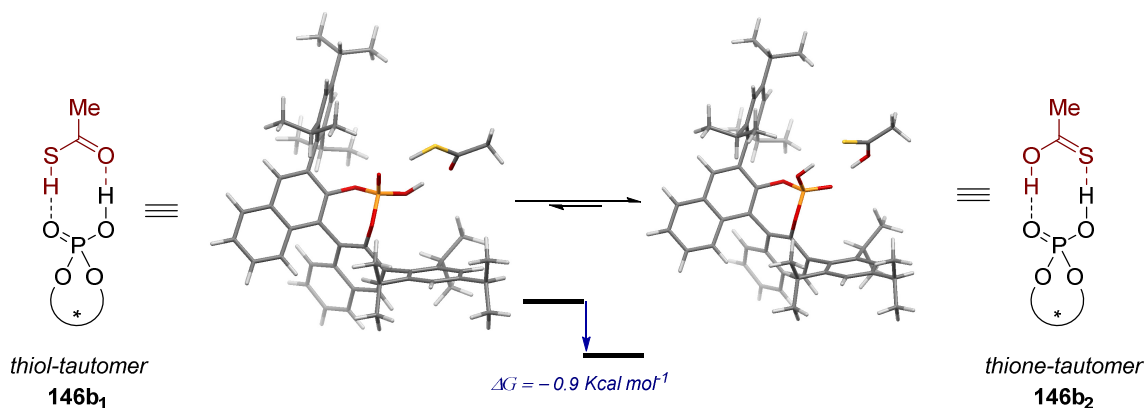
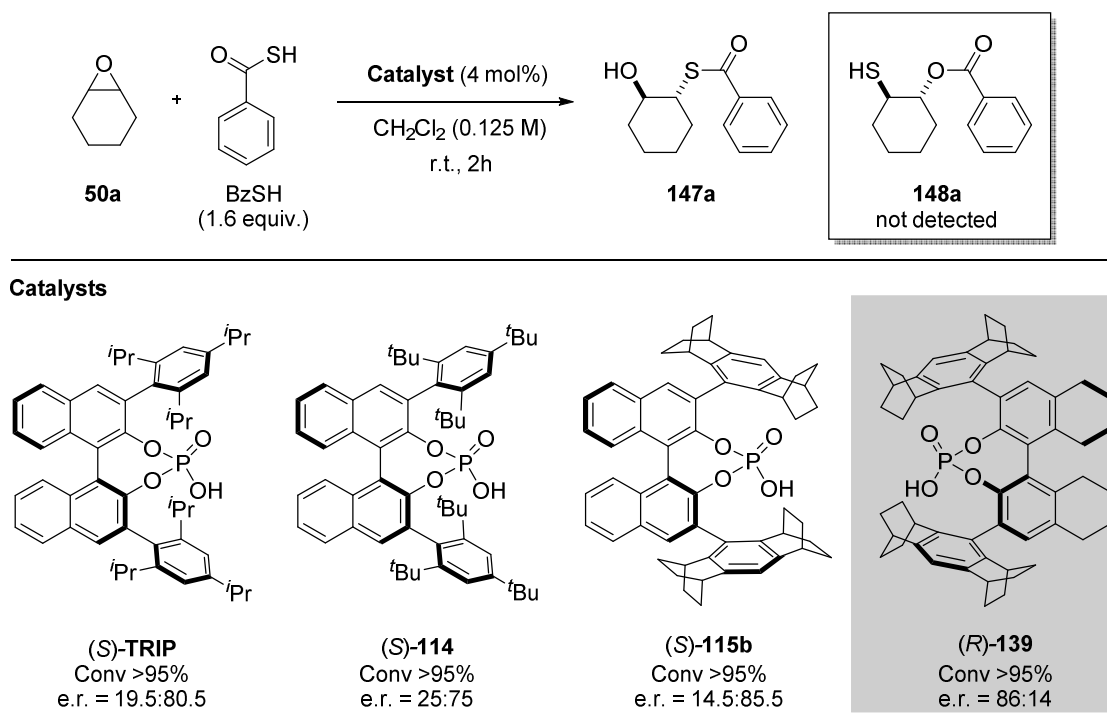


**Figure 4.10.** Models for heterodimer **TRIP·AcSH 146b**. Structures of thiol isomer **146b<sub>1</sub>** and the thione tautomer **146b<sub>2</sub>** computed at B3LYP/cc-pTVZ level.

#### 4.4.2. Preliminary studies and optimization of reaction conditions

With the confirmation of the non-covalent association, we commenced exploring the reactivity of this novel heterodimeric species, and started the investigations on the proposed methodology choosing cyclohexene oxide **50a** as model substrate (Scheme 4.30).



Conversion determined by <sup>1</sup>H-NMR; enantiomeric ratio determined by HPLC on chiral stationary phase.

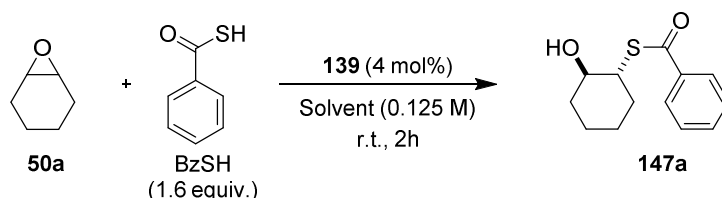
**Scheme 4.30.** Preliminary investigation on the ring opening of **50a** with thiobenzoic acid: evaluation of chiral phosphoric acid catalysts.

## 4. Results and Discussion

Indeed, the reaction catalyzed by **TRIP** gave full conversion of the starting material into ring opened product **147a** with promising enantioselectivity, yet the expected acyl transfer product was not observed under these conditions (Scheme 4.30). Gratifyingly, the transformation was remarkably fast and only traces of catalyst degradation were observed. The enantioselectivity of the transformation was found to be affected by the steric hindrance of the catalyst pocket. In fact, our novel polycyclic chiral phosphoric acid **139** was found to again outperform **TRIP** (er = 86:14, Scheme 4.30).

Despite not having obtained the expected organocascade product, we next performed a screening of various reaction parameters to identify suitable conditions for the epoxide opening reaction (Table 4.24).

**Table 4.24.** Optimization of conditions for the thio-carboxylolysis of **50a**.



entry	Solvent	Catalyst loading	temperature	Conv <sup>[a]</sup>	er <sup>[b]</sup>
1	CH <sub>2</sub> Cl <sub>2</sub>	4 mol%	rt	>95%	86:14
2	CHCl <sub>3</sub>	4 mol%	rt	>95%	85:15
3	benzene	4 mol%	rt	>95%	87.5:12.5
4	toluene	4 mol%	rt	>95%	90:10
5	toluene	1 mol%	rt	>95%	90:10
6	toluene	0.1 mol%	rt	>95%	89.5:10.5
7	toluene	0.01 mol%	rt	>95%	85:15
8	toluene	0.001 mol%	rt	48%	63:37
9 <sup>[c]</sup>	toluene	4 mol%	-40° C	>95%	96:4
10 <sup>[c]</sup>	toluene	0.1 mol%	-40° C	79%	96:4
11 <sup>[c]</sup>	toluene	4 mol%	-78° C	>95%	98:2
12 <sup>[c]</sup>	toluene	1 mol%	-78° C	89%	97.5:2.5

<sup>a</sup> Determined by <sup>1</sup>H-NMR; <sup>b</sup> Determined by HPLC on chiral stationary phase;

<sup>c</sup> Reaction time 48 h

Extensive screening of solvent and temperature revealed that full conversion and excellent level of enantioselectivity can be achieved in toluene under cryogenic conditions (entry 11, Table 4.24). Remarkably, the reaction could be promoted by 1 mol% of catalyst giving the product in 89% yield and 97.5:2.5 enantiomeric ratio (entry 12, Table 4.24), while

at room temperature 100 ppm of catalyst loading was found to be the threshold for this activity (entry 7, Table 4.24). Presumably the slight loss in enantioselectivity in this reaction ( $er = 85:15$ ) is derived from a slow background reactivity and taking this phenomenon into account, the turnover number is 4320.

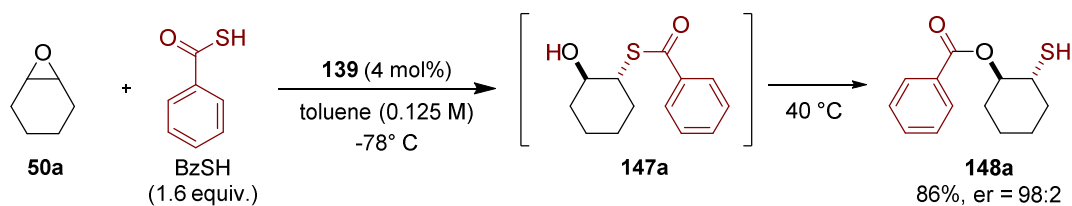
Having established the conditions for the asymmetric thiocarboxylation, we focused on the second step of the designed methodology in an effort to unlock the cascade transformation. We hypothesized that the *in situ* sequence had been hampered by a slow and rate-determining acyl transfer step. Therefore, mimicking the conditions at the end of the ring opening process, the fate of compound **147a** was monitored. Indeed, after prolonged reaction time a significant amount of thiol product **148a** was detected (60% yield; entry 1, Table 4.25). The catalytic role of the phosphoric acid catalyst in the transformation could be confirmed, since no relevant conversion was observed without. Intriguingly, the reaction was found to proceed more readily in the absence of thiocarboxylic acid. Two possible scenarios may explain this outcome: (1) the heterodimer is less active than the phosphoric acid monomer in this specific transformation or (2) the actual catalyst is the simple phosphoric acid and therefore the heterodimerization process inhibits its activity.

**Table 4.25.** Investigation on trans-acylation step for towards **148a**.

entry	Conditions		Conv <sup>[a]</sup>
	TRIP, <b>4a</b>	BzSH	
1	4 mol%	0.6 equiv.	60%
2	-	0.6 equiv.	traces
3	4 mol%	-	86%

<sup>a</sup> Determined by <sup>1</sup>H- NMR

Consequently, we reinvestigated the reaction by simply elevating the reaction temperature upon full consumption of the epoxide. Indeed, these conditions proved to be suitable for the catalytic activation of the thioester moiety, and the free thiol product was selectively obtained in good yield and without erosion of the enantiopurity (86% yield,  $er = 98:2$ , Scheme 4.31).



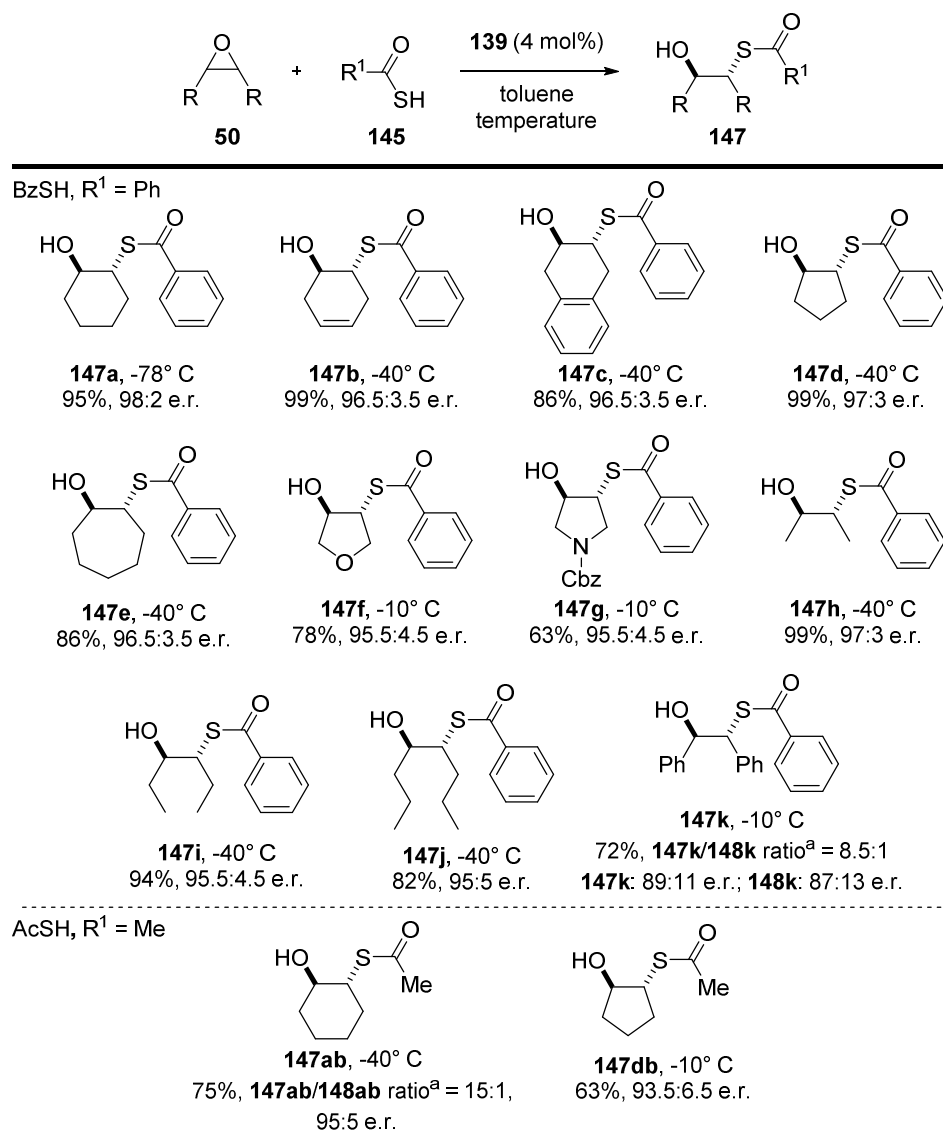
**Scheme 4.31.** Organocascade approach to thiol **148a**.

#### 4.4.3. Reaction scope

It is noteworthy that our transformation can either directly deliver organocascade products **148** or can be interrupted giving intermediates **147**. This reaction control enables isolation of the same 1,2-hydroxythiol scaffold either protected on sulfur or on oxygen. Due to the potential synthetic applicability of this divergence, we investigated both transformations.

At first we focused on the simple ring opening reaction. As shown in Scheme 4.32, the transformation is rather general and a large variety of *meso*-epoxides **50a-k** reacted with high level of stereocontrol. Six-membered ring substrates **50a-c** delivered the corresponding *S*-benzoyl  $\beta$ -hydroxythiols **147a-c** in good to outstanding yields and excellent enantioselectivities. It is noteworthy that the reaction outcome is essentially unaffected by the ring size of the starting materials as proven by the high yields and optical purity of products **147d,e**. The presence of heteroatoms in the substrate scaffold is well tolerated (products **147f,g**); however, a small influence on reactivity was detected and the reaction temperature had to be elevated to  $-10^\circ\text{C}$ . Acyclic substrates also reacted smoothly, providing *syn*-hydroxythioesters **147h-j** with excellent stereoselectivity. Notably, the isolation of product **147h** in outstanding yield and enantioselectivity (99%, er = 97:3) gave further confirmation of the remarkable capability of catalyst **139** in controlling the enantioselective transformation of very small substrates. Furthermore, reacting *cis*-stilbene oxide **50k**, the desired product **147k** was obtained under mild conditions in good yield and moderate optical purity concurrently with a minor amount of its thiol isomer (**147k**: er = 89:11; **148k**: er = 87:13).

## 4. Results and Discussion



Reactions were performed on a 0.1 mmol scale. Enantiomeric ratios were determined by HPLC on chiral stationary phase. <sup>a</sup> Determined by <sup>1</sup>H-NMR

### Scheme 4.32. Reaction scope of the asymmetric thiocarboxylation of *meso*-epoxides.

Remarkably the asymmetric carboxylation could also be extended to the use of thioacetic acid. Under similar conditions, products **147ab** and **147db** were obtained with high levels of stereocontrol, albeit with slightly diminished reactivity. X-ray analysis of a suitable crystal of compound **147ab** allowed the unambiguous assignment of the absolute configuration. As presented in Figure 4.11, in agreement with the related hydrolysis of epoxides, the compound exhibits (*R,R*)-stereochemistry.



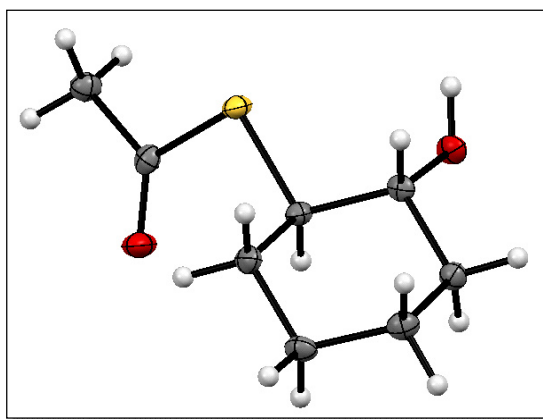
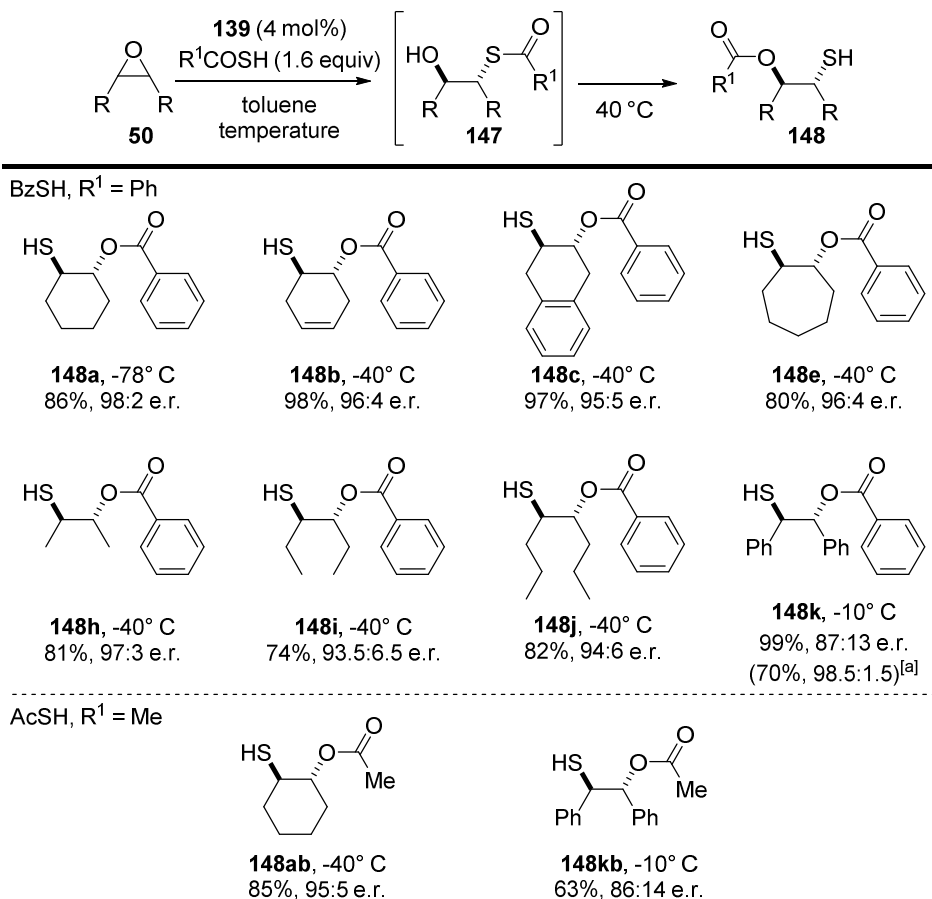


**Figure 4.11.** X-ray analysis of **147ab** showing (*R,R*) configuration.

We next focused on the cascade transformation and we reinvestigated all the previously tested substrates (Scheme 4.33).

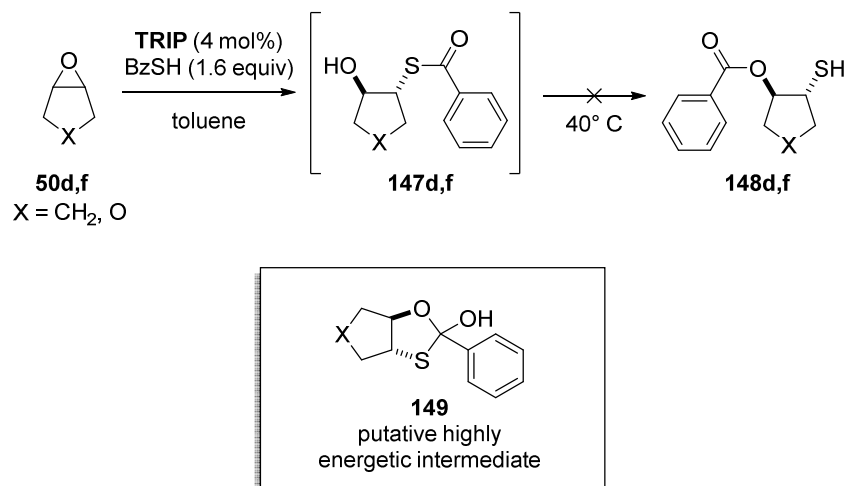


Reactions were performed on a 0.1 mmol scale. Enantiomeric ratios were determined by HPLC on chiral stationary phase. <sup>a</sup> After single recrystallization.

**Scheme 4.33.** Reaction scope of the organocascade reaction.

Six- and seven-membered ring substrates smoothly underwent the thiocarboxylisacyl transfer cascade affording the desired thiols **148a-c,e** in excellent yields and selectivities. Acyclic products **148h-j** were also efficiently obtained in good yields and enantiopurity. In some cases the enantiomeric ratio was found to be slightly lower than that of isolated alcohols **147** shown above. This may be due to the conversion of residual amount of the epoxide at higher temperature during the second step. Notably, when the isolated compound showed only moderate enantiomeric ratio, a single recrystallization could significantly improve the optical purity. This procedure allowed the isolation of thiol **148k** in 70% yield and 98.5:1.5 enantiomeric ratio, although initially obtained in near quantitative yield but with moderate enantiopurity.

This designed reaction sequence was unsuccessful for five-membered ring epoxides. Despite various attempts, as shown in Scheme 4.34, the reaction provided the corresponding alcohol intermediate and no acyl transfer could be detected even at elevated temperature. This outcome can be rationalized with the requirement for a *trans*-fused bicyclooctane intermediate **149**: presumably, the high energy associated with such species effectively prevents the intramolecular reaction.<sup>163</sup>



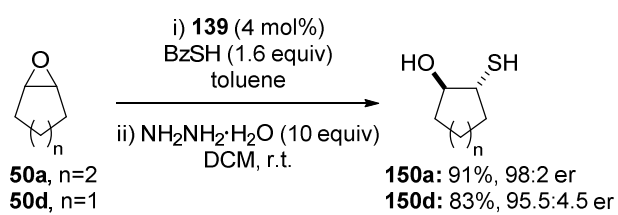
**Scheme 4.34.** Organocascade approach to thiol **148a**.

Finally, an *in situ* deprotection of the initially obtained products under mild conditions was also investigated. Coupling the asymmetric ring opening with an hydrazinolysis of the thioester functionality, enantioenriched 1,2-hydroxythiols were directly

## 4. Results and Discussion

---

obtained. The overall methodology constitutes an equivalent of the long sought after asymmetric sulphydrolysis of epoxides.



**Scheme 4.35.** Direct access to 1,2-thioalcohols.

#### 4.5. Mechanistic investigations

The study of the interaction between catalysts and substrate is often a crucial aspect for the development of asymmetric organocatalysis since it allows the codification and the establishment of novel activation modes.<sup>33</sup> In all the methodologies presented in this thesis, the heterodimerizing self-assembly between a phosphoric acid catalyst and a carboxylic acid (or thiocarboxylic acid) has been proposed as a new concept in Brønsted acid catalysis. Exploiting this system, we have developed highly enantioselective ring openings of epoxides and aziridines using (thio)-carboxylic acids as nucleophiles.<sup>113, 132, 158</sup> Detailed mechanistic investigations and theoretical analysis on heterodimeric species were undertaken to rationalize and establish the features and the principles of this novel catalytic mode.

*The kinetic studies by NMR analysis were performed in collaboration with M. Leutzsch. The theoretical investigations were performed in collaboration with Dr. D. Fazzi (AK Prof. Thiel, MPI Mülheim).*

##### 4.5.1. Studies on heterodimeric activation

The development of novel unprecedented transformations has been possible using the concept of the heterodimerization as a defined working model (Figure 4.12).

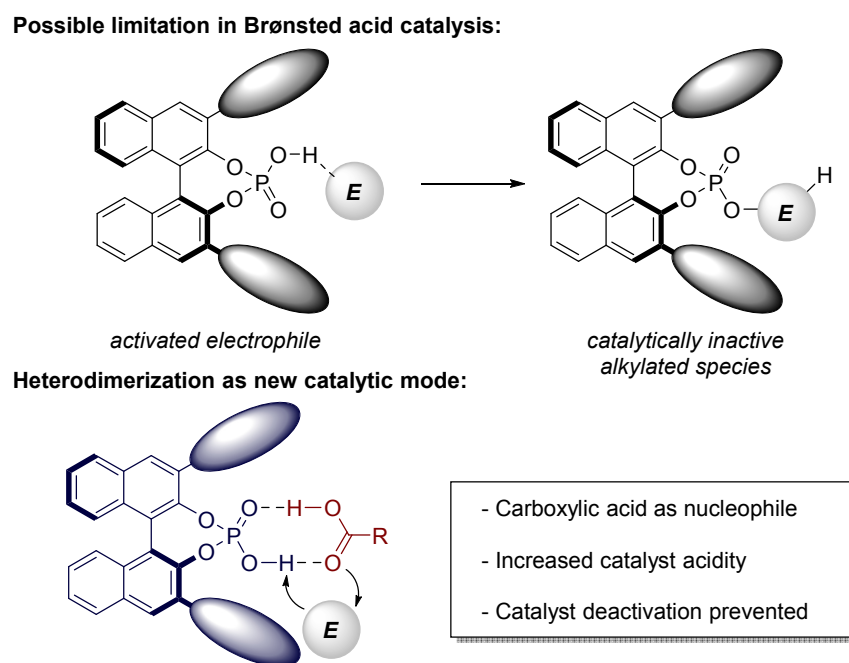


**Figure 4.12.** Heterodimerization as working model in Brønsted acid catalysis.

This idea was based on two main principles: on the one hand a favorable self-assembly with the nucleophile could prevent the deactivation of the catalyst, while on the other hand the expected acidity enhancement (heteroconjugation) could further facilitate the activation of the electrophile. In addition, during our analytic experiments (cf. paragraph 4.1), we observed an increased electron density on the carboxylate fragment and we speculated that its nucleophilicity may result enhanced. Aiming at a deeper understanding of the system, which could facilitate the exploitation of this reactivity, a theoretical investigation on the chemical properties of the heterodimeric species was performed. In particular, we evaluated the effects of the dimerization process on both the acidity of the species and on the frontier molecular orbitals using density functional theory calculations at the B3LYP/cc-pTVZ level.

Interestingly, comparing the orbitals of an acetic acid molecule with those of the same molecule in association with **TRIP**, a HOMO raising effect was observed rather than the possibly more intuitive LUMO lowering (Figure 4.13).

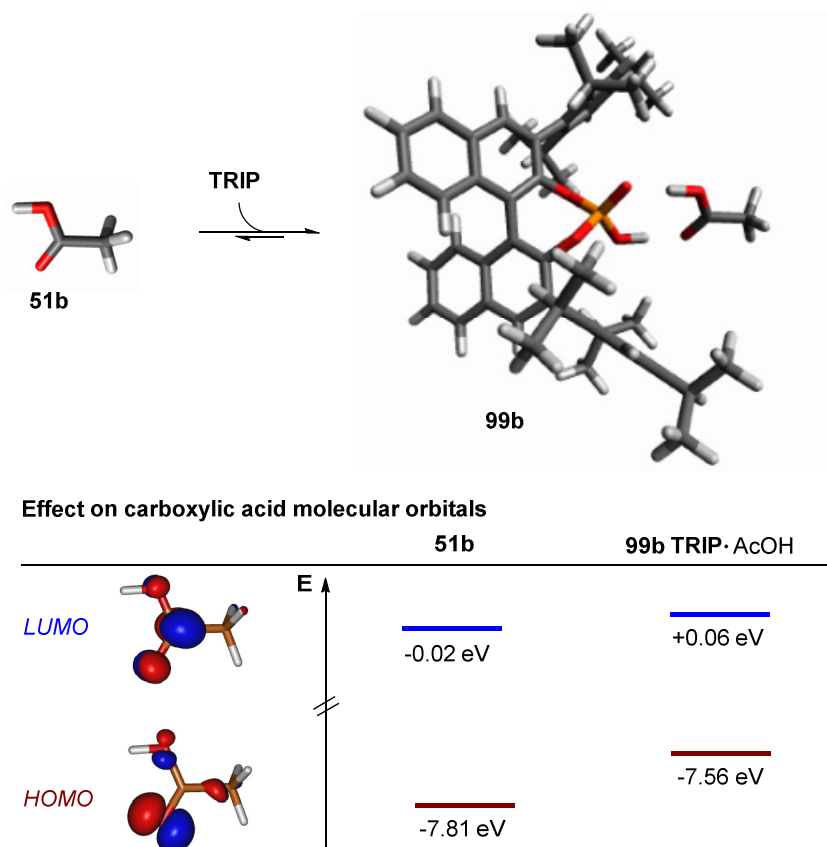


**Figure 4.13.** Evaluation of the effect of heterodimerization on the FMO of carboxylic acid. Structures computed at B3LYP/cc-pTVZ level.

Indeed, this outcome is in accordance with the reactivity observed, confirming an increase of the nucleophilic character of the carboxylic acid. Meaningfully, the observed upfield shift of the carboxylic acid protons signals in the titration experiments is in agreement with this finding. The phosphoric acid catalyst is both more acidic and more basic than acetic acid, and a “partial deprotonation” with concurrent HOMO raising is presumably the result of the overall pull-push effect.

The investigation of the Brønsted acidity upon heterodimerization was performed, using pyridine as indicator, to compare the acid strength of **TRIP** and the heterodimer **TRIP·AcOH** (Figure 4.14).

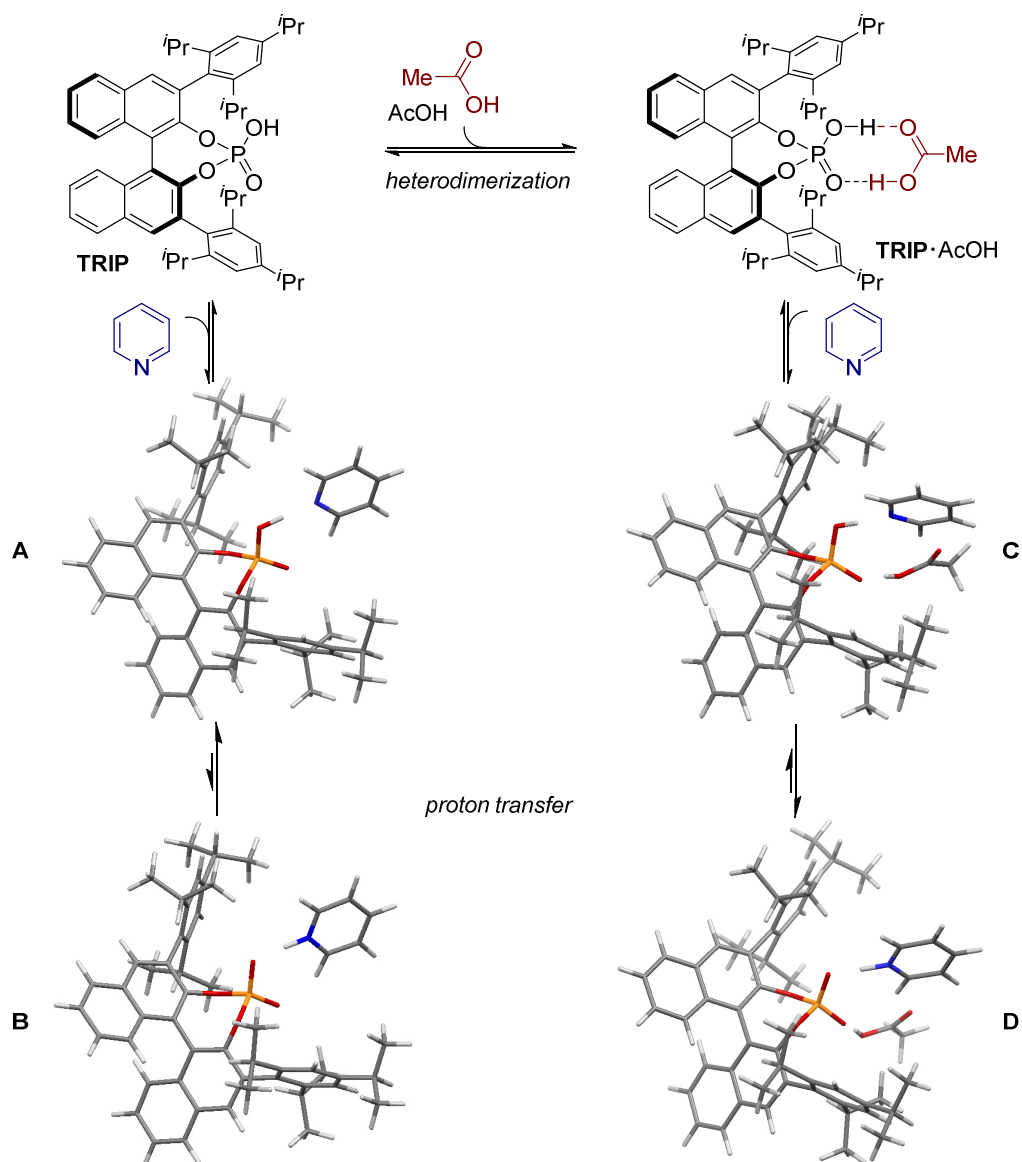


**Figure 4.14.** Evaluation of the effect of heterodimerization on Brønsted acidity using pyridine as sensor. Structures computed at B3LYP/cc-pTVZ level.

This analysis not only revealed that the trimeric species **C** is more stable than complex **A** ( $\Delta G = -5.76 \text{ kcal mol}^{-1}$ ), but also indicates that in this assembly the proton transfer is favored while in the absence of acetic acid it is not. In fact, complex **D** is more stable than **C** ( $\Delta G = -6.49 \text{ kcal mol}^{-1}$ ), while the corresponding species **B** is significantly disfavored with respect to **A** ( $\Delta G = +3.10 \text{ kcal mol}^{-1}$ ). Therefore, in agreement with the expected hetero-conjugation effect, these calculations confirm a significant acidity enhancement upon association.

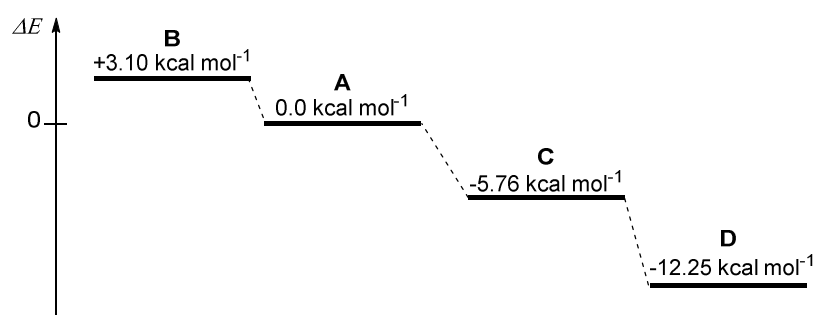


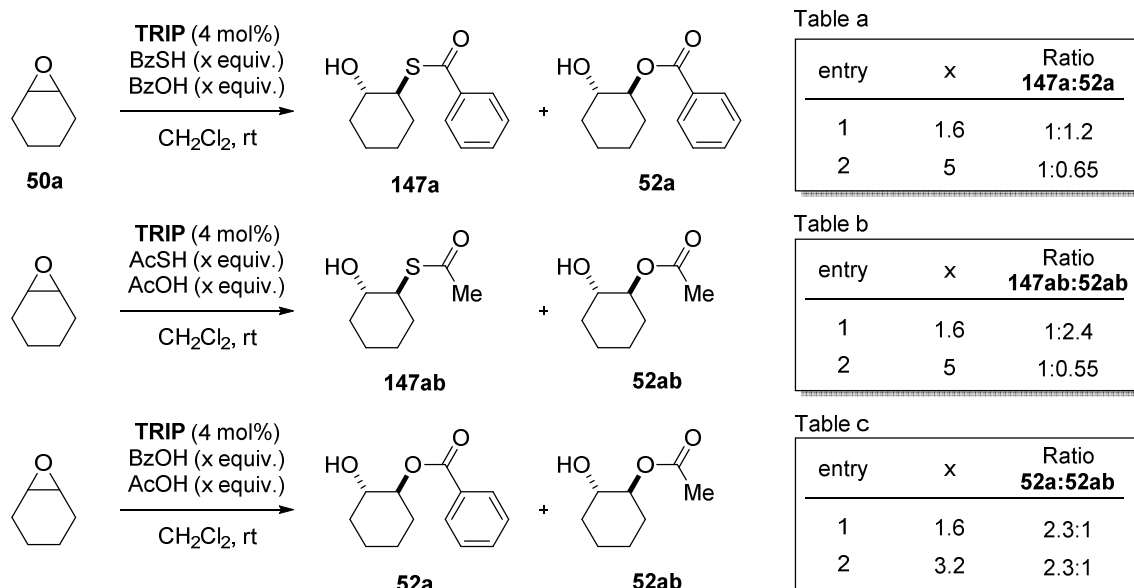
**Figure 4.15.** Energetic overview of the study on the Brønsted acidity.

#### 4.5.2 Studies on the catalytic cycle

Having gained further insights on the reactivity of heterodimeric species we undertook a thorough investigation on the mechanism of the transformation to experimentally elucidate the catalytic cycle. Despite our knowledge on the instability of oxiranium phosphate species,<sup>80</sup> which results in catalyst alkylation, competition experiments were initially performed to explore the possibility that the reactions involve a simple Brønsted acid activation of the epoxide substrates.<sup>39a, 44</sup>

As shown in Scheme 4.36, we performed the ring opening of cyclohexene oxide **50a** in the presence of a combination of different carboxylic acids and thiocarboxylic acids and **TRIP** as the catalyst. Although the reaction with thiobenzoic acid was expected to be faster than the corresponding reaction with benzoic acid, in equimolar amount of the two acids the products ratio was in favor of compound **52a** (entry 1, Table a, Scheme 4.36). Interestingly, by increasing the loading of both nucleophiles a remarkable effect was observed on the products distribution: with 5 equivalent of (thio)-carboxylic acids with respect to the epoxide substrate the product ratio favored **147a** (entry 2, Table a, Scheme 4.36). This effect could

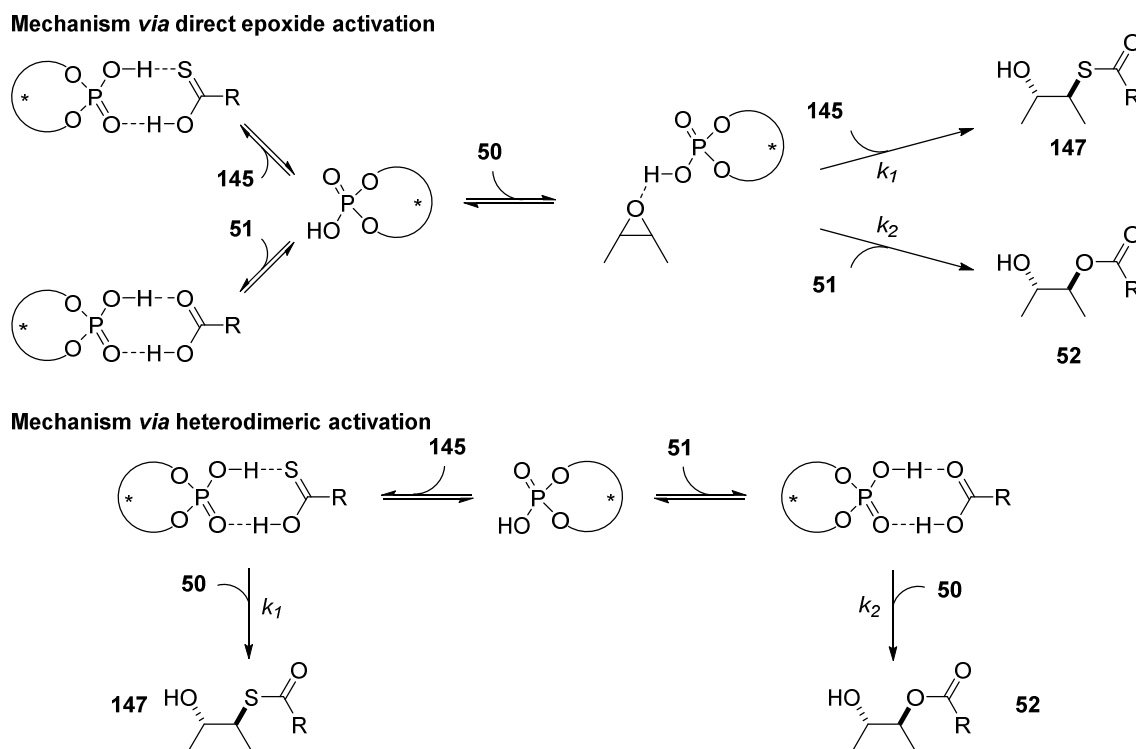
also be observed when performing the experiments with mixtures of acetic and thioacetic acid (Table b, Scheme 4.36). However, when similar experiments were performed using mixtures of benzoic and acetic acid, the product distribution was instead stable, and the benzoyl-protected diol **52a** was predominantly formed (ratio = 2.3:1, Table c, Scheme 4.36).



**Scheme 4.36.** Competition experiments for the ring opening of **50a**.

Based on these experimental results, a preliminary rationalization of the mechanism is possible (Scheme 4.37). If a common mechanism *via* direct activation of the epoxide was occurring, the product distribution would reflect the ratio between the two kinetic constants for the ring opening reaction ( $k_1$  and  $k_2$ ) and no change in the relative amount of the products should be detected by increasing the loading of both nucleophiles. However, the experiments (a) and (b) shown above are not in line with such pathway and therefore this mechanism should be discarded. Contrarily, a different mechanism occurring *via* heterodimer intermediates would be in agreement with the experimental observations. If the favored heterodimeric species with benzoic acid represented the resting state of the catalyst in the mixture, the rate of the formation of protected glycol **52** would be not dependent on the concentration of the carboxylic acid. Conversely, in this case the formation of the protected  $\beta$ -hydroxythiol **147** should instead be kinetically dependent on the concentration on the thiocarboxylic acid **145**. On the other hand, the competition experiment with carboxylic acids suggests that in such reaction mixture the two possible heterodimers are in equilibrium and none of them is selected as resting state.





**Scheme 4.37.** Analysis of possible mechanisms for the competition experiments.

We then focused on the analysis of the kinetic reaction profile. The carboxylolysis of epoxide **140i** with benzoic acid was selected due to the high reactivity, and the reaction progress could be studied by *in-situ*  $^1\text{H-NMR}$  measurements (Figure 4.16). Following the analytical method described by *Blackmond*, different experiments were performed to estimate the kinetic law.<sup>164</sup> The consumption of the epoxide was monitored during time and a mathematical fitting process was used to extrapolate the data. A linear relationship was observed between reaction rate and the concentration of the starting epoxide, thus suggesting a first-order reaction. Nevertheless, we performed three independent experiments employing different amounts of benzoic acid and an almost perfect overlay of the reaction profiles was obtained (Figure 4.16a). This result suggests that the carboxylic acid concentration does not influence the rate of the ring opening reaction. Next, using the method of the initial rates, we investigated the role of the epoxide in the kinetic law.<sup>165</sup> The linear plot obtained in this experiment accounts for a first-order dependence of the reaction rate with respect to the concentration of epoxide **140i** (Figure 4.16b). From this analysis the reaction rate equation of the carboxylolysis reaction and the observed kinetic constant were experimentally derived ( $K_{obs}=0.295 \text{ M}^{-1}\text{s}^{-1}$ ).

#### 4. Results and Discussion

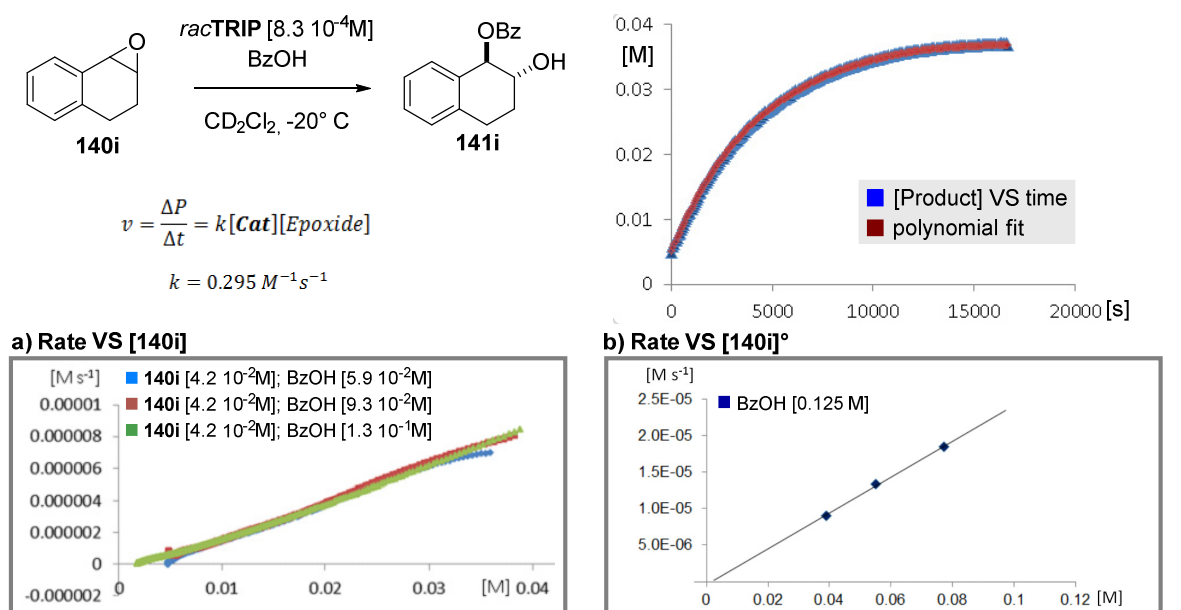


**Figure 4.16.** Kinetic studies on the ring opening of **140i**. Experiments followed by <sup>1</sup>H-NMR.

Aiming towards a more complete understanding of the system under investigation, we have also explored the deactivation pathway of the phosphoric acid catalyst in the absence of carboxylic acid. In this case we used <sup>31</sup>P-NMR analysis to follow the alkylation of **TRIP** with epoxide **50a** (Figure 4.17). The reaction was performed employing an excess (10 equiv.) of the epoxide for two reasons: (1) to mimic catalytic conditions for the phosphoric acid compound and (2) to reach pseudo-zeroth order dependence with respect to that substrate.

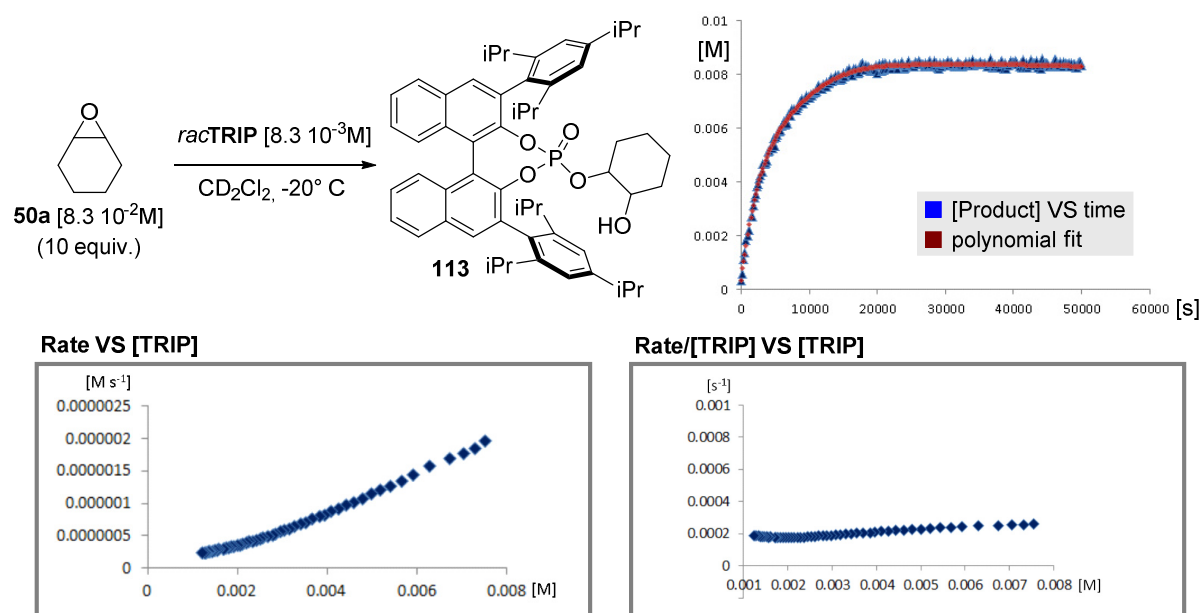
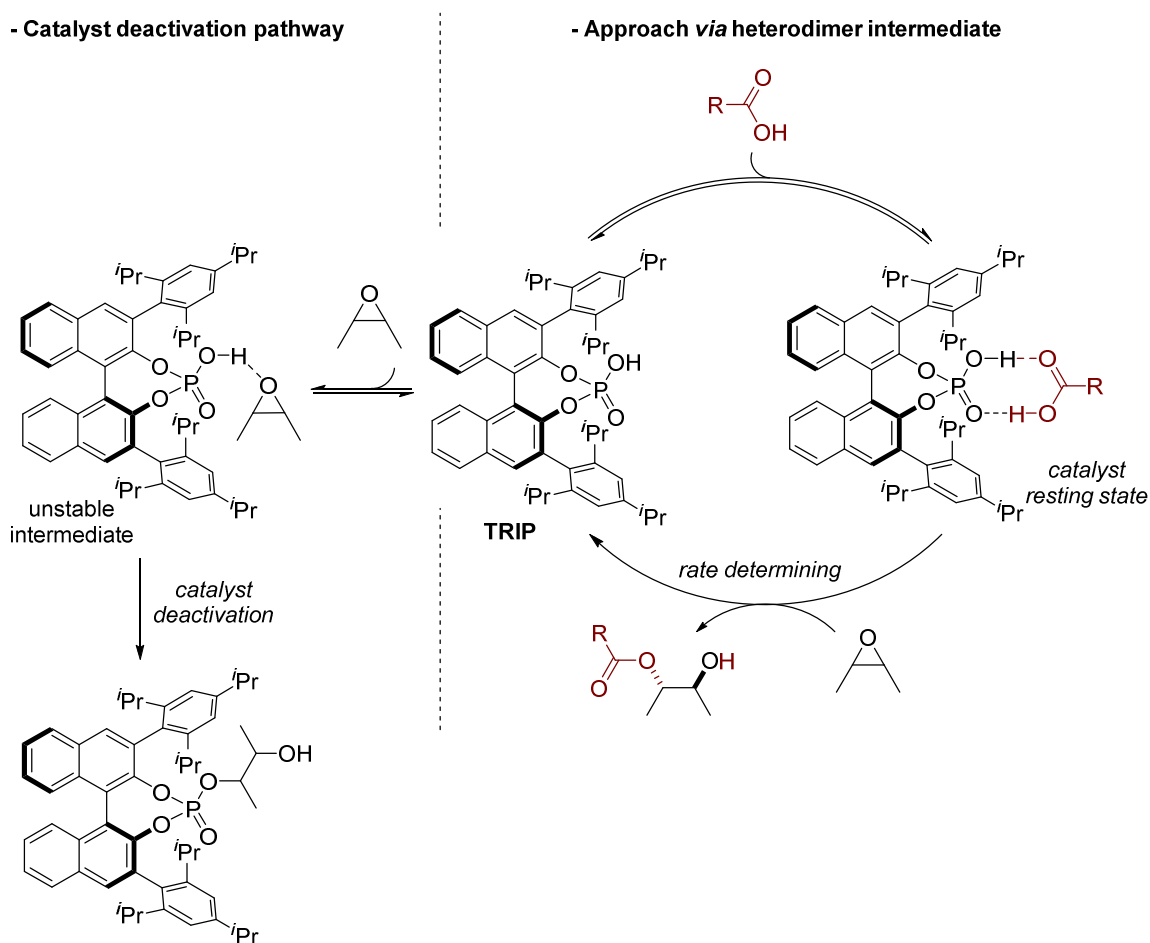


**Figure 4.17.** Kinetic studies on the deactivation pathway. Experiment followed by <sup>31</sup>P-NMR.

As shown in Figure 4.17, a linear relationship was observed between the decomposition rate and the concentration of **TRIP**, thus indicating a bimolecular reaction in which only one molecule of the phosphoric acid is involved in the reaction pathway.

According to this kinetic analysis a reaction mechanism can be proposed (Scheme 4.38). The interaction between the phosphoric acid catalyst and the epoxide leads to the direct alkylation of the catalyst. However, upon heterodimerization with carboxylic acids such undesired pathway is effectively prevented. The heterodimer then engages the asymmetric carboxylisis reaction due to the observed increased acidity and nucleophilicity, delivering the ring opening product and regenerating the “free” catalyst which is immediately associated again with another molecule of carboxylic acid. The resting state of the catalytic cycle is proposed to be the heterodimeric species (due to the observed zeroth order dependence on the carboxylic acid) while the ring opening reaction is the rate-determining step (first-order with respect to the epoxide).



**Scheme 4.38.** Proposed catalytic cycle

The catalytic cycle was also investigated by computational analysis. Using density functional theory calculations at the B3LYP/cc-pTVZ level, we followed the sequence of the different intermediates with particular interest in the energetic reaction pathway (Figure 4.18). We propose that the heterodimer resting state (II) is intercepted by the epoxide resulting in the formation of a trimolecular complex (III) in a reversible fashion. Next the  $S_N2$  ring opening reaction occurs *via* a bifunctional transition state (IV) delivering a catalyst-product complex (V) that gets eventually dissociated and the product gets replaced by a second molecule of carboxylic acid. The overall exothermicity of the reaction is in accordance with the release of the epoxide ring strain.

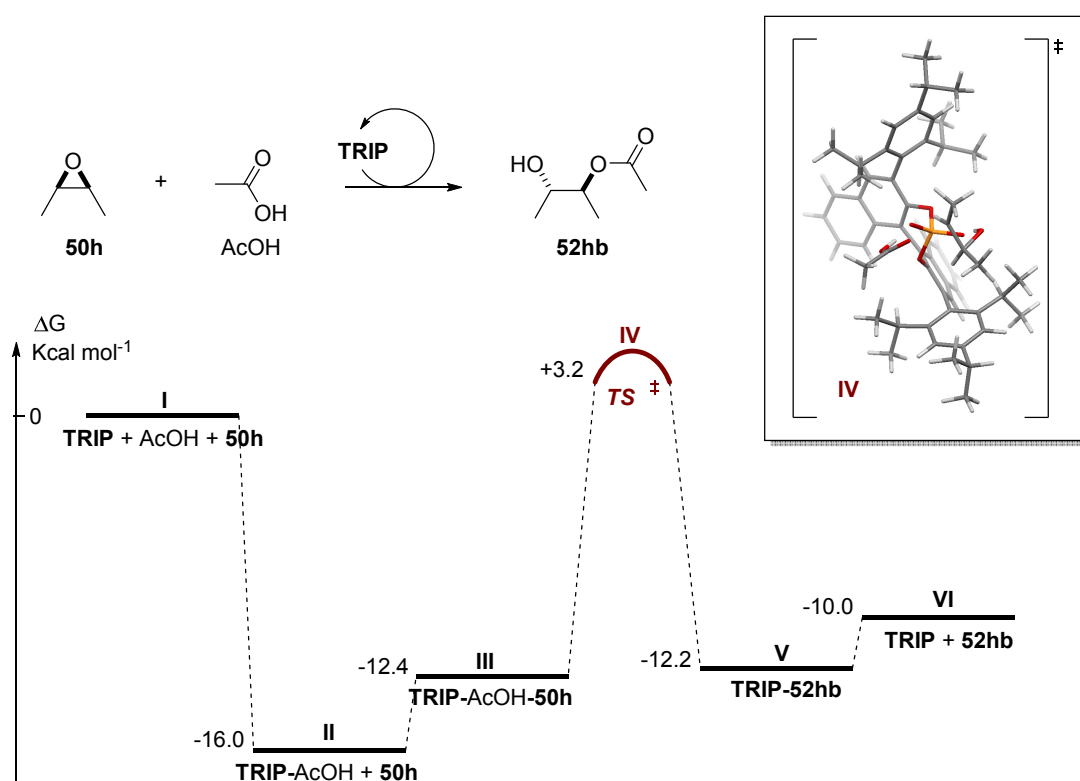


**Figure 4.18.** Theoretical plot of the catalytic cycle. Structures computed at B3LYP/cc-pTVZ level.

According to this analysis, the heterodimeric association plays a crucial role in the reaction, which is based on the inherent dichotomy between stability and reactivity. The apparent change of the polarity of the mechanism, in which the phosphoric acid catalyst primarily establishes an interaction with the nucleophile rather than with the electrophile, is somewhat peculiar. This kind of unconventional strategy represents a core feature of our approach to carboxylic acid activation.

### 4.5.3. Investigations on the transition states

During these studies, a pronounced influence of the structure of the phosphoric acid catalyst on the reaction outcome was observed. Sterically hindered catalysts usually outperformed less bulky phosphoric acids with significant influence on both reaction rate and enantioselectivity of the transformations. This simple experimental observation was realized during the investigations on the ring opening of aziridines and turned out to be crucial when we were studying the reaction on the epoxide system. A moderate selectivity was obtained with **TRIP**, whilst catalyst **139**, bearing rigid polycyclic substituents, was found to be optimal for the reaction. These results were similarly observed in the desymmetrization and kinetic resolution of epoxides with carboxylic acids and also in the reactions with thiocarboxylic acids. In order to understand the catalyst structure-selectivity relationship, we investigated the transition states for the ring opening of *meso*-epoxides using DFT calculations (structures at B3LYP/6-31G\* level) both with (*S*)-**TRIP** and with catalyst (*S*)-**139** (Figure 4.19 and 4.20 respectively). As mentioned before, the reaction is believed to be occurring through a bifunctional transition state in which both substrates are interacting with the phosphate moiety in the catalyst pocket.

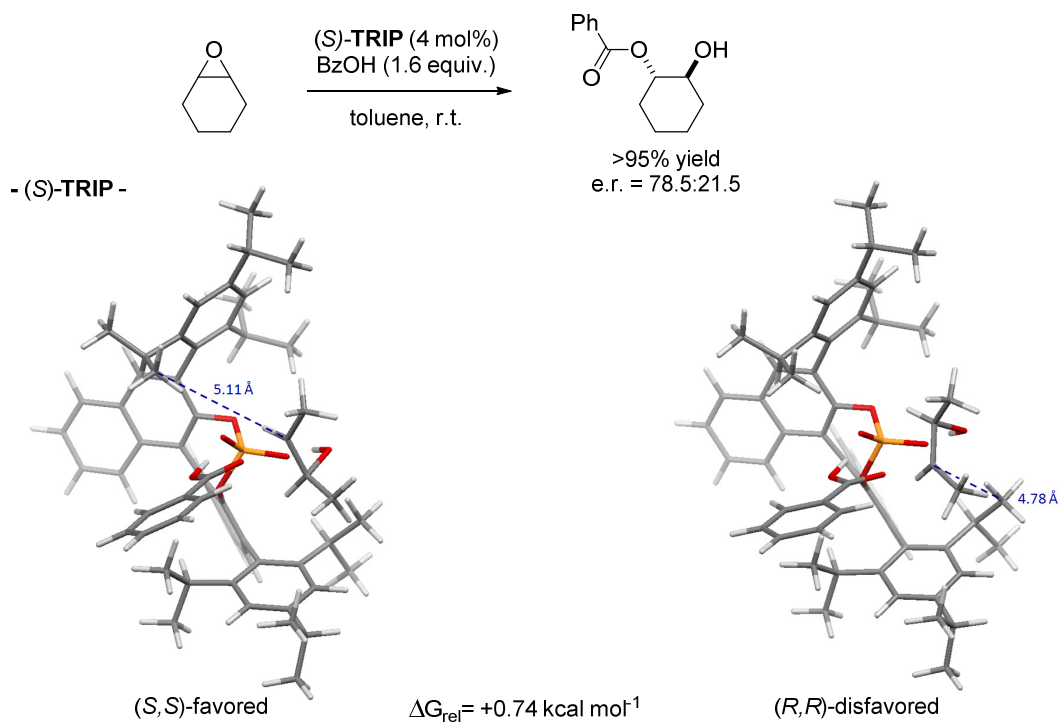


**Figure 4.19.** Transition states analysis for the carboxylation of *meso*-epoxides with **TRIP**. Structures computed at B3LYP/6-31G\* level.

The diastereomeric structures computed for the reaction catalyzed by **TRIP** phosphoric acid are in agreement with the experimental outcome, showing a lower energy for the transition state leading to the experimentally favored (*S,S*)-product ( $\Delta G = 0.74 \text{ kcal mol}^{-1}$ ). The origin of the selectivity observed may be ascribed to a different spatial arrangement: the closer distance between the reacting carbon center and the catalyst scaffold suggests a more energetic pathway for the formation of the minor enantiomer of the product ( $5.11 \text{ \AA}$  vs.  $4.78 \text{ \AA}$ ).

Similar considerations can be employed for the diastereomeric transition states for the reaction catalyzed by **139** (Figure 4.20).

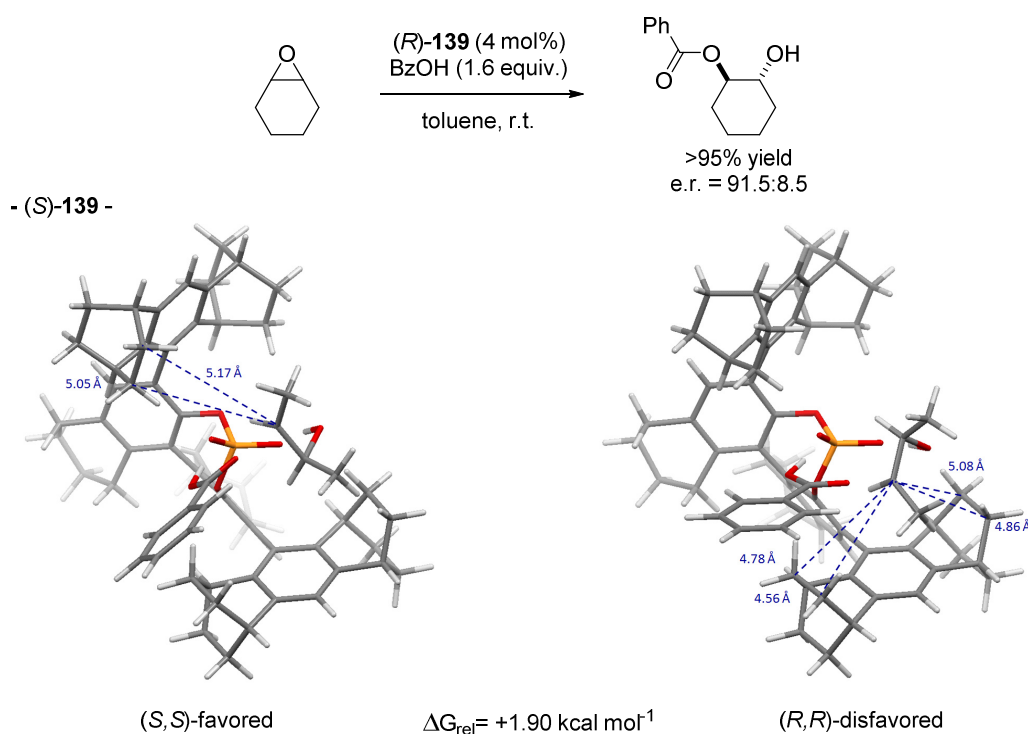


**Figure 4.20.** Transition states analysis for the carboxylation of *meso*-epoxides with catalyst **139**. Structures computed at B3LYP/6-31G\* level.

We have previously qualitatively investigated the catalytic pocket of our novel catalyst by X-ray diffraction analysis (cf. paragraph 4.3) observing a significantly congested active site. Indeed, in agreement with the experimental data, the calculation reveals a higher energy difference between the two transition states with respect to the reaction catalyzed by **TRIP** ( $\Delta G = 1.90 \text{ kcal mol}^{-1}$ ). It is noteworthy that in the disfavored transition state (leading to *R,R*-product), the reacting center is mainly surrounded by aliphatic portions of the

polycyclic substituent, which will presumably not provide any significant stabilization to the polar, partially charged reaction center, which is indeed placed almost equidistantly from the four aliphatic groups. Notably, the closest methylene group to the epoxide center is in the *meta*-position of the aryl substituent (4.56 Å), confirming the importance of the *ortho-meta* substitution pattern in our designed class of catalysts.

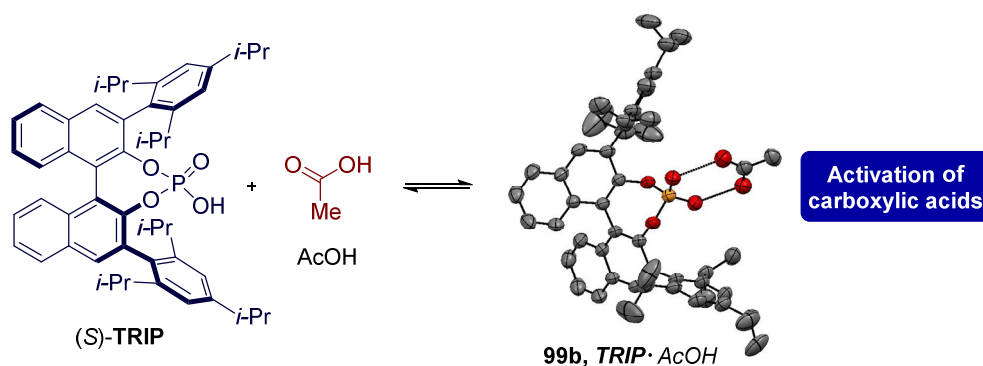
Having witnessed the potential of confinement in phosphoric acid catalysis, we predict that this class of catalysts may significantly contribute to a further advancement of asymmetric Brønsted acid organocatalysis.

## 5. Summary

### 5.1. Activation of carboxylic acids in asymmetric organocatalysis

Brønsted acid catalysis has had an enormous impact in organic chemistry and great interest remains in the development of highly enantioselective methodologies. However, several substrates classes are not prone to established asymmetric activation strategies and therefore their transformations remain elusive in this field. For this reason, an active research program in our laboratory is aimed at the development of novel catalytic modes for such challenging classes.

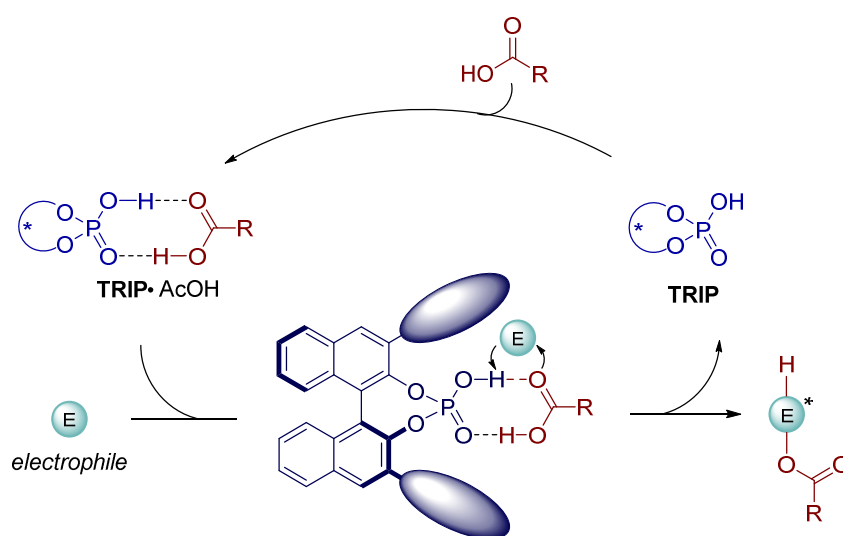
Due to the particular chemical features, the exploitation of carboxylic acid substrates in catalytic methodologies has been rather limited and this Ph.D. thesis describes the development of a new concept for the activation of this moiety in chiral Brønsted acid catalysis. Prior to this work, no general asymmetric system had been developed for the exploitation of carboxylic acids, whether organocatalytic or metal-based (cf. paragraph 2.3). In metal-free catalysis, the only successful methodologies were intramolecular lactonization reactions and the carboxylate moiety served only as nucleophilic handle to capture an electrophilic species, which had been generated in spatial proximity in an asymmetric fashion.<sup>68-71</sup> Yet, due to their easy accessibility and their high stability, carboxylic acids are remarkably useful compounds in organic synthesis and their transformations are widely employed on an industrial scale.<sup>61</sup> Focusing on the hampered homodimerization of chiral phosphoric acid catalysts, we developed a new activation strategy based on the heterodimerizing self-assembly with carboxylic acids.



**Scheme 5.1.** Heterodimerizing self-assembly between **TRIP** phosphoric acid and acetic acid.



The features of this novel recognition were established by various analytical techniques, while the properties could be explored by both theoretical and synthetic investigations. Our analyses confirmed that a highly acidic and reactive species was formed upon association, and the study of the frontier molecular orbital of the carboxylic acid molecule revealed that its nucleophilicity was enhanced (HOMO activation).<sup>32</sup> Exploiting this activation mode we investigated a novel catalytic mechanism, which exhibits an apparent reversed polarity from the usual Brønsted acid catalysis.<sup>39a</sup> In fact, the phosphoric acid catalyst primarily activates the nucleophile rather than directly interacting with the electrophilic partner (Scheme 5.2).



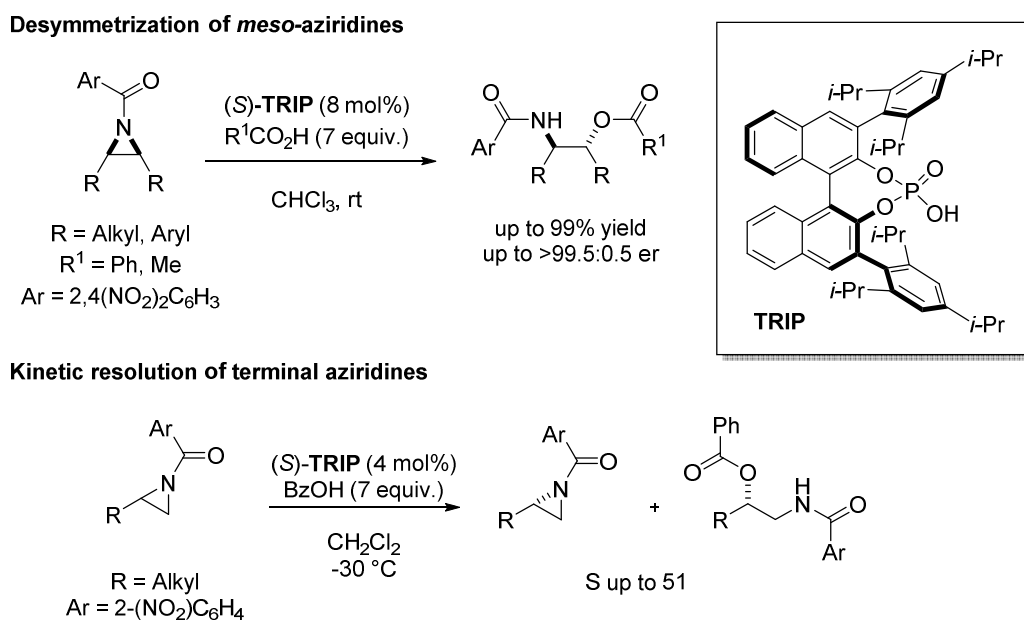
**Scheme 5.2.** A novel catalytic cycle in asymmetric phosphoric acid catalysis.

We have demonstrated that this self-assembly serves as useful tool in the organocatalysis of nucleophilic addition reactions of carboxylic acids with highly reactive, Lewis basic compounds. This association effectively overrides the instability of phosphoric acid catalysts towards aziridines and epoxides and was exploited for the asymmetric carboxylation of these important electrophiles.

As suggested in the introduction, the success of organocatalysis relies on the possibility to design novel transformations based on established activation modes.<sup>33</sup> From this point of view, our investigation may open new perspectives by not only providing a general strategy for the reactions of carboxylic acids, but also promoting the development of different heterodimeric activations.

## 5.2. Highly enantioselective carboxylsysis of aziridines<sup>113</sup>

Molecules containing a vicinal amino alcohol moiety are interesting synthetic targets, due to their abundance in naturally occurring molecules, pharmacologically active compounds, and their application as chiral ligands, auxiliaries, or catalysts in asymmetric transformations.<sup>112</sup> Stereoselective metal-based transformations of aziridines have been widely investigated in the last few years,<sup>78</sup> but an asymmetric catalytic conversion that leads to amino alcohols has been entirely elusive. Organocatalytic asymmetric ring opening of aziridines are instead significantly rare and in phosphoric acid catalysis these transformations face the alkylative deactivation of the catalyst as the major challenge. Exploiting the novel activation of carboxylic acids, and tuning the reactivity of the aziridine substrates by the judicious choice of the nitrogen protecting group, their first asymmetric conversion into protected 1,2-aminoalcohols was disclosed (Scheme 5.3).

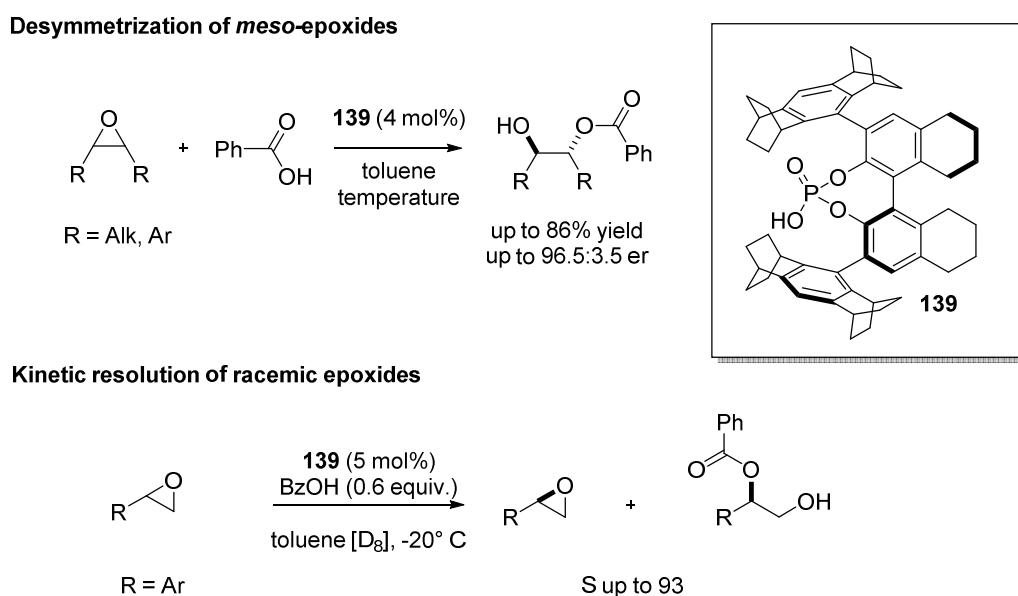


**Scheme 5.3.** Highly enantioselective carboxylsysis of aziridines

Catalyzed by **TRIP** phosphoric acid, a highly enantioselective desymmetrization of *meso*-aziridines was obtained and the desired products were generally isolated in excellent yields and enantioselectivities. Remarkably, this methodology was also successfully utilized for a kinetic resolution of terminal aziridines. Notably, in this transformation both products are synthetically valuable and could be obtained in excellent enantiopurity. The  $S_N2$  ring opening event occurs selectively at the most substituted carbon center, thus suggesting an asynchronous concerted mechanism.

### 5.3. Asymmetric, biomimetic hydrolysis of epoxides<sup>132</sup>

There is significant industrial interest in the asymmetric hydrolysis of epoxides as this transformation gives access to chiral 1,2-diol moieties,<sup>89</sup> which are widespread in natural and medicinal compounds.<sup>77</sup> Moreover, when applied to a kinetic resolution strategy, it provides enantiopure epoxides, which are considered linchpin intermediates in organic synthesis.<sup>152</sup> Exploring the reactivity of our heterodimeric species, we discovered that, even in this case, the deactivation of the catalyst was inhibited and that our novel carboxylic reaction could be used for the desymmetrization of *meso*-epoxides. Nevertheless, due to the absence of stereodiscriminating moieties in the substrate, the reaction catalyzed by **TRIP** was found only moderately enantioselective. Therefore, a novel confined phosphoric acid **139** was designed and synthesized, providing a suitable asymmetric environment for the transformation. We disclosed the first asymmetric ring opening of epoxides with an oxygen nucleophile, which proceeds under metal-free conditions. Both a desymmetrization and a kinetic resolution strategy were developed, providing monoacylated 1,2-diols and chiral epoxides in high enantiopurity (Scheme 5.4).

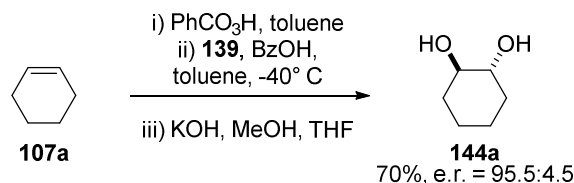


**Scheme 5.4.** Enantioselective carboxylolysis of epoxides: desymmetrization and kinetic resolution

This asymmetric carboxylolysis of epoxides could also be successfully applied to the development of an organocatalytic *anti*-dihydroxylation of simple olefins. Although asymmetric *syn*-dihydroxylation strategies have been widely investigated for many years,<sup>157</sup>

a similar transformation proceeding with *anti*-selectivity had been entirely elusive. We realized that the *Prilezhaev* oxidation of an alkene yields the corresponding epoxide with a stoichiometric amount of carboxylic acid byproduct. By simply adding the phosphoric acid catalyst **139** to the reaction mixture, the asymmetric ring-opening is performed and a following hydrolysis under mild basic conditions delivers the desired chiral 1,2-diol.

**Asymmetric *anti*-dihydroxylation of unactivated olefins**

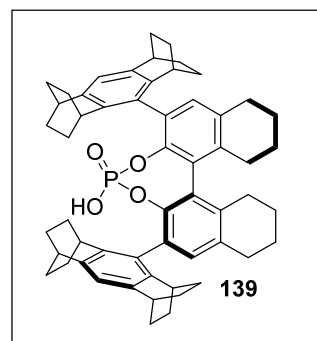
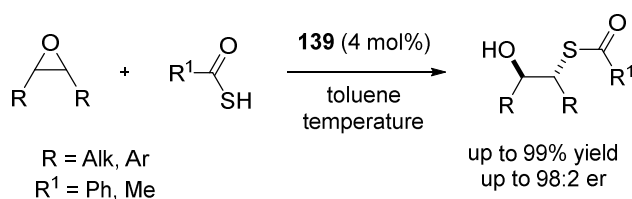
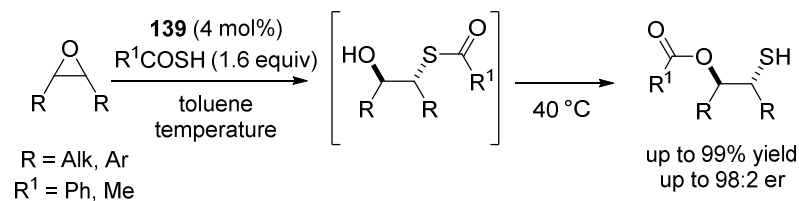


**Scheme 5.5.** First non-enzymatic asymmetric *anti*-dihydroxylation of unactivated olefins.

Mimicking the natural bio-synthetic pathway of 1,2-diols, which is a key transformation in the xenobiotic metabolism of living organisms, this methodology constitutes an elegant biomimetic approach.<sup>23, 91</sup>

#### 5.4. Enantioselective organocascade approach to $\beta$ -hydroxythiols

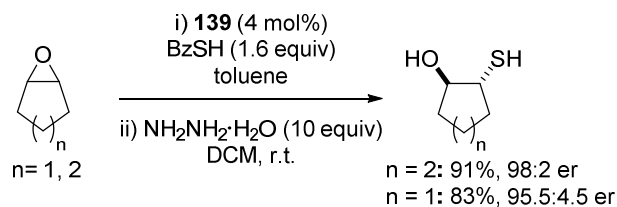
The synthesis of enantiopure thiols is of significant interest for industrial and academic applications. However, direct asymmetric approaches to free thiols have previously been elusive.<sup>100</sup> Despite having been intensively investigated, a straightforward and general asymmetric approach to the synthesis of chiral  $\beta$ -hydroxythiols was still not available.<sup>102-103</sup> Broadening the activation of carboxylic acids to its sulfur variant, we studied the asymmetric ring opening of *meso*-epoxides (Scheme 5.6). We disclosed a novel organocascade reaction that is catalyzed by our confined catalyst **139** and furnishes *O*-protected  $\beta$ -hydroxythiols with excellent enantioselectivities. The method relies on an asymmetric thiocarboxylation of *meso*-epoxides, followed by an intramolecular transesterification reaction. By varying the reaction conditions, the intermediate thioesters can also be obtained chemoselectively and enantioselectively. The opportunity to obtain the same scaffold either protected on sulfur or on oxygen by a simple modification is noteworthy and could open intriguing possibilities in synthetic medicinal chemistry.

Asymmetric thiocarboxylation of *meso*-epoxidesOrganocascade synthesis of *O*-protected  $\beta$ -hydroxythiols

**Scheme 5.6.** Asymmetric thio-carboxylation of *meso*-epoxides and organocascade approach to  $\beta$ -hydroxythiols.

In addition, the deprotection reaction can be performed *in situ* affording the free  $\beta$ -hydroxythiol under mild conditions and, as such, the methodology is an attractive alternative to hypothetical asymmetric sulfhydrolysis of epoxides (Scheme 5.7).

## Asymmetric variant to the sulfhydrolysis of epoxides



**Scheme 5.7.** Asymmetric variant to the sulfhydrolysis of *meso*-epoxides.

## 5.5. Exploration of novel classes of confined phosphoric acid catalysts

Chiral phosphoric acids represent the most exploited class of catalyst for asymmetric Brønsted acid catalysis. As discussed in the introduction (cf. paragraph 2.2.2), one of the crucial aspects which contributes to their success is represented by the possible modular nature of the geometrical properties of the active site. Among others, **TRIP** is recognized as one of the most useful and versatile phosphoric acid and, being significantly more hindered than its congeners, it is usually preferred when the reaction substrates lack big

stereodiscriminating groups.<sup>53</sup> The reduced size of the catalytic pocket limits the number of possible conformations in the transition states, thus reducing possible less-selective pathways. Nevertheless, the class of highly hindered catalysts is underrepresented and presumably this is due to challenging synthetic routes.

During our investigations on the hydrolysis of epoxides, in an effort towards the optimization of the selectivity of the reaction, we had the opportunity to further contribute to the field of asymmetric acid catalysis by developing a new family of chiral BINOL-derived phosphoric acids. We initially designed and synthesized catalyst **114** with bulky *tert*-butyl groups in the *ortho*-positions of the aryl substituents and then we introduced a novel class of catalysts (**115a-c**) characterized by a combined *ortho-meta* substitution pattern. All these catalysts bear the active phosphoric acid moiety in a congested environment and at the same time possess unique spatial arrangements. Although we observed a superior selectivity with the polycyclic catalyst **115b**, we expect that all these catalysts to find application in different asymmetric methodologies.

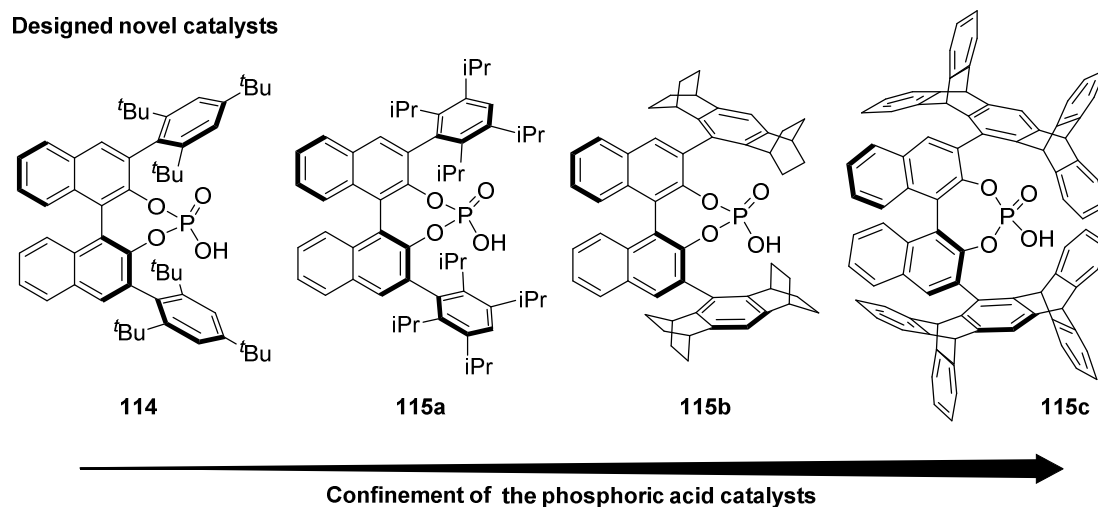


**Figure 5.1.** Designed novel confined phosphoric acid catalysts

As expected, modifying the axially chiral backbone of catalyst **115b**, a fine tuning of the selectivity was obtained. Phosphoric acid **139**, with a tetra-hydrogenated BINOL-scaffold, was found to be the optimal catalyst in both asymmetric transformations involving the ring opening of epoxides (Figure 5.2).

A combination of other chiral backbones (i.e. SPINOL, biphenol, etc.) and these newly introduced substituents can generate new successful entries to the class of confined phosphoric acids.

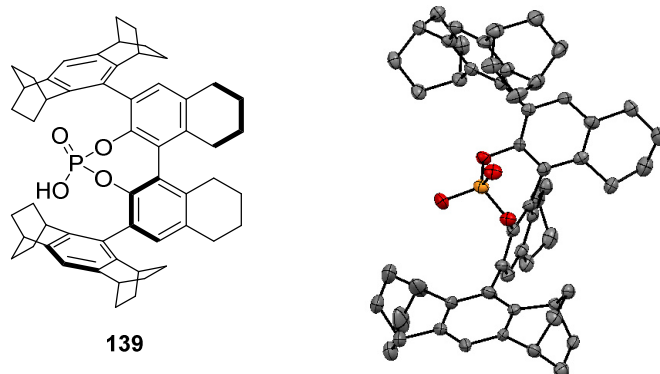


**Figure 5.2.** Catalyst **139** and X-ray crystal structure.

This work has been disclosed in part in the following publications:

- 1) "Activation of Carboxylic Acids in Asymmetric Organocatalysis"; M. R. Monaco, B. Poladura, M. Diaz de los Bernardos, M. Leutzsch, R. Goddard, B. List, *Angew. Chem. Int. Ed.* **2014**, *53*, 7063.
- 2) "An Organocatalytic Asymmetric Hydrolysis of Epoxides"; M. R. Monaco, S. Prévost, B. List, *Angew. Chem. Int. Ed.* **2014**, *53*, 8142.
- 3) "Catalytic Asymmetric Synthesis of Thiols"; M. R. Monaco, S. Prévost, B. List, *J. Am. Chem. Soc.* **2014**, *136*, 16982.

## 6. Outlook

The establishment of a novel activation mode in organocatalysis usually provides a useful entry to a variety of novel transformations which were previously elusive. We believe that the concepts described in this thesis can be exploited for the asymmetric reactions of carboxylic acids and thiocarboxylic acids with a large variety of electrophiles. Moreover, hydroxyl and thiol moieties are widespread in nature and, since carboxylate compounds can be used as valuable precursors, applications of these methodologies to total synthesis of natural products can be predicted.

Beyond these possible developments, which would be difficult to enumerate and to encompass all, some related applications can be envisioned not only in the field of asymmetric catalysis.

### 6.1. Enantioselective recognition of chiral carboxylic acids by heterodimerization.

Enantioselective recognition of the two enantiomers of chiral compounds is not only an important aspect in asymmetric catalysis, but it also holds an interesting potential for different applications in biology, material and pharmaceutical sciences.<sup>166</sup> For this reason, the design of synthetic, chiral receptors has become an important and growing field in applied chemistry.

Chiral carboxylic acids are important molecules in medicine.<sup>167</sup> For instance, a large family of non-steroidal anti-inflammatory drugs is represented by chiral derivatives of propionic acids and chirality is known to strongly influence the bioactivity of these compounds. As presented in the introductory section, a notable example is *naproxen*: the (*S*)-enantiomer is used to treat arthritis pain, while the (*R*)-isomer causes liver poisoning (cf. paragraph 1.1).<sup>9c</sup> Therefore the development of selective synthetic receptors for chiral carboxylic acids or carboxylate is highly investigated.<sup>168</sup>

The heterodimeric self-assembly with phosphoric acids holds discrete potential in this context. The wide commercial availability of chiral phosphoric acids seems to be particularly suitable to tune the properties of a supramolecular recognition.<sup>169</sup> Heterodimers of chiral phosphoric acids with the different enantiomers of carboxylic acids are diastereoisomeric



species and as such may exhibit significantly different stability and display different physico-chemical properties (Figure 6.1). Next to the classical uses of enantioselective recognition for optical resolution strategy (crystallization, partition methods, separation) an interesting application of this phenomenon is represented by the enantiopurity determination by chiral shift reagents. NMR would represent a sensitive, fast and non-destructive technique for the analysis of a scalemic mixture.

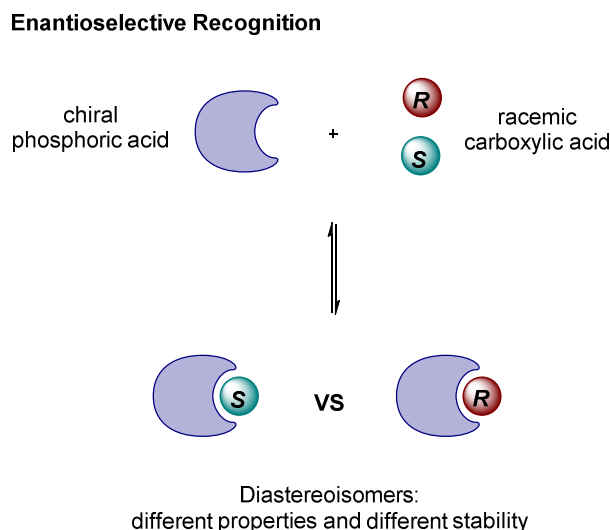


**Figure 6.1.** Enantioselective recognition of carboxylic acids *via* heterodimerization.

Indeed, preliminary investigations on mixture of **TRIP** phosphoric acid and racemic mandelic acid **51x**, confirms such opportunity (Table 6.1). The addition of the phosphoric acid to a solution of racemic carboxylic acid causes the split of the resonance signals of the enantiomers.

entry	ratio TRIP:51x	<sup>1</sup> H-NMR
1	0:1	
2	0.5:1	
3	1:1	
4	1.5:1	

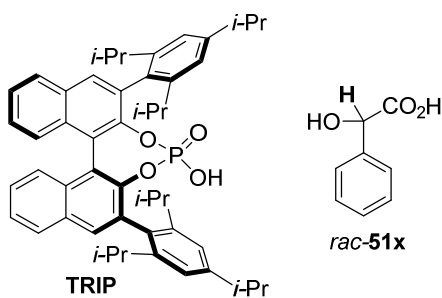


**Table 6.1.** NMR investigation of diastereoisomeric heterodimers.

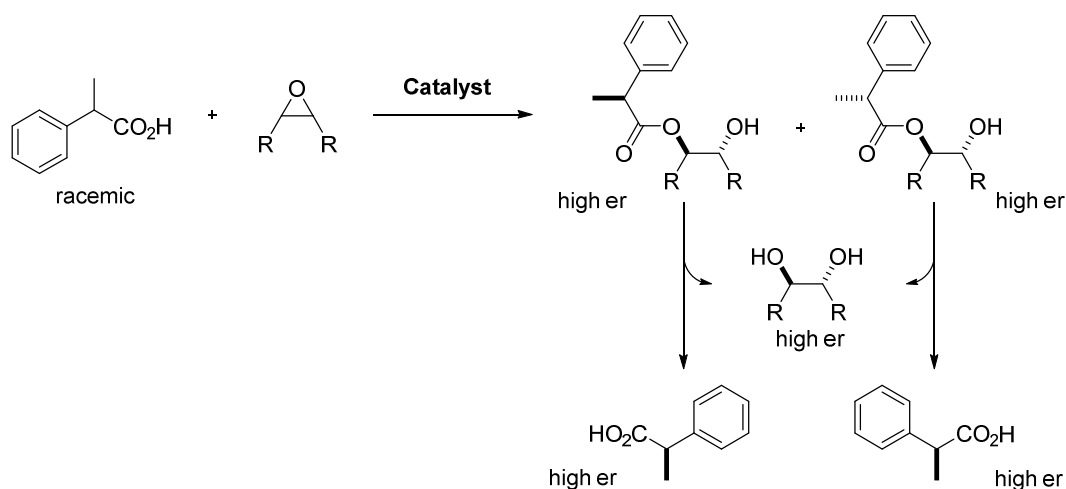
Intriguingly, the maximum gap between the signals is shown at an equimolar ratio between the two species (entry 3, Table 6.1) and upon saturation of the mandelic acid an overlap is obtained again (entry 4, Table 6.1). This observation suggests that the resonance splitting is due to a significant difference of binding constants rather than a different chemical shift of the complexes formed.

Further investigations on this phenomenon may provide interesting advances for industrial and analytical purposes.

## 6.2. Stereodivergent resolution of racemic carboxylic acids.

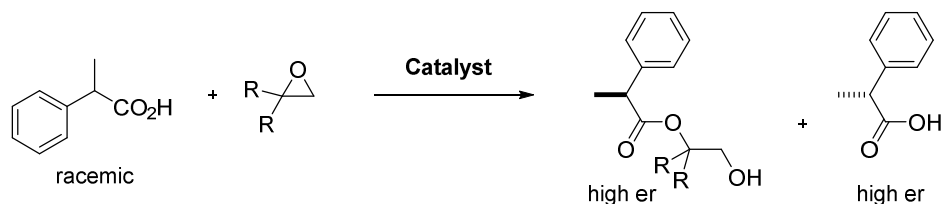
Notably, the disclosed asymmetric carboxylation of epoxides (cf. paragraph 4.3) is characterized by a perfect atom economy. However, in order to isolate the chiral 1,2-diol, the mild basic hydrolysis regenerates a stoichiometric amount of carboxylic acid as byproduct. To overcome this synthetic issue, we used inexpensive benzoic acid as preferred nucleophile. Nevertheless, the possible recovery of the carboxylic acid could avoid any waste.

In a parallel process, the stereodivergent resolution of chiral carboxylic acids can be realized.<sup>170</sup> The high enantiocontrol on the epoxide ring opening is presumably maintained when reacting both enantiomers of the nucleophile and a separable mixture of enantiopure diastereoisomeric products is expected (Scheme 6.1). Mild hydrolysis may eventually deliver at the same time the enantioenriched 1,2-diols and the resolved carboxylic acid enantiomers.



**Scheme 6.1.** Stereodivergent resolution of carboxylic acids *via* epoxide carboxylation.

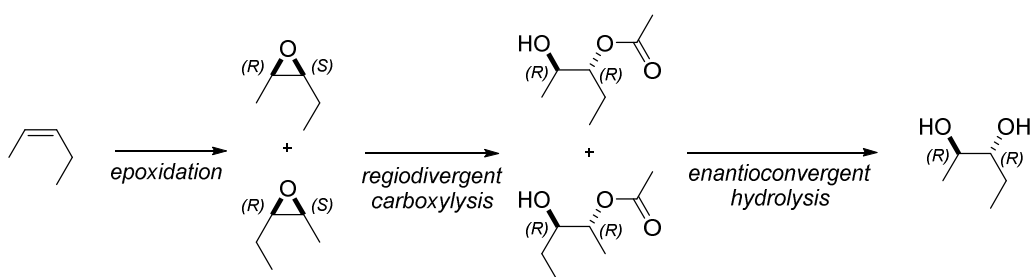
In this context a kinetic resolution of carboxylic acid *via* simple oxirane ring opening may also be hypothesized, although this reaction would face the ring opening at the methylene carbon as the major challenge (Scheme 6.2).



**Scheme 6.2.** Kinetic resolution of carboxylic acids *via* epoxide carboxylisis.

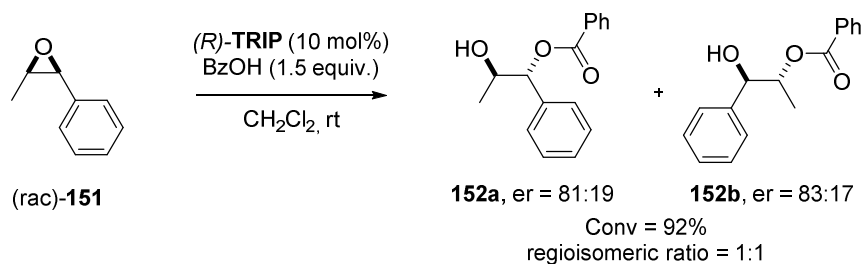
### 6.3. Regiodivergent, enantioconvergent dihydroxylation of unsymmetrical olefins.

The ring opening of epoxides, promoted by catalyst (*R*)-**139** exhibited a strong preference for the nucleophilic attack on the (*S*)-chiral center of the *meso*-epoxides, thus favoring the (*R,R*)-product. A similar selectivity was observed for the kinetic resolution of racemic epoxides, which preferentially reacts (*S*)-epoxides. Performing the reaction on a disubstituted epoxide, derived from an unsymmetrical olefin, can result in the regiodivergent ring opening of the two enantiomers (Scheme 6.3).<sup>171</sup> Notably, the two products would show the same absolute configuration (*R,R*) and the mild hydrolysis would therefore provide the same 1,2-diol. Such reaction design may be utilized to broaden the scope of our *anti*-dihydroxylation of olefin to a large variety of *cis*-alkenes.



**Scheme 6.3.** Regiodivergent and enantioconvergent *anti*-dihydroxylation strategy.

Indeed, a preliminary investigation on the carboxylisis of epoxide **151** using (*R*)-**TRIP** as the catalyst, confirmed that the catalytic regiodivergent process can be realized. Approaching full consumption of the epoxide starting material, the two regioisomers **152a,b** were obtained in an equimolar amount and with significant enantioenrichment (Scheme 6.4).



**Scheme 6.4.** Preliminary investigation on the regiodivergent carboxylation of unsymmetrical epoxides.

#### 6.4. Towards other heterodimeric self-assemblies.

*“...One of the most useful properties of scientific theories is that they can be used to make predictions about natural events or phenomena that have not yet been observed”*

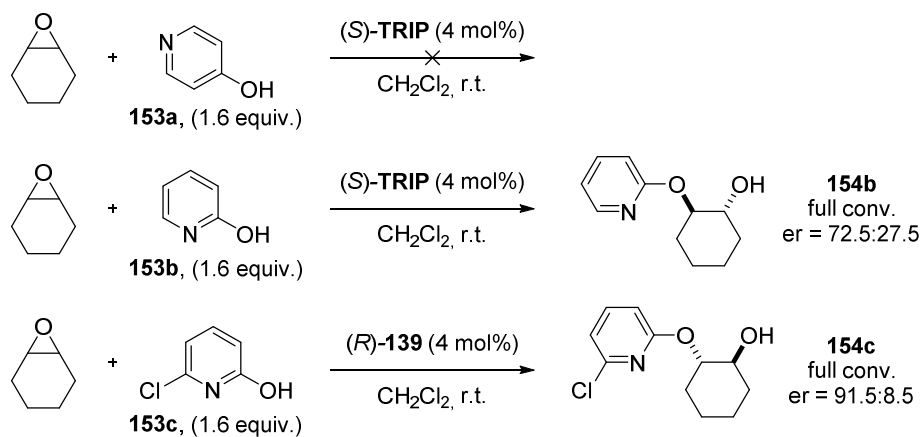
United States National Academy of Sciences, 2008

As we mentioned above, the activation *via* self-assembly heterodimerization may be applied to a variety of reactions of carboxylic acids and thiocarboxylic acids. Nonetheless, we expect that the catalytic principles investigated in this Ph.D. thesis may not be limited to these classes of nucleophiles. The formation of similar supramolecular entities could provide further intriguing possibilities in asymmetric organocatalysis.

For instance, we hypothesized that in analogy with carboxylic acids, 2-pyridone compounds represent suitable association partners for chiral phosphoric acids. In an attempt to preliminary explore our speculation, we selected the ring opening of epoxide as model reaction with **TRIP** as the catalyst. The products obtained in such transformation would have medicinal interest since they have been found active against certain type of cellular cancer growth through the inhibition of *prostaglandins-endoperoxide synthase*.<sup>172</sup>

Indeed, in this case we could not only observe the envisioned reactivity but once again verify the importance of the heterodimeric structure. While no reaction was observed with 4-pyridone, 2-pyridone smoothly gave the desired products in moderate enantioselectivity and no degradation of the phosphoric acid catalyst occurred (2 days, full conv., er = 72.5:27.5). Modifying the electronic properties of the pyridone nucleophile and

using **139** as the catalyst both reactivity and selectivity were improved (4 hours, full conv., er = 91.5:8.5).



**Scheme 6.5.** Preliminary studies on 2-pyridones reactivity.

Indeed, also in this case, the speculated interaction could be qualitatively confirmed by NMR analysis (Figure 6.2).

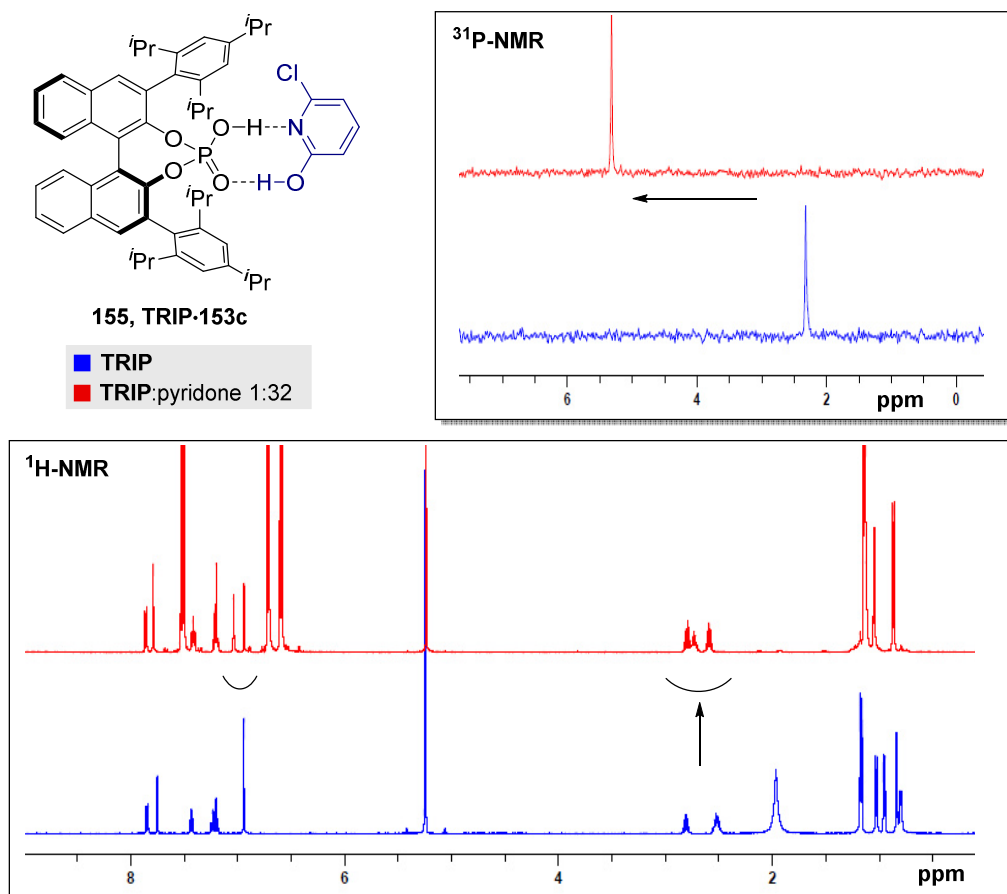


**Figure 6.2.** Spectroscopic investigations on the interaction of **TRIP** phosphoric acid and pyridones.

Given these results, it is presumable that the newly investigated catalytic mode also encompasses the asymmetric reactions of mercaptobenzothiazols, recently explored by the *Sun* group (cf. paragraph 2.5.1).<sup>173</sup>

## 7. Experimental Section

### 7.1. General experimental conditions

#### Solvents and reagents

All solvents used in the standard procedures were purified by distillation. Absolute diethyl ether, tetrahydrofuran and toluene were obtained by distillation over sodium with benzophenone as indicator; absolute chloroform and dichloromethane were obtained by distillation over calcium hydride, and ethanol, isopropanol and methanol were dried by distillation over magnesium. Absolute 1,4-dioxane, MTBE and DCE were purchased from Sigma-Aldrich and used as received. Commercial reagents were obtained from various sources and used without further purification.

#### Known Brønsted acid catalysts

Chiral Brønsted acid catalysts in Tables 4.2, 4.13 and 4.17 and **TRIP** were kindly supplied by the coworkers from the List group and were prepared according to the literature procedures. VAPOL-derived phosphoric acid **30** was purchased from Sigma-Aldrich.

#### Inert gas atmosphere

Air and moisture sensitive reactions were conducted under an atmosphere of argon (*Air Liquide*, >99.5% purity). Unless otherwise stated, all organocatalytic reactions were performed under an ambient atmosphere without the exclusion of moisture or air.

#### Thin layer chromatography (TLC)

Reactions were monitored by thin layer chromatography on silica gel or aluminum oxide precoated plastic sheets (0.2 mm, Macherey-Nagel). Visualization was accomplished by irradiation with UV light at 254 nm and different staining reagents; phosphomolybdic acid (PMA) stain: PMA (10 g) in EtOH (100 ml); *p*-anisaldehyde (PAA) stain: *p*-anisaldehyde (3.5 ml), glacial acetic acid (15 ml), EtOH (350 ml), conc. H<sub>2</sub>SO<sub>4</sub> (50 ml); KMnO<sub>4</sub> stain: KMnO<sub>4</sub> (1.5 g), K<sub>2</sub>CO<sub>3</sub> (10 g) and NaOH<sub>aq.</sub> (10%, 1.25 mL) in H<sub>2</sub>O (200 mL).

### **Column chromatography**

Column chromatography was performed under elevated pressure on silica gel (60, particle size 0.040-0.063 mm, Merck) using a specified solvent mixture.

### **High pressure liquid chromatography (HPLC)**

HPLC analyses on a chiral stationary phase were performed on a Shimadzu LC-2010C system equipped with a UV detector. Commercial HPLC-grade solvents were used, and measurements were conducted at 25 °C. The chiral stationary phase of the columns is specified in each experiment. The enantiomeric ratios were determined by comparing the samples with the appropriate racemic mixtures.

### **Gas chromatography (GC)**

GC analyses on a chiral stationary phase were performed on HP 6890 and 5890 series instruments equipped with a split-mode capillary injection system and a flame ionization detector (FID) using hydrogen as a carrier gas. Detailed conditions are given in the individual experiment. The enantiomeric ratios were determined by comparing the samples with the appropriate racemic mixtures.

### **Nuclear magnetic resonance spectroscopy (NMR)**

Proton, carbon, and phosphorus NMR spectra were recorded on Bruker AV-500 or Bruker AV-400 spectrometers in deuterated solvents at room temperature (298 K). Proton chemical shifts are reported in ppm ( $\delta$ ) relative to tetramethylsilane with the solvent resonance employed as the internal standard ( $\text{CD}_2\text{Cl}_2$ ,  $\delta$  5.32 ppm;  $\text{CDCl}_3$ ,  $\delta$  7.24 ppm;  $(\text{CD}_3)_2\text{SO}$ ,  $\delta$  2.50 ppm;  $\text{THF-}d_8$ ,  $\delta$  3.58, 1.72 ppm).  $^{31}\text{P}$  chemical shifts are reported in ppm relative to  $\text{H}_3\text{PO}_4$  as the external standard. Data are reported as follows: chemical shift, multiplicity (s = singlet, d = doublet, t = triplet, q = quadruplet, Q = quintuplet, sept = septuplet, m = multiplet), coupling constants (Hz) and integration. Slight shape deformation of the peaks in some cases due to weak coupling is not explicitly mentioned.  $^{13}\text{C}$  chemical shifts are reported in ppm from tetramethylsilane with the solvent resonance as the internal standard ( $\text{CD}_2\text{Cl}_2$ , 53.8 ppm;  $\text{CDCl}_3$ ,  $\delta$  77.0 ppm;  $(\text{CD}_3)_2\text{SO}$ ,  $\delta$  39.52 ppm;  $\text{THF-}d_8$ ,  $\delta$  67.21, 25.31 ppm).



### **Mass spectrometry (MS)**

Mass spectra were measured on a Finnigan MAT 8200 (70 eV) or MAT 8400 (70 eV) by electron ionization, chemical ionization or fast atom/ion bombardment techniques. Electrospray ionization (ESI) mass spectra were recorded on a Bruker ESQ 3000 spectrometer. High resolution mass spectra were obtained on a Finnigan MAT 95 or Bruker APEX III FT-MS (7 T magnet). All masses are given in atomic units/elementary charge (m/z).

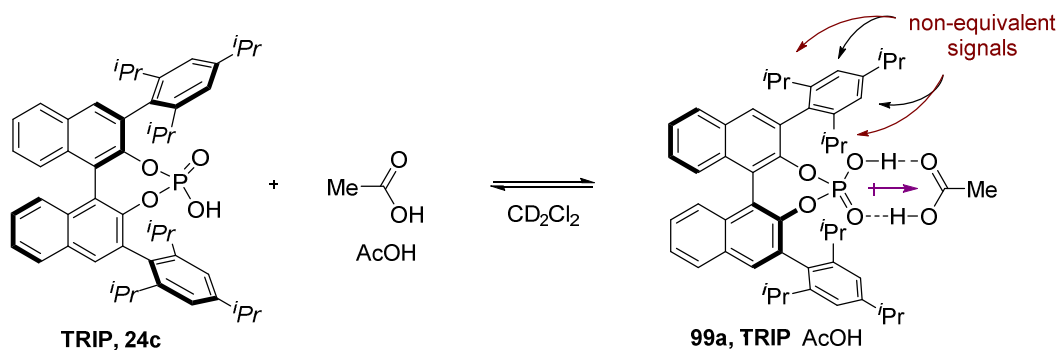
### **Specific rotation**

Optical rotations were determined with Autopol IV automatic polarimeter (Rudolph Research Analytical) using a 50 mm cell with temperature control. The measurements were performed at 25 °C at a wavelength  $\lambda = 589$  nm (sodium D-line). Concentrations (c) are given in g/100 ml.

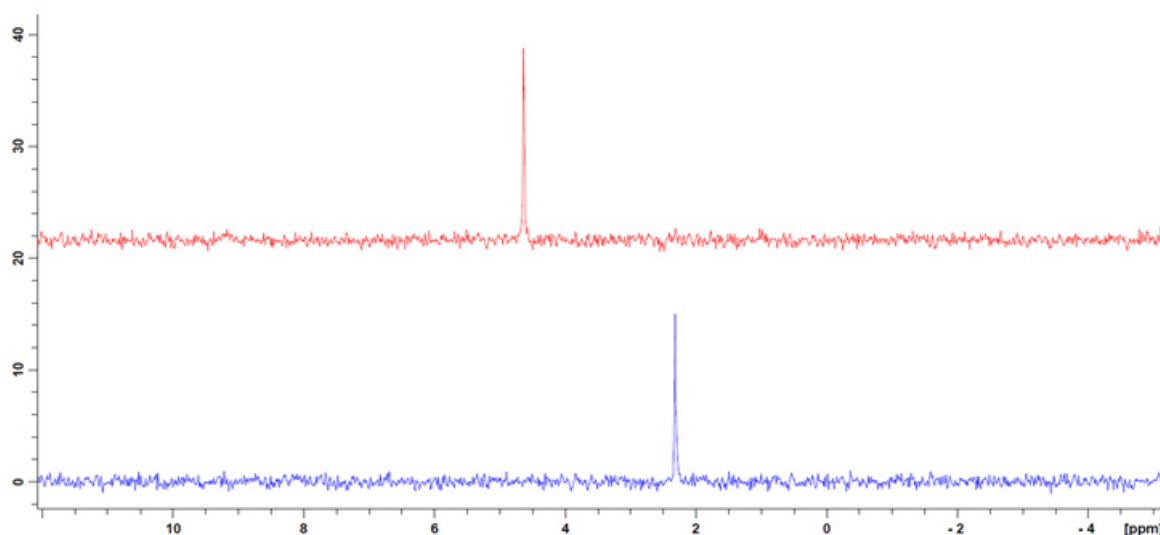
## 7.2. Studies on heterodimeric self-assembly

## 7.2.1. 1D-NMR studies

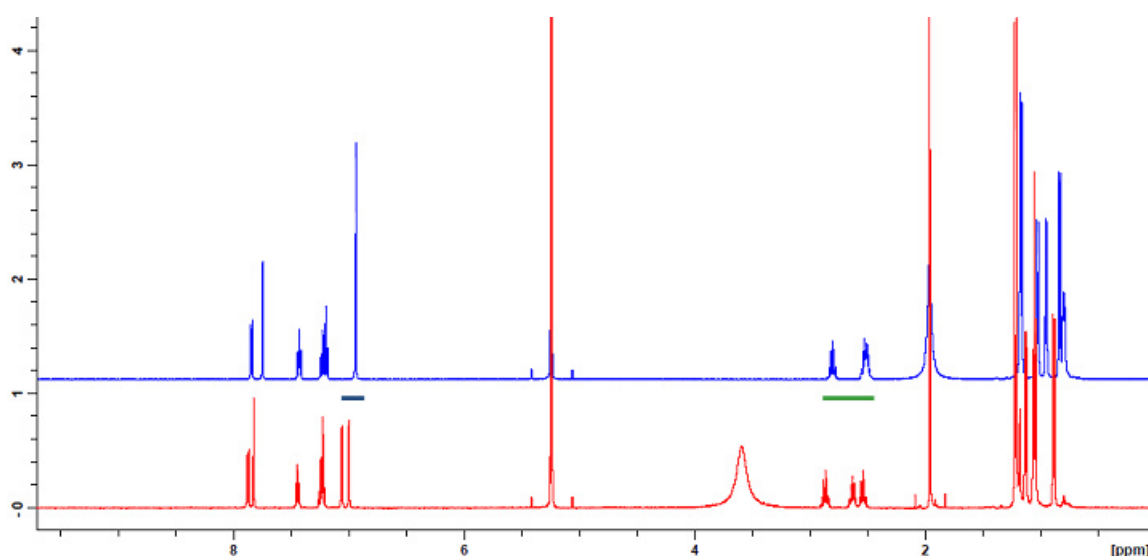
NMR spectroscopic experiments on mixtures of **TRIP** and acetic acid in deuterated dichloromethane were performed to investigate the formation of heterodimeric species **99a**. From these analyses some features of the non-covalent interaction could be appreciated.



*Experiment 1.* A solution of **TRIP** in  $\text{CD}_2\text{Cl}_2$  (0.0013 M) was prepared and analyzed by  $^1\text{H}$ -NMR and  $^{31}\text{P}$ -NMR (blue spectra). Next acetic acid (6 equiv.) was added to the solution. The  $^1\text{H}$ -NMR and  $^{31}\text{P}$ -NMR of the heterodimeric species were measured (red spectra) and compared with the previous data.

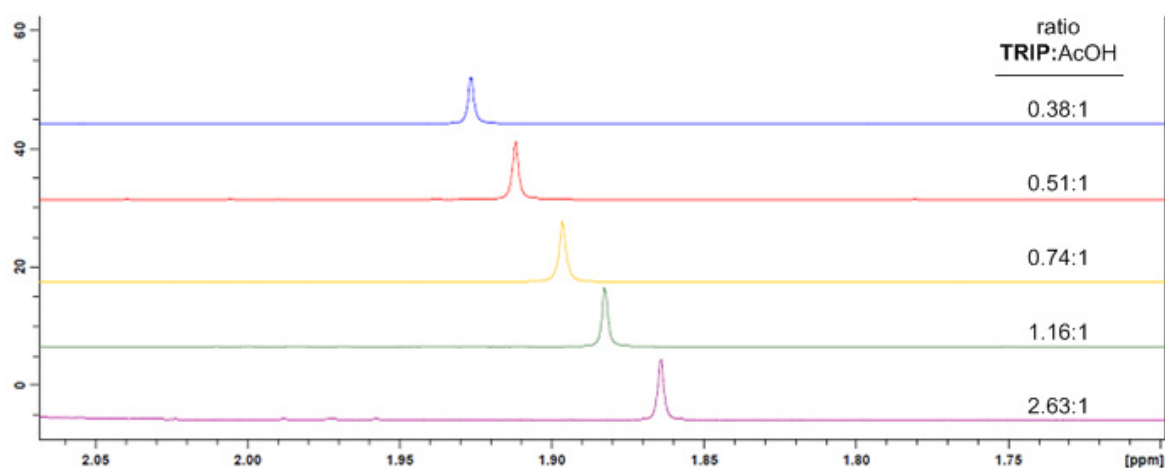
 $^{31}\text{P}$ -NMR

The phosphorous signal in the  $^{31}\text{P}$ -NMR shows a significant shift downfield, thus suggesting the establishment of a different chemical environment.

$^1\text{H-NMR}$ 

In the heterodimeric assembly, the proton signals of the phosphoric acid molecule are observed at lower fields, thus suggesting a lower electron density. In addition, the non-equivalent protons of the 3-3'aryl substituents, which were overlapping in the spectrum of the phosphoric acid monomer, are resolved. Presumably, this phenomenon is due to the presence in the catalytic pocket of the carboxylic acid molecule, which reduces the rotational freedom of the aryl substituent.

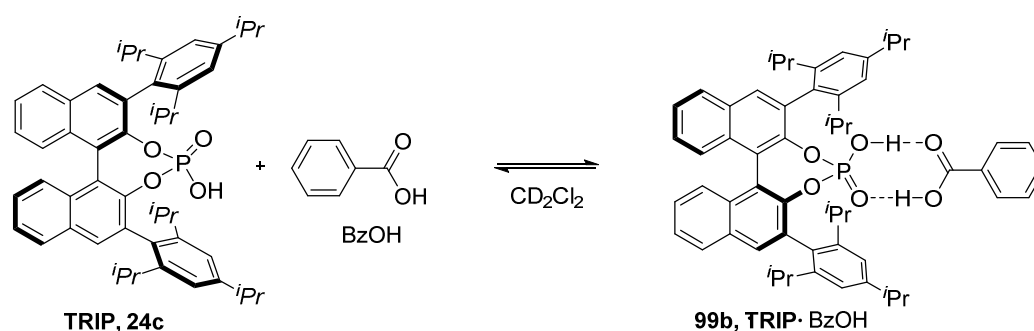
*Experiment 2.* Varying the relative ratio of the two components, mixtures of **TRIP** and acetic acid in deuterated dichlorometane were prepared and the chemical shift of the methyl group of the carboxylic acid was monitored in the  $^1\text{H-NMR}$ .



The establishment of the non-covalent interaction with the phosphoric acid causes an upfield shift of the proton signal of the methyl group of acetic acid. This outcome is in agreement with an increase of electron density on the carboxylic acid fragment. A shielding effect due to the ring current of the aryl substituent can also be hypothesized. However, the analysis of the crystal structure (*vide infra*) shows a significant distance ( $>7\text{\AA}$ ) between this group and the phenyl moiety and therefore, based on the *Johnson-Bovey* equation, a related influence should be minimal.<sup>174</sup>

### 7.2.2. 2D-DOSY studies<sup>115</sup>

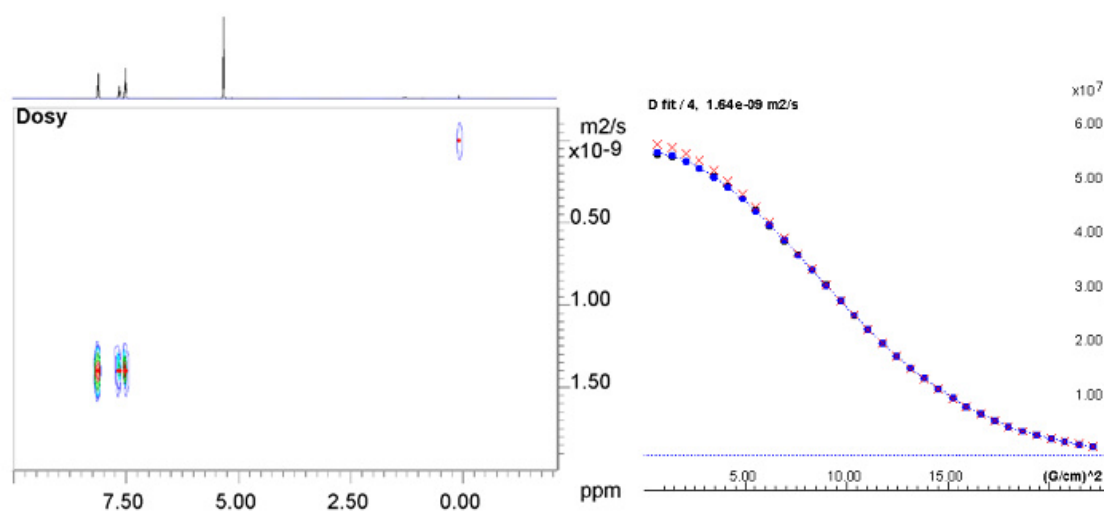
This study was performed to evaluate the effect of the heterodimerization process on the diffusion coefficients of benzoic acid and **TRIP**.



Three different DOSY experiments in deuterated dichloromethane were performed:

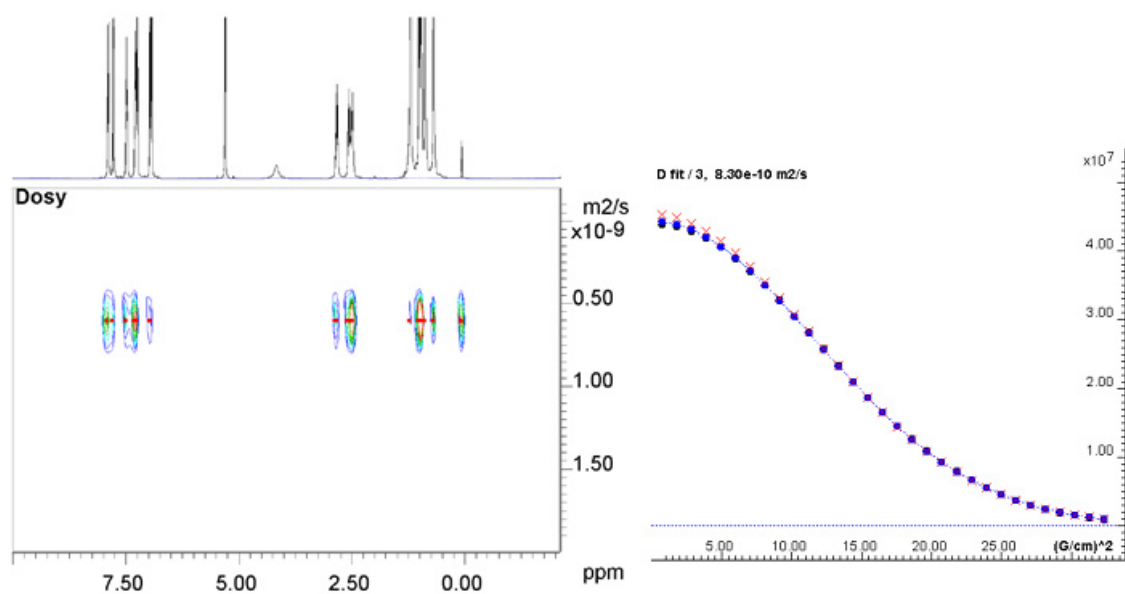
1. benzoic acid,
2. **TRIP**,
3. mixture of **TRIP** and benzoic acid in a 1:1 ratio.

*Experiment 1.* Benzoic acid in  $\text{CD}_2\text{Cl}_2$ .  $D_{\text{BzOH}} = 1.64 \times 10^{-9} \text{ m}^2/\text{s}$

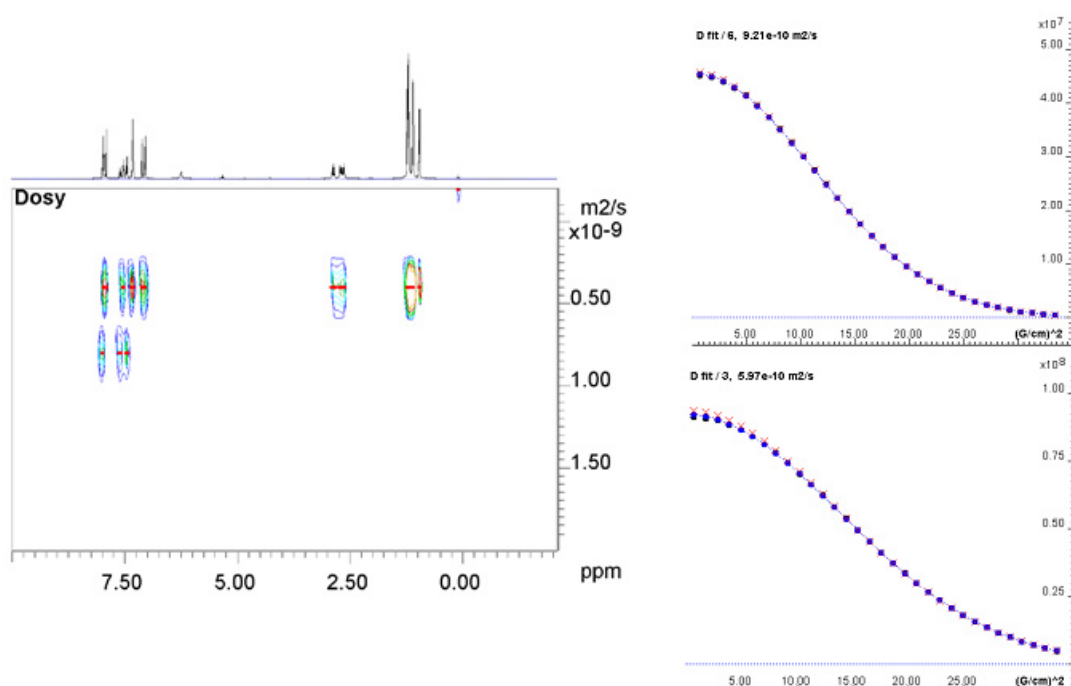


## 7. Experimental Section

Experiment 2. **TRIP** in  $\text{CD}_2\text{Cl}_2$ .  $D_{\text{TRIP}} = 8.30 \times 10^{-10} \text{ m}^2/\text{s}$ .



Experiment 3. Mixture 1:1 **TRIP**:BzOH in  $\text{CD}_2\text{Cl}_2$ .  $D_{\text{BzOH}} = 9.21 \times 10^{-10} \text{ m}^2/\text{s}$ ;  $D_{\text{TRIP}} = 5.97 \times 10^{-10} \text{ m}^2/\text{s}$ .



The diffusion coefficients of the two acids decrease in the third experiment with respect to their independent values in experiment 1 and 2. Being the heterodimeric species more voluminous than the two monomers, the establishment of an associative interaction is in agreement with the experimental outcome. Under these conditions, the equilibrium rate is

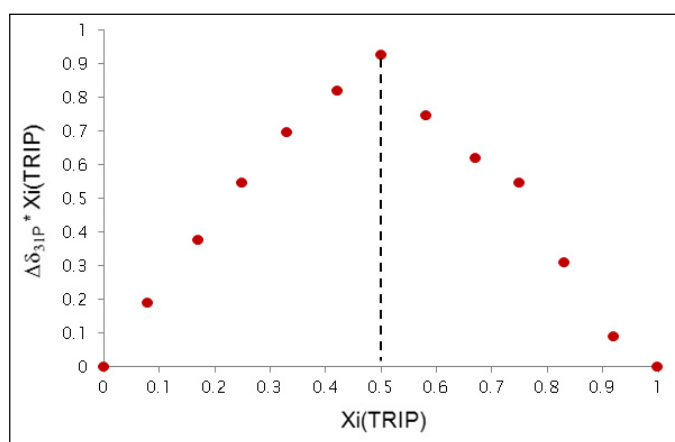
presumably faster than the NMR timescale and therefore the obtained diffusion coefficients are average values between the monomers and the heterodimer **99b**.

### 7.2.3. Binding isotherm studies

#### Determination of the stoichiometry of the complex by Job's method<sup>117</sup>

This experiment was designed to evaluate the stoichiometry of the self-assembly. Two equimolar (0.69 mM) solutions of **TRIP** and benzoic acid in deuterated dichloromethane were prepared. Then 12 samples were prepared with defined volumes of the two solutions to give a total volume of 0.6 mL. The <sup>31</sup>P-NMR spectra were measured referencing the peaks to an external standard (85% H<sub>3</sub>PO<sub>4</sub> in H<sub>2</sub>O) and the Job plot ( $\Delta\delta_{31P} * X_{TRIP}$  VS  $X_{TRIP}$ ) could be obtained [ $X_{TRIP}$  = mole fraction of **TRIP** in the mixture].

entry	$X_{TRIP}$	$X_{AcOH}$	$\delta_{TRIP}$	$\delta_{TRIP} * X_{TRIP}$
1	1	0	3.15	0.00
2	0.92	0.08	3.25	0.09
3	0.83	0.17	3.53	0.31
4	0.75	0.25	3.88	0.55
5	0.67	0.33	4.08	0.62
6	0.58	0.42	4.43	0.75
7	0.50	0.50	5.00	0.93
8	0.42	0.58	5.13	0.82
9	0.33	0.67	5.25	0.70
10	0.25	0.75	5.35	0.55
11	0.17	0.83	5.44	0.38
12	0.08	0.92	5.47	0.19



The plot showed a maximum for  $X_{TRIP}=0.5$ , thus confirming the 1:1 stoichiometry of the binding event.

#### Determination of association constants<sup>116</sup>

The experiments were designed for the evaluation of the binding constants of the complexes **TRIP**·AcOH and **TRIP**·BzOH. The chemical shift of the phosphorous signal of **TRIP** was monitored upon addition of the carboxylic acid. An accurate determination of the ratio between the two components in solution was obtained by integration of the <sup>1</sup>H-NMR signals.

The experimental data were plotted and, implementing equation 1, a non-linear regression approach was followed to obtain the binding isotherms and to determine the equilibrium constants (Origin 8.5 used as mathematical platform). All the experiments were performed twice and the average values are reported in the discussion section.

*Mathematical treatment.*

- [H<sub>0</sub>] = total concentration of **TRIP**.  
 [G<sub>0</sub>] = total concentration of carboxylic acid.  
 [H] = concentration of free **TRIP**.  
 [G] = concentration of free carboxylic acid.  
 [HG] = concentration of the heterodimer.  
 δ<sub>H</sub> = chemical shift of **TRIP**.  
 δ<sub>OBS</sub> = chemical shift observed.  
 δ<sub>HG</sub> = chemical shift of heterodimer.  
 K = binding constant.

$$(7.1) \quad K = \frac{[HG]}{[H][G]}$$

$$(7.2) \quad [H] = [H_0] - [HG]$$

$$(7.3) \quad [G] = [G_0] - [HG]$$

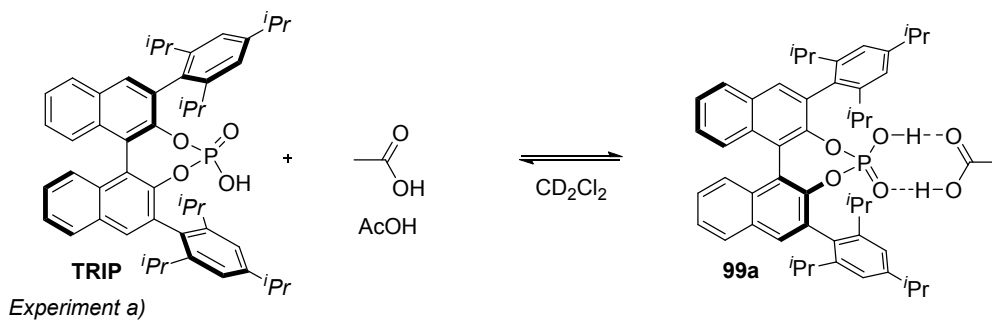
$$(7.4) \quad K = \frac{[HG]}{[H_0][G_0] - [H_0][HG] - [G_0][HG] + [HG]^2}$$

$$(7.5) \quad [HG]^2 - \left( [G_0] + [H_0] + \frac{1}{K} \right) [HG] + [H_0][G_0] = 0$$

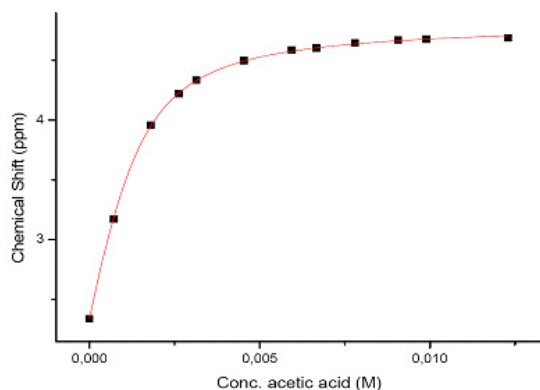
$$(7.6) \quad [HG] = \frac{\left( [G_0] + [H_0] + \frac{1}{K} \right) - \sqrt{\left( [G_0] + [H_0] + \frac{1}{K} \right)^2 - 4[H_0][G_0]}}{2}$$

$$(7.7) \quad [HG] = \frac{1}{2} \left( [G_0] + [H_0] + \frac{1}{K} \right) - \sqrt{\frac{1}{4} \left( [G_0] + [H_0] + \frac{1}{K} \right)^2 - [H_0][G_0]}$$

$$(7.8) \quad \delta_{OBS} = \frac{[HG]}{[H_0]} (\delta_{HG} - \delta_H) + \delta_H$$

Experiment 1. Determination of the binding constant of **TRIP**·AcOH.

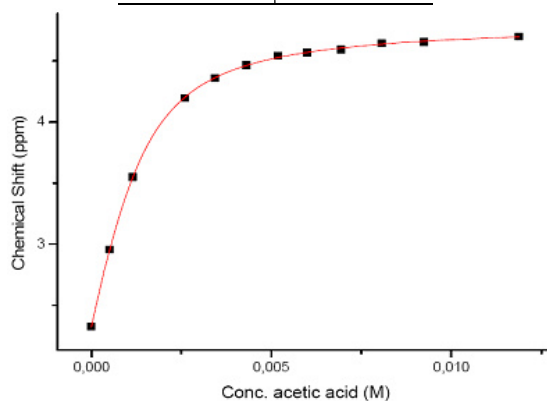
<b>TRIP</b> M.W.	752.98
mass (mg)	2.008
volume (ml)	2.00
<b>[TRIP]</b> (M)	0.001333369



entry	Ratio	[AcOH]	$\delta_{\text{OBS}}$
1	0	0	2.3388
2	0.541	0.000721352	3.1721
3	1.352	0.001802715	3.9574
4	1.975	0.002633403	4.2193
5	2.356	0.003141417	4.3346
6	3.403	0.004537454	4.4962
7	4.458	0.005944158	4.5833
8	5.003	0.006670844	4.6025
9	5.048	0.00779754	4.6414
10	6.798	0.009064241	4.6681
11	7.421	0.009894929	4.6741
12	9.220	0.01229366	4.6843

## Experiment b)

<b>TRIP</b> M.W.	752.98
mass (mg)	1.987
volume (ml)	2.00
<b>[TRIP]</b> (M)	0.001319424



entry	Ratio	[AcOH]	$\delta_{\text{OBS}}$
1	0	0	2.3223
2	0.384	0.000506659	2.9543
3	0.874	0.001153177	3.5492
4	1.969	0.002597946	4.1951
5	2.606	0.003438419	4.3584
6	3.269	0.004313198	4.4652
7	3.933	0.005189295	4.5403
8	4.544	0.005995463	4.5662
9	5.261	0.00694149	4.5945
10	6.114	0.008066959	4.6441
11	7.004	0.009241247	4.6549
12	9.010	0.011888012	4.7003

## - Calculations output

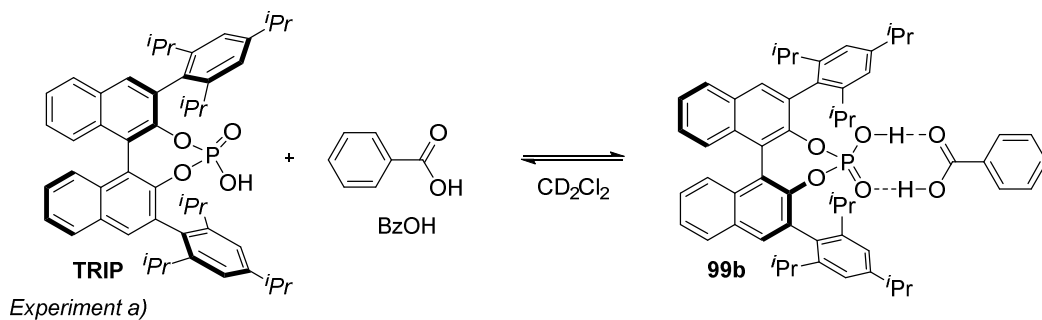
Exp. a	Value	Standard error
$\delta_{\text{H}}$	2.3388	0
$\delta_{\text{HG}}$	4.81037	0.00672
K	2003.57314	43.70165
$[\text{H}_0]$	0.00133	0

Exp. b	Value	Standard error
$\delta_{\text{H}}$	2.3223	0
$\delta_{\text{HG}}$	4.81322	0.00534
K	1917.89727	32.50106
$[\text{H}_0]$	0.00132	0



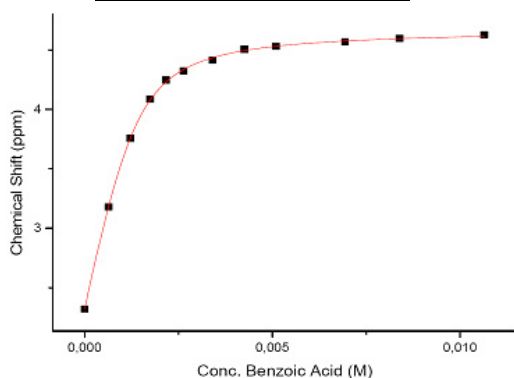
## 7. Experimental Section

### Experiment 2. Determination of the binding constant of **TRIP**·BzOH.



Experiment a)

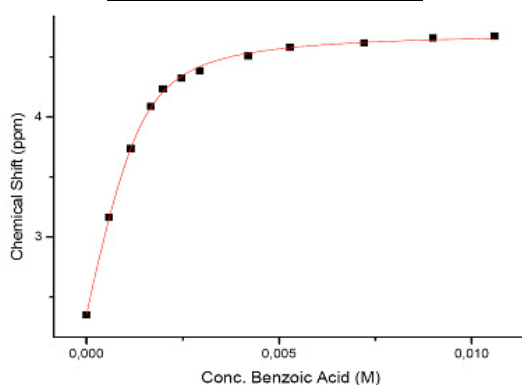
<b>TRIP</b> M.W.	752.98
mass (mg)	0.612
volume (ml)	0.60
<b>[TRIP]</b> (M)	0.001354618



entry	Ratio	[BzOH]	$\delta_{\text{OBS}}$
1	0	0	2.3201
2	0.474	0.000642089	3.1785
3	0.898	0.001216447	3.7557
4	1.292	0.001750166	4.085
5	1.599	0.002166034	4.2459
6	1.948	0.002638795	4.3225
7	2.515	0.003406863	4.413
8	3.143	0.004257563	4.5038
9	3.765	0.005100135	4.5297
10	5.123	0.006939706	4.5672
11	6.195	0.008391856	4.5966
12	7.864	0.010652713	4.6254

Experiment b)

<b>TRIP</b> M.W.	752.98
mass (mg)	0.612
volume (ml)	0.60
<b>[TRIP]</b> (M)	0.001354618



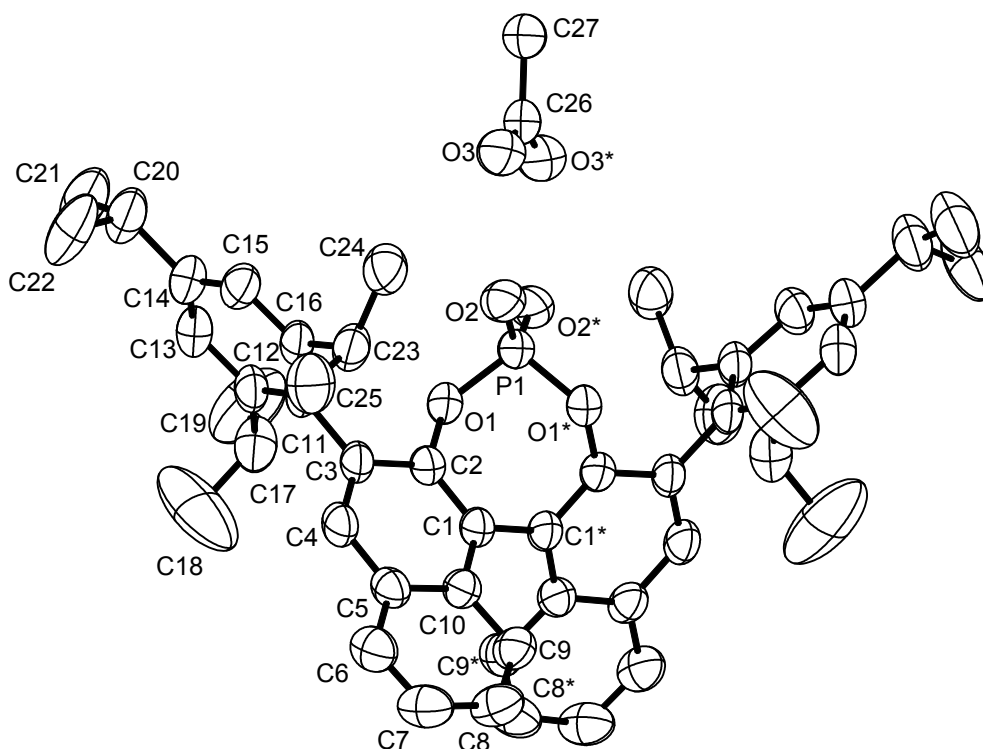
entry	Ratio	[AcOH]	$\delta_{\text{OBS}}$
1	0	0	2.3518
2	0.43	0.000582486	3.1618
3	0.85	0.001151425	3.7373
4	1.235	0.001672953	4.0891
5	1.469	0.001989933	4.2348
6	1.822	0.002468113	4.3246
7	2.173	0.002943584	4.3832
8	3.103	0.004203379	4.5105
9	3.902	0.005285718	4.5813
10	5.323	0.00721063	4.6187
11	6.641	0.008996016	4.6565
12	7.822	0.010595819	4.6738

#### - Calculations output

Exp. a	Value	Standard error
$\delta_{\text{H}}$	2.3201	0
$\delta_{\text{HG}}$	4.67506	0.00732
K	4000.71614	116.30241
[H <sub>0</sub> ]	0.00135	0

Exp. b	Value	Standard error
$\delta_{\text{H}}$	2.3518	0
$\delta_{\text{HG}}$	4.71895	0.01228
K	3934.77787	183.82194
[H <sub>0</sub> ]	0.00132	0

## 7.2.4. Crystal structure determination of TRIP·AcOH



The crystals were grown from a dichloromethane-acetic acid solution of **TRIP** by slow evaporation of the chlorinated solvent at room temperature. The molecular structure of **TRIP·AcOH** was determined at room temperature because the crystals become modulated when cooled. The dimeric complex sits on a crystallographic 2-fold axis which passes through the P atom and the two C atoms of the acetic acid molecule. Probability ellipsoids are shown at the 50% level and H atoms are omitted for clarity.

X-ray crystallographic data have been deposited in the Cambridge Crystallographic Data Centre database (<http://www.ccdc.cam.ac.uk/>) under accession code CCDC 1023462.

**Crystal data and structure refinement.**

Identification code	8214
Empirical formula	C <sub>52</sub> H <sub>61</sub> O <sub>6</sub> P
Color	colourless
Formula weight	812.97 g·mol <sup>-1</sup>
Temperature	296(2) K
Wavelength	0.71073 Å

## 7. Experimental Section

---

Crystal system	Tetragonal	
Space group	P 41 21 2, (no. 92)	
Unit cell dimensions	a = 12.807(2) Å	$\alpha = 90^\circ$ .
	b = 12.807(2) Å	$\beta = 90^\circ$ .
	c = 28.916(5) Å	$\gamma = 90^\circ$ .
Volume	4743.1(17) Å <sup>3</sup>	
Z	4	
Density (calculated)	1.138 Mg·m <sup>-3</sup>	
Absorption coefficient	0.105 mm <sup>-1</sup>	
F(000)	1744 e	
Crystal size	0.54 x 0.48 x 0.42 mm <sup>3</sup>	
$\theta$ range for data collection	1.739 to 28.521°.	
Index ranges	-17 ≤ h ≤ 17, -17 ≤ k ≤ 17, -38 ≤ l ≤ 38	
Reflections collected	100675	
Independent reflections	6003 [R <sub>int</sub> = 0.1037]	
Reflections with I > 2σ (I)	4247	
Completeness to $\theta = 25.242^\circ$	100.0 %	
Absorption correction	Semi-empirical from equivalents	
Max. and min. transmission	0.7457 and 0.3860	
Refinement method	Full-matrix least-squares on F <sup>2</sup>	
Data / restraints / parameters	6003 / 0 / 277	
Goodness-of-fit on F <sup>2</sup>	1.029	
Final R indices [I > 2σ (I)]	R <sub>1</sub> = 0.0543	wR <sup>2</sup> = 0.1278
R indices (all data)	R <sub>1</sub> = 0.0824	wR <sup>2</sup> = 0.1413
Absolute structure parameter	-0.02(19)	
Extinction coefficient	0	
Largest diff. peak and hole	0.228 and -0.217 e·Å <sup>-3</sup>	

### Atomic coordinates and equivalent isotropic displacement parameters (Å<sup>2</sup>).

U<sub>eq</sub> is defined as one third of the trace of the orthogonalized U<sub>ij</sub> tensor.

	x	y	z	U <sub>eq</sub>
C(1)	0.5691(2)	0.4701(2)	0.2726(1)	0.049(1)
C(2)	0.5035(2)	0.5197(2)	0.3027(1)	0.049(1)
C(3)	0.5324(3)	0.5484(2)	0.3483(1)	0.052(1)
C(4)	0.6316(3)	0.5245(2)	0.3613(1)	0.057(1)
C(5)	0.7055(3)	0.4805(2)	0.3313(1)	0.053(1)
C(6)	0.8101(3)	0.4632(3)	0.3448(1)	0.066(1)
C(7)	0.8819(3)	0.4281(3)	0.3145(1)	0.073(1)
C(8)	0.8537(3)	0.4084(3)	0.2688(1)	0.072(1)

## 7. Experimental Section

---

C(9)	0.7534(3)	0.4204(3)	0.2548(1)	0.061(1)
C(10)	0.6759(2)	0.4554(2)	0.2854(1)	0.051(1)
C(11)	0.4589(3)	0.5998(2)	0.3816(1)	0.054(1)
C(12)	0.3847(3)	0.5400(3)	0.4054(1)	0.057(1)
C(13)	0.3267(3)	0.5877(3)	0.4401(1)	0.063(1)
C(14)	0.3371(3)	0.6924(3)	0.4507(1)	0.064(1)
C(15)	0.4086(3)	0.7499(3)	0.4255(1)	0.065(1)
C(16)	0.4700(3)	0.7064(3)	0.3914(1)	0.058(1)
C(17)	0.3710(3)	0.4248(3)	0.3952(1)	0.073(1)
C(18)	0.4324(8)	0.3602(4)	0.4290(2)	0.198(4)
C(19)	0.2585(5)	0.3913(5)	0.3932(2)	0.148(3)
C(20)	0.2737(3)	0.7476(4)	0.4885(1)	0.085(1)
C(21)	0.1836(4)	0.6886(5)	0.5064(2)	0.114(2)
C(22)	0.3454(4)	0.7849(5)	0.5270(2)	0.121(2)
C(23)	0.5488(3)	0.7743(3)	0.3660(1)	0.065(1)
C(24)	0.5031(4)	0.8777(3)	0.3498(1)	0.081(1)
C(25)	0.6445(4)	0.7945(4)	0.3957(1)	0.092(1)
C(26)	0.1606(3)	0.8394(3)	0.2500	0.064(1)
C(27)	0.0791(3)	0.9209(3)	0.2500	0.078(2)
O(1)	0.4006(2)	0.5397(2)	0.2890(1)	0.056(1)
O(2)	0.2689(2)	0.6000(2)	0.2347(1)	0.063(1)
O(3)	0.1383(3)	0.7529(3)	0.2323(1)	0.079(1)
P(1)	0.3774(1)	0.6226(1)	0.2500	0.054(1)

---

### Bond lengths [Å] and angles [°].

C(1)-C(2)	1.365(4)	C(1)-C(10)	1.430(4)
C(1)-C(1)#1	1.488(5)	C(2)-O(1)	1.400(4)
C(2)-C(3)	1.419(4)	C(3)-C(4)	1.359(4)
C(3)-C(11)	1.499(4)	C(4)-C(5)	1.403(4)
C(4)-H(4)	0.9300	C(5)-C(6)	1.413(5)
C(5)-C(10)	1.417(4)	C(6)-C(7)	1.347(5)
C(6)-H(6)	0.9300	C(7)-C(8)	1.395(5)
C(7)-H(7)	0.9300	C(8)-C(9)	1.356(5)
C(8)-H(8)	0.9300	C(9)-C(10)	1.403(4)
C(9)-H(9)	0.9300	C(11)-C(12)	1.400(4)
C(11)-C(16)	1.402(5)	C(12)-C(13)	1.390(4)
C(12)-C(17)	1.515(5)	C(13)-C(14)	1.382(5)

## 7. Experimental Section

---

C(13)-H(13)	0.9300	C(14)-C(15)	1.384(5)
C(14)-C(20)	1.534(5)	C(15)-C(16)	1.379(4)
C(15)-H(15)	0.9300	C(16)-C(23)	1.521(5)
C(17)-C(18)	1.502(7)	C(17)-C(19)	1.505(7)
C(17)-H(17)	0.9800	C(18)-H(18A)	0.9600
C(18)-H(18B)	0.9600	C(18)-H(18C)	0.9600
C(19)-H(19A)	0.9600	C(19)-H(19B)	0.9600
C(19)-H(19C)	0.9600	C(20)-C(21)	1.474(6)
C(20)-C(22)	1.519(6)	C(20)-H(20)	0.9800
C(21)-H(21A)	0.9600	C(21)-H(21B)	0.9600
C(21)-H(21C)	0.9600	C(22)-H(22A)	0.9600
C(22)-H(22B)	0.9600	C(22)-H(22C)	0.9600
C(23)-C(25)	1.519(6)	C(23)-C(24)	1.521(5)
C(23)-H(23)	0.9800	C(24)-H(24A)	0.9600
C(24)-H(24B)	0.9600	C(24)-H(24C)	0.9600
C(25)-H(25A)	0.9600	C(25)-H(25B)	0.9600
C(25)-H(25C)	0.9600	C(26)-O(3)#1	1.253(4)
C(26)-O(3)	1.253(4)	C(26)-C(27)	1.477(7)
C(27)-H(27A)	0.9599(17)	C(27)-H(27B)	0.9598(17)
C(27)-H(27C)	0.9600(17)	O(1)-P(1)	1.578(2)
O(2)-P(1)	1.486(3)	O(2)-H(2)	0.69(7)
O(3)-H(3)	0.65(8)	P(1)-O(2)#1	1.486(3)
P(1)-O(1)#1	1.578(2)	P(1)-H(2)	1.84(7)
C(2)-C(1)-C(10)	119.0(2)	C(2)-C(1)-C(1)#1	120.6(2)
C(10)-C(1)-C(1)#1	120.37(18)	C(1)-C(2)-O(1)	119.0(2)
C(1)-C(2)-C(3)	123.5(3)	O(1)-C(2)-C(3)	117.4(2)
C(4)-C(3)-C(2)	116.3(3)	C(4)-C(3)-C(11)	120.4(2)
C(2)-C(3)-C(11)	123.2(3)	C(3)-C(4)-C(5)	123.3(3)
C(3)-C(4)-H(4)	118.4	C(5)-C(4)-H(4)	118.4
C(4)-C(5)-C(6)	122.2(3)	C(4)-C(5)-C(10)	119.4(3)
C(6)-C(5)-C(10)	118.4(3)	C(7)-C(6)-C(5)	121.4(3)
C(7)-C(6)-H(6)	119.3	C(5)-C(6)-H(6)	119.3
C(6)-C(7)-C(8)	120.0(3)	C(6)-C(7)-H(7)	120.0
C(8)-C(7)-H(7)	120.0	C(9)-C(8)-C(7)	120.5(3)
C(9)-C(8)-H(8)	119.8	C(7)-C(8)-H(8)	119.8
C(8)-C(9)-C(10)	121.3(3)	C(8)-C(9)-H(9)	119.4
C(10)-C(9)-H(9)	119.4	C(9)-C(10)-C(5)	118.3(3)
C(9)-C(10)-C(1)	123.7(2)	C(5)-C(10)-C(1)	117.9(3)

## 7. Experimental Section

---

C(12)-C(11)-C(16)	120.2(3)	C(12)-C(11)-C(3)	120.1(3)
C(16)-C(11)-C(3)	119.6(3)	C(13)-C(12)-C(11)	118.4(3)
C(13)-C(12)-C(17)	120.4(3)	C(11)-C(12)-C(17)	121.1(3)
C(14)-C(13)-C(12)	122.4(3)	C(14)-C(13)-H(13)	118.8
C(12)-C(13)-H(13)	118.8	C(13)-C(14)-C(15)	117.5(3)
C(13)-C(14)-C(20)	123.8(3)	C(15)-C(14)-C(20)	118.7(3)
C(16)-C(15)-C(14)	122.7(3)	C(16)-C(15)-H(15)	118.7
C(14)-C(15)-H(15)	118.7	C(15)-C(16)-C(11)	118.7(3)
C(15)-C(16)-C(23)	119.5(3)	C(11)-C(16)-C(23)	121.8(3)
C(18)-C(17)-C(19)	111.6(5)	C(18)-C(17)-C(12)	110.4(3)
C(19)-C(17)-C(12)	113.3(4)	C(18)-C(17)-H(17)	107.0
C(19)-C(17)-H(17)	107.0	C(12)-C(17)-H(17)	107.0
C(17)-C(18)-H(18A)	109.5	C(17)-C(18)-H(18B)	109.5
H(18A)-C(18)-H(18B)	109.5	C(17)-C(18)-H(18C)	109.5
H(18A)-C(18)-H(18C)	109.5	H(18B)-C(18)-H(18C)	109.5
C(17)-C(19)-H(19A)	109.5	C(17)-C(19)-H(19B)	109.5
H(19A)-C(19)-H(19B)	109.5	C(17)-C(19)-H(19C)	109.5
H(19A)-C(19)-H(19C)	109.5	H(19B)-C(19)-H(19C)	109.5
C(21)-C(20)-C(22)	112.3(3)	C(21)-C(20)-C(14)	115.3(4)
C(22)-C(20)-C(14)	110.2(4)	C(21)-C(20)-H(20)	106.1
C(22)-C(20)-H(20)	106.1	C(14)-C(20)-H(20)	106.1
C(20)-C(21)-H(21A)	109.5	C(20)-C(21)-H(21B)	109.5
H(21A)-C(21)-H(21B)	109.5	C(20)-C(21)-H(21C)	109.5
H(21A)-C(21)-H(21C)	109.5	H(21B)-C(21)-H(21C)	109.5
C(20)-C(22)-H(22A)	109.5	C(20)-C(22)-H(22B)	109.5
H(22A)-C(22)-H(22B)	109.5	C(20)-C(22)-H(22C)	109.5
H(22A)-C(22)-H(22C)	109.5	H(22B)-C(22)-H(22C)	109.5
C(25)-C(23)-C(16)	111.1(3)	C(25)-C(23)-C(24)	109.7(3)
C(16)-C(23)-C(24)	113.0(3)	C(25)-C(23)-H(23)	107.6
C(16)-C(23)-H(23)	107.6	C(24)-C(23)-H(23)	107.6
C(23)-C(24)-H(24A)	109.5	C(23)-C(24)-H(24B)	109.5
H(24A)-C(24)-H(24B)	109.5	C(23)-C(24)-H(24C)	109.5
H(24A)-C(24)-H(24C)	109.5	H(24B)-C(24)-H(24C)	109.5
C(23)-C(25)-H(25A)	109.5	C(23)-C(25)-H(25B)	109.5
H(25A)-C(25)-H(25B)	109.5	C(23)-C(25)-H(25C)	109.5
H(25A)-C(25)-H(25C)	109.5	H(25B)-C(25)-H(25C)	109.5
O(3)#1-C(26)-O(3)	124.7(5)	O(3)#1-C(26)-C(27)	117.6(3)
O(3)-C(26)-C(27)	117.6(3)	C(26)-C(27)-H(27A)	109.5(3)
C(26)-C(27)-H(27B)	109.5(3)	H(27A)-C(27)-H(27B)	109.5(3)

## 7. Experimental Section

C(26)-C(27)-H(27C)	109.5(3)	H(27A)-C(27)-H(27C)	109.5(3)
H(27B)-C(27)-H(27C)	109.5(3)	C(2)-O(1)-P(1)	120.13(18)
P(1)-O(2)-H(2)	110(6)	C(26)-O(3)-H(3)	117(8)
O(2)#1-P(1)-O(2)	116.8(2)	O(2)#1-P(1)-O(1)	112.34(13)
O(2)-P(1)-O(1)	104.94(13)	O(2)#1-P(1)-O(1)#1	104.94(13)
O(2)-P(1)-O(1)#1	112.34(13)	O(1)-P(1)-O(1)#1	104.96(15)
O(2)#1-P(1)-H(2)	96(2)	O(1)-P(1)-H(2)	116(2)
O(1)#1-P(1)-H(2)	121.7(19)		

### Anisotropic displacement parameters ( $\text{\AA}^2$ )

The anisotropic displacement factor exponent takes the form:

$$-2\pi^2[h^2a^{*2}U_{22} + \dots + 2hka^*b^*U_{12}].$$

	U <sub>11</sub>	U <sub>22</sub>	U <sub>33</sub>	U <sub>23</sub>	U <sub>13</sub>	U <sub>12</sub>
C(1)	0.061(2)	0.051(2)	0.035(1)	-0.003(1)	-0.004(1)	0.008(1)
C(2)	0.058(2)	0.052(2)	0.037(1)	-0.001(1)	-0.004(1)	0.007(1)
C(3)	0.071(2)	0.050(2)	0.033(1)	-0.001(1)	0.000(1)	0.005(1)
C(4)	0.078(2)	0.057(2)	0.037(1)	-0.005(1)	-0.010(1)	0.006(2)
C(5)	0.066(2)	0.047(2)	0.045(1)	-0.003(1)	-0.012(1)	0.005(1)
C(6)	0.074(2)	0.061(2)	0.063(2)	-0.011(2)	-0.022(2)	0.003(2)
C(7)	0.065(2)	0.065(2)	0.090(2)	-0.019(2)	-0.022(2)	0.009(2)
C(8)	0.063(2)	0.070(2)	0.083(2)	-0.023(2)	-0.004(2)	0.010(2)
C(9)	0.065(2)	0.064(2)	0.053(2)	-0.014(1)	-0.005(2)	0.008(2)
C(10)	0.060(2)	0.049(2)	0.043(1)	-0.006(1)	-0.005(1)	0.007(1)
C(11)	0.070(2)	0.062(2)	0.029(1)	-0.001(1)	0.000(1)	0.005(2)
C(12)	0.074(2)	0.064(2)	0.034(1)	0.001(1)	-0.002(1)	-0.001(2)
C(13)	0.072(2)	0.078(2)	0.040(1)	0.002(1)	0.004(1)	-0.006(2)
C(14)	0.076(2)	0.076(2)	0.041(1)	-0.006(1)	0.006(1)	0.003(2)
C(15)	0.088(2)	0.060(2)	0.048(2)	-0.007(1)	0.010(2)	0.007(2)
C(16)	0.081(2)	0.058(2)	0.034(1)	-0.001(1)	0.004(1)	0.007(2)
C(17)	0.099(3)	0.065(2)	0.056(2)	-0.002(2)	0.007(2)	-0.018(2)
C(18)	0.346(12)	0.063(3)	0.186(6)	0.031(4)	-0.134(8)	-0.020(5)
C(19)	0.135(5)	0.132(5)	0.176(5)	-0.079(5)	0.046(4)	-0.051(4)
C(20)	0.101(3)	0.102(3)	0.052(2)	-0.009(2)	0.019(2)	0.004(2)
C(21)	0.094(3)	0.179(5)	0.070(2)	-0.030(3)	0.017(2)	0.001(3)
C(22)	0.126(4)	0.162(5)	0.075(3)	-0.055(3)	0.029(3)	-0.017(4)
C(23)	0.090(3)	0.060(2)	0.046(2)	0.001(1)	0.016(2)	0.004(2)

## 7. Experimental Section

---

C(24)	0.122(3)	0.060(2)	0.061(2)	0.000(2)	0.011(2)	0.007(2)
C(25)	0.097(3)	0.100(3)	0.079(2)	0.015(2)	0.014(2)	-0.015(3)
C(26)	0.073(2)	0.073(2)	0.044(2)	0.007(2)	0.007(2)	0.012(3)
C(27)	0.084(2)	0.084(2)	0.065(3)	0.015(2)	0.015(2)	0.024(3)
O(1)	0.061(1)	0.069(1)	0.037(1)	0.000(1)	0.001(1)	0.011(1)
O(2)	0.065(2)	0.065(2)	0.060(1)	-0.006(1)	-0.011(1)	0.009(1)
O(3)	0.084(2)	0.079(2)	0.073(2)	-0.004(1)	-0.003(1)	0.015(2)
P(1)	0.061(1)	0.061(1)	0.040(1)	-0.003(1)	-0.003(1)	0.014(1)

---

**Hydrogen coordinates and isotropic displacement parameters ( $\text{\AA}^2$ )**

	x	y	z	$U_{\text{eq}}$
H(4)	0.6514	0.5381	0.3917	0.069
H(6)	0.8298	0.4764	0.3752	0.079
H(7)	0.9503	0.4169	0.3242	0.088
H(8)	0.9041	0.3868	0.2477	0.086
H(9)	0.7355	0.4052	0.2244	0.073
H(13)	0.2791	0.5477	0.4567	0.076
H(15)	0.4156	0.8207	0.4318	0.078
H(17)	0.4009	0.4120	0.3645	0.088
H(18A)	0.4993	0.3919	0.4340	0.238
H(18B)	0.4418	0.2911	0.4167	0.238
H(18C)	0.3952	0.3562	0.4578	0.238
H(19A)	0.2195	0.4277	0.4165	0.177
H(19B)	0.2538	0.3175	0.3985	0.177
H(19C)	0.2303	0.4075	0.3633	0.177
H(20)	0.2450	0.8107	0.4742	0.102
H(21A)	0.1406	0.6663	0.4811	0.171
H(21B)	0.1435	0.7323	0.5267	0.171
H(21C)	0.2079	0.6286	0.5232	0.171
H(22A)	0.3703	0.7259	0.5442	0.181
H(22B)	0.3077	0.8309	0.5472	0.181
H(22C)	0.4037	0.8215	0.5138	0.181
H(23)	0.5717	0.7359	0.3385	0.078
H(24A)	0.4944	0.9234	0.3758	0.122
H(24B)	0.4366	0.8655	0.3355	0.122
H(24C)	0.5496	0.9093	0.3278	0.122
H(25A)	0.6238	0.8291	0.4237	0.138



## 7. Experimental Section

---

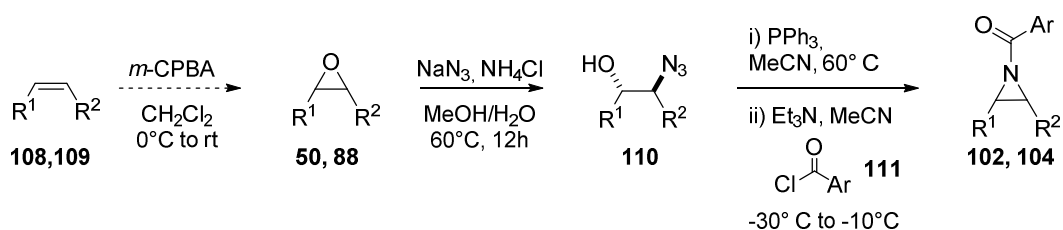
H(25B)	0.6927	0.8378	0.3791	0.138
H(25C)	0.6773	0.7292	0.4032	0.138
H(27A)	0.1096	0.9868	0.2582	0.093
H(27B)	0.0260	0.9031	0.2721	0.093
H(27C)	0.0486	0.9258	0.2197	0.093
H(2)	0.239(5)	0.645(5)	0.236(2)	0.04(2)
H(3)	0.175(6)	0.717(7)	0.233(3)	0.06(3)

---

### 7.3. Asymmetric carboxylation of aziridines

#### 7.3.1. Preparation of starting materials<sup>78e</sup>

When not commercially available, the starting epoxides **50** and **88** for the synthesis of aziridines **102** and **104** were prepared following the procedure reported in paragraph 7.4.2.



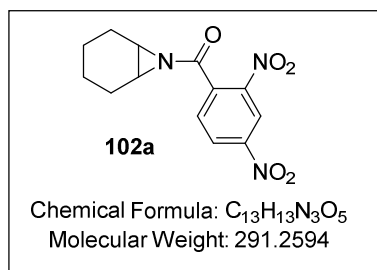
Sodium azide (2 equiv.) and ammonium chloride (1.5 equiv.) were added to a stirred solution of the corresponding epoxide (5 mmol) in a mixture of MeOH and H<sub>2</sub>O (3:1) [0.25 M]. The reaction was heated to 60 °C and stirred for 12 h. When the epoxide was completely converted into the corresponding azido alcohol (TLC mixtures: hexanes:MTBE, *p*-anisaldehyde stain) the reaction was cooled to room temperature and the methanol was removed by evaporation. Then the solution was extracted with dichloromethane and the organic phase was washed with brine solution, dried over anhydrous Na<sub>2</sub>SO<sub>4</sub>, filtered, and the solvent was removed in vacuum. The azido alcohol obtained was then used in the following step without further purification.

In a flame dried flask under argon, the desired benzoyl chloride was prepared by refluxing the corresponding benzoic acid (1 equiv.) in SOCl<sub>2</sub> (10 equiv.) overnight. The excess of thionyl chloride was then removed in vacuum to afford the desired benzoyl chloride as yellowish oil.

In a second flame dried flask a solution of the azido alcohol in acetonitrile [0.25 M] was degassed with argon (25-30 min), then triphenylphosphine (1 equiv.) was added and the mixture was stirred at 60 °C for 12 h. Then the reaction was cooled to -40 °C and triethylamine (1.2 equiv.) was added dropwise via syringe and then immediately a solution of the previously prepared benzoyl chloride in THF (5 ml) was slowly added to the mixture. The reaction was kept between -40 °C and -30 °C for 60 min and then the temperature was raised slowly to -10 °C and kept at this temperature for additional 30 min. Then water was added to the solution and the mixture was extracted with ethyl acetate. The organic layers were combined, washed with brine solution, and dried over anhydrous Na<sub>2</sub>SO<sub>4</sub>. The mixture

was filtered and the solvent was then removed by rotary evaporator. The crude product was purified immediately via flash column chromatography on silica gel [eluent: mixtures hexanes/AcOEt].

**7-(2,4-dinitrobenzoyl)-7-azabicyclo[4.1.0]heptane (102a):** Prepared from 5 mmol of cyclohexene oxide (812 mg, 2.5 mmol, 50% yield). Pale yellow solid.

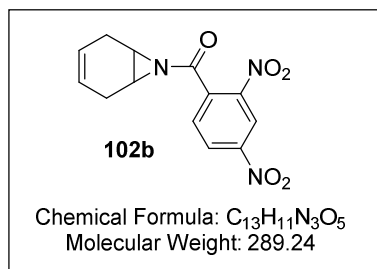


**<sup>1</sup>H-NMR** (500 MHz, CDCl<sub>3</sub>): δ 8.81 (d, *J* = 2.1 Hz, 1H), 8.54 (dd, *J* = 8.4, *J* = 2.1 Hz, 1H), 7.93 (d, *J* = 8.4 Hz, 1H), 3.05-2.95 (m, 2H), 1.95-1.8 (m, 4H), 1.55-1.45 (m, 2H), 1.38-1.28 (m, 2H).

**<sup>13</sup>C-NMR** (125 MHz, CDCl<sub>3</sub>): δ 176.0, 148.5, 147.7, 138.4, 130.9, 128.1, 120.1, 38.1, 23.8, 19.9.

**HRMS** (*m/z*) calcd for C<sub>13</sub>H<sub>13</sub>N<sub>3</sub>O<sub>5</sub> [M]<sup>+Na</sup>: 314.0747, found: 314.0747.

**7-(2,4-dinitrobenzoyl)-7-azabicyclo[4.1.0]hept-3-ene (102b):** Prepared from 5 mmol of 1,4-cyclohexadiene (311 mg, 1 mmol, 24% yield). Pale yellow solid.

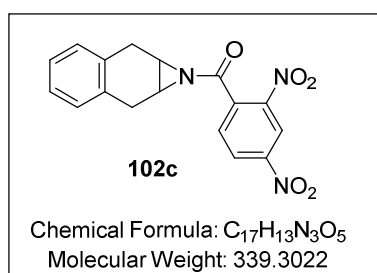


**<sup>1</sup>H-NMR** (500 MHz, CDCl<sub>3</sub>): δ 8.81 (d, *J* = 2.1 Hz, 1H), 8.53 (dd, *J* = 8.3, *J* = 2.1 Hz, 1H), 7.94 (d, *J* = 8.3 Hz, 1H), 5.53 (s, 2H), 3.13 (s, 2H), 2.45 (cm, 4H).

**<sup>13</sup>C-NMR** (125 MHz, CDCl<sub>3</sub>): δ 175.8, 148.6, 147.7, 138.3, 131.0, 128.1, 122.1, 120.0, 37.2, 24.1.

**HRMS** (*m/z*) calcd for C<sub>13</sub>H<sub>11</sub>N<sub>3</sub>O<sub>5</sub> [M]<sup>+Na</sup>: 312.0591, found: 312.0591.

**1-(2,4-dinitrobenzoyl)-1a,2,7,7a-tetrahydro-1H-naphtho[2,3-b]aziridine (102c):** Prepared from 5 mmol of 1,4-dihydronaphthalene (995 mg, 2.93 mmol, 59% yield). Red/brownish solid.

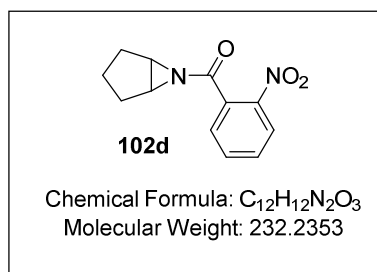


**<sup>1</sup>H-NMR** (500 MHz, CDCl<sub>3</sub>): δ 8.80 (d, *J* = 2.1 Hz, 1H), 8.47 (dd, *J* = 8.4, *J* = 2.1 Hz, 1H), 7.93 (d, *J* = 8.4 Hz, 1H), 7.24-7.18 (m, 2H), 7.10-7.02 (m, 2H), 3.39 (s, 2H), 3.26-3.12 (m, 4H).

**<sup>13</sup>C-NMR** (125 MHz, CDCl<sub>3</sub>): δ 175.4, 148.6, 147.7, 138.1, 131.9, 131.0, 129.4, 128.1, 127.2, 120.0, 38.2, 29.4.

**HRMS** (*m/z*) calcd for C<sub>17</sub>H<sub>13</sub>N<sub>3</sub>O<sub>5</sub> [M]<sup>+Na</sup>: 362.0747, found: 362.0747.

**6-(2-nitrobenzoyl)-6-azabicyclo[3.1.0]hexane (102d):** In this reaction the temperature of the acylation was constantly kept below  $-30^{\circ}\text{C}$  to avoid decomposition of the product. Prepared from 5 mmol of cyclopentane oxide (487.6 mg, 2.01 mmol, 42% yield). Yellow solid.

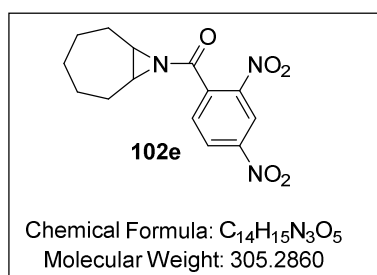


**$^1\text{H-NMR}$**  (500 MHz,  $\text{CDCl}_3$ ):  $\delta$  7.90 (d,  $J = 8.5$  Hz, 1H), 7.62-7.58 (m, 2H), 7.57 (t,  $J = 8.5$ , 1H), 3.30 (s, 2H), 2.05-1.95 (m, 2H), 1.75-1.55 (m, 3H), 1.50-1.35 (m, 1H).

**$^{13}\text{C-NMR}$**  (125 MHz,  $\text{CDCl}_3$ ):  $\delta$  176.8, 147.7, 133.4, 132.9, 130.9, 129.4, 124.2, 44.4, 27.1, 19.7.

**HRMS** ( $m/z$ ) calcd for  $\text{C}_{12}\text{H}_{12}\text{N}_2\text{O}_3$  [ $\text{M}$ ] $^{+\text{Na}}$ : 255.0740, found: 255.0742.

**8-(2,4-dinitrobenzoyl)-8-azabicyclo[5.1.0]octane (102e):** Prepared from 3.5 mmol of cycloheptane oxide (510 mg, 1.67 mmol, 48% yield). Pale red solid.

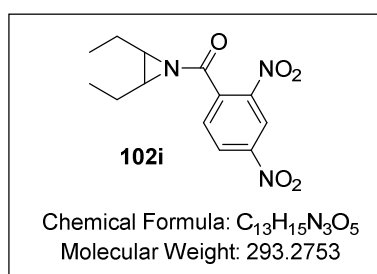


**$^1\text{H-NMR}$**  (500 MHz,  $\text{CD}_2\text{Cl}_2$ ):  $\delta$  8.76 (d,  $J = 2.2$  Hz, 1H), 8.53 (dd,  $J = 8.5$   $J = 2.2$ , 1H), 7.93 (d,  $J = 8.5$  Hz, 1H), 2.95 (cm, 2H), 1.98-1.82 (m, 4H), 1.70-1.46 (m, 5H), 1.30-1.17 (m, 1H).

**$^{13}\text{C-NMR}$**  (125 MHz,  $\text{CD}_2\text{Cl}_2$ ):  $\delta$  176.2, 148.7, 148.0, 138.3, 131.0, 128.3, 120.1, 43.2, 31.5, 28.9, 25.7.

**HRMS** ( $m/z$ ) calcd for  $\text{C}_{14}\text{H}_{15}\text{N}_3\text{O}_5$  [ $\text{M}$ ] $^{+\text{Na}}$ : 328.0904, found: 328.0905.

**cis-1-(2,4-dinitrobenzoyl)-2,3-diethylaziridine (102i):** Prepared from 5 mmol of cis-3-hexene (403 mg, 1.44 mmol, 27% yield). Yellow solid.

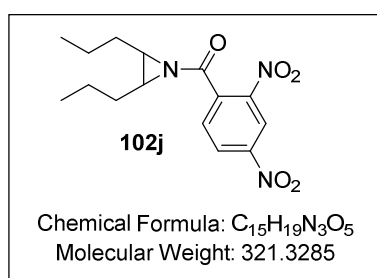


**$^1\text{H-NMR}$**  (500 MHz,  $\text{CD}_2\text{Cl}_2$ ):  $\delta$  8.83 (d,  $J = 2.1$  Hz, 1H), 8.54 (dd,  $J = 8.3$ ,  $J = 2.1$  Hz, 1H), 7.93 (d,  $J = 8.3$  Hz, 1H), 2.74 (cm, 2H), 1.65-1.48 (m, 4H), 0.95 (t,  $J = 7.5$  Hz, 6H).

**$^{13}\text{C-NMR}$**  (125 MHz,  $\text{CD}_2\text{Cl}_2$ ):  $\delta$  176.4, 148.6, 147.4, 138.6, 131.2, 128.4, 120.2, 45.1, 21.1, 11.8.

**HRMS** ( $m/z$ ) calcd for  $\text{C}_{13}\text{H}_{15}\text{N}_3\text{O}_5$  [ $\text{M}$ ] $^{+\text{Na}}$ : 316.0904, found: 316.0903.

**cis-1-(2,4-dinitrobenzoyl)-2,3-dipropylaziridine (102j):** Prepared from 5 mmol of cis-4-octene (465 mg, 1.44 mmol, 29% yield). Yellow solid.

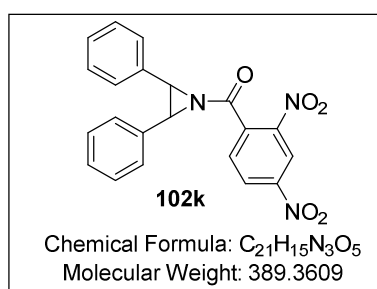


<sup>1</sup>H-NMR (500 MHz, CDCl<sub>3</sub>): δ 8.86 (d, *J* = 2.1 Hz, 1H), 8.54 (dd, *J* = 8.3, *J* = 2.1 Hz, 1H), 7.91 (d, *J* = 8.3 Hz, 1H), 2.82 (cm, 2H), 1.59-1.28 (m, 8H), 0.91 (t, *J* = 7.3 Hz, 6H).

<sup>13</sup>C-NMR (125 MHz, CDCl<sub>3</sub>): δ 171.4, 148.4, 147.1, 138.6, 130.9, 128.1, 120.1, 43.3, 29.7, 20.9, 13.9.

**HRMS** (*m/z*) calcd for C<sub>15</sub>H<sub>19</sub>N<sub>3</sub>O<sub>5</sub> [M]<sup>+Na</sup>: 344.1217, found: 344.1218.

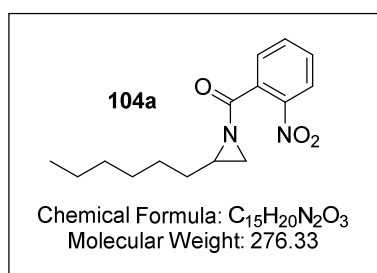
**cis-1-(2,4-dinitrobenzoyl)-2,3-diphenylaziridine (102k):** Prepared from 5 mmol of Z-stilbene (580 mg, 1.49 mmol, 30% yield). White solid.



<sup>1</sup>H-NMR (500 MHz, CDCl<sub>3</sub>): δ 8.88 (d, *J* = 2.1 Hz, 1H), 8.54 (dd, *J* = 8.4 Hz, *J* = 2.1 Hz, 1H), 8.08 (d, *J* = 8.4 Hz, 1H), 7.20-7.15 (m, 10H), 4.35 (s, 2H).

<sup>13</sup>C-NMR (125 MHz, CDCl<sub>3</sub>): 176.2, 148.7, 147.5, 137.7, 132.7, 130.6, 128.6, 128.6, 128.3, 128.1, 127.7, 120.3, 47.2.

**1-(2-nitrobenzoyl)-2-hexylaziridine (104a):** Prepared from 10 mmol of 1,2-epoxyoctane (1.55 g, 5.6 mmol, 56% yield). Colorless liquid.



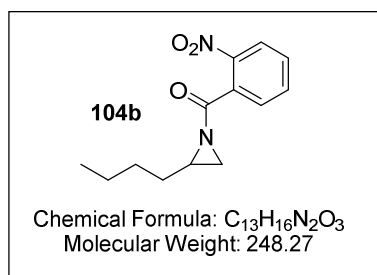
<sup>1</sup>H-NMR (CDCl<sub>3</sub>, 500 MHz): δ 7.97 (dd, *J* = 8.1 Hz, *J* = 0.8 Hz, 1H), 7.74-7.65 (m, 2H), 7.63-7.56 (m, 1H), 2.74 (dq, *J* = 6.0 Hz, *J* = 3.6 Hz, 1H), 2.63 (d, *J* = 6.0 Hz, 1H), 2.14 (d, *J* = 3.6 Hz, 1H), 1.60-1.46 (m, 2H), 1.38-1.12 (m, 8H), 0.84 (t, *J* = 6.8 Hz, 3H).

<sup>13</sup>C-NMR (CDCl<sub>3</sub>, 125 MHz): 177.9, 147.1, 133.6, 133.0, 130.8,

129.4, 124.3, 38.9, 32.2 [two peaks overlapped], 31.8, 28.9, 26.9, 22.7, 14.2.

**HRMS** (*m/z*) calcd for C<sub>15</sub>H<sub>20</sub>N<sub>2</sub>O<sub>3</sub> [M]<sup>+Na</sup>: 299.1366, found: 299.1369.

**1-(2-nitrobenzoyl)-2-butylaziridine (104b):** Prepared from 5 mmol of 1,2-epoxyhexane (820 mg, 3.3 mmol, 66% yield). Colorless liquid.

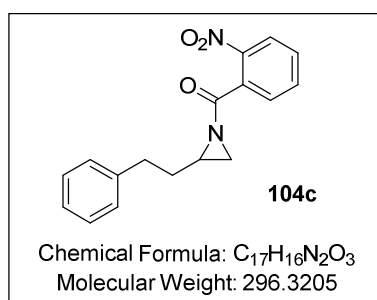


**$^1\text{H-NMR}$**  ( $\text{CD}_2\text{Cl}_2$ , 500 MHz):  $\delta$  7.93 (dd,  $J = 8.2$  Hz,  $J = 1.0$  Hz, 1H), 7.76-7.66 (m, 2H), 7.63-7.56 (m, 1H), 2.69 (dq,  $J = 6.2$  Hz,  $J = 3.7$  Hz, 1H), 2.59 (d,  $J = 6.2$  Hz, 1H), 2.14 (d,  $J = 3.7$  Hz, 1H), 1.62-1.45 (m, 2H), 1.38-1.20 (m, 4H), 0.84 (t,  $J = 7.2$  Hz, 3H).

**$^{13}\text{C-NMR}$**  ( $\text{CD}_2\text{Cl}_2$ , 125 MHz): 177.8, 147.7, 133.7, 132.9,

131.2, 129.8, 124.4, 39.1, 32.3, 32.1, 29.2, 22.6, 14.1.

**1-(2-nitrobenzoyl)-2-phenethylaziridine (104c):** Prepared from 5 mmol of but-3-en-1-ylbenzene (1.06 g, 3.6 mmol, 72% yield). Yellow oil.



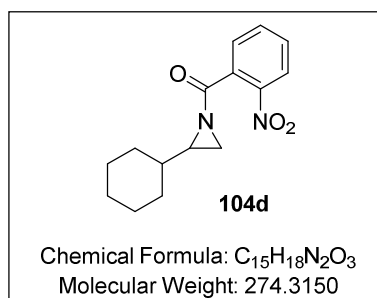
**$^1\text{H-NMR}$**  ( $\text{CDCl}_3$ , 500 MHz):  $\delta$  8.00 (dd,  $J = 8.3$  Hz,  $J = 0.8$  Hz, 1H), 7.75-7.67 (m, 2H), 7.64-7.58 (m, 1H), 7.28-7.22 (m, 2H), 7.20-7.15 (m, 1H), 7.10-7.05 (m, 2H), 2.80 (dq,  $J = 6.1$  Hz,  $J = 3.5$  Hz, 1H), 2.77-2.68 (m, 1H), 2.64 (d,  $J = 6.1$  Hz, 1H), 2.66-2.56 (m, 1H), 2.13 (d,  $J = 3.5$  Hz, 1H), 1.92-1.83 (m, 2H).

**$^{13}\text{C-NMR}$**  ( $\text{CDCl}_3$ , 125 MHz): 177.8, 147.2, 141.0, 133.7, 133.1,

130.9, 129.4, 128.7, 128.5, 126.3, 124.4, 38.4, 34.1, 33.2, 32.2.

**HRMS** ( $m/z$ ) calcd for  $C_{17}H_{16}N_2O_3$  [ $M$ ] $^{+\text{Na}}$ : 319.1053, found: 319.1055.

**1-(2-nitrobenzoyl)-2-cyclohexylaziridine (104d):** Prepared from 5 mmol of vinylcyclohexane (1.00 g, 3.65 mmol, 73% yield). Pale yellow oil.

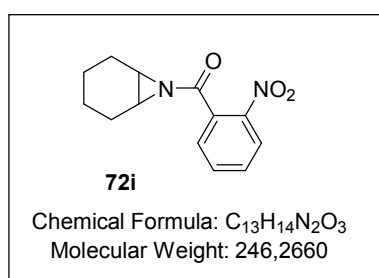


**$^1\text{H-NMR}$**  ( $\text{CDCl}_3$ , 500 MHz):  $\delta$  8.02 (d,  $J = 8.2$  Hz, 1H), 7.72-7.67 (m, 2H), 7.66-7.54 (m, 1H), 2.61 (d,  $J = 6.1$ , 1H), 2.69-2.54 (m, 1H), 2.18 (d,  $J = 3.6$  Hz, 1H), 1.76-1.58 (m, 5H), 1.28-0.85 (m, 6H).

**$^{13}\text{C-NMR}$**  ( $\text{CDCl}_3$ , 125 MHz): 178.2, 146.8, 133.8, 133.4, 130.6, 129.4, 124.4, 43.8, 40.2, 30.9, 30.5, 29.7, 26.3, 25.8, 25.7.

**HRMS** ( $m/z$ ) calcd for  $C_{15}H_{18}N_2O_3$  [ $M$ ] $^{+\text{Na}}$ : 297.1209, found: 297.1207.

**7-(2-nitrobenzoyl)-7-azabicyclo[4.1.0]heptane (72i)**: Prepared from 1 mmol of cyclohexene oxide (163 mg, 0.66 mmol, 66% yield). Pale yellow solid.

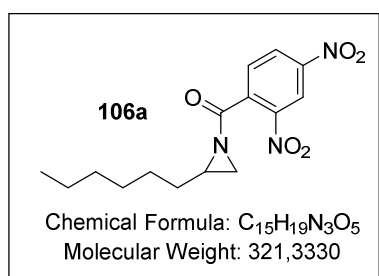


**<sup>1</sup>H-NMR** (500 MHz, CDCl<sub>3</sub>): δ 7.94 (d, *J* = 8.1 Hz, 1H), 7.74-7.64 (m, 2H), 7.60-7.54 (m, 1H), 2.94 (s, 2H), 1.94-1.75 (m, 4H), 1.53-1.42 (m, 2H), 1.38-1.21 (m, 2H);

**<sup>13</sup>C-NMR** (125 MHz, CDCl<sub>3</sub>): δ 178.4, 147.7, 133.6, 133.2, 130.9, 129.6, 124.4, 37.6, 24.0, 20.1.

**HRMS** (*m/z*) calcd for C<sub>13</sub>H<sub>14</sub>N<sub>2</sub>NaO<sub>3</sub> [M]<sup>+Na</sup>: 269.0902, found: 269.0910.

**1-(2,4-dinitrobenzoyl)-2-hexylaziridine (106a)**: Prepared from 10 mmol of 1,2-epoxyoctane (1.33 g, 4.2 mmol, 42% yield). Colorless liquid.

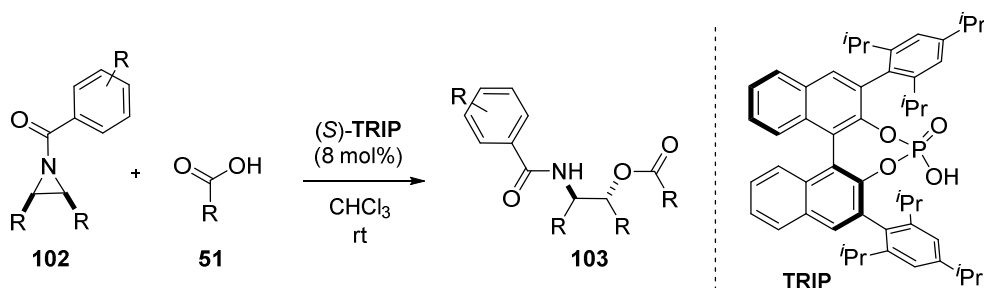


**<sup>1</sup>H NMR** (500 MHz, CDCl<sub>3</sub>): δ 8.84 (s, 1H), 8.55 (d, *J* = 8.35 Hz, 1H), 7.94 (d, *J* = 8.35 Hz, 1H), 2.81 (m, 1H), 2.68 (d, *J* = 6.3 Hz, 1H), 2.19 (d, *J* = 3.5 Hz, 1H), 1.59-1.53 (m, 2H), 1.37-1.20 (m, 9H), 0.86 (t, *J* = 6.3 Hz, 3H).

**<sup>13</sup>C-NMR** (125 MHz, CDCl<sub>3</sub>): δ 175.5, 148.5, 147.3, 138.3,

130.9, 128.2, 120.0, 39.5, 32.4, 32.1, 31.8, 28.9, 26.9, 22.7, 14.2.

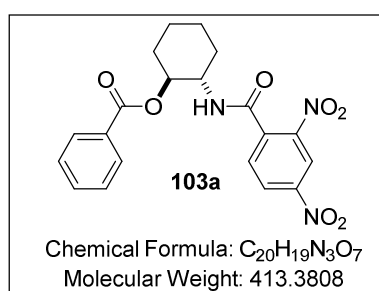
**HRMS** (*m/z*) calcd for C<sub>15</sub>H<sub>19</sub>N<sub>3</sub>O<sub>5</sub> [M]<sup>+Na</sup>: 344.1214, found: 344.1217.

7.3.2. General procedure for the desymmetrization of *meso*-aziridines

To the corresponding aziridine (0.2 mmol) a solution of benzoic acid (1.4 mmol, 7 equiv.) and (S)-TRIP phosphoric acid (8 mol%) in chloroform was added. The mixture was stirred at room temperature until complete product formation (TLC eluent: hexanes/MTBE = 2:3). The reaction was then diluted in hexanes and directly purified by flash column chromatography [eluent: mixtures hexanes/MTBE]. The enantiomeric ratios of products were analyzed by HPLC on a chiral stationary phase.

For analytical purpose, the racemic samples were prepared on 0.05 mmol scale using (RS)-TRIP as the catalyst.

**(*R,R*)-2-(2,4-dinitrobenzamido)cyclohexyl benzoate (103a)**: The reaction was performed at room temperature [conc. = 0.125M] and yielded the product as white solid. (81 mg, 98% yield, er > 99.5:0.5).



**$^1\text{H-NMR}$**  (500 MHz,  $\text{CDCl}_3$ ):  $\delta$  8.76 (d,  $J = 2.2$  Hz, 1H), 8.32 (dd,  $J = 8.4$  Hz, 2.2 Hz, 1H), 7.96 (d,  $J = 8.4$  Hz, 2H), 7.57 (t,  $J = 7.4$  Hz, 1H), 7.42 (t,  $J = 7.4$  Hz, 2H), 7.38 (d,  $J = 8.4$  Hz, 1H), 6.57 (d,  $J = 8.3$  Hz, 1H), 4.97 (td,  $J = 10.7$  Hz, 4.6 Hz, 1H), 4.28-4.15 (m, 1H), 2.42-2.30 (m, 1H), 2.22-2.10 (m, 1H), 1.95-1.78 (m, 2H), 1.75-1.63 (m, 1H), 1.55-1.34 (m, 3H).

**$^{13}\text{C-NMR}$**  (125 MHz,  $\text{CDCl}_3$ ):  $\delta$  167.9, 164.3, 148.2, 146.7, 138.1, 133.7, 130.2, 129.9, 129.8, 128.7, 128.3, 120.2, 75.5, 54.2, 31.9, 31.4, 24.4, 24.3.

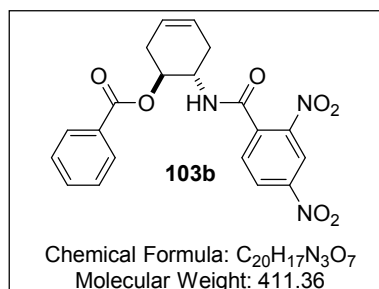
**HRMS** ( $m/z$ ) calcd for  $\text{C}_{20}\text{H}_{19}\text{N}_3\text{O}_7$  [ $\text{M}]^{+\text{Na}}$ : 436.1115, found: 436.1115.

**$[\alpha]_{\text{D}}^{25}$** : +3.3° ( $c = 0.8$ ,  $\text{CHCl}_3$ ).

The enantiomeric ratio was determined by HPLC analysis using a Daicel Chiralcel AD-3 column:  $n\text{Hept}:\text{PrOH} = 90:10$ , flow rate 1 mL/min,  $\tau_1 = 18.0$  min,  $\tau_2 = 27.5$  min.



**(*R,R*)-6-(2,4-dinitrobenzamido)cyclohex-3-en-1-yl benzoate (103b)**: The reaction was performed at room temperature [conc. = 0.125M] and yielded the product as white solid. (73.1 mg, 83% yield, er = 99:1).



1H, 2.26-2.15 (m, 1H).

$^1\text{H-NMR}$  (500 MHz,  $CDCl_3$ ):  $\delta$  8.76 (d, 2.1 Hz, 1H), 8.32 (dd,  $J$  = 8.3 Hz,  $J$  = 2.1 Hz, 1H), 7.98 (d,  $J$  = 7.8 Hz, 2H), 7.59 (t,  $J$  = 7.4 Hz, 1H), 7.44 (t,  $J$  = 7.4 Hz, 2H), 7.36 (d,  $J$  = 8.3 Hz, 1H), 6.59 (d,  $J$  = 8.7 Hz, 1H), 5.68 (cm, 2H), 5.32-5.24 (m, 1H), 4.58-4.48 (m, 1H), 2.86-2.82 (m, 1H), 2.68-2.57 (m, 1H), 2.55-2.46 (m, 1H), 2.26-2.15 (m, 1H).

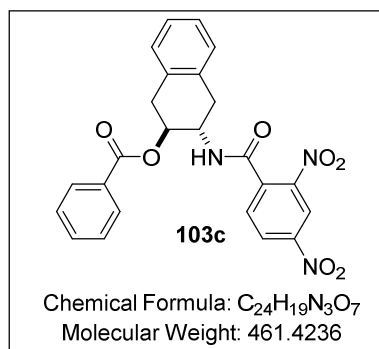
$^{13}\text{C-NMR}$  (125 MHz,  $CDCl_3$ ):  $\delta$  167.7, 164.5, 148.3, 146.6, 138.0, 133.8, 130.2, 129.9, 129.6, 128.8, 128.3, 124.7, 124.2, 120.2, 71.8, 50.3, 31.6, 31.1.

**HRMS** ( $m/z$ ) calcd for  $C_{20}H_{17}N_3O_7$  [ $M$ ] $^{+Na}$ : 434.0958, found: 434.0960.

$[\alpha]_D^{25}$ :  $-23.7^\circ$  ( $c$  = 0.295,  $CHCl_3$ ).

The enantiomeric ratio was determined by HPLC analysis using a Daicel Chiralcel AD-3 column:  $n\text{Hept}:i\text{PrOH}$  = 80:20, flow rate 1 mL/min,  $\tau_1$  = 10.5 min,  $\tau_2$  = 13.8 min.

**(*R,R*)-3-(2,4-dinitrobenzamido)-1,2,3,4-tetrahydronaphthalen-2-yl benzoate (103c)**: The reaction was performed at room temperature [conc. = 0.125M] and yielded the product as white solid. (91 mg, 99% yield, er = 98.5:1.5).



2.92 (dd,  $J$  = 16.5 Hz,  $J$  = 9.7 Hz, 1H).

$^1\text{H-NMR}$  (500 MHz,  $CDCl_3$ ):  $\delta$  8.76 (d,  $J$  = 2.0 Hz, 1H), 8.32 (dd,  $J$  = 8.2 Hz,  $J$  = 2.0 Hz, 1H), 8.01 (d,  $J$  = 7.6 Hz, 2H), 7.60 (t,  $J$  = 7.6 Hz, 1H), 7.50-7.40 (m, 3H), 7.22-7.05 (m, 4H), 6.70 (d,  $J$  = 8.3 Hz, 1H), 5.42 (td,  $J$  = 9.5 Hz,  $J$  = 5.9 Hz, 1H), 4.75-4.60 (m, 1H), 3.50 (dd,  $J$  = 16.5 Hz,  $J$  = 5.8 Hz, 1H), 3.32 (dd,  $J$  = 16.5 Hz,  $J$  = 5.8 Hz, 1H), 3.22 (dd,  $J$  = 16.5 Hz,  $J$  = 9.7 Hz, 1H), 2.92 (dd,  $J$  = 16.5 Hz,  $J$  = 9.7 Hz, 1H).

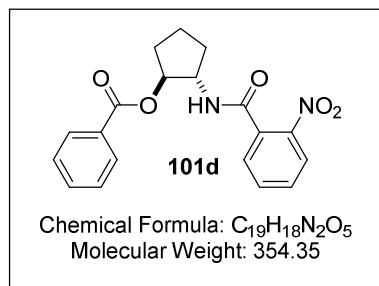
$^{13}\text{C-NMR}$  (125 MHz,  $CDCl_3$ ):  $\delta$  167.6, 164.6, 148.3, 146.7, 137.9, 133.9, 132.7, 132.6, 130.2, 129.9, 129.5, 129.1, 129.0, 128.8, 128.3, 127.0, 127.0, 120.3, 71.9, 50.7, 34.6, 34.3.

**HRMS** ( $m/z$ ) calcd for  $C_{24}H_{19}N_3O_7$  [ $M$ ] $^{+Na}$ : 484.1115, found: 484.1115.

$[\alpha]_D^{25}$ :  $-13.4^\circ$  ( $c$  = 1.0,  $CHCl_3$ ).

The enantiomeric ratio was determined by HPLC analysis using a Daicel Chiralcel OD-3 column:  $n\text{Hept}:i\text{PrOH}$  = 60:40, flow rate 1 mL/min,  $\tau_1$  = 10.5 min,  $\tau_2$  = 18.7 min.

**(*R,R*)-2-(2-nitrobenzamido)cyclopentyl benzoate (101d)**: The reaction was performed at -10 °C [0.1 mmol scale, conc. = 0.07M] and yielded the product as white solid. (34 mg, 96% yield, er = 98:2)



<sup>1</sup>H-NMR (500 MHz, CDCl<sub>3</sub>): δ 8.05-8.00 (m, 3H), 7.63 (td, *J* = 7.7 Hz, *J* = 1.0 Hz, 1H), 7.59-7.53 (m, 2H), 7.50 (td, *J* = 7.7 Hz, *J* = 1.0 Hz, 1H), 7.44 (t, *J* = 8.0 Hz, 2H), 6.44 (d, *J* = 7.6 Hz, 1H), 5.32 (q, *J* = 6.8 Hz, 1H), 4.45 (q, *J* = 7.6 Hz, 1H), 2.53-2.42 (m, 1H), 2.28-2.15 (m, 1H), 1.98-1.78 (m, 3H), 1.75-1.65 (m, 1H).

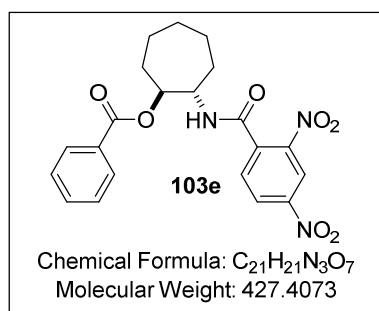
<sup>13</sup>C-NMR (125 MHz, CDCl<sub>3</sub>): δ 167.4, 166.7, 146.6, 133.9, 133.4, 133.1, 130.6, 130.1, 130.0, 128.9, 128.6, 124.7, 79.7, 57.5, 30.3, 29.7, 20.8.

HRMS (*m/z*) calcd for C<sub>19</sub>H<sub>18</sub>N<sub>2</sub>O<sub>5</sub> [M]<sup>+Na</sup>: 377.1108, found: 377.1104.

[α]<sub>D</sub><sup>25</sup>: -17.0° (*c* = 0.550, CHCl<sub>3</sub>).

The enantiomeric ratio was determined by HPLC analysis using a Daicel Chiralcel OD-3 column: *n*Hept:*i*PrOH = 90:10, flow rate 1 mL/min, τ<sub>1</sub> = 11.6 min, τ<sub>2</sub> = 15.9 min.

**(*R,R*)-3-(2,4-dinitrobenzamido)-1,2,3,4-tetrahydronaphthalen-2-yl benzoate (103e)**: The reaction was performed at room temperature [conc. = 0.125M] and yielded the product as white solid. (84 mg, 99% yield, er = 98.5:1.5).



<sup>1</sup>H-NMR (500 MHz, CDCl<sub>3</sub>): δ 8.81 (d, *J* = 2.1 Hz, 1H), 8.33 (dd, *J* = 8.3 Hz, *J* = 2.1 Hz, 1H), 8.01 (d, *J* = 7.6 Hz, 2H), 7.60 (t, *J* = 7.6 Hz, 1H), 7.46 (t, *J* = 7.6 Hz, 2H), 7.35 (d, *J* = 8.3 Hz, 1H), 6.46 (d, *J* = 8.0 Hz, 1H), 5.25-5.10 (m, 1H), 4.45-4.32 (m, 1H), 2.20-2.10 (m, 1H), 2.05-1.95 (m, 2H), 1.90-1.55 (m, 7H).

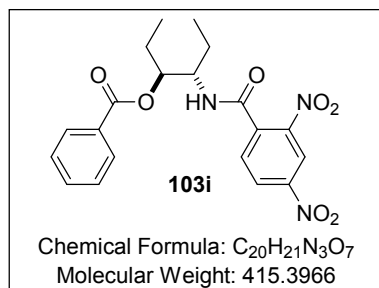
<sup>13</sup>C-NMR (125 MHz, CDCl<sub>3</sub>): δ 167.6, 164.0, 148.3, 146.8, 138.2, 133.8, 130.2, 129.9 (two peaks overlapping), 128.8, 128.2, 120.3, 78.1, 57.0, 31.7, 31.1, 27.8, 24.4, 22.7.

HRMS (*m/z*) calcd for C<sub>21</sub>H<sub>21</sub>N<sub>3</sub>O<sub>7</sub> [M]<sup>+Na</sup>: 450.1272, found: 450.1272.

[α]<sub>D</sub><sup>25</sup>: +17.8° (*c* = 1.0, CHCl<sub>3</sub>).

The enantiomeric ratio was determined by HPLC analysis using Daicel Chiralcel OD-3 column: *n*Hept:*i*PrOH = 80:20, flow rate 1 mL/min, τ<sub>1</sub> = 7.4 min, τ<sub>2</sub> = 10.7 min.

**(*R,R*)-4-(2,4-dinitrobenzamido)hexan-3-yl benzoate (103i)**: The reaction was performed at room temperature [conc. = 0.025M] and yielded the product as white solid. (82 mg, 99% yield, er = 93.5:6.5).



<sup>1</sup>H-NMR (500 MHz, CDCl<sub>3</sub>): δ 8.79 (d, *J* = 2.0 Hz, 1H), 8.38 (dd, *J* = 8.4 Hz, *J* = 2.0 Hz, 1H), 7.97 (d, *J* = 7.6 Hz, 2H), 7.56 (t, *J* = 7.6 Hz, 1H), 7.52 (d, *J* = 8.4 Hz, 1H), 7.42 (d, *J* = 7.6 Hz, 2H), 6.59 (d, *J* = 9.6 Hz, 1H), 5.25-5.15 (m, 1H), 4.42-4.32 (m, 1H), 1.92-1.80 (m, 2H), 1.80-1.68 (m, 1H), 1.65-1.50 (m, 1H), 1.07 (t, *J* = 7.4 Hz, 3H), 1.03 (t, *J* = 7.4 Hz, 3H).

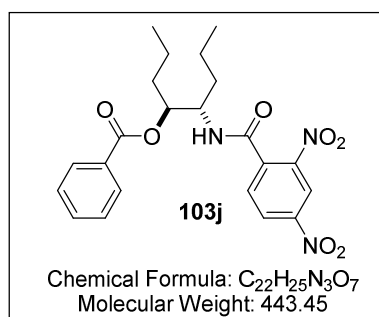
<sup>13</sup>C-NMR (125 MHz, CDCl<sub>3</sub>): δ 166.8, 164.5, 148.3, 146.9, 138.2, 133.6, 130.2, 129.8, 129.8, 128.7, 128.2, 120.3, 76.9, 54.1, 25.5, 25.0, 10.3, 10.0.

HRMS (*m/z*) calcd for C<sub>20</sub>H<sub>21</sub>N<sub>3</sub>O<sub>7</sub> [M]<sup>+Na</sup>: 438.1272, found: 438.1272.

[α]<sub>D</sub><sup>25</sup>: -75.5° (*c* = 1.100, CHCl<sub>3</sub>).

The enantiomeric ratio was determined by HPLC analysis using a Daicel Chiralcel AS-3 column: *n*Hept:*i*PrOH = 70:30, flow rate 1 mL/min, τ<sub>2</sub> = 8.0 min, τ<sub>1</sub> = 13.9 min.

**(*R,R*)-5-(2,4-dinitrobenzamido)octan-4-yl benzoate (103j)**: The reaction was performed at room temperature [conc. = 0.025M] and yielded the product as white solid. (83 mg, 94% yield, er = 94:6).



<sup>1</sup>H-NMR (500 MHz, CDCl<sub>3</sub>): δ 8.87 (s, 1H), 8.42 (d, *J* = 8.3 Hz, 1H), 8.01 (d, *J* = 7.5 Hz, 2H), 7.62-7.52 (t, *J* = 7.5 Hz, 1H), 7.54 (d, *J* = 8.3 Hz, 1H), 7.46 (t, *J* = 7.5 Hz, 2H), 6.04 (d, *J* = 9.5 Hz, 1H), 5.30 (cm, 1H), 4.54-4.46 (m, 1H), 1.92-1.74 (m, 2H), 1.74-1.62 (m, 1H), 1.62-1.42 (m, 5H), 1.02-0.95 (m, 6H).

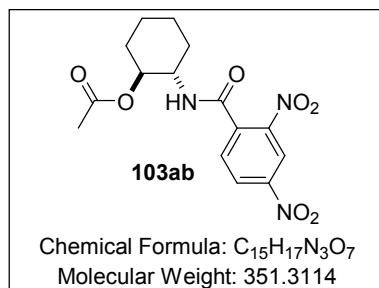
<sup>13</sup>C-NMR (125 MHz, CDCl<sub>3</sub>): δ 166.8, 164.4, 148.5, 147.1, 138.2, 133.7, 130.3, 129.9, 129.9, 128.8, 128.2, 120.4, 75.9, 52.9, 34.7, 34.1, 19.1, 18.9, 14.2, 14.1.

HRMS (*m/z*) calcd for C<sub>22</sub>H<sub>25</sub>N<sub>3</sub>O<sub>7</sub> [M]<sup>+Na</sup>: 466.1585, found: 466.1588.

[α]<sub>D</sub><sup>25</sup>: -89.9° (*c* = 0.345, CHCl<sub>3</sub>).

The enantiomeric ratio was determined by HPLC analysis using a Daicel Chiralcel AD-3 column: *n*Hept:*i*PrOH = 90:10, flow rate 1 mL/min, τ<sub>1</sub> = 13.8 min, τ<sub>2</sub> = 17.0 min.

**(*R,R*)-2-(2,4-dinitrobenzamido)cyclohexyl acetate (103ab)**: The reaction was performed at room temperature [conc. = 0.025M] and yielded the product as white solid. (66 mg, 94% yield, er = 97.5:2.5).



<sup>1</sup>H-NMR (500 MHz, CDCl<sub>3</sub>): δ 8.89 (d, *J* = 1.9 Hz, 1H), 8.50 (dd, *J* = 8.3 Hz, *J* = 1.9 Hz, 1H), 7.64 (d, *J* = 8.3 Hz, 1H), 6.32 (d, *J* = 7.8 Hz, 1H), 4.74 (td, *J* = 10.8 Hz, *J* = 4.6 Hz, 1H), 4.10-4.00 (m, 1H), 2.38-2.25 (m, 1H), 2.11 (s, 3H), 2.05-1.95 (m, 1H), 1.90-1.74 (m, 2H), 1.64-1.52 (m, 1H), 1.48-1.20 (m, 3H).

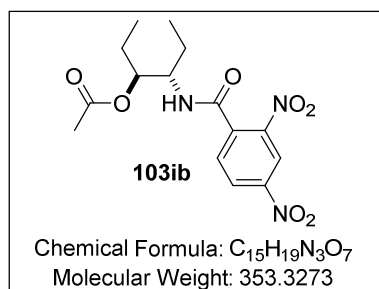
<sup>13</sup>C-NMR (125 MHz, CDCl<sub>3</sub>): δ 173.2, 164.2, 148.4, 146.9, 138.3, 130.3, 128.4, 120.4, 74.5, 54.7, 32.2, 31.5, 24.3, 24.3, 21.5.

HRMS (*m/z*) calcd for C<sub>15</sub>H<sub>17</sub>N<sub>3</sub>O<sub>7</sub> [M]<sup>+Na</sup>: 374.0958, found: 434.0960.

[α]<sub>D</sub><sup>25</sup>: +66.0° (*c* = 1.0, CHCl<sub>3</sub>).

The enantiomeric ratio was determined by HPLC analysis using a Daicel Chiralcel OD-3 column: *n*Hept:*i*PrOH = 80:20, flow rate 1 mL/min, τ<sub>1</sub> = 7.6 min, τ<sub>2</sub> = 10.2 min.

**(*R,R*)-4-(2,4-dinitrobenzamido)hexan-3-yl acetate (103ib)**: The reaction was performed at room temperature [conc. = 0.025M] and yielded the product as white solid. (62 mg, 88% yield, er = 92.5:7.5).



<sup>1</sup>H-NMR (500 MHz, CDCl<sub>3</sub>): δ 8.89 (d, *J* = 1.7 Hz, 1H), 8.52 (dd, *J* = 8.2 Hz, *J* = 1.7 Hz, 1H), 7.72 (d, *J* = 8.2 Hz, 1H), 6.04 (d, *J* = 9.0 Hz, 1H), 5.03-4.95 (m, 1H), 4.34-4.22 (m, 1H), 2.07 (s, 3H), 1.78-1.50 (m, 4H), 1.05 (t, *J* = 7.4 Hz, 3H), 0.98 (t, *J* = 7.4 Hz, 3H).

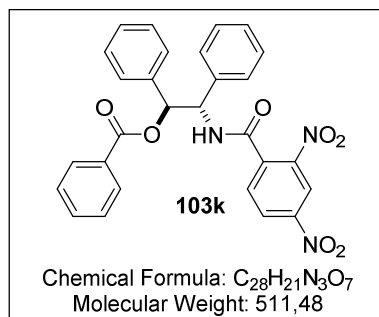
<sup>13</sup>C-NMR (125 MHz, CDCl<sub>3</sub>): δ 171.1, 164.5, 148.5, 147.0, 138.3, 130.3, 128.3, 120.4, 76.1, 53.6, 25.7, 24.9, 21.2, 10.4, 10.0.

HRMS (*m/z*) calcd for C<sub>15</sub>H<sub>19</sub>N<sub>3</sub>O<sub>7</sub> [M]<sup>+Na</sup>: 376.1115, found: 376.1117.

[α]<sub>D</sub><sup>25</sup>: -47.8° (*c* = 0.295, CHCl<sub>3</sub>).

The enantiomeric ratio was determined by HPLC analysis using a Daicel Chiralcel OD-3 column: *n*Hept:*i*PrOH = 85:15, flow rate 1 mL/min, τ<sub>1</sub> = 15.3 min, τ<sub>2</sub> = 19.3 min.

**(*R,R*)-2-(2,4-dinitrobenzamido)-1,2-diphenylethyl benzoate (103k)**: The reaction was performed at room temperature and yielded the product as white solid. (72 mg, 70% yield, er = 96:4).



<sup>1</sup>H-NMR (500 MHz, CD<sub>2</sub>Cl<sub>2</sub>): δ 8.78 (d, *J* = 2.2 Hz, 1H), 8.36 (dd, *J* = 8.1 Hz, *J* = 2.2 Hz, 1H), 8.04 (d, *J* = 7.6 Hz, 2H), 7.61 (t, *J* = 7.6 Hz, 1H), 7.46 (t, *J* = 7.6 Hz, 2H), 7.40-7.20 (m, 11 H), 7.02 (d, *J* = 8.3 Hz, 1H), 6.40 (d, *J* = 8.3 Hz, 1H), 5.73 (t, *J* = 8.3 Hz, 1H).

<sup>13</sup>C-NMR (125 MHz, CD<sub>2</sub>Cl<sub>2</sub>): δ 166.7, 164.1, 148.6, 147.0, 137.9, 137.6, 137.0, 134.0, 130.5, 130.1, 129.8, 129.0 (two peaks overlapping), 129.0, 128.9, 128.6, 128.5, 127.9, 127.6, 120.4, 78.4, 59.5.

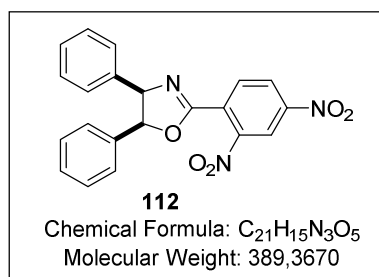
HRMS (*m/z*) calcd for C<sub>28</sub>H<sub>21</sub>N<sub>3</sub>O<sub>7</sub> [M]<sup>+Na</sup>: 510.1307, found: 510.1307.

[α]<sub>D</sub><sup>25</sup>: -19.8° (*c* = 1.050, CHCl<sub>3</sub>).

The enantiomeric ratio was determined by HPLC analysis using a Daicel Chiralcel IC-3 column: nHept:EtOH = 85:15, flow rate 1 mL/min, τ<sub>1</sub> = 8.1 min, τ<sub>2</sub> = 8.9 min,

**2-(2,4-dinitrophenyl)-4,5-diphenyl-4,5-dihydrooxazole (112)**: This compound was isolated as byproduct of the ring opening of aziridine **102k** (18 mg, 23% yield, er = 83:17) as a white solid.

Based on *NOE* correlation and on the value of the coupling constant between the oxazoline protons, the relative configuration was found to be *cis*; <sup>175</sup> the absolute stereochemistry was not assigned.

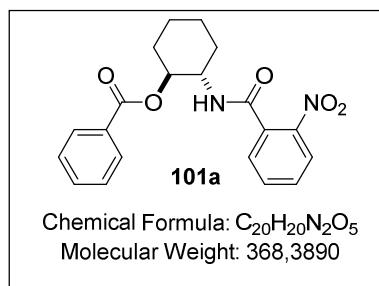


<sup>1</sup>H-NMR (500 MHz, CD<sub>2</sub>Cl<sub>2</sub>): δ 8.72 (d, *J* = 2.3 Hz, 1H), 8.55 (dd, *J* = 8.3 Hz, *J* = 2.3 Hz, 1H), 8.33 (d, *J* = 8.3 Hz, 2H), 7.15-6.9 (m, 10H), 6.09 (d, *J* = 10.4 Hz, 1H), 5.80 (d, *J* = 10.4 Hz, 1H).

<sup>13</sup>C-NMR (125 MHz, CD<sub>2</sub>Cl<sub>2</sub>) [peaks overlapping]: δ 161.0, 150.1, 149.6, 136.9, 135.6, 133.4, 128.5, 128.4, 128.3, 127.9, 127.1, 126.9, 120.0, 87.6, 75.2.

The enantiomeric ratio was determined by HPLC analysis using a Daicel Chiralcel IC-3 column: nHept:EtOH = 85:15, flow rate 1 mL/min, τ<sub>1</sub> = 11.2 min, τ<sub>2</sub> = 12.6 min,

**(*R,R*)-2-(2-nitrobenzamido)cyclohexyl benzoate (101a)**: This product was obtained during the optimization of the reaction conditions (Table 4.4). The reaction was performed at room temperature on 0.1 mmol scale [conc. = 0.125M] and yielded the product as white solid. (35 mg, 95% yield, er = 98.5:1.5).



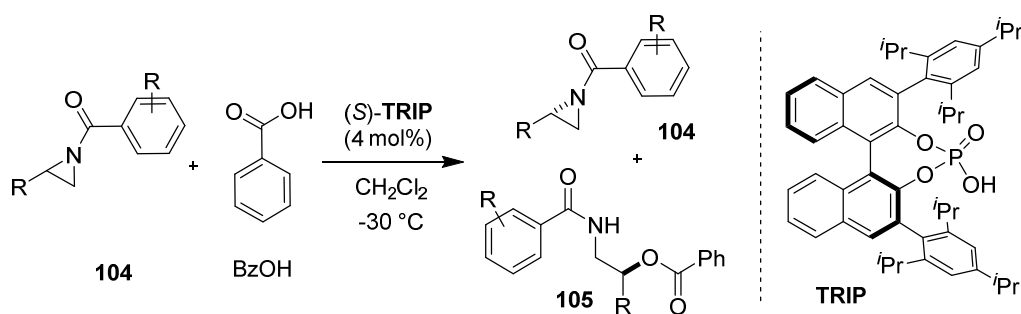
**<sup>1</sup>H-NMR** (500 MHz, CDCl<sub>3</sub>): δ 8.09-8.02 (m, 2H), 7.99-7.92 (m, 1H), 7.62-7.53 (m, 1H), 7.53-7.40 (m, 4H), 7.19-7.11 (m, 1H), 6.28 (d, *J* = 8.5 Hz, 1H), 4.99 (td, *J* = 10.8, 4.5 Hz, 1H), 4.30-4.18 (m, 1H), 2.44-2.32 (m, 1H), 2.21-2.11 (m, 1H), 1.92-1.77 (m, 2H), 1.69 (ddd, *J* = 15.8, 12.6, 3.8 Hz, 1H), 1.52-1.31 (m, 3H).

**<sup>13</sup>C-NMR** (125 MHz, CDCl<sub>3</sub>): δ 167.9, 166.5, 146.6, 133.9, 133.6, 133.3, 130.6, 130.5, 130.2, 130.1, 128.8, 128.8, 128.7, 124.8, 75.5, 54.0, 32.1, 31.6, 24.6, 24.5.

**HRMS**: (*m/z*) calcd for [C<sub>20</sub>H<sub>20</sub>N<sub>2</sub>O<sub>5</sub>] [M]<sup>+Na</sup>: 368.1372, found: 368.1372.

The enantiomeric ratio was determined by HPLC analysis using Daicel Chiralcel OD-3 column: *n*Hept:*i*PrOH = 90:10, flow rate 1 mL/min, τ<sub>1</sub> = 12.0 min, τ<sub>2</sub> = 15.5 min.

## 7.3.3. General procedure for the kinetic resolution of terminal aziridines

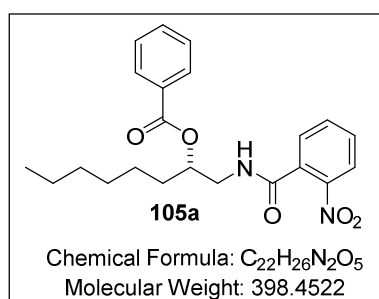


To a stirred solution of benzoic acid (0.7 mmol, 7 equiv.) and (*S*)-**TRIP** phosphoric acid (4 mol%) in  $\text{CH}_2\text{Cl}_2$  (4.25 ml) at  $-30\text{ }^\circ\text{C}$  a precooled solution of the aziridine (0.1 mmol) in  $\text{CH}_2\text{Cl}_2$  (2.0 ml) was added.

When the conversion was close to 50% (reaction time was optimized through a preliminary investigation), the reaction was quenched with MTBE (4.0 ml) and directly purified by flash column chromatography [eluent: mixtures hexanes/MTBE]. Both the enantiomeric ratios of the products and of the unreacted starting materials were analyzed by HPLC on a chiral stationary phase.

For analytical purpose, the racemic samples were prepared on 0.05 mmol scale using (*RS*)-**TRIP** as the catalyst.

**(*S*)-1-(2-nitrobenzamido)octan-2-yl benzoate (105a)** : The product was obtained as colorless oil (19 mg, 48% yield, er = 92.5:7.5), while the starting material was recovered as colorless oil (11.5 mg, 42% yield, er = 98:2). Reaction time: 2.5 h.



$^1\text{H-NMR}$  (500 MHz,  $\text{CDCl}_3$ ):  $\delta$  8.05-8.00 (m, 3H), 7.65-7.52 (m, 3H), 7.48-7.42 (m, 3H), 6.40-6.30 (m, 1H), 5.34-5.25 (m, 1H), 3.88-3.78 (m, 1H), 3.76-3.68 (m, 1H), 1.90-1.74 (m, 2H), 1.55-1.20 (m, 8H), 0.83 (t,  $J = 6.7\text{ Hz}$ , 3H).

$^{13}\text{C-NMR}$  ( $\text{CDCl}_3$ , 100 MHz):  $\delta$  167.2, 166.7, 146.7, 133.9, 133.5, 133.0, 130.7, 130.9, 129.9, 128.9, 128.7, 124.8, 74.4,

44.2, 32.4, 31.8, 29.3, 25.5, 22.7, 14.2.

**HRMS** ( $m/z$ ) calcd for  $\text{C}_{22}\text{H}_{26}\text{N}_2\text{O}_5$  [ $\text{M}$ ] $^{+\text{Na}}$ : 421.1734, found: 421.1733.

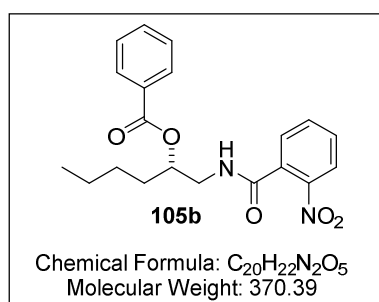
$[\alpha]_{\text{D}}^{25}$ :  $+13.7^\circ$  ( $c = 0.935$ ,  $\text{CHCl}_3$ ).

The enantiomeric ratio was determined by HPLC analysis:

**(S)-105a** - Daicel Chiralcel AD-3 column: *n*Hept:*i*PrOH = 90:10, flow rate 1 mL/min,  $\tau_1 = 11.7$  min,  $\tau_2 = 21.3$  min.

**(S)-1-(2-nitrobenzoyl)-2-hexylaziridine (104a)** - Daicel Chiralcel AD-3 column: *n*Hept:*i*PrOH = 98:2, flow rate 1 mL/min,  $\tau_1 = 8.0$  min,  $\tau_2 = 12.8$  min.  $[\alpha]_D^{25}$ :  $-44.8^\circ$  ( $c = 0.460$ ,  $\text{CHCl}_3$ ).

**(S)-1-(2-nitrobenzamido)hexyl-2-yl benzoate (105b)**: The product was obtained as colorless oil (18 mg, 49% yield, er = 94:6), while the starting material was recovered as colorless oil (11.5 mg, 46% yield, er = 95.5:4.5). Reaction time: 2.5 h.



$^1\text{H-NMR}$  (500 MHz,  $\text{CDCl}_3$ ):  $\delta$  8.08-7.98 (m, 3H), 7.66-7.52 (m, 3H), 7.50-7.40 (m, 3H), 6.26 (cm, 1H), 5.30 (m, 1H), 3.90-3.80 (m, 1H), 3.78-3.70 (m, 1H), 1.95-1.72 (m, 2H), 1.50-1.32 (m, 4H), 0.92 (t,  $J = 7.1$  Hz, 3H).

$^{13}\text{C-NMR}$  ( $\text{CDCl}_3$ , 100 MHz):  $\delta$  167.3, 166.7, 146.7, 133.9, 133.5, 133.0, 130.7, 130.1, 129.9, 128.9, 128.7, 124.8, 74.4,

44.3, 32.1, 27.7, 22.7, 14.1.

**HRMS** ( $m/z$ ) calcd for  $\text{C}_{20}\text{H}_{22}\text{N}_2\text{O}_5$   $[\text{M}]^{+\text{Na}}$ : 393.1421, found: 393.1422.

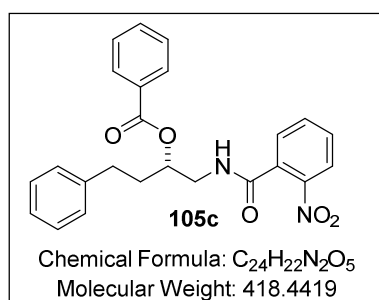
$[\alpha]_D^{25}$ :  $+3.3^\circ$  ( $c = 1.100$ ,  $\text{CHCl}_3$ ).

The enantiomeric ratio was determined by HPLC analysis:

**(S)-105b** - Daicel Chiralcel AD-3 column: *n*Hept:*i*PrOH = 90:10, flow rate 1 mL/min,  $\tau_1 = 11.7$  min,  $\tau_2 = 21.6$  min.

**(S)-1-(2-nitrobenzoyl)-2-butylaziridine (104b)** - Daicel Chiralcel AD-3 column: *n*Hept:*i*PrOH = 98:2, flow rate 1 mL/min,  $\tau_1 = 9.3$  min,  $\tau_2 = 13.7$  min.  $[\alpha]_D^{25}$ :  $-24.2^\circ$  ( $c = 0.685$ ,  $\text{CHCl}_3$ ).

**(S)-1-(2,4-dinitrobenzamido)-4-phenylbutan-2-yl benzoate (105c)**: The product was obtained as white solid (21.5 mg, 51% yield, er = 92.5:7.5), while the starting material was recovered as colorless oil (13 mg, 44% yield, er = 98.5:1.5). Reaction time: 12.5 h.



$^1\text{H-NMR}$  (500 MHz,  $\text{CDCl}_3$ ):  $\delta$  8.12-8.02 (m, 3H), 7.68-7.55 (m, 3H), 7.54-7.45 (m, 3H), 7.38-7.28 (m, 2H), 7.27-7.21 (m, 3H), 6.40 (cm, 1H), 5.35 (cm, 1H), 3.93-3.78 (m, 2H), 2.95-2.78 (m, 2H), 2.32-2.12 (m, 2H).



$^{13}\text{C-NMR}$  ( $\text{CDCl}_3$ , 100 MHz) [peaks overlapping]:  $\delta$  167.1, 166.8, 146.7, 141.0, 133.9, 133.6, 132.9, 130.7, 129.9, 128.9, 128.8, 128.7, 128.6, 126.4, 124.8, 73.7, 44.1, 33.9, 31.8.

**HRMS** ( $m/z$ ) calcd for  $\text{C}_{24}\text{H}_{21}\text{N}_2\text{O}_5$  [ $\text{M}]^{+\text{Na}}$ : 441.1421, found: 441.1420.

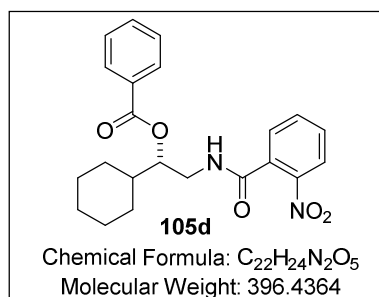
$[\alpha]_{\text{D}}^{25}$ :  $-8.1^\circ$  ( $c = 0.910$ ,  $\text{CHCl}_3$ ).

The enantiomeric ratio was determined by HPLC analysis:

**(S)-105c** - Daicel Chiralcel AD-3 column:  $n\text{Hept}:i\text{PrOH} = 80:20$ , flow rate 1 mL/min,  $\tau_1 = 7.3$  min,  $\tau_2 = 12.3$  min.

**(S)-1-(2-nitrobenzoyl)-2-phenethylaziridine (104c)**: Daicel Chiralcel AD-3 column:  $n\text{Hept}:i\text{PrOH} = 95:5$ , flow rate 1 mL/min,  $\tau_1 = 10.7$  min,  $\tau_2 = 12.3$  min.  $[\alpha]_{\text{D}}^{25}$ :  $-18.9^\circ$  ( $c = 0.530$ ,  $\text{CHCl}_3$ ).

**(S)-1-cyclohexyl-2-(2,4-dinitrobenzamido)ethyl benzoate (105d)**: The product was obtained as white solid (11 mg, 28% yield, er = 96:4), while the starting material was recovered as colorless oil (16 mg, 58% yield, er = 71.5:28.5). Reaction time: 18.5 h.



$^1\text{H-NMR}$  (500 MHz,  $\text{CDCl}_3$ ):  $\delta$  8.10-8.02 (m, 2H), 8.00-7.92 (dd,  $J = 8.2$  Hz,  $J = 1.0$  Hz, 1H), 7.70-7.52 (m, 3H), 7.50-7.40 (m, 3H), 6.32 (cm, 1H), 5.13 (cm, 1H), 3.90-3.78 (m, 1H), 3.75-3.65 (m, 1H), 1.95-1.20 (m, 11H).

$^{13}\text{C-NMR}$  ( $\text{CDCl}_3$ , 125 MHz):  $\delta$  167.3, 166.7, 146.7, 133.9, 133.5, 133.0, 130.7, 130.1, 129.9, 128.9, 128.7, 124.8, 74.4,

44.3, 32.1, 27.7, 22.7, 14.1.

$[\alpha]_{\text{D}}^{25}$ :  $+4.8^\circ$  ( $c = 0.800$ ,  $\text{CHCl}_3$ ).

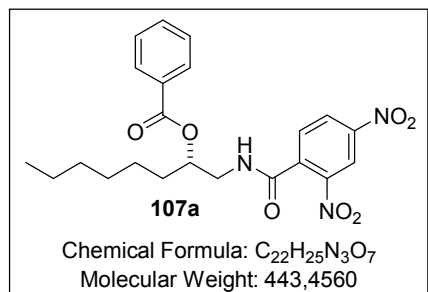
The enantiomeric ratio was determined by HPLC analysis:

**(S)-105d** - Daicel Chiralcel AD-3 column:  $n\text{Hept}:i\text{PrOH} = 80:20$ , flow rate 1 mL/min,  $\tau_1 = 8.9$  min,  $\tau_2 = 13.1$  min.

**(S)-1-(2-nitrobenzoyl)-2-cyclohexylaziridine (104d)**: Daicel Chiralcel AD-3 column:  $n\text{Hept}:i\text{PrOH} = 95:5$ , flow rate 1 mL/min,  $\tau_1 = 7.3$  min,  $\tau_2 = 10.0$  min.  $[\alpha]_{\text{D}}^{25}$ :  $-5.0^\circ$  ( $c = 0.800$ ,  $\text{CHCl}_3$ ).

**(S)-1-(2,4-dinitrobenzamido)octan-2-yl benzoate (107a)**: This product was obtained during the optimization of the reaction conditions (Table 4.7). Reaction time: 2.5 h.

Conversion 52%, S = 40.



<sup>1</sup>H-NMR (500 MHz, CDCl<sub>3</sub>): δ 8.77 (d, *J* = 2.1 Hz, 1H), 8.41 (dd, *J* = 8.2 Hz, *J* = 2.1 Hz, 1H), 7.9 (m, 2H), 7.62 (d, *J* = 8.2 Hz, 1H), 7.58 (m, 1H), 7.44 (m, 2H), 6.75 (m, 1H), 5.27 (m, 1H), 3.81 (m, 1H), 3.68 (m, 1H), 1.86-7.72 (m, 2H), 1.49-1.21 (m, 8H), 0.87 (t, *J* = 5Hz, 3H).

<sup>13</sup>C-NMR (CDCl<sub>3</sub>, 125 MHz): δ 167.4, 164.7, 148.3, 146.8,

137.9, 133.6, 130.4, 129.8, 128.7, 128.2, 120.2, 74.2, 44.5, 32.3, 31.7, 29.2, 25.4, 22.7, 14.2.

HRMS (*m/z*) calcd for C<sub>22</sub>H<sub>25</sub>N<sub>3</sub>O<sub>7</sub> [M]<sup>+Na</sup>: 466.1587, found: 466.1585.

[α]<sub>D</sub><sup>25</sup>: +13.9° (*c* = 0.245, CHCl<sub>3</sub>).

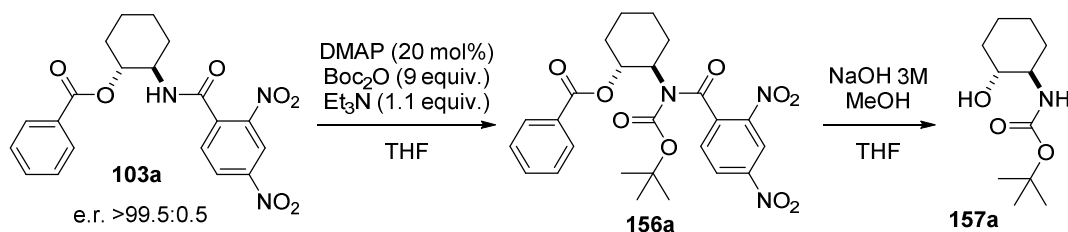
The enantiomeric ratio was determined by HPLC analysis:

**(S)-107a** - Daicel Chiralcel AS-3 column: *n*Hept:*i*PrOH = 70:30, flow rate 1 mL/min, τ<sub>1</sub> = 13.79 min, τ<sub>2</sub> = 20.64 min.

**(S)-1-(2,4-dinitrobenzoyl)-2-hexylaziridine (106a)**: The enantiomeric ratio was determined by HPLC analysis using Daicel Chiralcel AD-3 column: *n*Hept:*i*PrOH = 95:5, flow rate 1 mL/min, τ<sub>1</sub> = 8.88 min, τ<sub>2</sub> = 10.12 min.

## 7.3.4. Determination of the absolute configuration of products

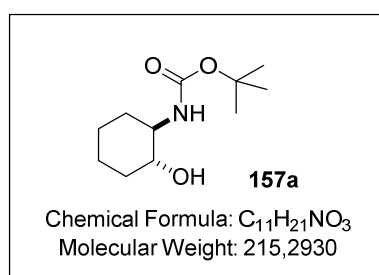
## 7.3.4.1. Determination of the absolute configuration of 103a

Preparation of intermediate **156a**

To a stirred solution of **103a** in THF (50 mg, 0.121 mmol in 0.5 mL of THF) was added  $\text{Boc}_2\text{O}$  (238 mg, 1.09 mmol, 9 equiv.), triethylamine (18  $\mu\text{L}$ , 0.133 mL, 1.1 equiv.) and DMAP (3 mg, 0.0242 mmol, 0.2 equiv.). When the substrate was fully reacted (1 hour, followed by TLC) the mixture was diluted with hexane and directly purified by column chromatography (eluent: mixtures of hexane:MTBE from 20:1 to 8:1). The product was collected and the solvent was evaporated to afford quantitatively the desired intermediate **156a**.

Preparation of compound **157a**

The previously isolated compound was dissolved in a mixture MeOH/THF 1:1 (3 mL) and 1.5 mL of a 3M aqueous solution of NaOH was added and the reaction was stirred for 20 hours at room temperature. Then dichloromethane was added and the organic phase was washed 3 times with a 3 M aqueous solution of NaOH. The organic phase was then dried over  $\text{Na}_2\text{SO}_4$  and the solvent was evaporated. The product was purified by column chromatography (eluent: mixtures hexane:MTBE from 2:1 to 1:2). 21.1 mg of the product **157a** were isolated as white solid (81% yield, 2 steps). The analysis of the optical rotation and the comparison with literature references allowed the assignment of the absolute configuration (*R,R*).<sup>128</sup>

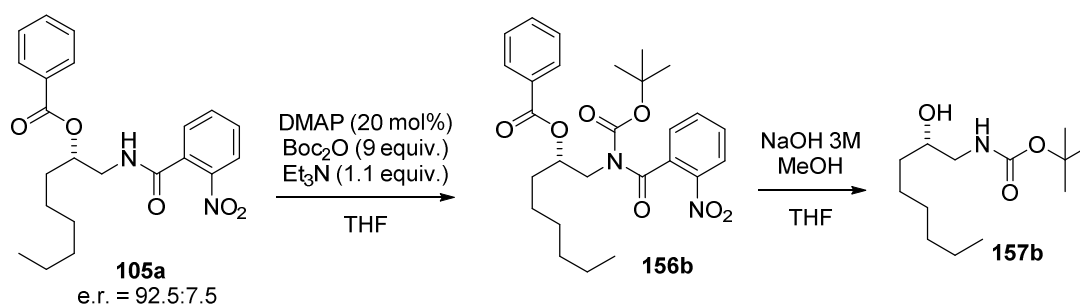


<sup>1</sup>H-NMR (500 MHz,  $\text{CD}_2\text{Cl}_2$ ):  $\delta$  4.80-4.20 (sb, 1H), 3.30-3.00 (m, 3H), 1.95-1.75 (m, 2H), 1.65-1.55 (m, 2H), 1.35 (s, 9H), 1.30-1.00 (m, 4H).

<sup>13</sup>C-NMR (125 MHz,  $\text{CD}_2\text{Cl}_2$ ):  $\delta$  157.5, 79.9, 75.6, 56.9, 34.5, 32.1, 28.4, 25.1, 24.4.

HRMS (*m/z*) calcd for  $\text{C}_{11}\text{H}_{21}\text{NO}_3\text{Na}$  [ $\text{M}$ ]<sup>+Na</sup>: 238.1414, found: 238.1414.

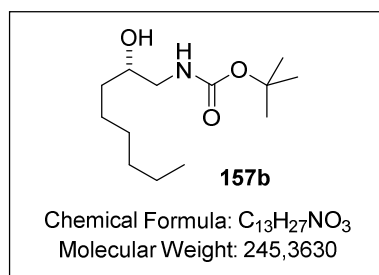
$[\alpha]_D^{25}$ : -26.1° (*c* = 0.850, MeOH).

7.3.4.2. Determination of the absolute configuration of **105a**Preparation of intermediate **156b**

To a stirred solution of **105a** in THF (19 mg, 0.048 mmol in 0.5 mL of THF) was added Boc2O (94.3 mg, 0.432 mmol, 9 equiv.), triethylamine (7.2  $\mu$ L, 0.052 mmol, 1.1 equiv.) and DMAP (1.2 mg, 0.01 mmol, 0.21 equiv.). When the substrate was fully reacted (1 hour, followed by TLC) the mixture was diluted with hexane and directly purified by column chromatography (eluent: mixtures of hexane:MTBE from 20:1 to 1:1). The product was collected and the solvent was evaporated to afford quantitatively the desired intermediate **156b**.

Preparation of compound **157b**

The previously isolated compound was dissolved in a mixture MeOH/THF 1:1 (1 mL) and 0.5 mL of a 2 M aqueous solution of NaOH was added and the reaction was stirred for 20 hours at room temperature. Then dichloromethane was added and the organic phase was washed 3 times with a 2 M aqueous solution of NaOH. The organic phase was then dried over Na2SO4 and the solvent was evaporated. The product was purified by column chromatography (eluent: mixtures hexane:MTBE from 2:1 to 1:1). 6.2 mg of the product **157b** were isolated (53% yield, 2 steps) as colorless oil. The analysis of the optical rotation and the comparison with literature references allowed the assignment of the absolute configuration (*S*).<sup>129</sup>



<sup>1</sup>H-NMR (500 MHz, CDCl3):  $\delta$  5.00-4.65 (sb, 1H), 3.70-3.50 (m, 1H), 3.35-3.10 (m, 1H), 3.00-2.85 (m, 1H), 2.30-2.10 (m, 1H), 1.45-1.15 (m, 10H), 1.38 (s, 9H), 0.85-0.75 (m, 3H).

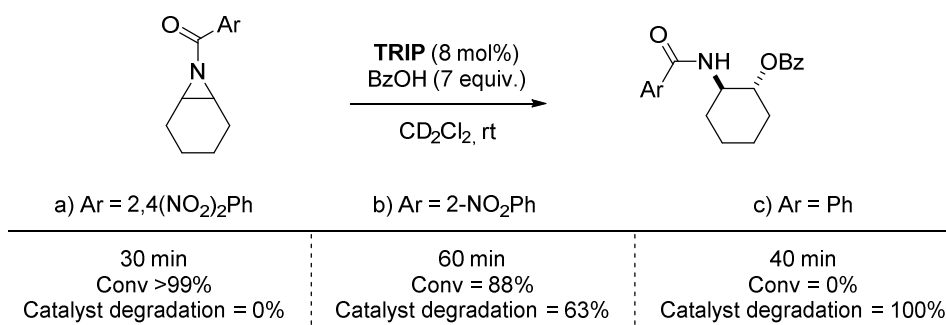
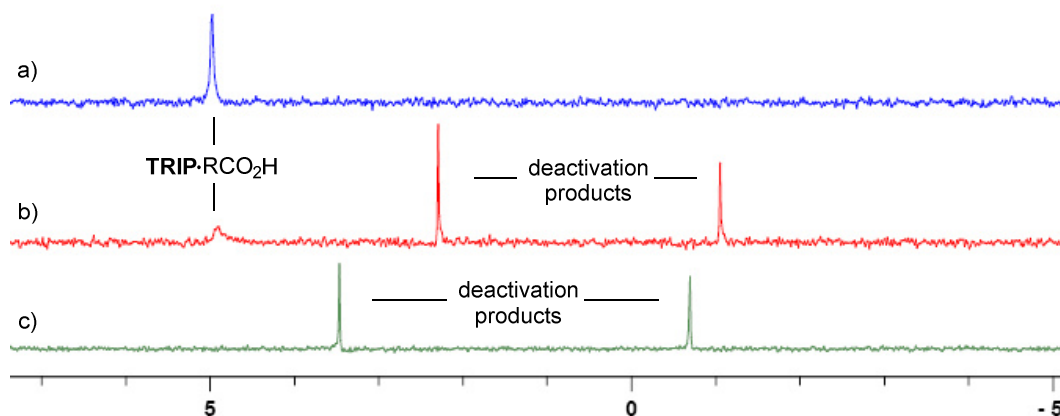
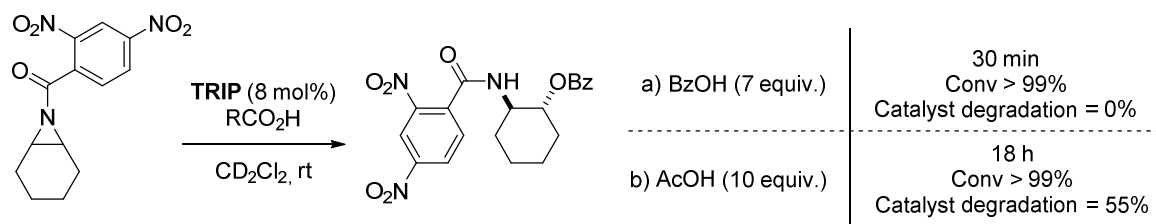
<sup>13</sup>C NMR (125 MHz, CDCl3):  $\delta$  157.3, 79.8, 71.9, 46.9, 35.1, 32.0, 29.5, 28.6, 25.7, 22.8, 14.3.

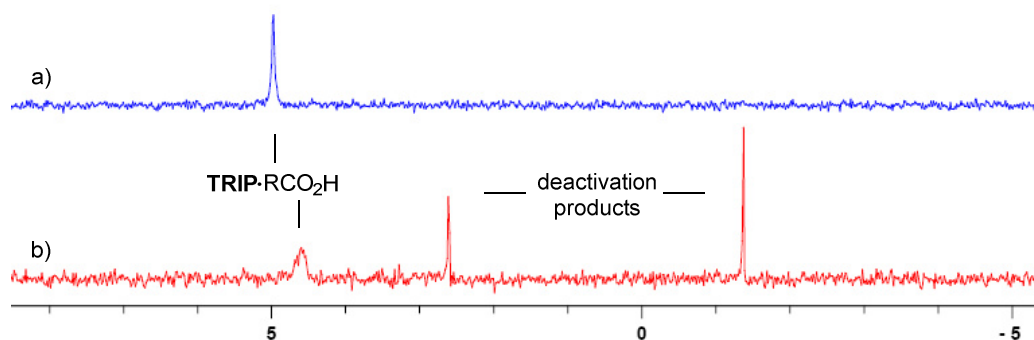
HRMS (*m/z*) calcd for C13H27NO3Na [ $M$ ]<sup>+Na</sup>: 268.1883, found: 268.1883.

$[\alpha]_D^{25}$ : +12.8° (*c* = 0.250, CHCl3).

## 7.3.5. Kinetic studies

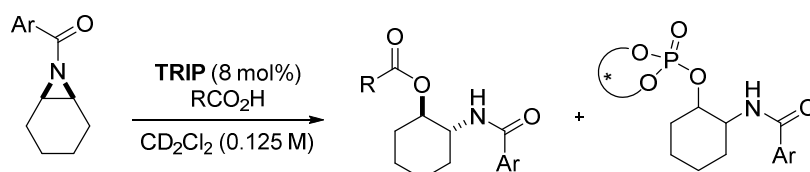
A comparative study for the evaluation of the protecting group of the aziridine and the carboxylic acid nucleophile was set out to investigate the influence of these parameters on the carboxylis reaction and on the degradation of the catalyst. The ring opening reactions were performed in deuterated dichloromethane under optimized conditions and they were analyzed by NMR spectroscopy. The yield of the desired product was determined by  $^1\text{H-NMR}$  while the catalyst alkylation could be measured by  $^{31}\text{P-NMR}$ .

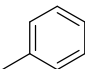
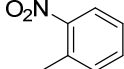
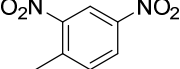
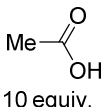
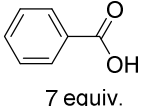
*Various protecting groups – benzoic acid* $^{31}\text{P-NMR}$ *2,4-dinitrobenzoyl protecting group – various carboxylic acids*

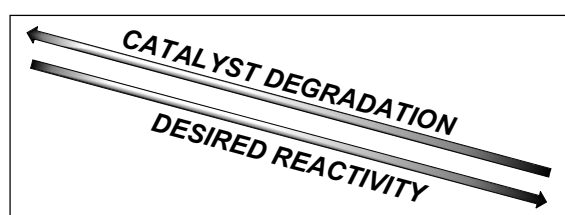
<sup>31</sup>P-NMR

These results highlight that reducing the basicity of the nitrogen protecting group the deactivation pathway is significantly lowered. On the other hand, using benzoic acid results in a double beneficial effect: the catalyst alkylation is lowered and the desired reactivity increased.

The results are summarized in the table below.



	Ar = 		
 10 equiv.	20 min Desired product Yield < 5% Degradation of the catalyst = full	10 min Desired product Yield = 15% Degradation of the catalyst > 95%	10 min Desired product Yield = 35% Degradation of the catalyst = 15%  18 h Desired product Yield > 95% Degradation of the catalyst = 55%
 7 equiv.	40 min Desired product Yield < 5% Degradation of the catalyst = full	5 min Desired product Yield = 48% Degradation of the catalyst = 20%  60 min Desired product Yield = 88% Degradation of the catalyst = 63%	10 min Desired product Yield = 88% Degradation of the catalyst = 0%  30 min Desired product Yield = quant Degradation of the catalyst = 0%

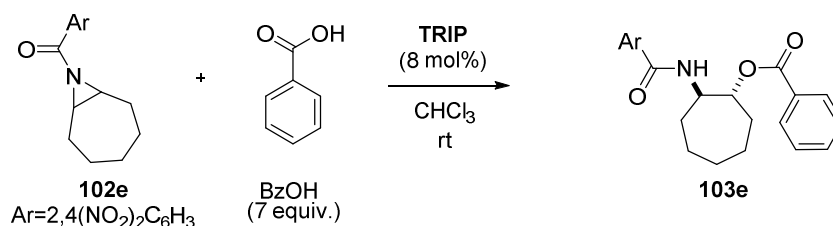


This study suggests the **TRIP** degradation is reduced by preventing the formation of an aziridinium phosphate species and in addition shows the importance of the carboxylic acid molecule in the tuning of the properties of the heterodimeric self-assembly.

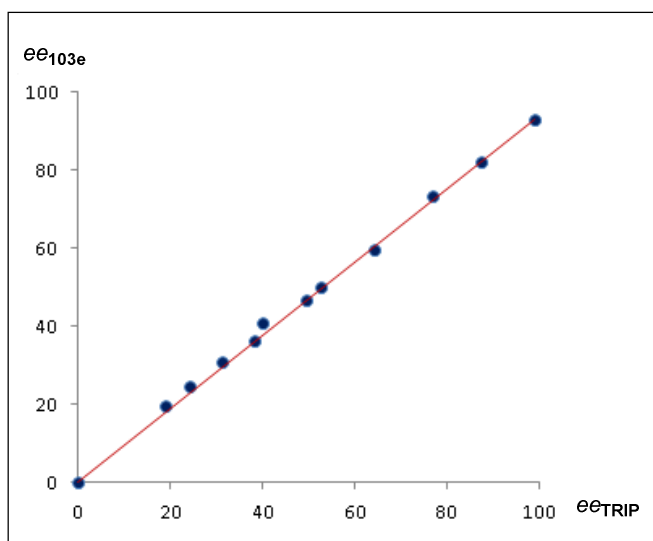
### 7.3.6. Non-linear effect studies

A non-linear effect investigation was performed to gain further insights on the transition state of the stereodiscriminating event.

Eleven reactions for the carboxylolysis of aziridine **102e** were performed, under optimized conditions, in the presence of scalemic mixtures of **TRIP** phosphoric acid as the catalyst. As shown in the table below, the enantioenrichment of the product was found to linearly depend on the catalyst enantiomeric ratio.



entry	$e_{\text{rTRIP}}$	$e_{\text{r103e}}$
1	99.6:0.4	96.5:3.5
2	93.8:6.2	91.2:8.8
3	88.4:11.6	86.7:13.3
4	82.1:17.9	79.8:20.2
5	76.4:23.6	75.0:25.0
6	74.8:25.2	73.4:26.6
7	70.1:29.9	70.4:29.6
8	69.1:30.9	68.2:31.8
9	65.6:34.4	65.5:34.5
10	62.2:37.8	62.4:37.6
11	59.5:40.5	59.8:40.2

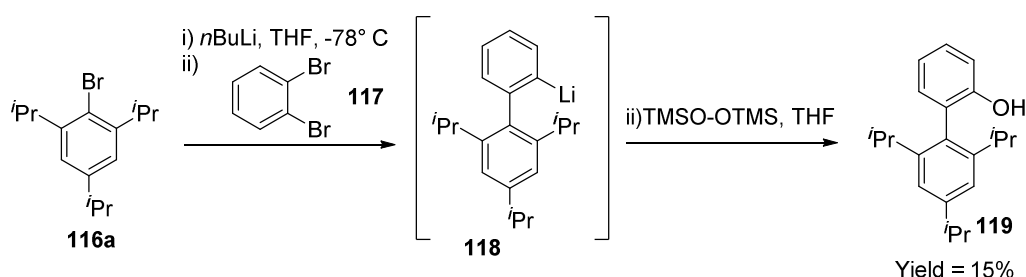


Determined by HPLC on chiral stationary phase

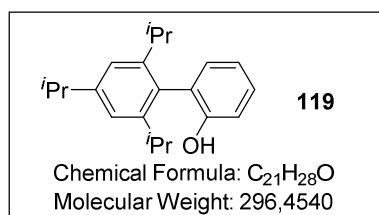
This experiment suggests that a single phosphoric acid molecule is involved in the enantioselective ring opening reaction.

## 7.4. Asymmetric hydrolysis of epoxides in organocatalysis

## 7.4.1. Preparation of catalysts

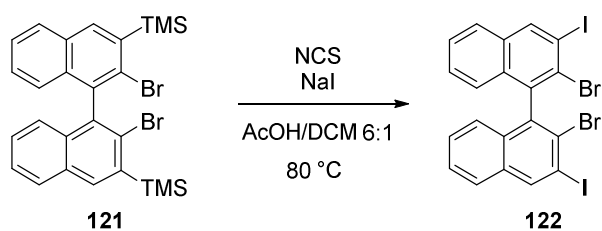
7.4.1.1 Preparation of **114**Model study for the biaryl coupling *via* aryne coupling

In a flame-dried round bottom flask, aryl bromide **116a** (283 mg, 1 mmol, 3 equiv.) was dissolved under Argon atmosphere in anhydrous THF (2 ml) and the temperature was cooled to  $-78^{\circ}\text{C}$ . Next a 2.5 M hexane solution of *n*-butyl lithium was slowly added (1.1 mmol, 3.3 equiv.), then temperature was raised to  $0^{\circ}\text{C}$  and the reaction was stirred for 30 minutes. After having lowered again the temperature to  $-78^{\circ}\text{C}$  a solution of dibromobenzene **117** (78 mg, 0.33 mmol, 1 equiv.) in THF (2 ml) was added dropwise and the mixture was left 20 minutes before the dropwise addition of a THF solution (1 ml) of TMS-peroxide (71.4 mg, 0.4 mmol, 1.2 equiv.). The stirred reaction was allowed to warm up to room temperature and after 12 hours a solution of MeOH:HCl<sub>conc</sub> (9:1, 10 ml) was added. MTBE was added and the organic phase was washed twice with water and then dried over Na<sub>2</sub>SO<sub>4</sub>. The organic solvent was evaporated in vacuo and next purification of the mixture was performed by flash chromatography on silica gel (eluent: hexane/DCM 4:1). The desired product **119** was isolated in 15% yield (14.5 mg, 0.049 mmol).

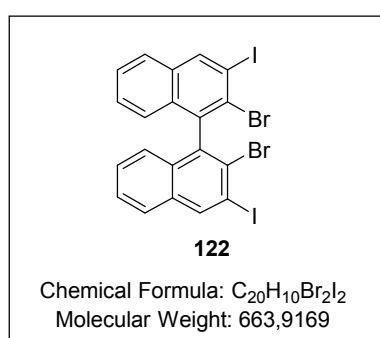
**2',4',6'-triisopropyl-[1,1'-biphenyl]-2-ol (119) –**

<sup>1</sup>H-NMR (500 MHz, CD<sub>2</sub>Cl<sub>2</sub>):  $\delta$  7.22-7.16 (m, 1H), 7.04 (s, 2H), 6.99-6.92 (m, 1H), 6.90-6.82 (m, 2H), 4.66 (s, 1H), 2.86 (sept,  $J = 7.0$  Hz, 1H), 2.48 (sept,  $J = 7.0$  Hz, 2H), 1.20 (d,  $J = 7.0$  Hz, 6H), 1.02 (d,  $J = 7.0$  Hz, 6H), 0.97 (d,  $J = 7.0$  Hz, 6H).



Synthesis of intermediate **122**

A round bottom flask, equipped with a reflux condenser, was charged with a solution of compound **121**<sup>141</sup> (2.250 g, 4.06 mmol, 1 equiv.) in 78 mL of a mixture AcOH/DCM 6:1. Next NCS (2.160 g, 4 equiv.) and NaI (2.435 g, 4 equiv.) were added at once and the resulting solution was stirred at 80 °C for 12 h (monitored by TLC to ensure full consumption of starting material. Eluent: hexane). Then DCM was added, the organic phase was washed with water, dried over Na<sub>2</sub>SO<sub>4</sub> and the solvent was removed in vacuo. Column chromatography (eluent: hexane/DCM 3:2) afforded the desired compound in 87% yield.

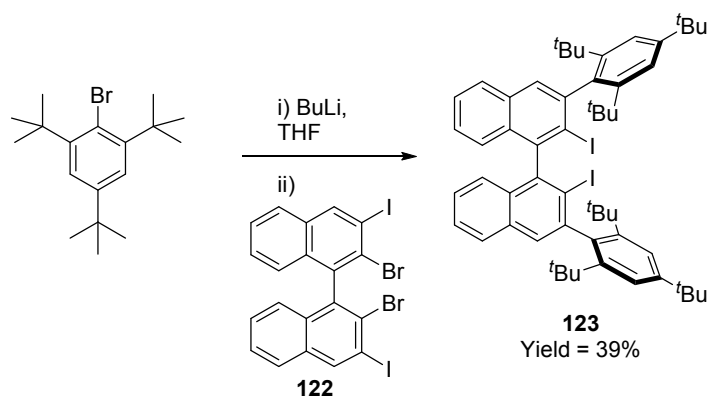
2,2'-dibromo-3,3'-diiodo-1,1'-binaphthalene (**122**) –

<sup>1</sup>H-NMR (500 MHz, CD<sub>2</sub>Cl<sub>2</sub>): δ 8.57 (s, 2H), 7.77 (d, *J* = 8.1 Hz, 2H), 7.45 (t, *J* = 8.1 Hz, 2H), 7.25 (t, *J* = 8.1 Hz, 2H), 6.89 (d, *J* = 8.1 Hz, 2H).

<sup>13</sup>C-NMR (125 MHz, CD<sub>2</sub>Cl<sub>2</sub>) [peaks overlapping]: δ 140.6, 139.9, 134.1, 132.3, 128.6, 128.5, 127.7, 126.1, 99.1.

HRMS (*m/z*) calcd for C<sub>20</sub>H<sub>10</sub>Br<sub>2</sub>I<sub>2</sub> [M]: 661.7239, found:

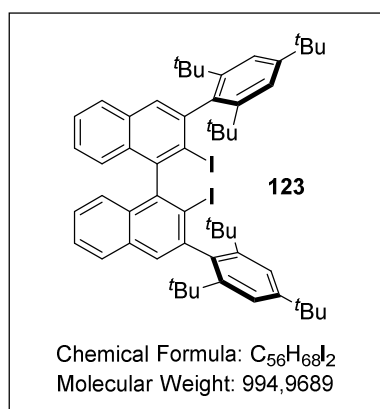
661.7243.

Synthesis of intermediate **123**

A flame-dried round bottom two neck flask was charged with a solution of 2-bromo-1,3,5-tri-*tert*-butylbenzene (2 g, 6.15 mmol, 5 equiv.) in dry THF (10.5 mL) under argon atmosphere.

The solution was cooled down to  $-78\text{ }^{\circ}\text{C}$  and BuLi (2.5 M in hexane, 2.45 mmol, 5.2 equiv.) was added dropwise. The solution was then stirred at  $0\text{ }^{\circ}\text{C}$  for 1h. Next the reaction was cooled at  $-78\text{ }^{\circ}\text{C}$  and a solution of intermediate **2** in THF (814 mg, 1.23 mmol, 1 equiv.) was added dropwise. [The color of the reaction turned orange and precipitation was observed (vigorous stirring is required)]. Next the reaction was left overnight allowing to reach rt, then DCM was added and the organic phase was washed with water, dried over  $\text{Na}_2\text{SO}_4$  and the solvent was removed in vacuo. Column chromatography on silica gel (eluent: hexane/DCM 10:1) afforded the desired compound in 39% yield.

### 2,2'-diiodo-3,3'-bis(2,4,6-tri-tert-butylphenyl)-1,1'-binaphthalene (**123**) –



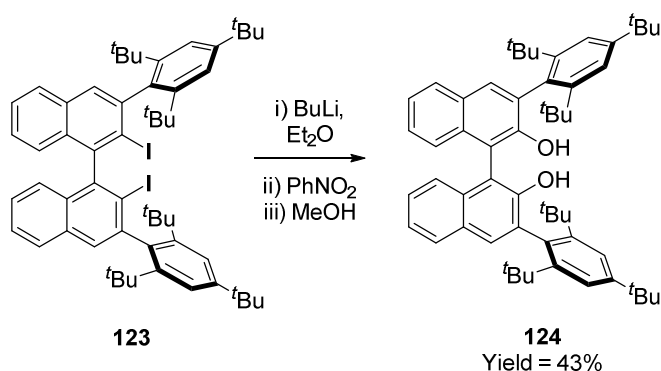
$^1\text{H-NMR}$  (500 MHz,  $\text{CD}_2\text{Cl}_2$ ):  $\delta$  7.99 (s, 2H), 7.83 (d, 2H), 7.52-7.40 (m, 6H), 7.18 (t, 2H), 7.05 (d, 2H), 1.29 (s, 18H), 1.14 (s, 36H).

$^{13}\text{C-NMR}$  (125 MHz,  $\text{CD}_2\text{Cl}_2$ ):  $\delta$  149.5, 147.8, 147.5, 146.1, 145.8, 140.2, 132.6, 132.3, 131.8, 128.7, 127.2, 127.1, 127.0, 124.1, 123.9, 114.5, 38.9, 38.8, 35.2, 35.0, 34.1, 31.6.

**HRMS** ( $m/z$ ) calcd for  $\text{C}_{56}\text{H}_{68}\text{I}_2$  [ $\text{M}$ ]: 994.3410, found:

994.3405.

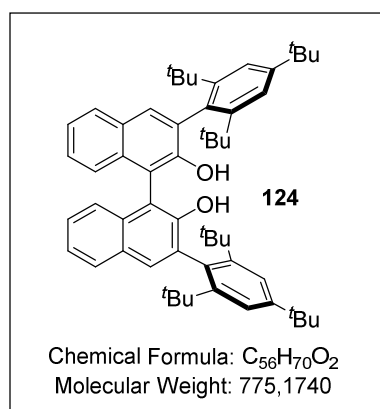
### Synthesis of intermediate **124**



In a flame-dried round bottom two neck flask, a 0.007 M solution of **123** in dry diethyl ether was added under argon atmosphere. Then the stirred solution was cooled down to  $-78\text{ }^{\circ}\text{C}$ , *n*-BuLi (2.5 M in hexane, 4 equiv.) was added dropwise and the reaction was stirred for 1h. Then the temperature was cooled down to  $-95\text{ }^{\circ}\text{C}$  and a 2.8 M solution of nitrobenzene in

diethyl ether was added dropwise. After 30 min methanol was added (1:1 with the reaction solvent), the temperature was raised to rt and stirred for 2 additional hours. DCM was added and the organic phase was washed with water, dried over  $\text{Na}_2\text{SO}_4$  and the solvent was removed in vacuo. Two purifications by column chromatography were needed (first eluent: pentane/MTBE, second eluent: mixtures hexane/DCM) to obtain the desired compound **124**.

**3,3'-bis(2,4,6-tri-tert-butylphenyl)-[1,1'-binaphthalene]-2,2'-diol (**124**)** – The reaction was performed on 0.25 mmol scale and the product was isolated in 43% yield.

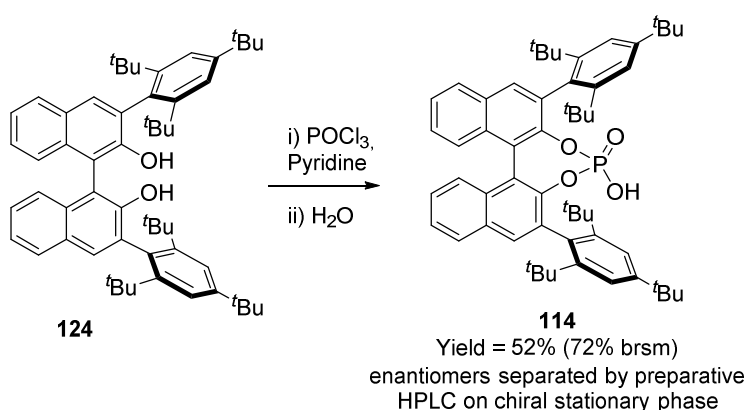


$^1\text{H-NMR}$  (500 MHz,  $\text{CD}_2\text{Cl}_2$ ):  $\delta$  7.82-7.75 (m, 4H), 7.58-7.48 (m, 4H), 7.29 (t, 2H), 7.20 (t, 2H), 7.10 (d, 2H), 4.89 (s, 2H), 1.29 (s, 18H), 1.14 (s, 18H), 1.05 (s, 18H).

$^{13}\text{C-NMR}$  (125 MHz,  $\text{CD}_2\text{Cl}_2$ ):  $\delta$  152.8, 149.5, 149.5, 134.1, 133.5, 132.4, 130.4, 128.3, 127.8, 126.6, 124.7, 123.7, 123.3, 123.3, 113.1, 38.1, 38.0, 35.1, 33.1, 33.0, 31.4.

**HRMS** ( $m/z$ ) calcd for  $\text{C}_{56}\text{H}_{70}\text{O}_2$   $[\text{M}]^{+\text{Na}}$ : 797.5268, found: 797.5269.

### Synthesis of **114**

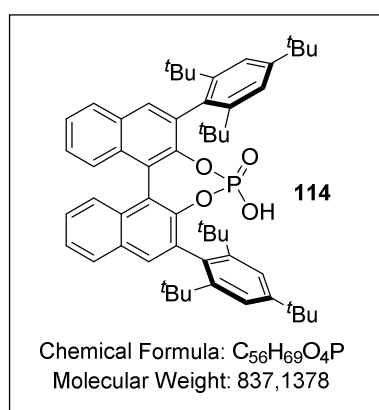


In a flame-dried round bottom two neck flask, equipped with a reflux condenser, a 0.025 M solution of the binol intermediate **124** in dry pyridine was added under argon atmosphere. Then the stirred solution was cooled down to  $0^\circ\text{C}$  and 10 equiv. of  $\text{POCl}_3$  were added. The reaction was then heated up to  $95^\circ\text{C}$  and 10 equiv. of  $\text{POCl}_3$  were added every 24 h until full consumption of starting material (TLC eluent: hexane/DCM 1:1). Then it was cooled to  $0^\circ\text{C}$  and 2.5 mL of water were added dropwise [careful: exothermic reaction]. Then the

temperature was raised to 100° C. After 3-4 hours the reaction was cooled to room temperature, DCM was added and the organic phase was washed with a 3 M HCl<sub>aq</sub> solution, water and brine. Then the organic layer was dried over anhydrous Na<sub>2</sub>SO<sub>4</sub> and the solvent evaporated in vacuo. Purification was accomplished by column chromatography (eluent: mixtures hexane:ethyl acetate). The isolated compound was then dissolved again in DCM and subjected to an acidic wash with a 6 M HCl<sub>aq</sub> solution to remove salt impurities and deliver the desired phosphoric acid catalysts **114**.

The separation of the enantiomers was performed *via* preparative HPLC on chiral stationary phase (Chiralpak QN-AX, 5 μm, 150x29 mm; eluent: Methanol/ (0.1 M NH<sub>4</sub>OAc)<sub>aq</sub>: 80:20)

**3,3'-bis(2,4,6-triterzbutyl-phenyl)-BINOL-derived phosphoric acid (114)** – The reaction was performed on 0.103 mmol scale and the product was isolated in 52% yield (72% brsm).



<sup>1</sup>H-NMR (500 MHz, CD<sub>2</sub>Cl<sub>2</sub>): δ 7.83 (s, 2H), 7.74 (d, *J* = 8.2 Hz, 2H), 7.40-7.33 (m, 6H), 7.09 (t, *J* = 8.2 Hz, 2H), 6.87 (d, *J* = 8.2 Hz, 2H), 6.32 (bs, 1H), 1.21 (s, 18H), 0.97 (s, 18H), 0.88 (s, 18H).

<sup>13</sup>C-NMR (125 MHz, CD<sub>2</sub>Cl<sub>2</sub>) [overlapping signals]: δ 149.3, 149.0, 148.7, 148.5, 148.4, 135.7, 135.7, 135.3, 133.2, 130.4, 130.3, 128.4, 127.6, 126.4, 125.9, 124.3, 123.5, 121.5, 38.9,

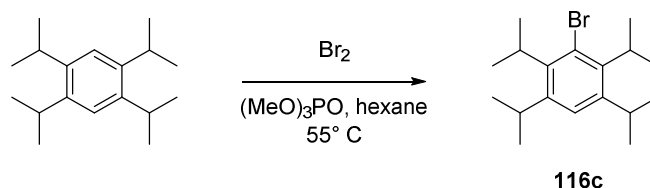
38.5, 35.1, 34.3, 33.6, 31.6.

<sup>31</sup>P NMR (202 MHz, CD<sub>2</sub>Cl<sub>2</sub>): δ -0.02 (s).

HRMS (*m/z*) calcd for C<sub>56</sub>H<sub>69</sub>O<sub>4</sub>P [M]<sup>-1</sup>: 835.4861, found: 835.4861.

#### 7.4.1.2. Synthesis of catalysts 115a-c and 139

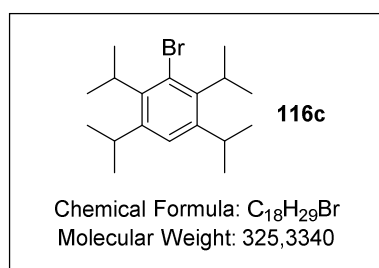
##### Synthesis of 116c



A flame-dried round bottom two neck flask, equipped with a reflux condenser was charged with a mixture of 1,2,4,5-tetraisopropyl benzene (1 g, 4 mmol), 8 ml of trimethyl phosphate

and 16 mL of hexane under argon atmosphere. The apparatus was then covered with aluminum foil to prevent light irradiation and a solution of Br<sub>2</sub> (1 mL, 20 mmol, 5 equiv.) in 8 mL of trimethyl phosphate was added dropwise at 0° C. Then the temperature was raised to 55° C and the reaction was stirred until full consumption of the starting material (TLC eluent: hexane). Next the reaction was cooled to room temperature and hexane and water were added. The mixture was washed twice with 1 M NaOH<sub>aq</sub> and twice with Na<sub>2</sub>S<sub>2</sub>O<sub>3</sub> to quench the unreacted bromine. The organic phase was then dried over Na<sub>2</sub>SO<sub>4</sub> and the solvent was removed in vacuo. The compound was purified by column chromatography on silica gel (eluent: hexane) and then crystallized in acetonitrile to yield the desired bromide **116c** as white solid in 75% yield.

**3-bromo 1,2,4,5 tetraisopropyl benzene (116c)** – Due to the presence of rotamers the spectra present a complicated pattern.



<sup>1</sup>H-NMR (500 MHz, CDCl<sub>3</sub>): δ 7.11 (s, 1H), 4.30-3.10 (4 multiplets due to rotamers, 4H), 1.55-1.18 (3 multiplets due to rotamers, 24H).

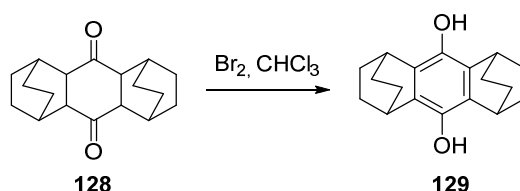
<sup>13</sup>C-NMR (125 MHz, CDCl<sub>3</sub>): δ 147.2, 146.8, 145.8, 142.2, 141.2, 129.4, 125.6, 123.7, 35.4, 33.5, 30.5, 29.7, 29.5, 24.9,

24.3, 22.0, 20.7. (peaks of the major rotamer are in *italic*).

HRMS (*m/z*) calcd for C<sub>18</sub>H<sub>29</sub>Br [M]: 324.1453, found: 324.1450.

### Synthesis of 116d

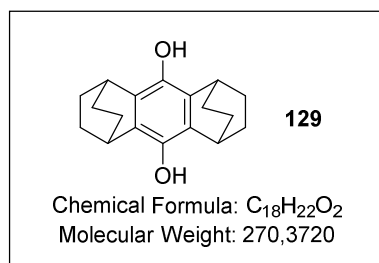
### Synthesis of hydroquinone 129



In a flame-dried round bottom flask equipped with a pressure equalizing addition funnel, dodecahydro-1,4:5,8-diethanoanthracene-9,10-dione **128** (12.60 g, 46.32 mmol), prepared following reported procedures,<sup>145</sup> was dissolved in 46 mL of chloroform. Then a solution of bromine (7.44 g, 46.5 mmol, 1.004 equiv.) in chloroform was added dropwise over a period

of 30 min at room temperature while argon was bubbled through the mixture to remove HBr. The resulted mixture was stirred for one additional hour and then cooled in an ice-acetone bath. The precipitate was filtered in vacuo and washed with cold chloroform to afford the desired hydroquinone **129** as a white solid in 68% yield.

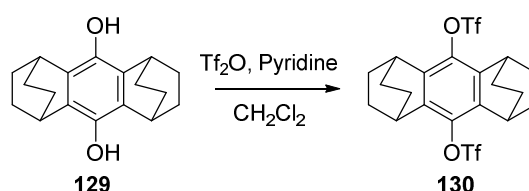
**octahydro-1,4:5,8-diethanoanthracene-9,10-diol (129) –**



<sup>1</sup>H-NMR (500 MHz, THF<sub>d8</sub>): δ 3.37 (bs, 4H), 1.69 (d, *J* = 7.2 Hz, 8H), 1.29 (d, *J* = 7.2 Hz, 8H)

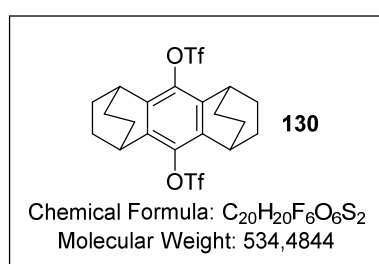
<sup>13</sup>C-NMR (125 MHz, THF<sub>d8</sub>): δ 139.7, 128.0, 27.2, 26.7

**Synthesis of bis-triflate 130**



In a flame-dried round bottom flask hydroquinone **129** (8.7 g, 31.5 mmol) was dissolved in 100 mL of dichloromethane. Argon was bubbled through the solution to remove oxygen. Then pyridine was added (7.46 g, 94.44 mmol, 3 equiv.) and the reaction was cooled at -10° C using an ice-acetone bath. To this stirred suspension was added dropwise a solution of Tf<sub>2</sub>O (21.33 g, 75.6 mmol, 2.4 equiv.) in 50 mL of dry chloroform. The reaction was allowed to reach room temperature and stirred for 12 h. Next the mixture was washed with water and 10% aqueous HCl and the desired compound was filtered off from the organic phase and isolated without further purification in 76% yield.

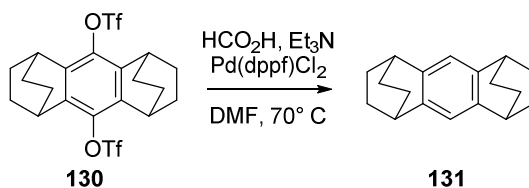
**octahydro-1,4:5,8-diethanoanthracene-9,10-diyl bis(trifluoromethanesulfonate) (130) –**



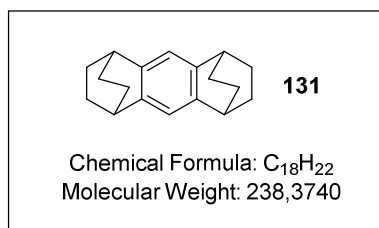
<sup>1</sup>H-NMR (500 MHz, CDCl<sub>3</sub>): δ 3.40 (bs, 4H), 1.90-1.70 (m, 8H), 1.50-1.35 (m, 8H).

<sup>13</sup>C-NMR (125 MHz, CDCl<sub>3</sub>): δ 137.7, 136.3, 118.8 (q, *J* = 320 Hz), 28.8, 25.1,

HRMS (*m/z*) calcd for C<sub>20</sub>H<sub>20</sub>O<sub>6</sub>F<sub>6</sub>S<sub>2</sub>Na [M]<sup>+Na</sup>: 557.0498, found: 557.0496.

Synthesis of intermediate **113**

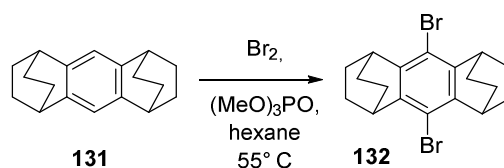
A flame-dried round bottom flask was charged with bis-triflate **130** (9.7 g, 18.2 mmol), 100 mL of DMF, 11 mL of formic acid (13.36 g, 290.4 mmol, 16 equiv.), 57 mL of dry triethylamine (44.08 g, 435.6 mmol, 24 equiv.) and 741 mg of Pd(dppf)Cl<sub>2</sub> (0.9 mmol, 5 mol%). The reaction was stirred at 70° C for 48 h, then brine was added. Next the precipitate was filtered off and washed with water and cold ethyl acetate. Purification was then accomplished by a second filtration on silica gel using toluene as the eluent. The desired compound was isolated as white solid in 72% yield.

octahydro-1,4:5,8-diethanoanthracene (**131**) –

<sup>1</sup>H-NMR (500 MHz, CDCl<sub>3</sub>): δ 6.89 (s, 2H), 2.94 (bs, 4H), 1.80-1.66 (m, 8H), 1.45-1.35 (m, 8H).

<sup>13</sup>C-NMR (125 MHz, CDCl<sub>3</sub>): δ 141.5, 119.2, 34.2, 26.9.

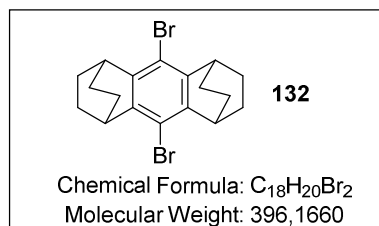
HRMS (*m/z*) calcd for C<sub>18</sub>H<sub>22</sub> [M]: 238.1722, found: 238.1718.

Synthesis of bis-bromide **132**

A flame-dried round bottom two neck flask, equipped with a reflux condenser was charged with a mixture of octahydro-1,4:5,8-diethanoanthracene **131** (2.5 g, 10.5 mmol), 20 mL of trimethyl phosphate and 100 mL of hexane under argon atmosphere. The apparatus was then covered with aluminum paper to prevent light irradiation and a solution of Br<sub>2</sub> (2.7 mL, 52.5 mmol, 5 equiv.) in 20 mL of trimethyl phosphate was added dropwise at 0° C. Then the temperature was raised to 55° C and the reaction was stirred until full consumption of the starting material (TLC eluent: hexane). Next the reaction was cooled to room temperature

and hexane and water were added. The mixture was washed twice with 1 M NaOH<sub>aq</sub> and twice with Na<sub>2</sub>S<sub>2</sub>O<sub>3</sub> to quench the unreacted bromine. The organic phase was then dried over Na<sub>2</sub>SO<sub>4</sub> and the solvent was removed in vacuo. The compound was purified by column chromatography on silica gel (eluent: hexane) to yield the desired bis-bromide **132** as white solid in 92% yield.

### 9,10-dibromo-octahydro-1,4:5,8-diethanoanthracene (**132**) –

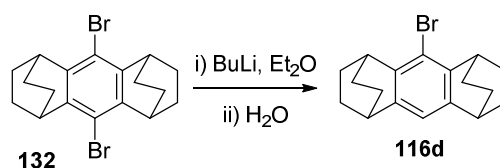


<sup>1</sup>H-NMR (500 MHz, CDCl<sub>3</sub>): δ 3.62 (bs, 4H), 1.84-1.75 (m, 8H), 1.44-1.30 (m, 8H).

<sup>13</sup>C-NMR (125 MHz, CDCl<sub>3</sub>): δ 114.9, 116.9, 34.1, 25.4.

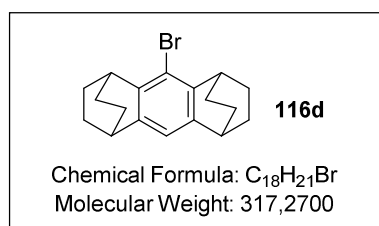
HRMS (*m/z*) calcd for C<sub>18</sub>H<sub>20</sub>Br<sub>2</sub> [M]: 393.9932, found: 393.9932.

### Synthesis of arylbromide **116d**



A flame-dried round bottom flask was charged with a mixture of bis-bromide **132** (1.7 g, 4.3 mmol) and 100 mL of dry diethyl ether under argon atmosphere. Then a 2.5 M solution of BuLi in hexane (1.72 mL, 4.3 mmol, 1 equiv.) was added dropwise at 0° C and the stirred mixture was allowed to reach room temperature. After 2 h, 20 mL of water were added to the suspension. The organic phase was separated, dried over Na<sub>2</sub>SO<sub>4</sub> and concentrated in vacuo to afford compound **116d** as a white solid in 97% yield.

### 9-bromo-octahydro-1,4:5,8-diethanoanthracene (**116d**) –



<sup>1</sup>H-NMR (500 MHz, CDCl<sub>3</sub>): δ 6.85 (m, 1H), 3.54 (m, 2H), 2.96 (s, 2H), 1.80-1.70 (m, 8H), 1.50-1.30 (m, 8H).

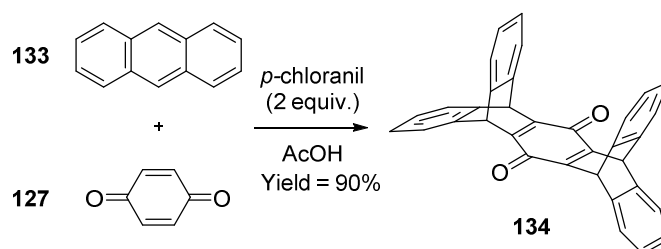
<sup>13</sup>C-NMR (125 MHz, CDCl<sub>3</sub>): δ 143.3, 139.8, 118.6, 117.3, 34.6, 33.1, 26.1, 25.6.

HRMS (*m/z*) calcd for C<sub>18</sub>H<sub>21</sub>Br [M]: 316.0827, found: 316.0826.

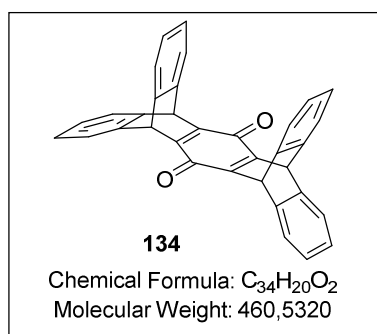


## Synthesis of 116e

## Synthesis of quinone 134



In a round bottom flask equipped with a reflux condenser, a mixture of anthracene **133** (7.13 g, 40 mmol, 2 equiv.), *p*-benzoquinone (2.16 g, 20 mmol, 1 equiv.) and *p*-chloranil (9.84 g, 40 mmol, 2 equiv.) were refluxed in acetic acid (240 ml) for 16 h. The resulting mixture was cooled at room temperature and the precipitate was filtered, washed with cold ether and dried under *vacuo* to give 8.34 g of the desired quinone **134** as a yellow solid (90% yield).

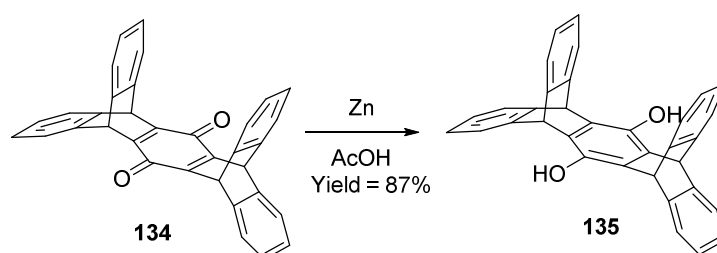
tetrahydro-5,14:7,12-bis([1,2]benzeno)pentacene-6,13-dione (**134**) –

<sup>1</sup>H-NMR (500 MHz, CDCl<sub>3</sub>): δ 7.35–7.25 (m, 8H), 6.95–6.85 (m, 8H), 5.68 (s, 4H).

<sup>13</sup>C-NMR (125 MHz, CDCl<sub>3</sub>): δ 180.0, 161.0, 143.6, 125.5, 124.3, 47.4.

HRMS (*m/z*) calcd for C<sub>34</sub>H<sub>20</sub>O<sub>2</sub> [M]<sup>+Na</sup>: 460.1463, found: 460.1462.

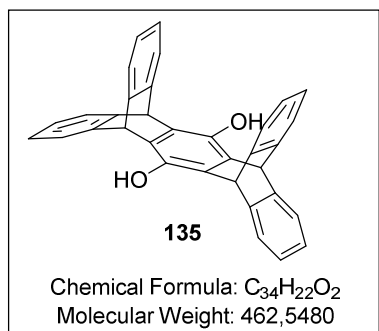
## Synthesis of hydroquinone 135



In a round bottom flask equipped with a reflux condenser, a mixture of quinone **134** (8.34 g, 17.95 mmol, 1 equiv.) and zinc powder (7.05 g, 107.7 mmol, 6 equiv.) was refluxed in acetic acid (50 ml). After 5 h the hot mixture was filtered, then the acetic acid solution was cooled down in an ice-aceton to induce the precipitation of hydroquinone **135**. The white solid was filtered off and dried under *vacuo*. The desired product was obtained in 94% yield (7.79 g)

and fast characterization *via* NMR was performed in deuterated chloroform, despite the tendency to re-oxidize into the starting material.

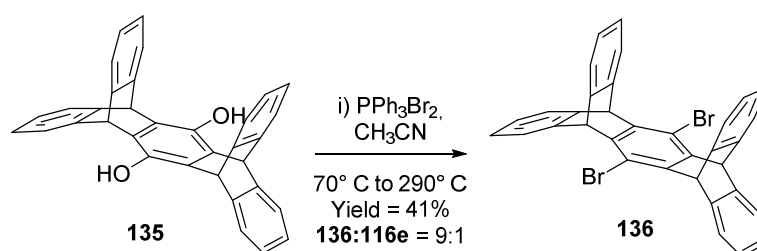
**tetrahydro-5,14:7,12-bis([1,2]benzeno)pentacene-6,13-diol (**135**) –**



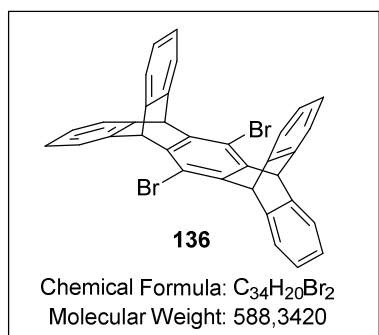
<sup>1</sup>H-NMR (500 MHz, CDCl<sub>3</sub>): δ 7.38-7.30 (m, 8H), 7.00-6.92 (m, 8H), 5.65 (s, 4H).

<sup>13</sup>C-NMR (125 MHz, CDCl<sub>3</sub>): δ 145.1, 139.8, 130.9, 125.2, 123.6, 47.6.

**Synthesis of dibromo intermediate **136****

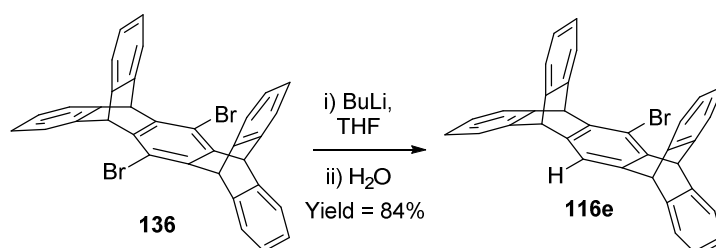


A flame-dried Schlenk-flask was purged with a suspension of hydroquinone **135** (2.0 g, 4.32 mmol, 1 equiv.) in anhydrous acetonitrile (7 ml) under argon atmosphere and next triphenylphosphine dibromide (4.56 g, 10.81 mmol, 2.5 equiv.) was added at 0° C. The temperature was raised to 30° C and the mixture was vigorously stirred for 30 min and then the solvent was distilled out at 70° C under reduced pressure. The Schlenk-flask was then equipped with an exhaust connected to a saturated sodium bicarbonate solution and a continuous Argon flow was provided before heating the solid mixture to 290° C. A strong evolution of HBr was observed for approximately 2 h, then the reaction was cooled to room temperature, DCM was added and the organic mixture was washed with brine and then dried over sodium sulfate. Evaporation of the solvent in *vacuo* and column chromatography was performed (eluent: hexane/DCM 10:1) to isolate a 9:1 mixture of **136:116e**. A final crystallization in THF/hexane gave the desired product (41% yield).

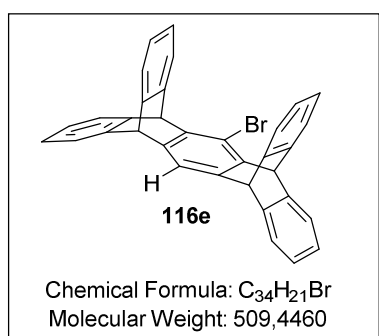
**6,13-dibromo-tetrahydro-5,14:7,12-bis([1,2]benzeno)pentacene (136) –**

<sup>1</sup>H-NMR (500 MHz, CDCl<sub>3</sub>): δ 7.38-7.32 (m, 8H), 6.98-6.90 (m, 8H), 5.85 (s, 4H).

<sup>13</sup>C-NMR (125 MHz, CDCl<sub>3</sub>): δ 144.3, 144.0, 125.6, 124.0, 116.0, 53.9.

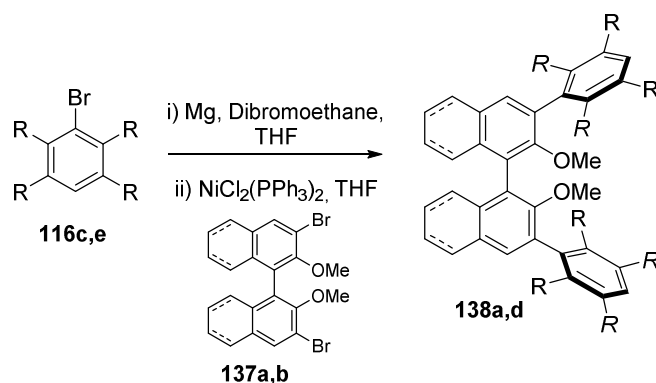
**Synthesis of arylbromide 116e**

In a flame-dried round bottom two neck flask, dibromide **136** (1.025 g, 1.75 mmol, 1 equiv.) was dissolved in anhydrous THF (120 ml) and cooled to 0° C. Then a 2.5 M hexane solution of *n*-BuLi was added dropwise, the temperature was allowed to reach room temperature and the and stirred for 1 h (milky suspension observed). Then water was added (5 ml) and the resulting clear solution was diluted with DCM. The organic phase was washed with brine and the solvent evaporated in *vacuo*. Purification was performed by flash chromatography on silica gel (eluent: mixtures hexane/DCM) and the desired product **116e** was be obtained in 84% yield.

**6-bromo-tetrahydro-5,14:7,12-bis([1,2]benzeno)pentacene (116e) –**

<sup>1</sup>H-NMR (500 MHz, CDCl<sub>3</sub>): δ 7.32-7.26 (m, 5H), 7.25-7.20 (m, 4H), 6.92-6.80 (m, 8H), 5.77 (s, 2H), 5.23 (s, 2H).

<sup>13</sup>C-NMR (125 MHz, CDCl<sub>3</sub>): [overlapping signals] δ 145.2, 144.8, 144.5, 141.8, 125.4, 125.3, 124.0, 123.5, 118.8, 54.3, 53.3.

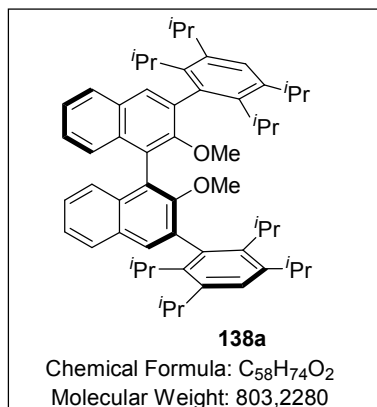
Catalysts **115a-c** and **139**Biaryl synthesis *via Kumada cross-coupling reaction*

A flame-dried round bottom two neck flask, equipped with a reflux condenser, was charged with activated Mg turnings (10 equiv.) under argon atmosphere. A 0.315 M solution of the desired aryl bromide **116a-c** (3.3 equiv.) in dry THF was prepared and 0.5 mL of it were immediately added in the reaction flask. Then 2 drops of dibromomethane were added with a syringe to the mixture and the rest of the solution was slowly added while carefully heating with a heat gun to facilitate the reaction. The mixture was stirred at reflux temperature under argon atmosphere for 2.5-4 hours and was monitored by TLC (eluent: hexane).

In a second flame-dried round bottom two neck flask, equipped with a reflux condenser, a 0.1 M solution of (*S*)-3,3'-dibromo-2,2'-dimethoxy-1,1'-binaphthalene **137a** (for catalysts **115a-c**) or the corresponding (*R*)-tetrahydrogenated compound **137b** (for catalyst **139**) in dry THF was prepared and then  $\text{NiCl}_2(\text{PPh}_3)_2$  was added under argon atmosphere. The warm solution (ca. 50° C) of the Grignard reagent prepared in the other flask was then added *via* syringe to this second flask and the reaction was stirred at reflux temperature under argon atmosphere for 12 h. Next the reaction mixture was cooled to room temperature and diluted with MTBE. The resulting solution was washed with water and brine and the organic phase was dried over anhydrous  $\text{Na}_2\text{SO}_4$ . The solvent was removed in vacuo and the product was purified by column chromatography (eluent: mixtures hexanes/DCM).

**138a** – Reaction performed on 0.29 mmol scale (49% yield).

**<sup>1</sup>H-NMR** (500 MHz, CD<sub>2</sub>Cl<sub>2</sub>): δ 7.89 (d, *J* = 8.3 Hz, 2H), 7.67 (s, 2H), 7.50-7.38 (cm, 2H), 7.28-7.35 (m, 6H), 3.58-3.40 (cm, 4H), 3.23 (s, 6H), 3.18-2.90 (m, 4H), 1.40-1.10 (m, 48H).

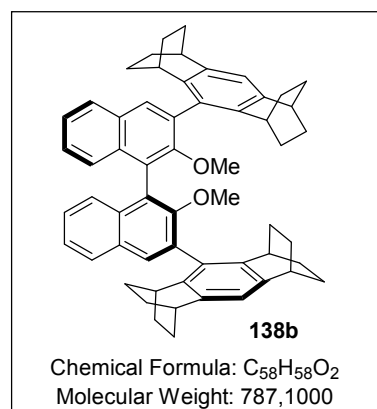


**<sup>13</sup>C-NMR** (125 MHz, CD<sub>2</sub>Cl<sub>2</sub>) [overlapping signals]: δ 155.1, 145.7, 140.8, 138.1, 137.7, 134.1, 130.7, 130.0, 128.3, 126.3, 125.8, 125.0, 124.2, 60.0, 32.4, 32.3, 29.7, 29.6, 25.0, 25.0, 24.9, 24.8, 22.8, 22.7, 22.6, 22.5.

**HRMS** (*m/z*) calcd for C<sub>58</sub>H<sub>74</sub>O<sub>2</sub>Na [M]<sup>+Na</sup>: 825.5581, found: 825.5586.

**138b** – Reaction performed on 0.81 mmol scale (91% yield).

**<sup>1</sup>H-NMR** (500 MHz, CD<sub>2</sub>Cl<sub>2</sub>): δ 7.95 (d, *J* = 8.3 Hz, 2H), 7.82 (s, 2H), 7.50-7.40 (m, 2H), 7.40-7.28 (m, 4H), 7.10 (s, 2H), 3.19 (s, 6H), 3.15-3.05 (m, 8H), 2.00-1.10 (m, 32H).

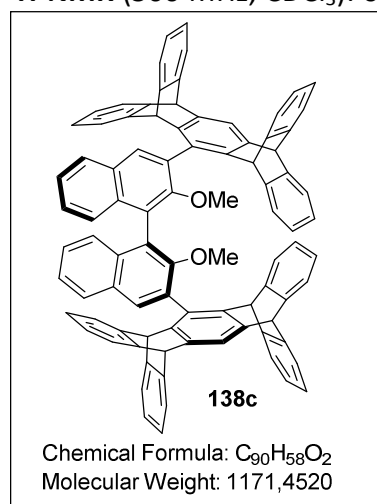


**<sup>13</sup>C-NMR** (125 MHz, CD<sub>2</sub>Cl<sub>2</sub>) [overlapping signals]: δ 155.8, 141.7, 141.7, 139.8, 139.7, 134.0, 133.2, 131.8, 130.9, 129.8, 128.4, 126.3, 126.0, 125.4, 125.0, 119.4, 60.5, 35.0, 31.7, 31.4, 27.1, 27.1, 27.0, 26.9, 26.3.

**HRMS** (*m/z*) calcd for C<sub>58</sub>H<sub>58</sub>O<sub>2</sub>Na [M]<sup>+Na</sup>: 809.4329, found: 809.4333.

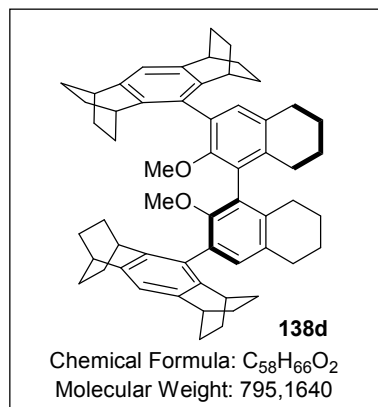
**138c** – Reaction performed on 0.5 mmol scale (60% yield).

**<sup>1</sup>H-NMR** (500 MHz, CDCl<sub>3</sub>): δ 8.10-7.92 (m, 2H), 7.83-7.75 (m, 4H), 7.58-7.52 (m, 4H), 7.47 (s, 2H), 7.35-7.20 (m, 10H), 7.15-7.10 (m, 2H), 7.09-7.00 (m, 4H), 6.95-6.80 (m, 10H), 6.78-6.70 (m, 4H), 6.62-6.57 (m, 2H), 5.47 (s, 2H), 5.43 (s, 2H), 5.36 (s, 2H), 5.33 (s, 2H), 2.78 (s, 6H).



**<sup>13</sup>C-NMR** (125 MHz, CDCl<sub>3</sub>) [overlapping signals]: δ 154.6, 145.9, 145.7, 145.6, 145.3, 145.3, 145.2, 142.7, 142.7, 141.3, 141.0, 134.2, 132.7, 130.8, 130.8, 130.4, 128.4, 126.6, 126.1, 126.0, 125.4, 125.2, 125.0, 124.9, 124.9, 124.7, 124.2, 123.6, 123.5, 123.3, 123.2, 119.5, 60.4, 54.4, 54.4, 52.0, 51.6.

**138d** – The reaction was performed on 0.945 mmol scale and the product was isolated in 70% yield.

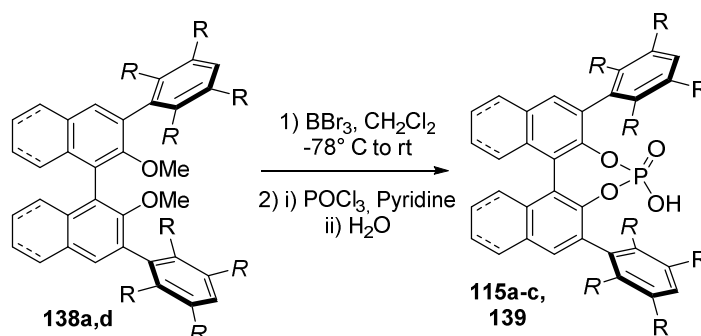


<sup>1</sup>H-NMR (500 MHz, CDCl<sub>3</sub>): δ 6.91 (s, 2H), 6.80 (s, 2H), 3.06 (s, 6H), 3.03-2.90 (m, 8H), 2.85-2.75 (m, 4H), 2.50-2.40 (m, 2H), 2.30-2.20 (m, 2H), 1.80-0.80 (m, 40H).

<sup>13</sup>C-NMR (125 MHz, CDCl<sub>3</sub>) [overlapping signals]: δ 154.0, 141.2, 141.1, 139.4, 139.0, 135.5, 131.9, 131.5, 130.8, 130.2, 128.9, 118.5, 59.9, 34.8, 31.2, 30.8, 29.7, 27.7, 27.0, 27.0, 26.9, 26.8, 26.8, 26.7, 26.0, 23.5, 23.4, 22.8.

HRMS (*m/z*) calcd for C<sub>58</sub>H<sub>66</sub>O<sub>2</sub>Na [M]<sup>+Na</sup>: 817.4955, found: 817.4954.

### Synthesis of catalysts **115a,c** and **139**

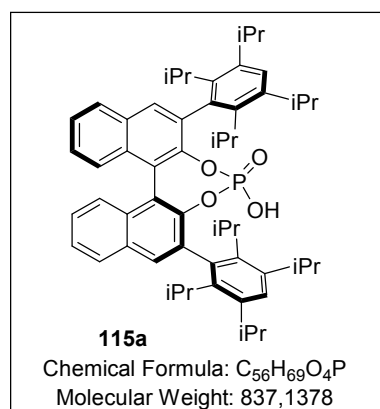


In a flame-dried round bottom two neck flask, a 0.025 M solution of the intermediate **138a,d** in DCM was added under argon atmosphere. Then the stirred solution was cooled down to -78° C and a 1 M solution of BBr<sub>3</sub> in DCM (6.25 equiv.) was added dropwise. The reaction was allowed to reach room temperature and stirred for additional 2-4 days until full conversion into the desired unprotected binol was obtained (TLC eluent: hexane:DCM 1:1). Then the reaction was cooled to 0° C and quenched with a saturated solution of NaHCO<sub>3</sub>. The organic phase was washed with water and brine and then dried over Na<sub>2</sub>SO<sub>4</sub> and the solvent removed in vacuo. The compound was subjected to a fast filtration through silica gel and used directly for the following step without further purification.

In a flame-dried round bottom two neck flask, equipped with a reflux condenser, a 0.025 M solution of the binol intermediate in dry pyridine was added under argon atmosphere. Then the stirred solution was cooled down to 0° C and 10 equiv. of POCl<sub>3</sub> were added. The

reaction was left for 24-48 hours at 95° C and when the starting material is completely converted (TLC eluent: hexane/DCM 1:1) it was cooled to 0° C and 3-5 mL of water were added dropwise [careful: exothermic reaction]. Then the temperature was raised to 100° C. After 3-4 hours the reaction was cooled to room temperature, DCM was added and the organic phase was washed with a 3 M HCl<sub>aq</sub> solution, water and brine. Then the organic layer was dried over anhydrous Na<sub>2</sub>SO<sub>4</sub> and the solvent evaporated in vacuo. Purification was accomplished by column chromatography (eluent: mixtures hexane:ethyl acetate). The isolated compound was then dissolved again in DCM and subjected to an acidic wash with a 6 M HCl<sub>aq</sub> solution to remove salt impurities and deliver the desired phosphoric acid catalysts.

**115a** – The reaction sequence was performed on 0.144 mmol scale and the product was isolated in 32% yield.



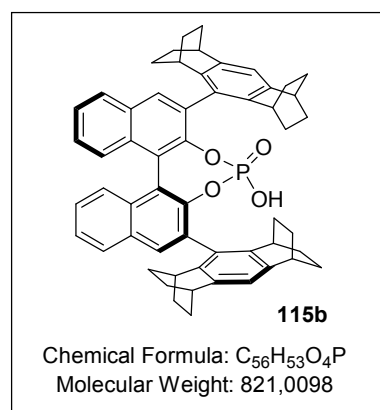
**<sup>1</sup>H-NMR** (500 MHz, CDCl<sub>3</sub>): δ 7.86 (d, *J* = 8.1 Hz, 2H), 7.69 (s, 2H), 7.46 (t, *J* = 8.1 Hz, 2H), 7.30-7.20 (m, 2H), 7.20-7.10 (m, 4H), 3.45-3.10 (m, 4H), 2.95-2.60 (m, 4H), 1.50-0.80 (m, 48H).

**<sup>13</sup>C-NMR** (125 MHz, CDCl<sub>3</sub>) [overlapping signals]: δ 146.4 (d, *J*<sub>CP</sub> = 7.8 Hz), 145.6, 144.8, 141.5, 140.8, 135.7, 135.6, 132.3, 131.8, 131.1, 128.2, 127.3, 126.5, 126.1, 125.6, 121.8, 32.2, 32.0, 29.3, 25.0, 25.0, 24.8, 23.5, 22.6, 22.2.

**<sup>31</sup>P-NMR** (202 MHz, CDCl<sub>3</sub>): δ 0.73 (s).

**HRMS** (*m/z*) calcd for C<sub>56</sub>H<sub>68</sub>O<sub>4</sub>P [M]<sup>-H</sup>: 835.4861, found: 835.4853.

**115b** – The reaction sequence was performed on 0.765 mmol scale and the product was isolated in 87% yield.



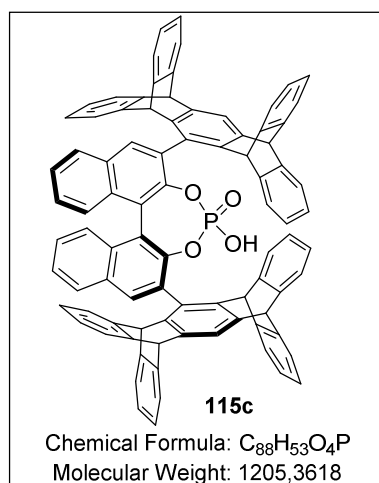
**<sup>1</sup>H-NMR** (500 MHz, CDCl<sub>3</sub>): δ 7.92 (d, *J* = 8.2 Hz, 2H), 7.75 (s, 2H), 7.58-7.46 (m, 4H), 7.40-7.32 (m, 2H), 6.81 (s, 2H), 2.90-2.60 (m, 8H), 1.80-0.60 (m, 32H).

**<sup>13</sup>C-NMR** (125 MHz, CDCl<sub>3</sub>) [overlapping signals]: δ 146.4 (d, *J*<sub>CP</sub> = 8.7 Hz), 141.9, 140.7, 140.2, 140.0, 133.2, 132.3, 131.8, 131.4, 128.3, 127.8, 126.2, 125.7, 122.6 (d, *J*<sub>CP</sub> = 1.9 Hz), 119.2, 34.8, 34.6, 31.5, 30.8, 26.8, 26.8, 26.6, 26.2, 25.9, 25.4.

$^{31}\text{P-NMR}$  (202 MHz,  $\text{CDCl}_3$ ):  $\delta$  1.89 (s).

**HRMS** ( $m/z$ ) calcd for  $\text{C}_{56}\text{H}_{52}\text{O}_4\text{P}$   $[\text{M}]^{\text{H}}$ : 819.3609, found: 819.3605.

**115c** – For compound **138d**, the ether cleavage was found significantly slow and the reaction was performed with 12 equiv. of  $\text{BBr}_3$  in dichloroethane under reflux (2 days). The reaction sequence was performed on 0.28 mmol scale and the product was isolated in 56% yield.



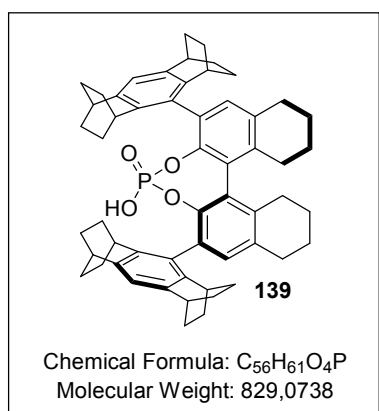
$^1\text{H-NMR}$  (500 MHz,  $(\text{CD}_3)_2\text{SO}$ ):  $\delta$  8.23 (d,  $J = 7.9$  Hz, 2H), 7.80-7.72 (m, 6H), 7.70-7.65 (m, 2H), 7.63 (s, 2H), 7.47 (t,  $J = 6.5$  Hz, 4H), 7.39 (d,  $J = 7.2$  Hz, 2H), 7.35 (d,  $J = 7.2$  Hz, 2H), 7.32 (d,  $J = 7.2$  Hz, 2H), 7.16-7.06 (m, 6H), 7.03 (t,  $J = 7.7$  Hz, 2H), 6.95-6.85 (m, 6H), 6.84-6.75 (m, 6H), 6.66 (t,  $J = 7.5$  Hz, 2H), 5.64 (s, 2H), 5.61 (s, 2H), 5.48 (s, 2H), 5.19 (s, 2H).

$^{13}\text{C-NMR}$  (100 MHz,  $(\text{CD}_3)_2\text{SO}$ ):  $\delta$  146.7, 146.6, 146.5, 146.3, 146.1, 145.6, 145.5, 145.2, 145.1, 145.0, 143.3, 142.3, 141.9, 141.5, 133.4, 132.6, 131.3, 130.2, 130.2, 129.6, 129.5, 128.0, 126.9, 126.7, 125.8, 125.7, 125.4, 125.3, 125.2, 125.2, 125.1, 125.0, 124.8, 124.8, 124.0, 123.8, 123.7, 123.4, 123.1, 123.1, 123.0, 120.0, 53.4, 53.2, 51.8, 51.7.

$^{31}\text{P-NMR}$  (202 MHz,  $(\text{CD}_3)_2\text{SO}$ ):  $\delta$  1.96 (s).

**HRMS** ( $m/z$ ) calcd for  $\text{C}_{88}\text{H}_{53}\text{O}_4\text{P}$   $[\text{M}]^{\text{H}}$ : 1203.3598, found: 1203.3615.

**139** – The reaction was performed on 0.654 mmol scale and the product was isolated in 70% yield.



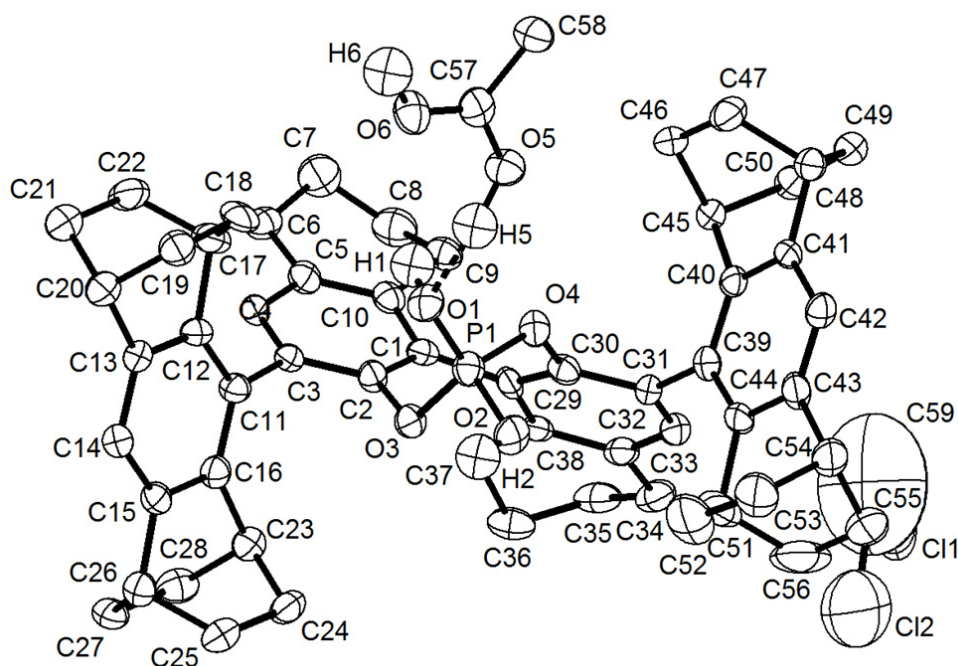
$^1\text{H-NMR}$  (500 MHz,  $\text{CDCl}_3$ ):  $\delta$  6.88 (s, 2H), 6.79 (s, 2H), 2.95-2.75 (m, 12H), 2.62 (bs, 2H), 2.50-2.35 (m, 2H), 2.00-1.00 (m, 40H).

$^{13}\text{C-NMR}$  (125 MHz,  $\text{CDCl}_3$ ) [overlapping signals]:  $\delta$  144.5 (d,  $J_{\text{CP}} = 9.0$  Hz), 141.5, 140.6, 139.7, 139.6, 136.3, 134.1, 133.0, 129.0 (d,  $J_{\text{CP}} = 3.3$  Hz), 128.0, 127.2, 118.8, 34.9, 34.6, 31.2, 30.9, 29.8, 28.1, 27.1, 27.0, 26.9, 26.5, 26.5, 25.6, 25.5, 23.2, 23.1.

$^{31}\text{P-NMR}$  (202 MHz,  $\text{CDCl}_3$ ):  $\delta$  0.75 (s).

**HRMS** ( $m/z$ ) calcd for  $\text{C}_{56}\text{H}_{60}\text{O}_4\text{P}$   $[\text{M}]^{\text{H}}$ : 827.4235, found: 827.4234.



7.4.1.1. Crystallographic data of compound **139**

The crystals were grown from a dichloromethane-acetic acid solution of **139** by slow evaporation of the chlorinated solvent at room temperature. The structure contains disordered hydrogen bonded chains of alternating phosphoric and acetic acid. The hydrophobic region of the crystal lattice appears to be filled with disordered dichloromethane, which sits on a crystallographic two-fold axis. P-O and C-O distances indicate that the hydroxyl H atoms are disordered. Probability ellipsoids are shown at the 50% level and H atoms are omitted for clarity.

**Crystal data and structure refinement.**

Identification code	MOA-MC-200-01 (9164)	
Empirical formula	$C_{117}H_{132}Cl_2O_{12}P_2$	
Color	colourless	
Formula weight	1863.06 g·mol <sup>-1</sup>	
Temperature	100 K	
Wavelength	1.54178 Å	
Crystal system	tetragonal	
Space group	P 4 <sub>3</sub> 2 <sub>1</sub> 2 (no. 96)	
Unit cell dimensions	a = 12.9475(3) Å	α = 90°.
	b = 12.9475(3) Å	β = 90°.
	c = 57.4120(15) Å	γ = 90°.
Volume	9624.4(5) Å <sup>3</sup>	

## 7. Experimental Section

---

Z	4	
Density (calculated)	1.286 Mg·m <sup>-3</sup>	
Absorption coefficient	1.434 mm <sup>-1</sup>	
F(000)	3976 e	
Crystal size	0.12 x 0.11 x 0.05 mm <sup>3</sup>	
θ range for data collection	3.079 to 67.663°.	
Index ranges	-13 ≤ h ≤ 15, -13 ≤ k ≤ 15, -60 ≤ l ≤ 68	
Reflections collected	143460	
Independent reflections	8581 [R <sub>int</sub> = 0.0651]	
Reflections with I > 2σ(I)	7316	
Completeness to θ = 67.663°	98.9 %	
Absorption correction	Gaussian	
Max. and min. transmission	0.95681 and 0.87519	
Refinement method	Full-matrix least-squares on F <sup>2</sup>	
Data / restraints / parameters	8581 / 6 / 622	
Goodness-of-fit on F <sup>2</sup>	1.798	
Final R indices [I > 2σ(I)]	R <sub>1</sub> = 0.0825	wR <sup>2</sup> = 0.2231
R indices (all data)	R <sub>1</sub> = 0.0957	wR <sup>2</sup> = 0.2290
Absolute structure parameter	0.063(6)	
Extinction coefficient	0	
Largest diff. peak and hole	0.683 and -0.903 e·Å <sup>-3</sup>	

### Atomic coordinates and equivalent isotropic displacement parameters (Å<sup>2</sup>).

U<sub>eq</sub> is defined as one third of the trace of the orthogonalized U<sub>ij</sub> tensor.

	x	y	z	U <sub>eq</sub>
C(1)	0.6692(4)	0.0616(4)	0.3677(1)	0.026(1)
C(2)	0.5787(4)	0.0248(4)	0.3575(1)	0.025(1)
C(3)	0.5588(4)	0.0287(4)	0.3338(1)	0.024(1)
C(4)	0.6336(4)	0.0746(4)	0.3199(1)	0.026(1)
C(5)	0.7227(4)	0.1210(4)	0.3295(1)	0.030(1)
C(6)	0.7991(5)	0.1723(5)	0.3132(1)	0.033(1)
C(7)	0.8770(5)	0.2393(6)	0.3241(1)	0.048(2)
C(8)	0.9155(5)	0.1923(5)	0.3468(1)	0.046(2)
C(9)	0.8280(4)	0.1777(5)	0.3641(1)	0.032(1)
C(10)	0.7387(4)	0.1160(4)	0.3535(1)	0.027(1)
C(11)	0.4630(4)	-0.0162(4)	0.3228(1)	0.027(1)
C(12)	0.3936(5)	0.0483(4)	0.3109(1)	0.029(1)
C(13)	0.3108(5)	0.0087(4)	0.2981(1)	0.032(1)
C(14)	0.2944(5)	-0.0993(4)	0.2975(1)	0.034(1)
C(15)	0.3608(4)	-0.1639(4)	0.3096(1)	0.029(1)

## 7. Experimental Section

---

C(16)	0.4440(4)	-0.1225(4)	0.3225(1)	0.028(1)
C(17)	0.3962(5)	0.1661(5)	0.3099(1)	0.041(2)
C(18)	0.2930(5)	0.2062(5)	0.3193(1)	0.043(2)
C(19)	0.2013(5)	0.1582(5)	0.3059(1)	0.040(2)
C(20)	0.2455(5)	0.0872(5)	0.2865(1)	0.040(2)
C(21)	0.3131(5)	0.1543(5)	0.2703(1)	0.044(2)
C(22)	0.4024(6)	0.1991(5)	0.2846(1)	0.047(2)
C(23)	0.5075(5)	-0.2065(5)	0.3340(1)	0.033(1)
C(24)	0.4342(5)	-0.2696(5)	0.3500(1)	0.036(1)
C(25)	0.3439(4)	-0.3147(5)	0.3353(1)	0.034(1)
C(26)	0.3554(4)	-0.2789(4)	0.3100(1)	0.030(1)
C(27)	0.4566(4)	-0.3225(4)	0.3006(1)	0.034(1)
C(28)	0.5473(5)	-0.2779(5)	0.3153(1)	0.038(2)
C(29)	0.6852(4)	0.0440(4)	0.3934(1)	0.026(1)
C(30)	0.6156(4)	0.0787(4)	0.4095(1)	0.029(1)
C(31)	0.6317(5)	0.0732(4)	0.4337(1)	0.030(1)
C(32)	0.7197(5)	0.0259(4)	0.4409(1)	0.033(1)
C(33)	0.7904(4)	-0.0189(4)	0.4254(1)	0.030(1)
C(34)	0.8853(5)	-0.0708(5)	0.4347(1)	0.038(2)
C(35)	0.9667(5)	-0.0923(5)	0.4167(1)	0.043(2)
C(36)	0.9162(5)	-0.1421(5)	0.3954(1)	0.040(2)
C(37)	0.8445(4)	-0.0663(5)	0.3837(1)	0.034(1)
C(38)	0.7730(4)	-0.0107(4)	0.4011(1)	0.026(1)
C(39)	0.5590(5)	0.1250(5)	0.4504(1)	0.033(1)
C(40)	0.5642(4)	0.2319(4)	0.4531(1)	0.026(1)
C(41)	0.4986(4)	0.2830(4)	0.4685(1)	0.024(1)
C(42)	0.4282(4)	0.2264(4)	0.4824(1)	0.029(1)
C(43)	0.4245(5)	0.1214(5)	0.4801(1)	0.033(1)
C(44)	0.4881(5)	0.0697(5)	0.4641(1)	0.039(2)
C(45)	0.6378(4)	0.3036(4)	0.4414(1)	0.026(1)
C(46)	0.5756(5)	0.3876(4)	0.4279(1)	0.032(1)
C(47)	0.4987(5)	0.4395(5)	0.4444(1)	0.036(1)
C(48)	0.5147(5)	0.3971(4)	0.4694(1)	0.031(1)
C(49)	0.6264(5)	0.4190(5)	0.4769(1)	0.034(1)
C(50)	0.7008(5)	0.3588(5)	0.4604(1)	0.032(1)
C(51)	0.4643(8)	-0.0446(5)	0.4640(1)	0.064(2)
C(52)	0.3425(7)	-0.0567(7)	0.4597(2)	0.071(3)
C(53)	0.2828(6)	-0.0068(6)	0.4784(1)	0.060(2)
C(54)	0.3562(5)	0.0524(5)	0.4947(1)	0.045(2)

## 7. Experimental Section

---

C(55)	0.4278(6)	-0.0276(5)	0.5070(1)	0.049(2)
C(56)	0.4893(8)	-0.0851(6)	0.4885(2)	0.079(3)
C(57)	0.3102(5)	0.3976(5)	0.3789(1)	0.036(2)
C(58)	0.3180(5)	0.5002(5)	0.3907(1)	0.039(2)
O(1)	0.3811(3)	0.1407(3)	0.3733(1)	0.035(1)
O(2)	0.3805(3)	0.0000(3)	0.4046(1)	0.037(1)
O(3)	0.5014(3)	-0.0159(3)	0.3724(1)	0.028(1)
O(4)	0.5254(3)	0.1278(3)	0.4015(1)	0.031(1)
O(5)	0.3677(3)	0.3275(3)	0.3887(1)	0.037(1)
O(6)	0.2522(3)	0.3785(4)	0.3625(1)	0.042(1)
P(1)	0.4409(1)	0.0667(1)	0.3872(1)	0.030(1)
Cl(1)	1.0095(5)	-0.0550(6)	0.4988(1)	0.113(2)
Cl(2)	0.7964(10)	-0.1535(8)	0.4988(3)	0.187(6)
C(59)	0.869(3)	-0.002(6)	0.4948(11)	0.34(3)

---

**Bond lengths [Å] and angles [°].**

---

C(1)-C(2)	1.396(8)	C(1)-C(10)	1.405(8)
C(1)-C(29)	1.503(8)	C(2)-C(3)	1.384(7)
C(2)-O(3)	1.417(6)	C(3)-C(4)	1.390(7)
C(3)-C(11)	1.506(8)	C(4)-C(5)	1.413(8)
C(4)-H(4)	0.9500	C(5)-C(10)	1.396(8)
C(5)-C(6)	1.516(8)	C(6)-C(7)	1.471(9)
C(6)-H(6A)	0.9900	C(6)-H(6B)	0.9900
C(7)-C(8)	1.523(10)	C(7)-H(7A)	0.9900
C(7)-H(7B)	0.9900	C(8)-C(9)	1.519(9)
C(8)-H(8A)	0.9900	C(8)-H(8B)	0.9900
C(9)-C(10)	1.532(8)	C(9)-H(9A)	0.9900
C(9)-H(9B)	0.9900	C(11)-C(16)	1.399(8)
C(11)-C(12)	1.405(8)	C(12)-C(13)	1.398(8)
C(12)-C(17)	1.526(8)	C(13)-C(14)	1.415(8)
C(13)-C(20)	1.480(8)	C(14)-C(15)	1.386(8)
C(14)-H(14)	0.9500	C(15)-C(16)	1.413(8)
C(15)-C(26)	1.490(8)	C(16)-C(23)	1.514(8)
C(17)-C(22)	1.518(9)	C(17)-C(18)	1.533(10)
C(17)-H(17)	1.0000	C(18)-C(19)	1.543(9)
C(18)-H(18A)	0.9900	C(18)-H(18B)	0.9900
C(19)-C(20)	1.556(9)	C(19)-H(19A)	0.9900

## 7. Experimental Section

---

C(19)-H(19B)	0.9900	C(20)-C(21)	1.543(9)
C(20)-H(20)	1.0000	C(21)-C(22)	1.530(9)
C(21)-H(21A)	0.9900	C(21)-H(21B)	0.9900
C(22)-H(22A)	0.9900	C(22)-H(22B)	0.9900
C(23)-C(28)	1.508(8)	C(23)-C(24)	1.555(8)
C(23)-H(23)	1.0000	C(24)-C(25)	1.555(8)
C(24)-H(24A)	0.9900	C(24)-H(24B)	0.9900
C(25)-C(26)	1.534(8)	C(25)-H(25A)	0.9900
C(25)-H(25B)	0.9900	C(26)-C(27)	1.526(8)
C(26)-H(26)	1.0000	C(27)-C(28)	1.555(9)
C(27)-H(27A)	0.9900	C(27)-H(27B)	0.9900
C(28)-H(28A)	0.9900	C(28)-H(28B)	0.9900
C(29)-C(30)	1.369(8)	C(29)-C(38)	1.412(8)
C(30)-C(31)	1.403(8)	C(30)-O(4)	1.409(7)
C(31)-C(32)	1.359(8)	C(31)-C(39)	1.502(8)
C(32)-C(33)	1.404(8)	C(32)-H(32)	0.9500
C(33)-C(38)	1.413(8)	C(33)-C(34)	1.501(8)
C(34)-C(35)	1.504(9)	C(34)-H(34A)	0.9900
C(34)-H(34B)	0.9900	C(35)-C(36)	1.528(9)
C(35)-H(35A)	0.9900	C(35)-H(35B)	0.9900
C(36)-C(37)	1.507(8)	C(36)-H(36A)	0.9900
C(36)-H(36B)	0.9900	C(37)-C(38)	1.541(8)
C(37)-H(37A)	0.9900	C(37)-H(37B)	0.9900
C(39)-C(40)	1.395(8)	C(39)-C(44)	1.407(8)
C(40)-C(41)	1.394(8)	C(40)-C(45)	1.490(7)
C(41)-C(42)	1.416(7)	C(41)-C(48)	1.492(8)
C(42)-C(43)	1.367(8)	C(42)-H(42)	0.9500
C(43)-C(44)	1.402(9)	C(43)-C(54)	1.511(8)
C(44)-C(51)	1.512(9)	C(45)-C(50)	1.541(8)
C(45)-C(46)	1.558(8)	C(45)-H(45)	1.0000
C(46)-C(47)	1.528(8)	C(46)-H(46A)	0.9900
C(46)-H(46B)	0.9900	C(47)-C(48)	1.553(8)
C(47)-H(47A)	0.9900	C(47)-H(47B)	0.9900
C(48)-C(49)	1.535(8)	C(48)-H(48)	1.0000
C(49)-C(50)	1.558(8)	C(49)-H(49A)	0.9900
C(49)-H(49B)	0.9900	C(50)-H(50A)	0.9900
C(50)-H(50B)	0.9900	C(51)-C(56)	1.535(12)
C(51)-C(52)	1.605(13)	C(51)-H(51)	1.0000
C(52)-C(53)	1.473(11)	C(52)-H(52A)	0.9900

## 7. Experimental Section

---

C(52)-H(52B)	0.9900	C(53)-C(54)	1.541(9)
C(53)-H(53A)	0.9900	C(53)-H(53B)	0.9900
C(54)-C(55)	1.557(10)	C(54)-H(54)	1.0000
C(55)-C(56)	1.522(11)	C(55)-H(55A)	0.9900
C(55)-H(55B)	0.9900	C(56)-H(56A)	0.9900
C(56)-H(56B)	0.9900	C(57)-O(6)	1.229(7)
C(57)-O(5)	1.301(7)	C(57)-C(58)	1.496(9)
C(58)-H(58A)	0.9800	C(58)-H(58B)	0.9800
C(58)-H(58C)	0.9800	O(1)-P(1)	1.468(4)
O(1)-H(1)	0.8400	O(2)-P(1)	1.533(4)
O(2)-H(2)	0.8400	O(3)-P(1)	1.576(4)
O(4)-P(1)	1.577(4)	O(5)-H(5)	1.10(16)
O(6)-H(6)	1.01(16)	Cl(1)-C(59)	1.96(4)
Cl(2)-C(59)	2.18(7)	C(59)-H(59A)	0.9900
C(59)-H(59B)	0.9900		
C(2)-C(1)-C(10)	117.6(5)	C(2)-C(1)-C(29)	118.6(5)
C(10)-C(1)-C(29)	123.8(5)	C(3)-C(2)-C(1)	124.0(5)
C(3)-C(2)-O(3)	118.4(5)	C(1)-C(2)-O(3)	117.6(5)
C(2)-C(3)-C(4)	116.8(5)	C(2)-C(3)-C(11)	123.3(5)
C(4)-C(3)-C(11)	119.9(5)	C(3)-C(4)-C(5)	121.7(5)
C(3)-C(4)-H(4)	119.1	C(5)-C(4)-H(4)	119.1
C(10)-C(5)-C(4)	119.2(5)	C(10)-C(5)-C(6)	122.3(5)
C(4)-C(5)-C(6)	118.5(5)	C(7)-C(6)-C(5)	116.2(5)
C(7)-C(6)-H(6A)	108.2	C(5)-C(6)-H(6A)	108.2
C(7)-C(6)-H(6B)	108.2	C(5)-C(6)-H(6B)	108.2
H(6A)-C(6)-H(6B)	107.4	C(6)-C(7)-C(8)	110.8(5)
C(6)-C(7)-H(7A)	109.5	C(8)-C(7)-H(7A)	109.5
C(6)-C(7)-H(7B)	109.5	C(8)-C(7)-H(7B)	109.5
H(7A)-C(7)-H(7B)	108.1	C(9)-C(8)-C(7)	111.5(5)
C(9)-C(8)-H(8A)	109.3	C(7)-C(8)-H(8A)	109.3
C(9)-C(8)-H(8B)	109.3	C(7)-C(8)-H(8B)	109.3
H(8A)-C(8)-H(8B)	108.0	C(8)-C(9)-C(10)	111.6(5)
C(8)-C(9)-H(9A)	109.3	C(10)-C(9)-H(9A)	109.3
C(8)-C(9)-H(9B)	109.3	C(10)-C(9)-H(9B)	109.3
H(9A)-C(9)-H(9B)	108.0	C(5)-C(10)-C(1)	120.2(5)
C(5)-C(10)-C(9)	118.8(5)	C(1)-C(10)-C(9)	120.9(5)
C(16)-C(11)-C(12)	117.7(5)	C(16)-C(11)-C(3)	122.1(5)
C(12)-C(11)-C(3)	120.1(5)	C(13)-C(12)-C(11)	122.0(5)

## 7. Experimental Section

---

C(13)-C(12)-C(17)	111.3(5)	C(11)-C(12)-C(17)	126.7(5)
C(12)-C(13)-C(14)	119.4(5)	C(12)-C(13)-C(20)	115.0(5)
C(14)-C(13)-C(20)	125.6(5)	C(15)-C(14)-C(13)	119.4(6)
C(15)-C(14)-H(14)	120.3	C(13)-C(14)-H(14)	120.3
C(14)-C(15)-C(16)	120.4(5)	C(14)-C(15)-C(26)	125.6(5)
C(16)-C(15)-C(26)	114.0(5)	C(11)-C(16)-C(15)	121.0(5)
C(11)-C(16)-C(23)	127.2(5)	C(15)-C(16)-C(23)	111.7(5)
C(22)-C(17)-C(12)	108.6(5)	C(22)-C(17)-C(18)	106.7(6)
C(12)-C(17)-C(18)	107.8(5)	C(22)-C(17)-H(17)	111.2
C(12)-C(17)-H(17)	111.2	C(18)-C(17)-H(17)	111.2
C(17)-C(18)-C(19)	111.0(5)	C(17)-C(18)-H(18A)	109.4
C(19)-C(18)-H(18A)	109.4	C(17)-C(18)-H(18B)	109.4
C(19)-C(18)-H(18B)	109.4	H(18A)-C(18)-H(18B)	108.0
C(18)-C(19)-C(20)	108.2(5)	C(18)-C(19)-H(19A)	110.1
C(20)-C(19)-H(19A)	110.1	C(18)-C(19)-H(19B)	110.1
C(20)-C(19)-H(19B)	110.1	H(19A)-C(19)-H(19B)	108.4
C(13)-C(20)-C(21)	109.5(5)	C(13)-C(20)-C(19)	107.0(5)
C(21)-C(20)-C(19)	107.9(5)	C(13)-C(20)-H(20)	110.8
C(21)-C(20)-H(20)	110.8	C(19)-C(20)-H(20)	110.8
C(22)-C(21)-C(20)	108.7(5)	C(22)-C(21)-H(21A)	109.9
C(20)-C(21)-H(21A)	109.9	C(22)-C(21)-H(21B)	109.9
C(20)-C(21)-H(21B)	109.9	H(21A)-C(21)-H(21B)	108.3
C(17)-C(22)-C(21)	111.4(5)	C(17)-C(22)-H(22A)	109.4
C(21)-C(22)-H(22A)	109.4	C(17)-C(22)-H(22B)	109.4
C(21)-C(22)-H(22B)	109.4	H(22A)-C(22)-H(22B)	108.0
C(28)-C(23)-C(16)	108.4(5)	C(28)-C(23)-C(24)	108.0(5)
C(16)-C(23)-C(24)	107.7(5)	C(28)-C(23)-H(23)	110.9
C(16)-C(23)-H(23)	110.9	C(24)-C(23)-H(23)	110.9
C(25)-C(24)-C(23)	109.5(4)	C(25)-C(24)-H(24A)	109.8
C(23)-C(24)-H(24A)	109.8	C(25)-C(24)-H(24B)	109.8
C(23)-C(24)-H(24B)	109.8	H(24A)-C(24)-H(24B)	108.2
C(26)-C(25)-C(24)	109.1(5)	C(26)-C(25)-H(25A)	109.9
C(24)-C(25)-H(25A)	109.9	C(26)-C(25)-H(25B)	109.9
C(24)-C(25)-H(25B)	109.9	H(25A)-C(25)-H(25B)	108.3
C(15)-C(26)-C(27)	108.9(5)	C(15)-C(26)-C(25)	108.8(5)
C(27)-C(26)-C(25)	107.8(5)	C(15)-C(26)-H(26)	110.4
C(27)-C(26)-H(26)	110.4	C(25)-C(26)-H(26)	110.4
C(26)-C(27)-C(28)	108.7(5)	C(26)-C(27)-H(27A)	110.0
C(28)-C(27)-H(27A)	110.0	C(26)-C(27)-H(27B)	110.0

## 7. Experimental Section

---

C(28)-C(27)-H(27B)	110.0	H(27A)-C(27)-H(27B)	108.3
C(23)-C(28)-C(27)	110.8(5)	C(23)-C(28)-H(28A)	109.5
C(27)-C(28)-H(28A)	109.5	C(23)-C(28)-H(28B)	109.5
C(27)-C(28)-H(28B)	109.5	H(28A)-C(28)-H(28B)	108.1
C(30)-C(29)-C(38)	118.7(5)	C(30)-C(29)-C(1)	121.5(5)
C(38)-C(29)-C(1)	119.7(5)	C(29)-C(30)-C(31)	123.8(5)
C(29)-C(30)-O(4)	118.1(5)	C(31)-C(30)-O(4)	118.0(5)
C(32)-C(31)-C(30)	116.6(5)	C(32)-C(31)-C(39)	122.1(5)
C(30)-C(31)-C(39)	121.1(5)	C(31)-C(32)-C(33)	122.6(5)
C(31)-C(32)-H(32)	118.7	C(33)-C(32)-H(32)	118.7
C(32)-C(33)-C(38)	119.4(5)	C(32)-C(33)-C(34)	119.4(5)
C(38)-C(33)-C(34)	121.2(5)	C(33)-C(34)-C(35)	114.1(5)
C(33)-C(34)-H(34A)	108.7	C(35)-C(34)-H(34A)	108.7
C(33)-C(34)-H(34B)	108.7	C(35)-C(34)-H(34B)	108.7
H(34A)-C(34)-H(34B)	107.6	C(34)-C(35)-C(36)	109.3(5)
C(34)-C(35)-H(35A)	109.8	C(36)-C(35)-H(35A)	109.8
C(34)-C(35)-H(35B)	109.8	C(36)-C(35)-H(35B)	109.8
H(35A)-C(35)-H(35B)	108.3	C(37)-C(36)-C(35)	110.1(5)
C(37)-C(36)-H(36A)	109.6	C(35)-C(36)-H(36A)	109.6
C(37)-C(36)-H(36B)	109.6	C(35)-C(36)-H(36B)	109.6
H(36A)-C(36)-H(36B)	108.1	C(36)-C(37)-C(38)	112.7(5)
C(36)-C(37)-H(37A)	109.1	C(38)-C(37)-H(37A)	109.1
C(36)-C(37)-H(37B)	109.1	C(38)-C(37)-H(37B)	109.1
H(37A)-C(37)-H(37B)	107.8	C(29)-C(38)-C(33)	118.5(5)
C(29)-C(38)-C(37)	120.9(5)	C(33)-C(38)-C(37)	120.5(5)
C(40)-C(39)-C(44)	118.3(5)	C(40)-C(39)-C(31)	119.0(5)
C(44)-C(39)-C(31)	122.7(5)	C(41)-C(40)-C(39)	120.9(5)
C(41)-C(40)-C(45)	112.4(5)	C(39)-C(40)-C(45)	126.7(5)
C(40)-C(41)-C(42)	120.3(5)	C(40)-C(41)-C(48)	114.0(5)
C(42)-C(41)-C(48)	125.7(5)	C(43)-C(42)-C(41)	118.9(5)
C(43)-C(42)-H(42)	120.6	C(41)-C(42)-H(42)	120.5
C(42)-C(43)-C(44)	121.1(5)	C(42)-C(43)-C(54)	123.7(5)
C(44)-C(43)-C(54)	115.2(5)	C(43)-C(44)-C(39)	120.5(5)
C(43)-C(44)-C(51)	110.5(5)	C(39)-C(44)-C(51)	128.9(6)
C(40)-C(45)-C(50)	107.8(4)	C(40)-C(45)-C(46)	109.2(4)
C(50)-C(45)-C(46)	107.6(4)	C(40)-C(45)-H(45)	110.7
C(50)-C(45)-H(45)	110.7	C(46)-C(45)-H(45)	110.7
C(47)-C(46)-C(45)	109.7(4)	C(47)-C(46)-H(46A)	109.7
C(45)-C(46)-H(46A)	109.7	C(47)-C(46)-H(46B)	109.7



## 7. Experimental Section

---

C(45)-C(46)-H(46B)	109.7	H(46A)-C(46)-H(46B)	108.2
C(46)-C(47)-C(48)	109.2(5)	C(46)-C(47)-H(47A)	109.8
C(48)-C(47)-H(47A)	109.8	C(46)-C(47)-H(47B)	109.8
C(48)-C(47)-H(47B)	109.8	H(47A)-C(47)-H(47B)	108.3
C(41)-C(48)-C(49)	108.9(5)	C(41)-C(48)-C(47)	107.5(5)
C(49)-C(48)-C(47)	108.6(5)	C(41)-C(48)-H(48)	110.6
C(49)-C(48)-H(48)	110.6	C(47)-C(48)-H(48)	110.6
C(48)-C(49)-C(50)	108.7(5)	C(48)-C(49)-H(49A)	110.0
C(50)-C(49)-H(49A)	110.0	C(48)-C(49)-H(49B)	110.0
C(50)-C(49)-H(49B)	110.0	H(49A)-C(49)-H(49B)	108.3
C(45)-C(50)-C(49)	109.6(5)	C(45)-C(50)-H(50A)	109.8
C(49)-C(50)-H(50A)	109.8	C(45)-C(50)-H(50B)	109.8
C(49)-C(50)-H(50B)	109.8	H(50A)-C(50)-H(50B)	108.2
C(44)-C(51)-C(56)	106.7(6)	C(44)-C(51)-C(52)	107.3(7)
C(56)-C(51)-C(52)	108.4(7)	C(44)-C(51)-H(51)	111.4
C(56)-C(51)-H(51)	111.4	C(52)-C(51)-H(51)	111.4
C(53)-C(52)-C(51)	111.1(6)	C(53)-C(52)-H(52A)	109.4
C(51)-C(52)-H(52A)	109.4	C(53)-C(52)-H(52B)	109.4
C(51)-C(52)-H(52B)	109.4	H(52A)-C(52)-H(52B)	108.0
C(52)-C(53)-C(54)	109.8(6)	C(52)-C(53)-H(53A)	109.7
C(54)-C(53)-H(53A)	109.7	C(52)-C(53)-H(53B)	109.7
C(54)-C(53)-H(53B)	109.7	H(53A)-C(53)-H(53B)	108.2
C(43)-C(54)-C(53)	108.4(5)	C(43)-C(54)-C(55)	107.2(6)
C(53)-C(54)-C(55)	108.2(6)	C(43)-C(54)-H(54)	111.0
C(53)-C(54)-H(54)	111.0	C(55)-C(54)-H(54)	111.0
C(56)-C(55)-C(54)	108.8(6)	C(56)-C(55)-H(55A)	109.9
C(54)-C(55)-H(55A)	109.9	C(56)-C(55)-H(55B)	109.9
C(54)-C(55)-H(55B)	109.9	H(55A)-C(55)-H(55B)	108.3
C(55)-C(56)-C(51)	111.2(7)	C(55)-C(56)-H(56A)	109.4
C(51)-C(56)-H(56A)	109.4	C(55)-C(56)-H(56B)	109.4
C(51)-C(56)-H(56B)	109.4	H(56A)-C(56)-H(56B)	108.0
O(6)-C(57)-O(5)	122.7(6)	O(6)-C(57)-C(58)	124.6(6)
O(5)-C(57)-C(58)	112.6(5)	C(57)-C(58)-H(58A)	109.5
C(57)-C(58)-H(58B)	109.5	H(58A)-C(58)-H(58B)	109.5
C(57)-C(58)-H(58C)	109.5	H(58A)-C(58)-H(58C)	109.5
H(58B)-C(58)-H(58C)	109.5	P(1)-O(1)-H(1)	109.5
P(1)-O(2)-H(2)	109.5	C(2)-O(3)-P(1)	115.2(3)
C(30)-O(4)-P(1)	121.3(3)	C(57)-O(5)-H(5)	111(7)
C(57)-O(6)-H(6)	129(9)	O(1)-P(1)-O(2)	116.9(2)

## 7. Experimental Section

O(1)-P(1)-O(3)	114.3(2)	O(2)-P(1)-O(3)	102.9(2)
O(1)-P(1)-O(4)	108.6(2)	O(2)-P(1)-O(4)	107.4(2)
O(3)-P(1)-O(4)	106.0(2)	Cl(1)-C(59)-Cl(2)	94(3)
Cl(1)-C(59)-H(59A)	112.9	Cl(2)-C(59)-H(59A)	112.9
Cl(1)-C(59)-H(59B)	112.9	Cl(2)-C(59)-H(59B)	112.9
H(59A)-C(59)-H(59B)	110.3		

### Anisotropic displacement parameters ( $\text{\AA}^2$ ).

The anisotropic displacement factor exponent takes the form:

$$-2\pi^2 [ h^2 a^2 U_{11} + \dots + 2 h k a^* b^* U_{12} ].$$

	$U_{11}$	$U_{22}$	$U_{33}$	$U_{23}$	$U_{13}$	$U_{12}$
C(1)	0.028(3)	0.019(3)	0.029(3)	-0.001(2)	0.001(2)	0.000(2)
C(2)	0.025(3)	0.028(3)	0.023(3)	-0.002(2)	0.003(2)	-0.005(2)
C(3)	0.028(3)	0.021(3)	0.024(3)	-0.002(2)	-0.001(2)	0.002(2)
C(4)	0.032(3)	0.024(3)	0.023(3)	-0.003(2)	-0.003(2)	0.001(2)
C(5)	0.032(3)	0.028(3)	0.029(3)	-0.004(2)	0.003(3)	0.006(2)
C(6)	0.034(3)	0.030(3)	0.035(3)	0.004(3)	0.005(3)	0.006(3)
C(7)	0.046(4)	0.050(4)	0.048(4)	0.001(3)	0.010(3)	-0.011(3)
C(8)	0.039(4)	0.040(4)	0.058(4)	-0.001(3)	-0.003(3)	-0.006(3)
C(9)	0.028(3)	0.029(3)	0.040(3)	-0.002(3)	-0.003(3)	-0.004(2)
C(10)	0.027(3)	0.025(3)	0.031(3)	-0.005(2)	-0.002(2)	0.006(2)
C(11)	0.030(3)	0.023(3)	0.027(3)	0.000(2)	0.002(2)	0.002(2)
C(12)	0.038(3)	0.020(3)	0.030(3)	0.001(2)	-0.005(3)	0.002(2)
C(13)	0.044(4)	0.029(3)	0.023(3)	0.002(2)	-0.005(3)	-0.001(3)
C(14)	0.047(4)	0.029(3)	0.026(3)	-0.002(2)	0.000(3)	0.000(3)
C(15)	0.034(3)	0.027(3)	0.026(3)	-0.003(2)	0.002(2)	0.005(2)
C(16)	0.031(3)	0.030(3)	0.024(3)	0.000(2)	0.002(2)	0.001(2)
C(17)	0.053(4)	0.023(3)	0.047(4)	-0.001(3)	-0.013(3)	-0.002(3)
C(18)	0.059(4)	0.020(3)	0.049(4)	-0.008(3)	-0.020(3)	0.015(3)
C(19)	0.049(4)	0.033(3)	0.038(4)	0.000(3)	-0.012(3)	0.011(3)
C(20)	0.053(4)	0.033(3)	0.035(3)	0.003(3)	-0.011(3)	0.003(3)
C(21)	0.058(4)	0.037(4)	0.038(4)	0.004(3)	-0.006(3)	-0.004(3)
C(22)	0.063(4)	0.032(3)	0.047(4)	0.012(3)	-0.021(3)	-0.016(3)
C(23)	0.036(3)	0.032(3)	0.031(3)	0.002(3)	-0.003(3)	0.000(3)
C(24)	0.043(3)	0.034(3)	0.031(3)	0.010(3)	-0.002(3)	-0.003(3)
C(25)	0.031(3)	0.035(3)	0.036(3)	0.010(3)	0.003(3)	0.003(3)
C(26)	0.027(3)	0.034(3)	0.030(3)	0.000(3)	-0.001(2)	-0.003(2)

## 7. Experimental Section

---

C(27)	0.040(3)	0.024(3)	0.037(3)	-0.002(3)	0.002(3)	0.004(3)
C(28)	0.033(3)	0.034(3)	0.048(4)	0.006(3)	0.007(3)	0.006(3)
C(29)	0.031(3)	0.025(3)	0.023(3)	-0.008(2)	-0.002(2)	-0.003(2)
C(30)	0.030(3)	0.026(3)	0.031(3)	-0.003(2)	-0.002(2)	-0.006(3)
C(31)	0.046(4)	0.024(3)	0.019(3)	0.000(2)	-0.002(3)	0.001(3)
C(32)	0.043(4)	0.029(3)	0.027(3)	0.001(2)	-0.007(3)	-0.006(3)
C(33)	0.033(3)	0.022(3)	0.036(3)	0.004(2)	-0.010(3)	-0.004(2)
C(34)	0.039(3)	0.032(3)	0.043(4)	0.011(3)	-0.010(3)	-0.003(3)
C(35)	0.040(4)	0.026(3)	0.063(5)	0.009(3)	-0.009(3)	0.001(3)
C(36)	0.028(3)	0.027(3)	0.064(4)	0.002(3)	0.001(3)	0.001(3)
C(37)	0.031(3)	0.030(3)	0.040(4)	0.000(3)	0.002(3)	-0.001(3)
C(38)	0.030(3)	0.017(3)	0.031(3)	0.000(2)	-0.002(2)	-0.002(2)
C(39)	0.047(4)	0.033(3)	0.020(3)	-0.004(2)	0.005(3)	0.001(3)
C(40)	0.029(3)	0.027(3)	0.021(3)	0.001(2)	-0.005(2)	-0.005(2)
C(41)	0.027(3)	0.022(3)	0.022(3)	-0.001(2)	-0.002(2)	-0.005(2)
C(42)	0.027(3)	0.036(3)	0.024(3)	0.002(2)	0.003(2)	-0.008(3)
C(43)	0.039(3)	0.038(3)	0.023(3)	-0.005(3)	0.003(3)	-0.013(3)
C(44)	0.066(4)	0.027(3)	0.024(3)	-0.002(3)	0.003(3)	-0.020(3)
C(45)	0.030(3)	0.025(3)	0.023(3)	0.001(2)	-0.001(2)	0.001(2)
C(46)	0.041(3)	0.023(3)	0.031(3)	0.004(2)	-0.001(3)	-0.002(3)
C(47)	0.041(4)	0.035(3)	0.034(3)	0.008(3)	-0.002(3)	0.005(3)
C(48)	0.040(3)	0.029(3)	0.026(3)	0.000(2)	0.006(3)	0.000(3)
C(49)	0.042(3)	0.030(3)	0.031(3)	0.002(2)	-0.005(3)	-0.001(3)
C(50)	0.031(3)	0.033(3)	0.033(3)	0.003(3)	-0.006(2)	-0.010(3)
C(51)	0.110(7)	0.031(4)	0.051(4)	-0.012(3)	0.033(4)	-0.011(4)
C(52)	0.083(6)	0.068(5)	0.063(5)	-0.011(4)	0.019(5)	-0.042(5)
C(53)	0.070(5)	0.057(5)	0.052(4)	0.001(4)	0.000(4)	-0.039(4)
C(54)	0.058(4)	0.043(4)	0.033(4)	0.003(3)	0.003(3)	-0.024(3)
C(55)	0.058(4)	0.043(4)	0.045(4)	0.008(3)	0.008(3)	-0.009(3)
C(56)	0.115(8)	0.031(4)	0.092(7)	0.013(4)	0.036(6)	-0.007(5)
C(57)	0.032(3)	0.043(4)	0.035(4)	-0.001(3)	0.009(3)	-0.007(3)
C(58)	0.040(4)	0.032(3)	0.045(4)	-0.002(3)	-0.002(3)	0.001(3)
O(1)	0.030(2)	0.038(2)	0.036(2)	0.002(2)	-0.005(2)	0.008(2)
O(2)	0.035(2)	0.044(3)	0.031(2)	0.002(2)	0.009(2)	-0.005(2)
O(3)	0.028(2)	0.030(2)	0.026(2)	-0.002(2)	0.006(2)	0.004(2)
O(4)	0.030(2)	0.035(2)	0.026(2)	-0.003(2)	-0.001(2)	0.003(2)
O(5)	0.032(2)	0.036(2)	0.044(2)	0.001(2)	-0.004(2)	0.005(2)
O(6)	0.039(2)	0.049(3)	0.039(3)	-0.009(2)	-0.002(2)	0.011(2)
P(1)	0.030(1)	0.033(1)	0.028(1)	-0.002(1)	0.003(1)	0.002(1)

## 7. Experimental Section

---

Cl(1)	0.140(5)	0.126(5)	0.074(3)	-0.032(4)	-0.017(4)	0.030(4)
Cl(2)	0.288(16)	0.160(8)	0.113(5)	-0.011(7)	0.080(12)	0.031(10)
C(59)	0.11(3)	0.54(7)	0.36(6)	-0.03(5)	-0.10(4)	0.04(4)

---

**Hydrogen coordinates and isotropic displacement parameters ( $\text{\AA}^2$ ).**

	x	y	z	$U_{\text{eq}}$
H(4)	0.6247	0.0747	0.3034	0.031
H(6A)	0.8356	0.1175	0.3044	0.039
H(6B)	0.7599	0.2140	0.3017	0.039
H(7A)	0.8465	0.3080	0.3272	0.058
H(7B)	0.9359	0.2488	0.3133	0.058
H(8A)	0.9481	0.1247	0.3436	0.055
H(8B)	0.9687	0.2380	0.3537	0.055
H(9A)	0.8024	0.2461	0.3692	0.039
H(9B)	0.8544	0.1410	0.3780	0.039
H(14)	0.2383	-0.1273	0.2889	0.041
H(17)	0.4556	0.1942	0.3191	0.049
H(18A)	0.2906	0.2823	0.3178	0.051
H(18B)	0.2871	0.1889	0.3360	0.051
H(19A)	0.1583	0.2134	0.2990	0.048
H(19B)	0.1577	0.1174	0.3167	0.048
H(20)	0.1884	0.0536	0.2775	0.048
H(21A)	0.3405	0.1118	0.2574	0.053
H(21B)	0.2713	0.2109	0.2636	0.053
H(22A)	0.4688	0.1755	0.2779	0.057
H(22B)	0.4005	0.2754	0.2836	0.057
H(23)	0.5658	-0.1761	0.3431	0.040
H(24A)	0.4730	-0.3265	0.3575	0.043
H(24B)	0.4063	-0.2244	0.3624	0.043
H(25A)	0.3452	-0.3911	0.3360	0.041
H(25B)	0.2770	-0.2907	0.3417	0.041
H(26)	0.2958	-0.3037	0.3004	0.036
H(27A)	0.4652	-0.3031	0.2840	0.041
H(27B)	0.4561	-0.3988	0.3017	0.041
H(28A)	0.5862	-0.3353	0.3225	0.046
H(28B)	0.5951	-0.2396	0.3049	0.046
H(32)	0.7340	0.0231	0.4571	0.040
H(34A)	0.8649	-0.1369	0.4421	0.046

## 7. Experimental Section

---

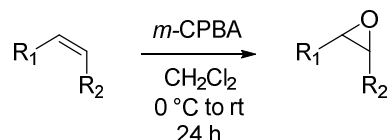
H(34B)	0.9156	-0.0265	0.4470	0.046
H(35A)	1.0197	-0.1392	0.4232	0.052
H(35B)	1.0009	-0.0270	0.4121	0.052
H(36A)	0.9703	-0.1641	0.3843	0.048
H(36B)	0.8769	-0.2040	0.4002	0.048
H(37A)	0.8018	-0.1035	0.3721	0.040
H(37B)	0.8861	-0.0143	0.3753	0.040
H(42)	0.3844	0.2608	0.4932	0.035
H(45)	0.6844	0.2648	0.4306	0.031
H(46A)	0.6236	0.4399	0.4215	0.038
H(46B)	0.5381	0.3554	0.4147	0.038
H(47A)	0.4272	0.4252	0.4391	0.044
H(47B)	0.5094	0.5152	0.4442	0.044
H(48)	0.4648	0.4299	0.4804	0.038
H(49A)	0.6370	0.3966	0.4932	0.041
H(49B)	0.6406	0.4940	0.4759	0.041
H(50A)	0.7503	0.4074	0.4532	0.039
H(50B)	0.7406	0.3074	0.4695	0.039
H(51)	0.5052	-0.0817	0.4518	0.077
H(52A)	0.3241	-0.0251	0.4445	0.086
H(52B)	0.3245	-0.1310	0.4590	0.086
H(53A)	0.2444	-0.0597	0.4873	0.071
H(53B)	0.2320	0.0417	0.4715	0.071
H(54)	0.3165	0.0937	0.5064	0.054
H(55A)	0.4754	0.0084	0.5178	0.059
H(55B)	0.3857	-0.0769	0.5161	0.059
H(56A)	0.4729	-0.1597	0.4893	0.095
H(56B)	0.5640	-0.0766	0.4916	0.095
H(58A)	0.2771	0.5512	0.3821	0.059
H(58B)	0.3904	0.5221	0.3911	0.059
H(58C)	0.2916	0.4945	0.4067	0.059
H(1)	0.4216	0.1816	0.3666	0.052
H(2)	0.3337	-0.0321	0.3975	0.055
H(5)	0.341(11)	0.250(12)	0.384(2)	0.056
H(6)	0.201(13)	0.426(13)	0.355(3)	0.064
H(59A)	0.8569	0.0284	0.4792	0.402
H(59B)	0.8483	0.0472	0.5072	0.402

---

### 7.4.2. Preparation of starting materials

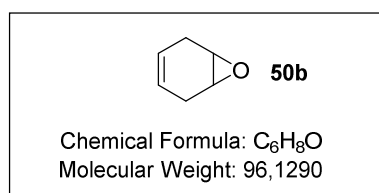
When not commercially available, the epoxides for the ring opening reaction were synthesized as described below, following literature procedures.

#### Procedure A



To a solution of *m*-chloroperbenzoic acid ([70%], 1.2 equiv.) in dichloromethane was added the corresponding olefin in dichloromethane at 0 °C and the reaction was stirred at room temperature for 24 h. After the olefin was completely converted (TLC), the reaction was diluted with dichloromethane and the solution was washed with a saturated aqueous solution of Na<sub>2</sub>S<sub>2</sub>O<sub>3</sub>, a saturated aqueous solution of NaHCO<sub>3</sub>, water and brine. The recovered organic phase was dried over Na<sub>2</sub>SO<sub>4</sub> and the solvent was removed with rotatory evaporator [for volatile epoxides the pressure was kept at 250 mBar and the temperature of the bath at 30 °C]. The crude product was purified by flash chromatography on silica gel (eluent: pentane/Et<sub>2</sub>O) to afford the desired epoxide.

***cis*-1,2-Epoxy-4-cyclohexene (50b)** – The reaction was performed on 5 mmol scale and the product was isolated in 61% yield.

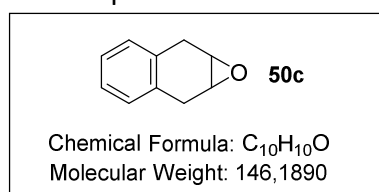


<sup>1</sup>H-NMR (500 MHz, CDCl<sub>3</sub>): δ 5.44 (s, 2H), 3.25 (s, 2H), 2.57 (d, *J* = 18.6 Hz, 2H), 2.44 (d, *J* = 18.5 Hz, 2H).

<sup>13</sup>C-NMR (125 MHz, CDCl<sub>3</sub>): δ 121.8, 51.2, 25.2.

HRMS (*m/z*) calcd for C<sub>6</sub>H<sub>8</sub>O [M]: 96.0575, found: 96.0574.

***cis*-2,3-Epoxy-1,4-dihydronaphthalene (50c)** – The reaction was performed on 5 mmol scale and the product was isolated in 75% yield.

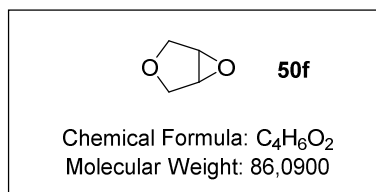


<sup>1</sup>H-NMR (500 MHz, CDCl<sub>3</sub>): δ 7.17-7.11 (m, 2H), 7.08-7.01 (m, 2H), 3.48 (s, 2H), 3.32 (d, *J* = 17.1 Hz, 2H), 3.20 (d, *J* = 17.6 Hz, 2H).

<sup>13</sup>C-NMR (125 MHz, CDCl<sub>3</sub>): δ 131.7, 129.5, 126.8, 52.0, 29.9.

HRMS (*m/z*) calcd for C<sub>10</sub>H<sub>10</sub>O [M]: 146.0732, found: 146.0731.

**6-Oxa-3-oxa-bicyclo[3.1.0]hexane (50f)** – The reaction was performed on 5 mmol scale and the product was isolated in 58% yield.

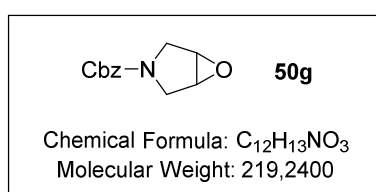


<sup>1</sup>H-NMR (500 MHz, CDCl<sub>3</sub>): δ 4.02 (d, *J* = 10.5 Hz, 2H), 3.78 (s, 2H), 3.65 (d, *J* = 10.5 Hz, 2H).

<sup>13</sup>C-NMR (125 MHz, CDCl<sub>3</sub>): δ 67.5, 56.1.

HRMS (*m/z*) calcd for C<sub>4</sub>H<sub>6</sub>O<sub>2</sub> [M]: 86.0368, found: 86.0368.

**Benzyl 6-oxa-3-azabicyclo[3.1.0]hexane-3-carboxylate (50g)** – The reaction was performed on 2.5 mmol scale and the product was isolated in 79% yield.

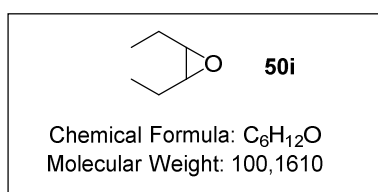


<sup>1</sup>H-NMR (500 MHz, CDCl<sub>3</sub>): δ 7.39-7.28 (m, 5H), 5.13 (d, *J* = 12.4 Hz, 1H), 5.09 (d, *J* = 12.4 Hz, 1H), 3.87 (dd, *J* = 24.5, *J* = 12.8 Hz, 2H), 3.71-3.66 (m, 2H), 3.39 (ddd, *J* = 7.9, *J* = 4.8, *J* = 0.8 Hz, 2H).

<sup>13</sup>C-NMR (125 MHz, CDCl<sub>3</sub>): δ 155.5, 136.8, 128.7, 128.3, 128.2, 67.2, 55.7, 55.2, 47.6, 47.4.

HRMS (*m/z*) calcd for C<sub>12</sub>H<sub>13</sub>NO<sub>3</sub> [M]<sup>+Na</sup>: 242.0788, found: 242.0785.

**cis-3,4-Epoxyhexane (50i)** – The reaction was performed on 5 mmol scale and the product was isolated in 37% yield.

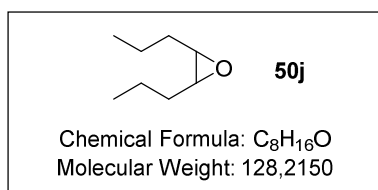


<sup>1</sup>H-NMR (500 MHz, CDCl<sub>3</sub>): δ 2.91-2.85 (m, 2H), 1.63-1.44 (m, 4H), 1.04 (t, *J* = 7.5 Hz, 6H).

<sup>13</sup>C-NMR (125 MHz, CDCl<sub>3</sub>): δ 58.7, 21.2, 10.8.

HRMS (*m/z*) calcd for C<sub>6</sub>H<sub>12</sub>O [M]: 100.0888, found: 100.0887.

**cis-4,5-Epoxyoctane (50j)** – The reaction was performed on 5 mmol scale and the product was isolated in 63% yield.

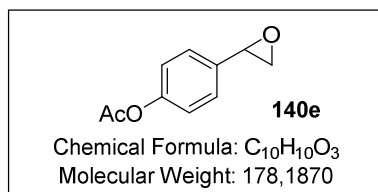


<sup>1</sup>H-NMR (500 MHz, CDCl<sub>3</sub>): δ 2.94-2.89 (m, 2H), 1.59-1.42 (m, 8H), 0.98 (t, *J* = 7.2 Hz, 6H).

<sup>13</sup>C-NMR (125 MHz, CDCl<sub>3</sub>): δ 57.2, 30.1, 20.1, 14.3.

HRMS (*m/z*) calcd for C<sub>8</sub>H<sub>16</sub>O [M]: 128.1201, found: 128.1202.

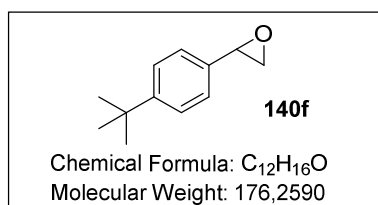
**4-(oxiran-2-yl)phenyl acetate (140e)** – The reaction was performed on 5 mmol scale and the product was isolated in 75% yield.



**<sup>1</sup>H-NMR** (500 MHz, CD<sub>2</sub>Cl<sub>2</sub>): δ 7.34-7.22 (m, 2H), 7.12-7.07 (m, 2H), 3.89 (dd, *J* = 4.0 Hz, *J* = 2.8 Hz, 1H), 3.16 (dd, *J* = 5.5 Hz, *J* = 4.0 Hz, 1H), 2.80 (dd, *J* = 5.5 Hz, *J* = 2.8 Hz, 1H), 2.32 (s, 3H).

**<sup>13</sup>C-NMR** (125 MHz, CD<sub>2</sub>Cl<sub>2</sub>): δ 169.4, 150.5, 135.2, 126.6, 121.7, 51.9, 51.2, 21.1.

**4-(tert-butyl)phenyl)oxirane (140f)** – The reaction was performed on 5 mmol scale and the product was isolated in 28% yield.

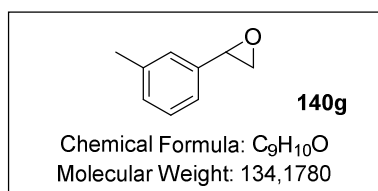


**<sup>1</sup>H-NMR** (500 MHz, CDCl<sub>3</sub>): δ 7.42-7.38 (m, 2H), 7.25-7.20 (m, 2H), 3.85 (dd, *J* = 4.1 Hz, *J* = 2.8 Hz, 1H), 3.14 (dd, *J* = 5.6 Hz, *J* = 4.1 Hz, 1H), 2.83 (dd, *J* = 5.6 Hz, *J* = 2.8 Hz, 1H), 1.33 (s, 9H).

**<sup>13</sup>C-NMR** (125 MHz, CDCl<sub>3</sub>): δ 151.3, 134.5, 125.4, 125.3,

52.3, 51.0, 34.6, 31.3.

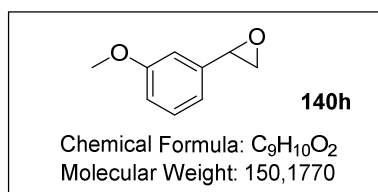
**2-(m-tolyl)oxirane (140g)** – The reaction was performed on 5 mmol scale and the product was isolated in 55% yield.



**<sup>1</sup>H-NMR** (500 MHz, CDCl<sub>3</sub>): δ 7.26-7.22 (m, 1H), 7.15-7.07 (m, 3H), 3.84 (dd, *J* = 2.6 Hz, *J* = 4.1 Hz, *J* = 2.6 Hz, 1H), 3.15 (dd, *J* = 5.6 Hz, *J* = 4.1 Hz, 1H), 2.81 (dd, *J* = 5.6 Hz, *J* = 2.6 Hz, 1H), 2.36 (s, 3H).

**<sup>13</sup>C-NMR** (125 MHz, CDCl<sub>3</sub>): δ 138.2, 137.5, 128.9, 128.4, 126.0, 122.7, 52.4, 51.1, 21.3.

**2-(3-methoxyphenyl)oxirane (140h)** – The reaction was performed on 5 mmol scale and the product was isolated in 84% yield.

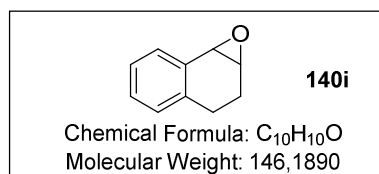


**<sup>1</sup>H-NMR** (500 MHz, CDCl<sub>3</sub>): δ 7.28-7.24 (m, 1H), 6.94-6.89 (m, 1H), 6.88-6.84 (m, 1H), 6.84-6.80 (m, 1H), 3.86 (dd, *J* = 4.1 Hz, *J* = 2.7 Hz, 1H), 3.82 (s, 3H), 3.14 (dd, *J* = 5.6 Hz, *J* = 4.1 Hz, 1H), 2.79 (dd, *J* = 5.6 Hz, *J* = 2.7 Hz, 1H).

**<sup>13</sup>C-NMR** (125 MHz, CDCl<sub>3</sub>): δ 159.9, 139.3, 129.6, 118.0, 113.9, 110.5, 55.2, 52.3, 52.1



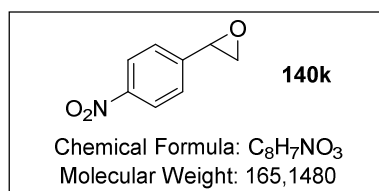
**1a,2,3,7b-tetrahydronaphtho[1,2-b]oxirene (140i)** – The reaction was performed on 5 mmol scale and the product was isolated in 77% yield.



<sup>1</sup>H-NMR (500 MHz, CDCl<sub>3</sub>): δ 7.41 (dd, *J* = 8.0 Hz, *J* = 1.3 Hz, 1H), 7.27 (td, *J* = 8.0 Hz, *J* = 1.3 Hz, 1H), 7.21 (tt, *J* = 8.0 Hz, *J* = 1.3 Hz, 1H), 7.10 (d, *J* = 8.0 Hz, 1H), 3.86 (d, *J* = 4.3 Hz, 1H), 3.77-3.72 (m, 1H), 2.80 (td, *J* = 6.7 Hz, *J* = 14.6 Hz, 1H), 2.57 (dd, *J* = 15.6 Hz, *J* = 5.6 Hz, 1H), 2.43 (dddd, *J* = 14.6 Hz, *J* = 6.7 Hz, *J* = 2.7 Hz, *J* = 1.6 Hz, 1H), 1.78 (cm, 1H).

<sup>13</sup>C-NMR (125 MHz, CDCl<sub>3</sub>): δ 136.7, 132.5, 129.5, 128.4, 128.4, 126.1, 55.1, 52.7, 24.4, 21.8.

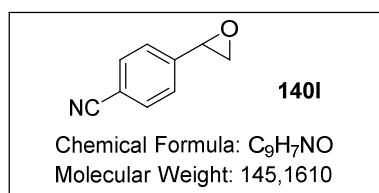
**2-(4-nitrophenyl)oxirane (140k)** – The reaction was performed on 5 mmol scale and the product was isolated in 84% yield.



<sup>1</sup>H-NMR (500 MHz, CDCl<sub>3</sub>): δ 8.28-8.20 (m, 2H), 7.50-7.42 (m, 2H), 3.99 (dd, *J* = 4.1 Hz, *J* = 2.6 Hz, 1H), 3.26 (dd, *J* = 5.6 Hz, *J* = 4.1 Hz, 1H), 2.80 (dd, *J* = 5.6 Hz, *J* = 2.6 Hz, 1H).

<sup>13</sup>C-NMR (125 MHz, CDCl<sub>3</sub>): δ 145.2, 144.1, 126.2, 123.9, 51.7, 51.5.

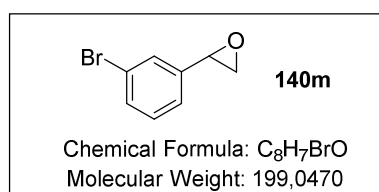
**2-(4-cyanophenyl)oxirane (140l)** – The reaction was performed on 5 mmol scale and the product was isolated in 50% yield.



<sup>1</sup>H-NMR (500 MHz, CDCl<sub>3</sub>): δ 7.59-7.55 (m, 2H), 7.34-7.30 (m, 2H), 3.84 (dd, *J* = 4.3 Hz, *J* = 2.6 Hz, 1H), 3.14 (dd, *J* = 5.4 Hz, *J* = 4.3 Hz, 1H), 2.69 (dd, *J* = 5.4 Hz, *J* = 2.6 Hz, 1H).

<sup>13</sup>C-NMR (125 MHz, CDCl<sub>3</sub>) [overlapping signals]: δ 143.3, 132.4, 126.1, 118.6, 119.9, 51.6.

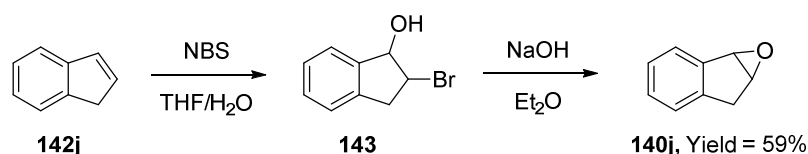
**2-(3-bromophenyl)oxirane (140m)** – The reaction was performed on 5 mmol scale and the product was isolated in 48% yield.



<sup>1</sup>H-NMR (500 MHz, CDCl<sub>3</sub>): δ 7.46-7.41 (m, 2H), 7.24-7.20 (m, 2H), 3.83 (dd, *J* = 4.2 Hz, *J* = 2.5 Hz, 1H), 3.15 (dd, *J* = 5.4 Hz, *J* = 4.2 Hz, 1H), 2.77 (dd, *J* = 5.4 Hz, *J* = 2.5 Hz, 1H).

<sup>13</sup>C-NMR (125 MHz, CDCl<sub>3</sub>): δ 140.0, 131.2, 130.1, 128.4, 124.2, 122.7, 51.6, 51.3.

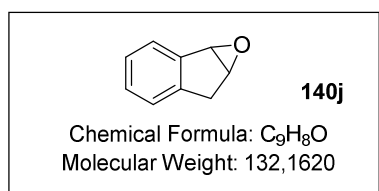
## Procedure B



In a round bottom flask, indene **142j** (580.8 mg, 5 mmol, 1 equiv.) was added to a mixture of tetrahydrofuran (10 mL) and water (3 mL). The resulting solution was cooled at 0 °C and N-Bromo succinimide (736.3 mg, 4.14 mmol, 0.83 equiv.) was added in portions. Next the reaction was allowed to reach room temperature and vigorously stirred for 20 h. Consumption of starting material was controlled by TLC and next ethyl acetate was added and the mixture was washed with brine. The resulting organic phase was dried over sodium sulfate and the solvent removed under vacuum. The obtained bromohydrin **143** (733 mg, white powder) was used without further purification in the following step.

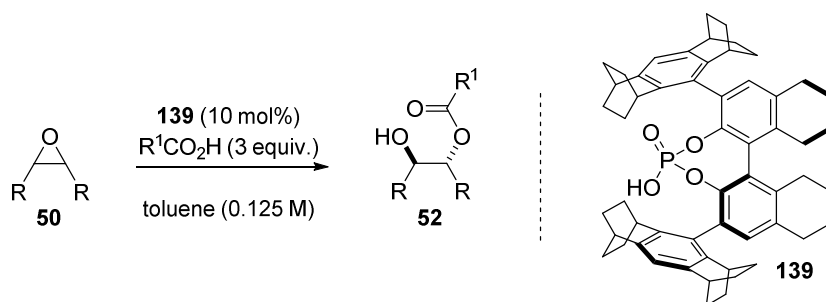
In a second round bottom flask, bromohydrin **143** (720 mg, 3.38 mmol, 1 equiv.) was dissolved in diethylether (10 mL). Next sodium hydroxide powder (338 mg, 8.45 mmol, 2.5 equiv.) was added at once and the solution was stirred at room temperature for 12 h. Water was added to the mixture and the separated aqueous phase was washed three times with diethyl ether. The collected organic phases were dried over sodium sulfate and the solvent was removed in under vacuum. Fast purification on column chromatography (mixtures hexane/MTBE) yielded the desired epoxide **140j**.

**1a,6a-dihydro-6H-indeno[1,2-b]oxirene (140j)** – The reaction was performed on 5 mmol scale and the product was isolated in 59% yield.



**<sup>1</sup>H-NMR** (500 MHz, CDCl<sub>3</sub>): δ 7.51 (d, *J* = 7.6 Hz, 1H), 7.30-7.22 (m, 2H), 7.21-7.18 (m, 1H), 4.30-4.27 (m, 1H), 4.14 (t, *J* = 2.90 Hz, 1H), 3.23 (d, *J* = 17.7 Hz, 1H), 3.00 (dd, *J* = 17.7 Hz, *J* = 3.0 Hz, 1H).

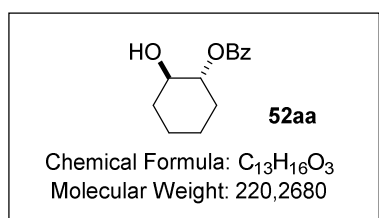
**<sup>13</sup>C-NMR** (125 MHz, CDCl<sub>3</sub>): δ 143.5, 128.5, 126.2, 126.0, 125.1, 59.1, 57.6, 34.6.

7.4.3. General procedure for the desymmetrization of *meso*-epoxides

A solution of the starting epoxide **50** (0.1 mmol) in 0.4 mL of toluene was placed in a screw-cap vial at the reaction temperature. To the stirred solution was added at once a pre-cooled solution of benzoic acid (0.3 mmol, 3 equiv.) and the catalyst (10 mol%) in toluene. The reaction was stirred for 4-6 days. Next 1 mL of MTBE was added to stop the reaction and the mixture was directly purified by flash column chromatography (eluent: mixtures hexane/MTBE). After purification the product was dissolved in DCM and submitted to an additional wash with 2 M NaOH<sub>aq</sub> to remove small impurities of benzoic acid. The enantiomeric ratios of products **52** were analyzed by HPLC on a chiral stationary phase.

For analytical purpose, the racemic samples were prepared on 0.05 mmol scale using (*RS*)-**TRIP** as the catalyst.

**(*R,R*)-2-hydroxycyclohexyl benzoate (52aa)** – The reaction was performed at  $-40^{\circ}$  C and the product was isolated as a white solid in 85% yield and e.r. = 96.5:3.5.



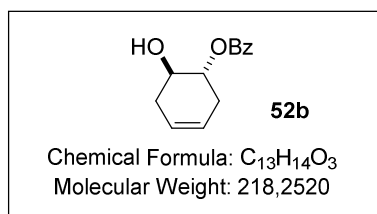
<sup>1</sup>H-NMR (500 MHz, CDCl<sub>3</sub>):  $\delta$  8.08-8.00 (m, 2H), 7.60-7.53 (m, 1H), 7.48-7.42 (m, 2H), 4.90-4.81 (cm, 1H), 3.80-3.68 (cm, 1H), 2.26 (bs, 1H), 2.20-2.05 (m, 2H), 1.85-1.70 (m, 2H), 1.50-1.20 (m, 4H).

<sup>13</sup>C-NMR (125 MHz, CDCl<sub>3</sub>):  $\delta$  166.9, 133.3, 130.5, 129.9, 128.6, 78.9, 73.0, 31.2, 30.2, 24.1, 23.9. HRMS (*m/z*) calcd for C<sub>13</sub>H<sub>16</sub>O<sub>3</sub>Na [M]<sup>+Na</sup>: 243.0992, found: 243.0992.

$[\alpha]_D^{25}$ :  $-48.0^{\circ}$  ( $c=0.870$ , CHCl<sub>3</sub>).

The enantiomeric ratio was determined by HPLC analysis using Daicel Chiralcel OD-3 column: *n*Hept:*i*PrOH = 98.5:1.5, flow rate 0.8 mL/min,  $\tau_1 = 16.9$  min,  $\tau_2 = 18.2$  min.

**(*R,R*)-6-hydroxycyclohex-3-en-1-yl benzoate (52b)** – The reaction was performed at  $-5^{\circ}\text{C}$  and the product was isolated as a colorless liquid in 86% yield and e.r. = 93.5:6.5.



$^1\text{H-NMR}$  (500 MHz,  $\text{CDCl}_3$ ):  $\delta$  8.10-8.02 (m, 2H), 7.62-7.55 (m, 1H), 7.48-7.42 (m, 2H), 5.68-5.55 (m, 2H), 5.18-5.12 (m, 1H), 4.12-4.02 (m, 1H), 2.78-2.58 (m, 2H), 2.30-2.15 (m, 3H).

$^{13}\text{C-NMR}$  (125 MHz,  $\text{CDCl}_3$ ):  $\delta$  166.8, 133.4, 130.3, 129.9,

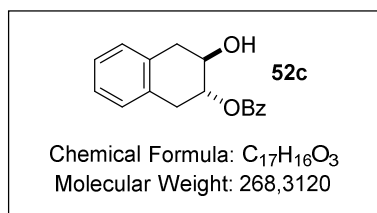
128.6, 124.5, 124.0, 75.0, 69.2, 33.1, 30.4.

**HRMS** ( $m/z$ ) calcd for  $\text{C}_{13}\text{H}_{14}\text{O}_3\text{Na}$   $[\text{M}]^{+\text{Na}}$ : 241.0835, found: 241.0833.

$[\alpha]_{\text{D}}^{25}$ :  $-106.2^{\circ}$  ( $c = 0.795$ ,  $\text{CHCl}_3$ ).

The enantiomeric ratio was determined by HPLC analysis using Daicel Chiralcel AS-3 column:  $n\text{Hept}:i\text{PrOH} = 85:15$ , flow rate 1.0 mL/min,  $\tau_1 = 4.5$  min,  $\tau_2 = 8.1$  min.

**(*R,R*)-3-hydroxy-1,2,3,4-tetrahydronaphthalen-2-yl benzoate (52c)** – The reaction was performed at  $-5^{\circ}\text{C}$  and the product was isolated as a colorless liquid in 73% yield and e.r. = 94.5:5.5.



$^1\text{H-NMR}$  (500 MHz,  $\text{CDCl}_3$ ):  $\delta$  8.10-8.02 (m, 2H), 7.62-7.55 (m, 1H), 7.48-7.42 (m, 2H), 7.22-7.08 (m, 4H), 5.30 (dt,  $J = 8.3$  Hz  $J = 8.5$  Hz,  $J = 5.7$  Hz, 1H), 4.30-4.22 (m, 1H), 3.42 (dd,  $J = 16.5$  Hz  $J = 5.7$  Hz, 1H), 3.29 (dd,  $J = 16.5$  Hz  $J = 5.7$  Hz, 1H), 3.00

(dd,  $J = 16.5$  Hz  $J = 8.5$  Hz, 1H), 2.95 (dd,  $J = 16.5$  Hz  $J = 8.5$  Hz, 1H), 2.44 (bs, 1H).

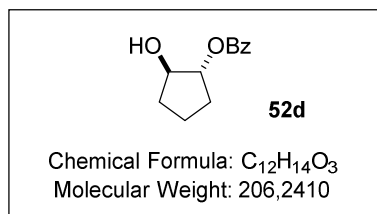
$^{13}\text{C-NMR}$  (125 MHz,  $\text{CDCl}_3$ ):  $\delta$  166.9, 133.6, 133.5, 133.2, 130.1, 129.9, 129.1, 128.9, 128.7, 126.8, 126.7, 75.5, 69.8, 36.3, 33.5.

**HRMS** ( $m/z$ ) calcd for  $\text{C}_{17}\text{H}_{16}\text{O}_3\text{Na}$   $[\text{M}]^{+\text{Na}}$ : 291.0992, found: 291.0991.

$[\alpha]_{\text{D}}^{25}$ :  $-78.5^{\circ}$  ( $c = 0.925$ ,  $\text{CHCl}_3$ ).

The enantiomeric ratio was determined by HPLC analysis using Daicel Chiralcel AS-3 column:  $n\text{Hept}:i\text{PrOH} = 85:15$ , flow rate 1.0 mL/min,  $\tau_1 = 4.6$  min,  $\tau_2 = 8.9$  min.

**(*R,R*)-2-hydroxycyclopentyl benzoate (52d)** – The reaction was performed at  $-20^{\circ}\text{C}$  and the product was isolated as a colorless liquid in 64% yield and e.r. = 95.5:4.5.



$^1\text{H-NMR}$  (500 MHz,  $\text{CDCl}_3$ ):  $\delta$  8.08-8.00 (m, 2H), 7.62-7.54 (m, 1H), 7.48-7.42 (m, 2H), 5.08-5.0 (cm, 1H), 4.30-4.20 (cm, 1H), 2.93 (s, 1H), 2.30-2.18 (m, 1H), 2.15-2.05 (m, 1H), 1.92-1.65 (m, 4H).

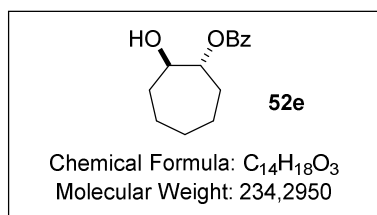
$^{13}\text{C-NMR}$  (125 MHz,  $\text{CDCl}_3$ ):  $\delta$  167.8, 133.4, 130.2, 129.9, 128.6, 84.8, 78.6, 32.9, 30.4, 22.0.

HRMS ( $m/z$ ) calcd for  $\text{C}_{12}\text{H}_{14}\text{O}_3\text{Na}$   $[\text{M}]^{+\text{Na}}$ : 229.0835, found: 229.0834.

$[\alpha]_{\text{D}}^{25}$ :  $+3.7^{\circ}$  ( $c = 0.375$ ,  $\text{CHCl}_3$ ).

The enantiomeric ratio was determined by HPLC analysis using Daicel Chiralcel OD-3 column:  $n\text{Hept}:$  $i\text{PrOH} = 98:2$ , flow rate 1.0 mL/min,  $\tau_1 = 8.1$  min,  $\tau_2 = 10.2$  min.

**(*R,R*)-2-hydroxycycloheptyl benzoate (52e)** – The reaction was performed at  $-5^{\circ}\text{C}$  and the product was isolated as a colorless liquid in 78% yield and e.r. = 95.5:4.5.



$^1\text{H-NMR}$  (500 MHz,  $\text{CDCl}_3$ ):  $\delta$  8.08-8.02 (m, 2H), 7.60-7.54 (m, 1H), 7.48-7.42 (m, 2H), 5.00-4.94 (m, 1H), 3.96-3.88 (m, 1H), 2.75 (bs, 1H), 2.00-1.30 (m, 10H).

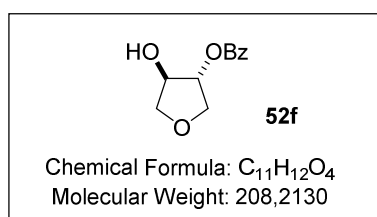
$^{13}\text{C-NMR}$  (125 MHz,  $\text{CDCl}_3$ ):  $\delta$  167.3, 133.3, 130.5, 129.9, 128.6, 83.0, 76.3, 33.0, 30.6, 28.5, 23.3, 23.2.

HRMS ( $m/z$ ) calcd for  $\text{C}_{14}\text{H}_{18}\text{O}_3\text{Na}$   $[\text{M}]^{+\text{Na}}$ : 257.1148, found: 257.1145.

$[\alpha]_{\text{D}}^{25}$ :  $-15.3^{\circ}$  ( $c = 0.770$ ,  $\text{CHCl}_3$ ).

The enantiomeric ratio was determined by HPLC analysis using Daicel Chiralcel OD-3 column:  $n\text{Hept}:$  $i\text{PrOH} = 98:2$ , flow rate 1.0 mL/min,  $\tau_1 = 8.8$  min,  $\tau_2 = 10.5$  min.

**(*R,R*)-4-hydroxytetrahydrofuran-3-yl benzoate (52f)** – The reaction was performed at  $10^{\circ}\text{C}$  and the product was isolated as a colorless liquid in 84% yield and e.r. = 95:5.



$^1\text{H-NMR}$  (500 MHz,  $\text{CDCl}_3$ ):  $\delta$  8.06-8.00 (m, 2H), 7.62-7.56 (m, 1H), 7.48-7.42 (m, 2H), 5.23 (cm, 1H), 4.48-4.42 (m, 1H), 4.26 (dd,  $J = 10.6$  Hz  $J = 5.1$  Hz, 1H), 4.12 (dd,  $J = 9.9$  Hz  $J = 5.1$  Hz, 1H), 4.00 (dd,  $J = 10.6$  Hz  $J = 2.3$  Hz, 1H), 3.81 (dd,  $J = 9.9$  Hz  $J = 2.8$  Hz, 1H), 2.69 (bs, 1H).

= 2.8 Hz, 1H), 2.69 (bs, 1H).

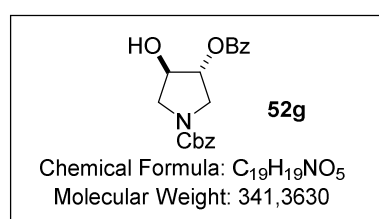
$^{13}\text{C-NMR}$  (125 MHz,  $\text{CDCl}_3$ ):  $\delta$  166.9, 133.7, 129.9, 129.5, 128.7, 81.8, 76.7, 73.8, 71.4.

**HRMS** ( $m/z$ ) calcd for  $\text{C}_{11}\text{H}_{12}\text{O}_4\text{Na}$   $[\text{M}]^{+\text{Na}}$ : 231.0628, found: 231.0629.

$[\alpha]_{\text{D}}^{25}$ :  $-20.3^\circ$  ( $c = 0.620$ ,  $\text{CHCl}_3$ ).

The enantiomeric ratio was determined by HPLC analysis using Daicel Chiralcel OD-3 column:  $n\text{Hept}:$  $i\text{PrOH} = 95:5$ , flow rate 1.0 mL/min,  $\tau_1 = 9.1$  min,  $\tau_2 = 10.4$  min.

**(*R,R*)-benzyl 3-(benzyloxy)-4-hydroxypyrrolidine-1-carboxylate (52g)** – The reaction was performed at room temperature and the product was isolated as a white solid in 83% yield and e.r. = 94:6.



$^1\text{H-NMR}$  (500 MHz,  $\text{CDCl}_3$ ):  $\delta$  7.98 (d,  $J = 7.6$  Hz, 2H), 7.58 (t,  $J = 7.6$  Hz, 1H), 7.44 (t,  $J = 7.6$  Hz, 2H), 7.40-7.27 (m, 5H), 5.34-5.26 (m, 1H), 5.20-5.13 (m, 2H), 4.42 (cm, 1H), 4.00-3.92 (m, 1H), 3.82-3.55 (m, 3H), 3.20 (bs, 1H).

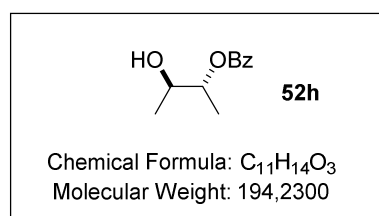
$^{13}\text{C-NMR}$  (125 MHz,  $\text{CDCl}_3$ ):  $\delta$  166.3, 166.2, 155.3, 155.3, 136.8, 136.7, 133.8, 129.9, 129.4, 128.7, 128.7, 128.2, 128.1, 78.4, 78.0, 73.9, 73.0, 67.3, 67.3, 52.5, 52.0, 49.7, 49.7 (8 additional peaks due to the presence of rotamers).

**HRMS** ( $m/z$ ) calcd for  $\text{C}_{19}\text{H}_{19}\text{NO}_5\text{Na}$   $[\text{M}]^{+\text{Na}}$ : 364.1155, found: 364.1156.

$[\alpha]_{\text{D}}^{25}$ :  $+24.4^\circ$  ( $c = 1.230$ ,  $\text{CHCl}_3$ ).

The enantiomeric ratio was determined by HPLC analysis using Daicel Chiralcel AS-3 column:  $n\text{Hept}:$  $i\text{PrOH} = 85:15$ , flow rate 1.0 mL/min,  $\tau_1 = 9.1$  min,  $\tau_2 = 11.2$  min.

**(*R,R*)-3-hydroxybutan-2-yl benzoate (52h)** – The reaction was performed at  $-20^\circ\text{C}$  and the product was isolated as a colorless liquid in 76% yield and e.r. = 95:5.



$^1\text{H-NMR}$  (500 MHz,  $\text{CDCl}_3$ ):  $\delta$  8.08-8.02 (m, 2H), 7.60-7.55 (m, 1H), 7.48-7.42 (m, 2H), 5.03 (Q,  $J = 6.4$  Hz, 1H), 3.91 (Q,  $J = 6.4$  Hz, 1H), 1.85 (bs, 1H), 1.35 (d,  $J = 6.4$  Hz, 3H), 1.26 (d,  $J = 6.4$  Hz, 3H).

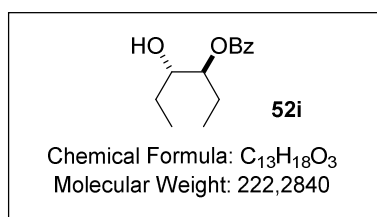
$^{13}\text{C-NMR}$  (125 MHz,  $\text{CDCl}_3$ ):  $\delta$  166.5, 133.3, 130.5, 129.8, 128.6, 75.7, 70.4, 19.3, 16.5.

**HRMS** ( $m/z$ ) calcd for  $\text{C}_{11}\text{H}_{14}\text{O}_3\text{Na}$   $[\text{M}]^{+\text{Na}}$ : 217.0835, found: 217.0833.

$[\alpha]_{\text{D}}^{25}$ :  $-39.3^\circ$  ( $c = 0.605$ ,  $\text{CHCl}_3$ ).

The enantiomeric ratio was determined by HPLC analysis using Daicel Chiralcel OD-3 column:  $n\text{Hept}:$  $i\text{PrOH} = 99:1$ , flow rate 1.0 mL/min,  $\tau_1 = 13.5$  min,  $\tau_2 = 15.4$  min.

**(S,S)-4-hydroxyhexan-3-yl benzoate (52i)** – The reaction promoted by catalyst **115b** was performed at  $-5^{\circ}\text{C}$  and the product was isolated as a colorless liquid in 85% yield and e.r. = 3.5:96.5.



$^1\text{H-NMR}$  (500 MHz,  $\text{CDCl}_3$ ):  $\delta$  8.09-8.04 (m, 2H), 7.60-7.55 (m, 1H), 7.49-7.43 (m, 2H), 5.06 (cm, 1H), 3.73-3.62 (m, 1H), 1.90-1.40 (m, 5H), 1.01 (t,  $J = 7.4$  Hz, 3H), 0.98 (t,  $J = 7.5$  Hz, 3H).

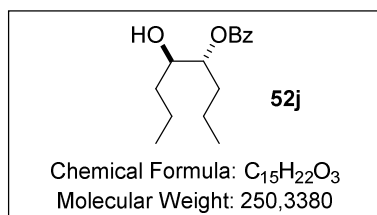
$^{13}\text{C-NMR}$  (125 MHz,  $\text{CDCl}_3$ ):  $\delta$  166.7, 133.3, 130.4, 129.9, 128.6, 78.4, 74.1, 25.9, 24.0, 10.3, 10.1.

**HRMS** ( $m/z$ ) calcd for  $\text{C}_{13}\text{H}_{18}\text{O}_3\text{Na}$   $[\text{M}]^{+\text{Na}}$ : 245.1148, found: 245.1148.

$[\alpha]_{\text{D}}^{25}$ :  $-10.1^{\circ}$  ( $c = 0.390$ ,  $\text{CHCl}_3$ ).

The enantiomeric ratio was determined by HPLC analysis using Daicel Chiralcel OD-3 column:  $n\text{Hept}:i\text{PrOH} = 99:1$ , flow rate 1.0 mL/min,  $\tau_1 = 8.7$  min,  $\tau_2 = 9.7$  min.

**(R,R)-5-hydroxyoctan-4-yl benzoate (52j)** – The reaction was performed at  $-5^{\circ}\text{C}$  and the product was isolated as a colorless liquid in 55% yield and e.r. = 95:5.



$^1\text{H-NMR}$  (500 MHz,  $\text{CDCl}_3$ ):  $\delta$  8.08-8.03 (m, 2H), 7.60-7.55 (m, 1H), 7.49-7.43 (m, 2H), 5.12 (Q,  $J = 4.1$  Hz, 1H), 3.74 (Q,  $J = 4.1$  Hz, 1H), 1.85-1.30 (m, 9H), 0.94 (t,  $J = 7.4$  Hz, 3H), 0.93 (t,  $J = 7.4$  Hz, 3H).

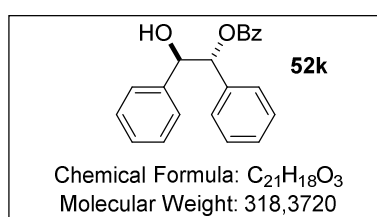
$^{13}\text{C-NMR}$  (125 MHz,  $\text{CDCl}_3$ ):  $\delta$  166.6, 133.3, 130.4, 129.9, 128.6, 77.3, 72.8, 36.1, 33.1, 19.1, 19.0, 14.2.

**HRMS** ( $m/z$ ) calcd for  $\text{C}_{15}\text{H}_{22}\text{O}_3\text{Na}$   $[\text{M}]^{+\text{Na}}$ : 273.1461, found: 273.1460.

$[\alpha]_{\text{D}}^{25}$ :  $+9.8^{\circ}$  ( $c = 0.615$ ,  $\text{CHCl}_3$ ).

The enantiomeric ratio was determined by HPLC analysis using Daicel Chiralcel OD-3 column:  $n\text{Hept}:i\text{PrOH} = 98.5:1.5$ , flow rate 1.0 mL/min,  $\tau_1 = 4.9$  min,  $\tau_2 = 6.1$  min.

**(R,R)-2-hydroxy-1,2-diphenylethyl benzoate (52k)** – The reaction was performed at room temperature and the product was isolated as a white solid in 85% yield and e.r. = 91:9.



$^1\text{H-NMR}$  (500 MHz,  $\text{CDCl}_3$ ):  $\delta$  8.14-8.06 (m, 2H), 7.62-7.56 (m, 1H), 7.50-7.43 (m, 2H), 7.26-7.15 (m, 10H), 6.11 (d,  $J = 7.3$  Hz, 1H), 5.10 (d,  $J = 7.3$  Hz, 1H), 2.63 (bs, 1H).

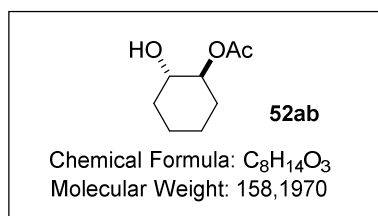
$^{13}\text{C-NMR}$  (125 MHz,  $\text{CDCl}_3$ ):  $\delta$  166.0, 139.2, 137.0, 133.5, 130.2, 130.0, 128.7, 128.5, 128.4, 128.4, 128.3, 127.5, 127.3, 80.8, 77.4.

**HRMS** ( $m/z$ ) calcd for  $\text{C}_{21}\text{H}_{18}\text{O}_3\text{Na}$  [ $\text{M}$ ] $^{+\text{Na}}$ : 341.1148, found: 341.1150.

$[\alpha]_{\text{D}}^{25}$ : +64.2° ( $c = 1.275$ ,  $\text{CHCl}_3$ ).

The enantiomeric ratio was determined by HPLC analysis using Daicel Chiralcel OD-3 column:  $n\text{Hept}:$  $i\text{PrOH} = 90:10$ , flow rate 1.0 mL/min,  $\tau_1 = 6.8$  min,  $\tau_2 = 7.7$  min.

**(*S,S*)-2-hydroxycyclohexyl acetate (52ab)** – This product was obtained during the optimization of the reaction conditions (Table 4.19).

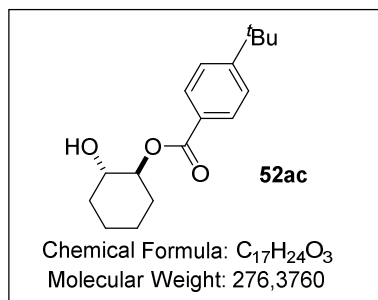


$^1\text{H-NMR}$  (500 MHz,  $\text{CDCl}_3$ ):  $\delta$  4.58-4.42 (m, 1H), 3.55-3.45 (m, 1H), 2.03 (s, 3H), 2.02-1.95 (m, 2H), 1.71-1.60 (m, 2H), 1.35-1.10 (m, 4H).

$^{13}\text{C-NMR}$  (125 MHz,  $\text{CDCl}_3$ ):  $\delta$  171.4, 78.4, 72.9, 33.1, 30.0, 23.9, 23.8, 21.4.

The enantiomeric ratio was determined by GC analysis using BGB 178/BGB 15 G 615 column [Gas: Hydrogen 0.50 bar, Temperature: 80 1,2/Min 140 18/Min 220 5 Min iso.  $\tau_1 = 30.3$  min,  $\tau_2 = 33.0$  min.]

**(*S,S*)-2-hydroxycyclohexyl 4-(tert-butyl)benzoate (52ac)** – This product was obtained during the optimization of the reaction conditions (Table 4.19).



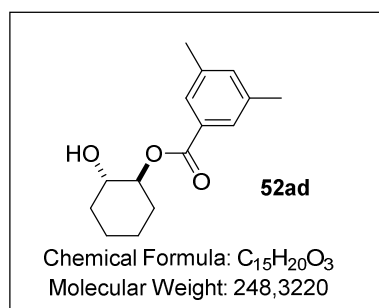
$^1\text{H-NMR}$  (500 MHz,  $\text{CDCl}_3$ ):  $\delta$  7.98-7.86 (m, 2H), 7.45-7.35 (m, 2H), 4.82-4.73 (m, 1H), 3.75-3.63 (m, 1H), 2.15-2.00 (m, 2H), 1.75-1.65 (m, 2H), 1.27 (s, 9H), 1.42-1.10 (m, 4H).

$^{13}\text{C-NMR}$  (125 MHz,  $\text{CDCl}_3$ ):  $\delta$  166.8, 156.8, 129.6, 127.5, 125.4, 78.6, 72.9, 35.1, 32.9, 31.1, 30.0, 23.9, 23.8.

The enantiomeric ratio was determined by HPLC analysis using Daicel Chiralcel OD-3 column:  $n\text{Hept}:$  $i\text{PrOH} = 98:2$ , flow rate 1.0 mL/min,  $\tau_1 = 7.1$  min,  $\tau_2 = 11.4$  min.



**(*S,S*)-2-hydroxycyclohexyl 3,5-dimethylbenzoate (52ad)** – This product was obtained during the optimization of the reaction conditions (Table 4.19).

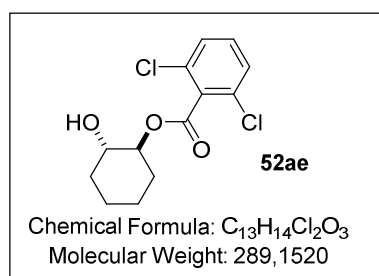


**$^1\text{H-NMR}$**  (500 MHz,  $\text{CDCl}_3$ ):  $\delta$  7.59 (s, 2H), 7.13 (s, 1H), 4.82-4.71 (m, 1H), 3.75-3.62 (m, 1H), 2.29 (s, 6H), 2.15-2.00 (m, 2H), 1.78-1.65 (m, 2H), 1.50-1.10 (m, 4H).

**$^{13}\text{C-NMR}$**  (125 MHz,  $\text{CDCl}_3$ ):  $\delta$  167.1, 138.1, 134.7, 130.1, 127.4, 78.7, 72.9, 33.0, 30.0, 24.0, 23.8, 21.2.

The enantiomeric ratio was determined by HPLC analysis using Daicel Chiralcel OD-3 column: *n*Hept:*i*PrOH = 99:1, flow rate 1.0 mL/min,  $\tau_1 = 17.4$  min,  $\tau_2 = 19.6$  min.

**(*S,S*)-2-hydroxycyclohexyl 2,6-dichlorobenzoate (52ae)** – This product was obtained during the optimization of the reaction conditions (Table 4.19).

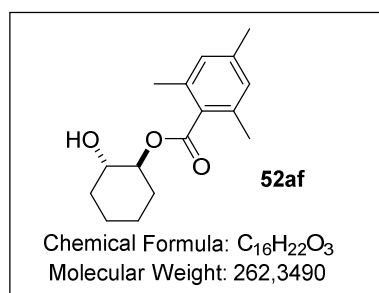


**$^1\text{H-NMR}$**  (500 MHz,  $\text{CDCl}_3$ ):  $\delta$  7.30-7.20 (m, 3H), 4.88-4.80 (m, 1H), 3.68-3.60 (m, 1H), 2.26-2.18 (m, 1H), 2.10-2.00 (m, 1H), 1.75-1.65 (m, 2H), 1.50-1.20 (m, 4H).

**$^{13}\text{C-NMR}$**  (125 MHz,  $\text{CDCl}_3$ ):  $\delta$  164.5, 133.7, 131.7, 130.9, 127.9, 80.7, 72.3, 32.4, 29.6, 23.9, 23.7.

The enantiomeric ratio was determined by HPLC analysis using Daicel Chiralcel OD-3 column: *n*Hept:*i*PrOH = 98:2, flow rate 1.0 mL/min,  $\tau_1 = 8.0$  min,  $\tau_2 = 8.9$  min.

**(*S,S*)-2-hydroxycyclohexyl 2,4,6-trimethylbenzoate (52af)** – This product was obtained during the optimization of the reaction conditions (Scheme 4.9).

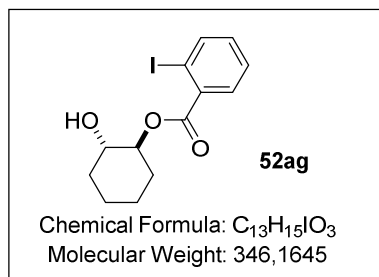


**$^1\text{H-NMR}$**  (500 MHz,  $\text{CDCl}_3$ ):  $\delta$  6.79 (s, 2H), 4.85-4.75 (m, 1H), 3.65-3.54 (m, 1H), 2.24 (s, 6H), 2.21 (s, 3H), 2.18-2.13 (m, 1H), 2.06-1.95 (m, 1H), 1.75-1.65 (m, 2H), 1.50-1.20 (m, 4H).

**$^{13}\text{C-NMR}$**  (125 MHz,  $\text{CDCl}_3$ ):  $\delta$  170.3, 139.4, 134.9, 131.1, 128.4, 78.9, 72.8, 33.2, 30.1, 24.0, 23.8, 21.1, 19.7.

The enantiomeric ratio was determined by HPLC analysis using Daicel Chiralcel OD-3 column: *n*Hept:*i*PrOH = 98.5:1.5, flow rate 0.8 mL/min,  $\tau_1 = 10.8$  min,  $\tau_2 = 11.4$  min.

**(S,S)- 2-hydroxycyclohexyl 2-iodobenzoate (52ag)** – This product was obtained during the optimization of the reaction conditions (Scheme 4.9).

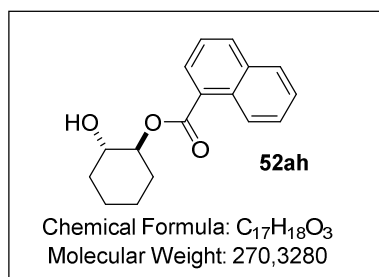


<sup>1</sup>H-NMR (500 MHz, CDCl<sub>3</sub>): δ 7.92 (dd, *J* = 7.7 Hz, *J* = 1.2 Hz, 1H), 7.72 (dd, *J* = 7.7 Hz, *J* = 1.7 Hz, 1H), 7.35 (td, *J* = 7.7 Hz, *J* = 1.2 Hz, 1H), 7.09 (td, *J* = 7.7 Hz, *J* = 1.7 Hz, 1H), 4.84-4.75 (m, 1H), 3.74-3.66 (m, 1H), 2.24-2.25 (m, 1H), 2.10-2.00 (m, 1H), 1.75-1.65 (m, 2H), 1.50-1.17 (m, 4H).

<sup>13</sup>C-NMR (125 MHz, CDCl<sub>3</sub>): δ 166.7, 141.1, 135.8, 132.6, 131.1, 128.0, 93.7, 80.0, 72.6, 32.9, 29.9, 23.9, 23.8.

The enantiomeric ratio was determined by HPLC analysis using Daicel Chiralcel OD-3 column: *n*Hept.:*i*PrOH = 98:2, flow rate 1.0 mL/min, τ<sub>1</sub> = 17.1 min, τ<sub>2</sub> = 19.4 min.

**(S,S)- 2-hydroxycyclohexyl 1-naphthoate (52ah)** – This product was obtained during the optimization of the reaction conditions (Scheme 4.9).

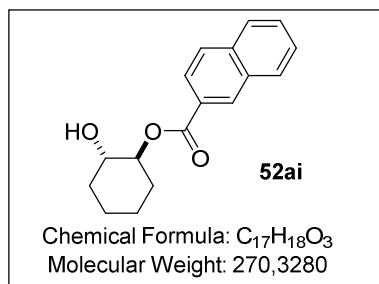


<sup>1</sup>H-NMR (500 MHz, CDCl<sub>3</sub>): δ 8.82 (d, *J* = 8.5 Hz, 1H), 8.11 (dd, *J* = 7.3 Hz, *J* = 1.2 Hz, 1H), 7.96 (d, *J* = 8.2 Hz, 1H), 7.82 (d, *J* = 8.2 Hz, 1H), 7.58-7.52 (m, 1H), 7.50-7.40 (m, 2H), 4.95-4.85 (m, 1H), 3.78-3.68 (m, 1H), 2.28-2.18 (m, 1H), 2.15-2.02 (m, 1H), 1.80-1.70 (m, 2H), 1.50-1.20 (m, 4H).

<sup>13</sup>C-NMR (125 MHz, CDCl<sub>3</sub>): δ 167.8, 133.8, 133.4, 131.3, 130.0, 128.6, 127.8, 127.5, 126.3, 125.8, 124.5, 78.9, 73.0, 33.2, 30.1, 24.0, 23.8.

The enantiomeric ratio was determined by HPLC analysis using Daicel Chiralcel OD-3 column: *n*Hept.:*i*PrOH = 98:2, flow rate 1.0 mL/min, τ<sub>1</sub> = 20.4 min, τ<sub>2</sub> = 24.1 min.

**(S,S)-2-hydroxycyclohexyl 2-naphthoate (52ai)** – This product was obtained during the optimization of the reaction conditions (Scheme 4.9).

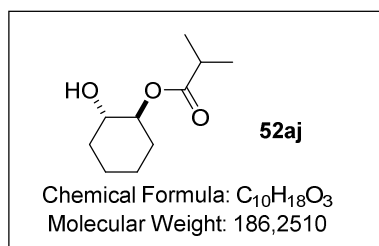


<sup>1</sup>H-NMR (500 MHz, CDCl<sub>3</sub>): δ 8.55 (s, 1H), 8.00 (dd, *J* = 8.6 Hz, *J* = 1.5 Hz, 1H), 7.89 (d, *J* = 8.0 Hz, 1H), 7.82 (m, 2H), 7.56-7.51 (m, 1H), 7.50-7.46 (m, 1H), 4.90-4.82 (m, 1H), 3.78-3.68 (m, 1H), 2.20-2.02 (m, 2H), 1.78-1.68 (m, 2H), 1.50-1.20 (m, 4H).

<sup>13</sup>C-NMR (125 MHz, CDCl<sub>3</sub>): δ 167.0, 135.6, 132.5, 131.2, 129.4, 128.3, 128.2, 127.8, 127.5, 126.7, 125.3, 78.9, 73.0, 33.1, 30.1, 24.0, 23.8.

The enantiomeric ratio was determined by HPLC analysis using Daicel Chiralcel OD-3 column: *n*Hept:*i*PrOH = 98:2, flow rate 1.0 mL/min,  $\tau_1 = 18.0$  min,  $\tau_2 = 23.5$  min.

**(*S,S*)-2-hydroxycyclohexyl isobutyrate (52aj)** – This product was obtained during the optimization of the reaction conditions (Table 4.19).



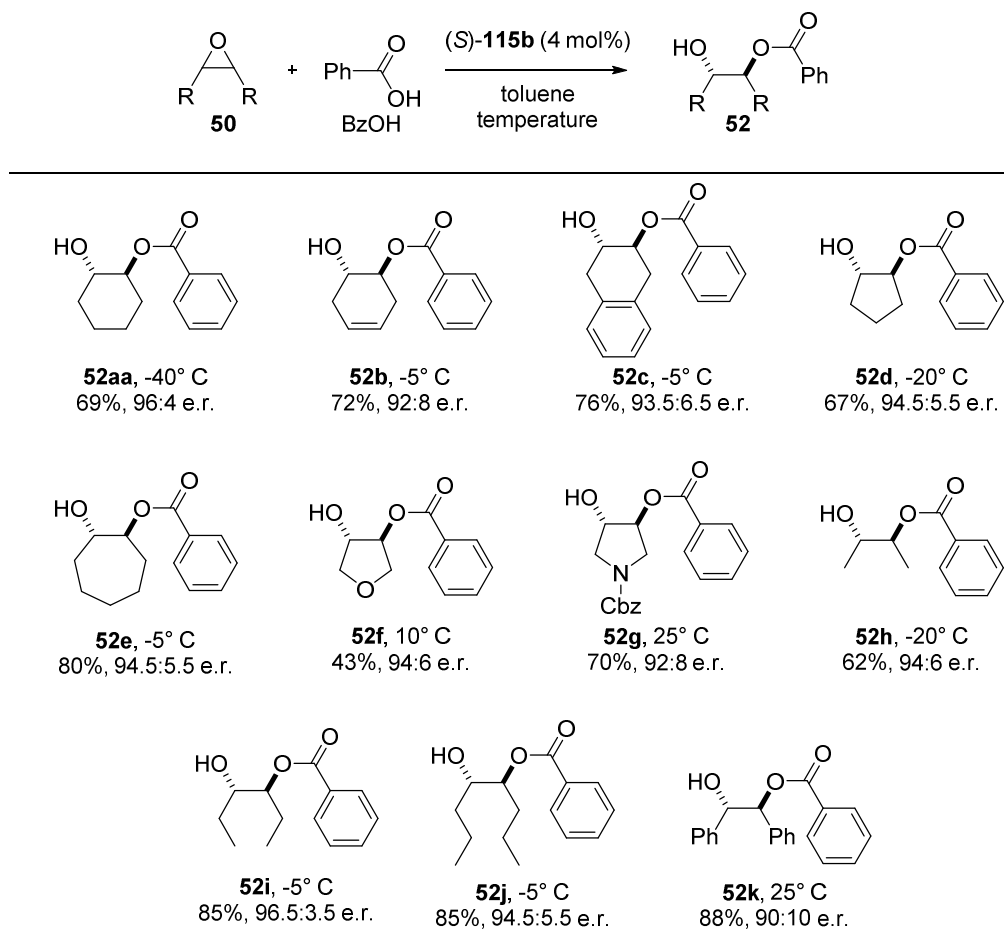
**<sup>1</sup>H-NMR** (500 MHz, CDCl<sub>3</sub>):  $\delta$  4.58-4.45 (m, 1H), 3.55-3.46 (m, 1H), 2.50 (sept,  $J = 7.1$  Hz, 1H), 2.05-1.90 (m, 2H), 1.70-1.60 (m, 2H), 1.38-1.20 (m, 4H), 1.12 (d,  $J = 7.1$  Hz, 3H), 1.11 (d,  $J = 7.1$  Hz, 3H).

**<sup>13</sup>C-NMR** (125 MHz, CDCl<sub>3</sub>):  $\delta$  177.5, 77.9, 72.9, 34.2, 33.0, 29.9, 23.9, 23.8, 19.1, 19.0.

The enantiomeric ratio was determined by GC analysis using Hydrodex BTBDAC G 625 column [Gas: Hydrogen 0.40 bar, Temperature: 115 40 min iso, 18/Min 220 5 Min iso.  $\tau_1 = 28.5$  min,  $\tau_2 = 29.3$  min.]

**7.4.3.1. Scope of the desymmetrization of *meso*-epoxide with catalyst (S)-115b**

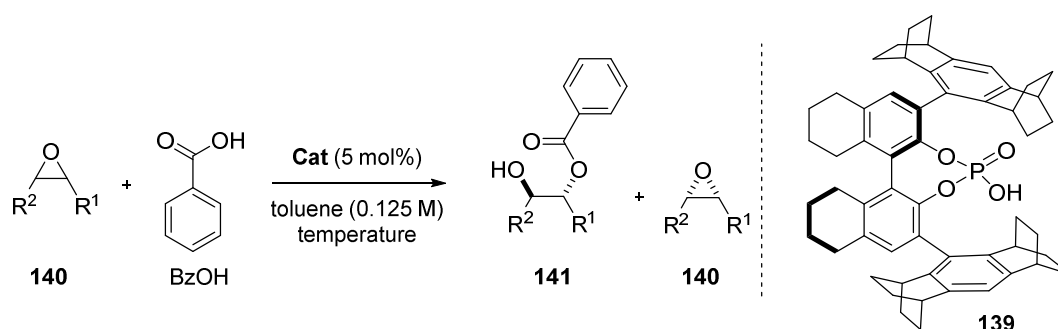
In order to explore the catalytic activity of phosphoric acid **115b**, we investigated the scope of the desymmetrization of *meso*-epoxides with benzoic acid. The same procedure described in paragraph 7.4.3. was used and the results are showed in the scheme below.



Reactions were performed on a 0.1 mmol scale. Enantiomeric ratios were determined by HPLC on chiral stationary phase.

Compared to **139**, phosphoric acid **115b** was found similarly active in the carboxylolysis reaction. However, with the only exception of product **52i**, catalyst **115b** generally afforded the desired products in reduced enantiopurities with respect to **139**.

## 7.4.4. General procedure for the kinetic resolution of racemic epoxides



In a screw-cap vial epoxide **140** (0.1 mmol) was dissolved in 0.4 mL of toluene and was cooled to the reaction temperature. Then a pre-cooled solution of benzoic acid (0.06 mmol, 0.6 equiv.) and catalyst **139** (4 mol%) in 0.4 mL of toluene was added and the reaction was stirred for 1-5 days. Next  $\text{NaHCO}_3$  (20 mg) was added to quench the reaction. The reaction mixture was then analyzed by NMR spectroscopy with internal standard and product **141** and unreacted starting material were isolated by preparative thin layer chromatography for the determination of the enantiomeric ratio.

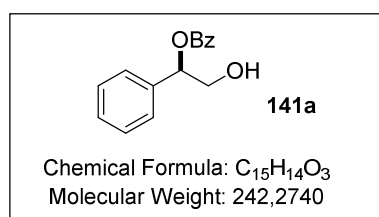
For analytical purpose, the racemic samples were prepared on 0.05 mmol scale using (*RS*)-**TRIP** as the catalyst.

**(*R*)-2-hydroxy-1-phenylethyl benzoate (141a)** – The reaction was performed at  $-20\text{ }^\circ\text{C}$ .

Product: 40% yield, e.r. = 95.7:4.3

Starting material: 55% yield, e.r. = 82.6:17.4.

$S = 43.7$ ;  $\text{conv}_{\text{calc}} = 41.6\%$



**$^1\text{H-NMR}$**  (500 MHz,  $\text{CDCl}_3$ ):  $\delta$  8.15-8.10 (m, 2H), 7.65-7.55 (m, 1H), 7.52-7.44 (m, 4H), 7.42-7.37 (m, 2H), 7.36-7.31 (m, 1H), 6.13 (dd,  $J = 7.5\text{ Hz}$ ,  $J = 3.8\text{ Hz}$ , 1H), 4.05 ((dd,  $J = 12.1\text{ Hz}$ ,  $J = 7.5\text{ Hz}$ , 1H), 3.96 (dd,  $J = 12.1\text{ Hz}$ ,  $J = 3.8\text{ Hz}$ , 1H), 2.04 (bs,

1H).

**$^{13}\text{C-NMR}$**  (125 MHz,  $\text{CDCl}_3$ ):  $\delta$  166.1, 137.0, 133.2, 129.9, 129.7, 128.7, 128.5, 128.4, 126.6, 77.4, 66.1.

**HRMS** ( $m/z$ ) calcd for  $\text{C}_{15}\text{H}_{14}\text{O}_3\text{Na}$  [ $\text{M}$ ] $^{+\text{Na}}$ : 265.0835, found: 265.0835.

The enantiomeric ratio was determined by HPLC analysis:

**141a** - Daicel Chiralcel AD-3 column: *n*Hept:*i*PrOH = 90:10, flow rate 1.0 mL/min,  $\tau_1 = 7.7$  min,  $\tau_2 = 13.9$  min.

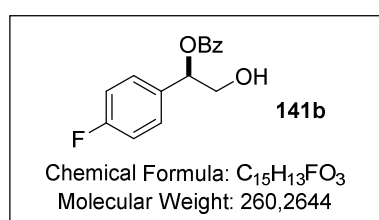
**(R)-2-phenyloxirane (140a)** - Daicel Chiralcel OD-3 column: *n*Hept:*i*PrOH = 99.5:0.5, flow rate 1.0 mL/min,  $\tau_1 = 5.2$  min,  $\tau_2 = 5.7$  min.

**(R)-1-(4-fluorophenyl)-2-hydroxyethyl benzoate (141b)** – Reaction performed at  $-20$  °C.

Product: 50% yield, e.r. = 93.3:6.7

Starting material: 46% yield, e.r. = 96.7:3.3.

S = 47.9;  $\text{conv}_{\text{calc}} = 51.9\%$



**$^1\text{H-NMR}$**  (500 MHz,  $\text{CDCl}_3$ ):  $\delta$  8.08-8.04 (m, 2H), 7.58-7.54 (m, 1H), 7.45-7.38 (m, 4H), 7.07-7.00 (m, 2H), 6.15 (dd,  $J = 7.5$  Hz,  $J = 3.9$  Hz, 1H), 4.00 (dd,  $J = 12.0$  Hz,  $J = 7.5$  Hz, 1H), 3.90 (dd,  $J = 12.0$  Hz,  $J = 3.9$  Hz, 1H).

**$^{13}\text{C-NMR}$**  (125 MHz,  $\text{CDCl}_3$ ):  $\delta$  166.0, 162.7 (d,  $J = 247.2$  Hz), 133.3, 133.0 (d,  $J = 3.4$  Hz), 129.8, 129.7, 128.5, 128.5 (d,  $J = 8.3$  Hz), 115.7 (d,  $J = 22.3$  Hz), 76.7, 66.0.

**HRMS** ( $m/z$ ) calcd for  $\text{C}_{15}\text{H}_{13}\text{FO}_3\text{Na}$   $[\text{M}]^{+\text{Na}}$ : 283.0741, found: 283.0741.

The enantiomeric ratio was determined by HPLC analysis:

**141b** - Daicel Chiralcel AD-3 column: *n*Hept:*i*PrOH = 90:10, flow rate 1.0 mL/min,  $\tau_1 = 7.3$  min,  $\tau_2 = 11.3$  min.

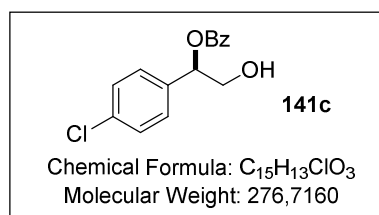
**(R)-2-(4-fluorophenyl)oxirane (140b)** - Daicel Chiralcel IA column: *n*Hept:*i*PrOH = 99.5:0.5, flow rate 1.0 mL/min,  $\tau_1 = 6.4$  min,  $\tau_2 = 6.9$  min.

**(R)-1-(4-chlorophenyl)-2-hydroxyethyl benzoate (141c)** – Reaction performed at  $-20$  °C.

Product: 30% yield, e.r. = 96.9:3.1

Starting material: 61% yield, e.r. = 73.5:26.5.

S = 49.8;  $\text{conv}_{\text{calc}} = 33.4\%$



**$^1\text{H-NMR}$**  (500 MHz,  $\text{CDCl}_3$ ):  $\delta$  8.08-8.04 (m, 2H), 7.56-7.52 (m, 1H), 7.46-7.38 (m, 2H), 7.37-7.27 (m, 4H), 6.03 (dd,  $J = 7.5$  Hz,  $J = 4.1$  Hz, 1H), 3.98 (dd,  $J = 12.2$  Hz,  $J = 7.5$  Hz, 1H), 3.89 (dd,  $J = 12.2$  Hz,  $J = 4.1$  Hz, 1H), 2.31 (bs, 1H).

**$^{13}\text{C-NMR}$**  (125 MHz,  $\text{CDCl}_3$ ):  $\delta$  166.0, 135.6, 134.3, 133.4, 129.7, 129.6, 128.9, 128.5, 128.0, 76.6, 65.9.

**HRMS** ( $m/z$ ) calcd for  $C_{15}H_{13}ClO_3Na$   $[M]^{+Na}$ : 299.0445, found: 299.0446.

The enantiomeric ratio was determined by HPLC analysis:

**141c** - Daicel Chiralcel AD-3 column:  $n$ Hept: $i$ PrOH = 90:10, flow rate 1.0 mL/min,  $\tau_1$  = 7.8 min,  $\tau_2$  = 12.1 min.

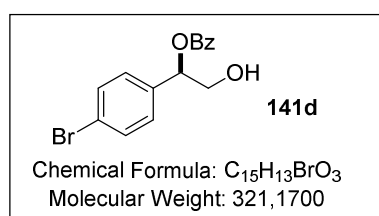
**(R)-2-(4-chlorophenyl)oxirane (140c)** - Daicel Chiralcel AS-3 column:  $n$ Hept: $i$ PrOH = 99:1, flow rate 1.0 mL/min,  $\tau_1$  = 6.3 min,  $\tau_2$  = 7.9 min.

**(R)-1-(4-bromophenyl)-2-hydroxyethyl benzoate (141d)** – Reaction performed at  $-20$  °C.

Product: 28% yield, e.r. = 97.0:3.0

Starting material: 51% yield, e.r. = 71.0:29.0.

$S$  = 48.9;  $conv_{calc}$  = 30.9%



**$^1H$ -NMR** (500 MHz,  $CDCl_3$ ):  $\delta$  8.06-8.03 (m, 2H), 7.58-7.52 (m, 1H), 7.51-7.40 (m, 4H), 7.32-7.26 (m, 2H), 6.01 (dd,  $J$  = 7.4 Hz,  $J$  = 4.1 Hz, 1H), 3.98 (dd,  $J$  = 12.2 Hz,  $J$  = 7.4 Hz, 1H), 3.90 (dd,  $J$  = 12.2 Hz,  $J$  = 4.1 Hz, 1H), 1.99 (bs, 1H).

**$^{13}C$ -NMR** (125 MHz,  $CDCl_3$ ):  $\delta$  166.0, 136.2, 133.4, 131.9, 129.7, 129.7, 128.5, 128.3, 122.5, 76.7, 65.9.

**HRMS** ( $m/z$ ) calcd for  $C_{15}H_{13}BrO_3Na$   $[M]^{+Na}$ : 342.9940, found: 342.9941.

The enantiomeric ratio was determined by HPLC analysis:

**141d** - Daicel Chiralcel AD-3 column:  $n$ Hept: $i$ PrOH = 90:10, flow rate 1.0 mL/min,  $\tau_1$  = 8.8 min,  $\tau_2$  = 14.3 min.

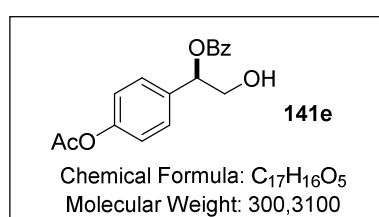
**(R)-2-(4-bromophenyl)oxirane (140d)** - Daicel Chiralcel AS-3 column:  $n$ Hept: $i$ PrOH = 99:1, flow rate 1.0 mL/min,  $\tau_1$  = 6.4 min,  $\tau_2$  = 8.2 min.

**(R)-1-(4-acetoxyphenyl)-2-hydroxyethyl benzoate (141e)** – Reaction performed at  $-20$  °C.

Product: 46% yield, e.r. = 93.4:6.6

Starting material: 45% yield, e.r. = 95.8:4.2.

$S$  = 45.6;  $conv_{calc}$  = 51.4%



**$^1H$ -NMR** (500 MHz,  $CDCl_3$ ):  $\delta$  8.13-8.08 (m, 2H), 7.62-7.54 (m, 1H), 7.50-7.42 (m, 4H), 7.14-7.06 (m, 2H), 6.10 (dd,  $J$  = 7.5 Hz,  $J$  = 4.0 Hz, 1H), 4.02 (dd,  $J$  = 12.2 Hz,  $J$  = 7.5 Hz, 1H), 3.93 (dd,  $J$  = 12.2 Hz,  $J$  = 4.0 Hz, 1H), 2.29 (s, 3H).

$^{13}\text{C-NMR}$  (125 MHz,  $\text{CDCl}_3$ ):  $\delta$  169.4, 166.0, 150.6, 134.7, 133.3, 129.8, 129.7, 128.5, 127.9, 121.9, 76.7, 66.0, 21.1.

**HRMS** ( $m/z$ ) calcd for  $\text{C}_{17}\text{H}_{16}\text{O}_5\text{Na}$  [ $\text{M}$ ] $^{+\text{Na}}$ : 323.0890, found: 323.0889.

The enantiomeric ratio was determined by HPLC analysis:

**141e** - Daicel Chiralcel AD-3 column:  $n\text{Hept}:i\text{PrOH}$  = 90:10, flow rate 1.0 mL/min,  $\tau_1$  = 12.7 min,  $\tau_2$  = 17.8 min.

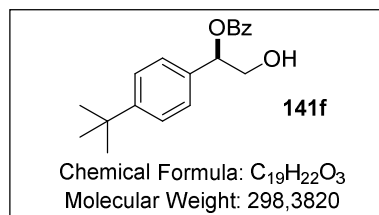
**(R)-4-(oxiran-2-yl)phenyl acetate (140e)** - Daicel Chiralcel OD-3 column:  $n\text{Hept}:i\text{PrOH}$  = 99:1, flow rate 1.0 mL/min,  $\tau_1$  = 9.5 min,  $\tau_2$  = 10.3 min.

**(R)-1-(4-(tert-butyl)phenyl)-2-hydroxyethyl benzoate (141f)** – Reaction performed at  $-40\text{ }^\circ\text{C}$ .

Product: 50% yield, e.r. = 95.3:4.7

Starting material: 47% yield, e.r. = 97.2:2.8.

$S$  = 73.2;  $\text{conv}_{\text{calc}}$  = 51%



$^1\text{H-NMR}$  (500 MHz,  $\text{CDCl}_3$ ):  $\delta$  8.13-8.07 (m, 2H), 7.60-7.54 (m, 1H), 7.48-7.42 (m, 2H), 7.41-7.35 (m, 4H), 6.11 (dd,  $J$  = 7.6 Hz,  $J$  = 4.0 Hz, 1H), 4.05 (dd,  $J$  = 12.1 Hz,  $J$  = 7.6 Hz, 1H), 3.95 (dd,  $J$  = 12.1 Hz,  $J$  = 4.0 Hz, 1H), 1.31 (s, 9H).

$^{13}\text{C-NMR}$  (125 MHz,  $\text{CDCl}_3$ ):  $\delta$  166.2, 151.4, 133.9, 133.2, 130.0, 129.7, 128.4, 126.4, 125.6, 77.3, 66.2, 34.6, 31.3.

**HRMS** ( $m/z$ ) calcd for  $\text{C}_{19}\text{H}_{22}\text{O}_3\text{Na}$  [ $\text{M}$ ] $^{+\text{Na}}$ : 321.1461, found: 321.1461.

The enantiomeric ratio was determined by HPLC analysis:

**141f** - Daicel Chiralcel AD-3 column:  $n\text{Hept}:i\text{PrOH}$  = 90:10, flow rate 1.0 mL/min,  $\tau_1$  = 5.7 min,  $\tau_2$  = 7.8 min.

**(R)-2-(4-(tert-butyl)phenyl)oxirane (140f)** - Daicel Chiralcel OJ-H column:  $n\text{Hept}:i\text{PrOH}$  = 99:1, flow rate 1.0 mL/min,  $\tau_1$  = 8.2 min,  $\tau_2$  = 8.9 min.

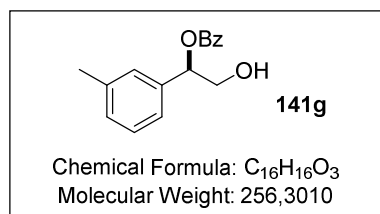


**(R)-2-hydroxy-1-(m-tolyl)ethyl benzoate (141g)** – Reaction performed at  $-20\text{ }^{\circ}\text{C}$ .

Product: 47% yield, e.r. = 94.3:5.7

Starting material: 44% yield, e.r. = 97.5:2.5.

S = 61.3;  $\text{conv}_{\text{calc}} = 51.7\%$



$^1\text{H-NMR}$  (500 MHz,  $\text{CDCl}_3$ ):  $\delta$  8.13-8.07 (m, 2H), 7.62-7.55 (m, 1H), 7.50-7.42 (m, 2H), 7.30-7.23 (m, 3H), 7.17-7.12 (m, 1H), 6.07 (dd,  $J = 7.6\text{ Hz}$ ,  $J = 4.0\text{ Hz}$ , 1H), 4.04 (dd,  $J = 12.0\text{ Hz}$ ,  $J = 7.6\text{ Hz}$ , 1H), 3.94 (dd,  $J = 12.0\text{ Hz}$ ,  $J = 4.0\text{ Hz}$ , 1H), 2.36 (s, 3H),

2.03 (bs, 1H).

$^{13}\text{C-NMR}$  (125 MHz,  $\text{CDCl}_3$ ):  $\delta$  166.1, 138.4, 136.9, 133.2, 130.0, 129.7, 129.3, 128.6, 128.4, 127.3, 123.6, 77.5, 66.2, 21.4.

**HRMS** ( $m/z$ ) calcd for  $\text{C}_{16}\text{H}_{16}\text{O}_3\text{Na}$   $[\text{M}]^{+\text{Na}}$ : 279.0992, found: 279.0991.

The enantiomeric ratio was determined by HPLC analysis:

**141g** - Daicel Chiralcel AD-3 column:  $n\text{Hept}:\text{iPrOH} = 90:10$ , flow rate 1.0 mL/min,  $\tau_1 = 6.9\text{ min}$ ,  $\tau_2 = 15.5\text{ min}$ .

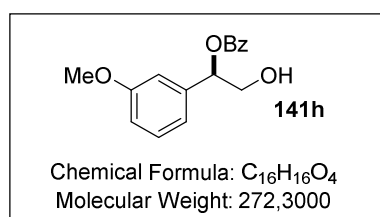
**(R)-2-(m-tolyl)oxirane (140g)** - Daicel Chiralcel OD-3 column:  $n\text{Hept}:\text{iPrOH} = 99.5:0.5$ , flow rate 1.0 mL/min,  $\tau_1 = 4.9\text{ min}$ ,  $\tau_2 = 5.2\text{ min}$ .

**(R)-2-hydroxy-1-(3-methoxyphenyl)ethyl benzoate (141h)** – Reaction performed at  $4\text{ }^{\circ}\text{C}$ .

Product: 48% yield, e.r. = 91.2:8.8

Starting material: 45% yield, e.r. = 93.2:6.8.

S = 28.7;  $\text{conv}_{\text{calc}} = 51.2\%$



$^1\text{H-NMR}$  (500 MHz,  $\text{CDCl}_3$ ):  $\delta$  8.14-8.08 (m, 2H), 7.62-7.55 (m, 1H), 7.50-7.42 (m, 2H), 7.30 (t,  $J = 7.7\text{ Hz}$ , 1H), 7.03 (d,  $J = 7.7\text{ Hz}$ , 1H), 6.99 (cm, 1H), 6.87 (dd,  $J = 7.7\text{ Hz}$ ,  $J = 2.7\text{ Hz}$ , 1H), 6.08 (dd,  $J = 7.6\text{ Hz}$ ,  $J = 4.0\text{ Hz}$ , 1H), 4.03 (dd,  $J = 12.1\text{ Hz}$ ,  $J =$

7.6 Hz, 1H), 3.95 (dd,  $J = 12.1\text{ Hz}$ ,  $J = 4.0\text{ Hz}$ , 1H), 3.81 (s, 3H).

$^{13}\text{C NMR}$  (125 MHz,  $\text{CDCl}_3$ ):  $\delta$  166.1, 159.7, 138.6, 133.2, 129.9, 129.8, 129.7, 128.4, 118.8, 113.6, 112.5, 77.3, 66.2, 55.2.

**HRMS** ( $m/z$ ) calcd for  $\text{C}_{16}\text{H}_{16}\text{O}_4\text{Na}$   $[\text{M}]^{+\text{Na}}$ : 295.0941, found: 295.0941.

The enantiomeric ratio was determined by HPLC analysis:

**141h** - Daicel Chiralcel AD-3 column: *n*Hept:*i*PrOH = 90:10, flow rate 1.0 mL/min,  $\tau_1 = 10.9$  min,  $\tau_2 = 17.0$  min.

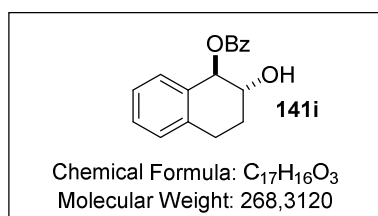
**(R)-2-(3-methoxyphenyl)oxirane (140h)** - Daicel Chiralcel AS-3 column: *n*Hept:*i*PrOH = 99:1, flow rate 1.0 mL/min,  $\tau_1 = 10.9$  min,  $\tau_2 = 17.0$  min.

**(R,R)-2-hydroxy-1,2,3,4-tetrahydronaphthalen-1-yl benzoate (141i)** – Reaction performed at -50 °C. Catalyst loading = 2 mol%

Product: 45% yield, e.r. = 98:2

Starting material: 55% yield, e.r. = 81.2:18.8.

S = 93.1;  $\text{conv}_{\text{calc}} = 39.4\%$



<sup>1</sup>H-NMR (500 MHz, CDCl<sub>3</sub>):  $\delta$  8.13-8.08 (m, 2H), 7.62-7.57 (m, 1H), 7.49-7.43 (m, 2H), 7.34-7.15 (m, 4H), 6.16 (d, *J* = 6.5 Hz, 1H), 4.28-4.16 (m, 1H), 3.05-2.92 (m, 2H), 2.88 (bs, 1H), 2.31-2.22 (m, 1H), 2.08-1.95 (m, 1H).

<sup>13</sup>C-NMR (125 MHz, CDCl<sub>3</sub>):  $\delta$  167.6, 137.0, 133.4, 133.0, 129.9, 129.8, 128.8, 128.5, 128.5, 128.1, 126.4, 77.1, 70.8.

HRMS (*m/z*) calcd for C<sub>17</sub>H<sub>16</sub>O<sub>3</sub>Na [M]<sup>+</sup>Na<sup>-</sup>: 291.0992, found: 291.0990.

The enantiomeric ratio was determined by HPLC analysis:

**141i** - Daicel Chiralcel AD-3 column: *n*Hept:*i*PrOH = 90:10, flow rate 1.0 mL/min,  $\tau_1 = 8.4$  min,  $\tau_2 = 9.0$  min.

**(1aS,7bR)-1a,2,3,7b-tetrahydronaphtho[1,2-b]oxirene (140j)** - Daicel Chiralcel OD-3 column: *n*Hept:*i*PrOH = 95:5, flow rate 1.0 mL/min,  $\tau_1 = 3.2$  min,  $\tau_2 = 3.6$  min.

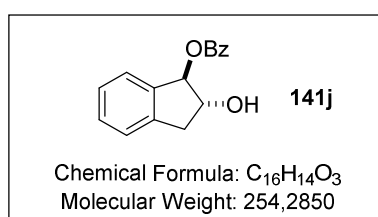
**(R,R)-2-hydroxy-2,3-dihydro-1H-inden-1-yl benzoate (141j)** – Reaction performed at -50 °C.

Catalyst loading = 2 mol%

Product: 53% yield, e.r. = 94.1:5.9

Starting material: 44% yield, e.r. = 99.6:0.4.

S = 86.5;  $\text{conv}_{\text{calc}} = 52.9\%$



<sup>1</sup>H-NMR (500 MHz, CDCl<sub>3</sub>):  $\delta$  8.11-8.06 (m, 2H), 7.62-7.57 (m, 1H), 7.49-7.39 (m, 3H), 7.36-7.22 (m, 3H), 6.10 (d, *J* = 5.1 Hz, 1H), 4.70-4.62 (m, 1H), 3.92 (bs, 1H), 3.42 (dd, *J* = 16.1 Hz, *J* = 7.9 Hz, 1H), 3.01 (dd, *J* = 16.1 Hz, *J* = 7.2 Hz, 1H).

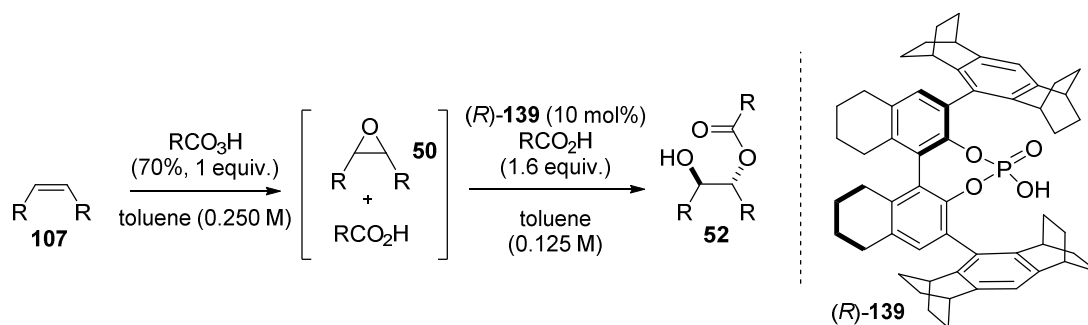
$^{13}\text{C-NMR}$  (125 MHz,  $\text{CDCl}_3$ ):  $\delta$  168.4, 140.4, 137.9, 133.5, 129.9, 129.5, 129.3, 128.5, 127.3, 125.0, 125.0, 87.3, 79.5, 38.4. HRMS ( $m/z$ ) calcd for  $\text{C}_{16}\text{H}_{14}\text{O}_3\text{Na}$   $[\text{M}]^{+\text{Na}}$ : 277.0835, found: 277.0835.

The enantiomeric ratio was determined by HPLC analysis:

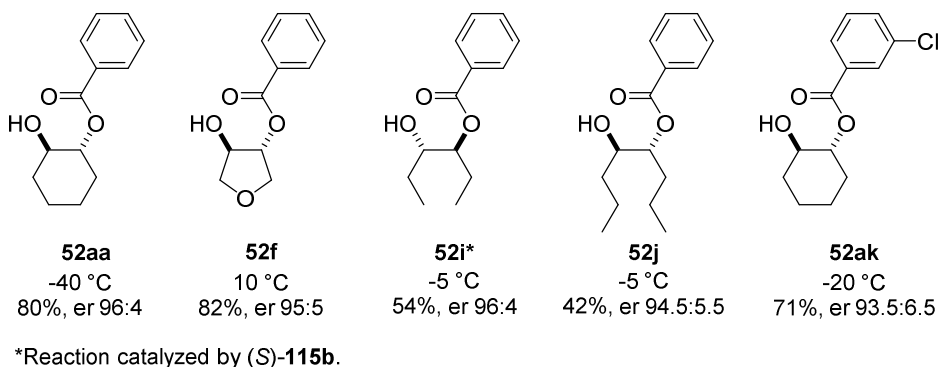
**141j** - Daicel Chiralcel OD-3 column:  $n\text{Hept}:$  $i\text{PrOH}$  = 90:10, flow rate 1.0 mL/min,  $\tau_1$  = 5.4 min,  $\tau_2$  = 6.2 min.

**(1aR,6aS)-1a,6a-dihydro-6H-indeno[1,2-b]oxirene (140j)** - Daicel Chiralcel OJ-H column:  $n\text{Hept}:$  $i\text{PrOH}$  = 98:2, flow rate 1.0 mL/min,  $\tau_1$  = 13.9 min,  $\tau_2$  = 16.4 min.

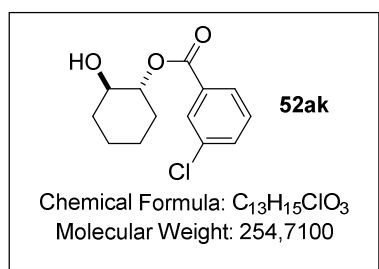
#### 7.4.5. General procedure for the *anti*-dihydroxylation strategy



A solution of the starting olefin **107** (0.1 mmol) in 0.4 mL of toluene was placed in a screw-cap vial. To the stirred solution 1 equiv. of peracid (70% in weight, 30% of related carboxylic acid) was added and the reaction was left 24 h to obtain full conversion into the desired epoxide intermediate. Next the reaction was cooled to reaction temperature and a pre-cooled toluene solution (0.4 mL) of the catalyst (10 mol%) and of the desired carboxylic acid (1.6 equiv.) was added at once. The reaction was stirred for additional 4-6 days and then 1 mL of MTBE was added to stop the reaction and the mixture was directly purified by flash column chromatography (eluent: mixtures hexane/MTBE). After purification the product was dissolved in DCM and submitted to an additional wash with 2 M  $\text{NaOH}_{\text{aq}}$  to remove small impurities of carboxylic acid. The enantiomeric ratios of products were analyzed by HPLC on a chiral stationary phase.



**(1R,2R)-2-hydroxycyclohexyl 3-chlorobenzoate (52ak)** – For this reaction no additional carboxylic acid was added after the epoxidation step. The ring opening step was performed at -20 °C and the product was isolated as a white solid in 71% yield and e.r. = 93.5:6.5.



<sup>1</sup>H-NMR (500 MHz, CDCl<sub>3</sub>): δ 8.02 (cm, 1H), 7.96-7.92 (m, 1H), 7.56-7.51 (m, 1H), 7.39 (t, *J* = 7.9 Hz, 1H), 4.89-4.81 (m, 1H), 3.78-3.68 (m, 1H), 2.19-2.06 (m, 3H), 1.82-1.74 (m, 2H), 1.50-1.20 (m, 4H). <sup>13</sup>C-NMR (125 MHz, CDCl<sub>3</sub>): δ 166.0, 135.0, 133.5, 132.5, 130.2, 130.2, 128.3, 79.6, 73.3, 33.6, 30.5, 24.4,

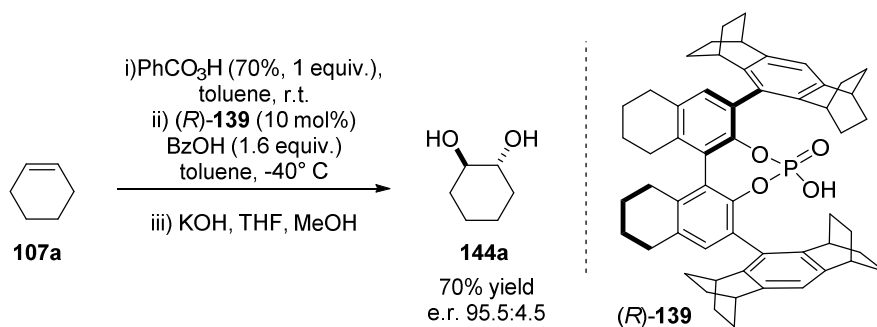
24.2.

**HRMS** (*m/z*) calcd for C<sub>13</sub>H<sub>15</sub>O<sub>3</sub>Na [M]<sup>+Na</sup>: 341.1148, found: 341.1150.

[α]<sub>D</sub><sup>25</sup>: -49.1° (*c* = 0.550, CHCl<sub>3</sub>).

The enantiomeric ratio was determined by HPLC analysis using Daicel Chiralcel OD-3 column: *n*Hept.:*i*PrOH = 99:1, flow rate 1.0 mL/min, τ<sub>1</sub> = 17.7 min, τ<sub>2</sub> = 21.1 min.

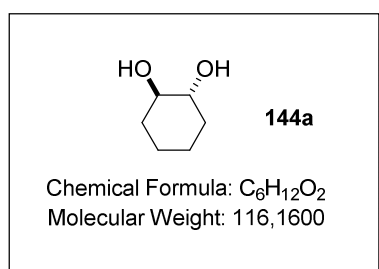
#### 7.4.6. Synthesis of *trans*-diol **144a** via organocatalytic biomimetic sequence



A solution of the starting olefin **107a** (0.1 mmol) in 0.4 mL of toluene was placed in a screw-cap vial. To the stirred solution 1 equiv. of peracid (70% in weight, 30% of related carboxylic

acid) was added and the reaction was left 24 h to obtain full conversion into the epoxide intermediate. Next the mixture was cooled to  $-40^{\circ}\text{C}$  and a pre-cooled solution of catalyst **139** (10 mol%) and benzoic acid (1.6 equiv.) was added at once. The reaction was stirred for additional 4 days and then the temperature was allowed to reach room temperature. Next 2 mL of THF, 100 mg of KOH and 0.1 mL of MeOH were added and the reaction was stirred for 12 h. Ethyl acetate was added and the organic phase was washed with a 2 M solution of  $\text{NaOH}_{\text{aq}}$ . The water phase was extracted three times more with ethyl acetate and the combined organic phase was dried over  $\text{Na}_2\text{SO}_4$ . The solvent was removed in vacuo and the diol was isolated in 70% yield and e.r. = 95.5:4.5 as a colorless crystalline solid.

**(1*R*,2*R*)-cyclohexane-1,2-diol (144a)**– The product was isolated as a white solid in 70% yield and e.r. = 95.5:4.5.



$^1\text{H-NMR}$  (500 MHz,  $\text{CDCl}_3$ ):  $\delta$  3.40-3.24 (m, 2H), 2.84-2.55 (m, 2H), 2.02-1.90 (m, 2H), 1.75-1.62 (m, 2H), 1.35-1.20 (m, 4H).

$^{13}\text{C-NMR}$  (125 MHz,  $\text{CDCl}_3$ ):  $\delta$  76.0, 33.0, 24.5.

The enantiomeric ratio was determined by GC analysis using IVADEX 7OV1701 G 573 column [Gas: Hydrogen 0.40 bar,

Temperature: 100 1/Min 125 12/Min 220 2 Min iso.  $\tau_1 = 16.5$  min,  $\tau_2 = 16.9$  min.]

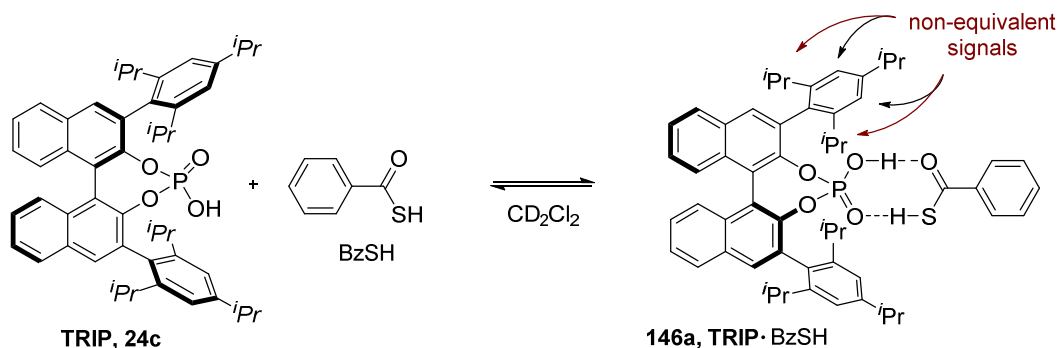
## 7.5. Asymmetric synthesis of $\beta$ -hydroxythiols

### 7.5.1. Heterodimer studies

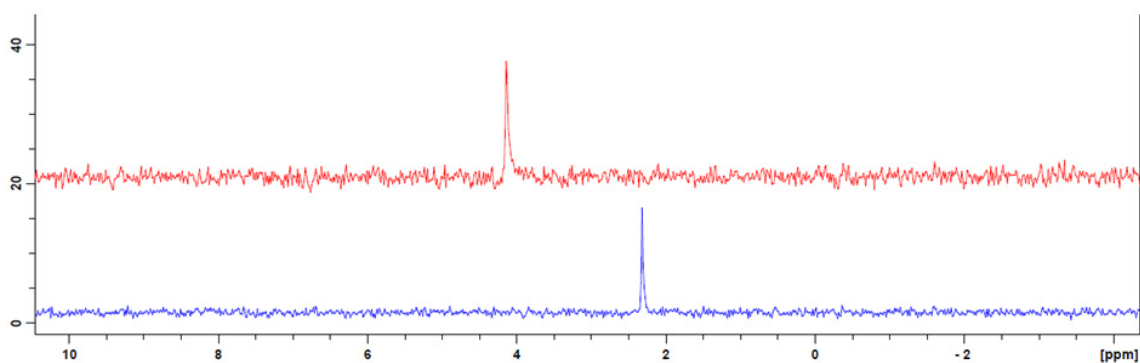
#### 7.5.1.1. 1D-NMR studies

This experiment was designed to investigate the hypothesized heterodimerization between chiral phosphoric acid catalysts and thiocarboxylic acids.

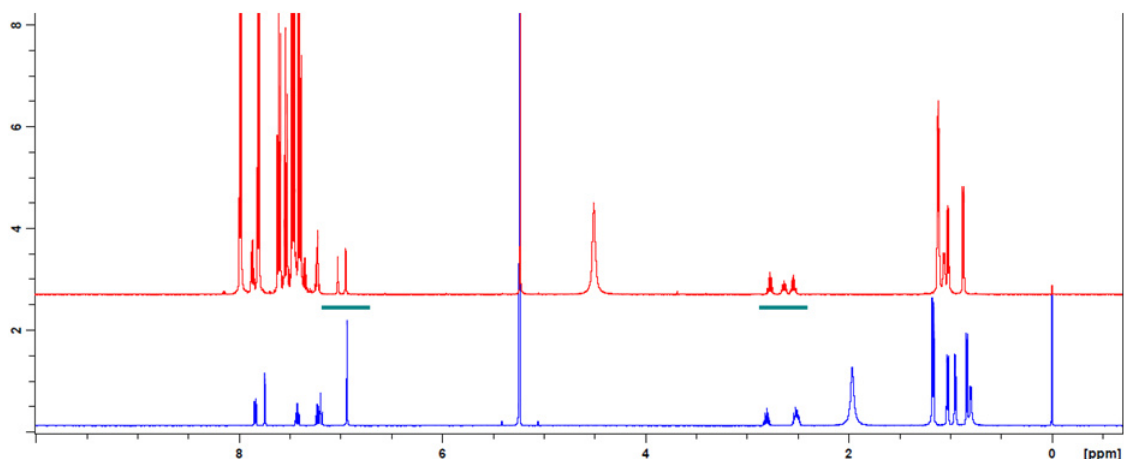
The effect of the addition of thiobenzoic acid (8.3 mg, 30 equiv.) to a solution of **TRIP** in deuterated dichloromethane (1.5 mg, 0.005 M) was analyzed by  $^1\text{H-NMR}$  and  $^{31}\text{P-NMR}$  spectroscopy (**TRIP**: blue spectra; **146a**: red spectra).



#### $^{31}\text{P-NMR}$



The phosphorous signal in the  $^{31}\text{P-NMR}$  shows a significant downfield shift, thus suggesting the establishment of a different chemical environment.

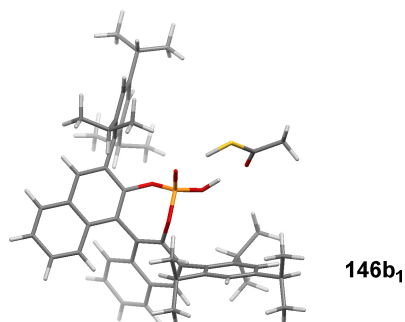
<sup>1</sup>H-NMR

The presence of thiobenzoic acid affects the chemical shift and the shape of the proton signals of the phosphoric acid molecule, thus suggesting the establishment of a new chemical environment. In particular, the non-equivalent protons of the 3,3'-aryl substituents, which were overlapping in the spectrum of the phosphoric acid monomer, are resolved. These data are in agreement with the previously investigated self-assembly of **TRIP** with carboxylic acids (cf. paragraph 7.2.1.).

7.5.1.2. Theoretical investigation on heterodimer **146a** by DFT calculation

This study was performed to evaluate the relative stability of the two possible tautomeric structures: thiol isomer **146b<sub>1</sub>** and thione isomer **146b<sub>2</sub>**.

Optimized geometries (B3LYP/cc-pVTZ, Cartesian coordinates in Å) and total electronic energy (E).

- **146b<sub>1</sub>**

C	4.257031	0.239247	-1.073365	C	4.243317	-0.491894	1.254089
C	3.756124	0.357846	0.240416	C	5.221307	-1.431731	0.927371

## 7. Experimental Section

---

C	5.730098	-1.565968	-0.357581	C	4.791860	0.297901	3.594456
C	5.230424	-0.718829	-1.341261	C	6.797731	-2.601881	-0.665309
C	2.755822	1.427575	0.561000	C	8.112064	-1.952672	-1.124255
C	1.405980	1.358534	0.125447	C	3.805674	1.151976	-2.208219
C	0.485132	2.370482	0.310930	C	3.201002	0.368227	-3.383101
C	0.862604	3.478171	1.140394	C	3.413885	-1.784628	3.295972
C	2.209916	3.567250	1.598554	C	4.950324	2.062376	-2.682684
C	3.128249	2.550108	1.257239	C	6.313141	-3.643961	-1.684231
C	-0.049938	4.476372	1.563666	O	0.520210	-1.469742	1.273575
C	0.355178	5.516692	2.359852	C	-5.327601	1.595313	2.634514
C	1.697591	5.624593	2.773909	C	-5.977175	-4.279813	1.722514
C	2.601526	4.666253	2.401640	C	-3.163567	-2.147652	-3.184590
C	-0.861228	2.303098	-0.324198	S	0.351470	-4.876427	-1.247845
C	-1.680022	1.210135	-0.124973	C	1.013353	-4.982226	0.386145
C	-3.029158	1.139745	-0.558799	C	1.501115	-6.355638	0.773552
C	-3.509793	2.209483	-1.271499	O	1.085991	-4.050847	1.169758
C	-2.694931	3.307473	-1.625946	H	-4.541332	2.203788	-1.597607
C	-1.345821	3.358351	-1.166190	H	-4.220921	4.302477	-2.775628
C	-3.190765	4.350155	-2.446232	H	-2.771388	6.173327	-3.466566
C	-2.384392	5.386853	-2.832776	H	-0.395254	6.223812	-2.743377
C	-1.038887	5.418348	-2.415847	H	0.499654	4.475794	-1.299814
C	-0.535052	4.435435	-1.603204	H	-5.656471	-1.348537	2.358319
C	-3.910926	-0.025820	-0.230360	H	-5.424879	-2.697288	-1.668467
C	-4.276094	-0.943893	-1.233838	H	-3.369127	1.527549	1.815768
C	-5.139961	-1.987785	-0.901782	H	-5.773183	2.125789	1.792094
C	-5.648619	-2.158609	0.378685	H	-5.063273	2.330594	3.397038
C	-5.270638	-1.239757	1.352777	H	-6.091481	0.939278	3.055491
C	-4.414560	-0.177238	1.078273	H	-3.137070	0.852061	4.151379
C	-3.776852	-0.836725	-2.670819	H	-2.525059	-0.426798	3.098210
C	-4.891864	-0.356103	-3.614920	H	-6.716433	-3.872641	-0.238346
C	-4.084507	0.802089	2.199200	H	-5.008781	-4.654435	1.389663
C	-3.421901	0.111978	3.401077	H	-6.636873	-5.134851	1.882412
C	-6.582675	-3.314642	0.692285	H	-5.830624	-3.788991	2.686260
C	-7.970013	-2.830946	1.140515	H	-7.911118	-2.272383	2.076302
O	-1.187956	0.129421	0.604586	H	-8.639198	-3.678289	1.301824
P	-0.052541	-0.815374	-0.030975	H	-8.421510	-2.179070	0.391930
O	-0.460538	-1.740728	-1.107628	H	-2.983846	-0.090912	-2.693879
O	1.032168	0.230133	-0.598863	H	-3.907790	-2.941667	-3.263897
C	3.760914	-0.412265	2.699416	H	-2.364209	-2.481219	-2.526778

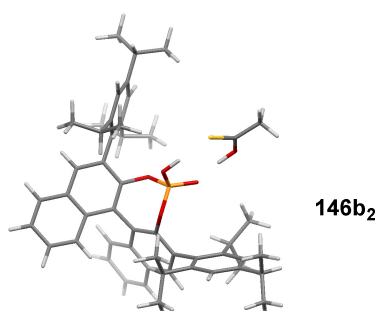


## 7. Experimental Section

H	-2.742654	-1.994951	-4.180301	H	5.399508	-4.132268	-1.344018
H	-4.098549	-0.597473	3.880146	H	7.072905	-4.412238	-1.840495
H	-5.713793	-1.073892	-3.648364	H	6.102365	-3.184504	-2.651386
H	-4.508886	-0.239257	-4.630554	H	7.981737	-1.419985	-2.067840
H	-5.304752	0.602025	-3.297933	H	8.883899	-2.709886	-1.274967
H	0.709710	-2.442690	1.184468	H	8.476724	-1.237264	-0.386489
H	4.156407	2.654983	1.575806	H	2.846929	0.179778	2.713138
H	3.631664	4.725356	2.729336	H	4.303591	-2.399608	3.442022
H	2.005957	6.455121	3.394482	H	2.723336	-2.337505	2.663193
H	-0.364533	6.259761	2.676285	H	2.946575	-1.655533	4.273695
H	-1.083683	4.409834	1.261827	H	5.727621	-0.263598	3.629242
H	5.614401	-0.799025	-2.350076	H	4.415874	0.385226	4.615718
H	5.599141	-2.085512	1.702894	H	5.022286	1.300106	3.234304
H	3.024178	1.806192	-1.826731	H	3.941184	-0.277859	-3.858158
H	5.353476	2.653071	-1.859107	H	0.918641	-6.698835	1.629652
H	4.596244	2.751191	-3.452175	H	2.540627	-6.277915	1.092089
H	5.770681	1.482213	-3.108398	H	1.415856	-7.075845	-0.035899
H	2.829287	1.056434	-4.144593	H	0.021820	-3.549840	-1.206913
H	2.369567	-0.253948	-3.054696				
H	7.003870	-3.129996	0.269753				

Energy = -3135.04743245 Hartree

**- 146b<sub>2</sub>**



C	4.273893	-0.848852	1.160041	C	0.730360	2.307920	0.401509
C	3.862156	0.095104	0.199094	C	1.182770	3.346815	1.281119
C	4.359483	0.018647	-1.118622	C	2.535869	3.326162	1.731056
C	5.255723	-0.995301	-1.443575	C	3.386972	2.272650	1.329769
C	5.681465	-1.936742	-0.511987	C	0.337216	4.376670	1.763386
C	5.177748	-1.840495	0.778328	C	0.811826	5.345115	2.610221
C	2.939651	1.212105	0.582270	C	2.160691	5.345995	3.017480
C	1.585333	1.251723	0.162340	C	3.000625	4.354274	2.587110

## 7. Experimental Section

---

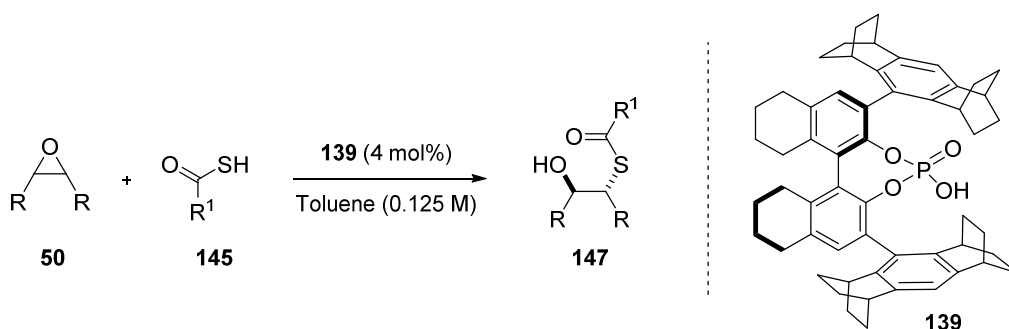
C	-0.616303	2.359149	-0.234754	S	-0.608888	-4.618445	-1.013784
C	-1.508665	1.315410	-0.095712	C	-0.156209	-5.069774	0.524588
C	-2.856434	1.358196	-0.538463	C	-0.145196	-6.506688	0.952015
C	-3.259114	2.495914	-1.192017	O	0.219193	-4.272435	1.484586
C	-2.370771	3.553939	-1.484564	H	4.421229	2.294423	1.645844
C	-1.023565	3.487738	-1.021758	H	4.034052	4.330702	2.908603
C	-2.791891	4.671651	-2.245873	H	2.524012	6.121232	3.678491
C	-1.915963	5.671128	-2.574021	H	0.142457	6.113806	2.972558
C	-0.573068	5.587749	-2.156089	H	-0.700572	4.391198	1.468197
C	-0.140139	4.529559	-1.399109	H	5.635202	-1.046711	-2.456072
C	-3.819292	0.239925	-0.278116	H	5.498108	-2.568383	1.512691
C	-4.255630	-0.584097	-1.334886	H	3.247107	1.714053	-1.777766
C	-5.193565	-1.580257	-1.062420	H	5.631456	2.390532	-1.766991
C	-5.709057	-1.794579	0.208843	H	4.888018	2.630822	-3.351704
C	-5.262339	-0.968074	1.234911	H	5.966564	1.262968	-3.079081
C	-4.331069	0.044062	1.021771	H	3.004383	1.113327	-4.134862
C	-3.760519	-0.419344	-2.768507	H	2.449877	-0.222096	-3.120267
C	-3.312703	-1.743594	-3.404905	H	6.820550	-3.633091	0.021868
C	-3.937567	0.930563	2.198107	H	5.141983	-4.407395	-1.640745
C	-5.124622	1.783721	2.674765	H	6.787530	-4.794290	-2.157087
C	-6.722831	-2.898018	0.457500	H	5.922908	-3.446997	-2.894539
C	-6.178754	-3.972926	1.410441	H	7.939585	-1.874637	-2.214468
O	-1.106284	0.168724	0.589432	H	8.728707	-3.284685	-1.510733
P	0.020740	-0.814106	0.012126	H	8.452033	-1.841944	-0.528349
O	-0.515983	-1.509436	-1.283692	H	2.934972	-0.140396	2.654652
O	1.123384	0.175578	-0.599633	H	4.090483	-2.917114	3.164679
C	3.980064	1.027166	-2.197416	H	2.522010	-2.587974	2.417868
C	5.189121	1.877096	-2.621557	H	2.836666	-2.092538	4.080250
C	6.660831	-3.037551	-0.881015	H	4.016972	-0.311755	-3.926214
C	6.092843	-3.976680	-1.955618	H	5.741615	-0.941650	3.555605
C	3.782720	-0.822240	2.603630	H	4.488571	-0.232003	4.575441
C	3.280371	-2.190150	3.087822	H	5.204381	0.709094	3.264882
O	0.467574	-1.728654	1.089912	H	-0.544598	-2.508775	-1.191675
C	3.323712	0.357755	-3.414543	H	-4.287414	2.579732	-1.516685
C	8.025356	-2.474998	-1.307065	H	-3.821646	4.712230	-2.577404
C	4.868079	-0.286856	3.553306	H	-2.246468	6.515866	-3.163157
C	-3.332240	0.129334	3.360543	H	0.125083	6.364399	-2.438213
C	-8.066161	-2.346437	0.958341	H	0.893486	4.483798	-1.093330
C	-4.824523	0.254081	-3.652782	H	-5.654916	-1.109539	2.233604

## 7. Experimental Section

---

H	-5.533223	-2.216664	-1.869529	H	-2.888557	0.232860	-2.747715
H	-3.170860	1.624627	1.858443	H	-4.151464	-2.421798	-3.566470
H	-5.528407	2.388777	1.862019	H	-2.580057	-2.253858	-2.783638
H	-4.813772	2.456774	3.476234	H	-2.856995	-1.552771	-4.377996
H	-5.934113	1.160692	3.058877	H	-5.720933	-0.365113	-3.722175
H	-2.998820	0.804443	4.150932	H	-4.442343	0.403928	-4.664386
H	-2.474268	-0.455254	3.031130	H	-5.124710	1.225007	-3.259076
H	-6.907018	-3.379671	-0.506562	H	-4.059941	-0.555008	3.799808
H	-5.247226	-4.397075	1.034879	H	0.867119	-6.780434	1.256267
H	-6.899898	-4.784296	1.526659	H	-0.481238	-7.161541	0.156335
H	-5.981165	-3.559997	2.401233	H	-0.785526	-6.624250	1.828350
H	-7.959724	-1.867922	1.933444	H	0.254597	-3.295802	1.241455
H	-8.796737	-3.150781	1.062618				
H	-8.471202	-1.606565	0.267190				

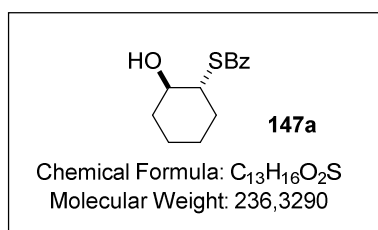
Energy = -3135.04887310 Hartree

7.5.2. General procedure for the thiocarboxylation of *meso*-epoxides

In a screw-cap vial, epoxide **50** (0.1 mmol) was dissolved in 0.4 mL of toluene and was cooled to the reaction temperature. Then a pre-cooled solution of thiocarboxylic acid **145** (0.16 mmol, 1.6 equiv.) and catalyst **139** (4 mol%) in 0.4 mL of toluene was added and the reaction was stirred for 2-5 days. Next, 1 mL of MTBE was added to the reaction and the cold mixture was directly purified by flash column chromatography (eluent: mixtures hexane/MTBE). The enantiomeric ratios of products **147** were measured by HPLC on a chiral stationary phase.

For analytical purpose, the racemic samples were prepared on 0.05 mmol scale using (*RS*)-**TRIP** as the catalyst.

***S*-((*R,R*)-2-hydroxycyclohexyl) benzothioate (**147a**)** – The reaction was performed at  $-78^{\circ}\text{C}$  and the product was isolated as a white solid in 95% yield and e.r. = 98:2.



**<sup>1</sup>H-NMR** (300 MHz,  $\text{CD}_2\text{Cl}_2$ ):  $\delta$  8.00-7.92 (m, 2H), 7.65-7.55 (m, 1H), 7.52-7.42 (m, 2H), 3.70-3.42 (m, 2H), 2.37 (d, 1H,  $J = 4.6$  Hz), 2.20-2.05 (m, 2H), 1.85-1.68 (m, 2H), 1.50-1.20 (m, 4H).

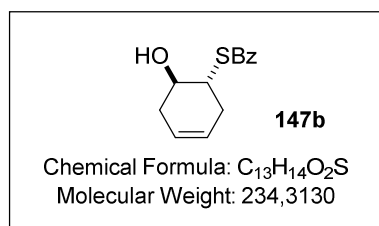
**<sup>13</sup>C-NMR** (75 MHz,  $\text{CD}_2\text{Cl}_2$ ):  $\delta$  192.6, 137.5, 133.9, 129.0, 127.7, 73.4, 50.7, 35.6, 32.6, 26.3, 24.6.

**HRMS** ( $m/z$ ) calcd for  $\text{C}_{13}\text{H}_{16}\text{O}_2\text{SNa}$  [ $\text{M}$ ]<sup>+Na</sup>: 259.0763, found: 259.0762.

**$[\alpha]_{\text{D}}^{25}$** :  $-39.6^{\circ}$  ( $c = 1.050$ ,  $\text{CHCl}_3$ ).

The enantiomeric ratio was determined by HPLC analysis using Daicel Chiralcel AD-3 column:  $n\text{Hept}:$ *i*PrOH = 95:5, flow rate 1.0 mL/min,  $\tau_1 = 13.0$  min,  $\tau_2 = 17.5$  min.

**S-((R,R)-6-hydroxycyclohex-3-en-1-yl) benzothioate (147b)** – The reaction was performed at  $-40^{\circ}\text{C}$  and the product was isolated as a colorless liquid in 99% yield and e.r. = 96.5:3.5.



$^1\text{H-NMR}$  (300 MHz,  $\text{CDCl}_3$ ):  $\delta$  8.05-7.92 (m, 2H), 7.64-7.55 (m, 1H), 7.50-7.42 (m, 2H), 5.75-5.60 (m, 2H), 4.05-3.82 (m, 2H), 2.78-2.55 (m, 2H), 2.45-2.18 (m, 3H).

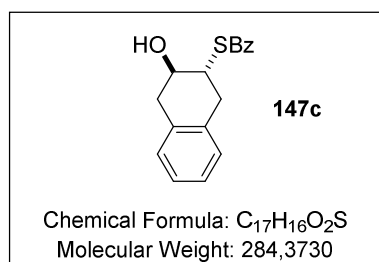
$^{13}\text{C-NMR}$  (75 MHz,  $\text{CDCl}_3$ ):  $\delta$  192.5, 137.1, 133.8, 128.8, 127.6, 125.3, 125.0, 69.6, 45.8, 34.1, 31.2.

**HRMS** ( $m/z$ ) calcd for  $\text{C}_{13}\text{H}_{14}\text{O}_2\text{SNa}$   $[\text{M}]^{+\text{Na}}$ : 257.0607, found: 257.0606.

$[\alpha]_{\text{D}}^{25}$ :  $-43.5^{\circ}$  ( $c = 1.200$ ,  $\text{CHCl}_3$ ).

The enantiomeric ratio was determined by HPLC analysis using Daicel Chiralcel AD-3 column:  $n\text{Hept}:$  $i\text{PrOH} = 95:5$ , flow rate 1.0 mL/min,  $\tau_1 = 13.4$  min,  $\tau_2 = 15.1$  min.

**S-((R,R)-3-hydroxy-1,2,3,4-tetrahydronaphthalen-2-yl) benzothioate (147c)** – The reaction was performed at  $-40^{\circ}\text{C}$  and the product was isolated as a colorless liquid in 86% yield and e.r. = 96.5:3.5.



$^1\text{H-NMR}$  (300 MHz,  $\text{CD}_2\text{Cl}_2$ ):  $\delta$  8.05-7.92 (m, 2H), 7.68-7.56 (m, 1H), 7.52-7.42 (m, 2H), 7.22-7.08 (m, 4H), 4.20-4.05 (m, 2H), 3.50-3.22 (m, 2H), 3.10-2.88 (m, 2H), 2.48 (bd,  $J = 3.5$  Hz, 1H).

$^{13}\text{C-NMR}$  (75 MHz,  $\text{CD}_2\text{Cl}_2$ ):  $\delta$  192.1, 137.3, 134.4, 134.2,

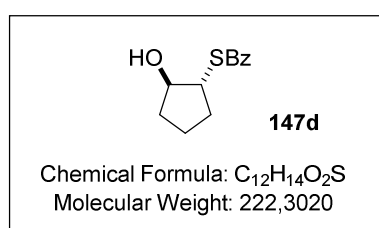
134.0, 129.5, 129.1, 128.6, 127.6, 126.8, 126.5, 70.1, 46.4, 37.5, 34.2.

**HRMS** ( $m/z$ ) calcd for  $\text{C}_{17}\text{H}_{16}\text{O}_2\text{SNa}$   $[\text{M}]^{+\text{Na}}$ : 307.0763, found: 307.0763.

$[\alpha]_{\text{D}}^{25}$ :  $-64.8^{\circ}$  ( $c = 1.225$ ,  $\text{CHCl}_3$ ).

The enantiomeric ratio was determined by HPLC analysis using Daicel Chiralcel AD-3 column:  $n\text{Hept}:$  $i\text{PrOH} = 95:5$ , flow rate 1.0 mL/min,  $\tau_1 = 22.7$  min,  $\tau_2 = 25.9$  min.

**S-((R,R)-2-hydroxycyclopentyl) benzothioate (147d)** – The reaction was performed at  $-40^{\circ}\text{C}$  and the product was isolated as a colorless liquid in 99% yield and e.r. = 97:3.



$^1\text{H-NMR}$  (300 MHz,  $\text{CD}_2\text{Cl}_2$ ):  $\delta$  8.00-7.90 (m, 2H), 7.65-7.54 (m, 1H), 7.52-7.43 (m, 2H), 4.25-4.15 (m, 1H), 3.72 (td,  $J = 8.1$  Hz,  $J = 4.5$  Hz, 1H), 2.91 (bs, 1H), 2.40-2.22 (m, 1H), 2.10-1.58 (m, 5H).

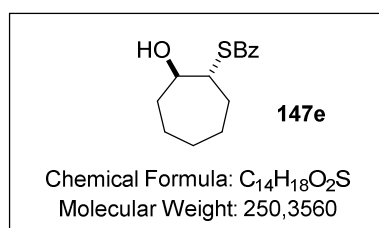
$^{13}\text{C-NMR}$  (75 MHz,  $\text{CD}_2\text{Cl}_2$ ):  $\delta$  194.5, 137.4, 133.9, 129.1, 127.6, 80.9, 51.4, 34.3, 30.8, 23.5.

**HRMS** ( $m/z$ ) calcd for  $\text{C}_{12}\text{H}_{14}\text{O}_2\text{SNa}$  [ $\text{M}$ ] $^{+\text{Na}}$ : 245.0607, found: 245.0607.

$[\alpha]_{\text{D}}^{25}$ : +37.5° ( $c = 1.100$ ,  $\text{CHCl}_3$ ).

The enantiomeric ratio was determined by HPLC analysis using Daicel Chiralcel AD-3 column:  $n\text{Hept}:$  $i\text{PrOH} = 95:5$ , flow rate 1.0 mL/min,  $\tau_1 = 10.5$  min,  $\tau_2 = 11.8$  min.

***S*-((*R,R*)-2-hydroxycycloheptyl) benzothioate (147e)** – The reaction was performed at  $-40^\circ\text{C}$  and the product was isolated as white solid in 86% yield and e.r. = 96.5:3.5.



$^1\text{H-NMR}$  (300 MHz,  $\text{CD}_2\text{Cl}_2$ ):  $\delta$  8.04-7.90 (m, 2H), 7.65-7.56 (m, 1H), 7.52-7.42 (m, 2H), 3.95-3.70 (m, 2H), 2.48 (bs, 1H), 2.15-1.40 (m, 10H).

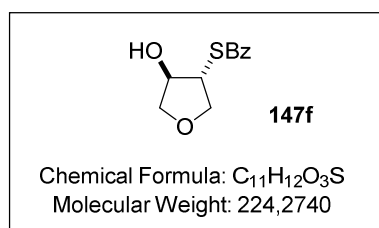
$^{13}\text{C-NMR}$  (75 MHz,  $\text{CD}_2\text{Cl}_2$ ):  $\delta$  192.9, 137.6, 133.8, 129.0, 127.6, 76.3, 53.6, 35.3, 32.1, 28.7, 26.9, 22.7.

**HRMS** ( $m/z$ ) calcd for  $\text{C}_{14}\text{H}_{18}\text{O}_2\text{SNa}$  [ $\text{M}$ ] $^{+\text{Na}}$ : 273.0920, found: 273.0919.

$[\alpha]_{\text{D}}^{25}$ : -28.2° ( $c = 0.985$ ,  $\text{CHCl}_3$ ).

The enantiomeric ratio was determined by HPLC analysis using Daicel Chiralcel AD-3 column:  $n\text{Hept}:$  $i\text{PrOH} = 95:5$ , flow rate 1.0 mL/min,  $\tau_1 = 13.4$  min,  $\tau_2 = 16.8$  min.

***S*-((*R,R*)-4-hydroxytetrahydrofuran-3-yl) benzothioate (147f)** – The reaction was performed at  $-10^\circ\text{C}$  and the product was isolated as a colorless liquid in 78% yield and e.r. = 95.5:4.5.



$^1\text{H-NMR}$  (300 MHz,  $\text{CD}_2\text{Cl}_2$ ):  $\delta$  8.00-7.90 (m, 2H), 7.68-7.58 (m, 1H), 7.55-7.45 (m, 2H), 4.48-4.32 (m, 2H), 4.08-3.92 (m, 2H), 3.80-3.70 (dd,  $J = 9.8$  Hz  $J = 4.1$  Hz, 2H), 2.78 (bd,  $J = 3.4$  Hz, 1H).

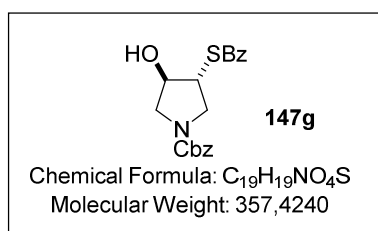
$^{13}\text{C-NMR}$  (75 MHz,  $\text{CD}_2\text{Cl}_2$ ):  $\delta$  192.8, 137.0, 134.2, 129.2, 127.6, 79.3, 74.6, 71.3, 50.7.

**HRMS** ( $m/z$ ) calcd for  $\text{C}_{11}\text{H}_{12}\text{O}_3\text{SNa}$  [ $\text{M}$ ] $^{+\text{Na}}$ : 247.0399, found: 247.0340.

$[\alpha]_{\text{D}}^{25}$ : +11.5° ( $c = 0.850$ ,  $\text{CHCl}_3$ ).

The enantiomeric ratio was determined by HPLC analysis using Daicel Chiralcel AD-3 column:  $n\text{Hept}:$  $i\text{PrOH} = 97:3$ , flow rate 1.0 mL/min,  $\tau_1 = 24.7$  min,  $\tau_2 = 26.6$  min.

**(*R,R*)-benzyl 3-(benzoylthio)-4-hydroxypyrrolidine-1-carboxylate (147g)** – Reaction performed at  $-10^{\circ}\text{C}$ . Product isolated as a colorless liquid in 63% yield and e.r. = 95.5:4.5.



$^1\text{H-NMR}$  (300 MHz,  $\text{CDCl}_3$ ):  $\delta$  7.95-7.88 (m, 2H), 7.65-7.57 (m, 1H), 7.52-7.43 (m, 2H), 7.42-7.27 (m, 5H), 5.17 (s, 2H), 4.44-4.35 (m, 1H), 4.18-4.00 (m, 2H), 3.92-3.36 (m, 3H), 2.80 (bs, 1H).

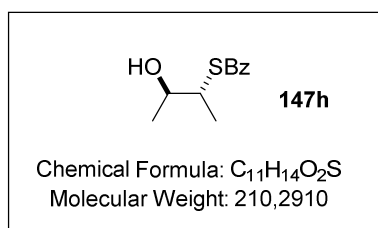
$^{13}\text{C-NMR}$  (75 MHz,  $\text{CDCl}_3$ ):  $\delta$  191.0, 154.9, 136.8, 136.6, 134.2, 129.0, 128.7, 128.3, 128.2, 127.6, 76.5, 75.3, 67.3, 52.7, 52.2, 49.1, 48.6 (additional peaks due to rotamers).

**HRMS** ( $m/z$ ) calcd for  $\text{C}_{19}\text{H}_{19}\text{NO}_4\text{SNa}$  [ $\text{M}$ ] $^{+\text{Na}}$ : 380.0927, found: 380.0928.

$[\alpha]_{\text{D}}^{25}$ :  $+53.4^{\circ}$  ( $c = 0.700$ ,  $\text{CHCl}_3$ ).

The enantiomeric ratio was determined by HPLC analysis using Daicel Chiralcel OD-3 column:  $n\text{Hept}:i\text{PrOH} = 85:15$ , flow rate 1.0 mL/min,  $\tau_1 = 12.2$  min,  $\tau_2 = 15.7$  min.

***S*-((*R,R*)-3-hydroxybutan-2-yl) benzothioate (147h)** – The reaction was performed at  $-40^{\circ}\text{C}$  and the product was isolated as a colorless liquid in 99% yield and e.r. = 97:3.



$^1\text{H-NMR}$  (300 MHz,  $\text{CD}_2\text{Cl}_2$ ):  $\delta$  8.10-7.95 (m, 2H), 7.65-7.52 (m, 1H), 7.52-7.42 (m, 2H), 4.00-3.89 (m, 1H), 3.83 (dq,  $J = 7.0$  Hz,  $J = 4.6$  Hz, 1H), 1.96 (bs, 1H), 1.43 (d,  $J = 7.2$  Hz, 3H), 1.26 (d,  $J = 6.2$  Hz, 3H).

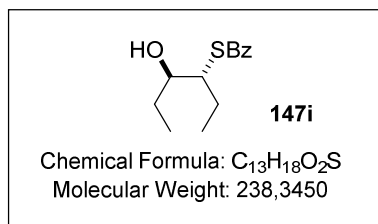
$^{13}\text{C-NMR}$  (75 MHz,  $\text{CD}_2\text{Cl}_2$ ):  $\delta$  191.9, 137.7, 133.8, 129.0, 127.6, 71.1, 46.8, 20.8, 18.0.

**HRMS** ( $m/z$ ) calcd for  $\text{C}_{11}\text{H}_{14}\text{O}_2\text{SNa}$  [ $\text{M}$ ] $^{+\text{Na}}$ : 233.0607, found: 233.0606.

$[\alpha]_{\text{D}}^{25}$ :  $-26.6^{\circ}$  ( $c = 1.175$ ,  $\text{CHCl}_3$ ).

The enantiomeric ratio was determined by HPLC analysis using Daicel Chiralcel AD-3 column:  $n\text{Hept}:i\text{PrOH} = 95:5$ , flow rate 1.0 mL/min,  $\tau_1 = 7.9$  min,  $\tau_2 = 8.9$  min.

***S*-((*R,R*)-4-hydroxyhexan-3-yl) benzothioate (147i)** – The reaction was performed at  $-40^{\circ}\text{C}$  and the product was isolated as a colorless liquid in 94% yield and e.r. = 95.5:4.5.



$^1\text{H-NMR}$  (300 MHz,  $\text{CD}_2\text{Cl}_2$ ):  $\delta$  8.04-7.95 (m, 2H), 7.64-7.55 (m, 1H), 7.52-7.43 (m, 2H), 3.83-3.70 (m, 2H), 2.00-1.40 (m, 5H), 1.04 (t,  $J = 7.4$  Hz, 3H), 0.98 (t,  $J = 7.4$  Hz, 3H).

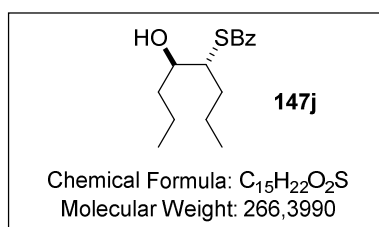
$^{13}\text{C-NMR}$  (75 MHz,  $\text{CD}_2\text{Cl}_2$ ):  $\delta$  192.2, 137.7, 133.7, 129.0, 127.7, 75.4, 52.5, 28.4, 26.1, 12.0, 10.4.

**HRMS** ( $m/z$ ) calcd for  $\text{C}_{13}\text{H}_{18}\text{O}_2\text{SNa}$  [ $\text{M}$ ] $^{+\text{Na}}$ : 261.0920, found: 261.0921.

$[\alpha]_{\text{D}}^{25}$ :  $-17.9^\circ$  ( $c = 1.050$ ,  $\text{CHCl}_3$ ).

The enantiomeric ratio was determined by HPLC analysis using Daicel Chiralcel AD-3 column:  $n\text{Hept}:i\text{PrOH} = 95:5$ , flow rate 1.0 mL/min,  $\tau_1 = 8.0$  min,  $\tau_2 = 8.6$  min.

***S*-((*R,R*)-5-hydroxyoctan-4-yl) benzothioate (**147j**)** – The reaction was performed at  $-40^\circ\text{C}$  and the product was isolated as a colorless liquid in 82% yield and e.r. = 95:5.



$^1\text{H-NMR}$  (300 MHz,  $\text{CD}_2\text{Cl}_2$ ):  $\delta$  8.02-7.96 (m, 2H), 7.64-7.55 (m, 1H), 7.52-7.43 (m, 2H), 3.88-3.76 (m, 2H), 1.90-1.30 (m, 9H), 0.98-0.88 (m, 6H).

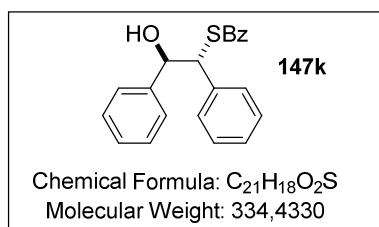
$^{13}\text{C-NMR}$  (75 MHz,  $\text{CD}_2\text{Cl}_2$ ):  $\delta$  192.0, 137.6, 133.7, 128.9, 127.6, 73.9, 50.8, 37.5, 34.9, 20.8, 19.5, 14.1, 14.0.

**HRMS** ( $m/z$ ) calcd for  $\text{C}_{15}\text{H}_{22}\text{O}_2\text{SNa}$  [ $\text{M}$ ] $^{+\text{Na}}$ : 289.1232, found: 289.1232.

$[\alpha]_{\text{D}}^{25}$ :  $+19.6^\circ$  ( $c = 1.100$ ,  $\text{CHCl}_3$ ).

The enantiomeric ratio was determined by HPLC analysis using Daicel Chiralcel OJ-H column:  $n\text{Hept}:i\text{PrOH} = 98:2$ , flow rate 1.0 mL/min,  $\tau_1 = 11.0$  min,  $\tau_2 = 12.1$  min.

***S*-((*R,R*)-2-hydroxy-1,2-diphenylethyl) benzothioate (**147k**)** – The reaction was performed at  $-10^\circ\text{C}$  and the product was isolated as a mixture 8.5:1 of compound **147k** and **148k** (white solid) in 72% yield and e.r. $_{147\text{k}}$  = 89:11, e.r. $_{148\text{k}}$  = 87:13.



$^1\text{H-NMR}$  (300 MHz,  $\text{CD}_2\text{Cl}_2$ ):  $\delta$  8.08-8.00 (m, 2H $_{148\text{k}}$ ), 7.90-7.80 (m, 2H $_{147\text{k}}$ ), 7.58-7.45 (m, 1H $_{147\text{k}}$  + 1H $_{148\text{k}}$ ), 7.45-7.32 (m, 2H $_{147\text{k}}$  + 2H $_{148\text{k}}$ ), 7.26-7.08 (m, 10H $_{147\text{k}}$  + 10H $_{148\text{k}}$ ), 6.13 (d,  $J = 8.5$  Hz, 1H $_{148\text{k}}$ ), 5.08-4.98 (m, 2H $_{147\text{k}}$ ), 4.50 (dd,  $J = 8.5$  Hz  $J = 5.2$  Hz, 1H $_{148\text{k}}$ ), 2.72 (bs, 1H $_{147\text{k}}$ ), 2.28 (d,  $J = 5.2$  Hz, 1H $_{148\text{k}}$ ).

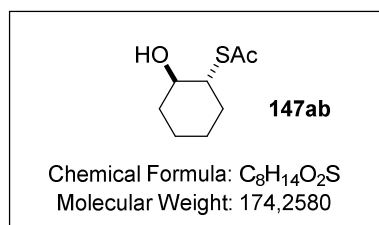
$^{13}\text{C-NMR}$  (75 MHz,  $\text{CD}_2\text{Cl}_2$ , compound 3k):  $\delta$  191.2, 141.7, 139.8, 137.2, 134.0, 129.1, 129.0, 128.8, 128.4, 128.2, 127.9, 127.7, 127.1, 77.6, 56.7.

**HRMS** ( $m/z$ ) calcd for  $\text{C}_{21}\text{H}_{18}\text{O}_2\text{SNa}$  [ $\text{M}$ ] $^{+\text{Na}}$ : 357.0920, found: 341.0919.



The enantiomeric ratio was determined by HPLC analysis using Daicel Chiralcel AD-3 column: *n*Hept:*i*PrOH = 85:15, flow rate 1.0 mL/min,  $\tau_1 = 13.2$  min,  $\tau_2 = 15.4$  min.

***S*-((*R,R*)-2-hydroxycyclohexyl) ethanethioate (**147ab**)** – The reaction was performed at  $-40^\circ$  C and the product was isolated as a mixture 15:1 of compound **147ab** and **148ab** in 75% yield and e.r.<sub>147ab</sub> = 95:5.



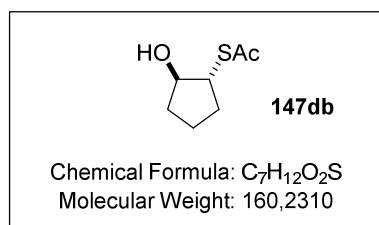
<sup>1</sup>H NMR (500 MHz, CD<sub>2</sub>Cl<sub>2</sub>):  $\delta$  3.35-3.20 (m, 2H), 2.25 (s, 3H), 2.17 (d, *J* = 4.5 Hz, 1H), 2.05-1.86 (m, 2H), 1.70-1.55 (m, 2H), 1.40-1.15 (m, 4H).

<sup>13</sup>C-NMR (125 MHz, CD<sub>2</sub>Cl<sub>2</sub>):  $\delta$  196.8, 73.2, 50.6, 35.4, 32.4, 31.1, 26.2, 24.5.

HRMS (*m/z*) calcd for C<sub>8</sub>H<sub>14</sub>O<sub>2</sub>SNa [M]<sup>+Na</sup>: 197.0607, found: 197.0608.

The enantiomeric ratio was determined by GC analysis using BGB-177/BG-15 column 30 m (60 min at 140 °C, 10 °C/min until 220°C, 3 min at 220 °C, 0.4 bar H<sub>2</sub>),  $\tau_1 = 24.7$  min,  $\tau_2 = 25.4$  min.

***S*-((*R,R*)-2-mercaptocyclopentyl) acetate (**147db**)** – The reaction was performed at  $-10^\circ$  C and the product was isolated as colorless liquid in 63% yield and e.r. = 93.5:6.5.



<sup>1</sup>H-NMR (500 MHz, CD<sub>2</sub>Cl<sub>2</sub>):  $\delta$  4.05-3.95 (m, 1H), 3.43 (td, *J* = 8.0 Hz, *J* = 4.5 Hz, 1H), 2.73 (bs, 1H), 2.24 (m, 3H), 2.18-2.05 (m, 1H), 1.92-1.80 (m, 1H), 1.78-1.65 (m, 1H), 1.62-1.50 (m, 2H), 1.48-1.35 (m, 1H).

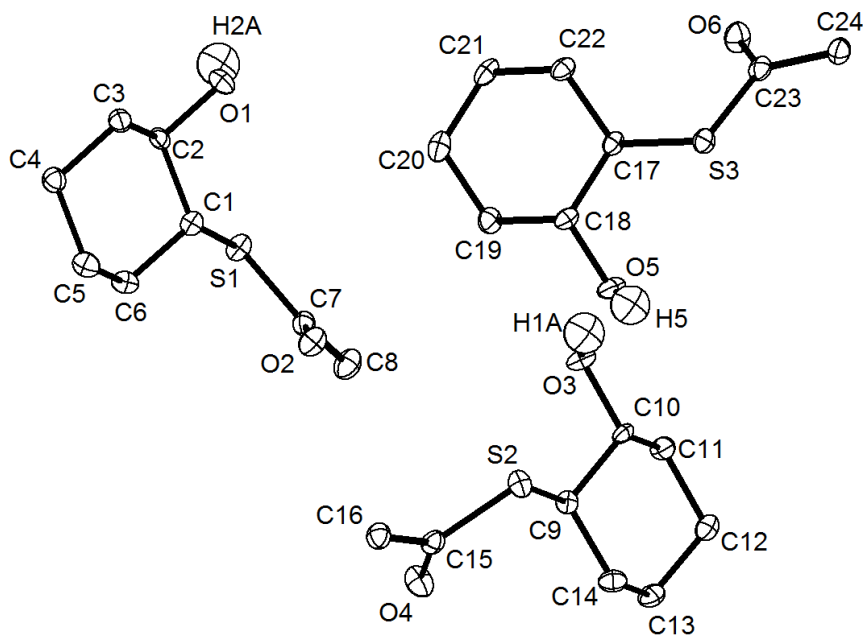
<sup>13</sup>C-NMR (125 MHz, CD<sub>2</sub>Cl<sub>2</sub>):  $\delta$  198.7, 80.7, 51.2, 34.0, 30.6, 30.4, 23.2.

HRMS (*m/z*) calcd for C<sub>7</sub>H<sub>12</sub>O<sub>2</sub>SNa [M]<sup>+Na</sup>: 183.0456, found: 183.0448.

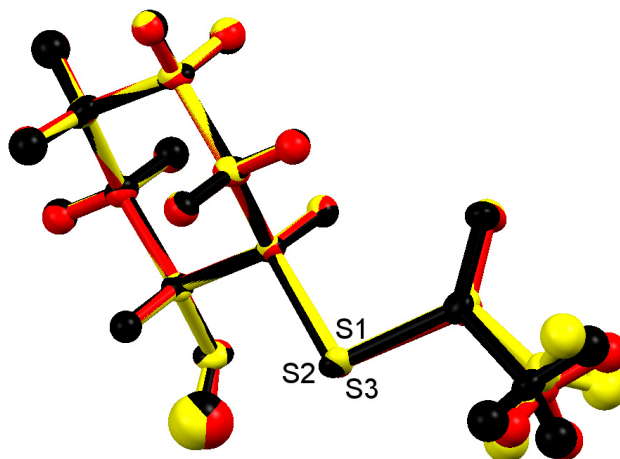
$[\alpha]_D^{25}$ : +81.1° (*c* = 0.375, CHCl<sub>3</sub>).

The enantiomeric ratio was determined by HPLC analysis using Daicel Chiralcel AD-3 column: *n*Hept:*i*PrOH = 90:10, flow rate 1.0 mL/min,  $\tau_1 = 5.1$  min,  $\tau_2 = 5.4$  min.

## 7.5.2.1. Crystallographic data of compound 147ab



Crystallization occurred by change of phase from a neat liquid state at room temperature. There are three independent molecules in the asymmetric unit, which differ only slightly in the conformation of the methyl carbonyl group attached to the sulfur atoms (Scheme below).



The Flack parameter is  $-0.004(4)$  and the absolute structure ( $R,R$ ) is therefore correct with a large degree of certainty.<sup>176</sup>

**Crystal data and structure refinement.**

Identification code	9133
Empirical formula	$C_8H_{14}O_2S$
	243

## 7. Experimental Section

---

Color	colourless	
Formula weight	174.25 g·mol <sup>-1</sup>	
Temperature	100 K	
Wavelength	1.54178 Å	
Crystal system	orthorhombic	
Space group	P 21 21 21, (no. 19)	
Unit cell dimensions	a = 5.2483(2) Å	α = 90°.
	b = 21.9303(7) Å	β = 90°.
	c = 22.8444(7) Å	γ = 90°.
Volume	2629.32(15) Å <sup>3</sup>	
Z	12	
Density (calculated)	1.321 Mg·m <sup>-3</sup>	
Absorption coefficient	2.878 mm <sup>-1</sup>	
F(000)	1128 e	
Crystal size	1.28 x 0.040 x 0.030 mm <sup>3</sup>	
θ range for data collection	2.793 to 67.904°.	
Index ranges	-6 ≤ h ≤ 5, -26 ≤ k ≤ 26, -26 ≤ l ≤ 27	
Reflections collected	116370	
Independent reflections	4701 [R <sub>int</sub> = 0.0809]	
Reflections with I > 2σ(I)	4556	
Completeness to θ = 67.679°	98.7 %	
Absorption correction	Gaussian	
Max. and min. transmission	0.91982 and 0.30765	
Refinement method	Full-matrix least-squares on F <sup>2</sup>	
Data / restraints / parameters	4701 / 0 / 313	
Goodness-of-fit on F <sup>2</sup>	1.153	
Final R indices [I > 2σ(I)]	R <sub>1</sub> = 0.0257	wR <sup>2</sup> = 0.0655
R indices (all data)	R <sub>1</sub> = 0.0270	wR <sup>2</sup> = 0.0662
Absolute structure parameter	-0.004(4)	
Extinction coefficient	0	
Largest diff. peak and hole	0.162 and -0.317 e·Å <sup>-3</sup>	

### Atomic coordinates and equivalent isotropic displacement parameters (Å<sup>2</sup>)

U<sub>eq</sub> is defined as one third of the trace of the orthogonalized U<sub>ij</sub> tensor.

	x	y	z	U <sub>eq</sub>
C(1)	0.8118(4)	0.7015(1)	0.3765(1)	0.014(1)
C(2)	0.8245(4)	0.7577(1)	0.4160(1)	0.014(1)
C(3)	0.6072(4)	0.8009(1)	0.4009(1)	0.016(1)
C(4)	0.6084(5)	0.8193(1)	0.3363(1)	0.017(1)
C(5)	0.6014(5)	0.7631(1)	0.2972(1)	0.018(1)

## 7. Experimental Section

---

C(6)	0.8204(5)	0.7202(1)	0.3119(1)	0.017(1)
C(7)	0.9362(5)	0.5800(1)	0.3667(1)	0.016(1)
C(8)	1.1152(5)	0.5264(1)	0.3678(1)	0.023(1)
C(9)	0.9079(5)	0.3328(1)	0.3664(1)	0.014(1)
C(10)	0.9142(5)	0.3244(1)	0.4328(1)	0.013(1)
C(11)	1.1316(5)	0.2825(1)	0.4499(1)	0.017(1)
C(12)	1.1187(5)	0.2206(1)	0.4190(1)	0.018(1)
C(13)	1.1066(5)	0.2294(1)	0.3528(1)	0.018(1)
C(14)	0.8854(5)	0.2709(1)	0.3358(1)	0.018(1)
C(15)	0.7570(5)	0.4114(1)	0.2781(1)	0.016(1)
C(16)	0.5810(5)	0.4577(1)	0.2514(1)	0.019(1)
C(17)	0.4267(4)	0.4741(1)	0.5878(1)	0.014(1)
C(18)	0.4172(5)	0.4739(1)	0.5209(1)	0.015(1)
C(19)	0.6289(5)	0.5142(1)	0.4965(1)	0.017(1)
C(20)	0.6136(5)	0.5794(1)	0.5200(1)	0.021(1)
C(21)	0.6199(5)	0.5788(1)	0.5866(1)	0.018(1)
C(22)	0.4077(4)	0.5393(1)	0.6116(1)	0.016(1)
C(23)	0.2740(5)	0.4157(1)	0.6895(1)	0.016(1)
C(24)	0.0897(5)	0.3791(1)	0.7257(1)	0.020(1)
O(1)	0.8030(4)	0.7415(1)	0.4764(1)	0.019(1)
O(2)	0.7182(3)	0.5764(1)	0.3497(1)	0.021(1)
O(3)	0.9502(3)	0.3813(1)	0.4624(1)	0.019(1)
O(4)	0.9571(3)	0.3954(1)	0.2566(1)	0.023(1)
O(5)	0.4502(4)	0.4137(1)	0.4981(1)	0.019(1)
O(6)	0.4744(3)	0.4347(1)	0.7079(1)	0.022(1)
S(1)	1.0723(1)	0.6490(1)	0.3927(1)	0.016(1)
S(2)	0.6454(1)	0.3831(1)	0.3465(1)	0.016(1)
S(3)	0.1681(1)	0.4270(1)	0.6163(1)	0.016(1)

---

### Bond lengths [Å] and angles [°]

C(1)-C(2)	1.529(3)	C(1)-C(6)	1.531(3)
C(1)-S(1)	1.825(2)	C(1)-H(1)	1.0000
C(2)-O(1)	1.430(3)	C(2)-C(3)	1.522(3)
C(2)-H(2)	1.0000	C(3)-C(4)	1.530(3)
C(3)-H(3A)	0.9900	C(3)-H(3B)	0.9900
C(4)-C(5)	1.522(3)	C(4)-H(4A)	0.9900
C(4)-H(4B)	0.9900	C(5)-C(6)	1.524(3)
C(5)-H(5A)	0.9900	C(5)-H(5B)	0.9900

## 7. Experimental Section

---

C(6)-H(6A)	0.9900	C(6)-H(6B)	0.9900
C(7)-O(2)	1.211(3)	C(7)-C(8)	1.507(3)
C(7)-S(1)	1.774(2)	C(8)-H(8A)	0.9800
C(8)-H(8B)	0.9800	C(8)-H(8C)	0.9800
C(9)-C(10)	1.530(3)	C(9)-C(14)	1.531(3)
C(9)-S(2)	1.823(2)	C(9)-H(9)	1.0000
C(10)-O(3)	1.432(3)	C(10)-C(11)	1.516(3)
C(10)-H(10)	1.0000	C(11)-C(12)	1.531(3)
C(11)-H(11A)	0.9900	C(11)-H(11B)	0.9900
C(12)-C(13)	1.524(3)	C(12)-H(12A)	0.9900
C(12)-H(12B)	0.9900	C(13)-C(14)	1.525(3)
C(13)-H(13A)	0.9900	C(13)-H(13B)	0.9900
C(14)-H(14A)	0.9900	C(14)-H(14B)	0.9900
C(15)-O(4)	1.211(3)	C(15)-C(16)	1.501(3)
C(15)-S(2)	1.780(2)	C(16)-H(16A)	0.9800
C(16)-H(16B)	0.9800	C(16)-H(16C)	0.9800
C(17)-C(18)	1.529(3)	C(17)-C(22)	1.534(3)
C(17)-S(3)	1.827(2)	C(17)-H(17)	1.0000
C(18)-O(5)	1.431(3)	C(18)-C(19)	1.524(3)
C(18)-H(18)	1.0000	C(19)-C(20)	1.531(3)
C(19)-H(19A)	0.9900	C(19)-H(19B)	0.9900
C(20)-C(21)	1.523(3)	C(20)-H(20A)	0.9900
C(20)-H(20B)	0.9900	C(21)-C(22)	1.522(3)
C(21)-H(21A)	0.9900	C(21)-H(21B)	0.9900
C(22)-H(22A)	0.9900	C(22)-H(22B)	0.9900
C(23)-O(6)	1.207(3)	C(23)-C(24)	1.504(3)
C(23)-S(3)	1.780(2)	C(24)-H(24A)	0.9800
C(24)-H(24B)	0.9800	C(24)-H(24C)	0.9800
O(1)-H(2A)	0.89(4)	O(3)-H(1A)	0.88(4)
O(5)-H(5)	0.82(4)		
C(2)-C(1)-C(6)	110.58(18)	C(2)-C(1)-S(1)	110.88(16)
C(6)-C(1)-S(1)	110.00(16)	C(2)-C(1)-H(1)	108.4
C(6)-C(1)-H(1)	108.4	S(1)-C(1)-H(1)	108.4
O(1)-C(2)-C(3)	108.34(18)	O(1)-C(2)-C(1)	111.47(17)
C(3)-C(2)-C(1)	109.58(18)	O(1)-C(2)-H(2)	109.1
C(3)-C(2)-H(2)	109.1	C(1)-C(2)-H(2)	109.1
C(2)-C(3)-C(4)	112.35(18)	C(2)-C(3)-H(3A)	109.1
C(4)-C(3)-H(3A)	109.1	C(2)-C(3)-H(3B)	109.1

## 7. Experimental Section

---

C(4)-C(3)-H(3B)	109.1	H(3A)-C(3)-H(3B)	107.9
C(5)-C(4)-C(3)	110.58(18)	C(5)-C(4)-H(4A)	109.5
C(3)-C(4)-H(4A)	109.5	C(5)-C(4)-H(4B)	109.5
C(3)-C(4)-H(4B)	109.5	H(4A)-C(4)-H(4B)	108.1
C(4)-C(5)-C(6)	110.65(19)	C(4)-C(5)-H(5A)	109.5
C(6)-C(5)-H(5A)	109.5	C(4)-C(5)-H(5B)	109.5
C(6)-C(5)-H(5B)	109.5	H(5A)-C(5)-H(5B)	108.1
C(5)-C(6)-C(1)	110.88(19)	C(5)-C(6)-H(6A)	109.5
C(1)-C(6)-H(6A)	109.5	C(5)-C(6)-H(6B)	109.5
C(1)-C(6)-H(6B)	109.5	H(6A)-C(6)-H(6B)	108.1
O(2)-C(7)-C(8)	122.9(2)	O(2)-C(7)-S(1)	122.94(19)
C(8)-C(7)-S(1)	114.15(18)	C(7)-C(8)-H(8A)	109.5
C(7)-C(8)-H(8B)	109.5	H(8A)-C(8)-H(8B)	109.5
C(7)-C(8)-H(8C)	109.5	H(8A)-C(8)-H(8C)	109.5
H(8B)-C(8)-H(8C)	109.5	C(10)-C(9)-C(14)	110.34(18)
C(10)-C(9)-S(2)	109.70(16)	C(14)-C(9)-S(2)	111.41(16)
C(10)-C(9)-H(9)	108.4	C(14)-C(9)-H(9)	108.4
S(2)-C(9)-H(9)	108.4	O(3)-C(10)-C(11)	107.96(18)
O(3)-C(10)-C(9)	111.48(17)	C(11)-C(10)-C(9)	110.12(18)
O(3)-C(10)-H(10)	109.1	C(11)-C(10)-H(10)	109.1
C(9)-C(10)-H(10)	109.1	C(10)-C(11)-C(12)	112.68(18)
C(10)-C(11)-H(11A)	109.1	C(12)-C(11)-H(11A)	109.1
C(10)-C(11)-H(11B)	109.1	C(12)-C(11)-H(11B)	109.1
H(11A)-C(11)-H(11B)	107.8	C(13)-C(12)-C(11)	110.33(18)
C(13)-C(12)-H(12A)	109.6	C(11)-C(12)-H(12A)	109.6
C(13)-C(12)-H(12B)	109.6	C(11)-C(12)-H(12B)	109.6
H(12A)-C(12)-H(12B)	108.1	C(12)-C(13)-C(14)	111.06(19)
C(12)-C(13)-H(13A)	109.4	C(14)-C(13)-H(13A)	109.4
C(12)-C(13)-H(13B)	109.4	C(14)-C(13)-H(13B)	109.4
H(13A)-C(13)-H(13B)	108.0	C(13)-C(14)-C(9)	110.76(18)
C(13)-C(14)-H(14A)	109.5	C(9)-C(14)-H(14A)	109.5
C(13)-C(14)-H(14B)	109.5	C(9)-C(14)-H(14B)	109.5
H(14A)-C(14)-H(14B)	108.1	O(4)-C(15)-C(16)	124.4(2)
O(4)-C(15)-S(2)	122.66(18)	C(16)-C(15)-S(2)	112.90(17)
C(15)-C(16)-H(16A)	109.5	C(15)-C(16)-H(16B)	109.5
H(16A)-C(16)-H(16B)	109.5	C(15)-C(16)-H(16C)	109.5
H(16A)-C(16)-H(16C)	109.5	H(16B)-C(16)-H(16C)	109.5
C(18)-C(17)-C(22)	110.77(18)	C(18)-C(17)-S(3)	109.31(16)
C(22)-C(17)-S(3)	110.68(15)	C(18)-C(17)-H(17)	108.7

## 7. Experimental Section

C(22)-C(17)-H(17)	108.7	S(3)-C(17)-H(17)	108.7
O(5)-C(18)-C(19)	108.22(18)	O(5)-C(18)-C(17)	111.25(18)
C(19)-C(18)-C(17)	109.90(18)	O(5)-C(18)-H(18)	109.1
C(19)-C(18)-H(18)	109.1	C(17)-C(18)-H(18)	109.1
C(18)-C(19)-C(20)	112.02(19)	C(18)-C(19)-H(19A)	109.2
C(20)-C(19)-H(19A)	109.2	C(18)-C(19)-H(19B)	109.2
C(20)-C(19)-H(19B)	109.2	H(19A)-C(19)-H(19B)	107.9
C(21)-C(20)-C(19)	109.90(19)	C(21)-C(20)-H(20A)	109.7
C(19)-C(20)-H(20A)	109.7	C(21)-C(20)-H(20B)	109.7
C(19)-C(20)-H(20B)	109.7	H(20A)-C(20)-H(20B)	108.2
C(22)-C(21)-C(20)	111.37(19)	C(22)-C(21)-H(21A)	109.4
C(20)-C(21)-H(21A)	109.4	C(22)-C(21)-H(21B)	109.4
C(20)-C(21)-H(21B)	109.4	H(21A)-C(21)-H(21B)	108.0
C(21)-C(22)-C(17)	110.47(18)	C(21)-C(22)-H(22A)	109.6
C(17)-C(22)-H(22A)	109.6	C(21)-C(22)-H(22B)	109.6
C(17)-C(22)-H(22B)	109.6	H(22A)-C(22)-H(22B)	108.1
O(6)-C(23)-C(24)	123.7(2)	O(6)-C(23)-S(3)	123.38(18)
C(24)-C(23)-S(3)	112.90(17)	C(23)-C(24)-H(24A)	109.5
C(23)-C(24)-H(24B)	109.5	H(24A)-C(24)-H(24B)	109.5
C(23)-C(24)-H(24C)	109.5	H(24A)-C(24)-H(24C)	109.5
H(24B)-C(24)-H(24C)	109.5	C(2)-O(1)-H(2A)	108(3)
C(10)-O(3)-H(1A)	111(2)	C(18)-O(5)-H(5)	108(3)
C(7)-S(1)-C(1)	99.71(11)	C(15)-S(2)-C(9)	100.46(11)
C(23)-S(3)-C(17)	100.46(11)		

### Anisotropic displacement parameters ( $\text{\AA}^2$ )

The anisotropic displacement factor exponent takes the form:

$$-2\pi^2 [ h^2 a^{*2} U_{11} + \dots + 2 h k a^* b^* U_{12} ].$$

	$U_{11}$	$U_{22}$	$U_{33}$	$U_{23}$	$U_{13}$	$U_{12}$
C(1)	0.010(1)	0.014(1)	0.018(1)	0.000(1)	-0.001(1)	0.001(1)
C(2)	0.014(1)	0.017(1)	0.011(1)	0.001(1)	0.002(1)	-0.003(1)
C(3)	0.016(1)	0.015(1)	0.016(1)	0.001(1)	0.002(1)	0.002(1)
C(4)	0.018(1)	0.017(1)	0.017(1)	0.002(1)	0.001(1)	0.002(1)
C(5)	0.015(1)	0.022(1)	0.016(1)	0.001(1)	-0.003(1)	0.003(1)
C(6)	0.014(1)	0.021(1)	0.016(1)	-0.002(1)	0.000(1)	0.000(1)
C(7)	0.016(1)	0.016(1)	0.017(1)	0.001(1)	0.002(1)	-0.001(1)
C(8)	0.019(1)	0.018(1)	0.033(1)	-0.001(1)	0.003(1)	0.001(1)

## 7. Experimental Section

---

C(9)	0.011(1)	0.014(1)	0.016(1)	0.001(1)	0.001(1)	0.001(1)
C(10)	0.014(1)	0.009(1)	0.016(1)	-0.003(1)	0.000(1)	-0.003(1)
C(11)	0.018(1)	0.015(1)	0.017(1)	-0.001(1)	-0.001(1)	0.001(1)
C(12)	0.019(1)	0.013(1)	0.022(1)	0.000(1)	0.000(1)	0.001(1)
C(13)	0.018(1)	0.015(1)	0.021(1)	-0.004(1)	0.002(1)	0.002(1)
C(14)	0.015(1)	0.020(1)	0.017(1)	-0.005(1)	-0.002(1)	0.001(1)
C(15)	0.016(1)	0.014(1)	0.018(1)	-0.001(1)	-0.003(1)	-0.002(1)
C(16)	0.019(1)	0.016(1)	0.021(1)	0.002(1)	0.001(1)	0.002(1)
C(17)	0.010(1)	0.012(1)	0.019(1)	0.000(1)	0.001(1)	-0.001(1)
C(18)	0.014(1)	0.012(1)	0.019(1)	-0.003(1)	0.000(1)	0.001(1)
C(19)	0.014(1)	0.018(1)	0.020(1)	0.001(1)	0.003(1)	-0.002(1)
C(20)	0.019(1)	0.015(1)	0.029(1)	0.004(1)	0.002(1)	-0.002(1)
C(21)	0.015(1)	0.011(1)	0.028(1)	-0.002(1)	0.001(1)	-0.002(1)
C(22)	0.014(1)	0.013(1)	0.021(1)	-0.003(1)	0.002(1)	0.001(1)
C(23)	0.017(1)	0.012(1)	0.021(1)	0.000(1)	0.002(1)	0.004(1)
C(24)	0.022(1)	0.015(1)	0.022(1)	0.001(1)	0.003(1)	-0.003(1)
O(1)	0.021(1)	0.024(1)	0.012(1)	0.002(1)	0.000(1)	0.001(1)
O(2)	0.015(1)	0.019(1)	0.028(1)	-0.001(1)	-0.002(1)	-0.001(1)
O(3)	0.019(1)	0.015(1)	0.022(1)	-0.007(1)	-0.002(1)	0.001(1)
O(4)	0.017(1)	0.028(1)	0.023(1)	0.005(1)	0.005(1)	0.007(1)
O(5)	0.018(1)	0.016(1)	0.023(1)	-0.008(1)	0.002(1)	-0.002(1)
O(6)	0.018(1)	0.023(1)	0.025(1)	0.003(1)	-0.004(1)	-0.006(1)
S(1)	0.011(1)	0.015(1)	0.023(1)	0.000(1)	-0.002(1)	0.001(1)
S(2)	0.012(1)	0.019(1)	0.018(1)	0.004(1)	0.002(1)	0.004(1)
S(3)	0.013(1)	0.016(1)	0.018(1)	0.000(1)	0.001(1)	-0.004(1)

---

**Hydrogen coordinates and isotropic displacement parameters ( $\text{\AA}^2$ )**

---

	x	y	z	$U_{eq}$
H(1)	0.6470	0.6800	0.3840	0.017
H(1A)	0.803(7)	0.3970(17)	0.4737(16)	0.048(11)
H(2)	0.9905	0.7790	0.4095	0.016
H(2A)	0.957(8)	0.7444(19)	0.4924(18)	0.053(11)
H(3A)	0.6211	0.8380	0.4254	0.019
H(3B)	0.4430	0.7809	0.4102	0.019
H(4A)	0.4585	0.8453	0.3279	0.021
H(4B)	0.7638	0.8433	0.3277	0.021
H(5A)	0.6140	0.7758	0.2557	0.021
H(5B)	0.4373	0.7416	0.3026	0.021

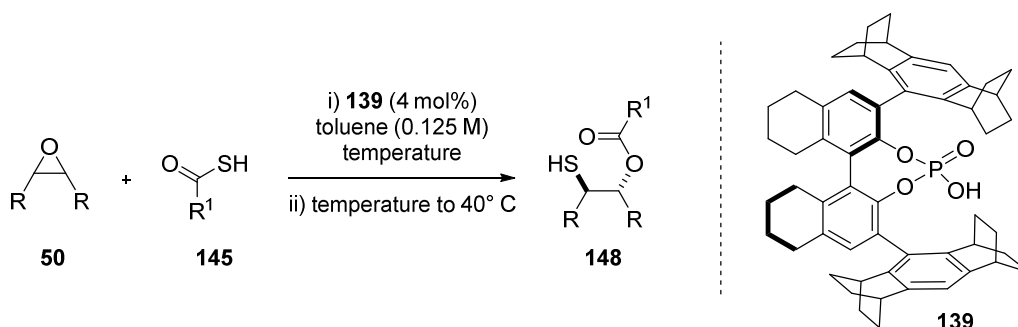


## 7. Experimental Section

---

H(5)	0.309(7)	0.4004(17)	0.4893(16)	0.045(11)
H(6A)	0.9845	0.7407	0.3035	0.021
H(6B)	0.8093	0.6833	0.2870	0.021
H(8A)	1.1362	0.5104	0.3281	0.035
H(8B)	1.0449	0.4944	0.3931	0.035
H(8C)	1.2812	0.5393	0.3831	0.035
H(9)	1.0712	0.3523	0.3539	0.017
H(10)	0.7497	0.3058	0.4459	0.016
H(11A)	1.1277	0.2759	0.4927	0.020
H(11B)	1.2952	0.3025	0.4401	0.020
H(12A)	1.2710	0.1962	0.4292	0.022
H(12B)	0.9660	0.1981	0.4324	0.022
H(13A)	1.0854	0.1892	0.3336	0.022
H(13B)	1.2685	0.2474	0.3389	0.022
H(14A)	0.7224	0.2513	0.3469	0.021
H(14B)	0.8850	0.2769	0.2929	0.021
H(16A)	0.6311	0.4652	0.2107	0.028
H(16B)	0.5912	0.4958	0.2736	0.028
H(16C)	0.4059	0.4422	0.2525	0.028
H(17)	0.5927	0.4562	0.6006	0.016
H(18)	0.2487	0.4902	0.5078	0.018
H(19A)	0.6169	0.5150	0.4533	0.021
H(19B)	0.7961	0.4964	0.5071	0.021
H(20A)	0.7588	0.6035	0.5048	0.025
H(20B)	0.4539	0.5989	0.5063	0.025
H(21A)	0.7867	0.5630	0.6000	0.022
H(21B)	0.6014	0.6210	0.6014	0.022
H(22A)	0.2403	0.5570	0.6010	0.019
H(22B)	0.4203	0.5386	0.6549	0.019
H(24A)	-0.0822	0.3958	0.7211	0.029
H(24B)	0.1396	0.3810	0.7670	0.029
H(24C)	0.0917	0.3365	0.7126	0.029

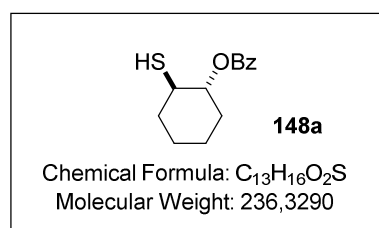
---

7.5.3. General procedure for the organocascade synthesis of thiols **148**.

In a screw-cap vial, epoxide **50** (0.1 mmol) was dissolved in 0.4 mL of toluene and was cooled to the reaction temperature. Then a pre-cooled solution of thiocarboxylic acid **145** (0.16 mmol, 1.6 equiv.) and catalyst **139** (4 mol%) in 0.4 mL of toluene was added and the reaction was stirred for 2-5 days. Next, the temperature was raised to room temperature and subsequently to 40 °C and the mixture was stirred for 1-2 days. The reaction mixture was directly purified by flash column chromatography (eluent: mixtures hexane/MTBE). The enantiomeric ratios of products were measured by HPLC on a chiral stationary phase.

For analytical purpose, the racemic samples were prepared on 0.05 mmol scale using (*RS*)-**TRIP** as the catalyst.

**(*R,R*)-2-mercaptocyclohexyl benzoate (148a)** – The reaction was performed at –78° C and the product was isolated as a colorless liquid in 86% yield and e.r. = 98:2.



<sup>1</sup>H-NMR (300 MHz, CDCl<sub>3</sub>): δ 8.12-8.02 (m, 2H), 7.62-7.53 (m, 1H), 7.52-7.40 (m, 2H), 4.95-4.80 (cm, 1H), 3.15-2.95 (m, 1H), 2.30-2.10 (m, 2H), 1.92-1.68 (m, 2H), 1.73 (d, *J* = 1.73 Hz, 1H), 1.62-1.20 (m, 4H).

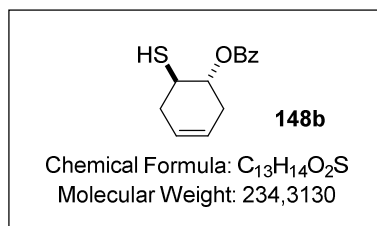
<sup>13</sup>C-NMR (75 MHz, CDCl<sub>3</sub>): δ 166.1, 133.1, 130.7, 129.9, 128.6, 79.0, 42.4, 35.1, 31.6, 25.6, 24.2.

HRMS (*m/z*) calcd for C<sub>13</sub>H<sub>16</sub>O<sub>2</sub>SNa [M]<sup>+Na</sup>: 259.0763, found: 259.0762.

[α]<sub>D</sub><sup>25</sup>: -89.7° (*c* = 0.925, CHCl<sub>3</sub>).

The enantiomeric ratio was determined by HPLC analysis using Daicel Chiralcel AD-3 column: *n*Hept:*i*PrOH = 98:2, flow rate 1.0 mL/min, τ<sub>1</sub> = 4.5 min, τ<sub>2</sub> = 5.0 min.

**(*R,R*)-6-mercaptocyclohex-3-en-1-yl benzoate (148b)** – The reaction was performed at  $-40^{\circ}$  C and the product was isolated as a colorless liquid in 98% yield and e.r. = 96:4.



$^1\text{H-NMR}$  (300 MHz,  $CD_2Cl_2$ ):  $\delta$  8.00-7.92 (m, 2H), 7.55-7.45 (m, 1H), 7.42-7.32 (m, 2H), 5.58 (cm, 2H), 5.10-5.00 (m, 1H), 3.32-3.18 (m, 1H), 2.78-2.58 (m, 2H), 2.25-2.05 (m, 2H), 1.77 (d,  $J = 7.1$  Hz, 1H).

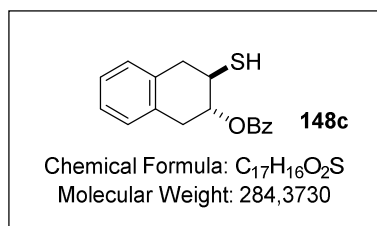
$^{13}\text{C-NMR}$  (75 MHz,  $CD_2Cl_2$ ):  $\delta$  166.1, 133.4, 130.8, 129.9, 128.8, 124.9, 124.3, 74.6, 37.6, 33.7, 30.0.

**HRMS** ( $m/z$ ) calcd for  $C_{13}H_{14}O_2SNa$  [ $M$ ] $^{+Na}$ : 257.0607, found: 257.0607.

$[\alpha]_D^{25}$ :  $-145.6^{\circ}$  ( $c = 1.100$ ,  $CHCl_3$ ).

The enantiomeric ratio was determined by HPLC analysis using Daicel Chiralcel AD-3 column:  $n\text{Hept}:i\text{PrOH} = 98:2$ , flow rate 1.0 mL/min,  $\tau_1 = 4.2$  min,  $\tau_2 = 4.6$  min.

**(*R,R*)-3-mercapto-1,2,3,4-tetrahydronaphthalen-2-yl benzoate (148c)** – Reaction performed at  $-40^{\circ}$  C. Product isolated as a colorless liquid in 97% yield and e.r. = 95:5.



$^1\text{H-NMR}$  (300 MHz,  $CDCl_3$ ):  $\delta$  8.10-8.02 (m, 2H), 7.65-7.54 (m, 1H), 7.50-7.40 (m, 2H), 7.25-7.08 (m, 4H), 5.37 (cm, 1H), 3.62-3.40 (m, 3H), 3.08-2.92 (m, 2H), 1.84 (d,  $J = 7.0$  Hz, 1H).

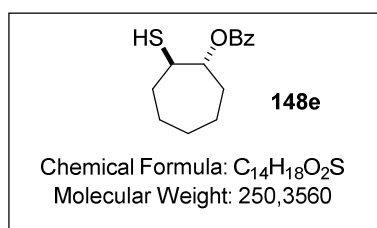
$^{13}\text{C-NMR}$  (75 MHz,  $CDCl_3$ ):  $\delta$  166.1, 133.4, 133.3, 133.0, 130.4, 129.9, 129.3, 128.9, 128.7, 126.9, 126.7, 74.9, 38.0, 36.7, 33.1.

**HRMS** ( $m/z$ ) calcd for  $C_{17}H_{16}O_2SNa$  [ $M$ ] $^{+Na}$ : 307.0763, found: 307.0763.

$[\alpha]_D^{25}$ :  $-132.2^{\circ}$  ( $c = 1.325$ ,  $CHCl_3$ ).

The enantiomeric ratio was determined by HPLC analysis using Daicel Chiralcel AD-3 column:  $n\text{Hept}:i\text{PrOH} = 98:2$ , flow rate 1.0 mL/min,  $\tau_1 = 8.0$  min,  $\tau_2 = 9.3$  min.

**(*R,R*)-2-mercaptocycloheptyl benzoate (148e)** – The reaction was performed at  $-40^{\circ}$  C and the product was isolated as a colorless liquid in 80% yield and e.r. = 96:4.



$^1\text{H-NMR}$  (300 MHz,  $CDCl_3$ ):  $\delta$  8.15-8.00 (m, 2H), 7.64-7.54 (m, 1H), 7.52-7.40 (m, 2H), 5.09 (dt,  $J = 7.8$  Hz,  $J = 3.1$  Hz, 1H), 3.38-3.25 (m, 1H), 2.20-2.00 (m, 2H), 1.95-1.50 (m, 9H).

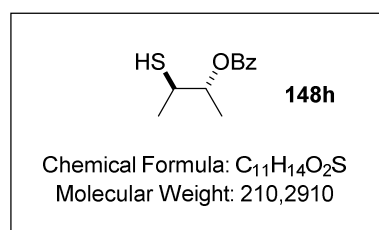
$^{13}\text{C-NMR}$  (75 MHz,  $CDCl_3$ ):  $\delta$  165.9, 133.2, 130.7, 129.8, 128.6, 81.9, 44.6, 33.8, 31.7, 28.0, 25.3, 22.4.

**HRMS** ( $m/z$ ) calcd for  $C_{14}H_{18}O_2SNa$   $[M]^{+Na}$ : 273.0919, found: 273.0920.

$[\alpha]_D^{25}$ :  $-76.2^\circ$  ( $c = 0.900$ ,  $CHCl_3$ ).

The enantiomeric ratio was determined by HPLC analysis using Daicel Chiralcel AD-3 column:  $nHept:iPrOH = 98:2$ , flow rate 1.0 mL/min,  $\tau_1 = 5.0$  min,  $\tau_2 = 5.5$  min.

**(*R,R*)-3-mercaptobutan-2-yl benzoate (148h)** – The reaction was performed at  $-40^\circ$  C and the product was isolated as a colorless liquid in 81% yield and e.r. = 97:3.



**$^1H$  NMR** (300 MHz,  $CDCl_3$ ):  $\delta$  8.13-8.05 (m, 2H), 7.65-7.55 (m, 1H), 7.50-7.42 (m, 2H), 5.19 (dq,  $J = 6.2$  Hz,  $J = 4.6$  Hz, 1H), 3.19 (dQ,  $J = 7.2$  Hz,  $J = 4.6$  Hz, 1H), 1.65 (d,  $J = 7.2$  Hz, 1H), 1.42 (cm, 6H).

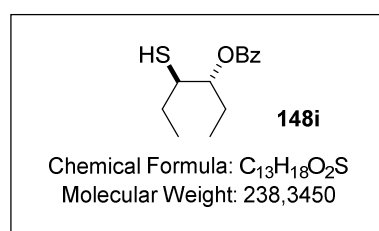
**$^{13}C$ -NMR** (125 MHz,  $CDCl_3$ ):  $\delta$  166.0, 133.2, 130.6, 129.8, 128.6, 75.2, 39.3, 20.9, 16.8.

**HRMS** ( $m/z$ ) calcd for  $C_{11}H_{14}O_2SNa$   $[M]^{+Na}$ : 233.0607, found: 233.0609.

$[\alpha]_D^{25}$ :  $-39.4^\circ$  ( $c = 0.350$ ,  $CHCl_3$ ).

The enantiomeric ratio was determined by HPLC analysis using Daicel Chiralcel OJ-H column:  $nHept:iPrOH = 99.5:0.5$ , flow rate 0.5 mL/min,  $\tau_1 = 14.6$  min,  $\tau_2 = 15.5$  min.

**(*R,R*)-4-mercaptohexan-3-yl benzoate (148i)** – The reaction was performed at  $-40^\circ$  C and the product was isolated as a colorless liquid in 74% yield and e.r. = 93.5:6.5.



**$^1H$ -NMR** (300 MHz,  $CD_2Cl_2$ ):  $\delta$  8.10-7.90 (m, 2H), 7.55-7.45 (m, 1H), 7.42-7.32 (m, 2H), 5.09 (cm, 1H), 2.84 (cm, 1H), 1.88-1.64 (m, 3H), 1.54-1.35 (m, 2H), 0.97 (t,  $J = 7.4$  Hz, 3H), 0.86 (t,  $J = 7.4$  Hz, 3H).

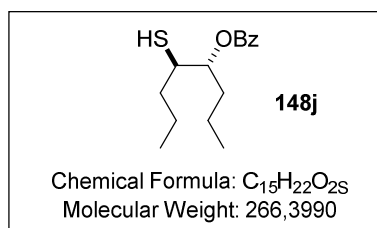
**$^{13}C$ -NMR** (75 MHz,  $CD_2Cl_2$ ):  $\delta$  166.3, 133.3, 130.9, 129.9, 128.8, 78.4, 46.0, 29.1, 25.1, 12.3, 10.2.

**HRMS** ( $m/z$ ) calcd for  $C_{13}H_{18}O_2SNa$   $[M]^{+Na}$ : 261.0920, found: 261.0921.

$[\alpha]_D^{25}$ :  $+12.0^\circ$  ( $c = 0.750$ ,  $CHCl_3$ ).

The enantiomeric ratio was determined by HPLC analysis using Daicel Chiralcel OJ-H column:  $nHept:iPrOH = 99.5:0.5$ , flow rate 0.5 mL/min,  $\tau_1 = 11.6$  min,  $\tau_2 = 12.3$  min.

**(*R,R*)-5-mercaptooctan-4-yl benzoate (148j)** – The reaction was performed at  $-40^{\circ}\text{C}$  and the product was isolated as a colorless liquid in 82% yield and e.r. = 94:6.



$^1\text{H-NMR}$  (300 MHz,  $\text{CDCl}_3$ ):  $\delta$  8.15-8.03 (m, 2H), 7.65-7.55 (m, 1H), 7.52-7.43 (m, 2H), 5.28 (cm, 1H), 3.08-2.95 (m, 1H), 1.95-1.30 (m, 9H), 0.96 (t,  $J = 7.4$  Hz, 3H), 0.91 (t,  $J = 7.4$  Hz, 3H).

$^{13}\text{C-NMR}$  (75 MHz,  $\text{CDCl}_3$ ):  $\delta$  166.3, 133.2, 130.5, 129.9, 128.6,

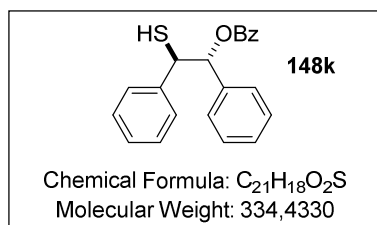
77.0, 44.0, 37.8, 33.9, 20.8, 19.1, 14.1, 13.9.

**HRMS** ( $m/z$ ) calcd for  $\text{C}_{15}\text{H}_{22}\text{O}_2\text{SNa}$  [ $\text{M}$ ] $^{+\text{Na}}$ : 289.1233, found: 289.1233.

$[\alpha]_{\text{D}}^{25}$ :  $+15.4^{\circ}$  ( $c = 0.350$ ,  $\text{CHCl}_3$ ).

The enantiomeric ratio was determined by HPLC analysis using Daicel Chiralcel OJ-3R column:  $\text{CH}_3\text{CN}:\text{H}_2\text{O} = 50:50$ , flow rate 1.0 mL/min,  $\tau_1 = 17.6$  min,  $\tau_2 = 18.6$  min.

**(*R,R*)-2-mercapto-1,2-diphenylethyl benzoate (148k)** – The reaction was performed at  $-10^{\circ}\text{C}$  and the product was isolated as a white solid in 99% yield and e.r. = 87:13. Single recrystallization in pentane afforded the product in 70% yield and e.r. = 98.5:1.5.



$^1\text{H-NMR}$  (300 MHz,  $\text{CDCl}_3$ ):  $\delta$  8.25-8.08 (m, 2H), 7.68-7.56 (m, 1H), 7.55-7.43 (m, 2H), 7.38-7.10 (m, 10H), 6.27 (d,  $J = 8.4$  Hz, 1H), 4.59 (dd,  $J = 8.4$  Hz  $J = 5.0$  Hz, 1H), 2.31 (d,  $J = 5.0$  Hz, 1H).

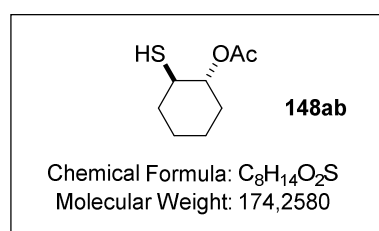
$^{13}\text{C-NMR}$  (75 MHz,  $\text{CDCl}_3$ ):  $\delta$  165.5, 139.4, 138.0, 133.4, 130.2, 130.0, 128.7, 128.7, 128.5, 128.4, 128.3, 128.0, 127.4, 80.7, 49.7.

**HRMS** ( $m/z$ ) calcd for  $\text{C}_{21}\text{H}_{18}\text{O}_2\text{SNa}$  [ $\text{M}$ ] $^{+\text{Na}}$ : 357.0920, found: 357.0921.

$[\alpha]_{\text{D}}^{25}$ :  $-2.7^{\circ}$  (e.r. = 87:13;  $c = 0.450$ ,  $\text{CHCl}_3$ ).

The enantiomeric ratio was determined by HPLC analysis using Daicel Chiralcel AD-3 column:  $n\text{Hept}:\text{iPrOH} = 85:5$ , flow rate 1.0 mL/min,  $\tau_1 = 6.0$  min,  $\tau_2 = 9.0$  min.

**(R,R)-2-mercaptocyclohexyl acetate (148ab)** – The reaction was performed at  $-40^{\circ}\text{C}$  and the product was isolated as a colorless liquid in 86% yield and e.r. = 95:5.



$^1\text{H-NMR}$  (500 MHz,  $\text{CD}_2\text{Cl}_2$ ):  $\delta$  4.47 (td,  $J = 4.4$  Hz,  $J = 10.0$  Hz, 1H), 2.80-2.70 (m, 1H), 2.06-1.90 (m, 2H), 1.97 (s, 3H), 1.70-1.58 (m, 2H), 1.62 (d,  $J = 6.1$  Hz, 1H), 1.43-1.15 (m, 4H).

$^{13}\text{C-NMR}$  (125 MHz,  $\text{CD}_2\text{Cl}_2$ ):  $\delta$  170.5, 78.5, 42.6, 35.5, 31.9,

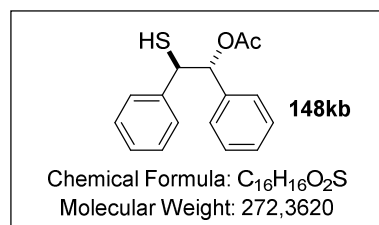
25.9, 24.5, 21.3.

**HRMS** ( $m/z$ ) calcd for  $\text{C}_8\text{H}_{14}\text{O}_2\text{SNa}$   $[\text{M}]^{+\text{Na}}$ : 197.0607, found: 197.0608.

$[\alpha]_{\text{D}}^{25}$ :  $-53.8^{\circ}$  ( $c = 0.520$ ,  $\text{CHCl}_3$ ).

The enantiomeric ratio was determined by GC analysis using BGB-177/BG-15 column 30 m ( $80^{\circ}\text{C}$ ,  $0.5^{\circ}\text{C}/\text{min}$  until  $120^{\circ}\text{C}$ ,  $10^{\circ}\text{C}/\text{min}$  until  $220^{\circ}\text{C}$ , 3 min at  $220^{\circ}\text{C}$ , 0.4 bar  $\text{H}_2$ ),  $\tau_1 = 64.0$  min,  $\tau_2 = 65.6$  min.

**(R,R)-2-mercapto-1,2-diphenylethyl acetate (148kb)** – The reaction was performed at  $10^{\circ}\text{C}$  and the product was isolated as a colorless liquid in 63% yield and e.r. = 86:14.



$^1\text{H-NMR}$  (500 MHz,  $\text{CD}_2\text{Cl}_2$ ):  $\delta$  7.20-7.00 (m, 10H), 5.87 (d,  $J = 8.90$  Hz, 1H), 4.31 (dd,  $J = 8.9$  Hz,  $J = 5.1$  Hz, 1H), 2.27 (d,  $J = 5.1$  Hz, 1H), 2.03 (s, 3H).

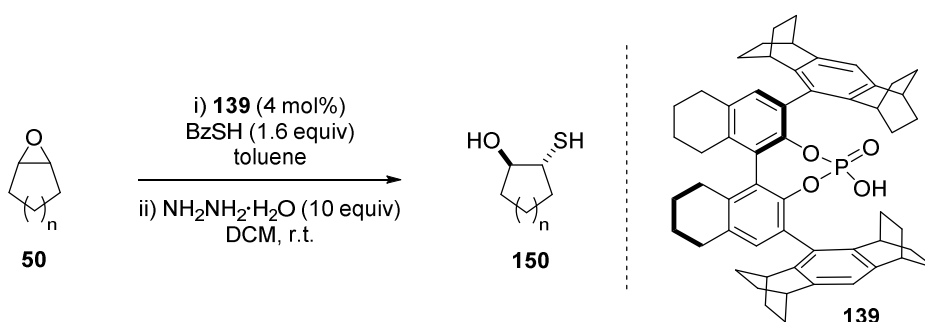
$^{13}\text{C-NMR}$  (125 MHz,  $\text{CD}_2\text{Cl}_2$ ):  $\delta$  170.1, 139.7, 138.4, 128.8,

128.5, 128.4, 128.4, 128.1, 127.5, 80.3, 49.4, 21.2.

**HRMS** ( $m/z$ ) calcd for  $\text{C}_{16}\text{H}_{16}\text{O}_2\text{SNa}$   $[\text{M}]^{+\text{Na}}$ : 295.0769, found: 295.0775.

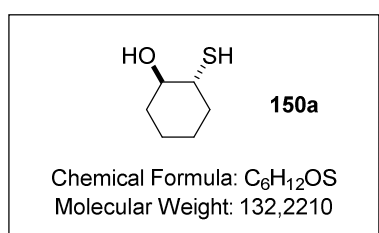
$[\alpha]_{\text{D}}^{25}$ :  $-59.5^{\circ}$  ( $c = 0.740$ ,  $\text{CHCl}_3$ ).

The enantiomeric ratio was determined by HPLC analysis using Daicel Chiralcel AD-3 column:  $n\text{Hept}:i\text{PrOH} = 90:10$ , flow rate 1.0 mL/min,  $\tau_1 = 5.6$  min,  $\tau_2 = 6.0$  min.

7.5.4. One-pot synthesis of 1,2-thioalcohols **150**

In a screw-cap vial, thiobenzoic acid (0.32 mmol, 1.6 equiv.) and catalyst **139** (4 mol%) were dissolved in 0.8 mL of toluene and cooled to the appropriate reaction temperature (**50a**:  $-78^\circ\text{C}$ , **50d**:  $-40^\circ\text{C}$ ). Then a pre-cooled solution of epoxide **50** (0.2 mmol) in 0.8 mL of toluene was added and the reaction was stirred for 2-3 days. Next, the reaction temperature was slowly raised to room temperature and a solution of hydrazine hydrate (100 mg, 2 mmol, 10 equiv.) in 0.5 mL of dichloromethane was added dropwise and the mixture was stirred for 2h at room temperature. The mixture was diluted with dichloromethane and the 1,2-thioalcohols were directly purified by column chromatography on silica gel (eluent: dichloromethane).

**(1R,2R)-2mercaptocyclohexanol (150a)** – Isolated in 91% yield (24 mg) and 98:2 er. Upon comparison with previous literature reports, the absolute configuration was confirmed to be *R,R*.<sup>103</sup>



$^1\text{H-NMR}$  (500 MHz,  $\text{CD}_2\text{Cl}_2$ ):  $\delta$  3.08 (m, 1H), 2.55 (d,  $J = 2.70$  Hz, 1H), 2.47-2.35 (m, 1H), 2.10-1.87 (m, 2H), 1.73-1.52 (m, 2H), 1.42 (d,  $J = 8.7$  Hz, 1H), 1.34-1.05 (m, 4H).

$^{13}\text{C-NMR}$  (125 MHz,  $\text{CD}_2\text{Cl}_2$ ):  $\delta$  76.9, 48.0, 36.8, 34.5, 26.9,

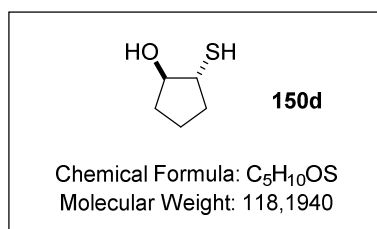
25.1.

**HRMS** ( $m/z$ ) calcd for  $\text{C}_6\text{H}_{12}\text{OS}$  [M]: 132.0609, found: 132.0609.

$[\alpha]_{\text{D}}^{25}$ :  $-73.3^\circ$  ( $c = 0.410$ ,  $\text{CHCl}_3$ ).

The enantiomeric ratio was determined by GC analysis using BGB-178-BG-15 column 30 m (115 min at  $75^\circ\text{C}$ ,  $10^\circ\text{C}/\text{min}$  until  $220^\circ\text{C}$ , 4 min at  $220^\circ\text{C}$ , 0.5 bar  $\text{H}_2$ ),  $\tau_1 = 99.9$  min,  $\tau_2 = 103.2$  min.

**(1*R*,2*R*)-2mercaptocyclopentanol (150d)** – Isolated in 83% yield (19.5 mg) and 95.5:4.5 er.



**<sup>1</sup>H-NMR** (500 MHz, CD<sub>2</sub>Cl<sub>2</sub>): δ 3.80 (c, 1H), 2.83 (Q, *J* = 7.1 Hz, 1H), 2.18-2.05 (m, 1H), 2.02-1.92 (m, 1H), 1.86 (d, *J* = 3.8 Hz, 1H), 1.75-1.60 (m, 2H), 1.52 (d, *J* = 7.1 Hz, 1H), 1.45-1.38 (m, 2H).

**<sup>13</sup>C-NMR** (125 MHz, CD<sub>2</sub>Cl<sub>2</sub>): δ 82.1, 46.4, 33.9, 32.6, 21.1.

**HRMS** (*m/z*) calcd for C<sub>5</sub>H<sub>9</sub>OS [M]<sup>-H</sup>: 117.0380, found: 117.0379.

**[α]<sub>D</sub><sup>25</sup>**: -45.5° (*c* = 0.440, CHCl<sub>3</sub>).

The enantiomeric ratio was determined by GC analysis using BGB-177/BGB-15 column 25 m (40 min at 100 °C, 10 °C/min until 220 °C, 3 min at 220 °C, 0.4 bar H<sub>2</sub>), τ<sub>1</sub> = 29.9 min, τ<sub>2</sub> = 30.7 min.



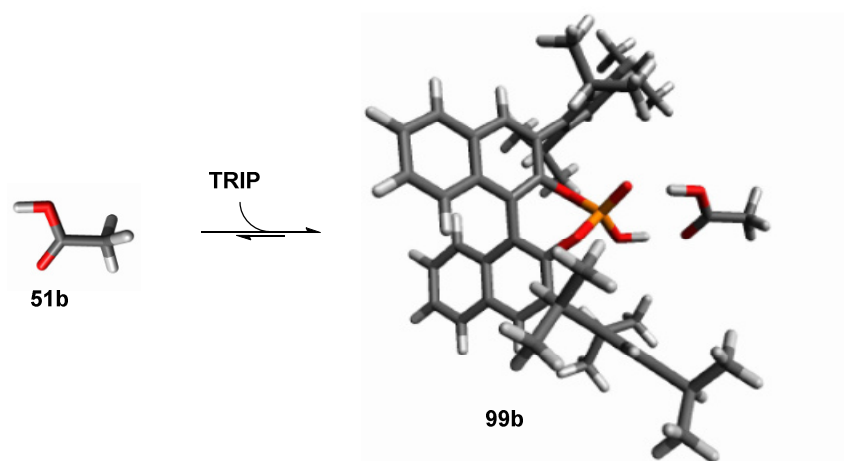
## 7.6. Mechanistic investigations

### 7.6.1. Molecular orbitals energies of acetic acid

This study was performed to investigate the effect of the heterodimerizing self-assembly on the energies of the frontier molecular orbitals of acetic acid (AcOH).

The geometries of acetic acid monomer and of the heterodimer **TRIP**·AcOH were optimized at the B3LYP/cc-pVTZ level.

The energies of the molecular orbitals were obtained from single-point calculations of the AcOH monomer, both in its optimum geometry and in the geometry adopted in the heterodimer complex.



Optimized (B3LYP/cc-pVTZ) geometry of acetic acid monomer.

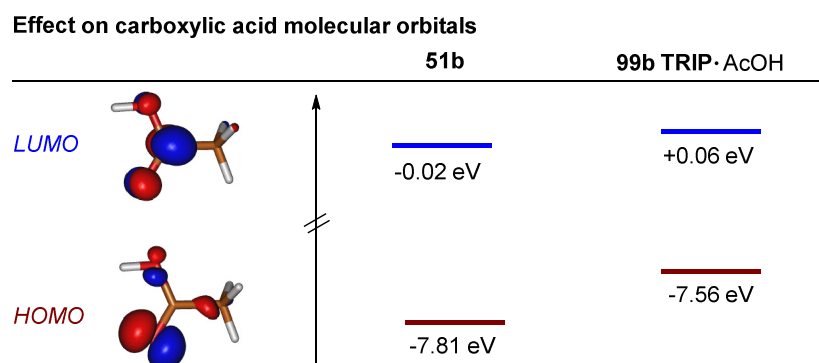
C	0.000000	0.155924	0.000000
O	0.186291	1.344228	0.000000
O	-1.243419	-0.385331	0.000000
H	-1.869140	0.354139	0.000000
C	1.063305	-0.905988	0.000000
H	2.043075	-0.439671	0.000000
H	0.951630	-1.542630	0.877792
H	0.951630	-1.542630	-0.877792

HOMO energy = -0.287108 Ha (-7.81 eV)  
LUMO energy = -0.000608 Ha (-0.02 eV)

B3LYP/cc-pVTZ geometry of acetic acid as extracted from the heterodimer.

C	-1.376743	-0.174484	-0.000723
C	0.099866	0.100302	-0.000531
O	0.830484	-0.990683	0.001157
O	0.550790	1.242042	0.000350
H	-1.634882	-0.786828	-0.864564
H	-1.930393	0.758345	-0.022584
H	-1.639960	-0.745733	0.889705
H	1.816308	-0.791561	-0.007084

HOMO energy = -0.277791 Ha (-7.56 eV)  
LUMO energy = +0.002263 Ha (+0.06 eV)



### 7.6.2. Brønsted acidity of TRIP·AcOH heterodimer

This study aimed at elucidating the effect of self-assembly on the acidity of the species. The stability of acid-base association complexes was evaluated using pyridine as indicator.

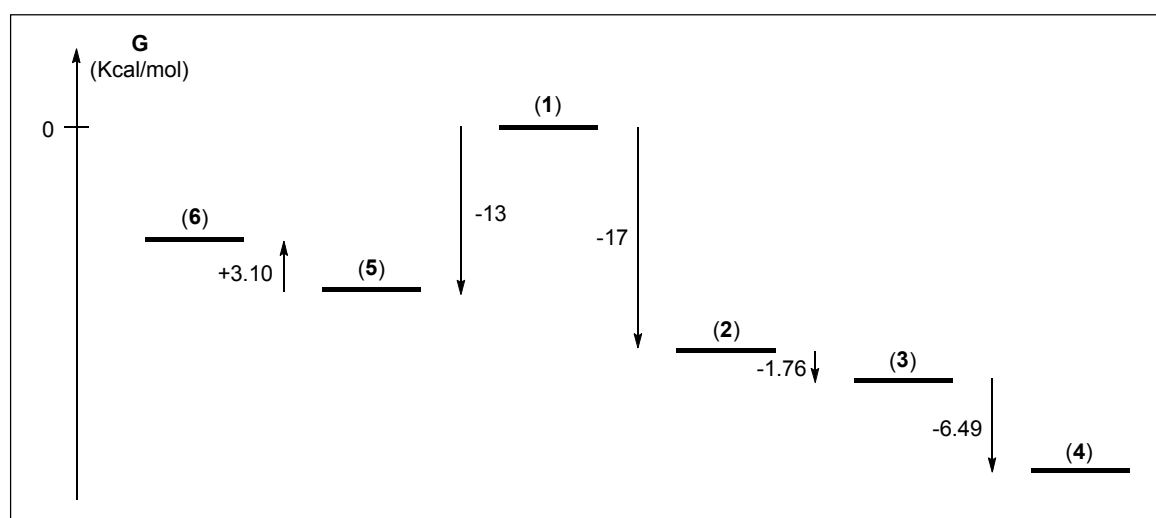
The following species were considered:

- 1) **TRIP/AcOH/pyridine**: the three molecules do not interact (i.e. they are at infinite distance). The energies of all other structures investigated presently are given relative to the reference energy of this non-interacting system.
- 2) **TRIP-AcOH/pyridine**: **TRIP-AcOH** heterodimer, no interaction with pyridine.
- 3) **TRIP-AcOH-pyridine**: complex between **TRIP-AcOH** and pyridine (with hydrogen bonding between neutral species).
- 4) **(TRIP-AcOH)<sup>-</sup>-pyridinium**: complex between **TRIP-AcOH** anion and pyridinium ion (with hydrogen bonding between ion pairs).
- 5) **TRIP-pyridine/AcOH**: **TRIP-pyridine** complex (with hydrogen bonding between neutral species), no interaction with AcOH.
- 6) **TRIP<sup>-</sup>-pyridinium/AcOH**: complex between **TRIP** anion and pyridinium ion (with hydrogen bonding between ion pairs), no interaction with AcOH.

## 7. Experimental Section

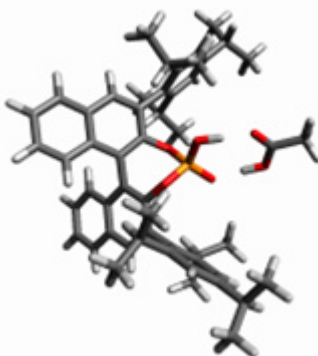
Gibbs free energies (G) computed at the B3LYP/cc-pVTZ (PCM, toluene) level for each system (1-6).

Complex	G (Hartree)
1) <b>TRIP</b> /AcOH/Py	-3060.46076803
2) <b>TRIP</b> -AcOH/Py	-3060.48789122
3) <b>TRIP</b> -AcOH-Py	-3060.49070734
4) ( <b>TRIP</b> -AcOH) <sup>-</sup> -Pyridinium <sup>+</sup>	-3060.50104359
5) <b>TRIP</b> -Py/AcOH	-3060.48177568
6) <b>TRIP</b> <sup>-</sup> -Pyridinium <sup>+</sup> /AcOH	-3060.47684770



The computational results highlight the increase of the overall acidity of the species upon heterodimeric association, in line with the expected heteroconjugation effect. They reveal not only that the trimeric species **4** is more stable than complex **5** ( $\Delta G = -12.25 \text{ kcal mol}^{-1}$ ), but also indicate that in this assembly the proton transfer is favored, yielding a stabilization compared with complex **3** ( $\Delta G = -6.49 \text{ kcal mol}^{-1}$ ). On the other hand, proton transfer is not favored for “free” **TRIP** and the ion pair complex **6** is found less stable than complex **5** with a standard hydrogen bonding interaction ( $\Delta G = +3.10 \text{ kcal mol}^{-1}$ ).

## Optimized structures (Cartesian coordinates, Å)



## (2) TRIP-AcOH/pyridine

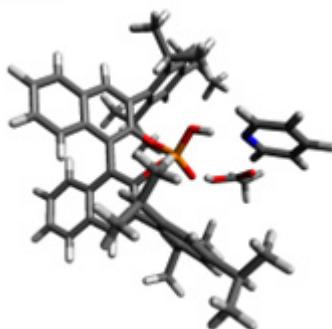
C	-4.677659	0.946715	-4.487945	C	-4.360709	1.983011	5.165858
C	-4.712616	-0.283129	-3.799808	C	-5.210795	3.072161	5.302045
C	-3.629075	-1.179696	-3.914038	C	-6.417967	3.040072	4.610774
C	-2.544011	-0.830293	-4.712571	C	-6.784904	1.964233	3.808059
C	-2.486849	0.375688	-5.403494	C	-3.671330	-0.267698	4.290336
C	-3.563653	1.243054	-5.274062	C	-2.258737	0.203531	3.913347
C	-5.915718	-0.667717	-2.993382	C	-8.146060	1.998374	3.121845
C	-5.888890	-0.721773	-1.574740	C	-9.290228	1.921761	4.146019
C	-6.947831	-1.151740	-0.800395	C	-4.817092	4.257575	6.166300
C	-8.199581	-1.402291	-1.454129	C	-4.580028	5.519922	5.322733
C	-8.254741	-1.352154	-2.878140	O	-5.928745	0.886579	0.833261
C	-7.091606	-1.020415	-3.607299	P	-4.544883	0.883013	0.016371
C	-9.403008	-1.660708	-0.751426	O	-3.275469	0.859119	0.748852
C	-10.578539	-1.890731	-1.418807	O	-4.686372	-0.391222	-0.954115
C	-10.619108	-1.884250	-2.827211	C	-3.618772	-2.542242	-3.230151
C	-9.479769	-1.617360	-3.537766	C	-3.715573	-3.681239	-4.258667
C	-6.793892	-1.330694	0.670533	C	-1.301681	0.738433	-6.281372
C	-6.337458	-0.294066	1.458126	C	0.015915	0.778899	-5.493892
C	-6.310201	-0.323190	2.875850	C	-5.816643	1.960446	-4.426812
C	-6.708897	-1.490097	3.478861	C	-5.335207	3.389037	-4.132333
C	-7.068894	-2.638102	2.738336	C	-2.400978	-2.727746	-2.312572
C	-7.101456	-2.574679	1.313755	C	-6.647196	1.948257	-5.722007
C	-7.382313	-3.857410	3.387359	C	-1.187400	-0.193380	-7.497768
C	-7.681451	-4.982636	2.667109	O	-4.797244	2.184666	-0.875322
C	-7.673754	-4.933996	1.258952	C	-8.307708	3.218874	2.203355
C	-7.395919	-3.763503	0.601018	C	-5.831623	4.526994	7.286824
C	-5.904827	0.868153	3.688551	C	-3.640001	-1.072586	5.600837
C	-4.672992	0.879585	4.371154	O	29.905076	18.565453	-1.574971

## 7. Experimental Section

---

C	30.621586	18.570233	-0.608709	H	-9.207054	1.027533	4.764916
C	32.081406	18.925023	-0.591738	H	-10.256899	1.894653	3.639157
O	30.175292	18.241681	0.629363	H	-9.286465	2.786961	4.810938
H	-7.140837	-1.025830	-4.687800	H	-9.265141	3.174581	1.680769
H	-9.500405	-1.589582	-4.619801	H	-7.515020	3.254006	1.456855
H	-11.551227	-2.076666	-3.341083	H	-3.866755	3.999380	6.641193
H	-11.484834	-2.075333	-0.857741	H	-3.831371	5.341896	4.550257
H	-9.395332	-1.666276	0.327529	H	-4.233712	6.343935	5.949625
H	-1.720671	-1.527155	-4.800657	H	-5.498555	5.841030	4.828054
H	-3.532489	2.185027	-5.806822	H	-6.802016	4.820725	6.882839
H	-4.503482	-2.612971	-2.600443	H	-5.485225	5.336177	7.932574
H	-4.607928	-3.580995	-4.877865	H	-5.982336	3.640880	7.904249
H	-3.760027	-4.648327	-3.754158	H	-3.997359	-0.941751	3.499612
H	-2.849706	-3.691426	-4.922662	H	-1.824101	0.840653	4.685458
H	-2.465770	-3.683949	-1.790132	H	-2.269425	0.748385	2.971980
H	-2.347465	-1.936770	-1.565769	H	-1.601096	-0.660204	3.796851
H	-1.486819	1.747493	-6.659785	H	-3.300441	-0.453069	6.433153
H	-0.051913	1.459294	-4.644579	H	-2.954664	-1.917633	5.512537
H	0.834498	1.113679	-6.133669	H	-4.624786	-1.462035	5.861087
H	0.280015	-0.207605	-5.109390	H	-8.283819	4.153200	2.766517
H	-0.992149	-1.222109	-7.189788	H	32.251672	19.761563	0.086047
H	-0.367899	0.120128	-8.147261	H	32.403807	19.185584	-1.594443
H	-2.106421	-0.190974	-8.084728	H	32.662899	18.081824	-0.218673
H	-6.475791	1.674038	-3.608716	H	29.235338	18.026833	0.537496
H	-4.746913	3.799780	-4.953893	H	-3.986265	2.700832	-0.952074
H	-4.726115	3.423660	-3.231026	N	29.692147	-13.371780	0.706619
H	-6.192193	4.048003	-3.983720	C	28.733463	-14.292825	0.601820
H	-1.466937	-2.725418	-2.876817	C	28.923518	-15.637595	0.899166
H	-6.037663	2.244835	-6.577700	C	30.177451	-16.049881	1.329140
H	-7.482873	2.646653	-5.647578	C	31.184836	-15.101463	1.442551
H	-7.052477	0.959300	-5.933724	C	30.891945	-13.781123	1.120465
H	-6.726330	-1.544789	4.559216	H	27.765792	-13.938836	0.263702
H	-7.365251	-3.885599	4.469399	H	28.107202	-16.339156	0.795013
H	-7.910255	-5.910614	3.173522	H	30.365472	-17.087689	1.570663
H	-7.884631	-5.830144	0.690879	H	32.177728	-15.374112	1.773071
H	-7.390008	-3.748759	-0.477963	H	31.656917	-13.016447	1.198545
H	-7.100098	3.875364	4.703145				
H	-3.416187	1.996507	5.694775				
H	-8.230531	1.115127	2.491334				

Energy = -3060.48789122 Hartree



## (3) TRIP-AcOH-pyridine

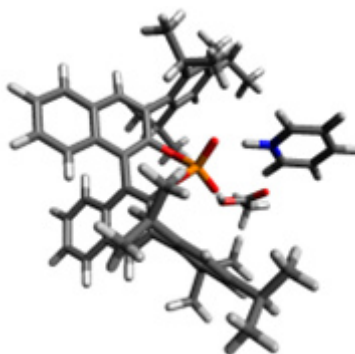
C	0.000000	0.000000	0.000000	C	-4.731326	-5.636913	3.860585
C	0.000000	0.000000	1.410818	C	-4.562224	-6.794332	3.076986
C	1.220855	0.000000	2.111969	C	-4.341099	-8.011584	3.721659
C	2.410997	0.013380	1.384581	C	-4.270603	-8.124420	5.103665
C	2.437836	0.018874	-0.003501	C	-4.429250	-6.964431	5.855396
C	1.218269	0.007577	-0.673124	C	-4.658274	-5.724127	5.266678
C	-1.301501	0.099153	2.148408	C	-4.621716	-6.771974	1.553493
C	-2.216657	-0.982137	2.232812	C	-3.427333	-7.487842	0.905512
C	-3.481894	-0.878564	2.774297	C	-4.051965	-9.477206	5.759467
C	-3.822131	0.335083	3.458212	C	-2.830274	-9.489570	6.689643
C	-2.907633	1.428225	3.417045	C	-4.846921	-4.513222	6.174177
C	-1.686805	1.285709	2.721323	C	-6.094952	-4.657257	7.059838
C	-3.235670	2.636314	4.079549	C	1.293786	-0.009059	3.634929
C	-4.402826	2.758619	4.784788	C	2.223116	-1.106538	4.175080
C	-5.291701	1.667906	4.859408	C	3.759186	0.025587	-0.752654
C	-5.012313	0.491819	4.211960	C	3.976202	-1.277147	-1.537860
O	-1.824795	-2.187365	1.654383	C	-1.284632	0.029682	-0.820256
P	-1.631077	-3.523866	2.519096	C	-1.455288	1.378881	-1.538233
O	-2.842523	-3.484189	3.584836	O	-0.380640	-3.270586	3.421127
C	-4.138865	-3.259287	3.122289	O	-1.611155	-4.710560	1.640255
C	-4.458433	-1.998248	2.661673	C	-5.943602	-7.364297	1.035997
C	-5.750927	-1.804242	2.073433	C	-3.598029	-4.228596	7.022269
C	-6.697096	-2.869729	2.127475	C	-5.310964	-9.955742	6.499989
C	-6.334956	-4.090156	2.739856	C	1.714166	1.362653	4.189605
C	-5.069462	-4.325925	3.217247	C	3.902402	1.249731	-1.668974
C	-6.123907	-0.615499	1.398096	C	-1.372351	-1.138970	-1.813133
C	-7.368055	-0.479535	0.837849	N	0.871392	-5.372734	4.486092
C	-8.314079	-1.520085	0.927323	C	1.156199	-5.458048	5.788807
C	-7.980870	-2.689183	1.557157	C	1.816136	-6.542697	6.345635

## 7. Experimental Section

---

C	2.199792	-7.585017	5.510507	H	-6.202138	1.757530	5.436814
C	1.907280	-7.500201	4.157119	H	-5.704656	-0.332591	4.286347
C	1.239873	-6.377667	3.682880	H	1.211755	0.011062	-1.755336
O	-0.443193	-5.417720	-0.680726	H	3.352458	0.016345	1.919401
C	0.594008	-6.249921	-0.609020	H	-2.126544	-0.071268	-0.138427
C	1.102908	-6.641656	-1.973586	H	-1.445616	2.208388	-0.829928
O	1.060574	-6.671442	0.427500	H	-2.402767	1.406800	-2.079958
H	-7.080311	-4.870385	2.818238	H	-0.653821	1.548510	-2.259374
H	-8.691869	-3.503398	1.616445	H	-2.333380	-1.122032	-2.330560
H	-9.294705	-1.396648	0.487836	H	-1.277808	-2.097857	-1.305060
H	-7.624176	0.433986	0.318075	H	4.548919	0.088133	0.000992
H	-5.410935	0.190249	1.313351	H	3.921415	-2.146538	-0.882170
H	-4.381628	-7.025179	6.935112	H	4.954509	-1.276500	-2.022551
H	-4.213118	-8.905178	3.124231	H	3.219764	-1.399101	-2.315105
H	-5.009982	-3.640392	5.544643	H	3.157604	1.237592	-2.466515
H	-6.988733	-4.826168	6.458105	H	4.888070	1.264666	-2.137940
H	-6.250269	-3.752262	7.650471	H	3.777678	2.178294	-1.110902
H	-5.999246	-5.493905	7.753927	H	0.295918	-0.225341	4.013741
H	-3.743060	-3.328326	7.622606	H	3.267705	-0.912970	3.926225
H	-2.724353	-4.077705	6.389374	H	1.953263	-2.081901	3.775251
H	-3.855340	-10.189716	4.953919	H	2.152008	-1.151848	5.263633
H	-1.932179	-9.162677	6.165125	H	2.719534	1.627450	3.856576
H	-2.653183	-10.495070	7.075997	H	1.716399	1.349761	5.281374
H	-2.976068	-8.829028	7.545912	H	1.039689	2.154577	3.864266
H	-5.565277	-9.279492	7.318282	H	-0.591027	-1.081826	-2.572659
H	-5.156133	-10.949884	6.924033	H	0.498967	-7.472750	-2.343308
H	-6.168920	-10.002227	5.828597	H	2.135763	-6.969428	-1.900579
H	-4.578210	-5.731777	1.234145	H	1.004963	-5.820922	-2.680730
H	-3.451816	-8.563556	1.088238	H	-0.796017	-5.205168	0.220441
H	-2.485921	-7.093545	1.280574	H	0.841195	-4.624347	6.404497
H	-3.448425	-7.339906	-0.175539	H	2.022767	-6.565589	7.406242
H	-3.383352	-5.051621	7.706021	H	2.717968	-8.446687	5.910152
H	-6.043499	-8.411090	1.329675	H	2.185946	-8.283742	3.467378
H	-5.982007	-7.317608	-0.053999	H	0.996982	-6.283940	2.631703
H	-6.808871	-6.828158	1.426375	H	0.051045	-4.030535	3.793452
H	-1.028512	2.141328	2.651421				
H	-2.535669	3.460546	4.027425				
H	-4.639731	3.683472	5.293263				

Energy = -3060.49070734 Hartree

(4) (TRIP-AcOH)<sup>-</sup>-pyridinium<sup>+</sup>

C	-0.169499	-4.474755	-2.548321	C	1.216029	3.512687	1.368195
N	-0.217975	-3.820775	-1.381092	C	3.015390	4.424886	2.766726
C	-0.158357	-4.459373	-0.207269	C	2.177144	5.401434	3.234574
C	-0.048394	-5.839667	-0.173114	C	0.837979	5.440132	2.797939
C	0.003753	-6.540925	-1.369074	C	0.372108	4.525649	1.888311
C	-0.056440	-5.849549	-2.576915	C	3.896992	0.328706	0.118573
O	-0.483584	-4.132973	2.818349	C	4.336889	-0.664185	1.015024
C	-0.583871	-3.267491	3.668338	C	5.267531	-1.604299	0.571166
O	-0.341100	-1.982574	3.462176	C	5.769356	-1.606642	-0.723157
C	-1.004885	-3.546895	5.089330	C	5.308432	-0.625337	-1.595070
O	-0.463476	-1.302897	-1.358232	C	4.386415	0.341589	-1.204731
P	0.019472	-0.582518	-0.118880	C	3.843136	-0.750710	2.454560
O	0.485903	-1.411287	1.034439	C	4.923415	-0.291892	3.448470
O	-1.116196	0.430867	0.462416	C	3.969444	1.396911	-2.223383
C	-1.465556	1.598765	-0.186857	C	3.290325	0.774628	-3.453133
C	-0.555351	2.637399	-0.246890	C	6.784876	-2.649050	-1.158713
C	-0.912059	3.808175	-0.995313	C	8.120746	-2.015576	-1.574827
C	-2.236182	3.920373	-1.513156	O	1.154714	0.449804	-0.669734
C	-3.151902	2.865276	-1.307094	C	-3.789192	0.589888	-0.515263
C	-2.793067	1.695728	-0.686021	C	-4.179085	-0.192821	-1.618513
C	0.001444	4.853089	-1.284652	C	-5.159002	-1.169203	-1.435069
C	-0.381472	5.952679	-2.009219	C	-5.761637	-1.401385	-0.206102
C	-1.702652	6.077882	-2.482348	C	-5.356527	-0.617882	0.870202
C	-2.606360	5.078474	-2.239370	C	-4.384773	0.370849	0.744464
C	0.770406	2.529537	0.425089	C	-3.590250	-0.003180	-3.012551
C	1.612254	1.470812	0.142478	C	-4.604711	0.654460	-3.963009
C	2.964095	1.409243	0.575777	C	-6.829982	-2.470843	-0.058867
C	3.408954	2.418073	1.392638	C	-8.192681	-1.874043	0.324561
C	2.558915	3.452243	1.844313	C	-4.042786	1.221219	1.962605



## 7. Experimental Section

---

C	-3.629123	0.379576	3.178092	H	0.340038	6.730187	-2.222497
C	-3.063140	-1.314208	-3.614377	H	1.019322	4.776681	-0.935272
C	-5.201621	2.169230	2.314202	H	-5.814886	-0.774535	1.838088
C	-6.415386	-3.572005	0.928498	H	-5.467570	-1.770039	-2.281861
C	5.155476	2.283390	-2.637057	H	-3.189792	1.847058	1.707933
C	6.238498	-3.557709	-2.270472	H	-5.463710	2.804786	1.467416
C	3.340472	-2.155152	2.819727	H	-4.927543	2.815358	3.150610
H	4.440204	2.416787	1.720044	H	-6.095494	1.612205	2.601079
H	4.041602	4.371444	3.107861	H	-3.325919	1.031108	3.999747
H	2.534302	6.133960	3.945977	H	-2.789565	-0.271996	2.940265
H	0.169123	6.196015	3.187621	H	-6.944292	-2.938937	-1.040627
H	-0.658801	4.568093	1.571579	H	-5.464266	-4.021317	0.641134
H	5.683753	-0.602479	-2.610298	H	-7.168997	-4.361301	0.964212
H	5.612492	-2.364812	1.260353	H	-6.302439	-3.176048	1.939172
H	3.237842	2.050898	-1.753650	H	-8.155489	-1.404200	1.308964
H	5.612978	2.761745	-1.770214	H	-8.958931	-2.651217	0.356804
H	4.824721	3.067123	-3.321434	H	-8.506960	-1.116179	-0.393744
H	5.929236	1.704442	-3.144161	H	-2.736756	0.666695	-2.926097
H	2.952400	1.557370	-4.135195	H	-3.865578	-2.031862	-3.794388
H	2.424723	0.181866	-3.160558	H	-2.329741	-1.764684	-2.949057
H	6.980766	-3.281495	-0.288404	H	-2.579795	-1.115322	-4.573267
H	5.308679	-4.037914	-1.963478	H	-5.483688	0.020748	-4.096612
H	6.959930	-4.338639	-2.519376	H	-4.158445	0.820447	-4.945601
H	6.035930	-2.990681	-3.180852	H	-4.947082	1.616727	-3.582087
H	8.000176	-1.379045	-2.453172	H	-4.451447	-0.240577	3.539728
H	8.853178	-2.786676	-1.822149	H	-0.227057	-3.214730	5.777105
H	8.531713	-1.401158	-0.773220	H	-1.189336	-4.608534	5.220950
H	2.993502	-0.077790	2.555718	H	-1.905669	-2.979639	5.324632
H	4.149323	-2.888266	2.825850	H	-0.049593	-1.800230	2.519491
H	2.575108	-2.485272	2.120659	H	-0.224779	-3.865443	-3.438403
H	2.901808	-2.142811	3.818908	H	-0.017388	-6.366439	-3.523949
H	3.976629	0.129753	-4.005425	H	0.090335	-7.619017	-1.366567
H	5.801011	-0.939951	3.401150	H	-0.008130	-6.333036	0.786013
H	4.539924	-0.322376	4.470210	H	-0.197465	-3.858711	0.691835
H	5.254817	0.726450	3.243950	H	-0.313773	-2.704696	-1.371825
H	-4.163957	2.980274	-1.672611				
H	-3.620304	5.151710	-2.612209				
H	-1.994456	6.954563	-3.044933				

Energy = -3060.50104359 Hartree



## (5) TRIP-pyridine / AcOH

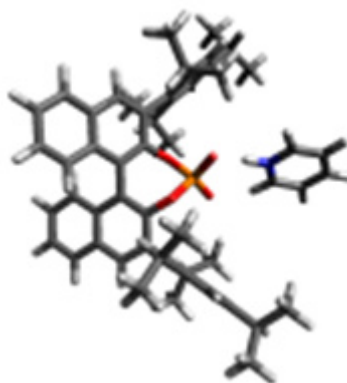
C	-4.234486	3.568402	-1.764112	C	-0.078827	-3.049623	0.700286
C	-4.974666	2.618827	-1.028360	C	1.209597	-2.526537	0.924554
C	-5.717155	3.031275	0.095705	C	1.851283	-2.823282	2.127384
C	-5.709521	4.381390	0.446550	C	1.267938	-3.607163	3.113333
C	-4.990253	5.333869	-0.262658	C	-0.007928	-4.106687	2.870826
C	-4.257392	4.901160	-1.363265	C	-0.694053	-3.846653	1.688244
C	-5.019188	1.191141	-1.481922	C	1.940999	-1.658203	-0.093888
C	-3.901879	0.321636	-1.360584	C	2.418583	-0.325083	0.501888
C	-3.877680	-0.964699	-1.865191	C	2.007235	-3.901131	4.407084
C	-5.102359	-1.512550	-2.371771	C	1.280946	-3.320173	5.629498
C	-6.240963	-0.662745	-2.491562	C	-2.070462	-4.472139	1.492178
C	-6.147242	0.683729	-2.076599	C	-1.980295	-6.003709	1.390733
C	-7.450555	-1.186477	-3.009797	C	-6.535782	2.063032	0.943655
C	-7.553644	-2.505116	-3.363188	C	-6.232919	2.191182	2.444089
C	-6.444081	-3.358994	-3.204327	C	-5.007444	6.791949	0.162445
C	-5.252686	-2.876567	-2.726490	C	-3.618609	7.277309	0.603899
O	-2.756793	0.844903	-0.778641	C	-3.436549	3.197898	-3.008999
P	-2.151771	0.277722	0.610019	C	-4.032485	3.843608	-4.270884
O	-2.341778	-1.321924	0.451466	O	-3.182759	0.583089	1.744428
C	-1.901991	-1.948615	-0.707939	O	-0.777250	0.772333	0.798559
C	-2.615666	-1.756666	-1.873843	C	3.116524	-2.417077	-0.732843
C	-2.096659	-2.327109	-3.082880	C	-3.065764	-4.048130	2.582609
C	-0.962559	-3.188623	-3.004856	C	2.277821	-5.402085	4.589838
C	-0.356766	-3.429387	-1.751781	C	-8.044131	2.227715	0.692517
C	-0.775010	-2.805350	-0.603090	C	-5.589772	7.705424	-0.926397
C	-2.629011	-2.045475	-4.365811	C	-1.945268	3.538234	-2.866222
C	-2.095645	-2.610651	-5.495734	N	-2.130204	1.832235	3.816531
C	-1.002480	-3.495375	-5.409614	C	-2.777127	2.051951	4.963967
C	-0.448601	-3.772250	-4.188581	C	-2.183871	2.682441	6.046866

## 7. Experimental Section

---

C	-0.864471	3.100956	5.929703	H	-6.533643	-4.406774	-3.458364
C	-0.190916	2.872055	4.738090	H	-4.416947	-3.548612	-2.606972
C	-0.859133	2.232708	3.702816	H	-3.688673	5.623522	-1.934667
O	34.472339	2.398988	-0.280247	H	-6.282379	4.703681	1.307160
C	35.141560	1.696318	-0.991242	H	-3.504970	2.120777	-3.147452
C	36.642742	1.663589	-1.042425	H	-5.080292	3.568977	-4.399382
O	34.594710	0.816305	-1.866617	H	-3.485897	3.519154	-5.158526
H	0.483881	-4.109079	-1.706342	H	-3.976992	4.932640	-4.226599
H	0.405467	-4.432895	-4.109578	H	-1.395852	3.202350	-3.747741
H	-0.596367	-3.940814	-6.307812	H	-1.514283	3.051749	-1.992423
H	-2.516152	-2.370990	-6.463283	H	-5.667815	6.859229	1.031537
H	-3.462427	-1.365901	-4.455044	H	-3.219217	6.652471	1.403328
H	-0.483704	-4.724627	3.621569	H	-3.667244	8.305941	0.966696
H	2.843120	-2.425937	2.304149	H	-2.908414	7.250543	-0.224250
H	-2.470692	-4.118930	0.543703	H	-4.966290	7.701623	-1.822107
H	-1.307578	-6.307045	0.587622	H	-5.652377	8.735826	-0.571117
H	-2.964153	-6.432009	1.188863	H	-6.590637	7.384287	-1.216617
H	-1.609945	-6.443749	2.318314	H	-6.261094	1.050877	0.651971
H	-4.054761	-4.459946	2.372215	H	-6.577804	3.144342	2.848477
H	-3.153819	-2.963543	2.630220	H	-5.164524	2.106777	2.632254
H	2.977196	-3.401389	4.335958	H	-6.741555	1.398414	2.995943
H	1.120712	-2.247298	5.518548	H	-8.380328	3.228121	0.972083
H	1.862653	-3.486373	6.538441	H	-8.612359	1.506145	1.282940
H	0.305192	-3.788821	5.769676	H	-8.297594	2.076553	-0.356582
H	1.346882	-5.963813	4.684750	H	-1.786824	4.613877	-2.770697
H	2.866025	-5.580568	5.492157	H	36.999594	0.660371	-0.809058
H	2.826591	-5.809575	3.740213	H	37.046255	2.377601	-0.332048
H	1.239294	-1.411512	-0.888406	H	36.984426	1.903115	-2.049468
H	3.164825	-0.474694	1.284341	H	33.633706	0.895730	-1.775755
H	1.580393	0.232570	0.913944	H	-3.803106	1.709181	5.009697
H	2.881114	0.283776	-0.277769	H	-2.745182	2.839136	6.956851
H	-2.762224	-4.409013	3.566897	H	-0.370507	3.596293	6.754881
H	3.870334	-2.673392	0.014138	H	0.836359	3.179940	4.605870
H	3.598166	-1.801673	-1.495121	H	-0.385166	2.019422	2.752863
H	2.791365	-3.345186	-1.204310	H	-2.780107	1.079095	2.552499
H	-7.005317	1.327800	-2.215364				
H	-8.300816	-0.523267	-3.106864				
H	-8.484989	-2.896336	-3.750050				

Energy = -3060.48177568 Hartree

(6)  $\text{TRIP}^-$ -pyridinium / AcOH

C	0.000000	0.000000	0.000000	C	-2.725445	2.561236	5.260524
N	0.000000	0.000000	1.338628	C	-3.009703	3.315352	6.569809
C	1.137276	0.000000	2.045520	C	-1.321836	6.479458	2.432981
C	2.360699	0.000078	1.409072	C	-2.005399	7.853617	2.490028
C	2.390948	0.001362	0.017237	C	-6.500528	-0.988983	1.856115
C	1.197380	0.001158	-0.694421	C	-5.452924	-1.763482	1.390653
O	-2.255782	-0.044745	2.417504	C	-5.635941	-2.877059	0.524254
P	-3.357484	-0.199439	1.371114	C	-6.912299	-3.149441	0.100108
O	-2.974145	-0.232831	-0.061697	C	-8.008785	-2.326320	0.436897
O	-4.486135	0.963289	1.545087	C	-7.808428	-1.216322	1.309609
C	-5.289771	1.036804	2.665014	C	-9.298292	-2.573674	-0.094294
C	-5.108612	2.169700	3.504411	C	-10.349773	-1.743545	0.188739
C	-5.922002	2.268785	4.605008	C	-10.147588	-0.620345	1.014745
C	-6.845550	1.257157	4.954080	C	-8.914758	-0.364526	1.558431
C	-7.011051	0.130761	4.094219	O	-4.185237	-1.518643	1.867795
C	-6.257348	0.073237	2.873280	C	-4.493496	-3.754682	0.116841
C	-7.595970	1.335126	6.152592	C	-4.025341	-3.736768	-1.211975
C	-8.449611	0.328725	6.518270	C	-2.992418	-4.604010	-1.570410
C	-8.582848	-0.805989	5.694116	C	-2.406003	-5.481858	-0.669371
C	-7.886598	-0.901160	4.516176	C	-2.882608	-5.479428	0.637920
C	-4.106986	3.239207	3.196397	C	-3.911234	-4.638195	1.051626
C	-4.293548	4.082654	2.081584	C	-4.601598	-2.813490	-2.280025
C	-3.386757	5.113716	1.852410	C	-5.452781	-3.601794	-3.289937
C	-2.297457	5.342938	2.687097	C	-1.284159	-6.407521	-1.108306
C	-2.126096	4.491483	3.770656	C	-1.667854	-7.888425	-0.970773
C	-2.997138	3.435370	4.040836	C	-4.400469	-4.741418	2.491342
C	-5.481210	3.937633	1.137735	C	-3.288030	-4.448346	3.508878
C	-5.043243	3.682703	-0.312379	C	-3.522019	-1.987748	-2.994734

## 7. Experimental Section

---

C	0.029754	-6.110648	-0.370005	H	-9.011122	0.395451	7.440568
C	-5.055119	-6.105900	2.762669	H	-9.237757	-1.612873	5.995346
C	-1.300612	1.989841	5.271461	H	-7.997910	-1.781970	3.903199
C	-0.560670	6.299869	1.110748	H	-3.541122	5.758900	0.996806
C	-6.423472	5.149519	1.227204	H	-1.275804	4.651218	4.422612
O	-4.605041	-9.909744	-34.307655	H	-6.056062	3.069056	1.452386
C	-3.455519	-9.595361	-34.955454	H	-6.770554	5.307027	2.249230
C	-3.482874	-10.061191	-36.383541	H	-7.298488	4.998429	0.591887
O	-2.549389	-9.015820	-34.416780	H	-5.929006	6.065553	0.898715
H	-7.086323	-4.005084	-0.539200	H	-5.916940	3.521380	-0.946797
H	-9.432621	-3.427606	-0.746434	H	-4.408524	2.800343	-0.378707
H	-11.328650	-1.938124	-0.228732	H	-0.584687	6.448637	3.240423
H	-10.971649	0.050902	1.217493	H	-0.041015	5.341366	1.083695
H	-8.781245	0.505838	2.182118	H	0.178671	7.092802	0.979537
H	-2.446583	-6.159011	1.359278	H	-1.238818	6.333064	0.256385
H	-2.629539	-4.593628	-2.590893	H	-2.745219	7.960637	1.694983
H	-5.171317	-3.988544	2.640640	H	-1.272971	8.654669	2.371104
H	-5.875242	-6.295189	2.068941	H	-2.517271	7.998963	3.441728
H	-5.454854	-6.141981	3.778057	H	-3.400621	1.709381	5.215608
H	-4.336794	-6.921223	2.658527	H	-0.547105	2.771216	5.393448
H	-3.690133	-4.469511	4.523721	H	-1.110128	1.452581	4.345010
H	-2.855017	-3.463786	3.337602	H	-1.186598	1.289608	6.101467
H	-1.112050	-6.213061	-2.170605	H	-2.356418	4.184170	6.673631
H	0.324323	-5.068251	-0.497941	H	-2.842021	2.665150	7.430875
H	0.836626	-6.742708	-0.747003	H	-4.039404	3.670424	6.612858
H	-0.067423	-6.299409	0.700612	H	-4.493313	4.532859	-0.720819
H	-1.838998	-8.157895	0.072803	H	-3.628947	-11.140867	-36.418327
H	-0.872119	-8.531042	-1.353221	H	-2.550542	-9.795101	-36.870583
H	-2.580385	-8.110538	-1.524693	H	-4.322659	-9.603381	-36.906449
H	-5.260451	-2.103223	-1.785283	H	-4.510619	-9.581561	-33.401285
H	-2.829225	-2.621341	-3.552183	H	1.035012	0.000587	3.121130
H	-2.962650	-1.392555	-2.275365	H	3.266632	-0.000885	1.995479
H	-3.989624	-1.307342	-3.709559	H	3.337632	0.001537	-0.505612
H	-2.489207	-5.190894	3.456715	H	1.181748	-0.000032	-1.773356
H	-4.853609	-4.332311	-3.837582	H	-0.983300	-0.009662	-0.459518
H	-5.914148	-2.931946	-4.018286	H	-0.891191	-0.007658	1.809567
H	-6.251753	-4.150557	-2.790273				
H	-5.841242	3.137787	5.245089				
H	-7.468936	2.204805	6.785155				

Energy = -3060.47684770 Hartree

### 7.6.3. Studies on the catalytic cycle

#### 7.6.3.1. Competition experiments

These experiments were designed to gain further insight on the mechanism of the asymmetric carboxylation of epoxides. In the presence of **TRIP** phosphoric acid, cyclohexene oxide was exposed to mixtures of different carboxylic acids and thiocarboxylic acids. The reaction mixture was directly analyzed by  $^1\text{H-NMR}$  spectroscopy in order to determine the product ratio.

**Experiment a.** Two different reactions were performed with mixtures of benzoic acid and thiobenzoic acid. Results are summarized in Table a in the following Scheme.

*Reaction a1.* A dichloromethane solution (0.4 ml) of benzoic acid (19.5 mg, 0.16 mmol, 1.6 equiv.), thiobenzoic acid (24.5 mg, 0.16 mmol, 1.6 equiv.) and **TRIP** (3 mg, 0.004 mmol, 4 mol%) was added to a stirred solution (0.4 ml) of cyclohexene oxide (9.8 mg, 0.1 mmol, 1 equiv.). After full consumption of the starting material (2 h) an aliquot of the reaction was diluted in deuterated dichloromethane and analyzed by NMR.

*Reaction a2.* Using 5 equivalents of benzoic and thiobenzoic acid, the above-mentioned protocol for reaction a1 was used.

**Experiment b.** Two different reactions were performed with mixtures of acetic acid and thioacetic acid. Results are summarized in Table b in the following Scheme.

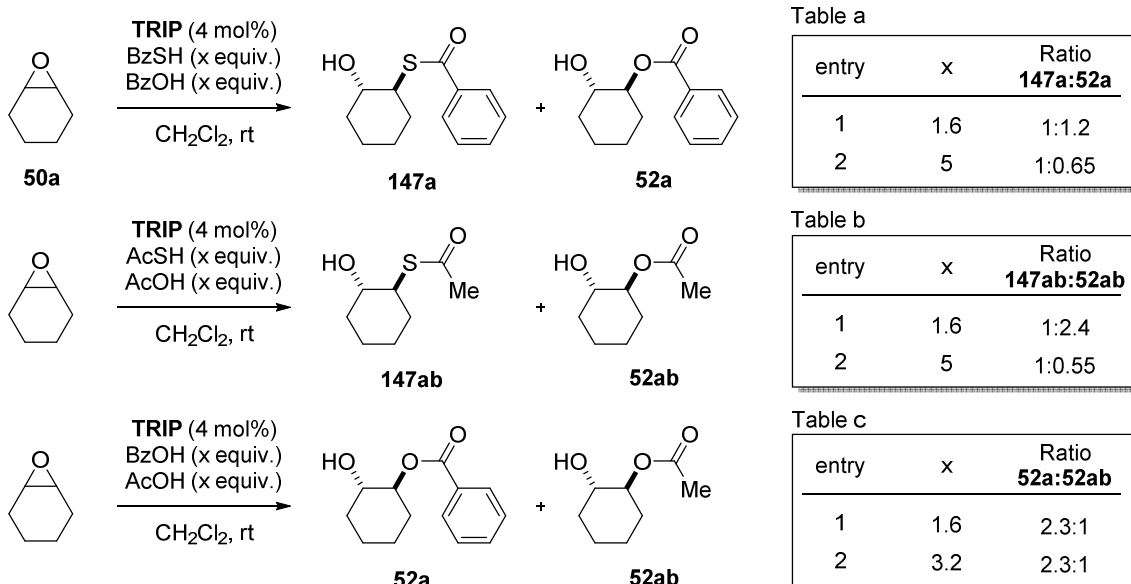
*Reaction b1.* A dichloromethane solution (0.2 ml) of acetic acid (4.8 mg, 0.08 mmol, 1.6 equiv.), thioacetic acid (6.1 mg, 0.08 mmol, 1.6 equiv.) and **TRIP** (1.5 mg, 0.002 mmol, 4 mol%) was added to a stirred solution (0.2 ml) of cyclohexene oxide (4.9 mg, 0.05 mmol, 1 equiv.). After full consumption of the starting material (2 h) an aliquot of the reaction was diluted in deuterated dichloromethane and analyzed by NMR.

*Reaction b2.* Using 5 equivalents of acetic and thioacetic acid, the above-mentioned protocol for reaction b1 was used.

**Experiment c.** Two different reactions were performed with mixtures of acetic acid and benzoic acid. Results are summarized in Table c in the following Scheme.

**Reaction c1.** A deuterated chloroform solution (0.8 ml) of acetic acid (4.8 mg, 0.08 mmol, 1.6 equiv.), benzoic acid (9.8 mg, 0.08 mmol, 1.6 equiv.) and **TRIP** (1.5 mg, 0.002 mmol, 4 mol%) was added to a stirred solution (0.7 ml) of cyclohexene oxide (4.9 mg, 0.05 mmol, 1 equiv.). After 15 h an aliquot of the reaction was analyzed by NMR.

**Reaction c2.** Using 3.2 equivalents of acetic and thioacetic acid, the above-mentioned protocol for reaction c1 was used.



As discussed in paragraph 4.5.2 these results suggest that a classical, direct activation of the epoxide moiety by the simple phosphoric acid catalyst is not involved in the transformation. The proposed mechanism *via* carboxylic acid activation is instead in agreement with these experimental data.

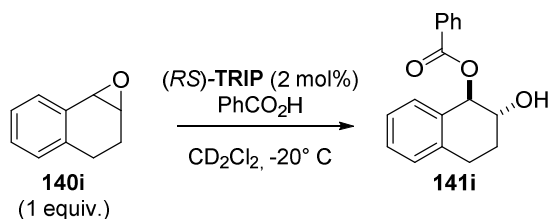
### 7.6.3.2. Kinetic studies

#### Carboxylisis of epoxides **140i**.

A series of kinetic experiments was performed to study the reaction mechanism of the ring opening reaction.

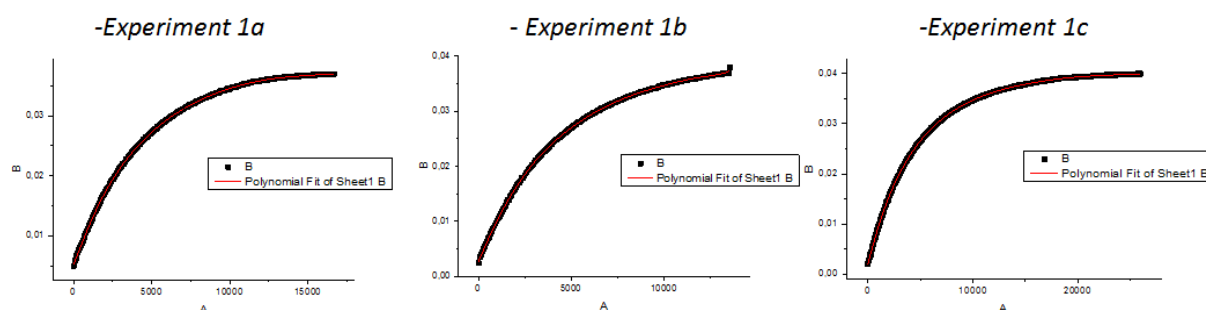
**Experiment 1.** This experiment was designed to evaluate the order dependence of the rate law with respect to the carboxylic acid.

## 7. Experimental Section

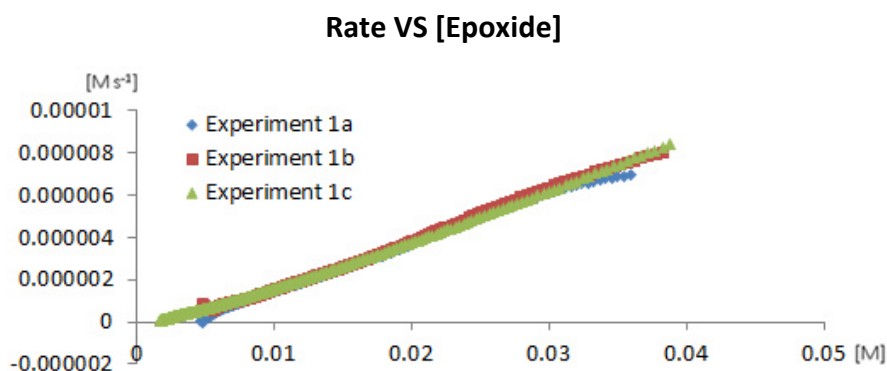


Epoxide **140i** (0.025 mmol, 1 equiv.),  $(RS)\text{-TRIP}$  (0.0005 mmol, 2 mol%) and benzoic acid (three different reactions. *1a*: 1.42 equiv.; *1b*: 2.24 equiv.; *1c*: 3.21 equiv.) were dissolved in  $\text{CD}_2\text{Cl}_2$  (0.6 mL) and the reaction was monitored using  $^1\text{H-NMR}$  spectroscopy.

The conversion was plotted as function of time and a 9<sup>th</sup> order polynomial function was used to fit the curve (see pictures below).



The calculated reaction rate ( $\Delta\text{conc}/\Delta t$ ) was plotted as a function of the epoxide concentration (see graph below).

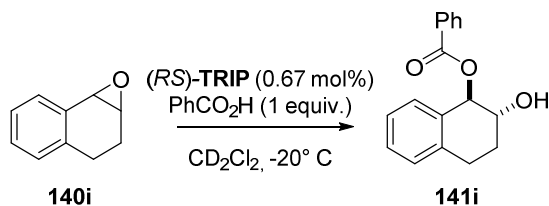


As shown above, the plots obtained from the three different experiments are linear and an almost perfect overlay is observed. This outcome is in accordance with a first order kinetic for the reaction and confirms that the concentration of the carboxylic acid does not influence the rate. This outcome suggests that the non-covalent self-assembly between the phosphoric acid and the carboxylic acid is the resting state of the catalytic cycle.



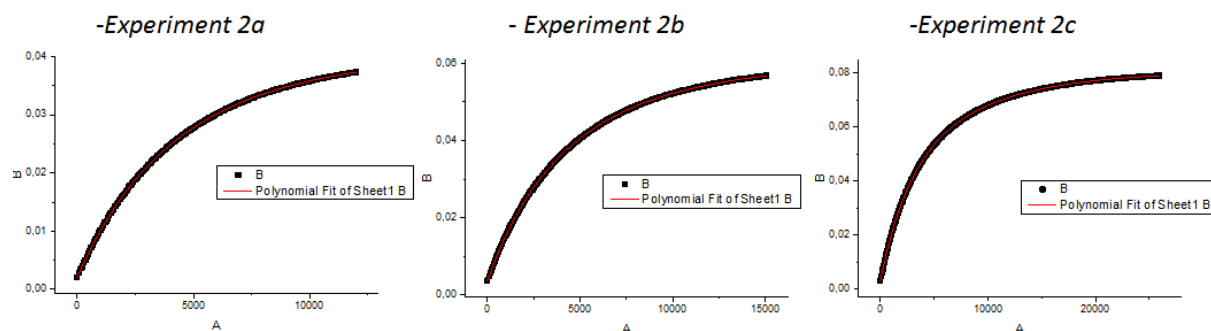
## 7. Experimental Section

*Experiment 2.* This experiment was designed to evaluate the order dependence of the rate law with respect to the epoxide.

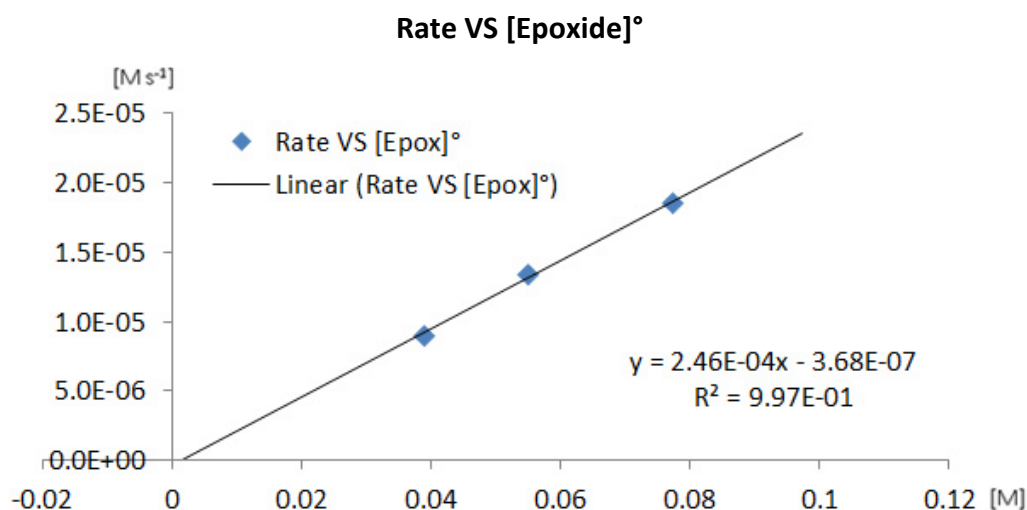


*Rac*TRIP (0.0005 mmol, 0.67 mol%), benzoic acid (0.075 mmol, 1 equiv.) and epoxide **140i** (three different experiments. *2a*: 0.31 equiv.; *2b*: 0.48 equiv.; *2c*: 0.64 equiv.) were dissolved in  $\text{CD}_2\text{Cl}_2$  (0.6 mL) and the reaction was monitored using  $^1\text{H-NMR}$  spectroscopy.

The conversion was plotted as function of time and a 9<sup>th</sup> order polynomial function was used to fit the curve.



Catalyst degradation affected the three experiments differently (the deactivation rate depends on the epoxide concentration [*vide infra*]). Nevertheless, the initial concentration of the catalyst was not affected by such phenomenon and therefore the method of the initial rates was used for the analysis.



A linear plot is obtained, thus accounting for a first-order dependence of the reaction rate with respect to the concentration of the epoxide. According to this result and based on *experiment 1*, the rate law is found to be:

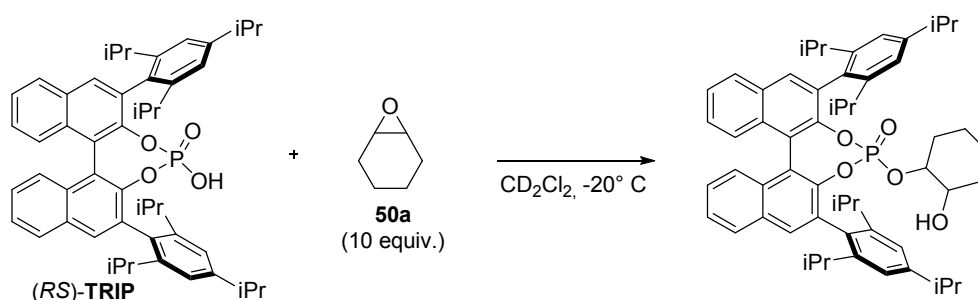
$$v = \frac{\Delta P}{\Delta t} = k[\mathbf{Cat}][\mathbf{Epoxide}]$$

In addition we could estimate the reaction constant  $k$  in these conditions:

$$k = 0.295 \text{ M}^{-1}\text{s}^{-1}$$

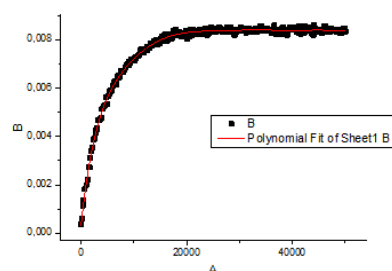
### Deactivation of TRIP catalyst.

This experiment was designed to evaluate the order dependence of the rate law with respect to the phosphoric acid catalyst in the degradation pathway. A large excess of the epoxide (10 equiv.) was used to reach a *pseudo-zero* order behavior and to mimic catalytic conditions.

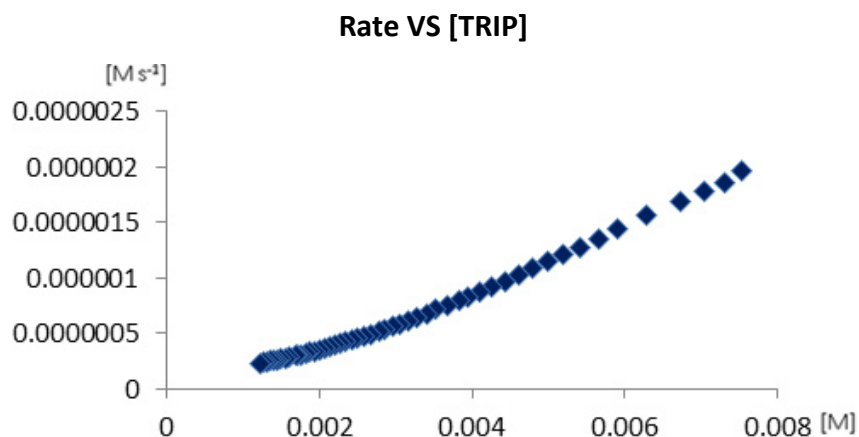


(*RS*)-**TRIP** (0.005 mmol, 1 equiv.) and epoxide **50a** (0.05 mmol, 10 equiv.) were dissolved in  $\text{CD}_2\text{Cl}_2$  (0.6 mL) and the reaction was monitored during time by  $^{31}\text{P}$ -NMR spectroscopy.

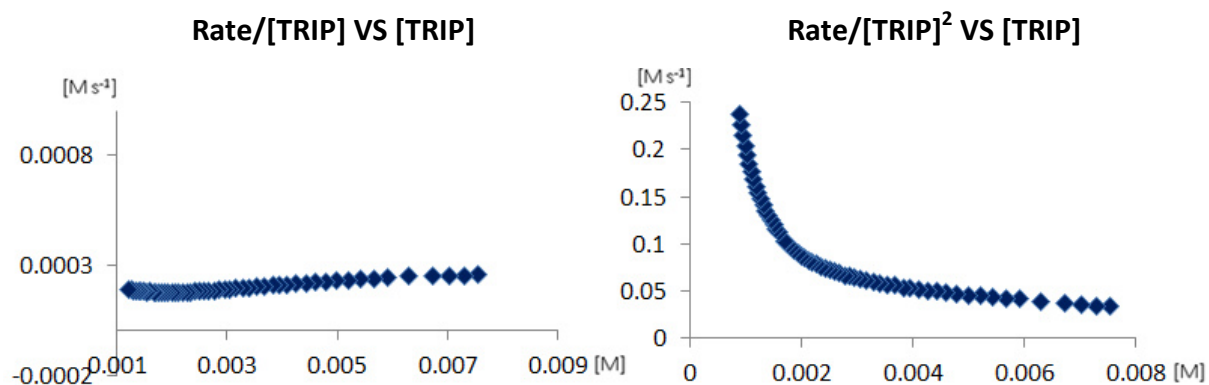
The conversion was plotted as function of time and a 9<sup>th</sup> order polynomial function was used to fit the curve (see picture below).



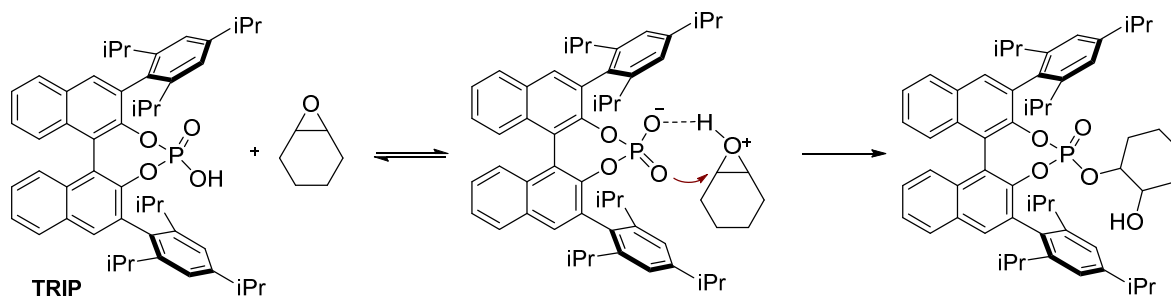
Then the calculated reaction rate ( $\Delta\text{conc}/\Delta t$ ) was plotted as a function of **TRIP** concentration (see graph below).



To evaluate the order of the phosphoric acid in the degradation reaction we examined the plots two following plots.

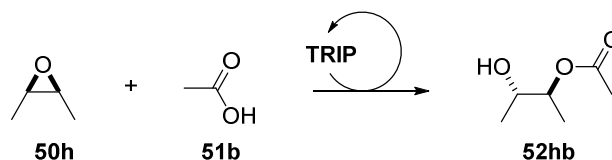


The first plot was found to be linear and constant, while the second appeared to be function of the **TRIP** concentration. This result suggests that **TRIP** degradation occur *via* the decomposition of the intermediate oxiranium phosphate and not with the nucleophilic attack of a second molecule of phosphoric acid (see scheme below).



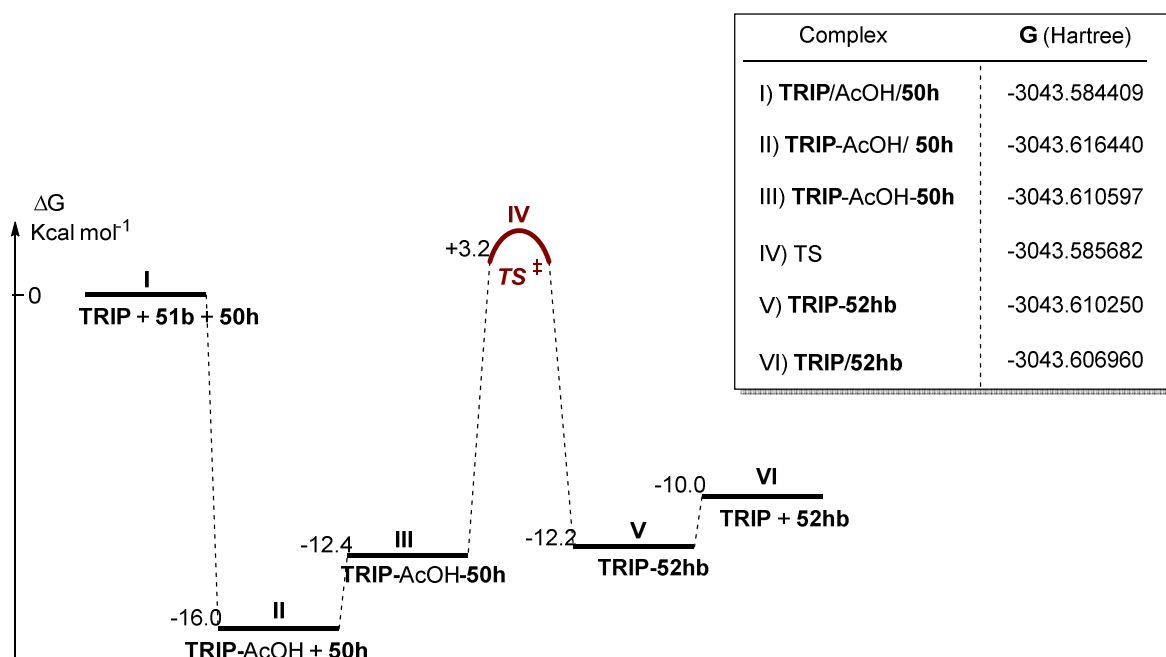
## 7.6.3.3. Theoretical investigation on the catalytic cycle

The objective of this study was to examine the sequence of events in the catalytic cycle for the reaction between epoxide **50h** and AcOH catalyzed by **TRIP** towards product **52hb**.



The following species were considered:

- (I) **TRIP/AcOH/50h**: the three molecules do not interact (i.e. they are at infinite distance). The energies of all other structures investigated are given relative to the reference energy of this non-interacting system.
- (II) **TRIP-AcOH/50h**: **TRIP-AcOH** heterodimer, no interaction with the epoxide.
- (III) **TRIP-AcOH-50h**: **TRIP**, AcOH and epoxide in a trimolecular complex.
- (IV) Transition state (TS).
- (V) **TRIP-52hb**: complex between **TRIP** and product.
- (VI) **TRIP/52hb**: no interaction between **TRIP** and product.



**Optimized structures (Cartesian coordinates, Å)****(I) TRIP/AcOH/50h**

C	7.794399	-1.920059	3.895177	C	2.369400	0.469103	-5.876303
C	7.377610	-0.582147	3.733290	C	2.371044	1.420192	-7.081971
C	6.278168	-0.095897	4.467308	O	6.374875	0.760416	-0.929134
C	5.630934	-0.959746	5.351171	P	5.856502	-0.319536	0.143022
C	6.023034	-2.279407	5.529649	O	4.731408	0.202216	0.924405
C	7.108363	-2.736971	4.788743	O	7.201502	-0.774169	0.895005
C	8.134871	0.327318	2.814864	C	5.771281	1.337605	4.347442
C	8.049990	0.211733	1.403924	C	6.128044	2.159451	5.597941
C	8.789898	0.967744	0.517813	C	5.278568	-3.184740	6.495817
C	9.567342	2.049171	1.049582	C	6.189238	-3.718173	7.611351
C	9.663326	2.196119	2.465107	C	8.995865	-2.497949	3.155303
C	8.968917	1.299669	3.307545	C	8.626633	-3.728774	2.313553
C	10.213747	3.012261	0.235555	C	4.263329	1.412212	4.064082
C	10.939029	4.036130	0.788655	C	10.148089	-2.816628	4.122407
C	11.066723	4.153105	2.186985	C	4.568462	-4.335787	5.766782
C	10.438141	3.252288	3.004057	O	5.566823	-1.674326	-0.652946
C	8.764019	0.666319	-0.941326	C	5.526773	-3.234443	-3.817875
C	7.568444	0.599515	-1.628533	C	1.193097	0.774561	-4.936138
C	7.470803	0.453419	-3.037661	C	6.287216	3.946001	-4.444736
C	8.647703	0.334705	-3.733827	O	-38.774951	-22.887630	-1.217418
C	9.903354	0.276375	-3.090089	C	-39.219871	-24.209017	-0.875709
C	9.972917	0.418612	-1.672962	C	-38.173807	-25.219832	-0.498255
C	11.092092	0.054428	-3.827584	C	-39.609992	-23.049324	-0.061045
C	12.301209	-0.063198	-3.196504	C	-39.023801	-22.694164	1.276357
C	12.367802	0.030477	-1.792223	O	-40.319807	27.428161	0.528307
C	11.238123	0.268366	-1.052232	C	-40.421609	28.607070	0.744811
C	6.150604	0.451165	-3.746444	C	-41.706087	29.366868	0.917874
C	5.413561	1.648357	-3.866718	O	-39.342650	29.420616	0.863083
C	4.204891	1.631493	-4.556443	H	9.079881	1.404613	4.378535
C	3.696022	0.474187	-5.136883	H	10.509859	3.342861	4.080413
C	4.442487	-0.690165	-5.012930	H	11.648422	4.961125	2.609702
C	5.658517	-0.734450	-4.330153	H	11.414040	4.764085	0.144672
C	5.913865	2.976616	-3.310623	H	10.123832	2.944633	-0.837624
C	4.914394	3.621177	-2.339051	H	7.436073	-3.761118	4.912349
C	6.410057	-2.061485	-4.269358	H	4.785580	-0.590664	5.917890
C	7.066105	-2.392925	-5.621235	H	9.365823	-1.741446	2.465354

## 7. Experimental Section

---

H	10.445268	-1.933117	4.688671	H	5.340156	4.529571	-1.908754
H	11.020375	-3.176408	3.573089	H	4.666815	2.944167	-1.522723
H	9.862950	-3.589485	4.838099	H	2.225908	-0.544549	-6.260487
H	9.493877	-4.073611	1.747130	H	1.163711	0.074860	-4.100282
H	7.830889	-3.495731	1.607054	H	0.244104	0.705259	-5.471235
H	4.506012	-2.573030	6.969426	H	1.269386	1.781858	-4.522989
H	3.885966	-3.957480	5.005213	H	2.484957	2.459247	-6.768431
H	3.992633	-4.940465	6.470213	H	1.431639	1.342569	-7.632330
H	5.286140	-4.993478	5.272862	H	3.186630	1.187600	-7.767369
H	6.973639	-4.362083	7.209746	H	7.205760	-1.962733	-3.532801
H	5.613967	-4.306482	8.328644	H	4.746666	-3.461874	-4.545337
H	6.671934	-2.902403	8.150516	H	5.049417	-3.025662	-2.862343
H	6.272254	1.799864	3.498344	H	6.133618	-4.133562	-3.698645
H	3.674254	1.025759	4.897547	H	6.311623	-2.523938	-6.399155
H	4.008589	0.854768	3.165327	H	7.640239	-3.318865	-5.551988
H	3.967508	2.452157	3.912191	H	7.740783	-1.602124	-5.948288
H	8.291763	-4.558171	2.938609	H	3.987278	3.901351	-2.841821
H	5.639073	1.753939	6.485810	H	-41.726985	29.839807	1.899811
H	5.801636	3.194499	5.480528	H	-42.546480	28.688649	0.812953
H	7.202088	2.163923	5.787208	H	-41.770218	30.161147	0.174082
H	8.615955	0.255563	-4.812069	H	-38.560182	28.862944	0.741232
H	11.022767	-0.035590	-4.904193	H	-40.621036	-22.675813	-0.213891
H	13.201611	-0.240989	-3.768845	H	-38.639003	-26.088497	-0.027193
H	13.319280	-0.089949	-1.291788	H	-37.650365	-25.566491	-1.391022
H	11.311479	0.332269	0.022343	H	-37.433666	-24.808212	0.184282
H	3.646289	2.554224	-4.645349	H	-39.649895	-23.086906	2.080483
H	4.061067	-1.596584	-5.465795	H	-38.015538	-23.083463	1.398442
H	6.826517	2.787687	-2.748813	H	-38.980268	-21.609418	1.388664
H	7.032289	3.508170	-5.110280	H	-39.977082	-24.590283	-1.558610
H	6.699240	4.870578	-4.035966	H	4.620002	-1.857173	-0.668848
H	5.416085	4.207693	-5.047901				Energy = -3043.584409 Hartree

### (II) TRIP-AcOH / 50h

C	-4.049120	2.951386	-0.693215	C	-3.837712	3.978451	-1.613674
C	-5.121050	3.067319	0.214536	C	-5.344969	2.022514	1.264796
C	-5.956859	4.203358	0.169491	C	-6.457589	1.141577	1.232808
C	-5.701437	5.193207	-0.774719	C	-6.760380	0.244293	2.236840
C	-4.645800	5.105495	-1.676541	C	-5.799505	0.062752	3.285596

## 7. Experimental Section

---

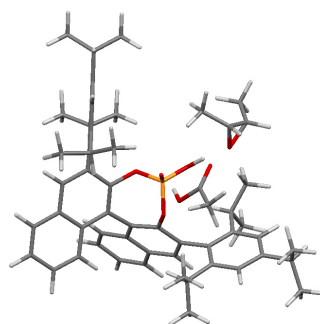
C	-4.663141	0.922445	3.333637	C	-7.165468	0.794888	-6.340682
C	-4.494768	1.908504	2.336662	H	-11.194826	-2.800188	2.240695
C	-5.901834	-0.960259	4.260791	H	-11.855525	-1.926290	4.408050
C	-4.954881	-1.100850	5.242638	H	-11.489631	-0.390556	6.301199
C	-3.855637	-0.222186	5.312011	H	-9.541872	1.151429	6.279252
C	-3.714969	0.765139	4.373943	H	-7.949097	1.111838	4.436180
C	-8.046309	-0.507856	2.223451	H	-8.802243	-5.843737	-1.589813
C	-8.411682	-1.265009	1.129243	H	-12.080651	-3.331910	-2.611028
C	-9.541961	-2.122113	1.098010	H	-7.746763	-3.751568	1.292234
C	-10.337992	-2.140166	2.216085	H	-9.103535	-5.723638	1.932001
C	-10.100317	-1.300625	3.326594	H	-7.372302	-6.067717	2.009091
C	-8.952022	-0.454786	3.334104	H	-8.336122	-6.675797	0.663314
C	-8.788092	0.433400	4.426177	H	-5.753934	-4.882714	0.443304
C	-9.685198	0.456308	5.462853	H	-6.351086	-3.740532	-0.763380
C	-10.794425	-0.412533	5.472837	H	-11.694161	-5.140510	-3.909589
C	-10.995822	-1.268542	4.423663	H	-9.403301	-4.737042	-4.790037
O	-7.591769	-1.250578	0.000707	H	-10.014534	-6.322094	-5.277698
P	-7.488331	0.063950	-0.913899	H	-8.824548	-6.193629	-3.984646
O	-8.643850	0.354237	-1.798172	H	-10.485627	-7.510424	-2.403093
C	-9.850179	-2.992926	-0.081367	H	-11.605188	-7.610377	-3.761943
C	-9.068564	-4.140192	-0.333490	H	-12.134407	-6.914058	-2.226444
C	-9.402782	-4.962447	-1.405524	H	-11.368558	-0.843462	0.047892
C	-10.484374	-4.692752	-2.238741	H	-12.514810	-1.166159	-2.761764
C	-11.237684	-3.558047	-1.970403	H	-11.016364	-0.320793	-2.350326
C	-10.947353	-2.695747	-0.912970	H	-12.566396	0.272916	-1.751592
C	-7.894127	-4.537526	0.553510	H	-6.628297	-5.471591	-0.966474
C	-6.581653	-4.664108	-0.233999	H	-13.757700	-2.504714	-0.878892
C	-10.844372	-5.602717	-3.400426	H	-13.829399	-0.998171	0.035874
C	-11.295171	-6.990418	-2.918551	H	-13.140421	-2.449706	0.768739
C	-11.839921	-1.477169	-0.701510	H	-6.184474	-0.015759	-2.635521
C	-13.220890	-1.883235	-0.159554	H	-3.652428	2.582388	2.414713
O	-7.326485	1.257285	0.148271	H	-2.864297	1.434015	4.403556
C	-7.109601	4.413538	1.145142	H	-3.120520	-0.338811	6.096857
C	-8.458625	4.577565	0.429089	H	-5.051148	-1.896835	5.968864
C	-4.371754	6.199639	-2.693575	H	-6.733637	-1.646884	4.223169
C	-3.995771	7.528161	-2.019948	H	-6.343962	6.063973	-0.799262
C	-3.098813	1.758219	-0.703577	H	-3.013870	3.895698	-2.311055
C	-1.740783	2.117955	-0.076461	H	-7.188797	3.528624	1.773600
C	-8.196643	-5.826950	1.334905	H	-5.902039	5.462947	2.632542
C	-9.704191	-5.718596	-4.422498	H	-7.643066	5.703026	2.813424
C	-11.988989	-0.627009	-1.971938	H	-6.763436	6.537040	1.532836
O	-6.126164	-0.171602	-1.637249	H	-9.266149	4.657700	1.159328
C	-6.835918	5.599010	2.085727	H	-8.667738	3.724577	-0.214988
C	-5.542726	6.389805	-3.668909	H	-3.507944	5.875757	-3.280577
C	-2.888496	1.172775	-2.108603	H	-5.791278	5.455420	-4.173027
O	-6.287731	0.241974	-4.185213	H	-5.292380	7.131348	-4.429909
C	-7.258496	0.577456	-4.857485	H	-6.438527	6.736568	-3.150920
O	-8.463591	0.781890	-4.377969	H	-4.826224	7.921769	-1.431206

## 7. Experimental Section

H	-3.734675	8.279040	-2.768195	C	81.293491	-0.196880	0.748124
H	-3.143334	7.404014	-1.351346	C	81.593457	-1.451091	1.520261
H	-3.543942	0.971120	-0.096645	C	81.411831	-0.052641	-0.710280
H	-2.338428	1.857672	-2.755643	C	81.853209	-1.136607	-1.652836
H	-3.835095	0.940656	-2.591585	H	81.592741	0.955599	-1.078680
H	-2.307698	0.251149	-2.043406	H	82.613177	-1.422142	1.910089
H	-1.236811	2.893891	-0.655788	H	80.914766	-1.537115	2.370727
H	-1.088711	1.242765	-0.050353	H	81.478773	-2.344071	0.909976
H	-1.849359	2.487990	0.942902	H	82.920788	-1.044784	-1.863583
H	-8.480475	5.479723	-0.184404	H	81.661169	-2.129716	-1.252881
H	-7.844996	0.112522	-6.851576	H	81.318423	-1.047809	-2.600137
H	-6.147771	0.631110	-6.679270	H	81.398024	0.717191	1.329907
H	-7.484660	1.808664	-6.582015				
H	-8.512933	0.624082	-3.386313				
O	80.126865	-0.195855	-0.087762				

Energy = -3043.616440 Hartree

### (III) TRIP-AcOH-50h



C	4.324202	-0.776538	1.130107	C	-2.147204	3.909874	-1.476574
C	3.940658	0.212189	0.203404	C	-0.816337	3.778226	-0.982406
C	4.462137	0.185233	-1.107047	C	-2.509274	5.069154	-2.205232
C	5.358003	-0.821021	-1.456634	C	-1.591072	6.048674	-2.472551
C	5.760928	-1.802433	-0.556402	C	-0.263848	5.902788	-2.022675
C	5.229628	-1.757798	0.725519	C	0.111861	4.802546	-1.295583
C	3.031232	1.328134	0.619470	C	-3.751513	0.619360	-0.424416
C	1.687533	1.419046	0.173277	C	-4.202139	-0.144451	-1.518760
C	0.857592	2.489284	0.438086	C	-5.209841	-1.086145	-1.308542
C	1.315545	3.477233	1.371234	C	-5.781638	-1.302769	-0.062312
C	2.655348	3.399082	1.853198	C	-5.314848	-0.540750	1.004092
C	3.487938	2.341689	1.424517	C	-4.313018	0.413585	0.853387
C	0.486368	4.509831	1.875722	C	-3.643445	0.024723	-2.927965
C	0.965078	5.427435	2.775251	C	-4.624964	0.785142	-3.836047
C	2.302252	5.372127	3.216162	C	-3.903383	1.241231	2.066235
C	3.125659	4.375998	2.764386	C	-3.510688	0.375985	3.272234
C	-0.469100	2.606990	-0.230170	C	-6.877215	-2.338947	0.116312
C	-1.397697	1.587648	-0.153740	C	-8.202914	-1.703690	0.562277
C	-2.732663	1.699996	-0.624241	O	-1.053357	0.405680	0.494903
C	-3.078968	2.875000	-1.243414	P	0.073328	-0.594205	-0.072534



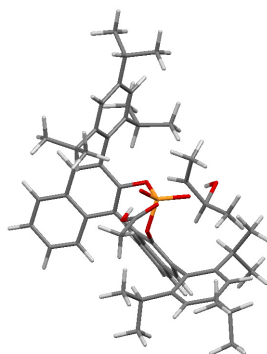
## 7. Experimental Section

---

O	0.476921	-1.532681	0.994775	H	4.155772	-0.037659	-3.925087
O	1.212151	0.390550	-0.639114	H	5.728686	-1.046218	3.551116
C	4.110997	1.239837	-2.150830	H	4.468355	-0.363606	4.580150
C	3.464670	0.625324	-3.401706	H	5.242498	0.633367	3.346198
C	6.747080	-2.889256	-0.948490	H	-4.096529	3.009272	-1.584727
C	8.119557	-2.312303	-1.326930	H	-3.527995	5.158681	-2.560548
C	3.797931	-0.814780	2.560624	H	-1.876297	6.926039	-3.037235
C	4.872810	-0.368558	3.566178	H	0.467690	6.664808	-2.256105
C	5.335653	2.091023	-2.524875	H	1.134350	4.709737	-0.963965
C	3.240980	-2.192868	2.946960	H	-5.746755	-0.688499	1.985295
C	6.200831	-3.787403	-2.068531	H	-5.562232	-1.675379	-2.145730
O	-0.426978	-1.217994	-1.416887	H	-3.024871	1.824556	1.797128
C	-5.005686	2.246004	2.442021	H	-5.249019	2.899489	1.603242
C	-6.455555	-3.463718	1.073721	H	-4.685905	2.871975	3.277529
C	-3.257078	-1.312819	-3.577338	H	-5.921887	1.732949	2.739970
O	-1.131108	-3.731093	-1.371251	H	-3.139111	1.007363	4.081418
C	-0.947808	-4.820134	-2.310068	H	-2.727946	-0.336146	3.014373
C	-0.210610	-4.529292	-3.585222	H	-7.045861	-2.791572	-0.864683
C	-0.334206	-4.885765	-0.975310	H	-5.529044	-3.934614	0.744331
C	1.120769	-4.668538	-0.689072	H	-7.229133	-4.232096	1.128823
O	-0.640921	-4.647430	2.215047	H	-6.293932	-3.083383	2.083853
C	-0.945626	-3.927813	3.140242	H	-8.109645	-1.245518	1.548465
C	-1.630256	-4.408282	4.394899	H	-8.990821	-2.457171	0.620158
O	-0.718007	-2.613341	3.173208	H	-8.523774	-0.929225	-0.135200
H	4.514891	2.321828	1.763962	H	-2.732899	0.617841	-2.856807
H	4.149385	4.309426	3.110089	H	-4.134722	-1.916460	-3.813317
H	2.669186	6.107757	3.919172	H	-2.612080	-1.896504	-2.924206
H	0.307849	6.198843	3.153770	H	-2.725139	-1.131933	-4.513157
H	-0.542765	4.566050	1.556032	H	-5.562354	0.235551	-3.941051
H	5.759133	-0.831094	-2.462075	H	-4.200458	0.917880	-4.833192
H	5.529701	-2.517544	1.435871	H	-4.863673	1.771437	-3.438837
H	3.379807	1.918612	-1.715730	H	-4.362199	-0.184122	3.662433
H	5.771783	2.564798	-1.644605	H	-1.049620	-4.119718	5.270938
H	5.053499	2.876857	-3.228194	H	-1.746939	-5.486951	4.361446
H	6.112453	1.486358	-2.995986	H	-2.607530	-3.932775	4.484192
H	3.169380	1.410774	-4.100161	H	-0.282098	-2.306488	2.339375
H	2.576065	0.051657	-3.141253	H	-0.848076	-5.472775	-0.223693
H	6.889406	-3.518851	-0.066071	H	0.065651	-5.466816	-4.072083
H	5.246310	-4.232391	-1.785937	H	-0.849440	-3.973933	-4.273321
H	6.901051	-4.595295	-2.289333	H	0.693149	-3.948802	-3.416329
H	6.045876	-3.221995	-2.989173	H	1.626671	-5.635506	-0.648532
H	8.051938	-1.679821	-2.213820	H	1.611034	-4.052317	-1.439847
H	8.827620	-3.114190	-1.544852	H	1.227625	-4.190942	0.282582
H	8.529849	-1.707433	-0.517688	H	-1.867034	-5.383294	-2.445407
H	2.970178	-0.110802	2.630745	H	-0.653931	-2.194412	-1.382582
H	4.026420	-2.948671	2.999913				
H	2.490700	-2.521988	2.231701				
H	2.770360	-2.141342	3.930211				

Energy = -3044.63202009 Hartree

## (IV) Transition State (TS)



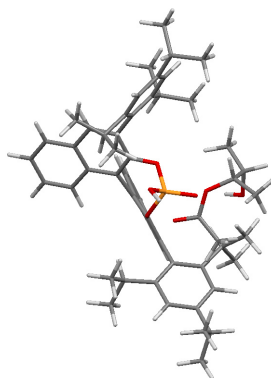
C	4.343245	-0.962696	0.922203	C	-4.679211	1.269360	-3.782804
C	3.959004	0.104511	0.086800	C	-6.834567	-2.203867	-0.134376
C	4.444359	0.165077	-1.236673	C	-8.161585	-1.583124	0.329234
C	5.299030	-0.835530	-1.690423	C	-3.815329	1.155907	2.117277
C	5.696730	-1.896213	-0.882782	C	-3.348252	0.178292	3.205290
C	5.206117	-1.935177	0.415444	C	4.101581	1.309452	-2.183626
C	3.089055	1.205969	0.612662	C	3.394203	0.818838	-3.455899
C	1.744128	1.375248	0.185263	C	6.638365	-2.975218	-1.388840
C	0.955867	2.447250	0.559477	C	8.024459	-2.411946	-1.737186
C	1.454128	3.330699	1.572887	C	3.863176	-1.095899	2.363369
C	2.794124	3.167053	2.032612	C	4.986846	-0.773283	3.362859
C	3.586536	2.125187	1.502231	O	0.488468	-1.543264	0.756838
C	0.665137	4.342304	2.175766	O	-0.511607	-1.091776	-1.583176
C	1.181090	5.161958	3.146611	C	-3.225821	-0.792338	-3.764066
C	2.518943	5.024341	3.567015	C	-4.933100	2.071938	2.643125
C	3.303910	4.044342	3.020898	C	-6.449215	-3.397288	0.751747
C	-0.373868	2.667659	-0.076393	C	5.346680	2.143248	-2.528354
C	-1.327884	1.667854	-0.076440	C	6.045853	-3.749617	-2.575638
C	-2.662007	1.858981	-0.527472	C	3.268194	-2.480514	2.659583
C	-2.983755	3.091587	-1.037340	O	-0.560018	-2.776758	2.717745
C	-2.027317	4.120400	-1.182608	C	-0.761989	-4.063220	2.648935
C	-0.696115	3.909972	-0.716325	O	-0.575131	-4.775639	1.659961
C	0.256213	4.934246	-0.947771	C	-1.269463	-4.650364	3.939468
C	-0.096157	6.105333	-1.568376	C	-0.154898	-4.303101	-0.458871
C	-1.423077	6.325977	-1.987914	C	-1.505572	-4.000151	-0.939956
C	-2.364458	5.349703	-1.799840	C	-2.483862	-5.099727	-1.252529
O	-1.005255	0.434642	0.460474	C	0.558405	-5.575146	-0.722998
P	0.043820	-0.559420	-0.293484	O	-0.776094	-3.547510	-2.105782
O	1.241630	0.454662	-0.716995	H	4.615208	2.042101	1.827163
C	-3.697527	0.781143	-0.423377	H	4.327983	3.914716	3.347825
C	-4.170788	0.134741	-1.582498	H	2.916716	5.683295	4.327133
C	-5.176607	-0.824021	-1.450583	H	0.553198	5.919464	3.596606
C	-5.727561	-1.167124	-0.222876	H	-0.363226	4.461522	1.871073
C	-5.242457	-0.516042	0.907379	H	5.670784	-0.777245	-2.705401
C	-4.242536	0.450100	0.835258	H	5.507342	-2.754523	1.056251
C	-3.648741	0.457599	-2.978961	H	3.410181	1.976305	-1.672665

## 7. Experimental Section

H	5.824600	2.531086	-1.627736	H	-2.985894	0.729722	4.074993
H	5.074961	2.991358	-3.159836	H	-2.537654	-0.454490	2.846799
H	6.087059	1.550465	-3.068335	H	-6.990027	-2.586267	-1.146974
H	3.107735	1.667422	-4.080276	H	-5.526217	-3.863735	0.404834
H	2.492373	0.259726	-3.210693	H	-7.236338	-4.153659	0.742285
H	6.772700	-3.686831	-0.569264	H	-6.298244	-3.090134	1.788051
H	5.077678	-4.181708	-2.320012	H	-8.079707	-1.190365	1.344331
H	6.711759	-4.560169	-2.878497	H	-8.959657	-2.328244	0.323951
H	5.900635	-3.099666	-3.440241	H	-8.459631	-0.760869	-0.321862
H	7.966756	-1.703416	-2.565312	H	-2.757978	1.073018	-2.867306
H	8.703653	-3.213875	-2.033333	H	-4.072895	-1.446917	-3.977261
H	8.463427	-1.891872	-0.885166	H	-2.475217	-1.358708	-3.217836
H	3.065756	-0.371274	2.517326	H	-2.792819	-0.499250	-4.722307
H	4.025557	-3.265569	2.620106	H	-5.590227	0.690922	-3.949111
H	2.482027	-2.719837	1.946702	H	-4.273450	1.541997	-4.758931
H	2.834833	-2.493406	3.661400	H	-4.962127	2.187185	-3.267151
H	4.043148	0.175590	-4.053042	H	-4.161036	-0.466878	3.543879
H	5.813179	-1.479948	3.263812	H	-0.169937	-2.326293	1.885247
H	4.616533	-0.832786	4.388323	H	-1.971579	-3.164115	-0.424126
H	5.389545	0.227863	3.208269	H	0.400774	-3.447033	-0.108587
H	-0.612429	-2.539090	-1.968991	H	-2.855319	-5.538912	-0.326240
H	-3.997888	3.279619	-1.364050	H	-3.328488	-4.687877	-1.802967
H	-3.383329	5.496473	-2.135601	H	-2.030297	-5.882909	-1.857602
H	-1.689881	7.257915	-2.468021	H	0.906547	-5.573729	-1.757069
H	0.653756	6.865904	-1.740781	H	1.427980	-5.651367	-0.075569
H	1.279175	4.784463	-0.638844	H	-0.083790	-6.440171	-0.574725
H	-5.662217	-0.756876	1.875686	H	-1.442320	-5.715851	3.828258
H	-5.548377	-1.319220	-2.339011	H	-0.541081	-4.469870	4.730057
H	-2.967792	1.796667	1.883535	H	-2.191582	-4.146906	4.229577
H	-5.234517	2.800250	1.889302				
H	-4.595750	2.617769	3.526435				
H	-5.817846	1.497493	2.923704				

Energy = -3044.60079443 Hartree  
Nimag = 1 (293i)

### (V) TRIP-52hb



C	4.295235	-0.447368	1.262311	C	4.417302	0.386777	-1.026906
C	3.883160	0.469806	0.275948	C	5.352515	-0.604065	-1.310908

## 7. Experimental Section

---

C	5.782030	-1.516293	-0.352090	C	-4.708681	0.434110	-3.739012
C	5.238664	-1.417092	0.921719	C	-8.210295	-1.792690	0.859058
C	2.928528	1.571376	0.622266	C	-3.376833	0.533907	3.295016
C	1.586884	1.587886	0.159692	O	0.626650	-3.333067	-1.983577
C	0.710205	2.631259	0.379858	C	0.575363	-4.338624	-1.291787
C	1.119512	3.677659	1.270722	C	1.815367	-5.154241	-1.053273
C	2.459355	3.679191	1.759037	O	-0.622224	-4.702471	-0.830387
C	3.336774	2.638177	1.383448	C	-0.950952	-5.554001	0.307704
C	0.245120	4.695709	1.726495	H	-2.009075	-5.741408	0.126495
C	0.680498	5.673447	2.583724	C	-0.819586	-4.722141	1.604952
C	2.016872	5.695607	3.029908	O	0.472441	-4.150245	1.685848
C	2.883469	4.715660	2.626115	C	-1.933756	-3.693367	1.746491
C	-0.621647	2.659138	-0.288154	H	-4.271545	2.833850	-1.631527
C	-1.502584	1.604043	-0.158431	H	-3.801384	4.952883	-2.722699
C	-2.845533	1.635594	-0.617832	H	-2.233751	6.768657	-3.291636
C	-3.246551	2.760801	-1.293776	H	0.121366	6.654060	-2.508314
C	-2.362523	3.822759	-1.585310	H	0.880274	4.795206	-1.127040
C	-1.025529	3.776393	-1.092077	H	-5.766793	-0.650461	2.179410
C	-2.778878	4.927433	-2.367825	H	-5.580875	-1.924081	-1.873522
C	-1.907204	5.933929	-2.686164	H	-3.190258	1.990024	1.758136
C	-0.573776	5.871393	-2.235366	H	-5.537800	2.788178	1.738203
C	-0.146221	4.825865	-1.457996	H	-4.819519	2.890485	3.348881
C	-3.822492	0.534056	-0.334615	H	-5.960311	1.601096	2.970355
C	-4.370112	0.404846	0.959126	H	-3.043443	1.221100	4.074912
C	-5.344029	-0.563618	1.186646	H	-2.520793	-0.062058	2.981094
C	-5.801279	-1.408024	0.180077	H	-7.059996	-2.956379	-0.512215
C	-5.238823	-1.269669	-1.081931	H	-5.524634	-3.996437	1.135030
C	-4.255162	-0.321940	-1.366449	H	-7.213954	-4.263804	1.580871
C	-3.968397	1.316934	2.113031	H	-6.254029	-3.056852	2.435155
C	-5.142015	2.200025	2.567085	H	-8.111405	-1.277264	1.815911
C	-3.706506	-0.241893	-2.787443	H	-8.991636	-2.547307	0.968161
C	-3.295993	-1.612858	-3.345795	H	-8.543580	-1.062294	0.121207
C	-6.883892	-2.442337	0.436628	H	-2.807665	0.372246	-2.762723
C	-6.441791	-3.502057	1.456555	H	-4.160693	-2.254477	-3.522477
O	-1.093364	0.462966	0.528046	H	-2.620226	-2.131442	-2.669334
P	0.046182	-0.504039	-0.066429	H	-2.785659	-1.486384	-4.302078
O	1.162380	0.519263	-0.624094	H	-4.113030	-0.137210	3.740831
C	4.041866	1.371218	-2.128971	H	-5.632602	-0.143824	-3.805956
C	5.233931	2.263716	-2.512095	H	-4.288853	0.511615	-4.743811
C	6.810359	-2.587121	-0.674871	H	-4.970347	1.438157	-3.406070
C	6.306016	-3.566612	-1.744864	H	4.360250	2.674131	1.732006
C	3.762907	-0.416982	2.691220	H	3.907653	4.708465	2.976894
C	3.237200	-1.782400	3.156830	H	2.349461	6.477660	3.699078
C	3.458069	0.671132	-3.365290	H	-0.010571	6.433010	2.924083
C	4.821867	0.113989	3.672363	H	-0.784000	4.693879	1.401794
C	8.163986	-1.982771	-1.077688	H	5.762772	-0.658168	-2.311233
O	-0.548426	-1.099894	-1.384750	H	5.559932	-2.123243	1.676847
O	0.506755	-1.453105	0.966383	H	3.267718	2.032204	-1.743621

## 7. Experimental Section

---

H	5.620864	2.800852	-1.645270	H	5.172736	1.107488	3.391959
H	4.934506	2.999308	-3.261258	H	4.195134	0.028370	-3.849327
H	6.052277	1.675877	-2.931415	H	2.623210	-4.693987	-1.612863
H	3.135025	1.411058	-4.100069	H	1.682073	-6.183744	-1.378246
H	2.598084	0.057794	-3.100165	H	2.054365	-5.148008	0.007542
H	6.968596	-3.159377	0.243254	H	-0.175088	-1.992717	-1.656092
H	5.367599	-4.031107	-1.440422	H	-2.903766	-4.187600	1.815948
H	7.037514	-4.358319	-1.918200	H	-1.785311	-3.105669	2.651357
H	6.132884	-3.059770	-2.695647	H	-1.957920	-3.012703	0.897169
H	8.080784	-1.405885	-2.000369	H	-0.899780	-5.438384	2.430412
H	8.903095	-2.768953	-1.243748	H	0.432986	-3.202754	1.453043
H	8.544277	-1.316750	-0.302547	C	-0.245985	-6.900722	0.370673
H	2.918298	0.269668	2.717418	H	-0.807825	-7.533835	1.058803
H	4.037244	-2.519836	3.239737	H	-0.243321	-7.396119	-0.599987
H	2.484416	-2.165599	2.472649	H	0.771453	-6.830792	0.744933
H	2.779781	-1.687632	4.143483				
H	5.691468	-0.545265	3.704936				
H	4.410723	0.173878	4.681932				

Energy = -3044.63202009 Hartree

### (VI) TRIP/52hb

C	16.041715	-3.530721	1.030699	C	22.828408	-1.257095	-0.947264
C	17.146452	-3.487499	0.158128	C	19.897648	3.653664	-0.265990
C	17.011236	-3.943389	-1.169794	C	19.686111	4.231261	1.004154
C	15.779929	-4.434839	-1.592927	C	19.014696	5.447219	1.090321
C	14.674546	-4.492329	-0.749560	C	18.541933	6.117435	-0.033527
C	14.832833	-4.036697	0.552045	C	18.762210	5.530620	-1.272395
C	18.476278	-3.002165	0.647536	C	19.428393	4.313578	-1.420376
C	19.017355	-1.754511	0.244488	C	20.211534	3.599496	2.288159
C	20.271303	-1.302450	0.601691	C	21.352706	4.436555	2.890434
C	21.003115	-2.060836	1.574407	C	19.636151	3.769633	-2.831153
C	20.480151	-3.316420	2.003342	C	18.334641	3.701846	-3.644243
C	19.242497	-3.766223	1.492071	C	17.813841	7.445580	0.076797
C	22.205905	-1.603580	2.168225	C	16.496132	7.316278	0.855734
C	22.868295	-2.359588	3.100862	O	18.864286	1.147521	0.607817
C	22.372138	-3.620132	3.488289	P	17.608275	0.392566	-0.052219
C	21.201039	-4.083288	2.951229	O	18.244246	-0.971238	-0.615787
C	20.833101	-0.063385	-0.005470	C	18.177410	-3.956648	-2.152322
C	20.134955	1.127189	0.038705	C	18.608951	-5.394128	-2.486775
C	20.665116	2.372913	-0.389254	C	13.334959	-5.029053	-1.222892
C	21.934743	2.362625	-0.910641	C	12.734662	-4.167971	-2.344605
C	22.665224	1.168817	-1.097185	C	16.110267	-3.060989	2.480190
C	22.106841	-0.070157	-0.665639	C	15.014430	-2.040449	2.823617
C	23.933690	1.180233	-1.727486	C	17.874723	-3.159851	-3.429976
C	24.614223	0.015774	-1.961710	C	16.064356	-4.252188	3.452511
C	24.044551	-1.214947	-1.579459	C	13.418242	-6.503178	-1.645908

## 7. Experimental Section

---

O	17.309232	1.104179	-1.451253	H	20.796918	-5.040264	3.255884
O	16.475829	0.333650	0.876665	H	22.909502	-4.210360	4.218227
C	20.692051	4.587735	-3.594609	H	23.778603	-1.982087	3.547061
C	18.704208	8.542063	0.680459	H	22.600038	-0.638134	1.890761
C	19.100779	3.356781	3.320732	H	15.685171	-4.787537	-2.611860
O	-104.035989	-0.667842	-1.901986	H	13.980392	-4.073133	1.218460
C	-105.108854	-0.529214	-1.376443	H	19.029497	-3.476955	-1.673898
C	-106.121633	-1.647544	-1.308664	H	18.871594	-5.947797	-1.584514
O	-105.418029	0.710673	-0.903183	H	19.478471	-5.389340	-3.146996
C	-106.336121	1.091661	0.148459	H	17.810438	-5.941060	-2.990973
H	-106.361864	2.176099	0.028219	H	18.754552	-3.131444	-4.075742
C	-105.706425	0.809701	1.524070	H	17.594072	-2.134071	-3.194123
O	-105.555878	-0.596215	1.739756	H	12.654377	-4.972448	-0.369058
C	-104.393306	1.549007	1.734733	H	12.640272	-3.126982	-2.034270
H	22.386198	3.296795	-1.216484	H	11.743263	-4.532371	-2.620734
H	24.348720	2.131347	-2.035854	H	13.358403	-4.193380	-3.239948
H	25.578735	0.035181	-2.450871	H	14.069011	-6.630869	-2.512763
H	24.569759	-2.136829	-1.790432	H	12.430537	-6.882132	-1.915417
H	22.408450	-2.210922	-0.667913	H	13.811675	-7.123519	-0.839991
H	18.864370	5.886888	2.067733	H	17.064690	-2.557512	2.625621
H	18.404034	6.042633	-2.156662	H	14.017842	-2.481423	2.764731
H	20.633191	2.627213	2.041047	H	15.058989	-1.182783	2.155858
H	22.167031	4.568423	2.176760	H	15.151012	-1.681497	3.845708
H	21.756702	3.947904	3.779122	H	15.120315	-4.793270	3.364589
H	21.005014	5.428370	3.184203	H	16.156353	-3.906616	4.483910
H	19.504610	2.839096	4.192759	H	16.869647	-4.962482	3.261085
H	18.302356	2.744424	2.904072	H	17.062242	-3.610410	-4.002050
H	17.562469	7.753409	-0.941869	H	-105.694464	-2.506742	-1.816555
H	15.845314	6.564120	0.408902	H	-107.049941	-1.360687	-1.800065
H	15.960277	8.267266	0.865190	H	-106.347565	-1.905227	-0.276790
H	16.675809	7.026486	1.892449	H	16.470886	1.579470	-1.412665
H	18.977310	8.307843	1.710848	H	-104.535428	2.627053	1.651943
H	18.182249	9.500733	0.686194	H	-103.998228	1.333838	2.727574
H	19.626240	8.660049	0.110387	H	-103.657437	1.253764	0.985245
H	20.009040	2.750344	-2.747860	H	-106.431640	1.145265	2.271374
H	17.919893	4.692453	-3.835808	H	-104.646298	-0.839934	1.541782
H	17.579999	3.110888	-3.128772	C	-107.768354	0.587426	0.023212
H	18.522669	3.233395	-4.611808	H	-108.399796	1.193766	0.674370
H	18.663522	4.293622	3.670094	H	-108.134696	0.708767	-0.995603
H	20.361720	5.618553	-3.735130	H	-107.881834	-0.449604	0.325094
H	20.871467	4.156330	-4.581267				
H	21.642631	4.617322	-3.062072				
H	18.875043	-4.735353	1.802399				

Energy = -3043.606960 Hartree

**7.6.3.4. Theoretical investigation on the transition states**

The analysis aimed at characterizing the transition state for the desymmetrization of *meso*-epoxide **50h** in the ring opening with benzoic acid catalyzed by (*S*)-**TRIP** or by (*S*)-**139**.

Optimized transition state structures, total electronic energies (*E*), thermal corrections (*T*<sub>c</sub>) at 300 K, Gibbs free energies (*G*), and the number of imaginary frequencies (*N*<sub>imag</sub>) are reported for the following cases:

- (*S*)-**TRIP**: (1): Reaction towards products (*S,S*)-**52h** (exp. favored)  
(2): Reaction towards products (*R,R*)-**52h** (exp. disfavored)
- (*S*)-**139**: (3): Reaction towards products (*S,S*)- **52h** (exp. favored)  
(4): Reaction towards products (*R,R*)- **52h** (exp. disfavored)

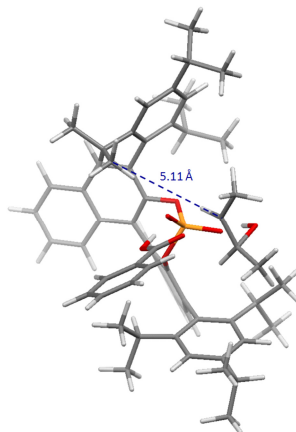
We considered the effects arising from the use of different DFT functionals, empirical dispersion corrections, and solvent treatments. The TS structures obtained at different levels of theory are similar. Averaging over all the bond lengths leads to RMS deviations of less than 0.001Å compared to the B3LYP/6-31G\* structures. The available experimental data indicate that the energy difference between the two diastereotopic transition states is higher for catalyst (*S*)-**139** than for **TRIP**. This result is in close agreement with the theoretical results obtained in vacuum at the B3LYP/6-31G\* level. This may be due to the fact that the catalyst pocket is sterically congested, which could make it difficult for solvent molecules to access the pocket.

B3LYP/6-31G* vacuum	<b>G</b>
1) ( <i>S</i> )- <b>TRIP</b> : Case 1	-3234.260969 Ha
2) ( <i>S</i> )- <b>TRIP</b> : Case 2	-3234.259790 Ha
( <i>S</i> )- <b>TRIP</b> : Δ <i>G</i>	<b>-0.74 kcal mol<sup>-1</sup></b>
3) ( <i>S</i> )- <b>139</b> : Case 3	-3465.204848
4) ( <i>S</i> )- <b>139</b> : Case 4	-3465.201819
( <i>S</i> )- <b>139</b> : Δ <i>G</i>	<b>-1.90 kcal mol<sup>-1</sup></b>

## Optimized transition state structures (B3LYP/6-31G\*):

## (S)-TRIP

## (1) - (S,S)-52h (exp. favored)



C	-3.435531	-1.974840	1.917636	C	5.231496	1.611730	1.815801
C	-2.981046	-2.176791	0.592671	C	5.216868	2.896591	1.266568
C	-3.754150	-1.706269	-0.496742	C	4.627752	3.057771	0.013116
C	-4.964581	-1.055510	-0.239998	C	4.050253	1.993706	-0.691275
C	-5.440535	-0.852860	1.058251	C	4.789278	-0.863637	1.813842
C	-4.657720	-1.318085	2.115351	C	4.094200	-0.905913	3.187820
C	-1.714510	-2.941115	0.332299	C	5.787927	4.094087	2.015044
C	-0.525147	-2.296256	-0.117323	C	7.257507	3.892717	2.426056
C	0.639283	-2.977329	-0.444290	C	3.417635	2.283361	-2.053430
C	0.701459	-4.387913	-0.163484	C	4.490164	2.608120	-3.112150
C	-0.482056	-5.056941	0.287311	C	-3.340004	-1.933160	-1.950436
C	-1.671232	-4.310710	0.487547	C	-3.272091	-0.621969	-2.755052
C	-0.440728	-6.453704	0.545605	C	-6.775799	-0.167760	1.320302
C	0.727098	-7.166137	0.402539	C	-7.955922	-0.987416	0.763990
C	1.908558	-6.500944	-0.000432	C	-2.663035	-2.474636	3.139722
C	1.896080	-5.151674	-0.277995	C	-3.311691	-3.748404	3.720357
O	-0.576971	-0.923191	-0.313854	O	0.318580	1.400518	-0.016501
P	0.264400	0.062666	0.697553	O	-0.254660	0.014929	2.110993
O	1.730580	-0.663633	0.738222	C	6.259523	-1.316409	1.919468
C	2.321884	-1.127797	-0.426764	C	2.365757	3.406356	-1.983875
C	1.793921	-2.249615	-1.050729	C	4.915592	4.451587	3.234820
C	2.381466	-2.671572	-2.295303	C	-4.267945	-2.957477	-2.633834
C	3.576293	-2.025761	-2.751101	C	-6.805992	1.274248	0.780264
C	4.125382	-0.960153	-1.993592	C	-2.518591	-1.408543	4.240878
C	3.509496	-0.469240	-0.861485	O	-1.382021	2.575433	-1.514220
C	1.813322	-3.680883	-3.121330	C	-1.936751	3.681902	-1.090541
C	2.411010	-4.052766	-4.305541	O	-1.811404	4.166568	0.051336
C	3.614289	-3.442323	-4.730169	C	-0.986255	3.392677	1.869530
C	4.179262	-2.447271	-3.966922	C	-2.098340	2.538364	2.326418
C	4.079023	0.701565	-0.114842	C	-3.350691	3.133548	2.925959
C	4.680993	0.510783	1.153416	C	-2.776562	4.374206	-2.107495



## 7. Experimental Section

---

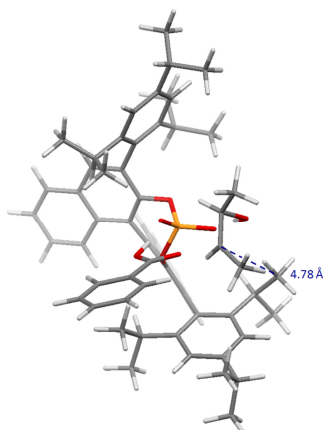
C	-2.903726	3.863375	-3.407589	H	-5.017404	-1.171867	3.131217
C	-3.694937	4.530402	-4.340521	H	-2.334498	-2.361856	-1.956755
C	-4.360021	5.705948	-3.983497	H	-4.272179	-3.910169	-2.092373
C	-4.234386	6.217388	-2.689006	H	-3.937870	-3.151693	-3.661737
C	-3.445166	5.554318	-1.753176	H	-5.301694	-2.593799	-2.676583
C	-0.634708	4.697029	2.499866	H	-2.902839	-0.820834	-3.768600
O	-1.149612	2.097771	3.326436	H	-2.596765	0.096917	-2.281155
H	5.047193	-0.498103	-2.337139	H	-6.901247	-0.112693	2.410600
H	5.092313	-1.952628	-4.290027	H	-5.994393	1.874036	1.207496
H	4.079932	-3.750735	-5.662229	H	-7.756711	1.761773	1.028062
H	1.950072	-4.820111	-4.921759	H	-6.696278	1.295032	-0.310454
H	0.887017	-4.153625	-2.816597	H	-7.903037	-1.069162	-0.328145
H	5.688927	1.457599	2.790043	H	-8.912015	-0.513174	1.017136
H	4.611259	4.051760	-0.428696	H	-7.958907	-2.003129	1.174080
H	4.280816	-1.591561	1.175840	H	-1.651039	-2.731312	2.814638
H	6.741648	-1.332909	0.935418	H	-3.483372	-1.148084	4.692986
H	6.319957	-2.325272	2.345538	H	-2.058810	-0.498636	3.849925
H	6.841647	-0.647062	2.564107	H	-1.877827	-1.790961	5.044226
H	4.142370	-1.918996	3.605658	H	-4.331249	-3.544888	4.070537
H	3.041434	-0.622252	3.101720	H	-2.731251	-4.119991	4.573540
H	5.755135	4.949654	1.326187	H	-3.371170	-4.550728	2.977483
H	3.876266	4.624062	2.933087	H	-4.258286	-0.151581	-2.851603
H	5.286616	5.357092	3.730419	H	-0.748280	2.102901	-0.854874
H	4.916685	3.639485	3.971551	H	-2.329158	1.733009	1.626039
H	7.365841	3.067333	3.139291	H	-0.240381	2.876372	1.274417
H	7.651365	4.797038	2.905538	H	-3.952185	3.597003	2.136998
H	7.884362	3.666566	1.556554	H	-3.939382	2.338765	3.393746
H	2.893046	1.381902	-2.381045	H	-3.124968	3.884828	3.687239
H	2.812302	4.371586	-1.716273	H	0.446286	4.778158	2.642483
H	1.596304	3.161777	-1.247717	H	-0.949430	5.496415	1.820931
H	1.881418	3.528698	-2.960471	H	-1.137164	4.838574	3.458431
H	4.575414	-0.230918	3.905945	H	-2.383463	2.950460	-3.674174
H	5.049617	3.513236	-2.845951	H	-3.792640	4.133291	-5.346914
H	4.026129	2.777305	-4.091587	H	-4.976096	6.223787	-4.713815
H	5.214434	1.792503	-3.216951	H	-4.751291	7.131669	-2.411315
H	-0.704110	1.263676	2.935561	H	-3.335631	5.936851	-0.744211
H	-2.569827	-4.838204	0.795870				
H	-1.352364	-6.946360	0.875639				
H	0.748714	-8.232307	0.611043				
H	2.837395	-7.058354	-0.086958				
H	2.812707	-4.656960	-0.576717				
H	-5.558874	-0.709317	-1.082164				

Energy = -3235.33620956 Hartree

Tc = 1.075241

G = -3234.260969 Hartree

Nimag = 1 (279i)

(2) - (*R,R*)-**52h** (exp. disfavored)

C	-2.534303	-4.251660	3.415888	C	3.396078	-2.250852	2.004267
C	-2.691346	-4.531227	2.050537	C	2.398677	-3.416355	1.866062
C	-3.495439	-5.606086	1.646759	C	6.024493	-3.843406	-2.001662
C	-4.138895	-6.392756	2.598403	C	5.312459	-4.155261	-3.331876
C	-3.982024	-6.110976	3.958202	C	0.525091	2.983426	0.469088
C	-3.180169	-5.041587	4.364719	C	-0.622812	2.282770	0.126734
C	-2.012281	-3.704576	1.013305	C	-1.821062	2.908532	-0.325641
O	-1.337640	-2.689857	1.494355	C	-1.800149	4.278994	-0.478595
O	-2.115127	-4.001245	-0.191225	C	-0.625736	5.045269	-0.266914
C	-1.896662	-2.841495	-2.010515	C	0.564571	4.396040	0.195037
C	-0.541561	-3.208720	-2.442491	C	1.743791	5.180641	0.326382
C	-0.272295	-4.542165	-3.094041	C	1.735424	6.530741	0.052723
O	-0.802123	-2.159001	-3.419510	C	0.547175	7.175819	-0.362852
C	-3.156783	-3.366990	-2.609707	C	-0.606110	6.443198	-0.521341
O	-0.279772	-0.013821	-2.109775	O	-0.649757	0.908069	0.311589
P	0.226239	-0.058641	-0.689001	O	0.290006	-1.399146	0.010910
O	1.678298	0.698734	-0.713157	C	4.438925	-2.554107	3.098431
C	2.247055	1.169917	0.460359	C	7.525250	-3.582581	-2.228276
C	3.447248	0.539908	0.902498	C	4.121170	1.108776	-3.108443
C	4.033036	1.031313	2.050238	C	-3.840503	1.638154	0.500335
C	3.446881	2.074453	2.811239	C	-3.420350	1.847781	1.954931
C	2.246181	2.699205	2.341954	C	-4.358204	2.847273	2.661249
C	1.685929	2.274634	1.085897	C	-5.048266	0.982982	0.242083
C	4.021231	2.497307	4.040318	C	-5.531705	0.795442	-1.055786
C	3.423991	3.474312	4.802361	C	-6.864067	0.105296	-1.319305
C	2.216023	4.064649	4.362864	C	-6.868971	-1.353247	-0.824733
C	1.645026	3.690683	3.166218	C	-4.755786	1.274487	-2.111257
C	4.072407	-0.591821	0.139777	C	-3.534671	1.932458	-1.912233
C	4.710421	-0.341545	-1.100188	C	-2.761983	2.429927	-3.134782
C	5.328812	-1.400550	-1.770738	C	-2.586217	1.342053	-4.210279
C	5.347784	-2.699884	-1.256561	C	-3.328700	0.524406	2.737061
C	4.715362	-2.920998	-0.033631	C	-8.045454	0.892163	-0.720500
C	4.069531	-1.900676	0.676596	C	-3.428374	3.680047	-3.744478
C	4.785180	1.054155	-1.719609	H	4.962893	0.590621	2.400135
C	6.239777	1.562183	-1.777534	H	4.939025	2.018734	4.374008

## 7. Experimental Section

---

H	3.868190	3.783967	5.744425	H	-2.642099	-0.175868	2.251489
H	1.730212	4.817868	4.977396	H	-7.005123	0.082566	-2.408818
H	0.714643	4.147709	2.850071	H	-6.058806	-1.928989	-1.287223
H	5.818929	-1.199939	-2.720495	H	-7.818156	-1.844856	-1.070292
H	4.721759	-3.927035	0.380119	H	-6.737085	-1.407460	0.262349
H	4.235359	1.745274	-1.074989	H	-7.979549	0.938350	0.372956
H	6.698063	1.569316	-0.782073	H	-8.999419	0.415514	-0.977002
H	6.273368	2.583724	-2.175372	H	-8.065094	1.920701	-1.096658
H	6.860625	0.931698	-2.425127	H	-1.758154	2.711890	-2.805535
H	4.147406	2.132524	-3.501484	H	-3.542090	1.050952	-4.662726
H	3.075920	0.791160	-3.053754	H	-2.111650	0.453383	-3.788778
H	5.939142	-4.736283	-1.366799	H	-1.945646	1.717113	-5.017262
H	4.253272	-4.383232	-3.168082	H	-4.441401	3.453082	-4.099215
H	5.775211	-5.016918	-3.828604	H	-2.847404	4.046358	-4.599566
H	5.366551	-3.303735	-4.020570	H	-3.507658	4.494402	-3.016379
H	7.685721	-2.711912	-2.875066	H	-4.306714	0.036166	2.827859
H	8.000034	-4.445853	-2.710233	H	-0.764155	-2.168574	0.819693
H	8.041478	-3.393322	-1.280797	H	-1.957115	-1.936084	-1.421679
H	2.818893	-1.380803	2.329276	H	0.226762	-2.912329	-1.728959
H	2.897360	-4.354322	1.593500	H	-3.064999	-4.408992	-2.922413
H	1.646343	-3.186506	1.107823	H	-3.964040	-3.279528	-1.879448
H	1.883438	-3.584164	2.819761	H	-3.419905	-2.754629	-3.478416
H	4.639247	0.465430	-3.829952	H	-0.300868	-5.332174	-2.336347
H	5.047581	-3.427631	2.834719	H	-1.003181	-4.769204	-3.875131
H	3.944546	-2.766703	4.054287	H	0.722689	-4.532174	-3.549028
H	5.121674	-1.710702	3.251025	H	-1.908740	-3.419992	3.719443
H	-0.507737	-1.272813	-2.991982	H	-3.057599	-4.823716	5.421911
H	-1.522587	6.920657	-0.860205	H	-4.484057	-6.725398	4.700891
H	0.552240	8.242780	-0.568343	H	-4.761801	-7.224886	2.282402
H	2.652955	7.104491	0.152127	H	-3.603303	-5.810605	0.587042
H	2.665384	4.701190	0.634668	H	-2.705796	4.791416	-0.792061
H	-5.635354	0.622713	1.083466	C	-3.076540	2.126992	-0.587843
H	-5.118216	1.135553	-3.127246				
H	-2.421160	2.290703	1.962490				
H	-4.380198	3.808412	2.135340				
H	-4.023235	3.029640	3.689707				
H	-5.386264	2.468043	2.705947				
H	-2.960575	0.711796	3.753073				

Energy = -3235.33440882 Hartree

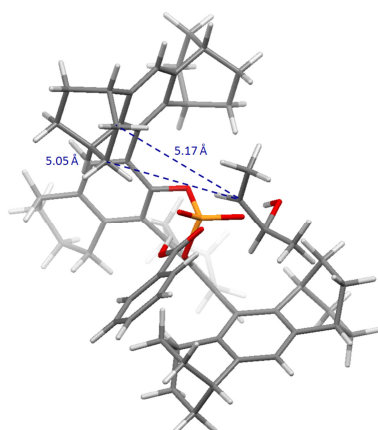
Tc = 1.074619

G = -3234.259790 Hartree

Nimag = 1 (311i)

(S)-139

(3) - (S,S)-52h (exp. favored)



C	2.206990	6.578202	0.821116	C	3.978039	-0.899464	0.922249
C	1.827550	5.347142	1.373927	C	-1.430784	-2.213387	1.347411
C	2.048820	5.095817	2.735848	C	-2.055927	-1.287050	0.493252
C	2.646975	6.069883	3.532824	C	-3.307275	-0.716725	0.764266
C	3.024511	7.295179	2.978046	C	-3.907112	-1.060666	1.982698
C	2.803548	7.548727	1.621578	C	-3.270229	-1.883122	2.910357
C	1.193173	4.324642	0.494611	C	-2.027021	-2.463859	2.602080
O	0.988626	4.569186	-0.707528	C	-3.880467	-2.205868	4.255125
O	0.897208	3.202612	1.106026	C	-3.783108	-3.717745	4.532735
C	0.498482	3.257210	-2.378639	C	-2.322469	-4.230047	4.448509
C	-0.125065	4.321076	-3.213647	C	-1.367120	-3.248594	3.718167
C	1.820149	2.661678	-2.627081	O	-1.412732	-0.952982	-0.695692
O	1.049836	1.832288	-3.534395	C	-3.989405	0.215813	-0.184790
C	2.911143	3.437318	-3.324188	C	-4.389716	-0.212722	-1.466454
O	-0.433073	1.405010	-0.148585	C	-5.070201	0.660060	-2.334475
P	-0.090387	0.009597	-0.635305	C	-5.361704	1.965752	-1.943863
O	0.582045	-0.138218	-1.979374	C	-4.972239	2.401453	-0.679241
O	0.779106	-0.675278	0.577822	C	-4.290666	1.538459	0.198945
C	0.947598	-2.058515	0.581534	H	-4.887513	-0.651342	2.214883
C	2.209891	-2.585296	0.273945	H	0.792559	0.993431	-2.993455
C	2.324577	-3.977123	0.278170	H	3.296288	-4.415346	0.060705
C	1.236847	-4.824777	0.509421	H	0.410374	2.497156	0.541386
C	-0.021246	-4.272838	0.811746	H	2.197729	2.076879	-1.786278
C	-0.150603	-2.865241	0.918204	H	-0.138491	2.690475	-1.706965
C	1.461261	-6.328483	0.448099	H	3.313656	4.197319	-2.646417
C	0.179754	-7.125978	0.187486	H	3.720446	2.757669	-3.607601
C	-0.927772	-6.651876	1.131239	H	2.544265	3.926141	-4.230630
C	-1.248659	-5.172066	0.890049	H	-0.786529	3.853106	-3.950305
C	3.387902	-1.724535	-0.054862	H	-0.741409	4.949738	-2.566124
C	3.969131	-1.760331	-1.338180	H	0.605334	4.944481	-3.732634
C	5.108285	-0.985734	-1.628763	H	1.751580	4.141647	3.155673
C	5.677049	-0.165736	-0.656023	H	2.818686	5.873402	4.587376
C	5.112983	-0.126550	0.618324	H	3.490538	8.052784	3.602551

## 7. Experimental Section

---

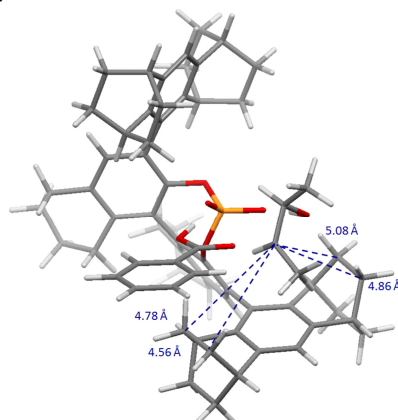
H	3.096250	8.501987	1.190374	C	-6.011008	3.649401	1.200604
H	2.026285	6.756519	-0.233451	C	-5.249829	2.705116	2.177066
C	3.559122	-0.767362	2.372315	H	-5.890916	2.637282	-2.619083
C	5.637150	0.670236	1.790634	H	-7.010090	3.258291	0.978934
C	3.261022	0.724557	2.673931	H	-6.149209	4.643320	1.644818
C	4.501878	1.590304	2.309106	H	-5.743834	4.416614	-0.832532
C	6.002040	-0.327154	2.922737	H	-5.872850	1.845444	2.449551
C	4.758980	-1.202648	3.257683	H	-5.003278	3.226312	3.110716
C	5.610307	-1.149667	-3.044785	H	-3.252400	4.552595	-0.699833
C	3.508063	-2.577249	-2.529662	H	-3.971279	5.397176	0.669261
C	4.467542	-0.750069	-4.013571	H	-2.835954	3.976434	2.140886
C	3.211057	-1.615730	-3.711146	H	-2.114619	3.127850	0.773751
C	5.935212	-2.649213	-3.276839	H	-3.396867	1.544493	2.180975
C	4.676117	-3.507182	-2.955188	H	-7.300534	-0.858817	-2.960929
H	6.561302	0.428254	-0.884817	H	-6.574842	-1.693952	-4.331700
H	4.803641	-0.885865	-5.049392	H	-6.191274	-2.288793	-1.482929
H	4.240947	0.315601	-3.890099	H	-5.501313	-3.153774	-2.853227
H	2.350829	-0.993145	-3.456643	H	-3.690363	-2.269098	-1.381583
H	2.931772	-2.212634	-4.588591	H	-5.958700	0.755795	-4.304479
H	6.780304	-2.943366	-2.644597	H	-4.394586	-0.949397	-5.293618
H	6.251244	-2.792976	-4.317843	H	-3.498838	0.388428	-4.579095
H	4.891434	-4.225499	-2.155747	H	-2.394692	-1.119798	-3.167168
H	4.368373	-4.090778	-3.831925	H	-3.324327	-2.449020	-3.852901
H	6.500164	-0.534030	-3.222525	H	1.894894	-6.661045	1.404204
H	2.617462	-3.165186	-2.297973	H	2.215474	-6.553899	-0.315989
H	2.380003	1.043533	2.111278	H	-0.143260	-6.982126	-0.853215
H	3.015556	0.827324	3.738871	H	0.373443	-8.198042	0.315216
H	4.861772	2.151431	3.180993	H	-1.838327	-7.248648	0.996860
H	4.246461	2.328947	1.541083	H	-0.604684	-6.799652	2.172305
H	4.973597	-2.263838	3.090069	H	-1.783423	-5.078730	-0.068306
H	4.481012	-1.096461	4.313894	H	-1.951916	-4.814306	1.643590
H	6.844436	-0.951288	2.604850	H	-4.924591	-1.874183	4.290394
H	6.335910	0.233793	3.804999	H	-3.353011	-1.656973	5.051233
H	2.683632	-1.380172	2.599821	H	-4.214568	-3.950930	5.513246
H	6.514288	1.263419	1.505825	H	-4.400194	-4.235801	3.788657
C	-4.208536	-1.592979	-2.065056	H	-1.923018	-4.405852	5.454344
C	-5.440252	0.035919	-3.660037	H	-2.307696	-5.202451	3.943066
C	-3.410171	-1.458139	-3.389177	H	-0.475986	-3.774769	3.369616
C	-4.140894	-0.466976	-4.341031	H	-1.009646	-2.512356	4.454175
C	-6.346009	-1.192611	-3.382759				
C	-5.614582	-2.158442	-2.405452				
C	-3.937336	2.214907	1.509516				
C	-5.204110	3.784833	-0.117137				
C	-3.064306	3.460314	1.199689				
C	-3.823863	4.404811	0.224064				

Energy = -3466.38995502 Hartree

Tc = 1.185107

G = -3465.204848 Hartree

Nimag = 1 (295i)

(4) - (*R,R*)-**52h** (exp. disfavored)

C	2.002237	6.513703	0.861648	C	0.577492	-6.867739	1.888994
C	1.228454	5.426437	1.290812	C	-0.773506	-6.397250	1.345996
C	0.613709	5.461875	2.550889	C	-1.004626	-4.926389	1.713922
C	0.777364	6.575457	3.372099	C	3.469813	-1.538759	0.022097
C	1.550592	7.656465	2.941483	C	4.021570	-0.542210	0.851595
C	2.162077	7.624899	1.685272	C	5.098786	0.245524	0.408690
C	1.072755	4.245628	0.394824	C	5.639092	0.054740	-0.863766
O	1.603526	4.246171	-0.733610	C	5.111388	-0.938401	-1.688154
O	0.366485	3.272059	0.907421	C	4.037401	-1.738295	-1.251739
C	2.126243	2.641268	-2.049054	O	0.834423	-0.503812	0.492838
C	1.021590	2.685734	-3.021024	C	-4.013465	-0.020319	-0.365282
C	0.950288	3.770604	-4.068333	C	-4.424801	-0.736756	-1.507037
C	3.519761	3.093137	-2.315090	C	-5.193745	-0.112597	-2.506010
O	1.640310	1.471560	-3.521237	C	-5.566637	1.224637	-2.383439
O	-0.449896	1.373278	-0.551799	C	-5.162356	1.944835	-1.261760
P	-0.081232	-0.074544	-0.809392	C	-4.386952	1.334162	-0.258637
O	0.581417	-0.414111	-2.121000	H	-4.828231	-0.432402	2.175108
O	-1.359081	-1.087627	-0.680114	H	1.207883	0.682633	-3.026580
C	-1.978081	-1.234686	0.558848	H	0.132820	2.485754	0.277251
C	-1.302373	-1.956517	1.561302	H	1.980523	1.952304	-1.227697
C	-1.873954	-1.991998	2.851049	H	0.056706	2.479714	-2.557050
C	-3.140799	-1.419220	3.066175	H	3.599948	3.732449	-3.195439
C	-3.828297	-0.826597	2.009095	H	3.877056	3.641714	-1.439587
C	-3.258707	-0.694652	0.735899	H	4.162239	2.214552	-2.433675
C	-1.153262	-2.495725	4.085927	H	0.666994	4.718269	-3.598761
C	-2.039804	-3.330237	5.050547	H	1.902532	3.900797	-4.589735
C	-3.530542	-2.913205	5.032877	H	0.190503	3.507891	-4.810647
C	-3.722203	-1.497701	4.459243	H	0.016001	4.617043	2.873623
C	-0.002786	-2.627423	1.232893	H	0.301271	6.600823	4.348251
C	1.056809	-1.856411	0.734558	H	1.676192	8.523817	3.584170
C	2.333949	-2.386029	0.499456	H	2.762437	8.465961	1.349905
C	2.497425	-3.752766	0.729339	H	2.467992	6.472375	-0.117032
C	1.441805	-4.584692	1.118976	H	3.480486	-4.190362	0.568259
C	0.173907	-4.027975	1.364350	C	3.628119	-0.233873	2.282476
C	1.706636	-6.080538	1.216708	C	5.595995	1.230343	1.442250

## 7. Experimental Section

---

C	3.244557	1.264367	2.391683	H	-6.167231	1.701769	-3.157001
C	4.416727	2.143536	1.866120	H	-6.096876	3.824227	-1.786767
C	4.875233	-0.471897	3.177885	H	-7.171307	2.972788	0.307143
C	6.049466	0.427540	2.691191	H	-6.425451	4.541652	0.600430
C	3.636328	-2.777376	-2.280872	H	-5.851620	2.053971	2.000634
C	5.602092	-1.284891	-3.074685	H	-5.050833	3.603076	2.242372
C	4.414700	-1.142832	-4.063180	H	-3.631702	4.181472	-1.843679
C	3.247566	-2.061608	-3.600795	H	-4.345523	5.215801	-0.608486
C	6.051870	-2.770324	-3.070407	H	-2.317489	3.111615	-0.228632
C	4.878267	-3.663863	-2.570877	H	-2.970442	4.203162	0.994011
H	6.482043	0.657937	-1.200278	H	-3.389161	1.826611	1.608093
H	6.358893	1.127911	3.477236	H	-6.144526	-0.492423	-4.411563
H	6.927278	-0.177792	2.440172	H	-3.572192	-2.678658	-1.028252
H	6.426732	1.829932	1.051455	H	-4.485094	-2.259140	-5.092043
H	4.616913	-0.244565	4.219768	H	-3.673786	-0.741976	-4.713257
H	5.155552	-1.530325	3.143090	H	-2.418148	-1.833432	-3.065429
H	4.096552	2.751399	1.011294	H	-3.255812	-3.341477	-3.422053
H	4.759809	2.844261	2.637630	H	-7.319618	-1.874254	-2.699728
H	2.324635	1.449241	1.830987	H	-6.580067	-2.927445	-3.903067
H	3.026910	1.498791	3.441255	H	-5.346906	-3.971860	-2.213226
H	2.798899	-0.860240	2.619596	H	-6.063436	-2.896083	-1.016384
H	4.752241	-1.411460	-5.072318	H	-3.225370	-0.768533	5.119008
H	4.087907	-0.097782	-4.104238	H	-4.784367	-1.227249	4.444465
H	3.029646	-2.823336	-4.360136	H	-4.101330	-3.609078	4.406110
H	2.328680	-1.493701	-3.441783	H	-3.957218	-2.976855	6.040846
H	6.931826	-2.886491	-2.428095	H	-1.961091	-4.394765	4.802400
H	6.357448	-3.056504	-4.084661	H	-1.629345	-3.224972	6.061867
H	5.166441	-4.211493	-1.666062	H	-0.245792	-3.045393	3.827378
H	4.611990	-4.414205	-3.325548	H	-0.811570	-1.603381	4.632402
H	6.433782	-0.635389	-3.373528	H	-1.907927	-4.548222	1.222215
H	2.802904	-3.391319	-1.932856	H	-1.210061	-4.873652	2.790891
C	-4.158847	-2.196610	-1.813494	H	-0.791023	-6.518306	0.253706
C	-5.555321	-1.024657	-3.655362	H	-1.592906	-7.006906	1.745805
C	-3.408674	-2.284440	-3.169481	H	0.604689	-6.710294	2.976765
C	-4.241246	-1.569657	-4.273691	H	0.720859	-7.942050	1.721535
C	-6.357684	-2.225443	-3.089393	H	2.656525	-6.247530	1.741440
C	-5.525336	-2.916663	-1.970677	H	1.855787	-6.474700	0.200037
C	-5.475595	3.397990	-0.990218				
C	-4.012964	2.301383	0.847427				
C	-4.136419	4.170684	-0.871146				
C	-3.245414	3.489228	0.207138				
C	-6.207782	3.490029	0.374283				
C	-5.315231	2.857067	1.482182				

Energy = -3466.38847500 Hartree

Tc = 1.186656

G = -3465.201819 Hartree

Nimag = 1 (309i)

## 8. Bibliography

- [1] W. T. Kelvin, *The molecular tactics of a crystal* Clarendon: Oxford, **1984**.
- [2] E. L. Eliel, S. H. Wilen, *Stereochemistry of organic compounds*, John Wiley: Chichester, **1994**.
- [3] J.-B. Biot, *Ann. Chim. Phys.* **1838**, 69, 27.
- [4] L. Pasteur, *Compt. Rend. Acad. Sci.* **1848**, 34, 535.
- [5] J. H. van't Hoff, *Arch. Neerl. Sci. Exactes Nat.* **1874**, 9, 445.
- [6] J. A. Le Bel, *Bull. Soc. Chim. France* **1874**, 22, 331.
- [7] M. Klusmann, D. G. Blackmond, in *Chemical Evolution II: From the Origins of Life to Modern Society*, L. Zaikowski, J. M. Friedrich, S. R. Seidel (Eds.), ACS Symposium Series, **2009**, vol. 1025, chapter 7, pp. 133-145.
- [8] (a) E. Fischer, *Ber. Dtsch. Chem. Ges.* **1894**, 27, 2985; (b) E. Fischer, *Ber. Dtsch. Chem. Ges.* **1894**, 27, 3479; (c) E. Fischer, *J. Chem. Soc., Trans.* **1907**, 91, 1749.
- [9] (a) R. S. Shallenberger, *Taste Chemistry*, Chapman & Hall: Glasgow, **1993**; (b) J. C. Brookes, A. P. Horsefield, A. M. Stoneham, *J. R. Soc. Interface*, **2009**, 6, 75; (c) M. D. Joesten, J. L. Hogg, M. E. Castellion, *The World of Chemistry: Essentials: Essentials*, Thomson Brooks/Cole, Belmont: **2007**.
- [10] M. Eichelbaum, A. S. Gross *Adv. Drug Res.* **1996**, 28, 1.
- [11] W. Lenz, *Teratology* **1988**, 38, 203.
- [12] Food and Drug Administration, *Chirality* **1992**, 4, 338.
- [13] I. Agranat, H. Caner, J. Caldwell, *Nat. Rev. Chem. Discov.* **2002**, 1, 753.
- [14] J. Jacques, A. Collet, S. H. Wilen, *Enantiomers, racemates, and resolutions*, Wiley: Chichester, **1981**.
- [15] P. Walsh, M. Kowzowski, *Fundamentals in Asymmetric Catalysis*, University Science Books: Sausalito, **2008**.



- [16] A. D. McNaught, A. Wilkinson, *IUPAC. Compendium of Chemical Terminology, 2nd ed. (the "Gold Book")*. Blackwell Scientific Publications: Oxford, **1997**.
- [17] (a) W. S. Knowles, M. J. Sabacky, *Chem. Commun.* **1968**, 1445; (b) B. D. Vineyard, W. S. Knowles, M. J. Sabacky *J. Mol. Catal.* **1983**, *19*, 159.
- [18] W. S. Knowles, *Asymmetric Hydrogenations*; R. J. Noyori, *Asymmetric Catalysis: Science and Opportunities*; K. B. Sharpless, *Searching for Reactivity in Les Prix Nobel. The Nobel Prizes 2001* ed. T. Frängsmyr, Nobel Foundation: Stockholm **2002**.
- [19] B. List, E. A. Lerner, C. F. Barbas III, *J. Am. Chem. Soc.* **2000**, *122*, 2395.
- [20] K. A. Ahrendt, C. J. Borths, D. W. C. MacMillan, *J. Am. Chem. Soc.* **2000**, *122*, 4243.
- [21] B. List, *Chem. Rev.* **2007**, *107*, 5413.
- [22] F. Xu, *Organocatalysis for Asymmetric Synthesis: From Lab To Factory in Sustainable Catalysis: Challenges and Practices for the Pharmaceutical and Fine Chemical Industries* eds. P. J. Dunn, K. K. Hii, M. J. Krische, M. T. Williams, John Wiley & Sons: Hoboken, New Jersey **2013**.
- [23] (a) P. Ball, *Nanotechnology* **2002**, *13*, 15; (b) R. Breslow, *J. Biol. Chem.* **2009**, *284*, 1337.
- [24] D. L. Nelson, M. M. Cox Lehninger, *Principles of Biochemistry* W.H. Freeman and Company: New York **2008**.
- [25] B. List, *Angew. Chem. Int. Ed.* **2010**, *49*, 1730.
- [26] J. von Liebig, *Liebigs Ann. Chem.* **1860**, *113*, 246.
- [27] G. Bredig, P. S. Fiske, *Biochem. Z.* **1912**, *46*, 7.
- [28] H. Pracejus, *Justus Liebigs Ann. Chem.*, **1960**, *634*, 9.
- [29] For Hajos-Parrish-Eder-Sauer-Wiechert reaction: (a) Z. G. Hajos, D. R. Parrish, *J. Org. Chem.* **1974**, *39*, 1615; (b) U. Eder, G. Sauer, R. Wiechert, *Angew. Chem. Int. Ed.* **1971**, *10*, 496. For Julia-Colonna epoxidation: (a) S. Julia, J. Masana, J. C. Vega, *Angew. Chem. Int. Ed.* **1980**, *19*, 929; (b) S. Julia, J. Guixer, J. Masana, J. Rocas, S. Colonna, R. Annunziata, H.

Molinari, *J. Chem. Soc., Perkin Trans. 1* **1982**, 1317. For Shi epoxidation: Y. Tu, Z.-X. Wang, Y. Shi *J. Am. Chem. Soc.* **1996**, *118*, 9806.

[30] 10851 publications. Data are based on a SciFinder® search of publications containing the concept 'organocatalysis'. The search was performed on April 2<sup>nd</sup>, 2015.

[31] For comprehensive reviews about asymmetric organocatalysis, see: (a) A. Berkessel, H. Gröger (Eds.), *Asymmetric Organocatalysis*, Wiley-VCH: Weinheim, **2005**. (b) P. I. Dalko (Ed.), *Enantioselective Organocatalysis: Reactions and Experimental Procedures*, Wiley-VCH: Weinheim, **2007**.

[32] (a) K. Fukui *Science* **1982**, *218*, 747; (b) *Frontier orbitals and organic chemical reactions I*. Fleming, John Wiley & Sons, Chichester, **2010**.

[33] (a) B. List, J. W. Yang, *Science* **2006**, *313*, 1584; (b) D. W. C. MacMillan *Nature* **2008**, *455*, 304.

[34] S. Mukherjee, J. W. Yang, S. Hoffmann, B. List, *Chem. Rev.* **2007**, *107*, 5471.

[35] A. Erkkilä, I. Majander, P. M. Pihko, *Chem. Rev.* **2007**, *107*, 5416.

[36] H. Jang, J. Hong, D. W. C. MacMillan, *J. Am. Chem. Soc.* **2007**, *129*, 7004.

[37] (a) D. Enders, O. Niemeier, A. Henseler, *Chem. Rev.* **2007**, *107*, 5606; (b) J. L. Moore, T. Rovis, *Top. Curr. Chem.* **2010**, *291*, 77.

[38] (a) A. G. Doyle, E. N. Jacobsen, *Chem. Rev.* **2007**, *107*, 5713; (b) J. Alemán, A. Parra, H. Jiang, K. A. Jørgensen, *Chem. Eur. J.* **2011**, *17*, 6890.

[39] (a) D. Kampen, C. M. Reisinger, B. List, *Top. Curr. Chem.* **2010**, *291*, 395; (b) T. Akiyama, J. Itoh, K. Fuchibe, *Adv. Synth. Catal.* **2006**, *348*, 999; (c) M. Terada, *Synthesis* **2010**, 1929.

[40] (a) M. Mahlau, B. List, *Angew. Chem. Int. Ed.* **2013**, *52*, 518; (b) R. J. Phipps, G. L. Hamilton, F. D. Toste, *Nature Chem.* **2012**, *4*, 603; (c) K. Brak, E. N. Jacobsen, *Angew. Chem. Int. Ed.* **2013**, *52*, 534.

[41] J. Seayad, B. List, *Org. Biomol. Chem.* **2005**, *3*, 719.

[42] S. Bahmanyar, K. N. Houk, H. J. Martin, B. List, *J. Am. Chem. Soc.* **2003**, *125*, 2475.

- [43] (a) J. N. Brønsted, *Recl. Trav. Chim. Pays-Bas* **1923**, *42*, 718; (b) T. M. Lowry, *Chem. and Ind.* **1923**, *42*, 43.
- [44] M. S. Taylor, E. N. Jacobsen, *Angew. Chem. Int. Ed.* **2006**, *45*, 1520.
- [45] M. Sinnott, *Comprehensive Biological Catalysis: A Mechanistic Reference* Academic Press: London **1998**.
- [46] M. Sigman, E. N. Jacobsen, *J. Am. Chem. Soc.* **1998**, *120*, 4901.
- [47] Y. Huang, A. K. Unni, A. N. Thadani, V. H. Rawal, *Nature* **2003**, *424*, 146.
- [48] H. Yamamoto, K. Futatsugi, *Angew. Chem. Int. Ed.* **2005**, *44*, 1924.
- [49] T. Akiyama, J. Itoh, K. Yokota, K. Fuchibe, *Angew. Chem. Int. Ed.* **2004**, *43*, 1566.
- [50] (a) D. Uraguchi, M. Terada, *J. Am. Chem. Soc.* **2004**, *126*, 5356; (b) M. Hatano, K. Moriyama, T. Maki, K. Ishihara, *Angew. Chem. Int. Ed.* **2010**, *49*, 3823.
- [51] D. Parmar, E. Sugiono, S. Raja, M. Rueping, *Chem. Rev.* **2014**, *114*, 9047.
- [52] R. Noyori, I. Tomino, Y. Tanimoto, *J. Am. Chem. Soc.* **1979**, *101*, 3129.
- [53] M. Klussmann, L. Ratjen, S. Hoffmann, V. Wakchaure, R. Goddard, B. List, *Synlett* **2010**, 2189.
- [54] (a) X.-H. Chen, X.-Y. Xu, H. Liu, L.-F. Cun, L.-Z. Gong, *J. Am. Chem. Soc.* **2006**, *128*, 14802; (b) G. B. Rowland, H. Zhang, E. B. Rowland, S. Chennamadhavuni, Y. Wang, J. C. Antilla, *J. Am. Chem. Soc.* **2005**, *127*, 15696; (c) K. Mori, K. Ehara, K. Kurihara, T. Akiyama, *J. Am. Chem. Soc.* **2011**, *133*, 6166; (d) Q.-S. Guo, D.-M. Du, J. Xu, *Angew. Chem. Int. Ed.* **2008**, *47*, 759; (e) T. Akiyama, Y. Saitoh, H. Morita, K. Fuchibe, *Adv. Synth. Catal.* **2005**, *347*, 1523; (f) I. Čorić, S. Müller, B. List, *J. Am. Chem. Soc.* **2010**, *132*, 17370; (g) F. Xu, D. Huang, C. Han, W. Shen, X. Lin, Y. Wang, *J. Org. Chem.* **2010**, *75*, 8677; (h) J. Stemper, K. Isaac, J. Pastor, G. Frison, P. Retailleau, A. Voiturez, J.-F. Betzer, A. Marinetti, *Adv. Synth. Catal.* **2013**, *355*, 3613; (j) D. Enders, M. Ludwig, G. Raabe, *Chirality* **2012**, *24*, 215.
- [55] (a) M. Terada, K. Sorimachi, D. Uraguchi, *Synlett* **2006**, 133; (b) G. Pousse, A. Devineau, V. Dalla, L. Humphreys, M.-C. Lasne, J. Rouden, J. Blanchet, *Tetrahedron* **2009**, *65*, 10617; (c) N. D. Shapiro, V. Rauniyar, G. L. Hamilton, J. Wu, F. D. Toste, *Nature* **2011**, *470*, 245; (d) D.

Nakashima, H. Yamamoto, *J. Am. Chem. Soc.* **2006**, *128*, 9626; (e) C. H. Cheon, H. Yamamoto, *Chem. Commun.* **2011**, *47*, 3043; (e) S. Vellalath, I. Čorić, B. List, *Angew. Chem. Int. Ed.* **2010**, *49*, 9749.

[56] (a) T. Hashimoto, K. Maruoka, *J. Am. Chem. Soc.* **2007**, *129*, 10054; (b) D. Kampen, A. Ladépêche, G. Claßen, B. List, *Adv. Synth. Catal.* **2008**, *350*, 962; (c) M. Hatano, T. Maki, K. Moriyama, M. Arinobe, K. Ishihara, *J. Am. Chem. Soc.* **2008**, *130*, 16858; (d) P. García-García, F. Lay, P. García-García, C. Rabalakos, B. List, *Angew. Chem. Int. Ed.* **2009**, *48*, 4363; (e) S. Prévost, N. Dupré, M. Leutzsch, Q. Wang, V. Wakchaure, B. List *Angew. Chem. Int. Ed.* **2014**, *53*, 8770; (f) I. Čorić, B. List, *Nature* **2012**, *483*, 315; (g) J. H. Kim, I. Čorić, S. Vellalath, B. List, *Angew. Chem. Int. Ed.* **2013**, *52*, 4474; (h) S. Liao, I. Čorić, Q. Wang, B. List *J. Am. Chem. Soc.* **2012**, *134*, 10765.

[57] (a) B. M. Nugent, R. A. Yoder, J. N. Johnston, *J. Am. Chem. Soc.* **2004**, *126*, 3418; (b) H. Xu, S. J. Zuend, M. G. Woll, Y. Tao, E. N. Jacobsen, *Science* **2010**, *327*, 986.

[58] S. Patai, *The chemistry of carboxylic acids and esters* Interscience Publishers: New York **1969**.

[59] M. A. Ogliaruso, J. F. Wolfe, *The synthesis of carboxylic acids and esters and their derivatives* eds S. Patai, Z. Rappoport, Wiley-Interscience: New York **1991**.

[60] J. March, *Advanced organic chemistry* Wiley-Interscience: New York **1992**.

[61] (a) L. J. Gooßen, N. Rodriguez, K. Gooßen, *Angew. Chem. Int. Ed.* **2008**, *47*, 3100; (b) L. J. Gooßen, K. Gooßen, N. Rodriguez, M. Blanchot, C. Linder, B. Zimmermann, *Pure Appl. Chem.* **2008**, *80*, 1725; (c) L. J. Gooßen, F. Collet, K. Gooßen, *Isr. J. Chem.* **2010**, *50*, 617.

[62] (a) T. Ohta, H. Takaya, M. Kitamura, K. Nagai, R. Noyori, *J. Org. Chem.* **1987**, *52*, 3174; (b) T. Ohta, H. Takaya, R. Noyori, *Tetrahedron Lett.* **1990**, *31*, 7189.

[63] E. N. Jacobsen, F. Kakiuchi, R. G. Konsler, J. F. Larrow, M. Tokunaga, *Tetrahedron Lett.* **1997**, *38*, 773.

[64] D. D. Ford, L. P. C. Nielsen, S. J. Zuend, C. B. Musgrave, E. N. Jacobsen, *J. Am. Chem. Soc.* **2013**, *135*, 15595.

- [65] (a) Z. Ning, R. Jin, J. Ding, L. Gao, *Synlett* **2009**, 2291; For recent reports on metal-catalyzed iodolactonization see: (b) T. Arai, S. Kajikawa, E. Matsumura, *Synlett* **2013**, 2045; (c) L. Filippova, Y. Stenstrøm, T. V. Hansen, *Tetrahedron Lett.* **2014**, *55*, 419.
- [66] H.-J. Lee, D. -Y Kim, *Tetrahedron Lett.* **2012**, *53*, 6984.
- [67] (a) L. Yin, M. Kanai, M. Shibasaki, *J. Am. Chem. Soc.* **2009**, *131*, 9610; (b) L. Yin, M. Kanai, M. Shibasaki, *Tetrahedron* **2012**, *68*, 6497.
- [68] (a) T. Dohi, A. Maruyama, N. Takenaga, K. Senami, Y. Minamitsuji, H. Fujioka, S. B. Caemmerer, Y. Kita, *Angew. Chem. Int. Ed.* **2008**, *47*, 3787; (b) T. Dohi, N. Takenaga, T. Nakae, Y. Toyoda, M. Yamasaki, M. Shiro, H. Fujioka, A. Maruyama, Y. Kita, *J. Am. Chem. Soc.* **2013**, *135*, 4558; (c) M. Uyanik, T. Yasui, K. Ishihara, *Angew. Chem. Int. Ed.* **2010**, *49*, 2175.
- [69] (a) M. Wang, L. X. Gao, W. P. Mai, A. X. Xia, F. Wang, S. B. Zhang, *J. Org. Chem.* **2004**, *69*, 2874; (b) D. C. Whitehead, R. Yousefi, A. Jaganathan, B. Borhan, *J. Am. Chem. Soc.* **2010**, *132*, 3298; (c) G. E. Veitch, E. N. Jacobsen, *Angew. Chem. Int. Ed.* **2010**, *49*, **7332**; (d) L. Zhou, C. K. Tan, X. Jiang, F. Chen, Y.-Y. Yeung, *J. Am. Chem. Soc.* **2010**, *132*, 15474; (e) K. Murai, T. Matsushita, A. Nakamura, S. Fukushima, M. Shimura, H. Fujioka, *Angew. Chem. Int. Ed.* **2010**, *49*, 9174.
- [70] (a) W. Zhang, S. Zheng, N. Liu, J. B. Werness, I. A. Guzei, W. Tang, *J. Am. Chem. Soc.* **2010**, *132*, 3664; (b) M. C. Dobish, J. N. Johnston, *J. Am. Chem. Soc.* **2012**, *134*, 6068; (c) D. H. Paull, C. Fang, J. R. Donald, A. D. Pansick, S. F. Martin, *J. Am. Chem. Soc.* **2012**, *134*, 11128.
- [71] M. Sakuma, A. Sakakura, K. Ishihara, *Org. Lett.* **2013**, *15*, 2838.
- [72] (a) G. S. Cortez, R. L. Tennyson, D. Romo, *J. Am. Chem. Soc.* **2001**, *123*, 7945. (b) V. C. Purohit, R. D. Richardson, J. W. Smith, D. Romo, *J. Org. Chem.* **2006**, *71*, 4549. (c) G. S. Cortez, S. H. Oh, D. Romo, *Synthesis* **2001**, 1731. For a related review article on ammonium enolate organocatalysis see: (d) M. J. Gaunt, C. C. C. Johansson, *Chem. Rev.* **2007**, *107*, 5596.
- [73] (a) A. K. Yudin (Ed.), *Aziridines and Epoxides in Organic Synthesis*, Wiley-VCH: Weinheim, 2006; (b) A. Padwa, S. S. Murphree, *Arkivoc* **2006**, *3*, 6.
- [74] (a) R. D. Bach, O. Dimitrenko *J. Org. Chem.* **2002**, *67*, 3884; (b) H. C. Kolb, M. G. Finn, K. B. Sharpless, *Angew. Chem. Int. Ed.* **2001**, *40*, 2004.

- [75] E. M. McGarrigle, E. L. Myers, O. Illa, M. A. Shaw, S. L. Riches, V. K. Aggarwal, *Chem. Rev.* **2007**, *107*, 5841.
- [76] (a) Q.-H. Xia, H.-Q. Ge, C.-P. Ye, Z.-M. Liu, K.-X. Su, *Chem. Rev.* **2005**, *105*, 1603; (b) H. M. I. Osborn, J. Sweeney, *Tetrahedron: Asymmetry* **1997**, *8*, 1693; (c) Y. Zhu, Q. Wang, R. G. Cornwall, Y. Shi, *Chem. Rev.* **2014**, *114*, 8199.
- [77] For review articles on metal-catalyzed enantioselective ring opening of epoxides see: (a) I. Pastor, M. Yus, *Curr. Org. Chem.* **2005**, *9*, 1; (b) C. Schneider, *Synthesis* **2006**, 3919.
- [78] For selected examples of metal-catalyzed enantioselective ring opening of aziridines see: (a) B. Wu, J. R. Parquette, T. V. RajanBabu, *Science* **2009**, *326*, 1662; (b) B. Wu, J. C. Gallucci, J. R. Parquette, T. V. RajanBabu, *Angew. Chem. Int. Ed.* **2009**, *48*, 1126; (c) Y. Xu, L. Lin, M. Kanai, S. Matsunaga, M. Shibasaki, *J. Am. Chem. Soc.* **2011**, *133*, 5791; (d) S. Peruncheralthan, H. Teller, C. Schneider, *Angew. Chem. Int. Ed.* **2009**, *48*, 4849; (e) Y. Fukuta, T. Mita, N. Fukuda, M. Kanai, M. Shibasaki, *J. Am. Chem. Soc.* **2006**, *128*, 6312; (f) Z. Li, M. Fernández, E. N. Jacobsen, *Org. Lett.* **1999**, *1*, 1611.
- [79] J. Biggs, N. B. Chapman, A. F. Finch, V. Wray, *J. Chem. Soc. B* **1971**, 55.
- [80] (a) T. H. Chan, P. Di Raddo, *Tetrahedron Lett.* **1979**, *22*, 1947; (b) P. Di Raddo, T. H. Chan, *J. Chem. Soc. Chem. Commun.* **1983**, 16; (c) O. Meyer, S. Ponaire, M. Rohmer, C. Grosdemange-Billiard, *Org. Lett.* **2006**, *8*, 4347.
- [81] (a) K. Misiura, R. W. Kinas, W. J. Stec, H. Kusnierczyk, C. Radzikowski, A. Sonodas, *J. Med. Chem.* **1988**, *31*, 226; (b) J.-Y. Goujon, D. Gueyrard, P. Compain, O. R. Martin, K. Ikeda, A. Katoc, N. Asano, *Bioorg. Med. Chem.* **2005**, *13*, 2313; (c) A. Alcaide, A. Llebaria, *J. Org. Chem.* **2014**, *79*, 2993.
- [82] T. Mita, E. N. Jacobsen, *Synlett*, **2009**, 1680.
- [83] M. Zhuang, H. Du, *Org. Biomol. Chem.* **2013**, *11*, 1460.
- [84] (a) E. B. Rowland, G. B. Rowland, E. Rivera-Otero, J. C. Antilla, *J. Am. Chem. Soc.* **2007**, *129*, 12084; (b) A. Lattanzi, G. Della Sala, *Eur. J. Org. Chem.* **2009**, 1845; (c) G. Della Sala, A. Lattanzi, *Org. Lett.* **2009**, *11*, 3330; (d) M. Senatore, A. Lattanzi, S. Santoro, C. Santi, G. Della

Sala, *Org. Biomol. Chem.* **2011**, *9*, 6205; (e) S. E. Larson, J. C. Baso, G. Li, J. C. Antilla, *Org. Lett.* **2009**, *11*, 5186.

[85] G. Della Sala, *Tetrahedron* **2013**, *69*, 50.

[86] For transformations of epoxides and aziridines in Lewis basic organocatalysis see: (a) R. Chawla, A. K. Singh, L. D. S. Yadav, *RSC Adv.* **2013**, *3*, 11385; (b) P.-A. Wang, *Beilstein J. Org. Chem.* **2013**, *9*, 1677.

[87] (a) S. E. Denmark, P. A. Barsanti, K.-T. Wong, R. A. Stavenger, *J. Org. Chem.* **1998**, *63*, 2428; (b) B. Tao, M. M.-C. Lo, G. C. Fu, *J. Am. Chem. Soc.* **2001**, *123*, 353; (c) M. Nakajima, M. Saito, M. Uemura, S. Hashimoto, *Tetrahedron Lett.* **2002**, *43*, 8827; (d) E. Tokuoka, S. Kotani, H. Matsunaga, T. Ishizuka, S. Hashimoto, M. Nakajima, *Tetrahedron: Asymmetry* **2005**, *16*, 2391; (e) N. Takenaka, R. S. Sarangthem, B. Captain, *Angew. Chem. Int. Ed.* **2008**, *47*, 9708.

[88] (a) Y. Zhang, C. W. Kee, R. Lee, X. Fu, J. Y.-T. Soh, E. M. F. Loh, K.-W. Huang, C.-H. Tan, *Chem. Commun.* **2011**, *47*, 3897; (b) A. Lattanzi, G. Della Sala, *Eur. J. Org. Chem.* **2009**, 1845; (c) Z. Wang, X. Sun, S. Ye, W. Wang, B. Wang, J. Wu, *Tetrahedron: Asymmetry* **2008**, *19*, 964.

[89] (a) H. C. Kolb, M. S. VanNieuwenhze, K. B. Sharpless, *Chem. Rev.* **1994**, *94*, 2483. (b) H. – U. Blaser, E. Schmidt (Eds), *Asymmetric Catalysis on Industrial Scale: Challenges, Approaches and Solutions*, Wiley-VCH: Weinheim, **2004**; (c) P. Kumar, P. Gupta, *Synlett* **2009**, 1367.

[90] (a) W. B. Jakoby, D. M. Ziegler, *J. Biol. Chem.* **1990**, *265*, 20715; (b) F. P. Guengerich, *Chem. Res. Toxicol.* **2008**, *21*, 70.

[91] (a) J. K. Beetham, D. Grant, M. Arand, J. Garbarino, T. Kiosue, F. Pinot, F. Oesch, W. R. Belknap, K. Shinozaki, B. D. Hammock, *DNA Cell Biol.* **1995**, *14*, 61; (b) J. W. Newman, C. Morisseau, B. D. Hammock, *Prog. Lipid. Res.* **2005**, *44*, 1; (c) M. T. Reetz, C. Torre, A. Eipper, R. Lohmer, M. Hermes, B. Brunner, A. Maichele, M. Bocola, M. Arand, A. Cronin, Y. Genzel, A. Archelas, R. Furstoss, *Org. Lett.* **2004**, *6*, 177; (d) M. T. Reetz, M. Bocola, L.-W. Wang, J. Sanchis, A. Cronin, M. Arand, J. Zou, A. Archelas, A. –L. Bottalla, A. Naworyta, S. L. Mowbray, *J. Am. Chem. Soc.* **2009**, *131*, 7334.

- [92] (a) M. Arand, H. Wagner, F. Oesch, *J. Biol. Chem.* **1996**, *271*, 4223; (b) B. K. Biswal, C. Morisseau, G. Garen, M. M. Cherney, C. Garen, C. Niu, B. D. Hammock, M. N. G. James, *J. Mol. Biol.* **2008**, *381*, 897.
- [93] T. Watabe, S. Suzuki, *Biochem. Biophys. Res. Commun.* **1971**, *43*, 1252.
- [94] (a) M. Tokunaga, J. F. Larrow, F. Kakiuchi, E. N. Jacobsen, *Science* **1997**, *277*, 936. (b) J. M. Ready, E. N. Jacobsen, *Angew. Chem. Int. Ed.* **2002**, *41*, 1374; (c) D. E. White, P. M. Tadross, Z. Lu, E. N. Jacobsen, *Tetrahedron* **2014**, *70*, 4165.
- [95] A. Berkessel, E. Ertürk, *Adv. Synth. Catal.* **2006**, *348*, 2619.
- [96] S. Matsunaga, J. Das, J. Roels, E. M. Vogl, N. Yamamoto, T. Iida, K. Yamaguchi, M. Shibasaki, *J. Am. Chem. Soc.* **2000**, *122*, 2252.
- [97] C. Schneider, A. R. Sreekanth, E. Mai, *Angew. Chem. Int. Ed.* **2004**, *43*, 5691.
- [98] (a) E. A. Ilardi, E. Vitaku, J. T. Njardarson, *J. Med. Chem.* **2014**, *57*, 2832; (b) L. K. Moran, J. M. Gutteridge, G. J. Quinlan, *Curr. Med. Chem.* **2001**, *8*, 763; (c) K. Pachamuthu, R. R. Schmidt, *Chem. Rev.* **2006**, *106*, 160.
- [99] (a) R. J. Cremlin, *An Introduction to Organosulfur Chemistry*, John Wiley & Sons Ltd: Chichester, **1996**. (b) A. Q. Acton, *Sulfur Compounds: Advances in Research and Application*, Scholarly Edition: Atlanta, GA, **2012**. (c) J. Clayden, P. MacLellan, *Beilstein J. Org. Chem.* **2011**, *7*, 582. (d) D. J. Procter, *J. Chem. Soc., Perkin Trans. 1*, **2001**, 335; (e) T. Kondo, T. Mitsudo, *Chem. Rev.* **2000**, *100*, 3205.
- [100] For alternative routes to enantioenriched thiols see: (a) A. Peschiulli, B. Procuranti, C. J. O' Connor, S. J. Connon, *Nat. Chem.* **2010**, *2*, 380; (b) C. Palomo, M. Oiarbide, F. Dias, R. López, A. Linden, *Angew. Chem. Int. Ed.* **2004**, *43*, 3307; (c) C. Palomo, M. Oiarbide, R. López, P. B. González, E. Gómez-Bengoia, J. M. Saá, A. Linden, *J. Am. Chem. Soc.* **2006**, *128*, 15236; (d) L. E. Overman, S. W. Roberts, H. F. Sneddon, *Org. Lett.* **2008**, *10*, 1485; (e) P. Chauhan, S. Mahajan, D. Enders, *Chem. Rev.* **2014**, *114*, 8807; (f) A. F. Meindertsma, M. M. Pollard, B. L. Feringa, J. G. de Vries, A. J. Minnaard, *Tetrahedron: Asymmetry* **2007**, *18*, 2849; (g) K. L. Kimmel, M. T. Robak, J. A. Ellman, *J. Am. Chem. Soc.* **2009**, *131*, 8754; (h) J. P. Phelan, E. J. Patel, J. A. Ellman, *Angew. Chem. Int. Ed.* **2014**, *53*, 11329; (i) S. Diosdado, J. Etxabe, J.



Izquierdo, A. Landa, A. Mielgo, I. Olaizola, R. López, C. Palomo, *Angew. Chem. Int. Ed.* **2013**, *52*, 11846.

[101] (a) T. A. Blizzard, F. DiNinno, H. Y. Chen, S. Kim, J. Y. Wu, W. Chan, E. T. Birzin, Y. T. Yang, L.-Y. Pai, E. C. Hayes, C. A. DaSilva, S. P. Roher, J. M. Scheffer, M. L. Hammond, *Bioorg. Med. Chem.* **2005**, *15*, 3912; (b) J. M. Bailey, *Prostaglandins, Leukotrienes and Lipoxins Biochemistry, Mechanism of Action and Clinical Applications*, Plenum Press: New York, **1985**; (c) T. Nagao, M. Sato, H. Nakajima, A. Kiyomoto, *Chem. Pharm. Bull.* **1973**, *21*, 92; (d) M. Ono, E. Takamura, K. Shinozaki, T. Tsumura, T. Hamano, Y. Yagi, K. Tsubota, *Am. J. Ophthalmol.* **2004**, *138*, 6.

[102] (a) H. Yamashita, T. Mukaiyama, *Chem. Lett.* **1985**, 1643; (b) T. Iida, N. Yamamoto, H. Sasai, M. Shibasaki, *J. Am. Chem. Soc.* **1997**, *119*, 4783; (c) C. Ogawa, N. Wang, S. Kobayashi, *Chem. Lett.* **2007**, *36*, 34; (d) M. V. Nandakumar, A. Tschöp, H. Krautscheid, C. Schneider, *Chem. Commun.* **2007**, 2756; (e) M. H. Wu, E. N. Jacobsen, *J. Org. Chem.* **1998**, *63*, 5252; (f) J. Wu, X.-L. Hou, L.-X. Dai, L.-J. Xia, M.-H. Tang, *Tetrahedron: Asymmetry* **1998**, *9*, 3431; (g) J. Sun, F. Yuan, M. Yang, Y. Pan, C. Zhu, *Tetrahedron Lett.* **2009**, *50*, 548.

[103] Z. Wang, W. K. Law, J. Sun, *Org. Lett.* **2013**, *15*, 5964.

[104] N. V. Sidgwick, *Inorganic chemistry. Ann. Rep.* **1933**, *30*, 144.

[105] A. Kütt, I. Leito, I. Kaljurand, L. Sooväli, M. V. Vlasov, L. M. Yagupolskii, I. A. Koppel, *J. Org. Chem.* **2006**, *71*, 2829.

[106] G. M. Barrow, *J. Am. Chem. Soc.* **1956**, *78*, 5802.

[107] D. F. Peppard, J. R. Ferraro, G. W. Mason, *J. Inorg. Nucl. Chem.* **1957**, *4*, 371.

[108] (a) F. Chu, L. S. Flatt, E. V. Anslyn, *J. Am. Chem. Soc.* **1994**, *116*, 4194; (b) J. DeFord, F. Chu, E. V. Anslyn, *Tetrahedron Lett.* **1996**, *37*, 1925.

[109] M. Rueping, E. Sugiono, C. Azap, T. Theissmann, M. Bolte, *Org. Lett.* **2005**, *7*, 3781.

[110] (a) T. Akiyama, Y. Tamura, J. Itoh, H. Morita, K. E. Fuchibe, *Synlett* **2006**, 141; (b) M. Rueping, C. Azap, *Angew. Chem. Int. Ed.* **2006**, *45*, 7832; (c) M. Rueping, E. Sugiono, F. R. Schoepke, *Synlett* **2007**, 1441; (d) G. Li, J. C. Antilla, *Org. Lett.* **2009**, *11*, 1075.

- [111] D. F. Peppard, J. R. Ferraro, G. W. Mason, *J. Inorg. Nucl. Chem.* **1958**, 7, 231.
- [112] S. C. Bergmeier, *Tetrahedron* **2000**, 56, 2561.
- [113] M. R. Monaco, B. Poladura, M. Diaz de los Bernardos, M. Leutzsch, R. Goddard, B. List *Angew. Chem. Int. Ed.* **2014**, 53, 7063.
- [114] (a) H. Friebolin, *Basic One- and Two-dimensional NMR Spectroscopy*, Wiley-VCH, Weinheim, **1998**; (b) C. Schalley (Ed.), *Analytical Methods in Supramolecular Chemistry*, Wiley-VCH: Weinheim, **2007**.
- [115] (a) K. F. Morris, C. S. Johnson, Jr., *J. Am. Chem. Soc.* **1992**, 114, 3139; (b) C. S. Johnson, Jr., *Prog. Nucl. Magn. Reson. Spectrosc.* **1999**, 34, 203.
- [116] L. Fielding, *Tetrahedron*, **2000**, 56, 6151.
- [117] J. S. Renny, L. L. Tomasevich, E. H. Tallmadge, D. B. Collum, *Angew. Chem. Int. Ed.* **2013**, 52, 11998.
- [118] K. Takeda, H. Yamashita, M. Akiyama, *Solvent Extr. Ion Exch.* **1987**, 5, 29.
- [119] C. C. Price, M.-T. L. Yip, *J. Biol. Chem.* **1974**, 249, 6849.
- [120] M. Kumar, S. Gandhi, S. Singh Kalra, V. K. Singh, *Synth. Commun.* **2008**, 38, 1527.
- [121] G. E. Ham, *J. Org. Chem.*, **1964**, 29, 3052.
- [122] V. Rauniyar, Z. J. Wang, H. E. Burks, F. D. Toste, *J. Am. Chem. Soc.* **2011**, 133, 8486.
- [123] (a) W. McCoull, F. A. Davis, *Synthesis* **2000**, 1347; (b) D. Tanner, *Ange. Chem. Int. Ed.* **1994**, 33, 599.
- [124] H. B. Kagan, J. C. Fiaud, *Topics in Stereochemistry* E. L. Eliel (Ed), Wiley & Sons: New York, **1988**.
- [125] Y. Ittah, Y. Sasson, I. Shahak, S. Tsaroom, J. Blum, *J. Org. Chem.* **1978**, 43, 4271.
- [126] N. Prieschajew, *Ber. Dtsch. Chem. Ges.* **1909**, 42, 4811.

- [127] (a) H. W. Heine, *Angew. Chem. Int. Ed.* **1962**, *1*, 528; (b) T. Nishiguchi, H. Tochio, A. Nabeya, Y. Iwakura, *J. Am. Chem. Soc.* **1969**, *91*, 5835; (c) D. Ferraris, W. J. Drury III, C. Cox, T. Lectka, *J. Org. Chem.* **1998**, *63*, 4568.
- [128] (a) F. J. Quijada, F. Rebolledo, V. Gotor, *Tetrahedron* **2012**, *68*, 7670; (b) M. Okano, J. Mito, Y. Maruyama, H. Masuda, T. Niwa, S.-I. Nakagawa, Y. Nakamura, A. Matsuura, *Bioorg. Med. Chem.* **2009**, *17*, 119.
- [129] N. J. Adderley, D. J. Buchanan, D.J. Dixon, D.I. Lainé, *Angew. Chem. Int. Ed.* **2003**, *42*, 4241.
- [130] (a) R. P. Bell, *Proc. R. Soc. London, Ser. A* **1936**, *154*, 414; (b) M. G. Evans, M. Polanyi, *J. Chem. Soc., Faraday Trans.* **1936**, *32*, 1333.
- [131] C. Girard, H. B. Kagan, *Angew. Chem. Int. Ed.* **1998**, *37*, 2922.
- [132] M. R. Monaco, S. Prévost, B. List, *Angew. Chem. Int. Ed.* **2014**, *53*, 8142.
- [133] F. Rived, M. Roses, E. Bosch, *Anal. Chim. Acta* **1998**, *374*, 309.
- [134] (a) H. Mandai, K. Murota, K. Mitsudo, S. Suga, *Org. Lett.* **2012**, *14*, 3486; (b) X. Cheng, S. Vellalath, R. Goddard, B. List, *J. Am. Chem. Soc.* **2008**, *130*, 15786; (c) X. Cheng, R. Goddard, G. Buth, B. List, *Angew. Chem. Int. Ed.* **2008**, *47*, 5079.
- [135] B. R. Steele, M. Micha-Screttas, C. G. Screttas, *Tetrahedron Lett.* **2004**, *45*, 9537.
- [136] A. Schmidt, A. Rahimi, *Chem. Commun.* **2010**, *46*, 2995.
- [137] T. E. Barder, S. D. Walker, J. R. Martinelli, S. L. Buchwald, *J. Am. Chem. Soc.* **2005**, *127*, 4685.
- [138] L. Salvi, N. R. Davis, S. Z. Ali, S. L. Buchwald, *Org. Lett.* **2012**, *14*, 170.
- [139] (a) F. R. Leroux, L. Bonnafoux, C. Heiss, F. Colobert, A. Lanfranchi, *Adv. Synth. Catal.* **2007**, *349*, 2705; (b) F. Leroux and M. Schlosser, *Angew. Chem. Int. Ed.* **2002**, *41*, 4272.
- [140] L. Camici, P. Dembech, A. Ricci, G. Seconi, M. Taddei, *Tetrahedron* **1988**, *44*, 4197.
- [141] M. Widhalm, C. Aichinger, K. Mereiter, *Tetrahedron Lett.* **2009**, *50*, 2425.

- [142] D. S. Wilbur, W. E. Stone, K. W. Anderson, *J. Org. Chem.* **1983**, *48*, 1542.
- [143] C. Stanciu, M. M. Olmstead, A. D. Phillips, M. Stender, P. P. Power, *Eur. J. Inorg. Chem.* **2003**, 3495.
- [144] For a different stepwise approach to **116d** see: H. Tomioka, H. Mizuno, H. Itakura, K. Hirai, *Chem. Commun.* **1997**, 2261.
- [145] R. Rathore, J. K. Kochi, *J. Org. Chem.* **1995**, *60*, 4399.
- [146] P. Ganji, H. Ibrahim, *J. Org. Chem.* **2012**, *77*, 511.
- [147] S. K. Kundu, W. S. Tan, J.-L. Yan, J.-S. Yang, *J. Org. Chem.* **2010**, *75*, 4640.
- [148] J. Cao, H.-Y. Lu, C.-F. Chen, *Tetrahedron* **2009**, *65*, 8104.
- [149] M. Fuchs, Y. Simeo, B. T. Ueberbacher, B. Mautner, T. Netscher, K. Fabe, *Eur. J. Org. Chem.* **2009**, 833.
- [150] C.-F. Chen, Y.-X. Ma, *Iptycenes chemistry*, Springer-Verlag: Berlin **2013**.
- [151] T. T. –L. Au-Yeung, S. –S. Chan, A. S. Chan, *Adv. Synth. Catal.* **2003**, *345*, 537.
- [152] (a) W. Zhang, J. L. Loebach, S. R. Wilson, E. N. Jacobsen, *J. Am. Chem. Soc.* **1990**, *112*, 2801; (b) R. Irie, K. Noda, Y. Ito, N. Matsumoto, T. Katsuki, *Tetrahedron: Asymmetry* **1991**, *7*, 481; (c) M. Colladon, A. Scarso, P. Sgarbossa, R. A. Michelin, G. Strukul, *J. Am. Chem. Soc.* **2006**, *128*, 14006; (d) S. Liao, B. List, *Angew. Chem. Int. Ed.* **2010**, *49*, 628; (e) A. Berkessel, T. Günther, Q. Wang, J.-M. Neudörfl, *Angew. Chem. Int. Ed.* **2013**, *52*, 8467.
- [153] (a) S. I. Kozhushkov, D. S. Yufit, A. de Meijere, *Adv. Synth. Catal.* **2005**, *347*, 255; (b) M. J. Palmer, J. A. Kenny, T. Walsgrove, A. M. Kawamoto, M. Wills, *J. Chem. Soc. Perkin Trans. 1* **2002**, 416.
- [154] (a) L. P. Hammett, *J. Am. Chem. Soc.* **1937**, *59*, 96; (b) C. Hansch, A. Leo, R. W. Taft, *Chem. Rev.* **1991**, *91*, 165.
- [155] P. Lu, *Tetrahedron* **2010**, *66*, 2549.
- [156] E. N. Jacobsen, I. Marko, W. S. Mungall, G. Schröder, K. B. Sharpless, *J. Am. Chem. Soc.* **1988**, *110*, 1968.

- [157] (a) S. Trudeau, J. B. Morgan, M. Shrestha, J. P. Morken, *J. Org. Chem.* **2005**, *70*, 9538; (b) B. Plietker, M. Niggeman, *Org. Lett.* **2003**, *5*, 3353; (c) K. Suzuki, P. D. Oldenburg, L. Que Jr., *Angew. Chem. Int. Ed.* **2008**, *47*, 1887; (d) R. A. Bhunnoo, Y. Hu, D. I. Lainé, R. C. D. Brown, *Angew. Chem. Int. Ed.* **2002**, *41*, 3479; (e) J. W. de Boer, W. R. Browne, S. R. Harutyunyan, L. Bini, T. D. Tiemersma-Wegman, P. L. Alsters, R. Hage, B. L. Feringa, *Chem. Commun.* **2008**, 3747; for a review on Osmium-free *syn*-dihydroxylation of alkenes, see (f) C. J. R. Bataille, T. J. Donohoe, *Chem. Soc. Rev.* **2011**, *40*, 114.
- [158] M. R. Monaco, S. Prévost, B. List, *J. Am. Chem. Soc.* **2014**, *136*, 16982.
- [159] For organocascade transformations see: (a) J. W. Yang, M. T. Hechavarria Fonseca, B. List, *J. Am. Chem. Soc.* **2005**, *127*, 15036; (b) Y. Huang, A. M. Walji, C. H. Larsen, S. W. C. MacMillan, *J. Am. Chem. Soc.* **2005**, *127*, 15051; (c) M. Marigo, T. Schulte, J. Franzén, K. A. Jørgensen, *J. Am. Chem. Soc.* **2005**, *127*, 15710. (d) C. Grondal, M. Jeanty, D. Enders, *Nature Chem.* **2010**, *2*, 167; (e) S. B. Jones, B. Simmons, A. Mastracchio, D. W. C. MacMillan, *Nature* **2011**, *475*, 183.
- [160] (a) D. Wu, D. Jia, *Int. J. Quant. Chem.* **2010**, *111*, 3018; (b) A. S. N. Murthy, C. N. R. Rao, B. D. N. Rao, P. Venkateswarlu, *Trans. Faraday Soc.* **1962**, *58*, 855.
- [161] D. A. Clabo, Jr., H. D. Dickson, T. L. Nelson, *J. Mol. Model.* **2000**, *6*, 341.
- [162] S. Nagaoka, T. Terao, F. Imashiro, A. Saika, N. Hirota, S. Hayashi, *J. Phys. Chem.* **1983**, *79*, 4694.
- [163] S.-j. Chang, D. McNally, S. Shary-Tehrany, M. J. Hickey, R. H. Boyd, *J. Am. Chem. Soc.* **1970**, *92*, 3109.
- [164] D. G. Blackmond, *Angew. Chem. Int. Ed.* **2005**, *44*, 4302.
- [165] J. Casado, M. A. Lopez-Quintela, F. M. Lorenzo-Barral, *J. Chem. Educ.* **1986**, *63*, 450.
- [166] T. H. Webb, C. S. Wilcox, *Chem. Soc. Rev.* **1993**, *22*, 383.
- [167] A. J. Lewis, D. E. Furst, *Nonsteroidal Anti Inflammatory Drugs: Mechanisms and Clinical Uses*, Marcel Dekker, New York: **1994**.

- [168] (a) A. Akdeniz, L. Mosca, T. Minami, P. Anzenbacher Jr., *Chem. Commun.* **2015**, 51, 5770; (b) Q. Ma, M. Ma, H. Tian, X. Ye, H. Xiao, L.-h. Chen, X. Lei, *Org. Lett.* **2012**, 14, 5813.
- [169] G. Adair, S. Mukherjee, B. List, *Aldrichimica Acta* **2008**, 41, 31.
- [170] (a) E. Vedejs, M. Jure, *Angew. Chem. Int. Ed.* **2005**, 44, 3974; (b) J. H. Kim, I. Čorić, C. Palumbo, B. List, *J. Am. Chem. Soc.* **2015**, 137, 1778.
- [171] Y. Xu, K. Kaneko, M. Kanai, M. Shibasaki, S. Matsunaga, *J. Am. Chem. Soc.* **2014**, 136, 9190.
- [172] R. Friesen, D. Dube, D. Deschenes, R. Fortin, PCT Int. Appl., WO 99/14194, **1999**.
- [173] (a) Z. Wang, Z. Chen, J. Sun, *Angew. Chem. Int. Ed.* **2013**, 52, 6685; (b) Z. Wang, F. K. Sheong, H. H. Y. Sung, I. D. Williams, Z. Lin, J. Sun, *J. Am. Chem. Soc.* **2015**, 137, 5895.
- [174] C. E. Johnson Jr., F. A. Bovey, *J. Phys. Chem.* **1958**, 29, 1012.
- [175] F. Shibahara, A. Yoshida, T. Murai, *Chem. Lett.* **2008**, 37, 646.
- [176] H. D. Flack, *Acta Cryst.* **1983**, A39, 876.

## 9. Appendix

### 9.1. Erklärung/Declaration

“Ich versichere, dass ich die von mir vorgelegte Dissertation selbständig angefertigt, die benutzten Quellen und Hilfsmittel vollständig angegeben und die Stellen der Arbeit – einschließlich Tabellen, Karten und Abbildungen –, die anderen Werken im Wortlaut oder dem Sinn nach entnommen sind, in jedem Einzelfall als Entlehnung kenntlich gemacht habe; dass diese Dissertation noch keiner anderen Fakultät oder Universität zur Prüfung vorgelegen hat; dass sie – abgesehen von unten angegebenen Teilpublikationen – noch nicht veröffentlicht worden ist sowie, dass ich eine solche Veröffentlichung vor Abschluss des Promotionsverfahrens nicht vornehmen werde. Die Bestimmungen der Promotionsordnung sind mir bekannt. Die von mir vorgelegte Dissertation ist von Herrn Professor Dr. Benjamin List betreut worden.“

Mülheim an der Ruhr, August 2015

---

(Mattia Riccardo Monaco)

Bisher sind folgende Teilpublikationen veröffentlicht worden:

- 1) “*Activation of Carboxylic Acids in Asymmetric Organocatalysis*”; M. R. Monaco, B. Poladura, M. Diaz de los Bernardos, M. Leutzsch, R. Goddard, B. List, *Angew. Chem. Int. Ed.* **2014**, *53*, 7063.
- 2) “*An Organocatalytic Asymmetric Hydrolysis of Epoxides*”; M. R. Monaco, S. Prévost, B. List, *Angew. Chem. Int. Ed.* **2014**, *53*, 8142.
- 3) “*Catalytic Asymmetric Synthesis of Thiols*”; M. R. Monaco, S. Prévost, B. List, *J. Am. Chem. Soc.* **2014**, *136*, 16982.

## 9.2. Lebenslauf/CV

### Mattia Riccardo Monaco

Geboren am 8. September 1987

in Neapel, Italien

Staatsangehörigkeit Italienisch

### Akademischer Werdegang

#### Promotion

11.2011-10.2015 Dissertation im Arbeitskreis von Prof. Dr. Benjamin List  
Max-Planck-Institut für Kohlenforschung in Mülheim an der Ruhr  
Titel: "Activation of Carboxylic acids *via* Self-Assembly Organocatalysis"

#### Hochschulstudium

10.2009-07.2011 M.Sc. im Arbeitskreis von Dr. Marco Bella  
Sapienza, University of Rome  
Titel: "Biomimetic Organocatalytic Synthesis: A New Enantioselective Approach towards the Class of Piperidine Alkaloids"  
*GIC* award 2011 – Italian Chemical Society für "excellent achievements in the field of catalysis"

10.2006-09.2009 B.Sc. im Arbeitskreis von Dr. Marco Bella  
Sapienza, University of Rome  
Titel: "Synthesis of Aminocarbonyl Compounds: The Rediscovery of Rabe Amination"

#### Schulbildung

09.2001-07.2006 Liceo Aristotele, naturwissenschaftliches Gymnasium, Rom, Italien

09.1998-07.2001 C. A. Dalla Chiesa, Sekundarschule, Rom, Italien

09.1993-07.1998 Europa, Grundschule, Rom, Italien